SYNOPSIS

Investigations into the Mechanical Cutting Characteristics of Some Medium and High Strength Rocks.

by

NUH BILGIN

The method of analysis developed by Protodyakanov and Teder has shown that different cutting tools behaved in substantially the same manner in the wide range of rocks tested. An overall picture of the cutting performance for picks, discs and roller cutters has been built up, and the work reported in this thesis has been an attempt to increase the available knowledge on cutting characteristics of a range of rocks. The data obtained is basic to the design of the cutting systems for the excavation of these rock materials.

INVESTIGATIONS INTO THE MECHANICAL CUTTING CHARACTERISTICS OF SOME MEDIUM AND HIGH STRENGTH ROCKS

A THESIS

Submitted for the Degree of

Ph.D in Applied Science of the

University of Newcastle upon Tyne

by

NUH BILGIN, B.Sc., I.T.U.

JUNE 1977

CONTENTS PAGE

Acknowledgements ... ...

List of Illustrations ... ...

CHAPTER ONE

1. Introduction 1

CHAPTER TWO

2. Objectives of Research 5

CHAPTER THREE

3. Previous Research in Rock Cutting ... 7

3.1 Disc Cutters 7

3.1.1 Disc Cutting Theories ... 7

3.1.2 Laboratory Investigations of Disc Cutting Performance ... 10

3.1.3 Wear of Disc Cutters ... 11

3.1.4 Correlation of Labcratory Cutting Data with Actual Tunnel Boring Machine Performance ... 13

3.1.5 Relationships between Tunnelling Machine Performance and Operational Variables 14

3.1.6 Correlation cf Rock Physical Properties with Machine Performance ... 17

3.2 Toothed Roller Cutters ... 20

3.2.1 Theoretical Studies ... 20

3.2.2 Experimental Results ... 23

3.2.3 Wear Performance of Toothed Roller Cutters 24

PAGE

3.3 Tungsten Carbide Studded Roller Cutters 25

3.3.1 Prediction of Raise and Tunnel Boring Machine Performance ... 25

3.4 Pick Cutters 29

3.4.1 Theoretical Studies ... 29

3.4.2 Laboratory Investigations ... 33

3.4.3 Wear Performance of Pick Cutters 34

3.4.4 Correlation of rock properties and the cutting performance of road headers 35

CHAPTER FOUR

4. Planning of the Experiments ... 36

4.1 The Design of the Partial Factorial Experiment 37

4.2 Analysis of the Experimental Data ... 40

CHAPTER FIVE

5. Experimental Equipment 48

5.1 Rock Cutting Rigs 48

5.2 Instrumentation 53

5.3 Cutting Tools 56

CHAPTER SIX

6. Mechanical and Physical Properties of the Experimental Rocks 61

6.1 Description of Each Rock ... 61

6.2 Description of Each Test and Results... 64

PAGE

CHAPTER SEVEN

7. Cutting Rocks with Discs 78

7.1 Experimental Programme ... 78

7.2 Results of Unrelieved Cutting Experiments 82

7.3 Results of Relieved Cutting Experiments 97

7.4 Conclusions 113

CHAPTER EIGHT

8. Correlation of Rock Properties with the Measured Performance of Disc Cutters ... 116

8.1 Prediction of Mean Thrust Force ... 118

8.2 Prediction of Mean Rolling Force ... 122

8.3 Prediction of Peak Thrust and Rolling Forces 128

8.4 Prediction of Disc Groove Angle ... 131

8.5 The Comparison of the Predicted and Measured Performance of Disc Cutters ... 134

8.6 The Comparison of Predicted and Measured Performance of Rocks Tested in U.S.B.M. 137

8.7 Conclusions 140

CHAPTER NINE

9. Effect of Edge Radius on the Cutting Performance of Disc Cutters 141

9.1 Experimental Technique and Procedure... 143

9.2 Effect of Edge Radius on Thrust Force 146

9.3 Effect of Edge Radius on Rolling Force 152

9.4 The effect of Edge Radius on Yield, Specific Energy and Coarseness Index ... 155

PAGE

9.5 Relieved Cutting in Bunter Sandstone with Blunt Discs 158

9.6 Conclusions 166

CHAPTER TEN

10. Toothed Roller Cutters 167

10.1 Experimental Technique and Procedure... 168

10.2 Unrelieved Cutting 169

10.3 Relieved Cutting 175

CHAPTER ELEVEN

11. Cutting High Strength Rocks with Picks ... 178

11.1 Experimental Programme ... 178

11.2 Results of Unrelieved Cutting Experiments 183

11.3 Comparison of Experimental Results with Evans' Tensile Theory ... 186

11.4 Relieved Cutting Results ... 197

11.5 Conclusions 200

CHAPTER TWELVE

12. Effect of Rock Properties on the Wear Performance of a Single Pick 202

12.1 Experimental Programme ... 203

12.2 Some Theoretical Considerations on the Wear Performance of Pick Cutters ... 205

12.3 Experimental Results and Conclusions... 209

PAGE

CHAPTER THIRTEEN

13. Relative Efficiency of Picks and Roller Cutters 213

13.1 Unrelieved Cutting 214

13.2 Relieved Cutting 215

13.3 Tool Wear 216

13.4 Conclusions 218

CHAPTER FOURTEEN

14. Conclusions and Recommendations for Future Research 221

Appendices 227

References 316

* * *

List of Illustrations

1-2 Hydraulic Rock Cutting.

3 Disc Cutters.

4 Disc Cutting Theory (after Roxborough and Phillips).

5 Disc Life versus Disc Position on Head.

6 Advance Rate versus Specific Energy.

7 Advance Rate versus Rotary Speed.

8 Specific Energy versus Compressive Strength.

9 Toothed Roller Cutters.

10 Geometrical Parameters of Toothed Roller Cutters.

11 Definition of Skew Angle.

12 Tungsten Carbide Studded Roller Cutters.

13 Penetration Rate versus Button Penetration Index.

14 Variation in Penetration Rate with Rock Compressive Strength.

15 Pick Cutters.

16 Illustration of Evans' Theory.

17 Orthoganal Latin Squares.

18 Mean Thrust Force versus Disc Penetration, Disc Edge Angle, Disc Diameter.

19 Predicted Values versus Actual Values of FT.

20 Butler Shaping Machine.

21 Modified Kelly Shaping Machine with Instrumentation.

22 Ultra Violet Chart Recorder.

23 Typical U.V. Traces.

24 Some Toolholders.

25 Some Tungsten Carbide Inserts.

26 Standard Tool Holder for Negative Tungsten Carbide Inserts.

27 Some Experimental Discs.

28 Mohr Envelopes for Experimental Rocks.

29 Disc Cutter Parameters.

30 Variation in Disc Forces with Penetration.

31 Variation in $\frac{FT}{FR}$ Ratios with Penetration.

32 Variation in Yield with Penetration.

33 Variation in Specific Energy and Coarseness Index with Disc Penetration.

34 Variation in Disc Forces with Edge Angle.

35 Variation in $\frac{FT}{FR}$ Ratios with Edge Angle.

36 Variation in Yield with Disc Edge Angle.

37 Variation in Specific Energy and Coarseness Index with Disc Penetrations.

38 Variation in Disc Forces with Disc Diameters.

39 Variation in Yield with Disc Diameter.

40 Variation in Specific Energy and Coarseness Index with Disc Diameter.

41 Effect of Spacing on Disc Forces.

42 Force Relieved/Force Unrelieved Ratios versus s/p.

43 Variation in Yield with Spacing.

44 Relieved/Unrelieved Yield Ratios.

45 Variation in Specific Energy with Spacing.

46 Effect of Spacing on Empirical Specific Energy Values.

47 Variation in Ccarseness Index with Spacing.

48 Gecmetry of Disc Penetration.

49 Mean Thrust Force versus Projected Contact Area.

50 Variation in Measured and Predicted Forces with Disc Penetration.

51 Variation in Measured and Predicted Forces with Disc Edge Angle.

52 Variation in Measured and Predicted Forces with Disc Diameter.

53 The Projected Area of the Disc in the Direction of Movement.

54 The Relationship between the Groove Angle, the sum of the Internal Friction Angle and the Sliding Friction Angle.

55 Mean Rolling and Thrust Forces versus Disc Penetration.

56 Mean Thrust Force versus Disc Penetration.

57 Definition of Disc Bluntness (after Rad).

58 Disc Cutters with Different Edge Radius.

59 Blunt Disc Analysis.

60 Relationship between the Projected Area of Disc Contact and Edge Radius.

61 Relationship between % Increase in Mean Thrust Force and % Increase in Projected Area of Disc Contact.

62 Variation in Rolling Forces with Edge Radius.

63 Decrease of the Effect of Edge Radius on Rolling Force with Deeper Penetrations.

64 Variation in Yield and Specific Energy with Edge Radius.

65 Variation in Coarseness Index with Edge Radius.

66 Variation in Thrust Forces with s/p for Different Edge Radius.

67 Variation in Rolling Forces with s/p for Different Edge Radius.

68 Variation in Yield with s/p for Different Edge Radius.

69 Variation in Specific Energy with s/p for Different Edge Radius.

70 Variation in Thrust Forces with Penetration, 12 Toothed Roller Cutt Experiment.

71 Variation in Rolling Forces with Penetration, 12 Toothed Roller Cutter Experiment.

72 Variation in Yield with Penetration, 12 Toothed Roller Cutter Experiment.

73 Variation in Specific Energy with Penetration, 12 Toothed Roller Cutter Experiment.

74 Peak Force/Mean Force Ratios for 4 Rocks.

75 Variation in Yield with Spacing, 12 Toothed Roller Cutter Experiment.

76 Variation in Specific Energy with Spacing, 12 Toothed Roller Cutter Experiment.

77 Pick Cutter Parameters.

78 Variation in Forces with Pick Cutter Parameters in Anhydrite.

79 Variation in Yield and Specific Energy with Pick Cutter Parameters in Anhydrite.

80 Variation in Forces with Pick Cutter Parameters in Limestone.

81 Variation in Yield and Specific Energy with Pick Cutter Parameters in Limestone.

82 Variation in Forces with Pick Cutter Parameters in Greywacke.

83 Variation in Yield and Specific Energy with Pick Cutter Parameters in Greywacke.

84 Variation in Forces with Pick Cutter Parameters in Granite.

85 Variation in Yield and Specific Energy with Pick Cutter Parameters in Granite.

86 Variation in Coarseness Index with Depth of Cut and Rake Angle.

87 Effect of Tool Wear in Granite.

88 Variation in Specific Energy with Spacing.

89 Worn Tips.

90 Failure of Rock Specimen between Quartz grains.

91 Theoretical consideration of Cutting a Quartz Grain.

92 Relation between Tip Weight loss and Rock Properties (after Schimazek).

93 Theoretical Wear Curves.

94 Effect of Quartz Content and Quartz Grain size on Tool Wear.

95 Effect of Cutting Distance on Wear Flat.

96 Variation in Specific Energy with Wear Flat.

* * *

ACKNOWLEDGEMENTS

The author would like to express his appreciation to the following people without whose help much of the research work would have been impossible.

Professor E.L.J. Potts, Milburn Professor of Mining Engineering at the University of Newcastle upon Tyne, for providing him the opportunity to carry out the research.

Professor F.F. Roxborough who introduced the author to the rock cutting field.

Dr. R.J. Fowell for his supervision and encouragement.

Dr. H.R. Phillips for his supervision, guidance in the research, assistance in data processing and analysis.

Dr. A. Rispin for his advice and assistance in the understanding of this wcrk.

Mr. G. Leach and Mr. D. Price for assistance in experimental work.

Mr. R. Sciville, Excavation Labcratory Technician, for his help in the construction of apparatus.

Mr. T. Pollock for providing both a technical service and a reliable source of advice.

The Ministry of Education of Turkey for the financial

maintenance of the author.

Finally, my thanks to Mrs. Edna Gannie for typing this Thesis so speedily.

* * *

CHAPTER ONE

INTRODUCTION

The increasing rate of industrial and environmental development demands more tunnels. It is estimated that the annual rate of sub-surface excavation which was $3.8 \times 10^8 m^3$ in 1960 - 1970 will increase to $8.1 \times 10^8 m^3$ in 1970 - 1980 and $16.2 \times 10^8 m^3$ in 1980 - 1990[1].

By its nature, tunnelling is a complex and often expensive undertaking, but the advantages that a tunnel facility offers make it a highly desirable method of construction for urban rapid-transit systems, utility conduits, sewers and acqueducts. Most of these tunnels will be more suited to machine tunnelling than conventional tunnelling, as a minimum amount of disturbances from subsidence and noise will be essential under urban areas.

A full-face tunnel boring machine usually promises high advance rates compared with cyclic excavation methods. There are other numerous advantages to be gained by tunnel boring. There is increased safety as there are no explosives, little danger of collapse, less labour is required and overbreak is usually less than 5%. All these advantages of tunnel boring have attracted the mining industry as well as the civil engineering field. Recently, Mr. Tregelles, Director of Mining Research and Development, N.C.B., emphasised this point as "...it is appreciated that the mining roadheader extraction rates are seldom more than $12 m^3/h$ (which is three times the mining national average) compared with the rates achieved by civil engineering tunnelling machines, which, in similar sized roadways, have average performances of the order of

$30.6m^3/h$. It, therefore, seems clear that work should be carried cut to transfer civil engineering technology as rapidly as pcssible so as to be available for use in coal mining[2]".

However, in spite of the advantages of continuous boring as compared with cyclic blasting, there is still considerable room for improvement in tunnelling machines to make them more cost-effective. The limiting factors to handling hard rocks are cutter bearing capacity, and the ability of cutter edge material to resist high cutter loads and the abrasive grinding action. The cutter cost is one of the most important factors in determining the economic success of a hard rock tunnel bore. Typical examples for a medium strength and abrasive sandstone is 3-5£/m^3[3,4] and for a high strength and very abrasive rock is 57£/m^3[5]. A careful study of the cutting and the wear performance of cutting tools in abrasive and hard rocks could be a considerable help in designing more economic tunnel boring machines.

New exotic methcds of rock machining have been undergoing tests for several years in different research laboratories. Hydraulic cutting was used with success in California in 1852 for working an Auriferous Alluvicn[6], Fig.2. Since then, it has attracted the attention of different research workers. Recently a project funded by the National Science Foundation and U.S.B.M. was contracted to the Colarado School of Mines, Flaw Research, Inc., and the Robbins Company[7]. The main cbjective was to design and field test a high pressure water-jet-assisted tunnelling machine in hard rock (Fig.1). The results are promising, since the advance rate of the machine increased ccnsiderably compared with the advance rate achieved by the machine without use cf the water jets.

The Department of Mining Engineering of the University of Newcastle upon Tyne has developed its research interests in the general field of rock excavation over the last ten years. Initially, the work was supported by firms such as Austin Hoy Limited, but recently, T.R.R.L and the Wolfson Foundation have been major supporters of our research. This Thesis is concerned with the cutting performance of picks, discs and gear cutters. A large programme of cutting tests has been carried out with these cutting tools to determine the influence of changes in both design and operational variables on efficient cutting.

* * *

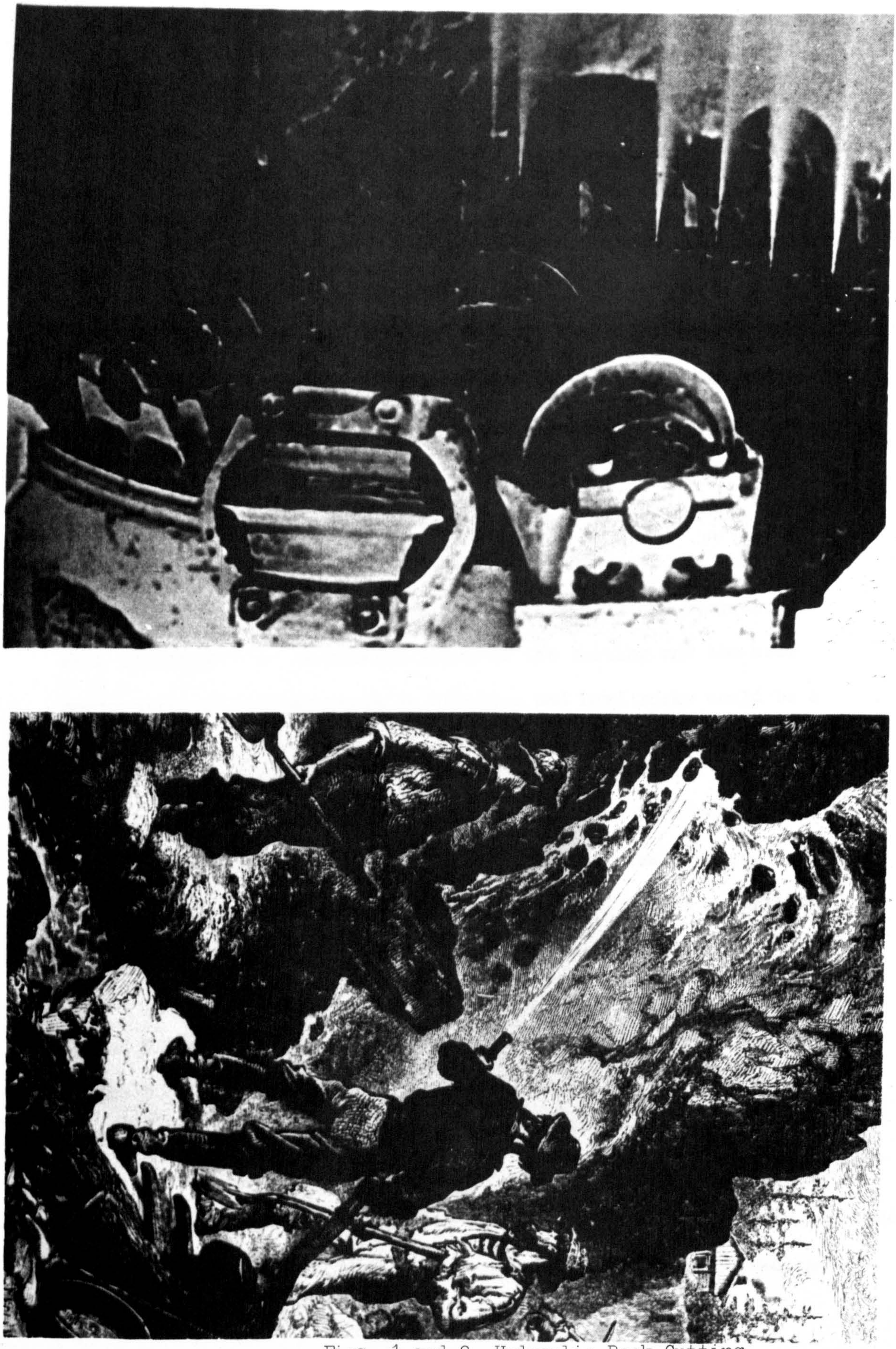

Figs. 1 and 2 Hydraulic Rock Cutting.

CHAPTER TWO

OBJECTIVES OF RESEARCH

Disc cutters are the most commonly used tool for full-face tunnel bcring machines, but their successful application is hindered by lack of understanding of the fundamental breakage phenomena which govern their efficient use. Labcratory cutting experiments can give the basic data to choose the most suitable cutting tool and to design a cutting head of a tunnel bcring machine for a given rock mass. In several countries research workers have investigated the effects of geometrical and operational variables on disc cutting performance, but such experiments are mostly time consuming and expensive. Due to this fact, there are many advantages of finding some relationship between rock properties and the performance cf rock cutting tools. Discs with different gecmetries have been tested in many contrasting rocks in order to fulfil these requirements.

A sharp edge on a disc cutter can not resist the high forces to which it is subjected when cutting hard rock. Hence, in practice, discs with different edge radii are used in abrasive and hard formations in crder to prolong disc life. Although the impcrtance of edge radius to the effective performance of a disc cutter has been acknowledged by different research workers, few results are available. One of the cbjectives of this Thesis is to clarify the laws governing the cutting performance of blunt discs.

Design and metallurgical improvements have jointly contributed to the development of the present-day toothed roller cutters in use in

blast hole drilling and in the oil industry. Such cutters are now in common use on tunnel boring machines. Some cutting tests, using this type of cutter, have been included in the research programme in order to compare their efficiency with that of discs and picks.

Picks are the primary excavating tools in coal mining since they are widely used in shearers, ploughs, road headers etc. and are gaining application in the harder and more abrasive rocks. The effect of design and operational variables are investigated in four high strength rocks. Two further medium strength rocks are also included in the cutting programme to provide data for the comparison of the efficiency of discs and picks.

Picks are more susceptible to wear than any type of roller cutters since each point on the cutting edge is in continuous contact with rock. There are many factors affecting wear performance of pick cutters. Seven rocks with different degrees of abrasiveness and hardness were tested with one single pick. A theoretical approach has been used to explain the relationship between wear rate and rock physical properties.

* * *

CHAPTER THREE

PREVIOUS RESEARCH IN ROCK CUTTING

3.1 Disc Cutters

Disc Cutters are the most commonly used tool for full-face tunnel boring machines (Fig.3), since they have several advantages compared to other types of cutters. They operate as a free rolling wheel, so that any point on the disc is in contact with the rock only once per revolution, ensuring that the rate of wear of the cutting edge is much less than that of a drag pick. They are more efficient than button cutters, since the rock degradation is more by cutting, rather than a grinding action.

3.1.1 Disc Cutting Theories

Evans, in an attempt to compare relative efficiency of picks and discs for cutting rock, suggested that the force on a wedge required for penetration is identical in form with the calculation of passive earth pressure against a retaining wall in soil mechanics[8]. He formulated thrust force FT, and groove angle α as:

$$FT = \frac{2.c.p.\cos\phi.\sin(\theta+\psi)}{\sin^2\left(\frac{\pi}{4} - \frac{1}{2}\overline{\theta+\psi+\phi}\right)}$$

$$\alpha = \frac{\pi}{2} + \theta+\psi+\phi$$

where FT = Thrust Force

c = Cohesion

ϕ = Angle of Internal Friction

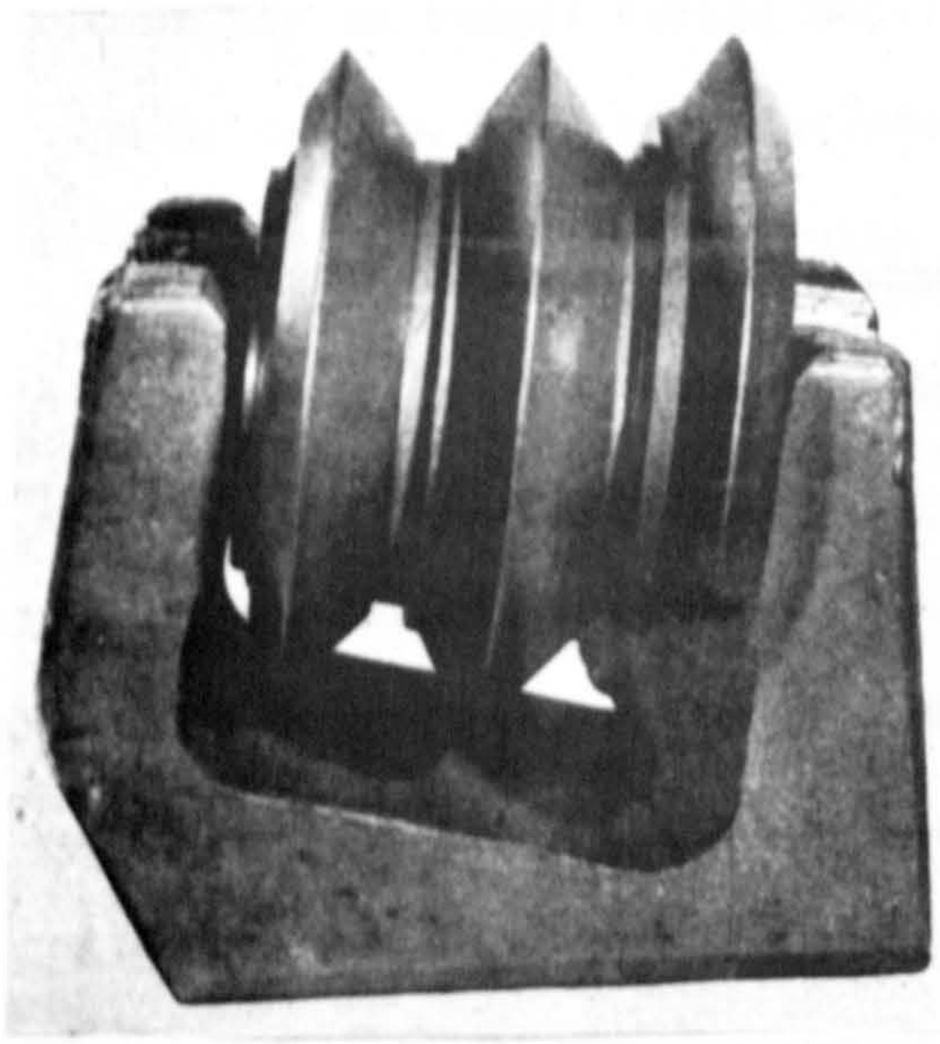

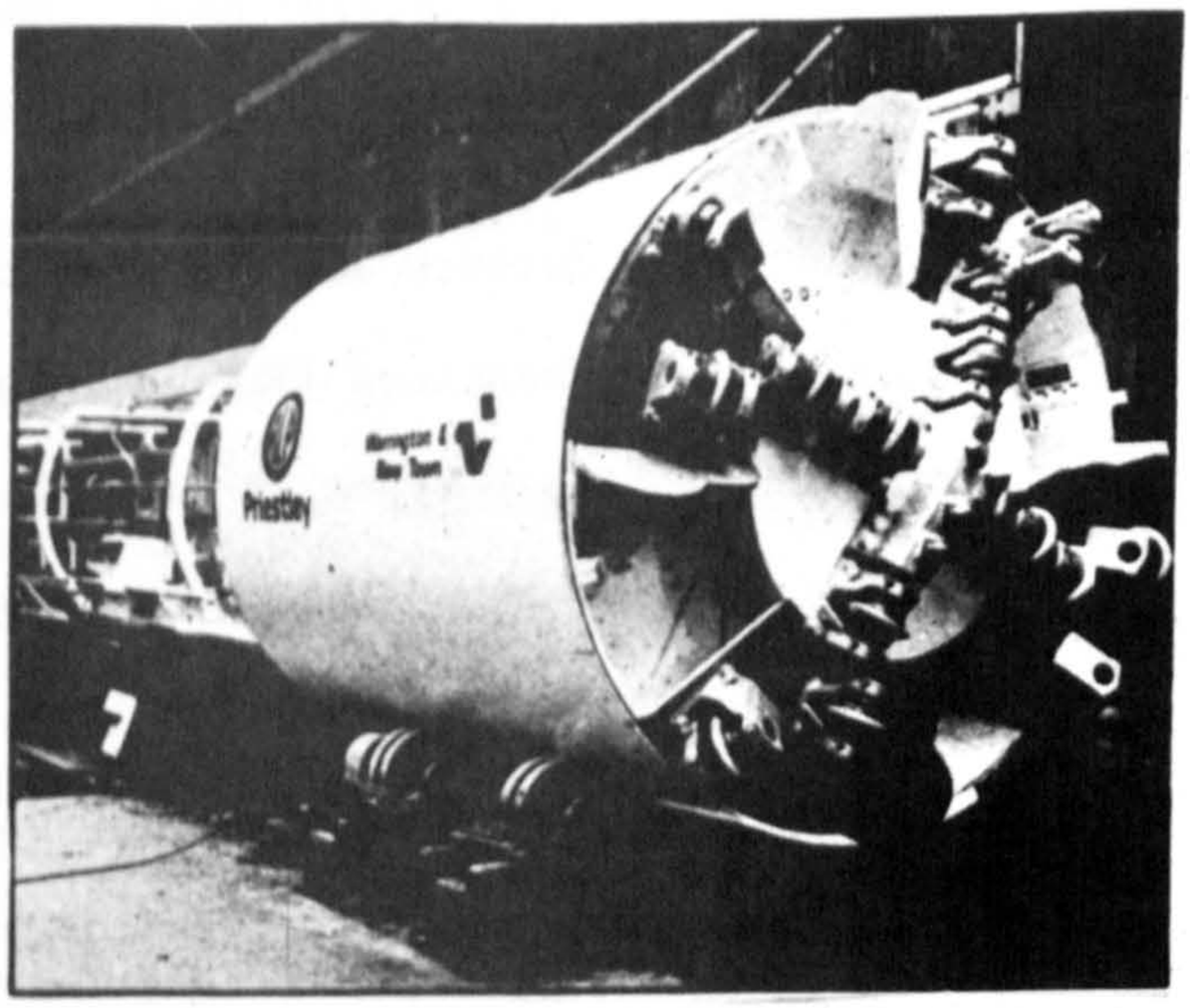

Fig.3 Disc Cutters.

p = Disc Penetration

θ = Semi Edge Angle

ψ = Angle of Friction between Wedge and Rock

α = Groove Angle.

Another theoretical approach to the prediction of disc cutting performance is that of Roxborough and Phillips[9]. They assumed that thrust force equals the uniaxial compressive strength of the rock times the disc contact projected area (A), (Fig.4). The resultant force is assumed to pass through the centre of the disc, and to bisect the arc of contact.

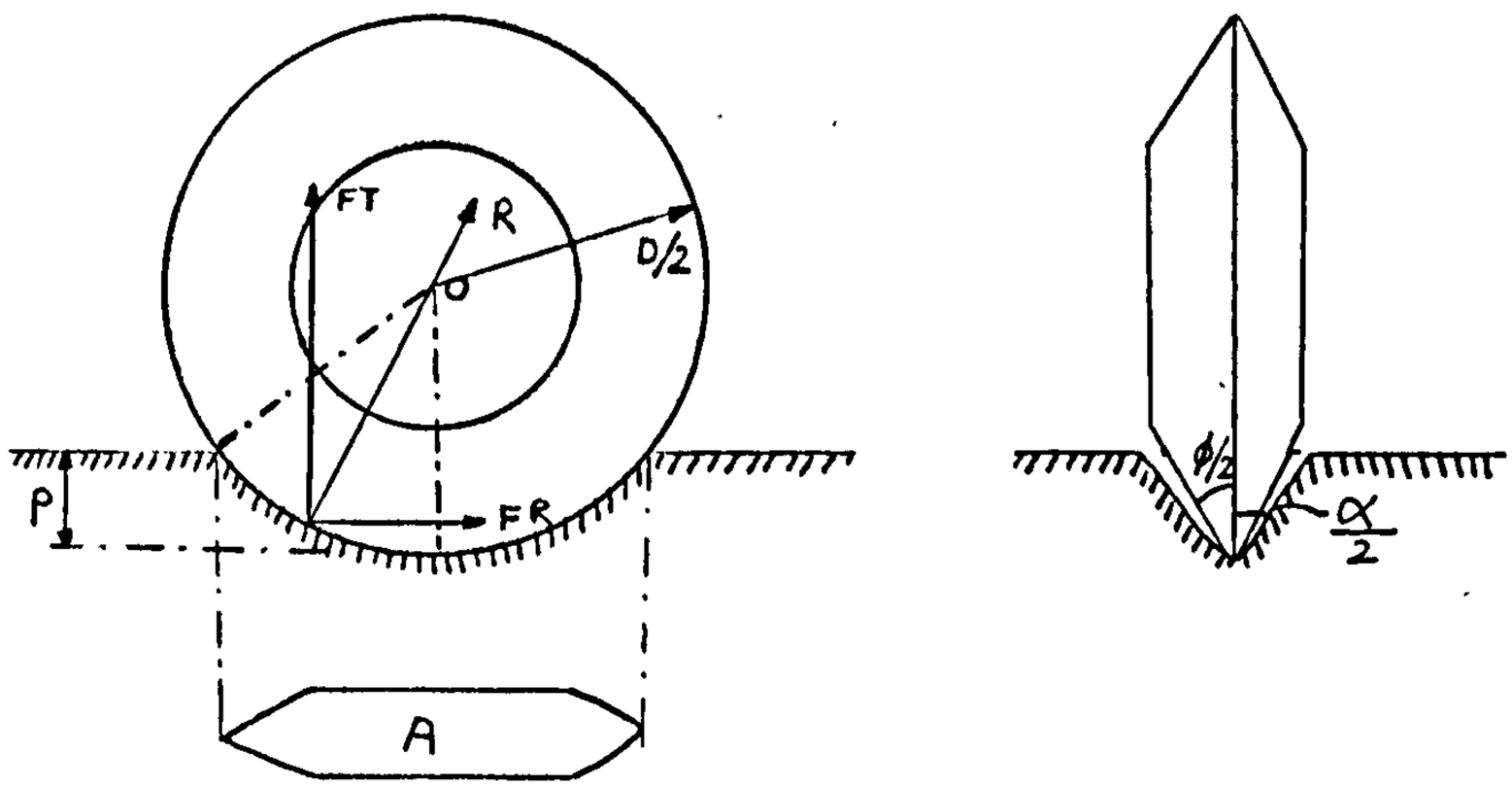

Fig.4 Disc Cutting Theory (After Roxborough and Phillips)

The projected area was estimated by Hewitt[10] and Phillips[11] to be 50% less than the area originally formulated by Roxborough and Phillips. Optimum spacing/penetration ratio, thrust and rolling forces were derived of the following form:

$$FT = 4.\sigma_c.\tan\frac{\phi}{2}\sqrt{D.p^3 - p^4}$$

$$FR = 4.\sigma_c.p^2.\tan\frac{\phi}{2}$$

$$\frac{s}{p} \leq \frac{\sigma_c}{\sigma_s}$$

where σ_c = Uniaxial compressive strength

σ_s = Shear strength.

3.1.2 Laboratory Investigations of Disc Cutting Performance

In several countries research workers investigated the effect of geometrical and operational variables on disc cutting performance. The first research in this respect was carried out by Baron et al.[12] in Russia in 1962. He used two disc cutters with 40° edge angle, 0.5mm edge radius at 96, 150mm diameters. He concluded that increasing penetration causes a rapid increase in both thrust and rolling forces and a decrease in specific energy consumption. The thrust force is affected by disc diameter, but not rolling force. Cutting speed does not have any effect on disc forces. His results are in good agreement with the results given by the research workers in the University of Newcastle upon Tyne[9,10,11,13], in Japan[14,15] and in the U.S.A.[16,17,18,19].

In Newcastle and at the Colarado School of Mines, cutting speed[9,10,11,13,19] and disc diameter [9,10,11,13] showed no effect on yield and specific energy. This is contradicted by Rad[20,21], who suggests that yield increases and specific energy decreases with increasing diameter and cutting speed.

All the research workers agree that there is an optimum spacing[9,10,11,13,19,20,22,23] and the disc with the smallest edge angle is more efficient than the others[9,10,11,13,14,15,16,17].

The Twin Cities Mining Research Centre of the U.S. Bureau of Mines attempted to correlate the rock physical properties with disc cutter performance parameters[16,17]. The predictor equations they developed gave high correlation coefficients, but their major drawback was the failure to consider the effect of disc geometry on tool performance. Experiments were only undertaken with one diameter of disc. The U.S.B.M. suggested that the most significant physical properties for use in empirical equations were:

1. Shore Scleroscope Hardness
2. Density
3. Tensile Strength
4. Compressive Strength
5. Young's Modulus.

3.1.3 Wear of Disc Cutters

When tunnelling in hard rock, the most important consideration when comparing the economics of mechanised boring with those of conventional drilling and blasting techniques is the cost of cutters for the drive.

Many manufacturers calculate cutter costs by first taking

the sum of radii of travel of all cutters to find mean cutter radius. The cutter life is defined as it should cut a given number of linear metres before wearing out. Typical figures are 120,000m for sandstones and 210,000 to 300,000m for shale[24].

It should be noted that the gauge cutters fail more frequently than the inner cutters[25] due to their higher loading and greater distance of travel (Fig.5).

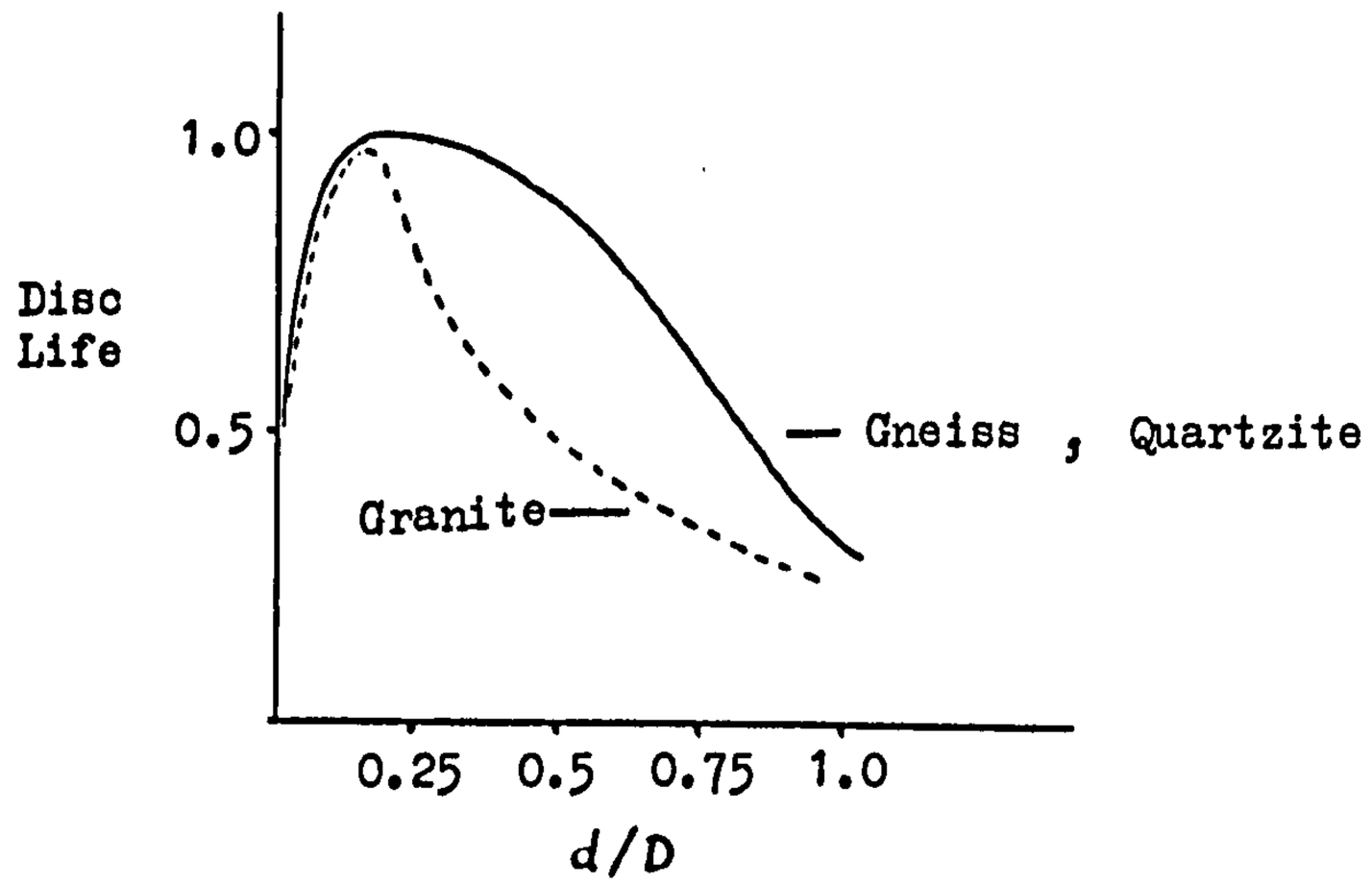

Fig.5 Disc Life versus Disc Position on Head Expressed as Ratio Disc Path Diameter/ Head Diameter (After Innaurato, Mancini and Pelizza).

Different research workers have investigated the effect of cutting distance and edge radius on the wear performance of disc cutters.

Baron found that steel discs sharpened themselves and

the disc performance did not change in an abrasive concrete[12], but deteriorated quickly in granite and basalt.

Rad[26] used several blunt discs with different edge radius and concluded that measuring the diameter of disc cutters and comparing it with the original diameter provides a very good tool for determination of bluntness and wear.

Özdemir showed that[19] the increase in the forces with a 105^{o} edge angle blunt disc is bigger than the increase of forces with a 90^{o} edge angle blunt disc if both of them have the same diameter and the same wear flat.

3.1.4 Correlation of Laboratory Cutting Data with Actual Tunnel Boring Machine Performance

To achieve cheap and quick results laboratory tests are preferred but they should truly represent the actual situation.

The T.R.R.L. recently supported rock cutting research in the University of Newcastle upon Tyne, in order to compare laboratory results with those of a pilot-scale investigation and a full face instrumented tunnel boring machine[27,28]. It is reported that the correlation between predicted and actual results was reasonably good[28]. Rad suggested that a satisfactory correlation existed between laboratory cutting results and field performance data[29].

Some of the investigations at the Colarado School of Mines concluded that it was not possible to predict the performance of a full face machine by using a small linear cutting rig and

15cm diameter rock cores[19,30,31,32]. Wang found an excellent agreement between laboratory results performed on a large cutting rig and field results at high penetration. He suggests that a scale factor existed between a small and a large rock cutting machine[19,33].

3.1.5 Relationships between Tunnelling Machine Performance and Operational Variables

Investigation into the performance of tunnelling machines can be carried out at several levels. The most accurate but time consuming and expensive method consists of instrumenting the cutting tools of a tunnelling machine by strain gauges. Examples of this method are the work of Gobetz and T.R.R.L.[34,35,36]. Hustrulid, Rad, Wang and Mellor prefer to obtain the specification and performance of machines from shift and manufacturer reports and to interpret the data for the prediction of the machine performance[29,31,32,37,38].

This method of predicting machine performance is not accurate, since the data taken from manufacturers' catalogues and contractors' shift reports represents average values for different geological strata and states of wear of cutters. Both these factors are known to have an important effect on advance rate.

Nizamoğlu[39] has refined this technique by systematically changing the operational variables of a Wirth TBV-580 H tunnel boring machine. Thrust and rotational speed were varied while torque and the time necessary to cut a given distance were measured.

The main conclusions of this research are summarised below.

(a) Penetration is related to torque in a linear manner.

(b) Penetration increases with increasing thrust but the relationship is not quite linear.

(c) The torque generated is proportional to the applied thrust.

Mellor[37,38] has found, for a range of machines, that torque is proportional to tunnel face diameter raised to a power of approximately 2.3, i.e.

$$T = K.D^{2.3} \quad (T \text{ in ft.lb, } D \text{ in ft}).$$

An essential factor for the assessment of boring machine performance is the specific energy consumption, i.e. the energy consumed in excavating unit volume of rock. In Fig.6[29,31,32] specific energy is plotted against advance rate for two tunnels driven in the United States. It can be seen that lower S.E. values can be obtained with higher advance rates.

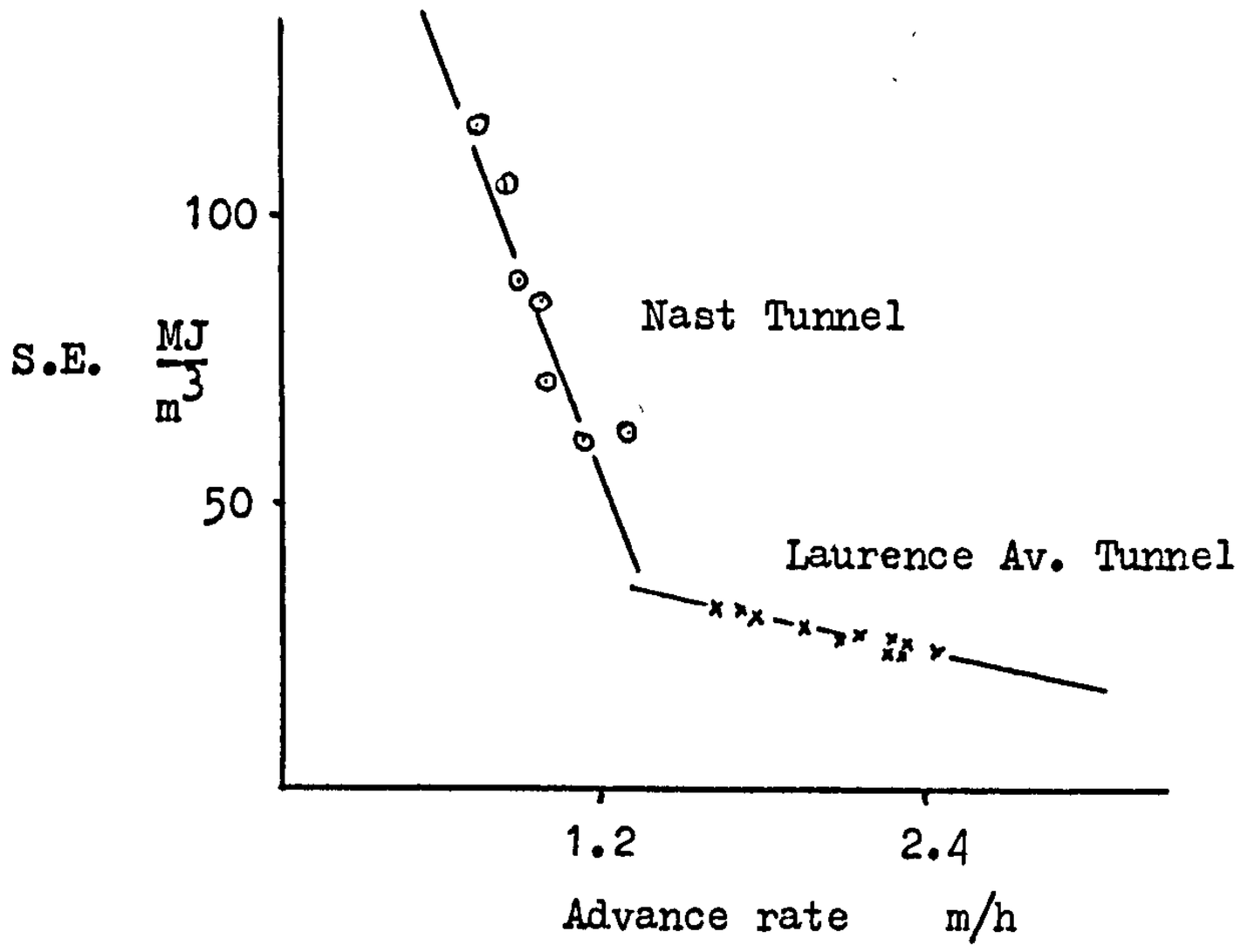

Fig. 6 Advance Rate versus Specific Energy
(after Wang, Hustrulid and Rad)

Although Gaye[40] shows advance rate to be a linear function of thrust force, Nizamoğlu has fitted a power law curve to his data[39].

Rotary speed is a factor in the determination of machine power. The higher the power the greater the possible head speed under constant thrust force. Rotary speeds of current tunnelling machines are in the range of 3 to 12 rev/min with 9 rev/min a common speed for medium size machines[37]. Low rotary speeds are not specially advantageous from a rock cutting point of view since, as shown in Fig.7, boring rate increases with increasing rotary speed.

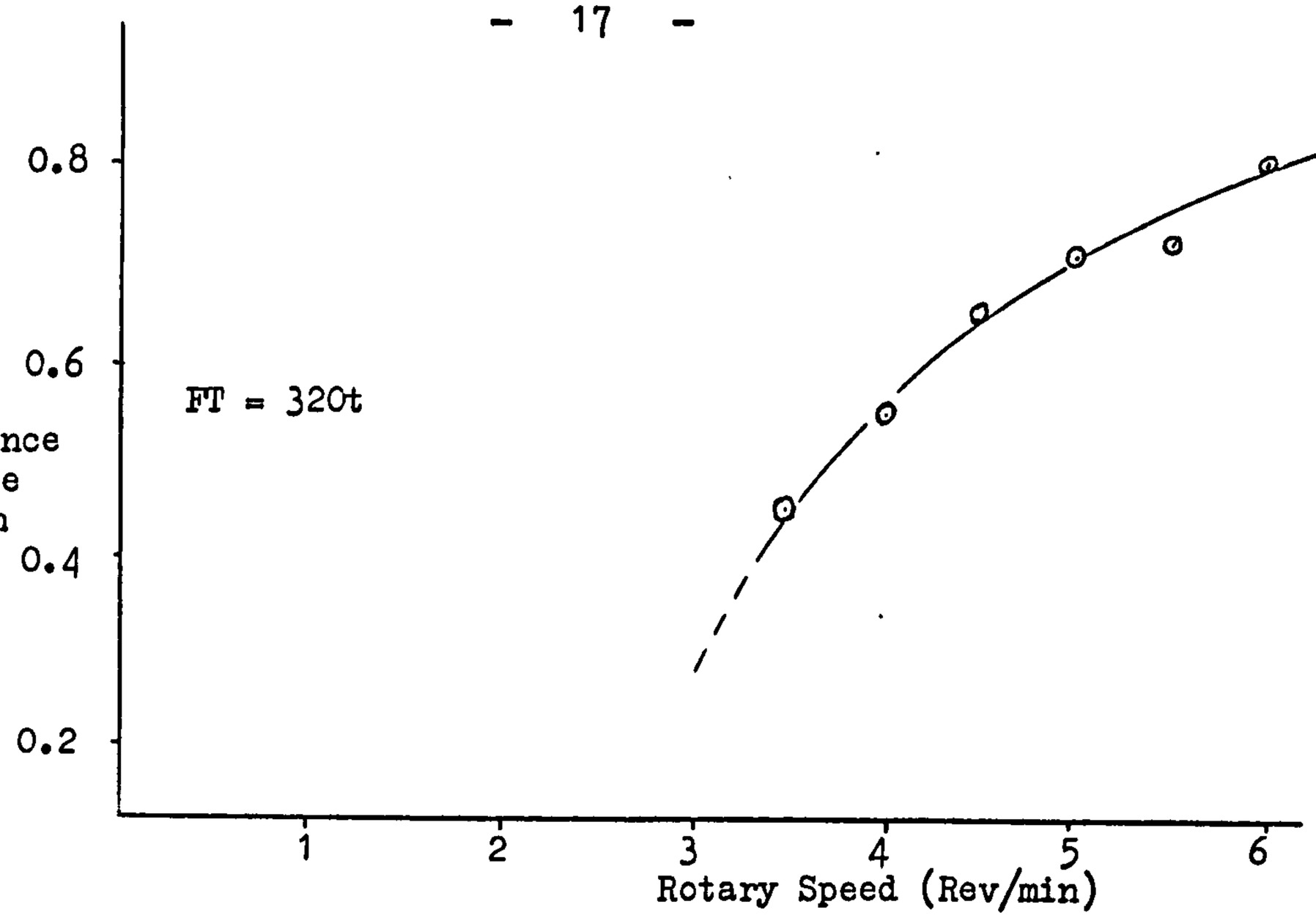

Fig.7 Advance Rate versus Rotary Speed (after Nizamoğlu)

3.1.6 Correlation of Rock Physical Properties with Machine Performance

The physical and structural characteristics of a rock mass play a major role in determining the requirements of a rock fragmentation process. It has long been recognised that hardness, variation in rock strength, joints and bedding planes all contribute to affect both boring rate and cutter change frequency. Research has been carried out to determine whether there are statistically significant correlations between the physical properties of the rock and machine performance.

If a fair comparison is to be made between machines working in different types of rock, then the strength of the rock must be

taken into consideration. Unconfined compressive strength is the most commonly used because it is easily determined[40,41]. Fig.8 represents an attempt to correlate specific energy values to rock hardness in terms of compressive strength and may serve as a first guide to prediction[42].

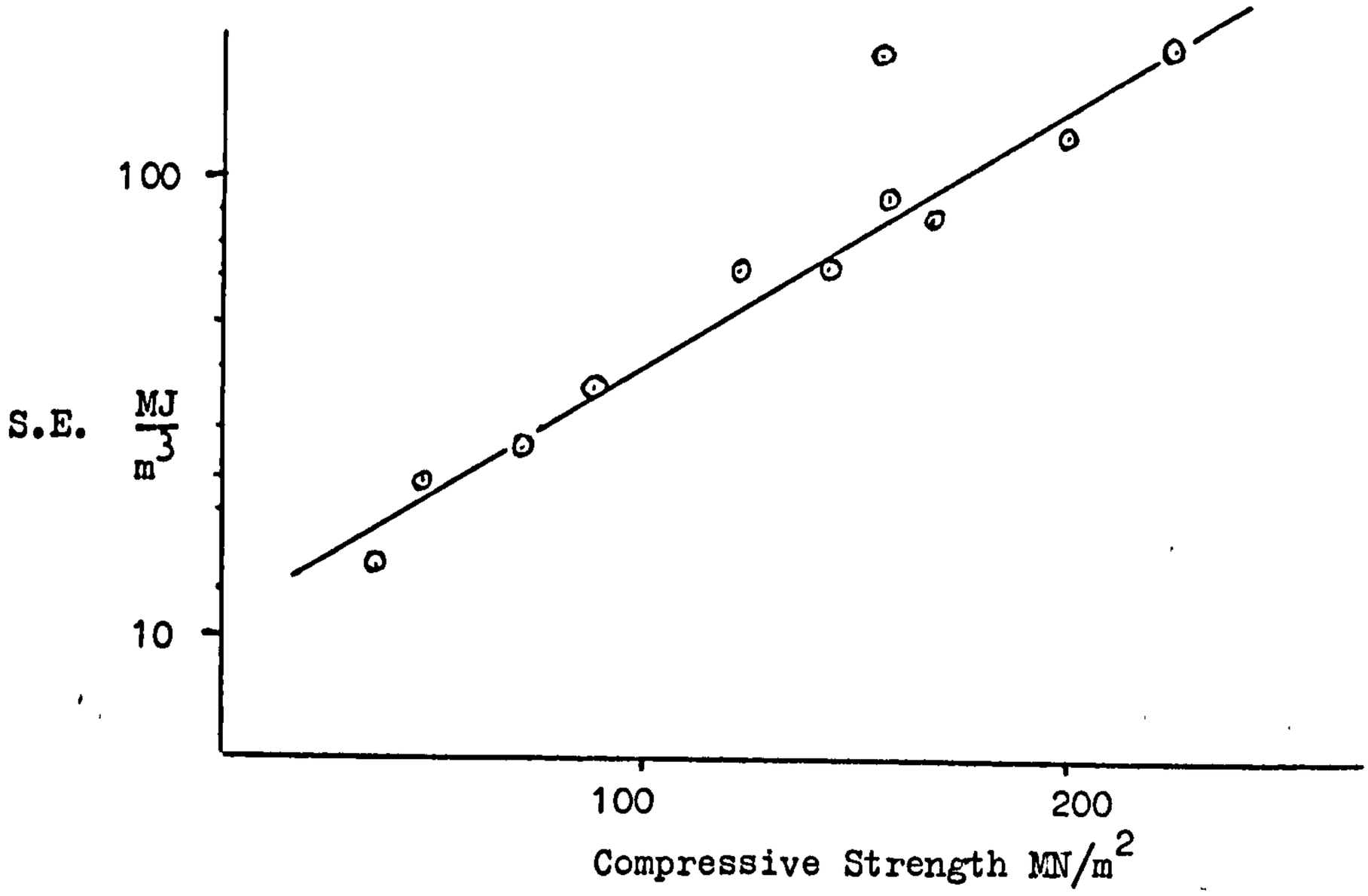

Fig.8 Variation in Specific Energy with Compressive Strength, (after Hibbard, Hyman, Murphy)

The correlations were generally not good between σ_c and boring rate[43,44], which suggests that the other rock properties must be considered.

Miller[45] has used the Schmidt Hammer to estimate uniaxial compressive strength and found that it was relatively insensitive to high strength rocks and relatively oversensitive to low strength rocks.

It appears that other physical properties, such as grain hardness, interact with compressive strength to effect the Rebound Number. This might explain why the Schmidt Hammer gives such good correlations with machine performance in some rocks and a great deal of scatter in others[43,44,46].

Tarkoy[43,44] modified a Taber Abrasor to take a rock sample of 5.54cm diameter and $\frac{1}{4}$cm thickness. He correlated weight loss of the sample and abrasor disc with boreability of the rock. He defines the abrasiveness AR, Abrasion hardness HA and total hardness HT as follows:-

$$AR = \frac{1}{\text{Av. weight loss (gm) of 4 Abrasor discs}} \qquad HA = \frac{1}{\text{Av. weight loss of 2 rock specimens}}$$

$$HT = HR\sqrt{HA}$$ HR is Schmidt Rebound Number

Cerchar has defined hardness as the time taken in seconds to drill a hole of 1cm deep under a constant normal load of 20kg and a rotational speed of 190 rev/min. Abrasivity by definition is the diameter of wear flat of a mild steel tip (cone angle 90°) which is dragged a distance of 1cm in a rock sample. Normal load applied against the rock is 7kg. Selected unit of abrasivity corresponds to 0.1mm measured on the diameter of the wear flat.

Combes found a correlation between boring rate of a Wirth tunnelling machine and the Cerchar hardness and abrasivity index[47].

* * *

3.2 Toothed Roller Cutters

Toothed roller cutters have long been used in the oil industry for cutting larger diameter boreholes to great depths and now they are commonly used on tunnel boring machines (Fig.9). These tools are suitable for soft to medium hard formations such as soft to medium shale, clay, limestcne, sandstone, etc.

Different research workers have investigated the effect of the large number of variables which are likely to influence the performance of toothed roller cutters in any given rock material. The information obtained from these studies is reported in this section. The studies offer a start in answering some of the more general questions involved in the rock cutting process.

3.2.1 Theoretical Studies

The relationship between the different geometrical parameters of this type of cutter has been defined by Teale[48] and this analysis gives a useful guide to the design criteria to be employed. The following parameters, as detailed in Fig.10 are relevant to the analysis.

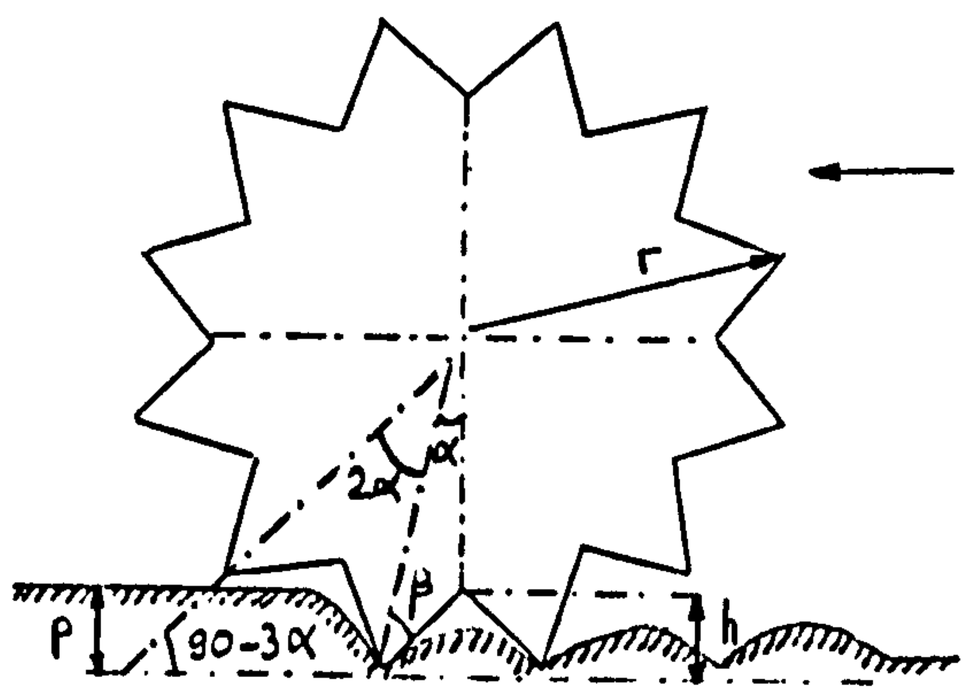

Fig.10 Geometrical Parameters of Toothed Roller Cutters (after Teale)

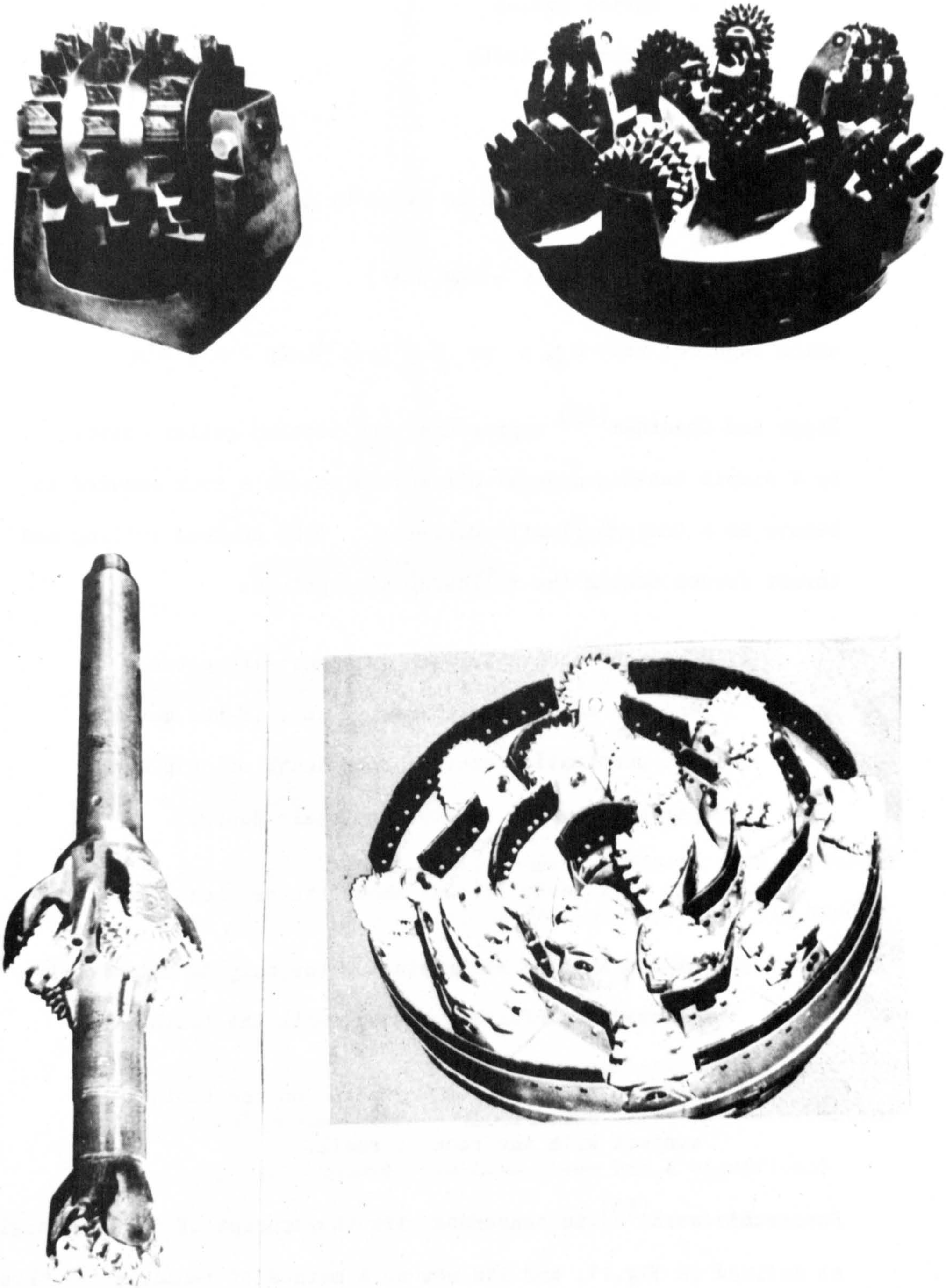

Fig.9 Toothed Roller Cutters.

2β = Wedge Angle

r = Cutter Radius

N = Number of teeth

$\alpha = \frac{\pi}{N}$

Maximum penetration p is given by the following formula

$$p = r(\cos\alpha - \cos 3\alpha)$$

which requires that $h \geqslant p$ or $\beta \leqslant (\cot^{-1} 2\sin 2\alpha) - \alpha$

Biggs and Cheatham[49] represented the toothed roller cutter by a simple two-dimensional bit moving across a rock assumed to behave as a Coulomb Plastic Material. They derived rolling and thrust forces making the following assumptions:

1. Chipping occurs between the penetrating tool and the adjacent withdrawing tool if the maximum bit penetration exceeds both depth of chip and a parameter which is given in their paper.

2. The rock never 'flows' above its original surface.

3. At the instant of fracturing the chip is immediately removed from further contact with the tooth.

4. Horizontal motion of any point on the tooth in contact with the rock is small.

Peterson's work[50] is concerned with the concept of the skew angle, as defined in Fig.11, and its use as a method of reducing the thrust required for a given boring rate or penetration rate. His theoretical description of thrust force shows a reasonable agreement with his experimental results.

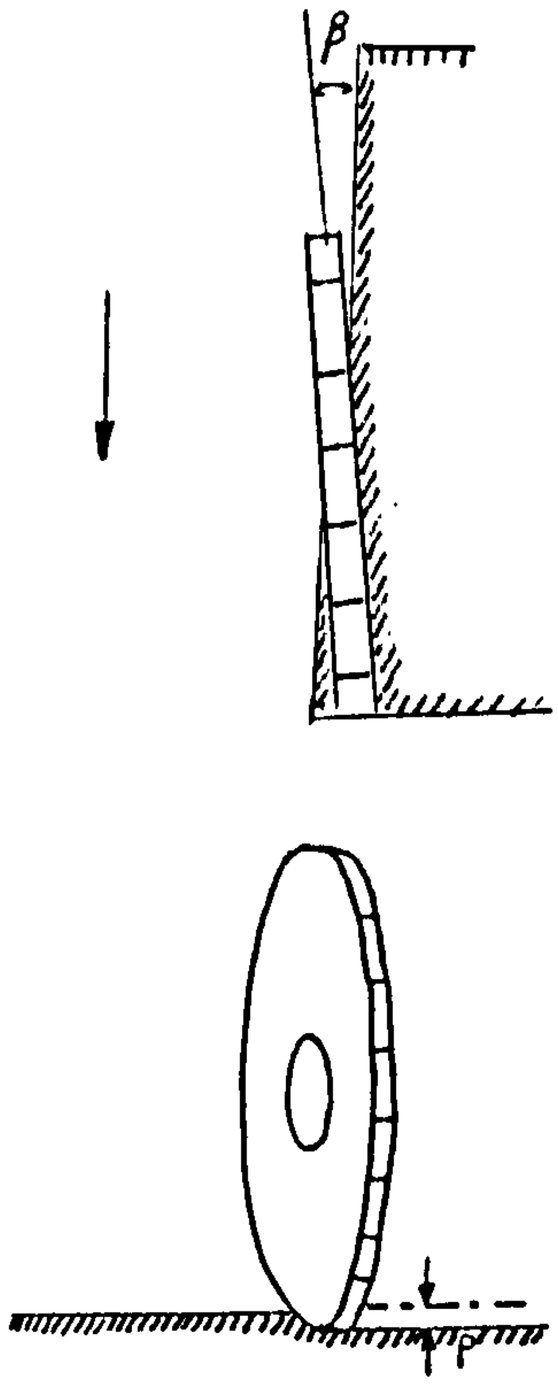

Fig.11 Definition of Skew Angle (after Peterson)

3.2.2 Experimental Results

Peterson[50] conducted his experiments in four different rocks with a range of compressive strengths of 40 - 219 MN/m^2. The low capacity of the dynamometer limited the penetration of the roller cutter, which varied from 0.5mm to 2mm. He concluded that the ratio of side to thrust force and rolling to thrust force is independent of rock type. Skew angle has no effect on the rolling force ~~and the sideways force~~ but a significant reduction in thrust force is obtained with increased skew angle.

The research at the M.R.D.E. of the N.C.B.[48,51] was designed to measure only the thrust force and yield. For the 12 toothed roller cutter, the thrust force was found to be directly proportional to the penetration, but for the 30 toothed roller cutter, the penetration levels off as the thrust force is increased. For a given penetration, the yield for the 30 toothed cutter is bigger than the yield for 12 toothed roller cutter.

The experiments done in chalk at the University of Newcastle upon Tyne[52] showed that the 12 toothed roller cutter provided the lowest specific energy values for all the disc cutters but debris tended to pack in between adjacent teeth, requiring very high thrusts to maintain the level of penetration. Thrust to Rolling force ratios were found to be 5.4 in dry chalk and 2.3 in wet chalk.

3.2.3 Wear Performance of Toothed Roller Cutters

The results of different research workers are in good agreement in this respect.

Peterson[50] artificially blunted the teeth of the 30cm diameter cutter. He found that there is very little increase in the force required as the wear flat increases. Price and Shepperd[51] assessed the tooth wear by examining the variation in penetration per cut with the number of cuts made since their initial sharpening. Quantitatively after a cutting distance of 65m at a mean thrust of 1.5 ton the efficiency of the cutter is reduced by only 10%.

* * *

3.3 Tungsten Carbide Studded Roller Cutters

The cutting tools which successfully and econcmically excavate extremely hard igneous formations such as granite, quartzite and basalt are tungsten carbide studded roller cutters (button cutters) (Fig.12). A high penetration force into the rock surface causes rock degradation by crushing rather than cutting and these tools work on that principle.

Although laboratory studies proved that button cutters are nct very efficient[14,19,53], the poor life of the other type of cutters in hard rocks[54,55] means that button cutters are commonly used on tunnel and raise boring machines.

3.3.1 Prediction of Raise and Tunnel Boring Machine Performance

Dresser O.M.E. have developed a boreability Index[56] by pressing hydraulically a sphero-conical tungsten carbide insert into a flat rock surface. The crater depth divided by the ram load constitutes the boreability index. Handewith, using similar techniques claims that actual tunnel boring rate can be predicted within an accuracy of ± 12 per cent[57,58].

A semi-empirical methcd of predicting the boring rate and cutter life was suggested by Morris[59]. He combines button penetration index with the other factors to predict machine performance.

Lightfoot found a good correlation between the performance of security Model 480 Raise Drill and the results of Morris[60]. Fig.13 shows the relation between button penetration index and bcring rate.

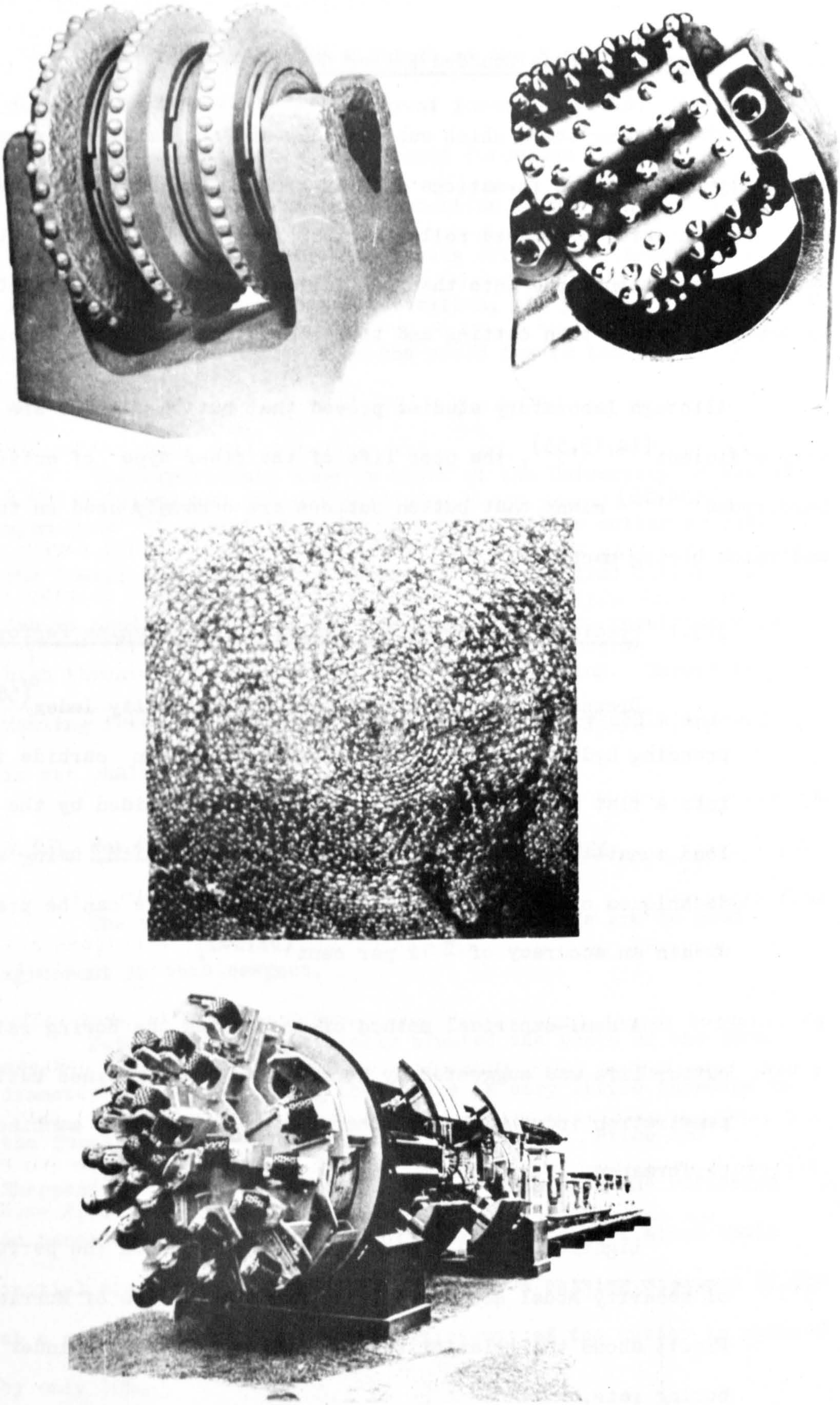

Fig.12 Tungsten Carbide Studded Roller Cutters.

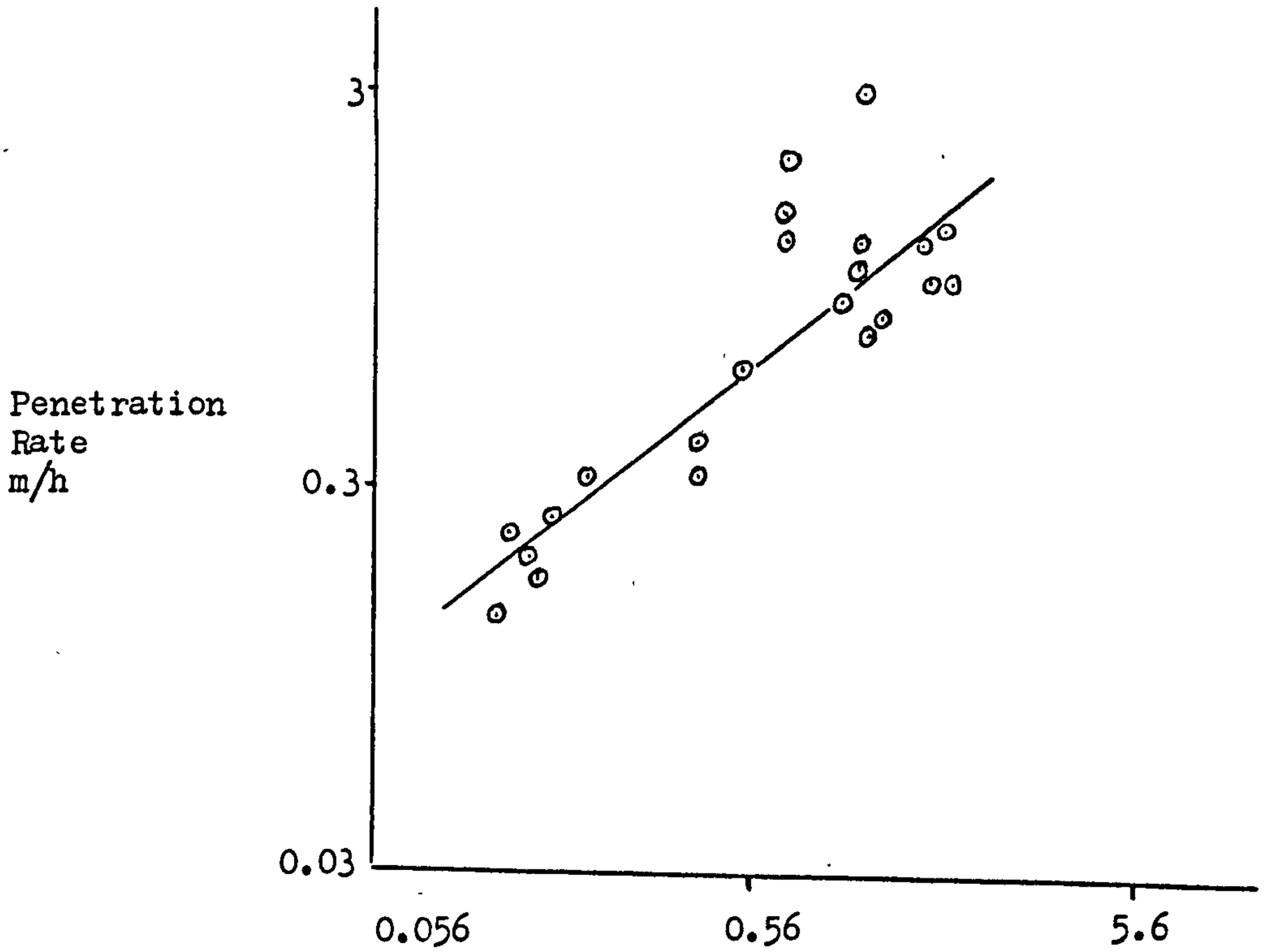

Fig.13 Penetration Rate versus Button Penetration Index (after Lightfoot)

Calder tried to predict boring rate from drilling studies[61]. His empirical rotary drilling equation relates boring rate to uniaxial compressive strength of the rock, thrust force and hole diameter.

As can be seen from Fig.14, the predicted results are roughly 50 per cent higher than those actually being achieved.

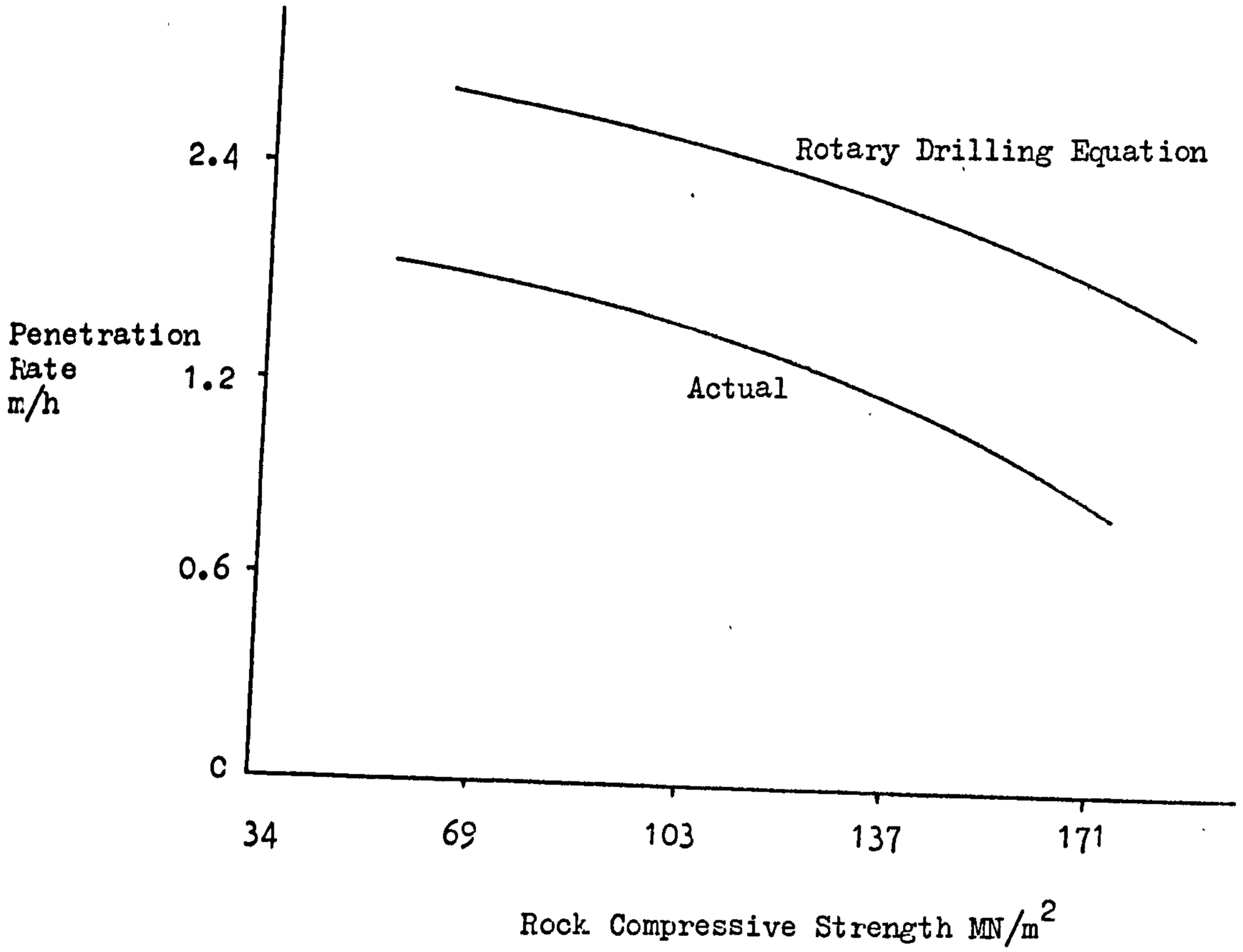

Fig.14 Variation in Penetration Rate with Rock Compressive Strength (after Calder)

* * *

3.4 Pick Cutters

The basic cutting tool used in shearers, trepanners, ploughs, continuous miners and partial face tunnel boring machines is the pick cutter. Extensive studies in developing the rationalised use of this type of cutter have been carried out in England and elsewhere. The following section is a brief summary of this work.

3.4.1 Theoretical Studies

The most acceptable theory for coal and rock cutting is that of Evans. His theory is based on the observation that the penetration of wedges normal to the surface of coal produces cracks attributed to tensile breakage. Fig.16 illustrates the assumptions of his breakage theory. The full theory of symmetrical and asymmetrical attack is given elsewhere[62].

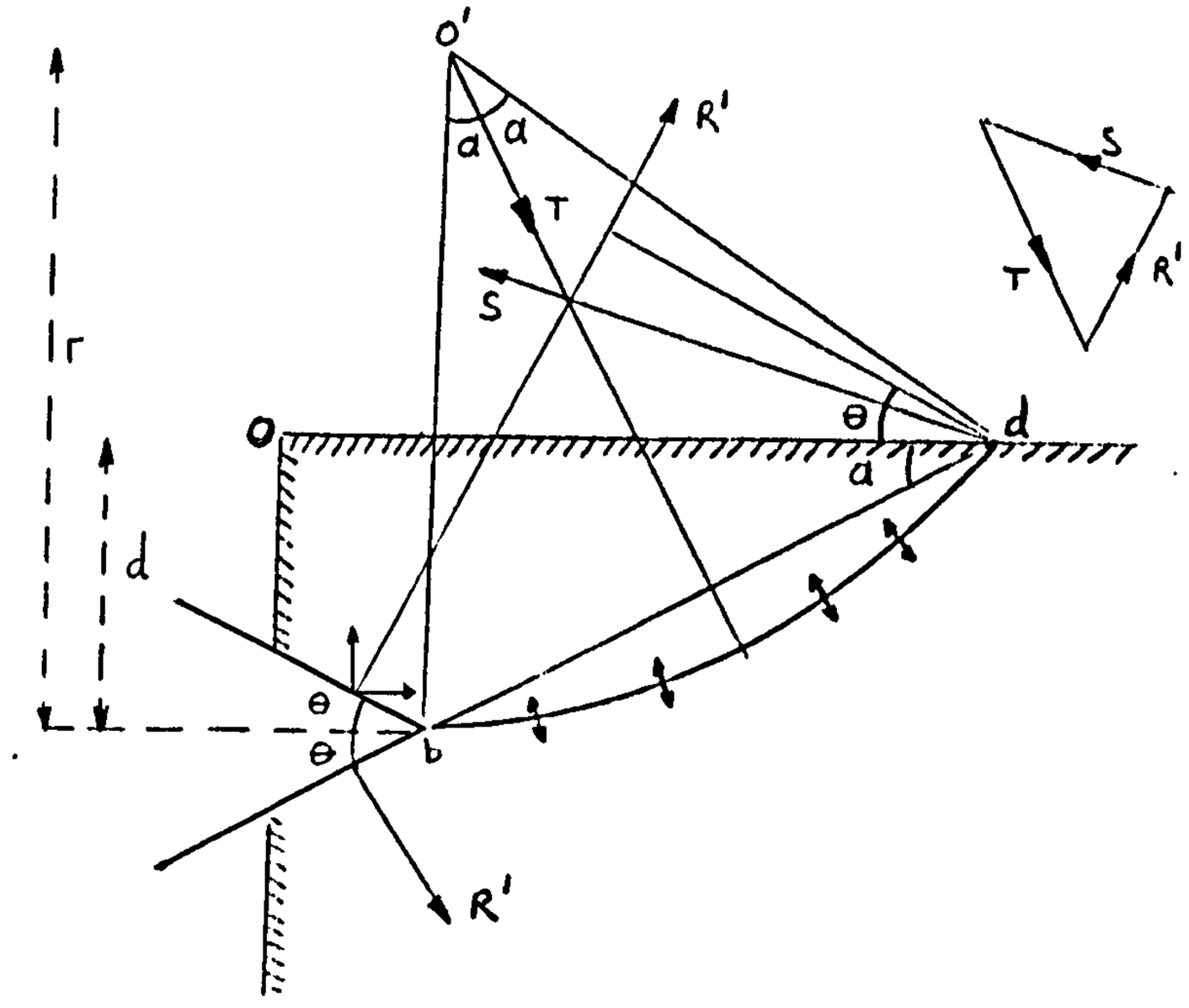

Fig.16 Illustrating assumptions of Evans' Theory.

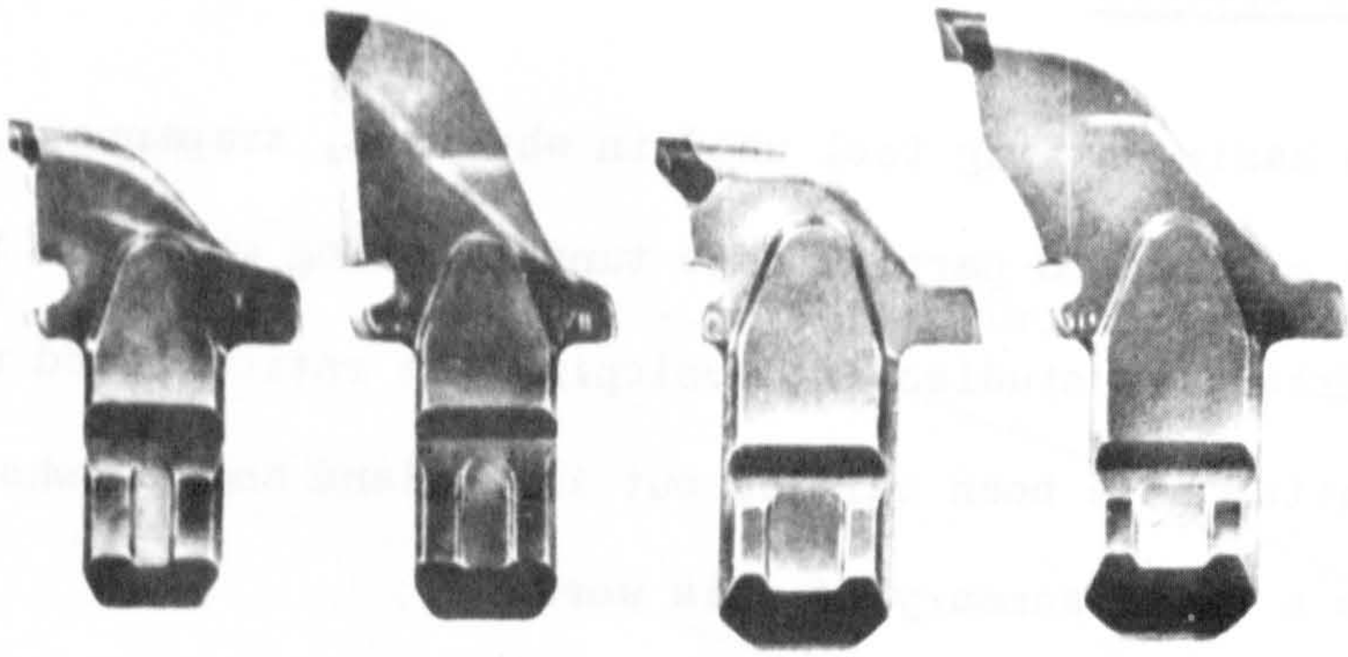

SP227
2"-50mm
gauge

SP300
3"-75mm
gauge

HSP200
2"-50mm
gauge

HSP300
3"-75mm
gauge

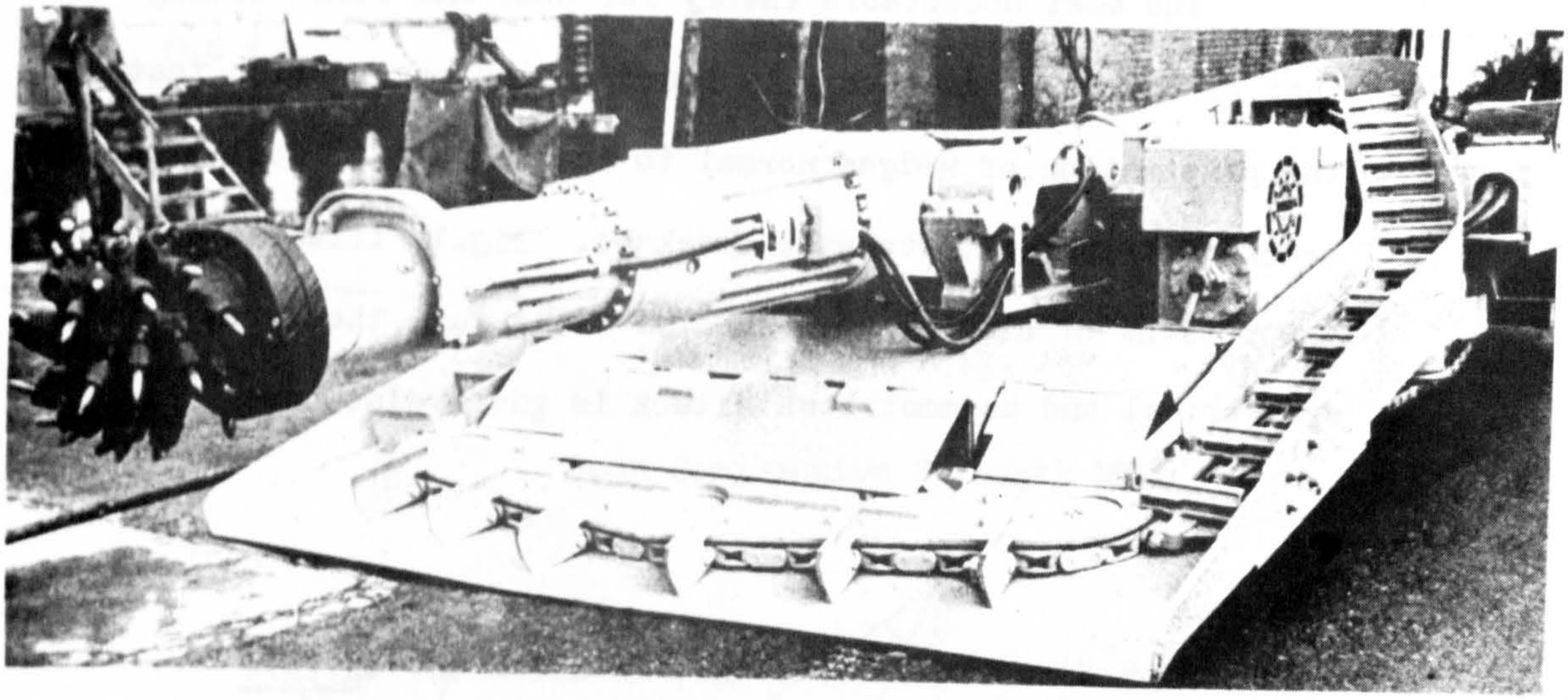

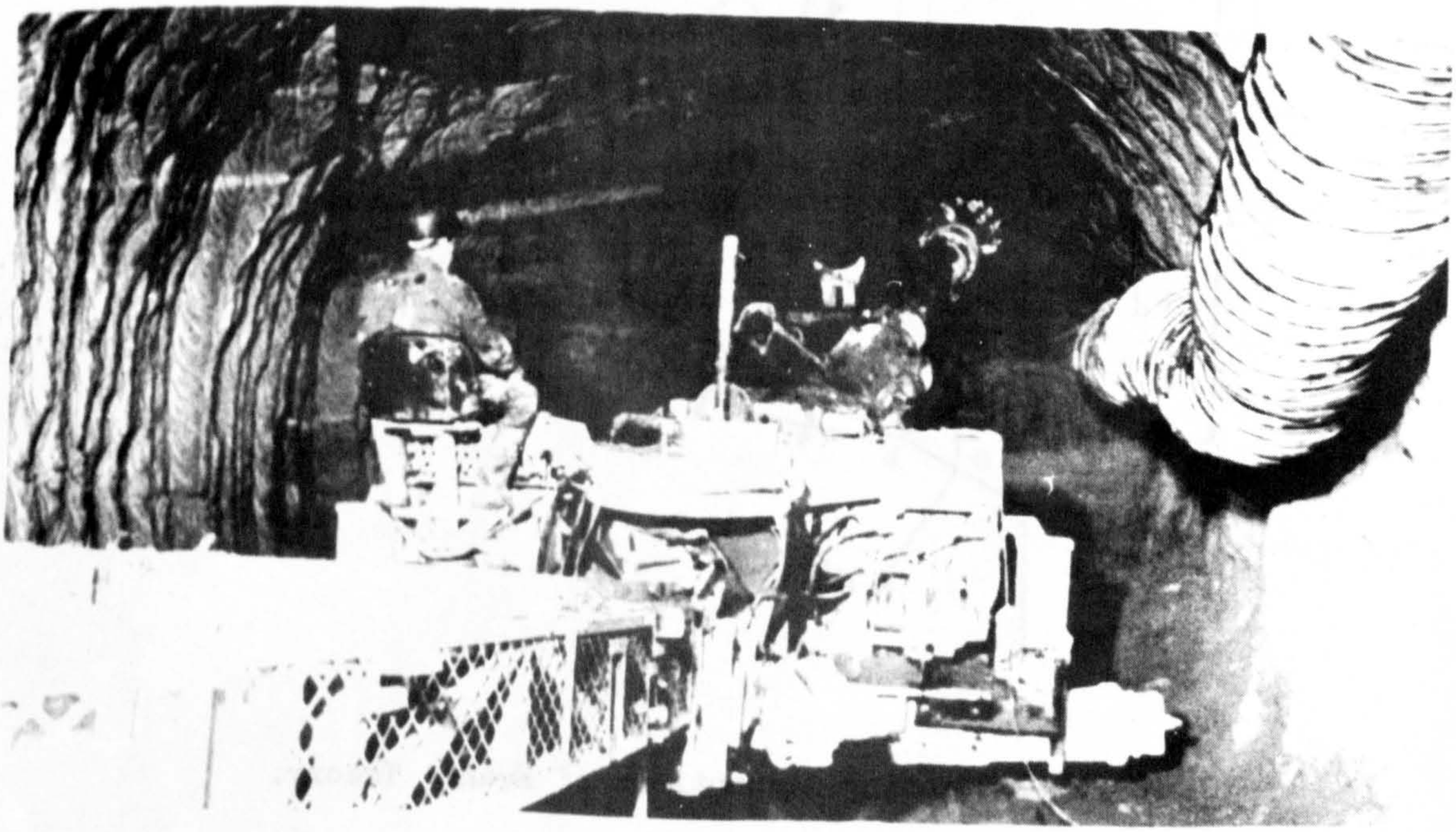

Fig.15 Pick Cutters.

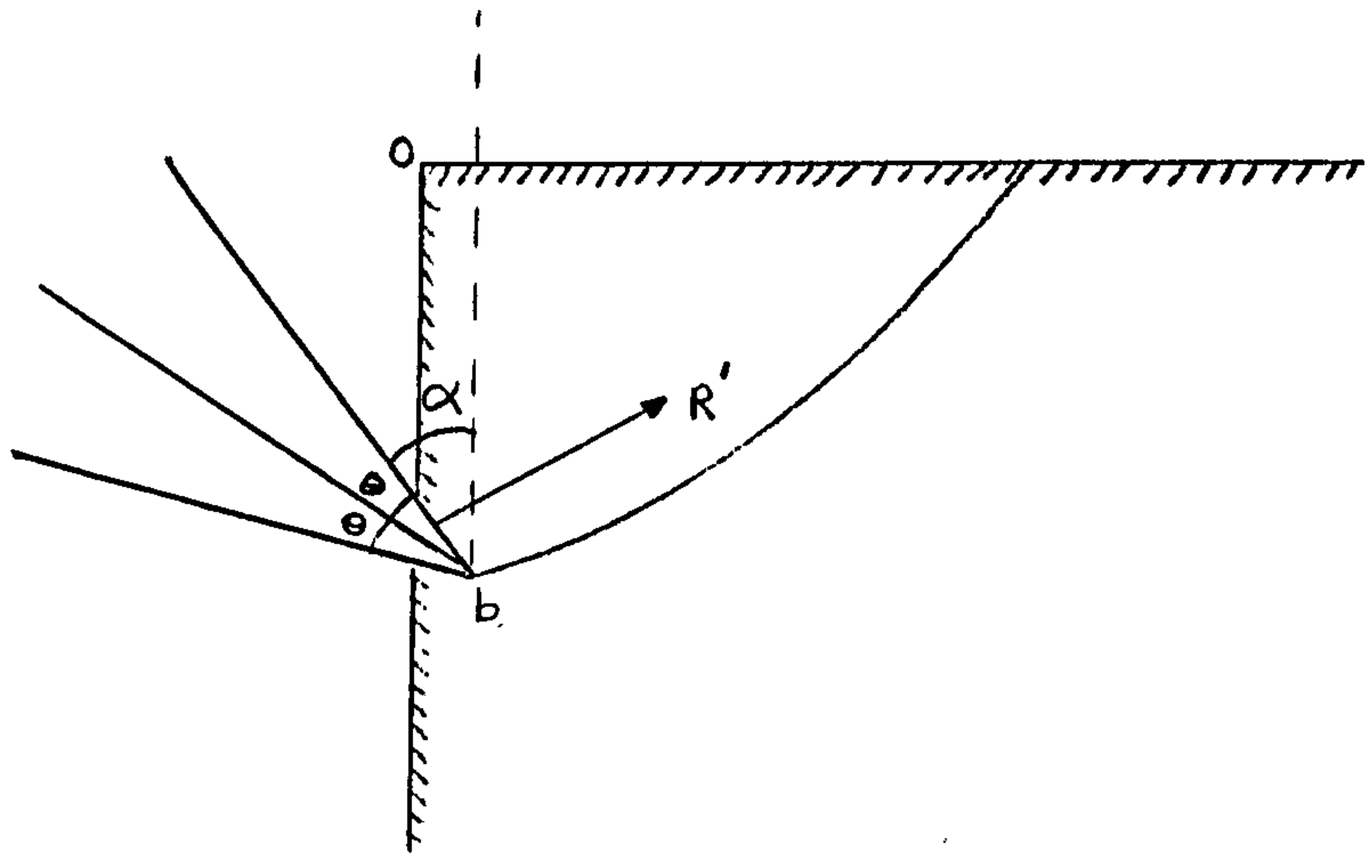

Fig.16 A Illustration of Asymmetrical Attack.

Evans formulates peak cutting force for unit width of tool as

$$F'C = \frac{2\sigma t.d.\sin\theta}{1-\sin\theta} \qquad \text{or} \qquad F'C = \frac{2\sigma t.d.\sin(\theta+\varphi)}{1-\sin(\theta+\varphi)}$$

where $F'C$ = Peak cutting force

σt = Tensile strength of the rock

d = Depth of cut

θ = Semi wedge angle

φ = Friction angle between steel and rock.

However, Evans has shown that the above equation may be adapted for chisel picks as:

$$F'C = \frac{2\,\sigma t.d.\sin\left\{\frac{1}{2}\left(\frac{\pi}{2}-\alpha\right)+\varphi\right\}}{1-\sin\left\{\frac{1}{2}\left(\frac{\pi}{2}-\alpha\right)+\varphi\right\}}$$

where α is rake angle as defined in Fig.16A.

Roxborough has found that cutting experiments carried out in Sandstone, Limestone, Anhydrite and dry chalk gave results of the same magnitude as values calculated from Evans' theory[63]. However, there was no evidence of the tensile arc of failure when cutting wet chalk and the formula adapted from Merchant Metal Cutting Theory by Potts and Shuttleworth gave reasonable predicted values[64]. The Merchant Theory assumes failure to occur in shear. This phenomenon is explained by Evans as his cutting theory is based upon the assumption that $\sigma t/\sigma c$ is small and for higher values of $\sigma t/\sigma c$ there is a theoretical possibility that shear breakage may take place more easily than tensile breakage[65]. Using the same basic assumption of shear failure as Merchant Theory, Nishimatsu used Mohr's criterion of failure and obtained an expression for the resultant force[66]. He observed discontinuous cutting in rock and proposed a failure process which involved a primary and secondary crushed zone associated with coarse chip formation. This is a semi empirical approach since it is necessary to carry out a few cutting experiments in order to calculate the angle of friction of rock cutting, which is found to be a function of rake angle.

3.4.2 Laboratory Investigations

The earliest work was carried out at the Research Establishment of the National Coal Board and much of the work is described in a monograph published by Evans and Pcmeroy[62]. The following conclusions were obtained.

- Energy to excavate unit volume of cutting material is reduced considerably as depth cf cut increases.

- Cutting efficiency increases with increase in rake angle.

- There is an optimum spacing/depth ratio when the distance between adjacent cuts is considered.

- Cutting speed does not significantly affect pick forces and yield.

- Groove deepening is highly inefficient.

- Simple chisel picks are more efficient than the other types of picks.

- The back clearance angle should be not less than 6 degrees

- Simulating overburden stress on coal specimens during cutting experiments tended to increase pick forces for the first increment of stress. Further stress increase caused a peak value beyond which the cutting forces fell rapidly.

- The most efficient orientation of the cleats is 45 degrees to the line of attack.

The later investigations of the N.C.B. are reported by Barker[67,68].

At the University of Newcastle upon Tyne the investigations were initially concerned with the ploughability of coal[69,70,71], but much more of the later work has been carried out in medium and high strength rocks. Allington carried out tests using various commercial picks in Sandstone, Limestone and Anhydrite[72]. Rispin tested chisel picks in Quartzites taken from South African Mines[73]. Powell's main interest was percussively activated cutting tools in high strength and abrasive rocks[74]. A more comprehensive study of the symmetrical and asymmetrical shaped picks was done by Roxborough and Phillips[75] in Bunter Sandstone. Dunn[76] investigated cutting performance of picks in groove deepening, stressed rock and corner cutting situations. His major conclusion, confining stress has no significant effect on tool forces and yield in Bunter Sandstone, contradicts the coal cutting results reported by Evans and Pomeroy. Research workers at the Mining Technology Laboratories, Chamber of Mines of South Africa, have recently completed a series of tests in cutting a strong rock with a drag bit assisted by high pressure water jets[77]. Hood reports that high pressure water jets directed immediately ahead of drag picks reduce the magnitude of the forces on the bits significantly.

3.4.3 Wear Performance of Pick Cutters

Picks are more susceptible to wear than any type of roller

cutters since each point on the cutting edge is in continuous contact with rock. Any improvement in prolonging pick cutter life will have a big effect on the economics of mechanical excavation. Several investigations were carried out in this respect. Evans extended his cutting theory to blunt wedges and found good correlation with his theory and the results obtained by Dalziel and Davies[62]. Most of the experimental work done at M.R.D.E., Bretby is summarised by Kenny and Johnson in two technical papers[78,79]. At the University of Newcastle upon Tyne an extensive wear testing programme started by Rispin[73] and Fowell[74] is being continued by Harle, who is studying the effect of various pick metallurgical and operational parameters in different types of rock[80].

3.4.4 Correlation of rock properties and the cutting performance of road headers

Long term in-situ and laboratory studies have been recently completed by Fowell and McFeat-Smith[81,82]. The main approach has been to represent in-situ conditions of beds by one rock material property, deformation coefficient, and one rock mass property, break index. They predict the performance of road headers in massive beds from a few simple hardness and mineralogical tests.

* * *

CHAPTER FOUR

PLANNING OF THE EXPERIMENTS

Any experiment is carried out to determine the variation of a dependent variable due to changes in one or a number of independent variables. For example, we may wish to determine the relationship between a dependent variable FT, and the independent variables, p, ϕ, D and S. The independent variables here may be such that the magnitude of the effect of each on FT varies with the magnitude of the others. This variation, commonly termed interaction, should be investigated throughout the experiment, so that the desired information can be obtained with sufficient precision.

Conventional factorial experimental designs measure the affect of a varying single factor while the other factors are kept constant, so that any variation in the results of the experiment can be directly attributed to the factor which is being altered. Such designs are limited in the application by the large number of tests which the design requires to be performed. For example, if disc penetration, disc edge angle, disc diameter and cutting speed are each studied at five levels, it would be necessary to carry out 5^4 tests. When working on rocks, a measure of replication is essential in order to gain greater statistical integrity and four replications of any test is considered a minimum[73].

The factcrial experiment previously discussed would require 2500 individual cutting tests and several blocks of experimental rock would have to be used. Clearly, a more efficient experimental design is desirable for this type of investigation. The partial factorial method of Protodyakanov and Teder[83,84] has been used for the design cf some of the experiments described in this Thesis. By the manipulation of

orthogonal latin squares, this method reduces the required tests from 2500 to 100. When combined and averaged in the correct manner, the results of the partial factorial method may be analysed to produce a mathematical model to describe the effects of the independent variables on the dependent variable. This method is widely and successfully used in the U.S.S.R.

4.1 The Design of the Partial Factorial Experiment

Each combination of the influencing factors occurs once and only once in the experimental matrix. This can be done graphically or by using numerical matrices. The second method, which is basically a manipulation of orthogonal latin squares, is chosen for the experiments carried out.

Latin squares have been used a great deal in agricultural experimental work[85] and they have been found to be useful in other scientific and industrial experiments. A latin square is defined as a square consisting of figures in which each number occurs once and only once in each column and in each row. Two latin squares of the same size are orthogonal to each other if they are superimposed, every letter of one square appears once and only once, with every letter of the other. This is shcwn in Fig.17A below:

1	2	3	4	5
2	3	4	5	1
3	4	5	1	2
4	5	1	2	3
5	1	2	3	4

1	3	5	2	4
2	4	1	3	5
3	5	2	4	1
4	1	3	5	2
5	2	4	1	3

11	23	35	42	54
22	34	41	53	15
33	45	52	14	21
44	51	13	25	32
55	12	24	13	43

Fig.17A Orthogonal Latin Squares

The number of columns must be equivalent to the number of levels of each variable and an odd number of levels is necessary in order to maintain the symmetry of the squares.

The orthogonal squares used to generate the experimental combinations are obtained from one original square by displacement of the columns and a circular rotation of the numbers[83,84]. The five orthogonal squares generated from one square are given in Fig.17B.

(a) Edge Angle

1	1	1	1	1
2	2	2	2	2
3	3	3	3	3
4	4	4	4	4
5	5	5	5	5

(b) Disc Diameter

1	2	3	4	5
2	3	4	5	1
3	4	5	1	2
4	5	1	2	3
5	1	2	3	4

(c) Penetration

1	3	5	2	4
2	4	1	3	5
3	5	2	4	1
4	1	3	5	2
5	2	4	1	3

(d) Cutting Speed

1	4	2	5	3
2	5	3	1	4
3	1	4	2	5
4	2	5	3	1
5	3	1	4	2

1	5	4	3	2
2	1	5	4	3
3	2	1	5	4
4	3	2	1	5
5	4	3	2	1

Fig.17B Orthogonal Latin Squares

These squares are used for the experimental design.

* * *

4.2 Analysis of the Experimental Data

The levels of the three disc cutter variables studied are detailed in Table 1.

Table 1 Independent Variables and their Levels.

Factor or Independent Variable	Units	Levels				
Disc Diameter (D)	mm	100	125	150	175	200
Disc Edge Angle (ϕ)	Degrees	60	70	80	90	100
Penetration (p)	mm	10	8	6	4	2

Each square represents one of three variables. The corresponding number in each of the 3 squares are the experimental levels of each factor. For the first test, the first figure in each square is taken as the level of that factor, i.e. all factors are at level 1 (Fig.17B). For the ninth test, the ninth figure in each square is taken, i.e. disc edge angle is set at level 2, disc diameter at level 5, penetration at level 3. The 25 combinations obtained by working across the rows are given in Table 2.

If these 25 tests are carried out, with suitable replication, it is possible to analyse the results in such a manner that the relationship between the dependent variable, such as $\overline{FT}$, and the 3 variables, ϕ, D and p, is fully defined. The experiment undertaken in Gypsum provides the values of mean thrust force ($\overline{FT}$) which are given in the first column of Table 3 and which will be used in this example.

Initially the mean values of $\overline{FT}$ for each level of penetration, disc edge angle and disc diameter are calculated. To obtain the effect

of penetration alone on the mean thrust force, all the $\overline{FT}$ results at each level of penetration are averaged. Because of the unique experimental design this gives the five $\overline{FT,p}$ values which are independent of the effects of ϕ and D. All the averaged values are given in Table 4 and plotted in Fig.18 against the respective variables.

The variations in FT with penetration, disc edge angle and diameter are clearly linear and of the form:

$$\overline{FT,p} = Ap+B \quad - - (1) \qquad \overline{FT,\phi} = C\phi+E \quad - - - (2)$$

$$\overline{FT,D} = FD+G \quad - - (3)$$

The second stage of the analsyis is designed to combine the partial equations to produce a single general equation relating $\overline{FT}$ to the 3 variables. This equation can be stated in general terms as

$$\overline{FT} = f(p) \cdot f(\phi) \cdot f(D) \quad - - - (4).$$

The first part of equation (4) is defined by Fig.18A where $\overline{FT,p}$ is plotted against penetration. The best fitting straight line is obtained by normal regression procedures, thus defining the constants A and B in equation (1).

However, since the effect of penetration is dominant, its affect must be eliminated from the data set before the true effects of ϕ and D may be determined.

Equation (1) may be re-written as:

$$\overline{FT,p} = A\left(p + \frac{B}{A}\right)$$

where B/A is the ratio of intercept/slope from Fig.18A. Consequently, in order to eliminate the effect of p from the data set, each of the

25 values of $\overline{FT}$ in Table 3 must be divided by $(p + \frac{B}{A})$. This produces a new set shown in the next column. Grouping this new data according to disc edge angle, gives 5 new values of $\frac{\overline{FT}}{p+B/A}$, ϕ which are shown in Table 5, column 2. By regressing these calculated values against disc edge angle, an equation of the form $C\phi+E$ can be calculated, i.e. $f\phi = \phi+\frac{E}{C}$. In order to determine the contribution of D to the general equation it is necessary to eliminate the effect of ϕ from data set. $\frac{\overline{FT}}{p+B/A}$ values are divided by $\phi + \frac{E}{C}$ to give a new set (Table 3, Column 3). This new set is averaged according to the levels of D and these new mean values of $\frac{\overline{FT}}{(p+B/A)(\phi+E/C)}$, D (Table 5, Column 3) are regressed against D. This gives the final constants to define the general equation for this example.

From Table 5, the combined equation can be presented as:

$$\overline{FT} = (p - 0.93)(\phi - 20.198)(2.3\times10^{-4}D+0.07) \quad - - - (5)$$

The validity of this equation may be checked by comparing the measured values with those predicted by equation (5). This can be presented graphically as seen in Fig.19. If the actual and predicted values of $\overline{FT}$ are regressed the correlation coefficient obtained is 0.988, indicating a highly significant predictor equation.

* * *

Table 2. Experimental Conditions

Test No.	Disc Edge Angle (Ø)	Disc Diameter D (mm)	Penetration p (mm)
1	60	100	10
2	60	125	6
3	60	150	2
4	60	175	8
5	60	200	4
6	70	125	8
7	70	150	4
8	70	175	10
9	70	200	6
10	70	100	2
11	80	150	6
12	80	175	2
13	80	200	8
14	80	100	4
15	80	125	10
16	90	175	4
17	90	200	10
18	90	100	6
19	90	125	2
20	90	150	8
21	100	200	2
22	100	100	8
23	100	125	4
24	100	150	10
25	100	175	6

Table 3 Actual and Predicted Values of $\overline{FT}$

Test No.	Actual Values $\overline{FT}$ (kN)	$\frac{\overline{FT}}{p + \frac{A}{B}}$	$\frac{\overline{FT}}{(p+\frac{A}{B})\ (\phi + \frac{E}{C})}$	Predicted Values $\overline{FT}=f(p).f(\phi).f(D)$
1	35.86	3.954	0.099	33.80
2	19.49	3.844	0.097	20.08
3	6.11	5.712	0.144	4.49
4	34.21	4.839	0.122	31.29
5	12.75	4.154	0.104	14.30
6	30.94	4.376	0.088	35.03
7	14.38	4.685	0.094	16.11
8	44.75	4.934	0.099	50.23
9	26.70	5.267	0.106	29.55
10	6.32	5.908	0.119	4.99
11	29.43	5.805	0.097	31.94
12	7.48	6.993	0.117	7.11
13	45.56	6.444	0.108	49.49
14	14.25	4.642	0.078	17.19
15	48.92	5.394	0.090	53.96
16	21.95	7.151	0.102	23.83
17	78.76	8.684	0.124	74.10
18	24.81	4.894	0.070	33.14
19	10.44	9.760	0.140	7.43
20	51.31	7.258	0.104	51.99
21	11.24	10.508	0.132	9.99
22	47.66	6.741	0.084	52.83
23	23.61	7.691	0.096	24.37
24	75.38	8.311	0.104	76.25
25	46.89	9.249	0.116	44.99

Table 4 Mean Values of $\overline{FT}$ to Plot Fig.18

Variable p (mm)	Test No.	$\overline{FT,p}$ (kN)	Variable ($\phi°$)	Test No.	$\overline{FT,\phi}$ (kN)	Variable D (mm)	Test No.	$\overline{FT,D}$ (kN)
2	3,10, 12,19, 21	8.32	60	1,2, 3,4, 5	21.69	100	1, 10 14,18 22	25.78
4	5, 7, 14,16, 23	17.39	70	6,7, 8,9, 10	24.62	125	2, 6, 15,19 23	26.68
6	2, 9, 11,18 25	29.47	80	11,12 13,14 15	29.13	150	3, 7, 11,20 24	35.32
8	4, 6, 13,20; 22	41.94	90	16,17 18,19 20	37.46	175	4, 8, 12,16 25	31.06
10	1, 8, 15,17, 24	56.73	100	21,22 23,24. 25	40.96	200	5, 9, 13,17 21	35.00

Table 5 Partial Factorial Equation for $\overline{FT}$

p(mm)	$f(p)=p+\frac{B}{A}$	ϕ (°)	$f(\phi)=\frac{\overline{FT}}{p+\frac{B}{A}},\phi$	D (mm)	$f(D)=\frac{\overline{FT}}{(p+\frac{B}{A})(\phi+\frac{E}{C})},D$
2	1.070	60	4.500	100	0.090
4	3.070	70	5.034	125	0.102
6	5.070	80	5.856	150	0.109
8	7.070	90	7.549	175	0.111
10	9.070	100	8.500	200	0.115

$f(p) = (p - 0.93)$; $f(\phi) = (\phi - 20.198)$; $f(D) = (2.3\times10^{-4}D+0.07)$

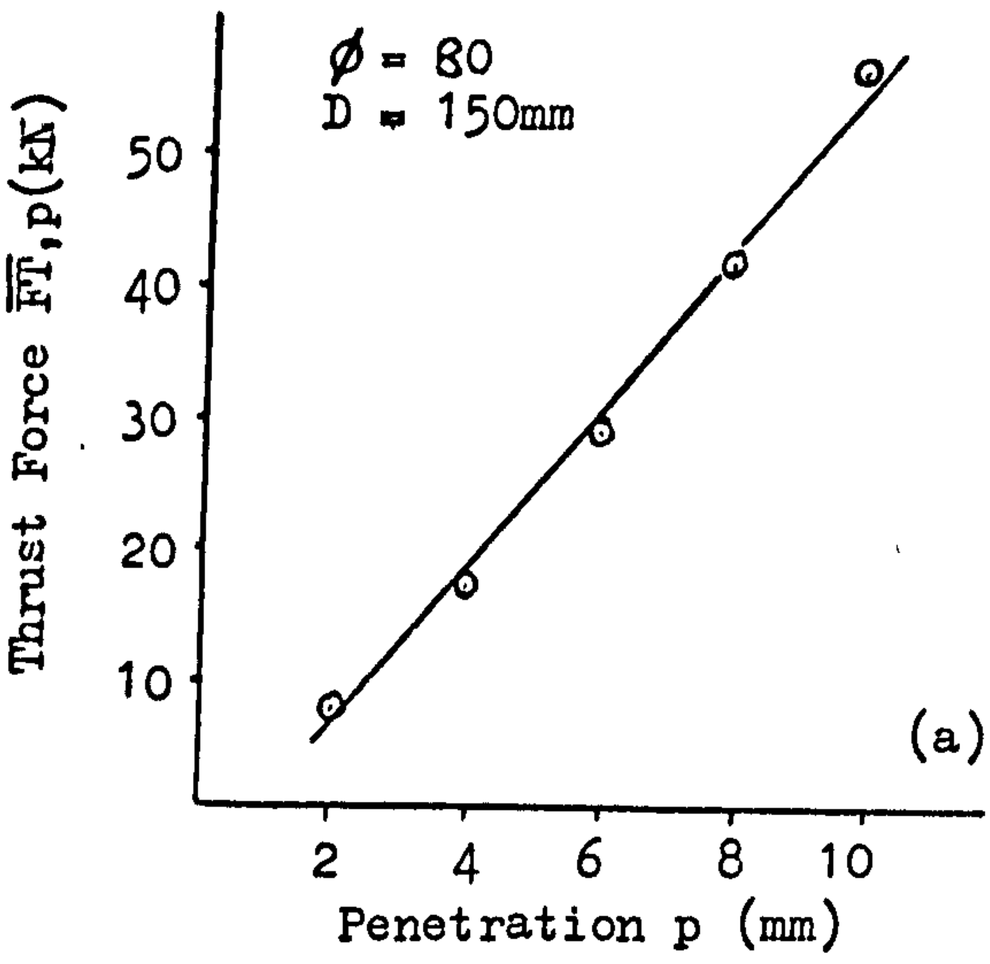

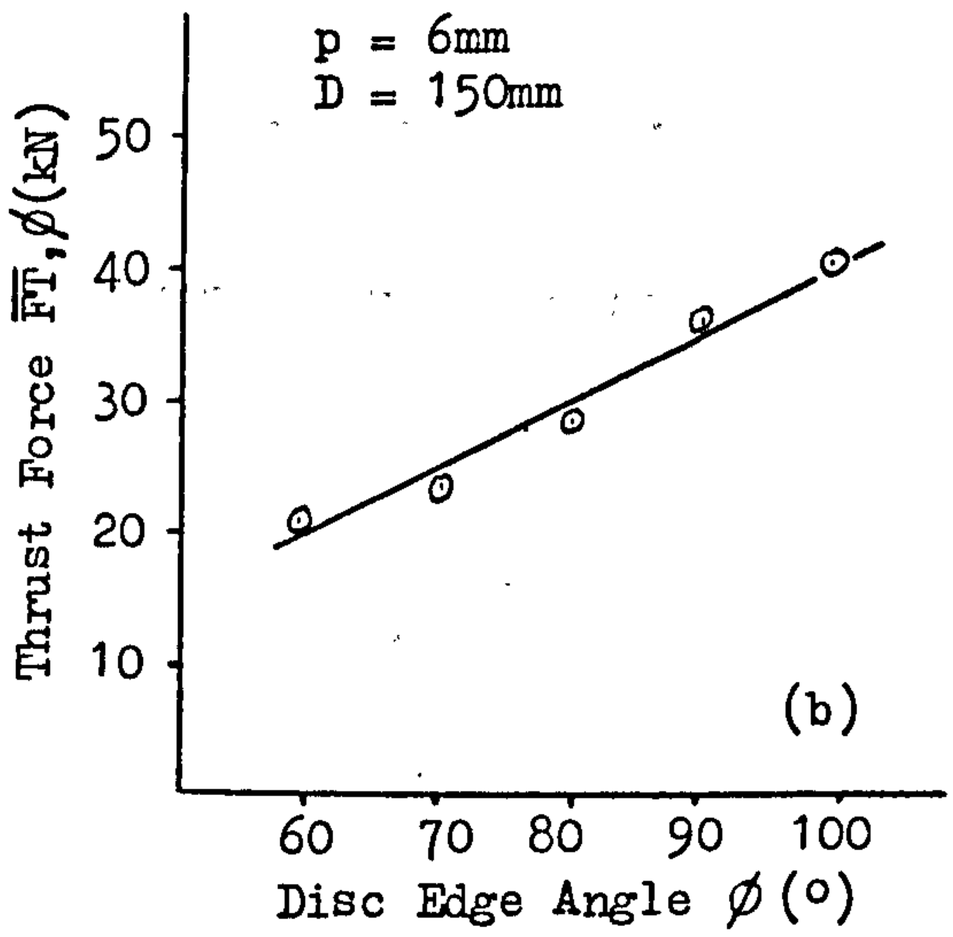

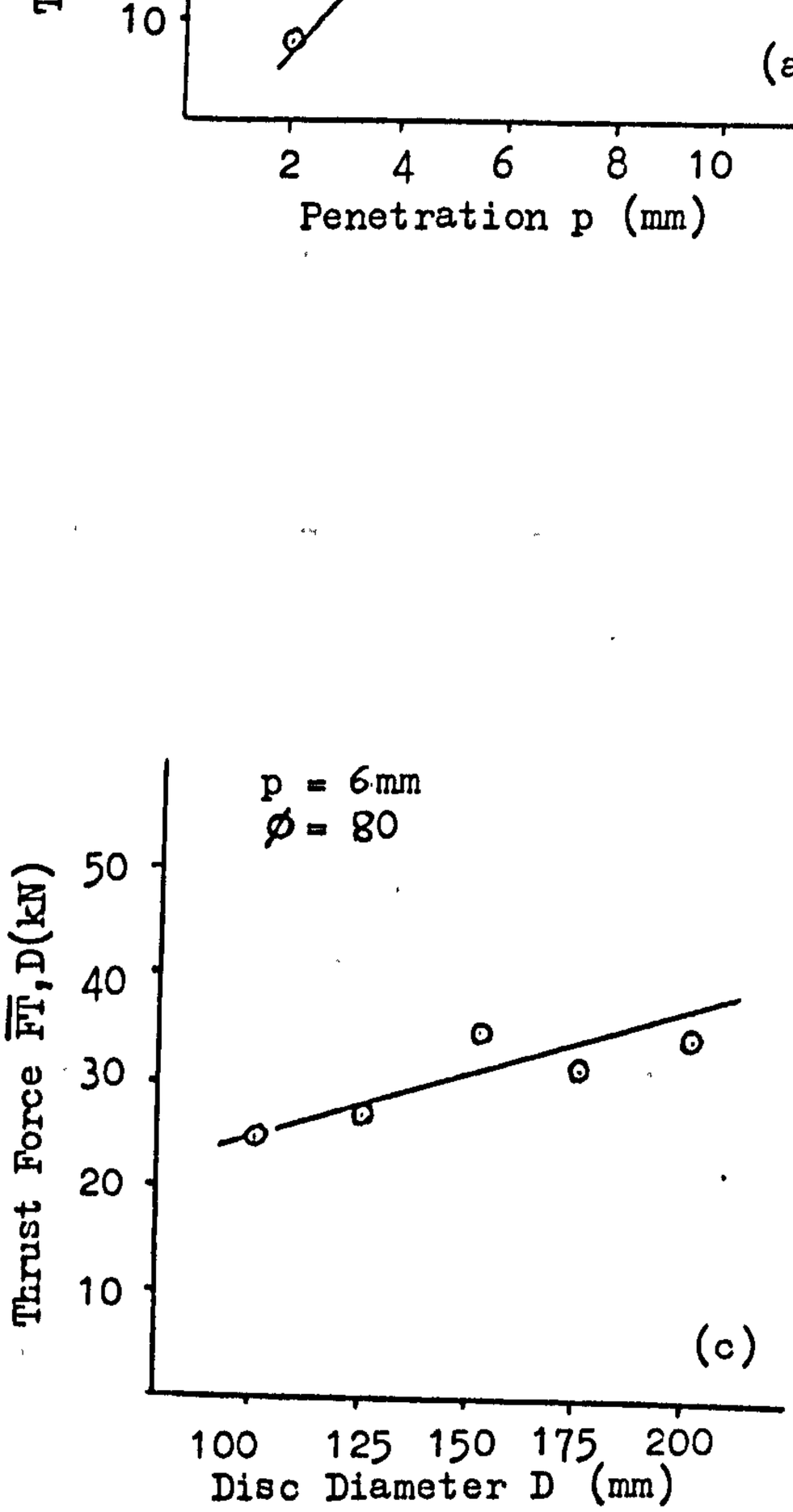

Fig.18. Mean Thrust Force versus Disc Penetration, Disc Edge Angle, Disc Diameter.

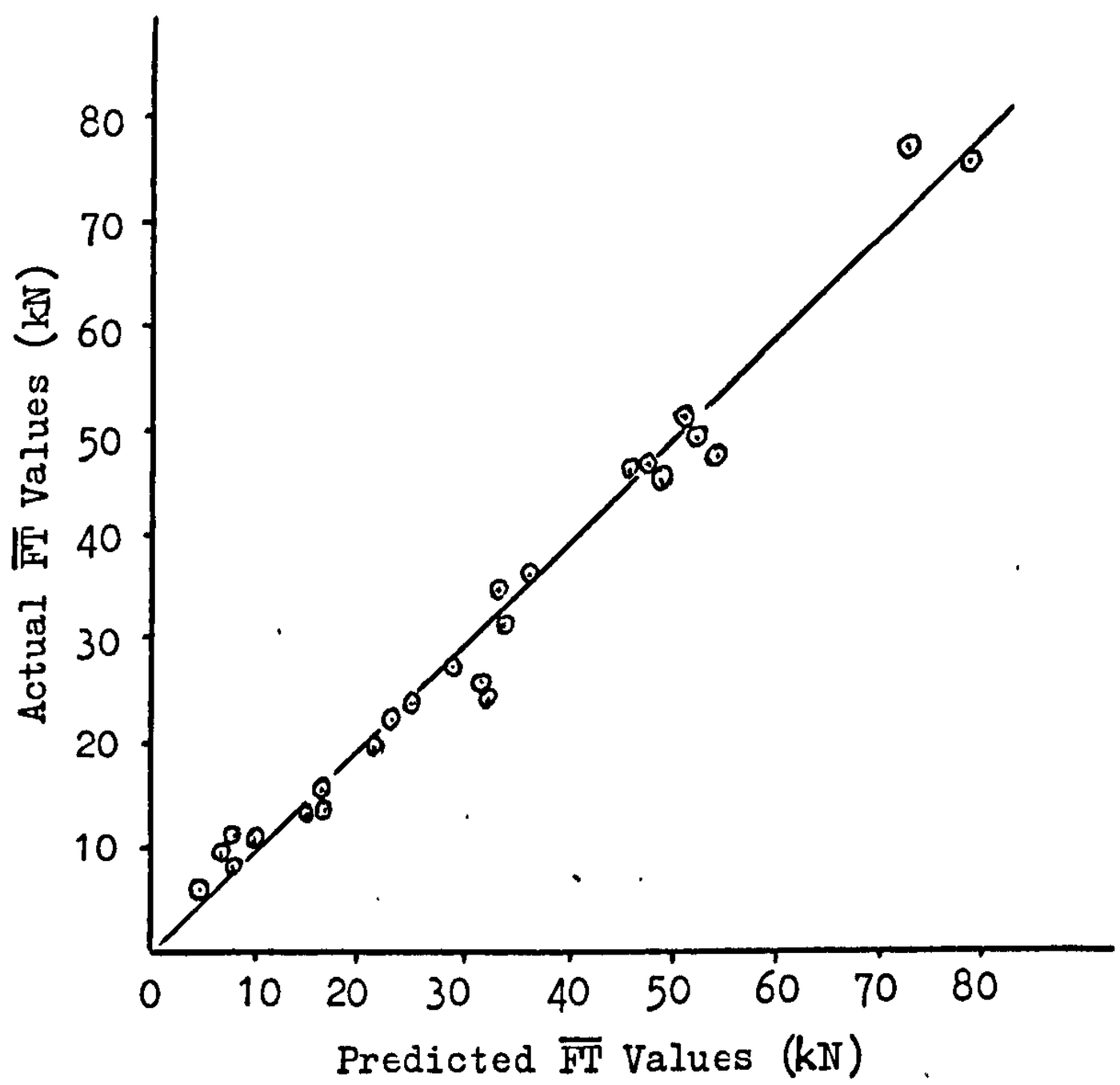

Fig.19 Predicted Values versus Actual Values of $\overline{FT}$.

CHAPTER FIVE

EXPERIMENTAL EQUIPMENT

5.1 Rock Cutting Rigs

The 9kW Butler Shaping Machine (Fig.20) was used to conduct the experiments with picks in low strength rocks. This machine has a maximum stroke cf 660mm, a speed range of 0.13 to 0.63m/sec., and a work table which could be raised, lowered and traversed horizontally. The head of the machine had been modified to accept the mounting of a dynamometer tool holder.

A modified Kelly Shaping Machine (Fig.21) having a stroke of 800mm was used in disc cutting experiments and in pick cutting experiments for high strength rocks. A few design changes have been made, such as including thrust frame to give the rig a high degree of rigidity[74]. This strong steel framewcrk limited the deflection cf the tool during cutting to 10% of the penetration at very high vertical loads. A maximum in-line thrust force of 10 tons can be provided on the machine. A rock specimen of 0.5m square by 0.3m high can be accommodated by the machine and lowered and laterally traversed with respect to the cutting tool, so the required depth of cut could be set up, using a dial gauge. Cutting speed can be changed up to 0.2 m/s.

Experimental rocks were fixed to prepared steel plates with araldite AY103 and allowed to cure for 24 hours, and this was then bolted onto the machine table.

At deep penetrations the rock specimens tended to split from the cut to the base plate and so it was necessary to confine the blocks using wcod packing and securing bolts within a large steel frame fixed to the work table. In order to eliminate the impact action of the disc,

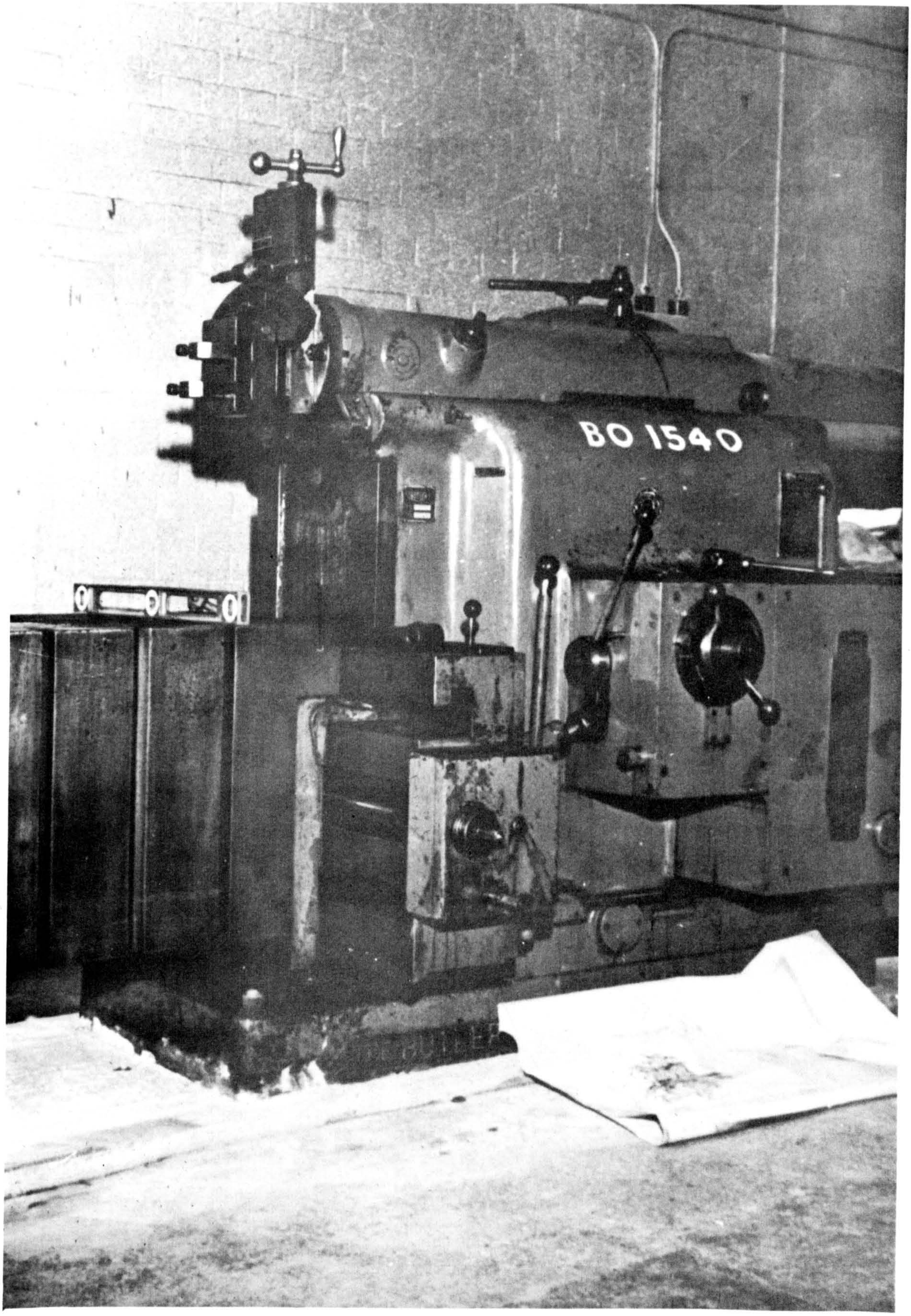

Fig.20 Butler Shaping Machine.

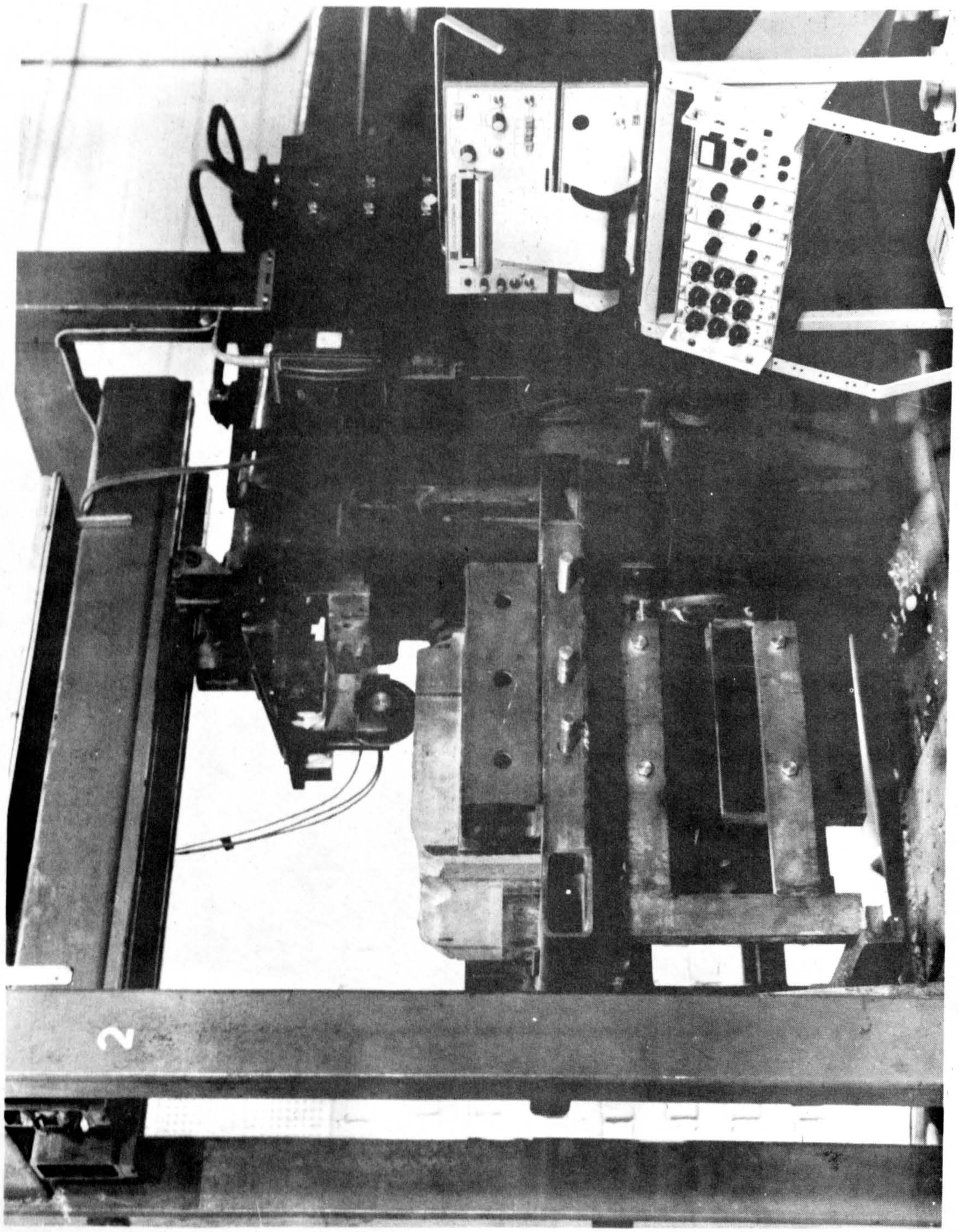

Fig.21A Modified Kelly Shaping Machine with Instrumentation.

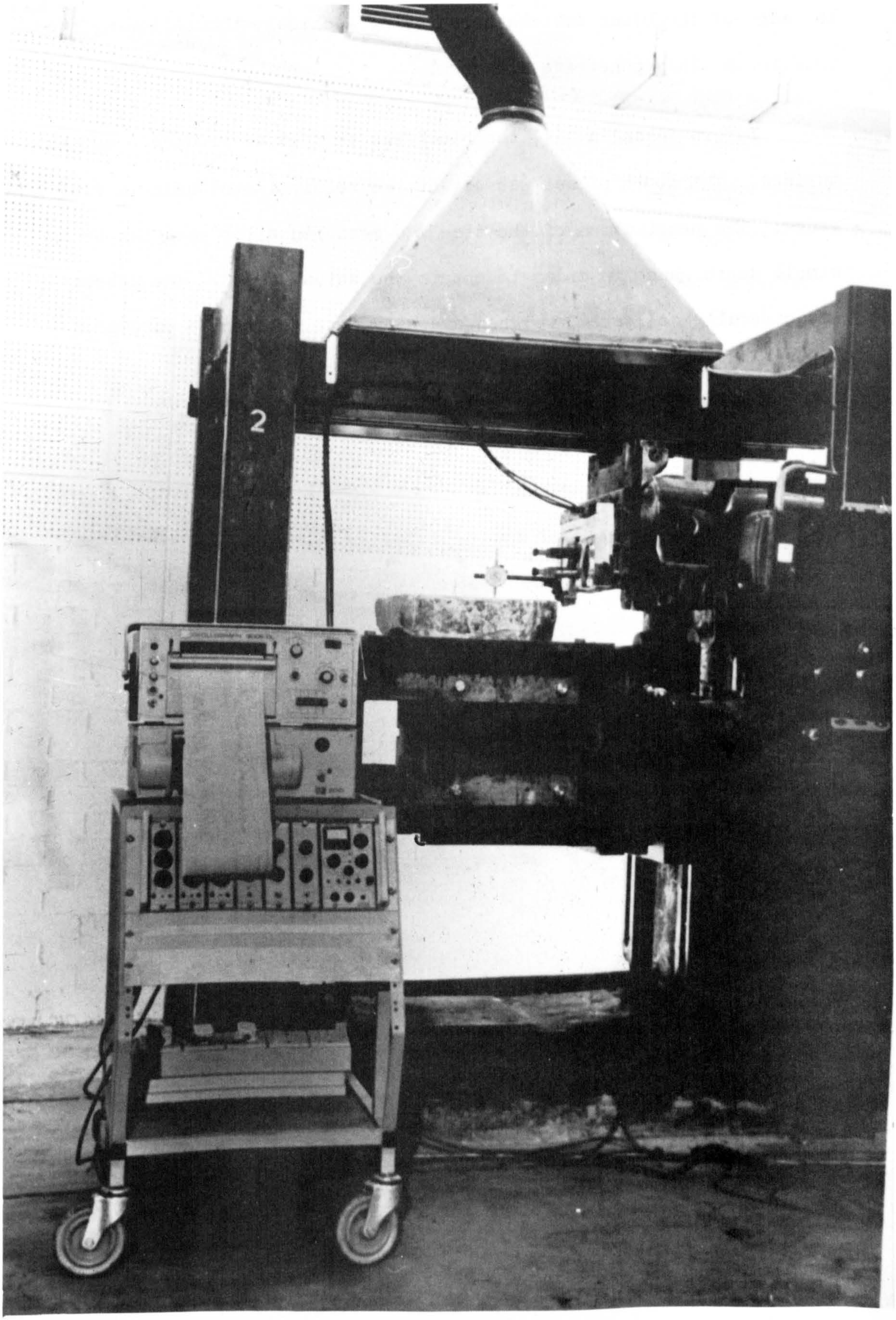

Fig.21B Modified Kelly Shaping Machine with Instrumentation.

the edge of the block was chambered using a chisel, thus allowing the tool to smoothly penetrate the rock.

Before taking a cut, the block was trimmed to produce a smooth surface. The depth of cut was set at the required level using a dial gauge. The penetration of the disc was measured after each cut by a simple depth gauge in order to obtain the actual depth. The debris was carefully collected, weighed and sieved to obtain the values of yield, specific energy and coarseness index.

* * *

5.2 Instrumentation

The experimental cutting tool is clamped in the tool holder of a 100 kN capacity steel dynamometer which is designed and manufactured in the Department's laboratory[72]. The output from the dynamometer is amplified using an S.E.4000 Carrier Amplifier system and is displayed on an S.E.3006 Ultra Violet Chart Recorder (Fig.22). A typical U.V. Recording is shown in Fig.23.

The dynamometer resolves the instantaneous force on a cutting tool into three mutually orthogonal components, each measured by a strain-gauged bridge circuit. The instrumentation for each of the three forces consists of an amplifier and integrator, which gives a measure of the mean force level in any cut. The U.V. charts showed the instantaneous and integrated values of two force compcnents during a cut. U.V. trace analysis was carried out using a D-Mac Digital Table, which provides a punched card deck for each cut. Further analysis of the cut data was performed on the Department's Wang 720 B Mini-computer and the University's Hewlett-Packard Computer 2000 E, using specially developed data handling programs.

* * *

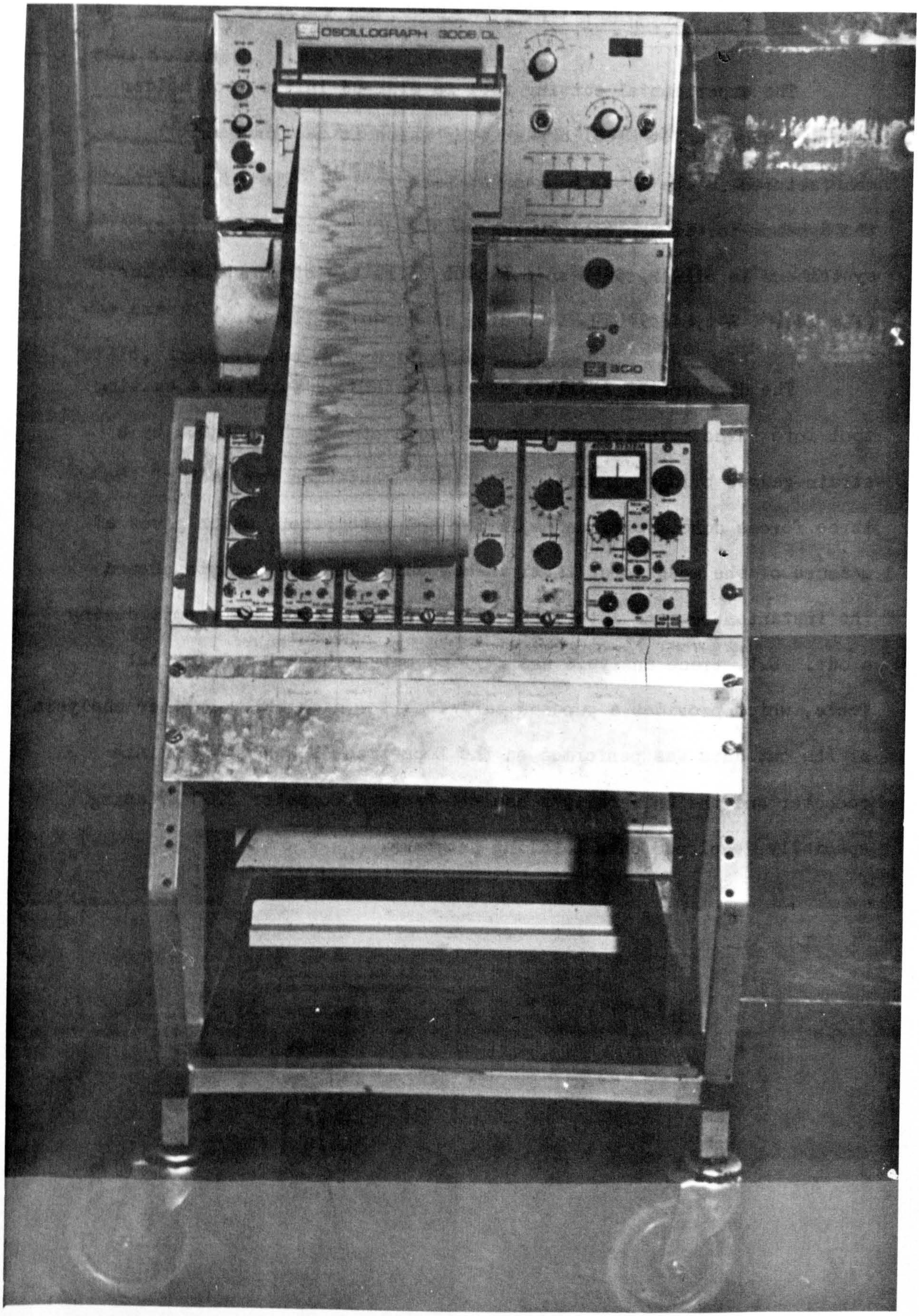

Fig.22 Ultra Violet Chart Recorder.

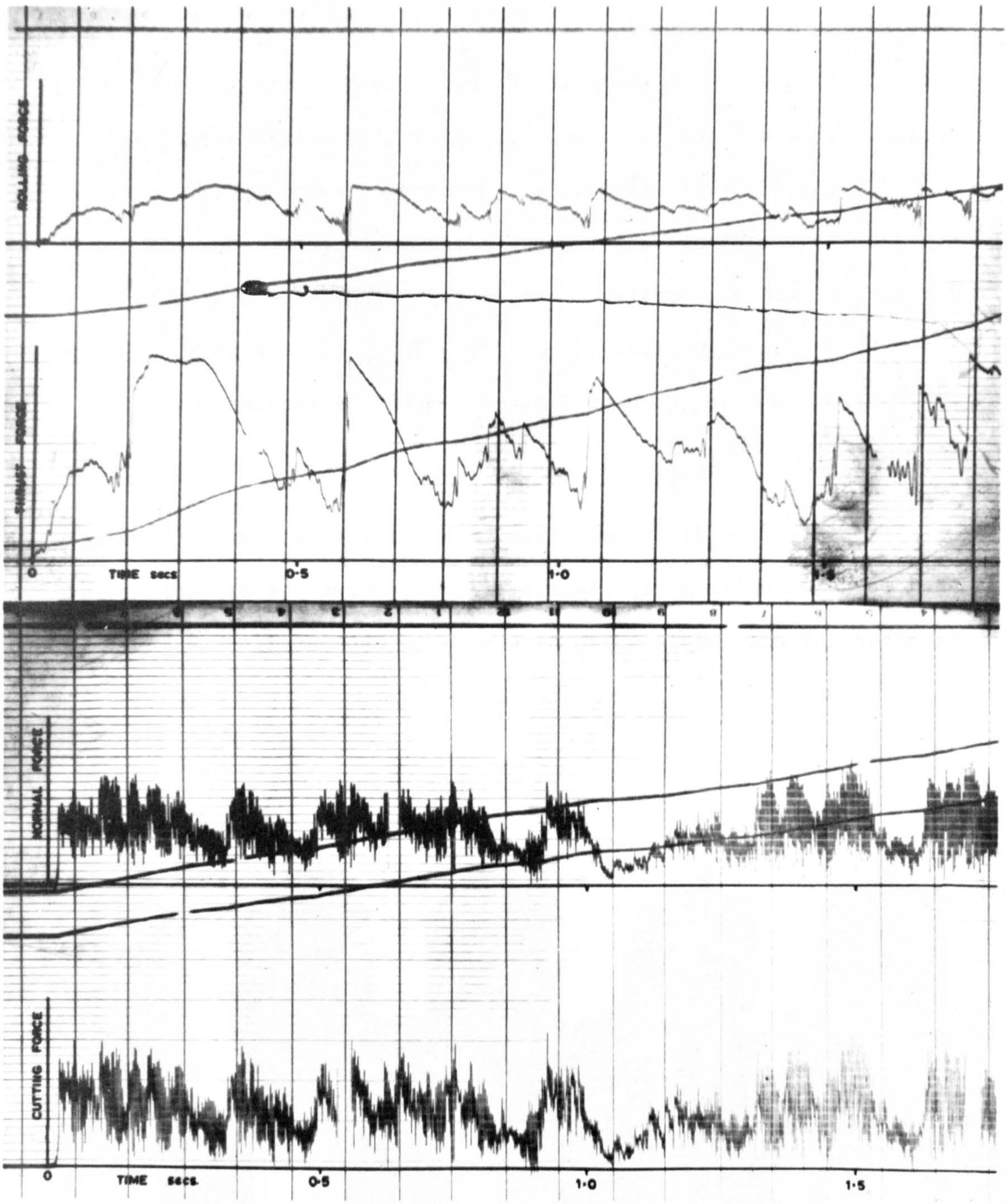

Fig. 23 Typical U.V. Traces.

5.3 Cutting Tools

Initially 25 toolholders for pick experiments were manufactured, each having different width and rake angle. The carbide tips were securely clamped in these toolholders. Due to cutting experience in Anhydrite, it was felt that new, stronger tool shanks should be designed for high strength rocks. A range of negative rake tools were considered as most suitable, since these would posses an inherent strength in their geometry. Some of the toolholders and carbide inserts are shown in Figs. 24 and 25. The basic design for 25 negative rake angle tools is shown in Fig.26 with the dimensions given in Appendix 1.

Twenty five discs made from high quality tool steel have been used for disc cutting experiments. Fig.27 shows the variations in diameter and edge angle which have been incorporated.

* * *

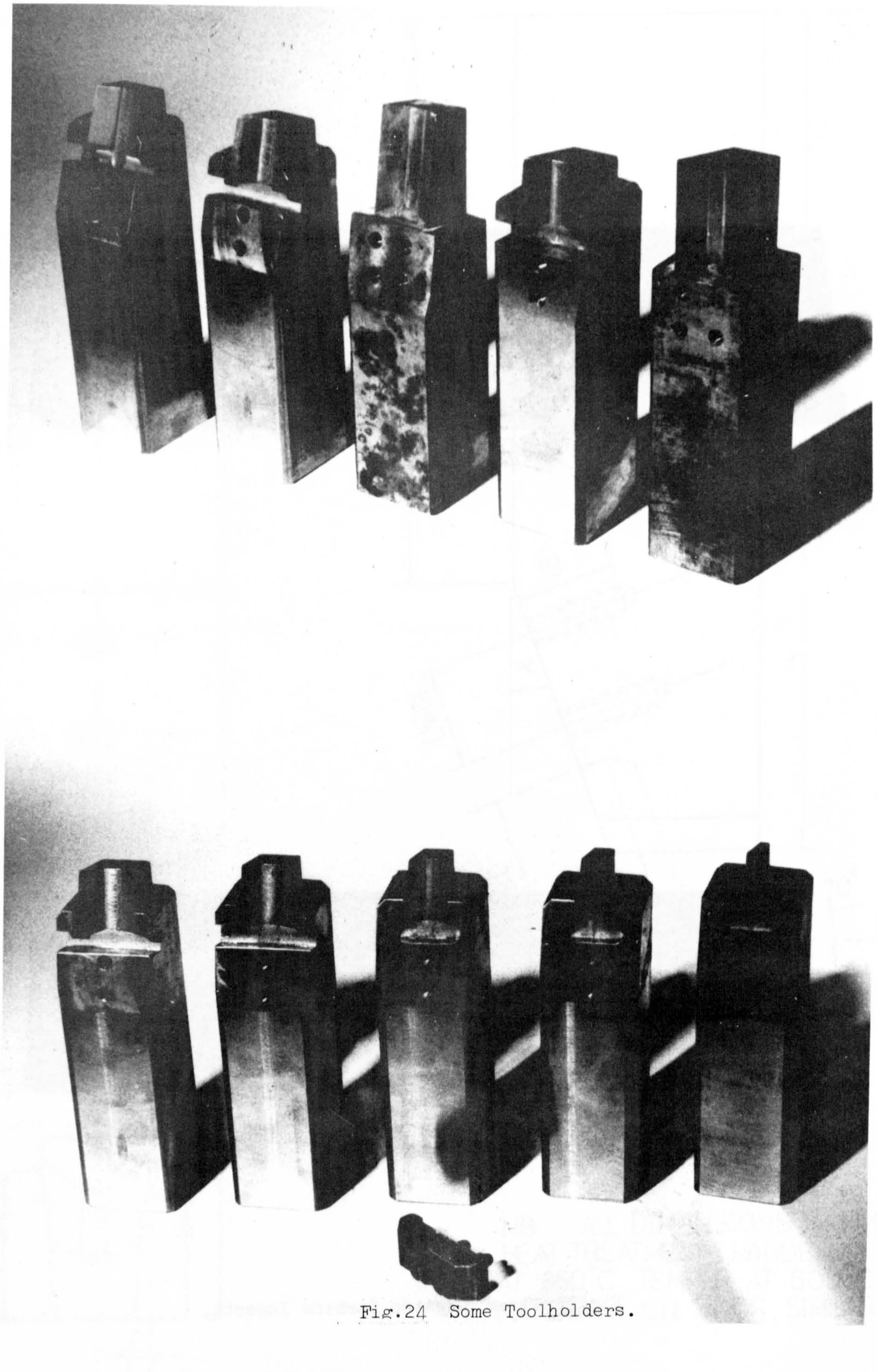

Fig.24 Some Toolholders.

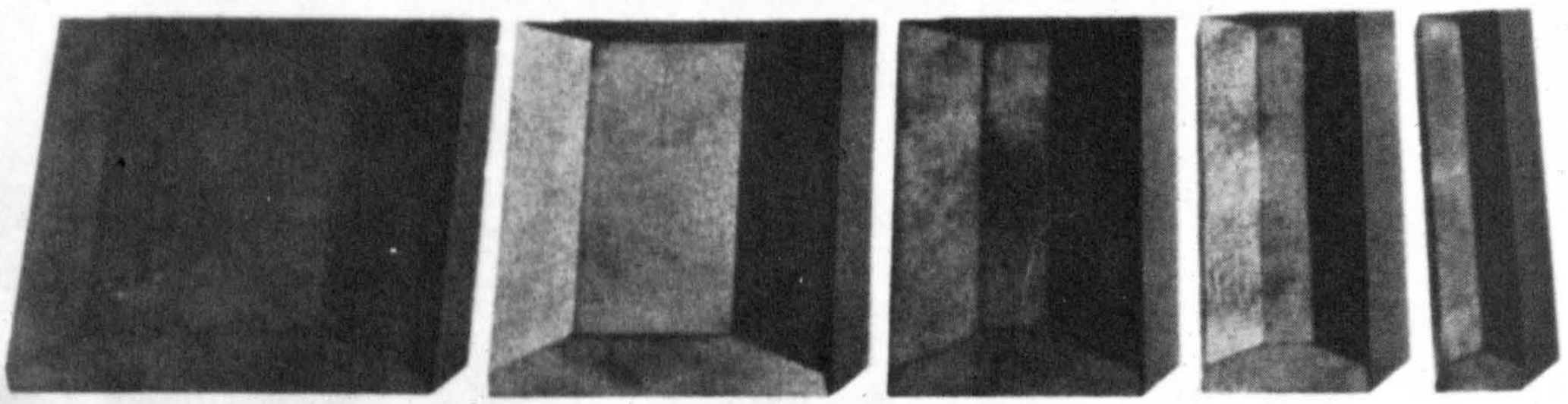

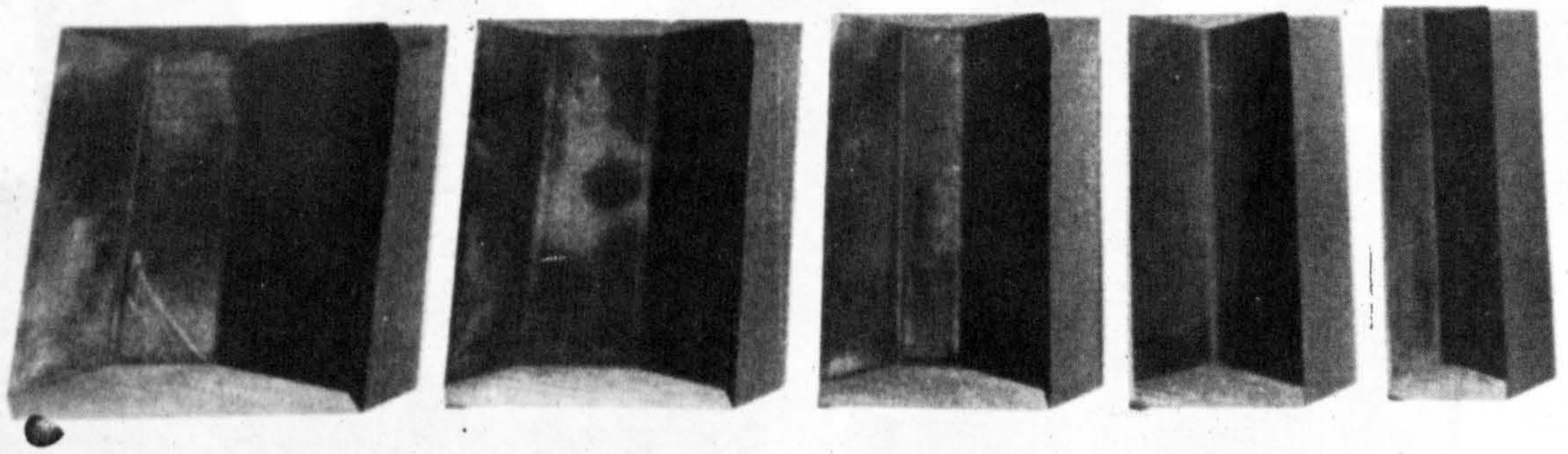

Fig.25 Some Tungsten Carbide Inserts.

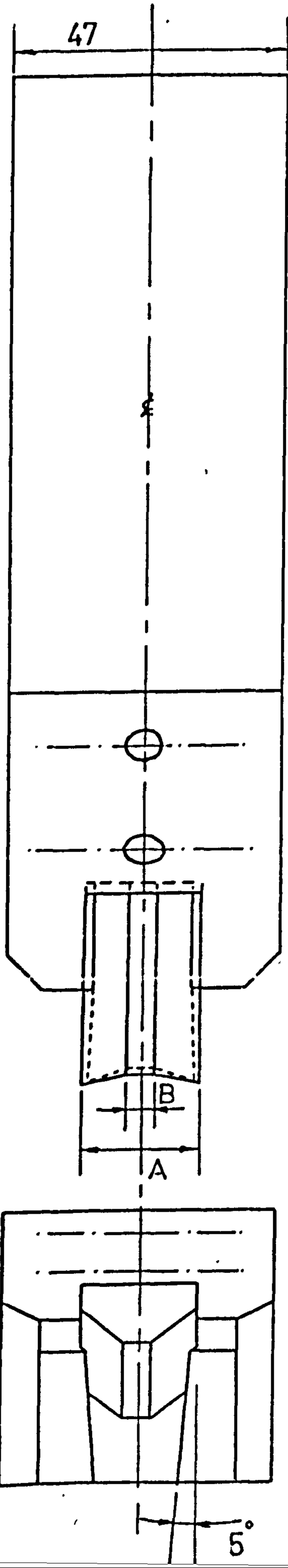

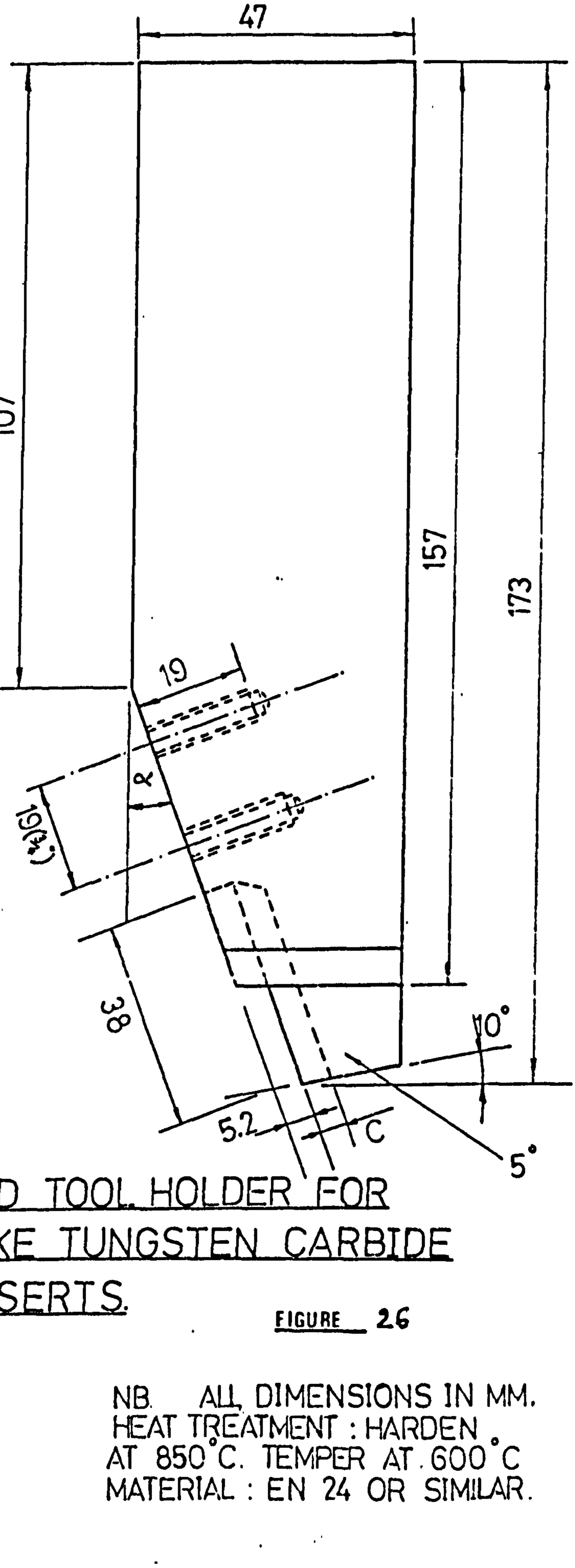

STANDARD TOOL HOLDER FOR -VE RAKE TUNGSTEN CARBIDE INSERTS.

FIGURE 26

NB. ALL DIMENSIONS IN MM.
HEAT TREATMENT : HARDEN AT 850°C. TEMPER AT 600°C
MATERIAL : EN 24 OR SIMILAR.

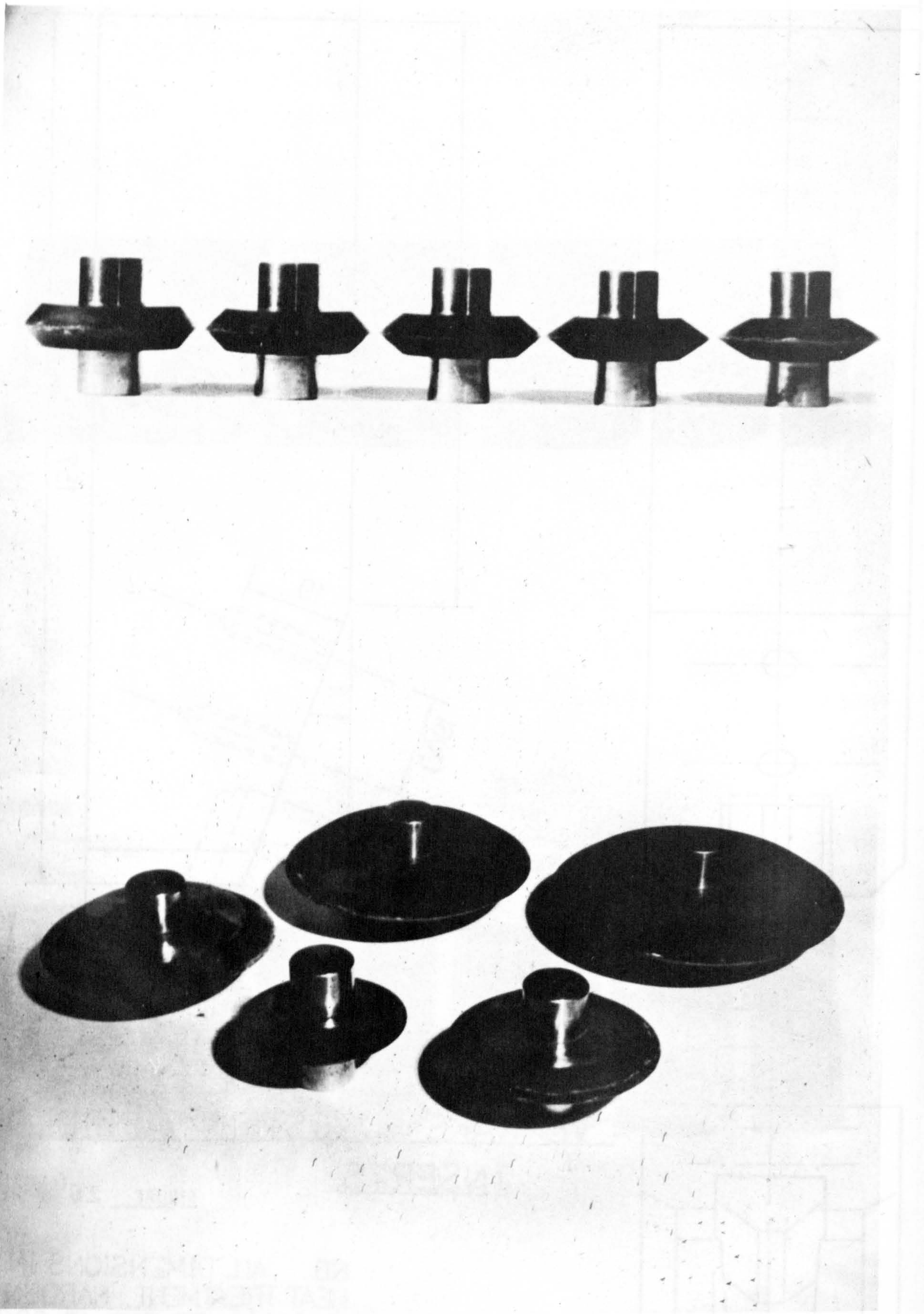

Fig.27 Some Experimental Discs.

CHAPTER SIX

MECHANICAL AND PHYSICAL PROPERTIES OF THE EXPERIMENTAL ROCKS

One of the objectives of this Thesis is to try and predict cutter performance from tool and rock properties. To this end, each rock which has been tested for its cutting properties has also been subjected to a wide range of physical tests. In this Chapter, each rock is described, as is each physical test, and the results are stated for future correlations with the cutting tests.

6.1 Description of Each Rock

Gypsum

Gypsum is widely distributed in the United Kingdom, occurring mainly in rocks of Permian and Triassic age in the East Midlands and Northern England[86]. Gypsum ($CaSO_4,2H_2O$) is a very important raw material for the building industry, being used principally in the manufacture of plaster and as retarder in portland cement. The samples were obtained from the British Gypsum mine, located at Sherburn in Elmet, Yorkshire. No quartz occurs in the rock.

Bunter Sandstone

The rock samples were obtained from Woolton Quarry of Liverpool Contractors Limited. Iron oxide is the predominant cementing material and accounts for the deep red colour. Quartz content is 82%. This rock has been used for one of the major projects for T.R.R.L. The mechanical and physical properties are fully described elsewhere[75].

Dunhouse Sandstone

Dunhouse Sandstone is a typical coal measures sandstone of a type that underlies several towns in the North of England. It is exploited at Dunhouse Quarry, near Bishop Auckland, Co. Durham, for use in the building industry. It is light yellow in colour, a fact reflecting the presence of limonite cement. The sphericity, roundness and the well sorted nature of the grains indicate a water-deposited marine environment. Quartz grains are 0.2mm in size, the content is 76%. This rock should be classified as a fine-grained sandstone.

Mansfield Sandstone

Samples have been taken from Mansfield where the rock is known as Mansfield Whitestone. Very thin, grey clay bands are found in the material in disoriented directions. It is cemented with a free quartz content of about 14%. Quartz grain size is 0.2mm. This rock would best be termed a siliceous dolomite.

Anhydrite

Anhydrite is used in the manufacture of sulphuric acid. The anhydrite ($CaSO_4$) belongs to St. Bees Evaporites of the Upper Permian in Cumberland and is best described by Arthurton and Hemingway[87]. The predominant colour is grey with red and white interstital filling. Usually termed nodulus Anhydrite, it contains whitish and relatively opaque nodules, mostly ovate with occasional pale interstital material. The samples were obtained from the Whitehaven mine of Laporte Industries.

Weardale Limestone

This is a dark grey chemically deposited Limestone. It does nct contain any quartz, consists almost totally of calcite-sparite, thin to moderately bedded, fine to medium christalline bands. Samples were obtained from a commercial quarry situated near Stanhcpe, where the rock reaches a thickness of 10m.

Creetown Granite

This is coarse-grained, igneous rock in which the feldspars are rather weathered. Apart from quartz and feldspar the other constituents include biotite, muscovite and opaques - magnetite. The quartz crystals have very irregular boundaries and this is typical of the last crystals to form. The quartz content is 38% with 1mm in grain size.

Greywacke

This is a very poorly sorted sediment with quartz, feldspar grains and rock fragments, cemented by a finer grain matrix. The quartz content of this rock is 32% with 0.35mm average in size. The samples were obtained from a commercial quarry located near Peebles.

* * *

6.2 Description of Each Test and Results

Uniaxial Compressive Strength

In order to compare the different rock types and the performance of the cutters in these rocks, tests must be carried out under standard conditions.

The cylindrical specimens of 41mm diameter, having a length to diameter ratio of 2, were tested under the nominal loading rate of 0.69 MN/m^2 per second. The samples were dried and dry steel platens were used throughout the experiments. The results are given in Table 6.

Table 6 Uniaxial Compressive Strength Values

Rock	No. of Tests	$\sigma c (MN/m^2) \pm$ s.d.
Gypsum	10	45.02 ± 5.9
Dunhouse Sandstone	10	55.84 ± 0.6
Mansfield Sandstone	10	71.30 ± 3.9
Anhydrite	10	112.91 ± 7.2
Weardale Limestone	10	127.25 ±16.9
Creetown Granite	10	179.10 ± 2.0
Greywacke	10	183.86 ±19.5

Uniaxial Tensile Strength

Measuring the tensile strength of the rocks is of extreme importance, because values are necessary in order to compare actual cutting results with Evans' Rock Cutting Theory[62]. The Brazilian Disc method was used for dry rocks. This tests consists of compressing a circular solid

disc to failure across a diameter. Discs were carefully prepared, having a diameter of 41mm and thickness of 20mm. A loading rate of 0.69 MN/m^2 was applied, using dry steel platens. The results are tabulated in Table 7.

Table 7 Tensile Strength Values

Rock	No. of Tests	$\sigma t (MN/m^2) \pm$ s.d.
Gypsum	10	2.75 ± 0.47
Dunhouse Sandstone	10	3.12 ± 0.10
Mansfield Sandstone	10	4.41 ± 0.01
Anhydrite	10	5.47 ± 0.99
Weardale Limestone	10	7.45 ± 1.55
Granite	10	10.77 ± 0.67
Greywacke	10	16.45 ± 2.18

Triaxial Strength

In the triaxial test an axial compressive load is applied by a testing machine while a lateral hydraulic pressure stresses the specimen uniformly. The rock specimen is enclosed in a rubber membrane which protects it from contact with the hydraulic fluid. For Gypsum, Dunhouse and Mansfield Sandstones a triaxial cell which will accommodate a cylindrical specimen of 150mm in length and 75mm in diameter was used. Load was applied to the specimen axially using a 100 ton Avery Testing Machine. A triaxial Hook Cell was bought to test the other rocks in order

to minimise the time necessary to complete each test. A 25 or 100 ton testing machine was used and rock specimens were of 30mm diameter and 60mm length.

The results have been plotted to produce the Mohr Envelopes shown in Fig.28. The levels of confining pressure and failure stress are given in Table 8.

Table 8 Triaxial Strength Values

	Rock		
	Gypsum	Dunhouse Sandstone	Mansfield Sandstone
	(a) (b)	(a) (b)	(a) (b)
a) Confining Pressure b) Failure stress in MN/m^2	0 - 35.6 3.4 - 61.2 6.9 - 75.4 10.3 - 80.3 13.8 - 82.7 20.7 - 101.3 34.5 - 124.1	0 - 54.5 3.4 - 80.3 6.9 - 116.3 13.8 - 114.7 20.6 - 175.0	0 - 53.0 3.4 - 78.0 6.9 - 101.5 13.8 - 144.7

	Rock							
	Anhydrite		Limestone		Granite		Greywacke	
	(a)	(b)	(a)	(b)	(a)	(b)	(a)	(b)
a) Confining pressure b) Failure stress in MN/m^2	0	113.9	0	127.3	0	179.10	0	185.2
	3.4	137.2	8.3	188.2	6.9	219.27	6.9	218.0
	10.3	170.4	13.8	220.7	13.8	289.90	13.8	242.2
	20.69	219.2	19.38	231.3	27.58	373.50	20.7	270.0
	27.58	250.4	31.14	287.9	41.38	417.30	27.58	285.0
	34.48	258.1	41.52	331.0	55.16	49 51	55.16	365.0
	55.16	311.1	55.36	376.9				

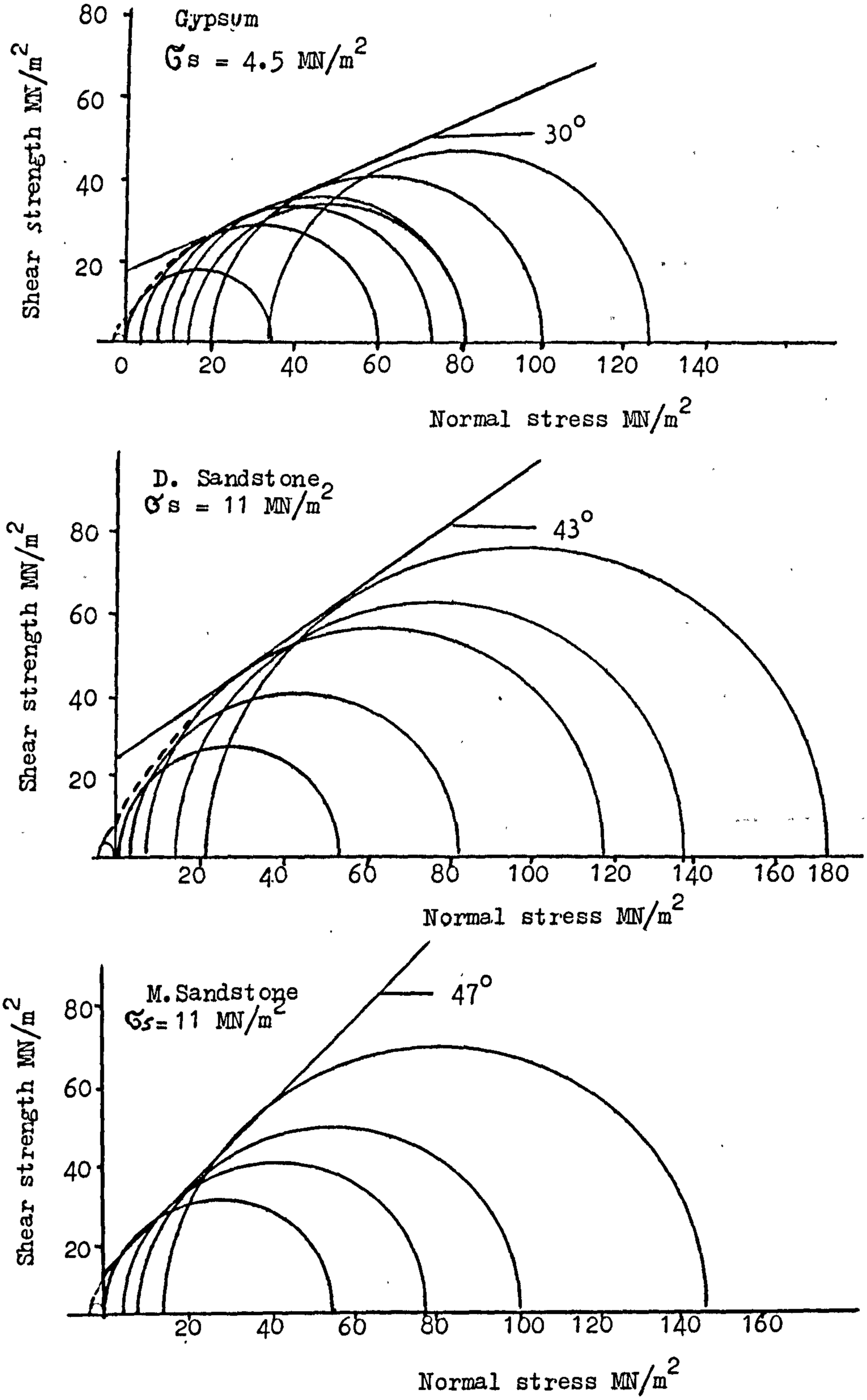

Fig.28A Mohr Envelopes for Experimental Rocks.

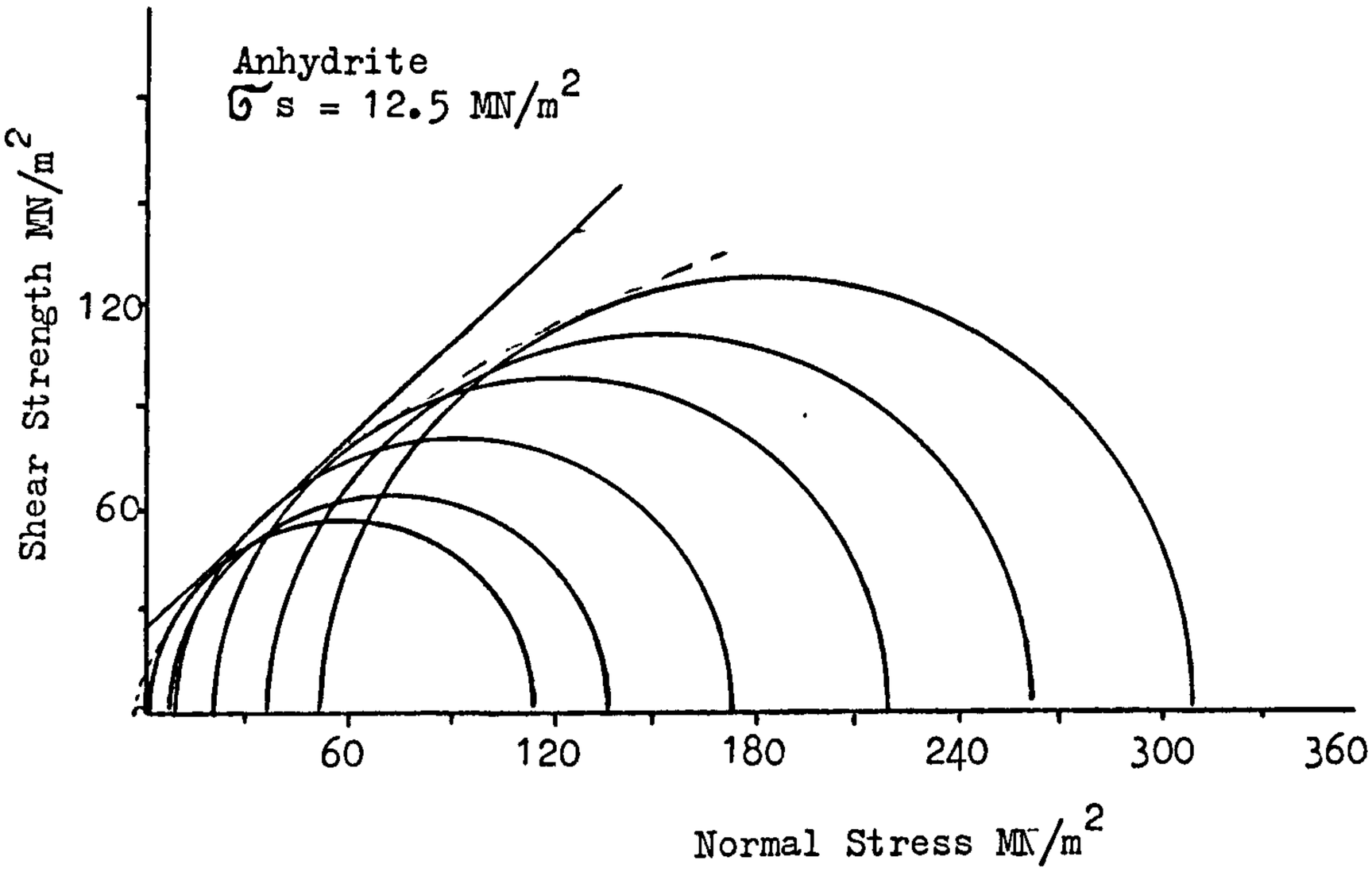

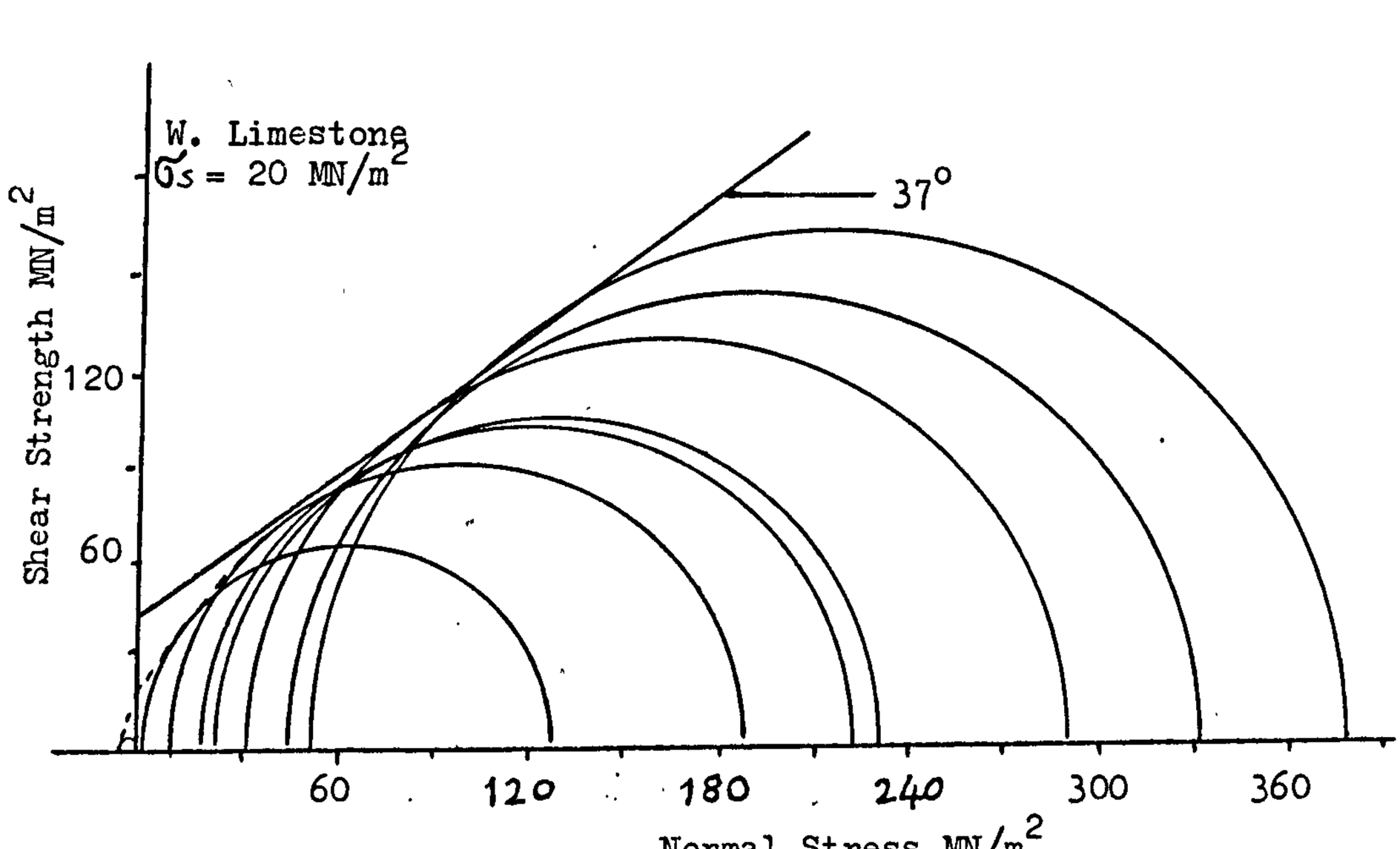

Fig.28B Mohr Envelopes for Experimental Rocks.

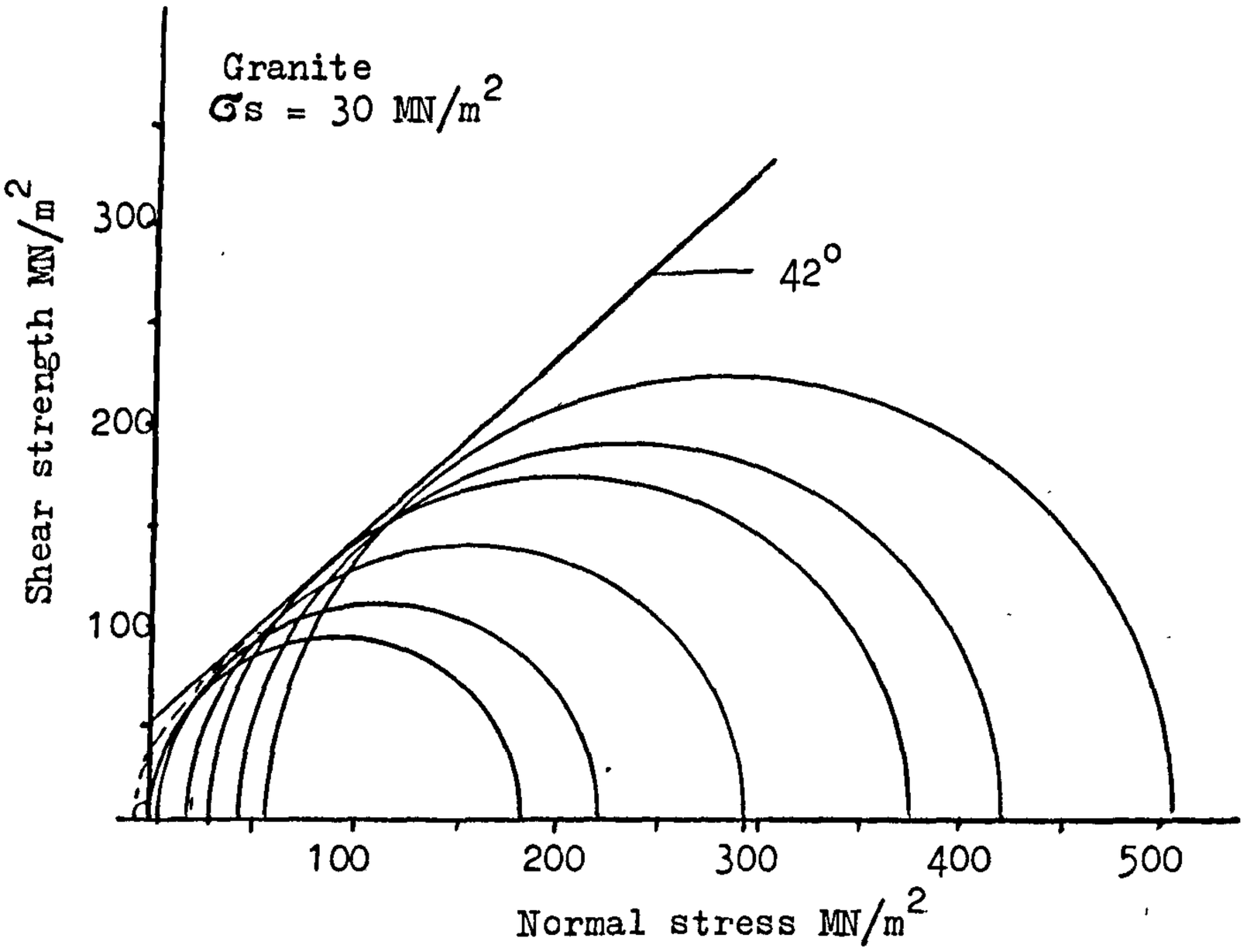

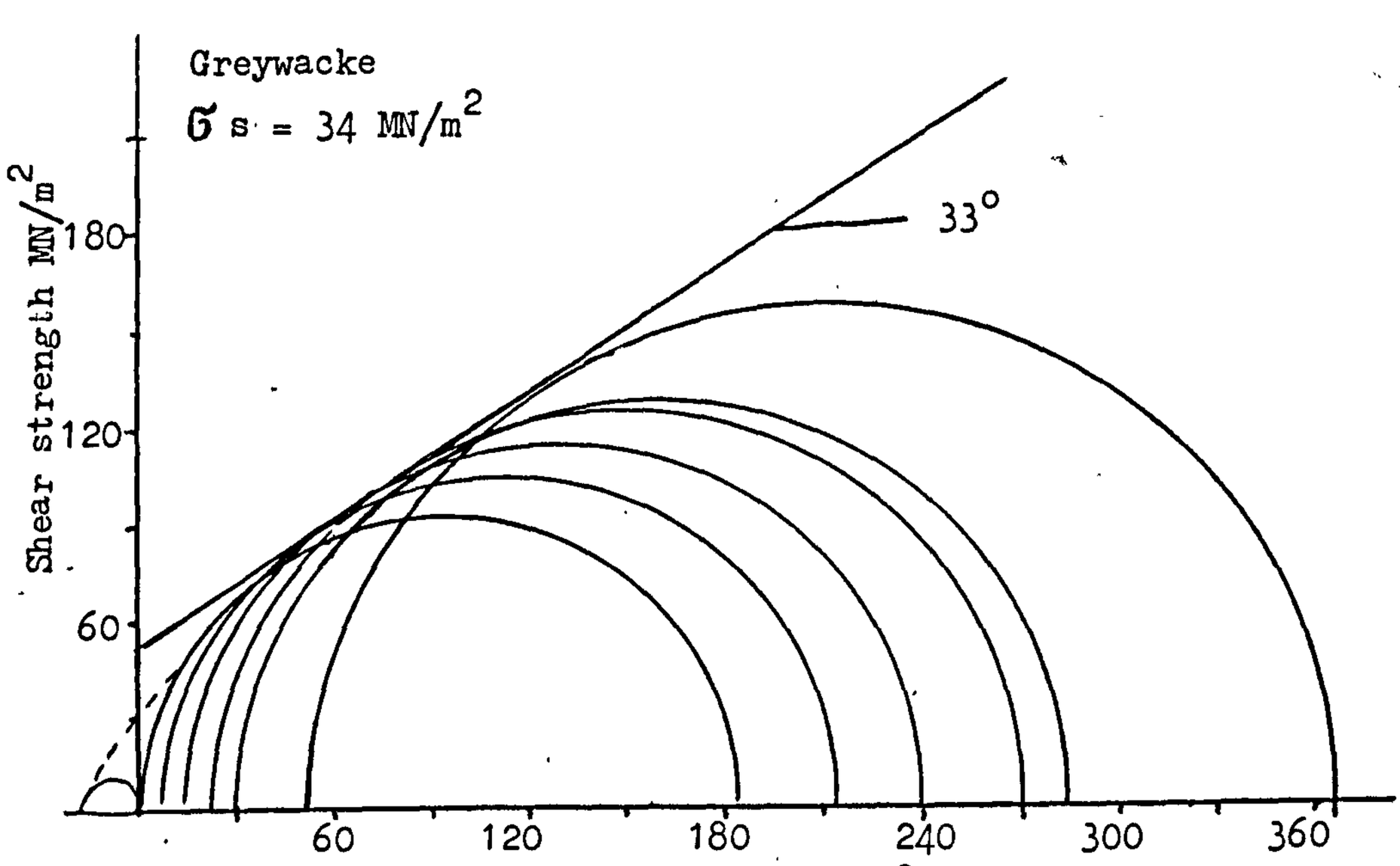

Fig. 28C Mohr Envelopes for Experimental Rocks.

Elastic Properties

The elasticity of the material is a measure of the resistance to deformation. For each rock the stress-strain relation in uniaxial compression up to failure load was recorded and the static elastic modulus was determined from the slope of the tangent drawn at 50% failure load.

Dynamic modulus was also measured for dry rock specimen using the laboratory's 'Pundit Sonic Testing Equipment'.

The elastic modulus values for each rock are calculated using the following formula. The results are given in Table 9.

$$ED = (V)^2 \times D \times 10^6$$

where

ED is Dynamic Young's Modulus in MN/m^2

V is wave velocity in m/s

D is Bulk Density of the Rock in Kg/m^3

Table 9 Elastic Modulus Values.

Rock	Static E. Modulus 10^4 MN/m^2	Dynamic E. Modulus 10^4 MN/m^2
Gypsum	5.0	4.26
Dunhouse Sandstone	1.2	1.25
Mansfield Sandstone	5.33	5.91
Anhydrite	10.95	10.35
Weardale Limestone	6.00	10.51
Granite	6.78	11.00
Greywacke	6.11	7.66

Sliding Friction

In order to understand the basic mechanism of cutting action of picks made of tungsten carbide and the discs made of hardened steel it is necessary to know how sliding friction changes from one rock to the other. A study has been made of the friction between hardened steel and tungsten carbide on the experimental rocks for different normal loads using elementary equipment. It is interesting to notice that the coefficient of friction for tungsten carbide is always higher than for hardened steel. The results are given in Table 10.

Table 10 Sliding Friction Values

Rock	Tungsten Carbide	Hardened Steel
Gypsum	0.960	0.900
Durhouse Sandstone	0.429	0.183
Mansfield Sandstone	0.321	0.169
Anhydrite	0.736	0.391
Weardale Limestone	0.633	0.432
Granite	0.393	0.266
Greywacke	0.436	0.200

Density and Porosity

Bulk Density was calculated using air-dried specimens at 100°C for one week. The same specimens were then immersed in water and placed in a vacuum pump which displaces all the air from the voids. Apparent

porosity of the rock was calculated by multiplying the moisture content by the dry bulk density. The results are given in Table 11.

Table 11 Density and Porosity Values

Rock	Bulk Density g/cc	Apparent Porosity %
Gypsum	2.26	0
Dunhouse Sandstone	2.19	11.83
Mansfield Sandstone	2.37	9.53
Anhydrite	2.92	0.20
Weardale Limestone	2.66	0.62
Granite	2.69	0.14
Greywacke	2.67	0.90

Indirect Rock Testing

Schmidt Rebound Number

The Schmidt Hammer was originally designed to test the compressive strength of concrete and it is successfully used for measuring rock strength in sites underground. The Schmidt Hammer is a portable hand operated device. The measurement is recorded by means of the rebounding mass and a pointer on a linear scale.

Miller has used the Schmidt Hammer to estimate uniaxial compressive strength and found that it was relatively insensitive to high strength

rocks and oversensitive to low strength rocks[88]. 'Type N' instrument is used throughout the tests and the results are illustrated in Table 12.

Table 12 Schmidt Hammer Values

Rock	Number of Tests	Schmidt Hammer Rebound Number ± s.d.
Gypsum	30	39.03 ± 3.58
Dunhouse Sandstone	30	47.23 ± 3.01
Mansfield Sandstone	30	40.43 ± 2.86
Anhydrite	30	49.80 ± 4.44
Weardale Limestone	30	60.20 ± 1.10
Granite	30	63.05 ± 2.18
Greywacke	30	56.43 ± 3.22

Shore Hardness

The test consists of dropping a diamond-tipped mass on the surface of the rock specimen. The mass is fitted into a vertical guide tube and set at a predetermined height; after striking the surface the mass rebounds and rebound values are measured on a graduated tube.

Since the presence of a large number of hard and non-hard crystals in the same material contributes highly difference hardness values, it is necessary to take a large number of readings. Local compacting of material during the test causes the rebound values to increase gradually and after a certain strike the values stay constant. An average of 30 readings were taken from each test point. The difference between the first reading and the average value gives the plasticity of the rock which

is calculated as follows[89]:

$$p = \frac{H30 - H1}{H30} \times 100$$

p is the coefficient of plasticity of rock

H1 is first Shore Hardness value

H30 is the average of 30 readings.

Shore Hardness and the plasticity of the experimental rocks are tabulated in Table 13.

Table 13 Shore Hardness and Plasticity Values

Rock	No. of Tests	Shore Hardness ± s.d.	Plasticity Coefficient ± s.d.
Gypsum	50	33.90 ± 3.80	16.9 ± 4.40
Dunhouse Sandstone	50	60.39 ± 3.66	28.15± 4.93
Mansfield Sandstone	50	53.54 ± 6.57	21.45± 8.72
Anhydrite	50	53.03 ± 9.74	18.26± 11.00
Weardale Limestone	50	76.95 ± 7.30	18.07± 6.70
Granite	50	88.14 ± 9.30	6.81± 3.90
Greywacke	50	69.50 ± 5.58	17.58± 5.00

Cone Indenter

The National Coal Board Cone Indenter was designed at M.R.D.E. to determine the resistance of the rock to indentation by a tungsten carbide

60° cone. The indenters can accommodate any small flat specimen up to 25 x 25 x 6mm. A standard load is applied to the tip and the hardness value is obtained by dividing the force by the amount of penetration which has occurred during the test. A modified load is applied when testing hard rock samples to modify cone indenter hardness. Details of the instrument and its use appear elsewhere[90]. Cone indenter values are given in Table.14.

Table 14. Cone Indenter Values

Rock	No. of Tests	Cone Indentor Hardness ± s.d.
Gypsum	10	1.39 ± 0.15
Dunhouse Sandstone	10	1.43 ± 0.02
Mansfield Sandstone	10	2.33 ± 0.68
Anhydrite	10	1.98 ± 0.23
Weardale Limestone	10	5.37 ± 0.36 (Im)
Granite	10	6.59 ± 2.54 (Im)
Greywacke	10	3.76 ± 13.60

Impact Strength Index (I.S.I.)

The test is similar to that described by Evans and Pomeroy[62]. The apparatus consists of a vertical steel cylinder of 4.45cm internal diameter. A steel plunger, which weighed 1.8kg fits loosely inside the hollow cylinder. The rock specimen of 100gm in the $\frac{3}{8}$ - $\frac{1}{8}$ inch size range is poured gently into I.S.I. apparatus. The plunger is dropped 20

times into the cylinder from the maximum height of 30.5cm. The dropping rate must not be faster than one per second. Finally the rock specimen is removed from the apparatus and sieved. The mass of rock in grams remaining on the $\frac{1}{8}$ inch sieve is the Impact Strength Index of the rock. The test results obtained for different rocks are tabulated in Table 15.

Table 15 I.S.I. Results

Rock	Number of Tests	I.S.I. ± s.d.
Gypsum	5	80.28 ± 0.94
Dunhouse Sandstone	5	50.70 ± 1.53
Mansfield Sandstone	5	71.04 ± 2.87
Anhydrite	5	75.16 ± 1.98
Weardale Limestone	5	79.88 ± 2.71
Granite	5	82.23 ± 1.20
Greywacke	5	87.95 ± 2.51

* * *

CHAPTER SEVEN

CUTTING ROCKS WITH DISCS

With ever rising labour costs mining engineers and underground civil engineers are looking at excavation systems to increase production. Research is being undertaken in Britain and elsewhere to create novel systems to improve the performance of the existing generation of excavation machines. The research described in this Chapter is concerned with discs for relieved and unrelieved cutting in a wide range of rocks. Discs are widely used as the primary excavation tool on full face tunnelling machines, but their application is hindered by lack of understanding of the fundamental breakage phenomena which govern their efficient use. This type of research is a logical extension of initial investigations into the efficiency of disc cutters[52,75], of the type undertaken in the Department of Mining Engineering of the University of Newcastle upon Tyne.

7.1 Experimental Programme

A partial factorial experimental technique developed by Protodyakonov and Teder has been used in these experiments. This technique was described in Chapter Four. Disc cutter parameters are defined in Fig.29.

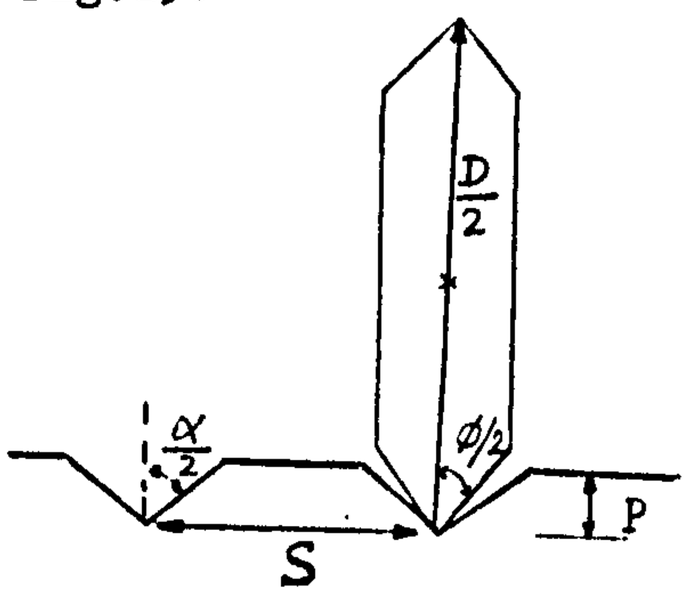

D = Disc Diameter

ϕ = Disc Edge Angle

α = Groove Angle

p = Disc Penetration

S = Spacing.

Fig. 29 Disc Cutting Parameters.

The effect of edge angle (ϕ) diameter of disc (D) and penetration (p) on the cutting performance of 25 different discs has been studied in four medium strength rocks. Similar experimental programmes in the Weardale Limestone and Greywacke caused damage to the more acute-angled discs and the partial factorial experiment was abandoned. The cutting speed did not show any significant effect on the cutting performance of discs in previous experiments[75] and so it was not included in these later investigations.

A constant cutting speed of 150mm/sec was used for these experiments and each of the 25 experimental levels was replicated four times. The experimental programmes carried out for Gypsum, Dunhouse Sandstone, Mansfield Sandstone, Anhydrite, Weardale Limestone and Greywacke are given below:

Table 16 Experimental Programme for Relieved and Unrelieved Cutting in Medium Strength Rocks.

Independent Variables	Levels				
Disc Diameter, D(mm)	100	125	150	175	200
Disc Edge Angle, ϕ (°)	60	70	80	90	100
Penetration, p(mm)					
in Gypsum & D.Sandstone	10	8	6	4	2
in Mansfield Sandstone	7.5	6	4.5	3	1.5
in Anhydrite	5	4	3	2	1
Spacing, S(mm)					
in Gypsum & D.Sandstone	12	24	36	48	60
in Mansfield Sandstone	9	18	27	36	45
in Anhydrite	6	12	18	24	30

Table 17 Experimental Programme for Relieved and Unrelieved Cutting in High Strength Rocks $\phi = 60^{\circ}$, D = 150mm

Rock	Penetration, p (mm)				
Weardale Limestone	1	3	4	5	7
Greywacke	1	3	4	5	
Rock	S/p				
Weardale Limestone (p = 3 and 7mm)	1	3	5	7	9
Greywacke					

The measured and calculated parameters obtained for each experimental cut are defined as follows:

(a) Mean Thrust Force, $\overline{FT}$ (kN)

The average force acting normal to the direction of cutting which maintains the disc at the required level of penetration.

(b) Mean Peak Thrust Force, F'T (kN)

The average of the peak forces acting as above.

(c) Mean Rolling Force, $\overline{FR}$ (kN)

The average force on the disc in the direction of cutting which causes the disc to roll at the required level of penetration.

(d) Mean Peak Rolling Force, F'R (kN)

The average of the peak forces acting on the tool in the direction of cutting.

(e) Yield, Q (m^3/km)

The volume of rock excavated by the disc per unit distance travelled.

(f) Rolling Specific Energy, SE (MJ/m^3)

The work done per unit volume of each cut.

$$SE = \frac{\text{Mean Rolling Force}}{\text{Yield}}$$

(g) Coarseness Index (C.I.)

Coarseness Index is a non-dimensional number used for the comparison of debris size and is the sum of the cumulative weight percentages retained in each sieve during the analysis of the debris. The value depends upon the size of sieves used. The sieves used in these experiments have the following specifications: 25mm, 8mm, 8 mesh, 130 mesh, 120 mesh. Note that the maximum possible value for 6 size fractions is 600, corresponding to all material being larger than 25mm. Similarly the minimum value must be 100, corresponding to all material being - 120 mesh.

* * *

7.2 Results of Unrelieved Cutting Experiments

All the experimental data is given in Appendices 2 - 6.

Effect of Penetration

Thrust and rolling forces, as shown in Fig.30, increased rapidly with penetration. Thrust/Rolling Force ratios are a function of penetration (Fig.31), having a value of 10-13 for shallow cuts and 5-4 for deep cuts. For each experimental rock, yield increase was approximately proportional to the square of the penetration (Fig.32). The improvement in cutting efficiency, as seen from Fig.33, is most pronounced over the first few levels of p and, although this improvement continues, the rate does fall at higher penetrations. Figs.33, 37 and 40 show that the only experimental variable which affects the coarseness index is the penetration. It was observed that all grooves excavated by a single disc cutter are approximately triangular so the groove angle α is related to yield by the equation

$$Q = p^2 \tan \frac{\alpha}{2} \qquad ---(6)$$

The groove angle α was calculated for each level of penetration and experimental rock.

As it can be seen from Table 18, α is independent of p.

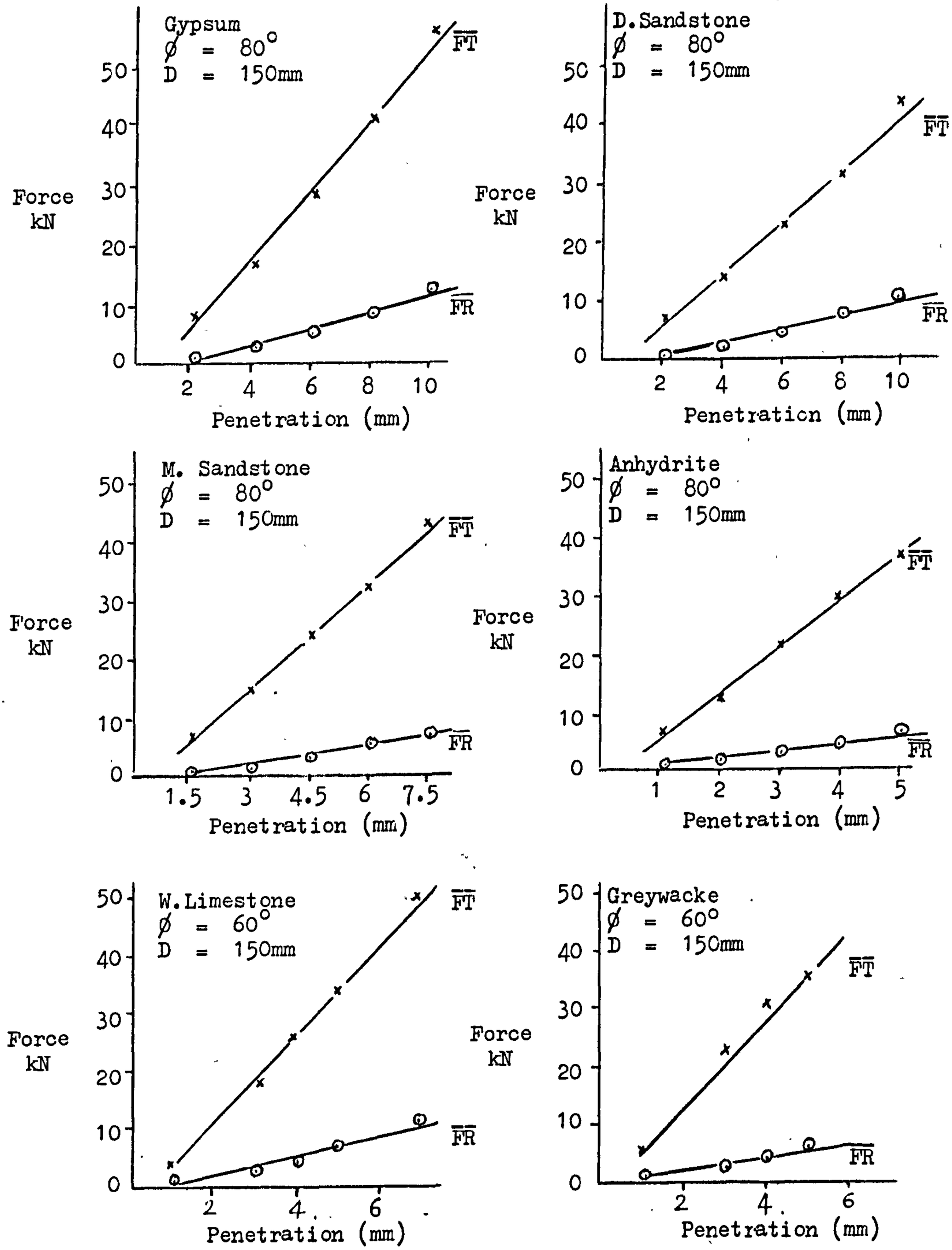

Fig.30 Variation in Disc Forces with Penetration.

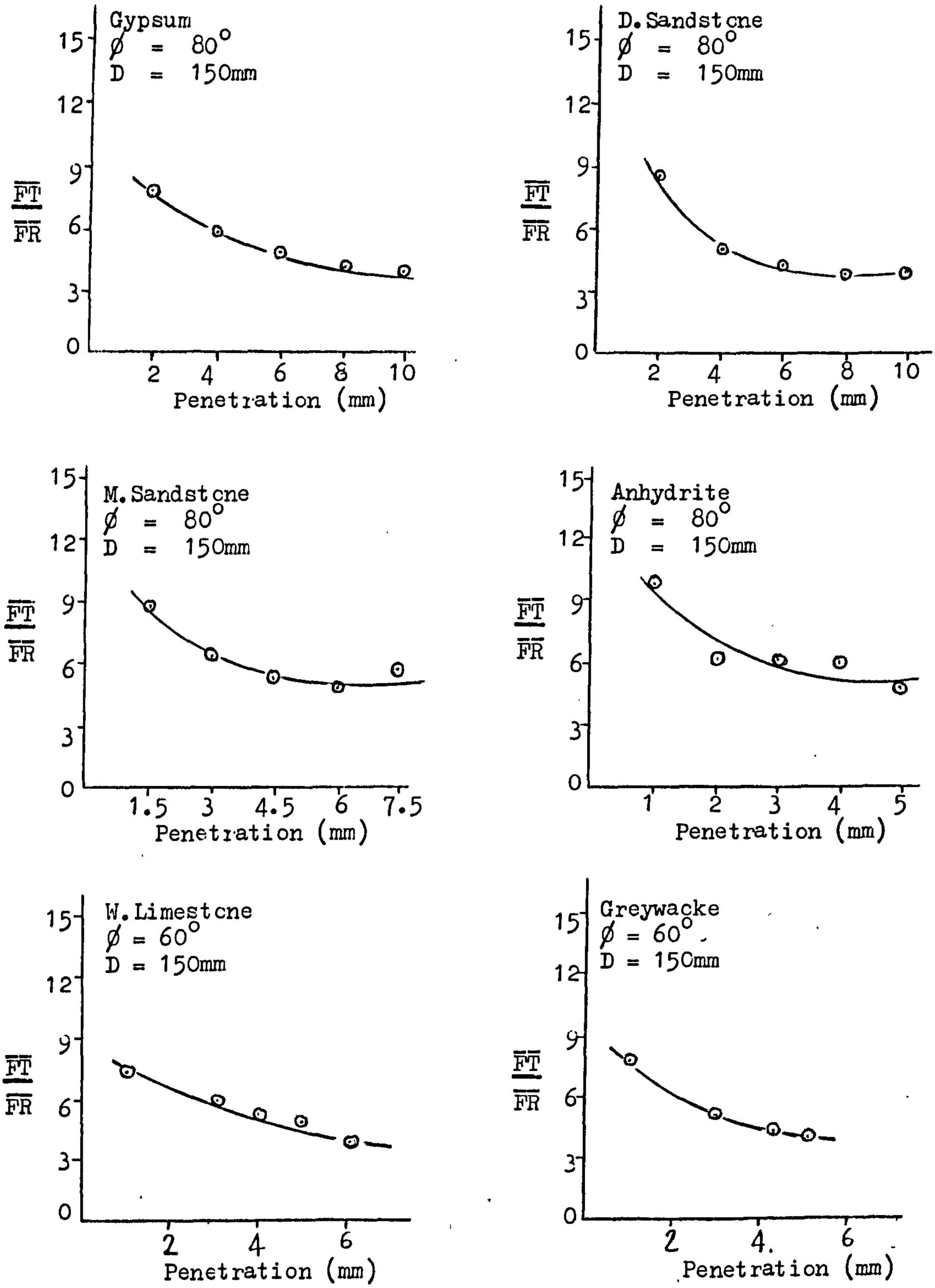

Fig.31. Variation in $\frac{\overline{FT}}{\overline{FR}}$ Ratios with Penetration.

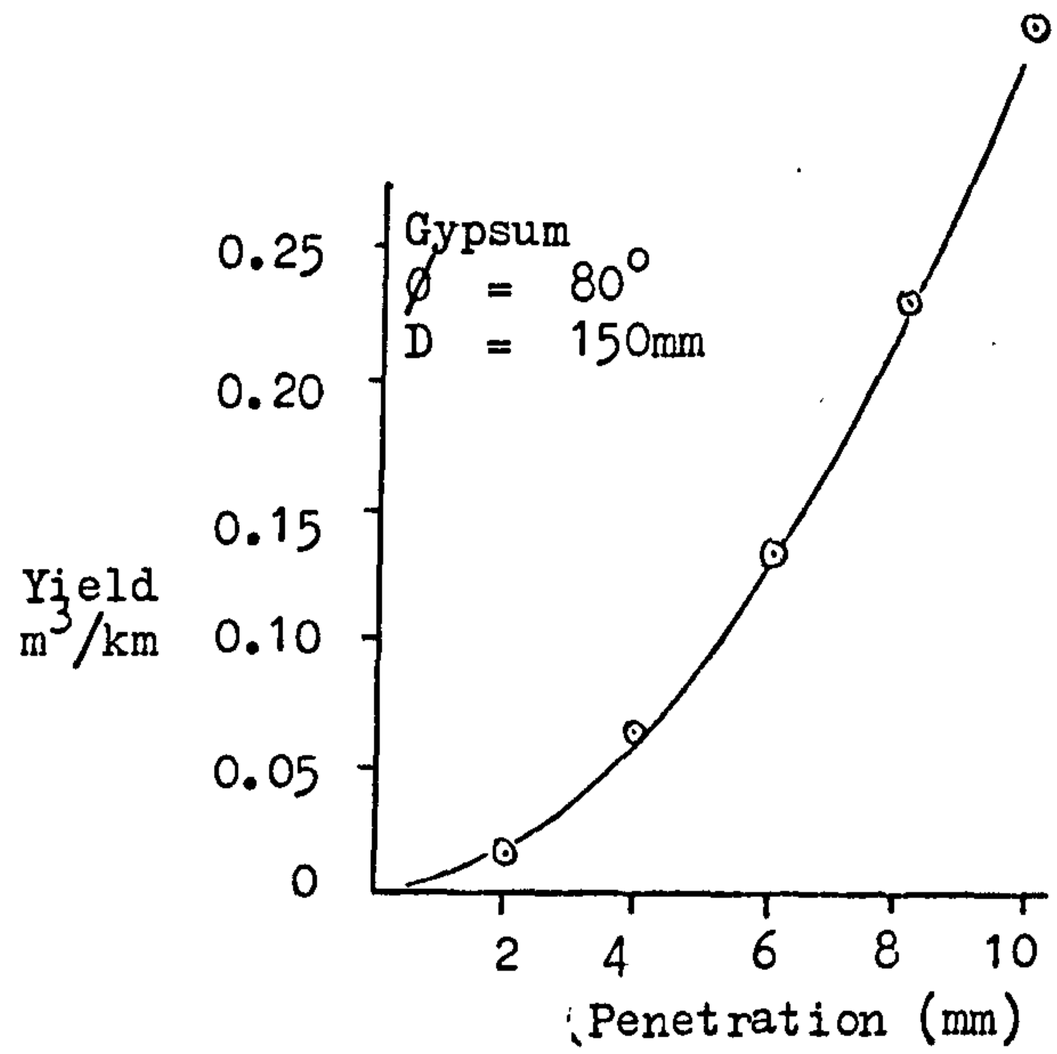

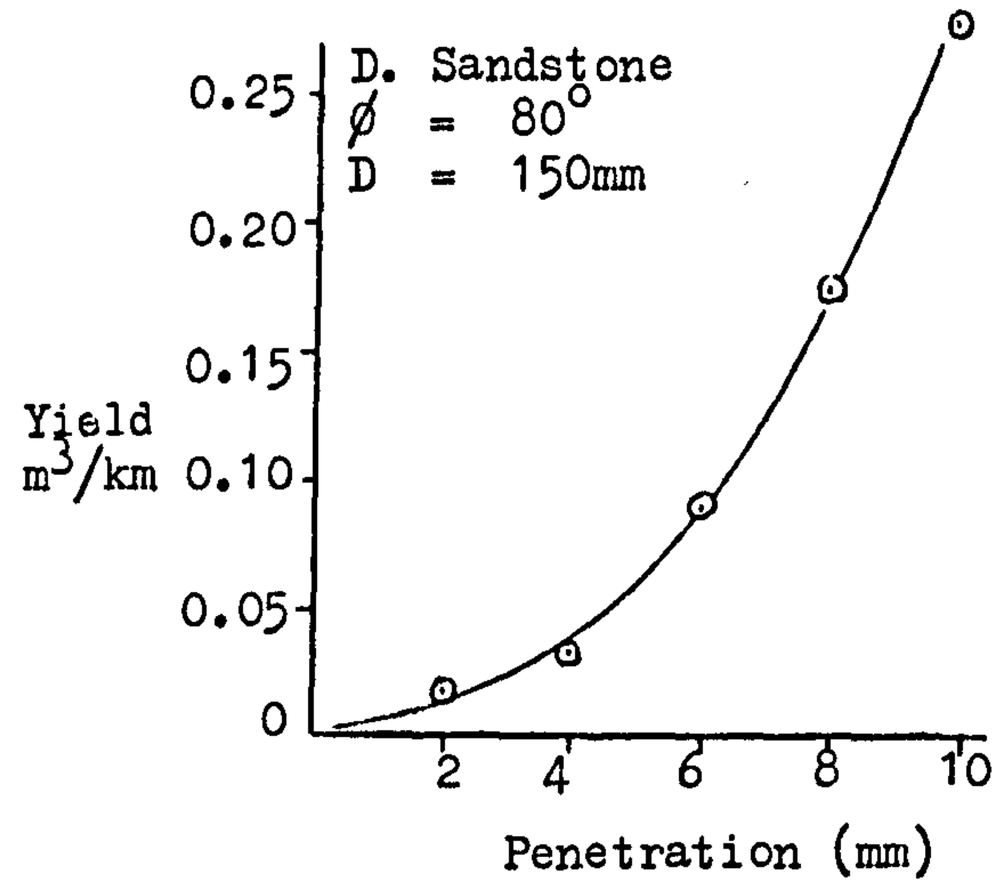

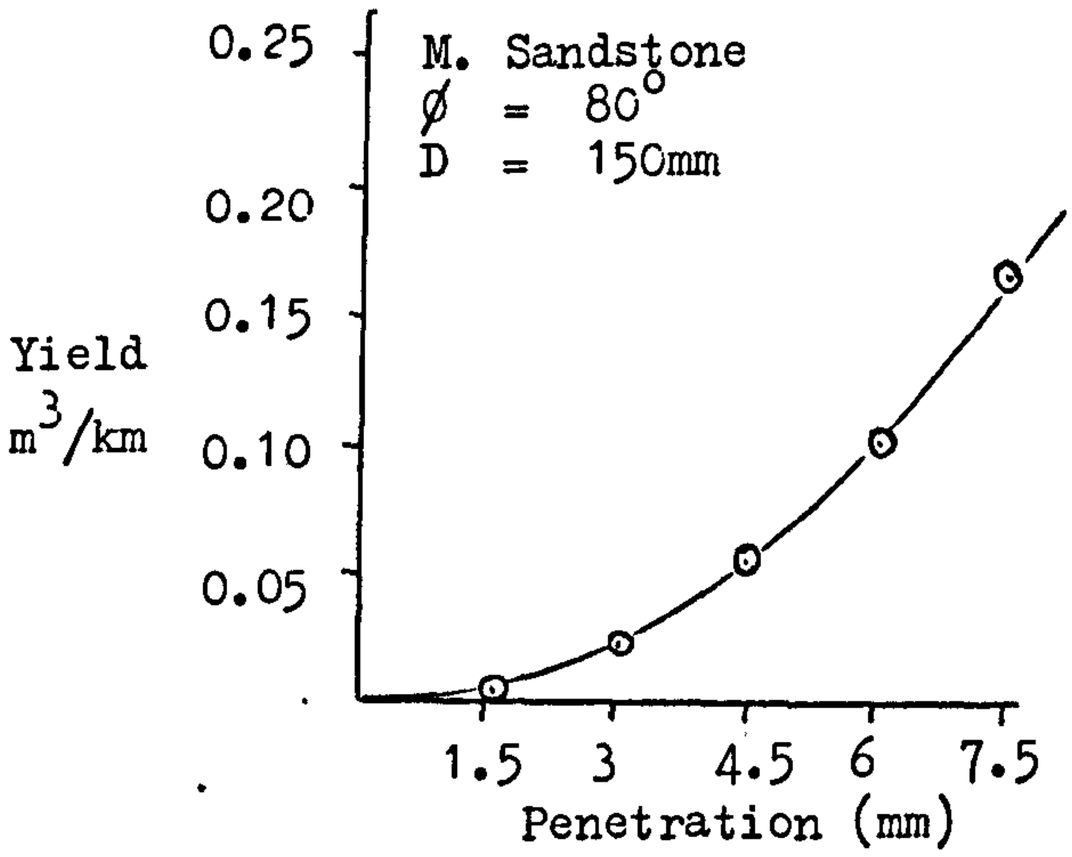

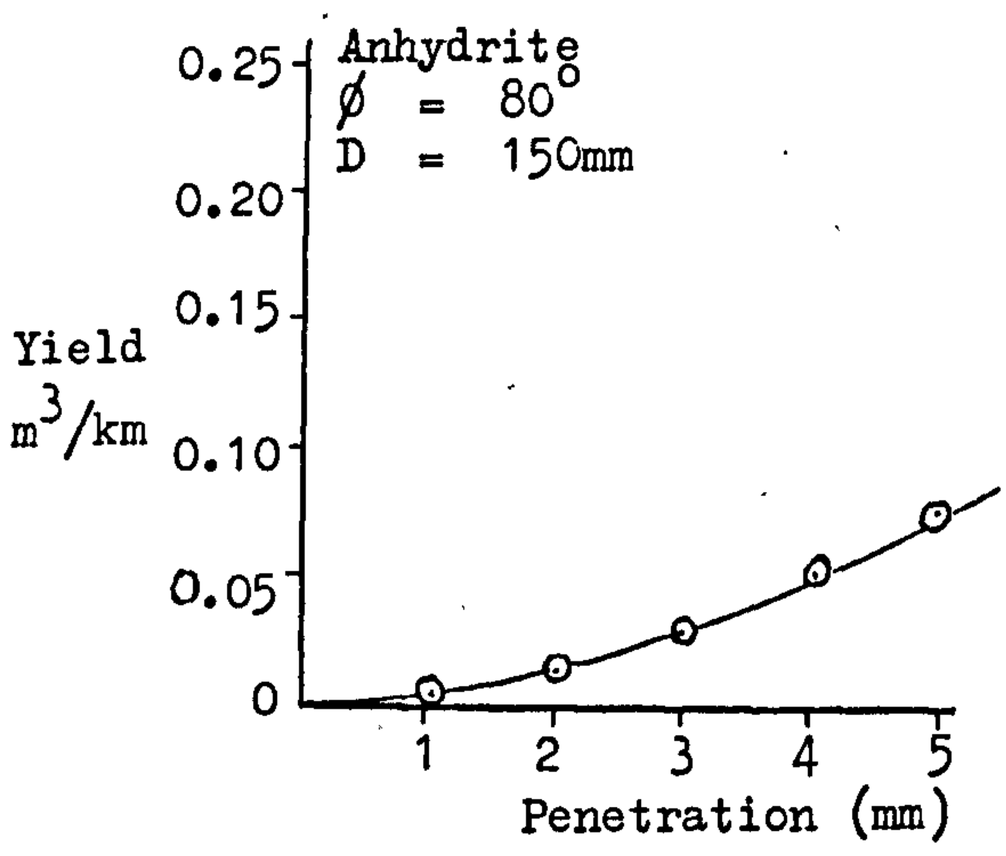

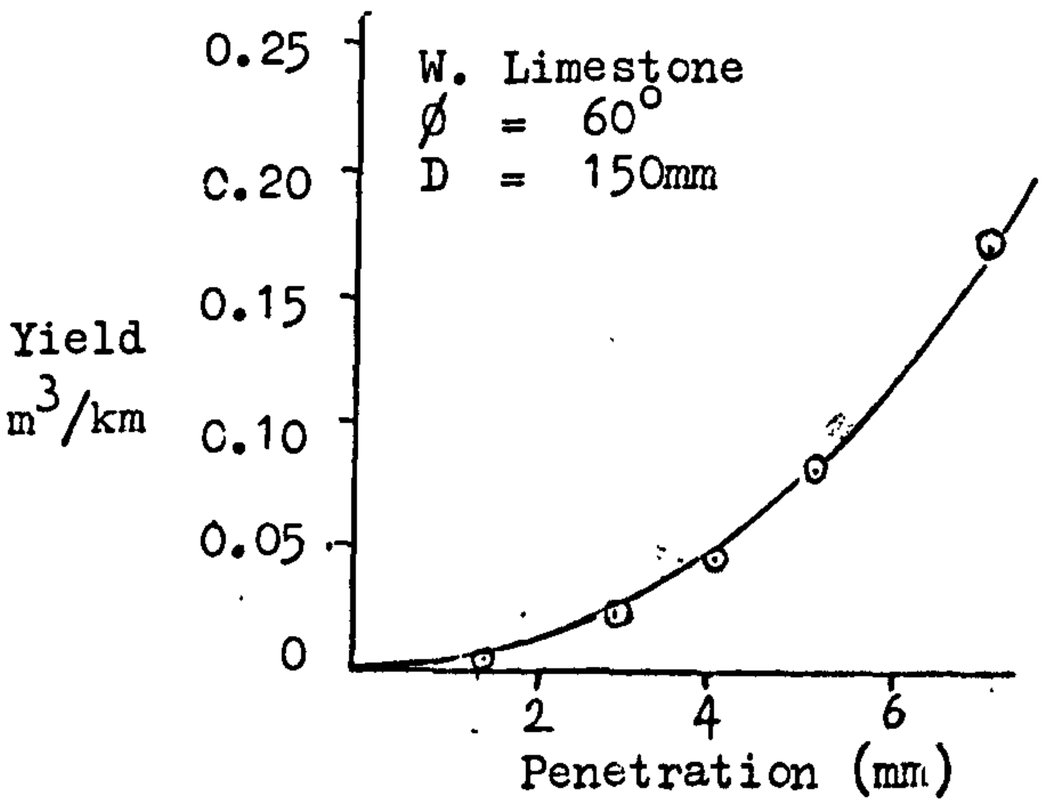

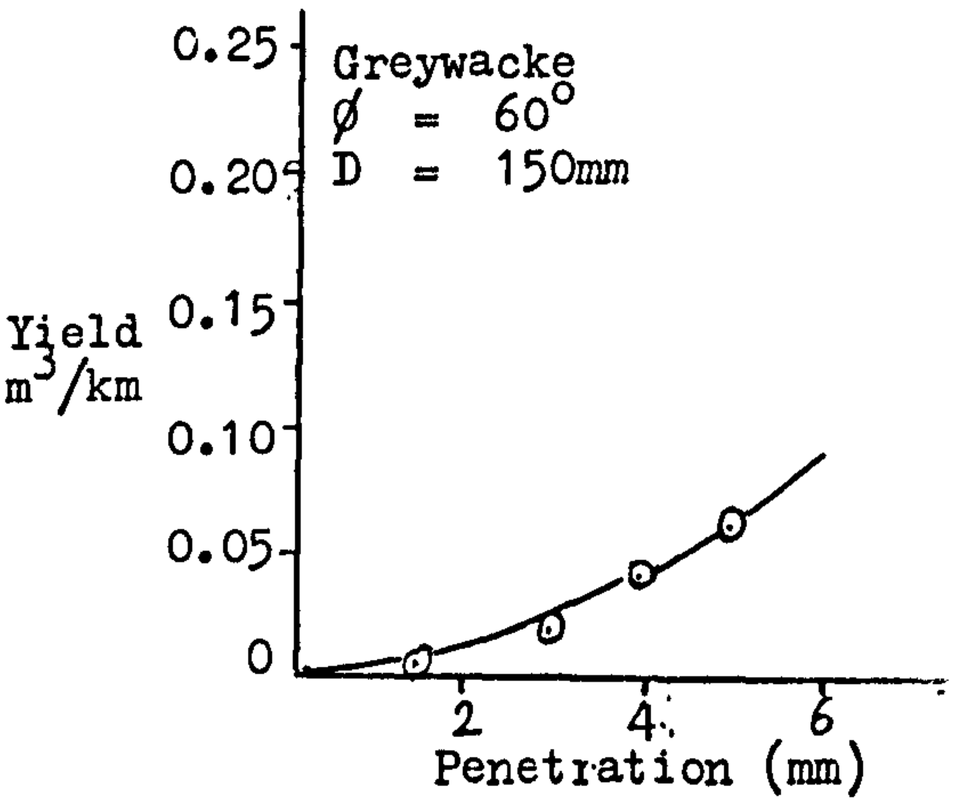

Fig.32 Variation in Yield with Disc Penetration.

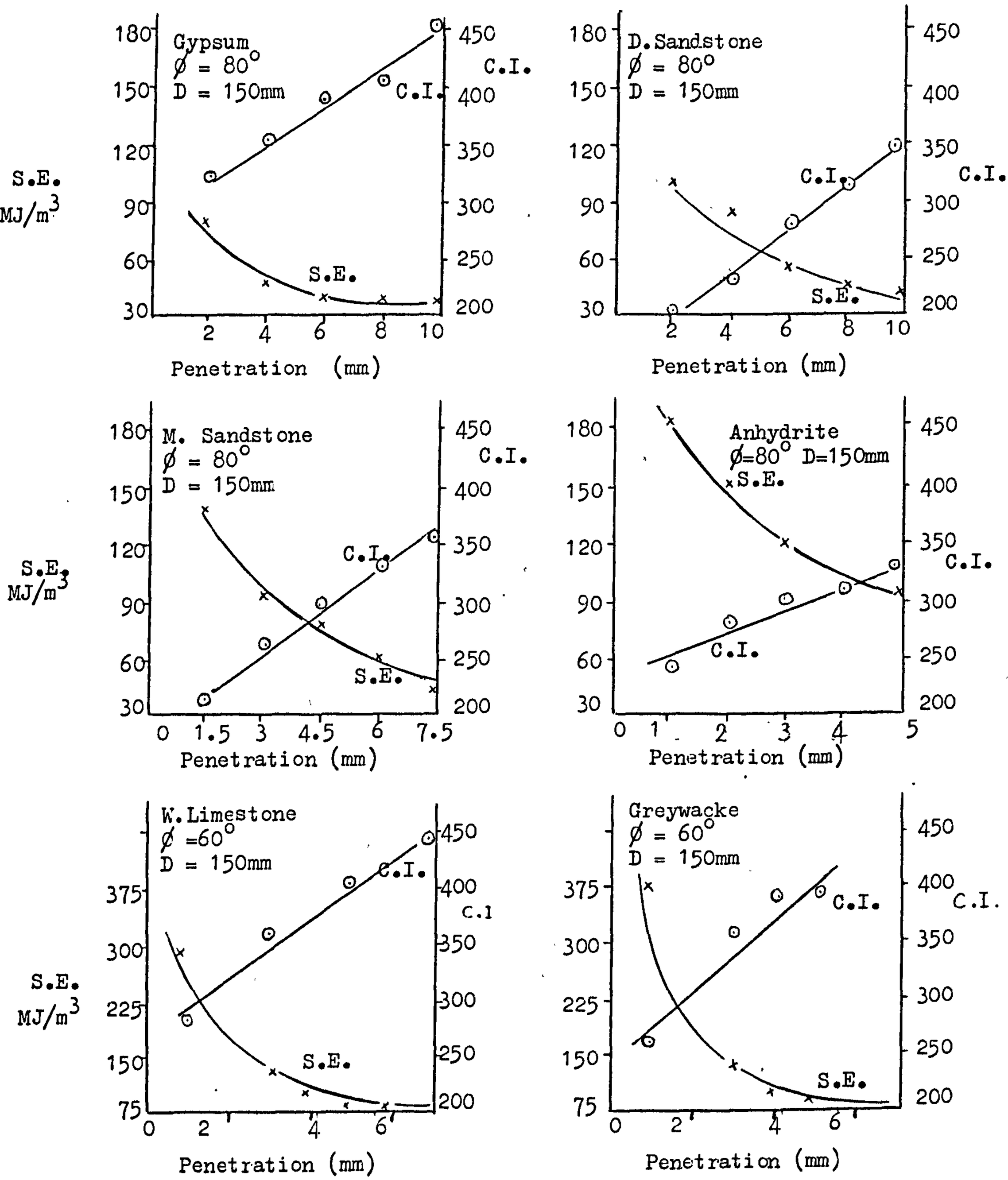

Fig.33. Variation in Specific Energy and Coarseness Index with Disc Penetration.

Table 18. Groove angle for different levels of penetration at mean level of disc diameter and edge angle.

p (mm)	Gypsum (α°)	Dunhouse Sandstone (α°)	p (mm)	Mansfield Sandstone (α°)	p (mm)	Anhydrite (α°)	p (mm)	Weardale Limestone (α°)	Greywacke (α°)
2	143.1	138.2	1.5	136.1	1	151.0	1	119.0	120.0
4	149.0	128.9	3.0	139.1	2	146.5	3	140.2	136.5
6	148.4	126.3	4.5	138.4	3	143.6	4	142.0	139.1
8	147.4	132.6	6.0	142.1	4	144.2	5	148.2	133.1
10	146.7	139.7	7.5	142.7	5	142.3	7	145.9	-

Note that for 1mm of penetration the breakout angle in Weardale Limestone and Greywacke is small if compared to higher penetrations. This angle does nct represent the real breakout angle, since, rather than chip formation, crushing probably occurs because the depth of cut is of similar magnitude to the grain size of the rock.

Effect of Edge Angle

Fig.34 shows that both thrust and rolling forces increase linearly with edge angle in all rocks. Thrust/Rolling force ratios are independent of disc edge angle (Fig.35). Although edge angle appears to have no effect on yield for Dunhcuse Sandstone and Anhydrite, as demonstrated in Fig.36, there is a significant increase in yield for Mansfield Sandstone and Gypsum This fact is reflected in the groove angles, which are tabulated below at mean level of penetration and disc diameter. As it can be easily seen from Table 19, groove angle increases with disc edge angle in Gypsum and Mansfield Sandstone.

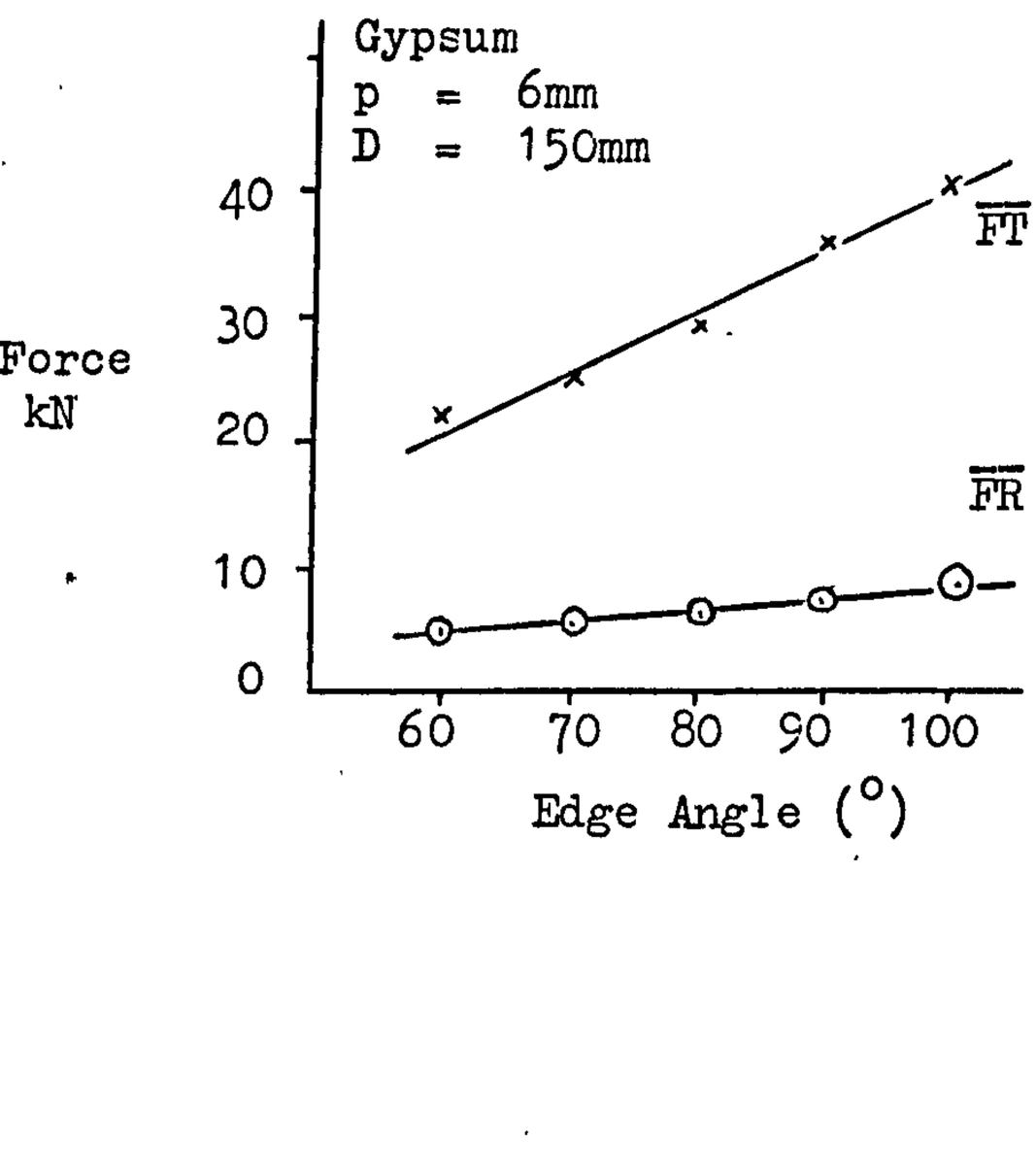

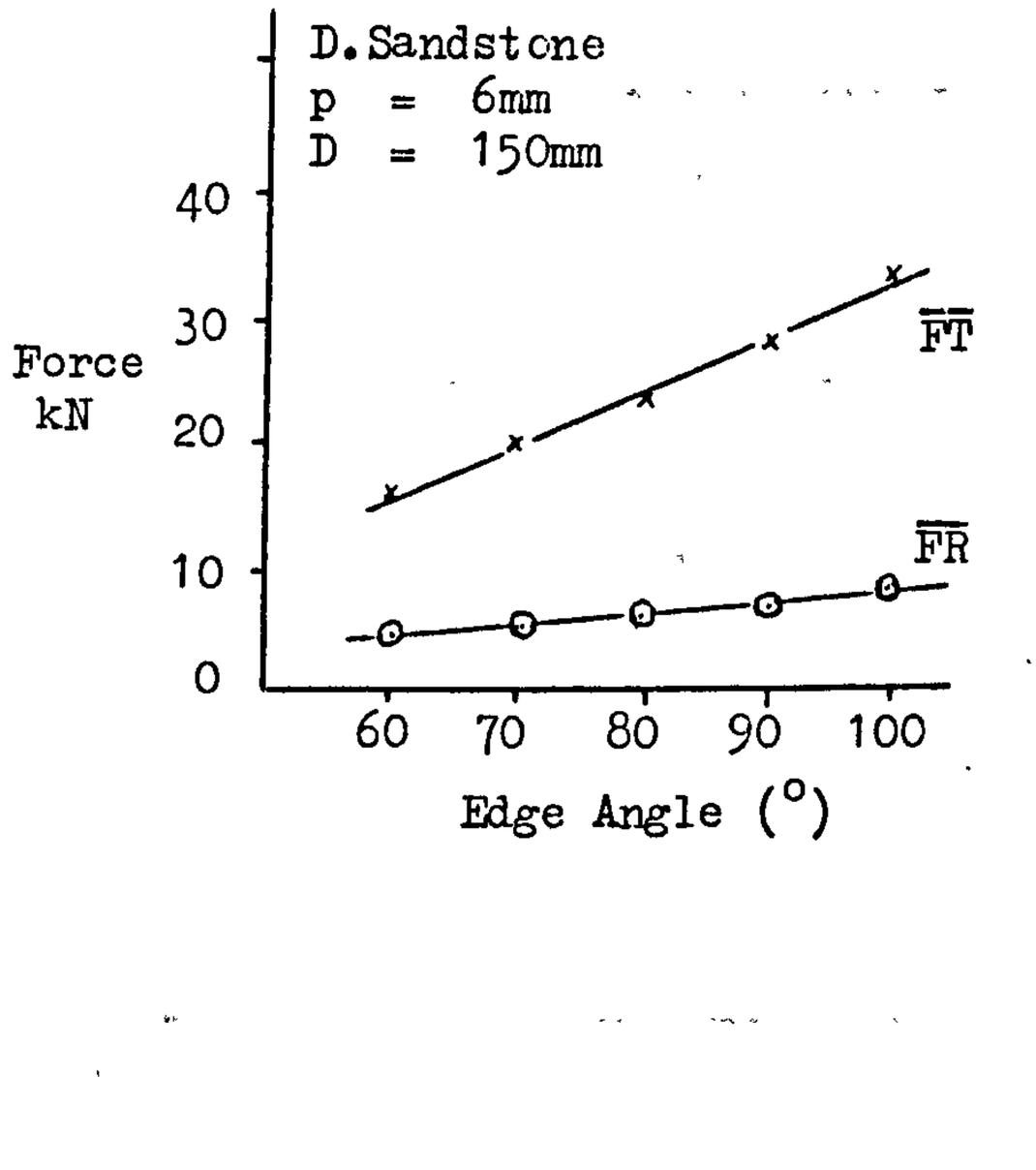

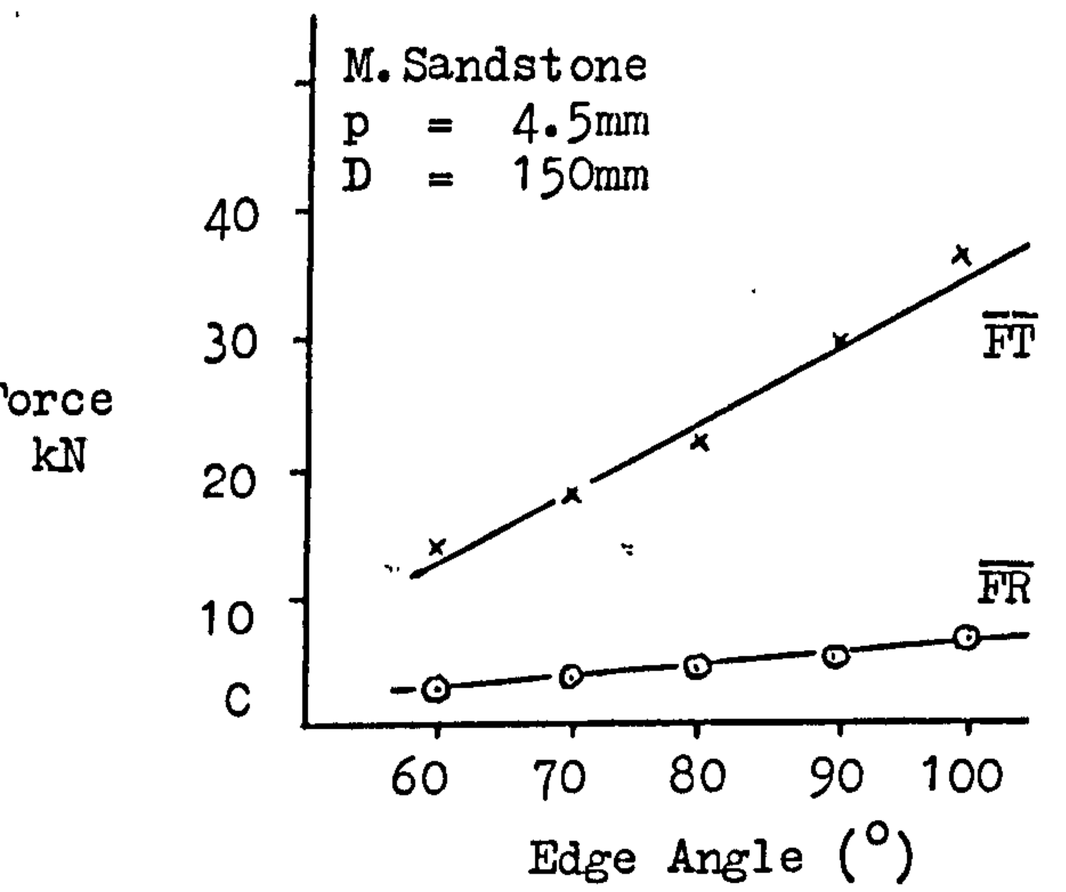

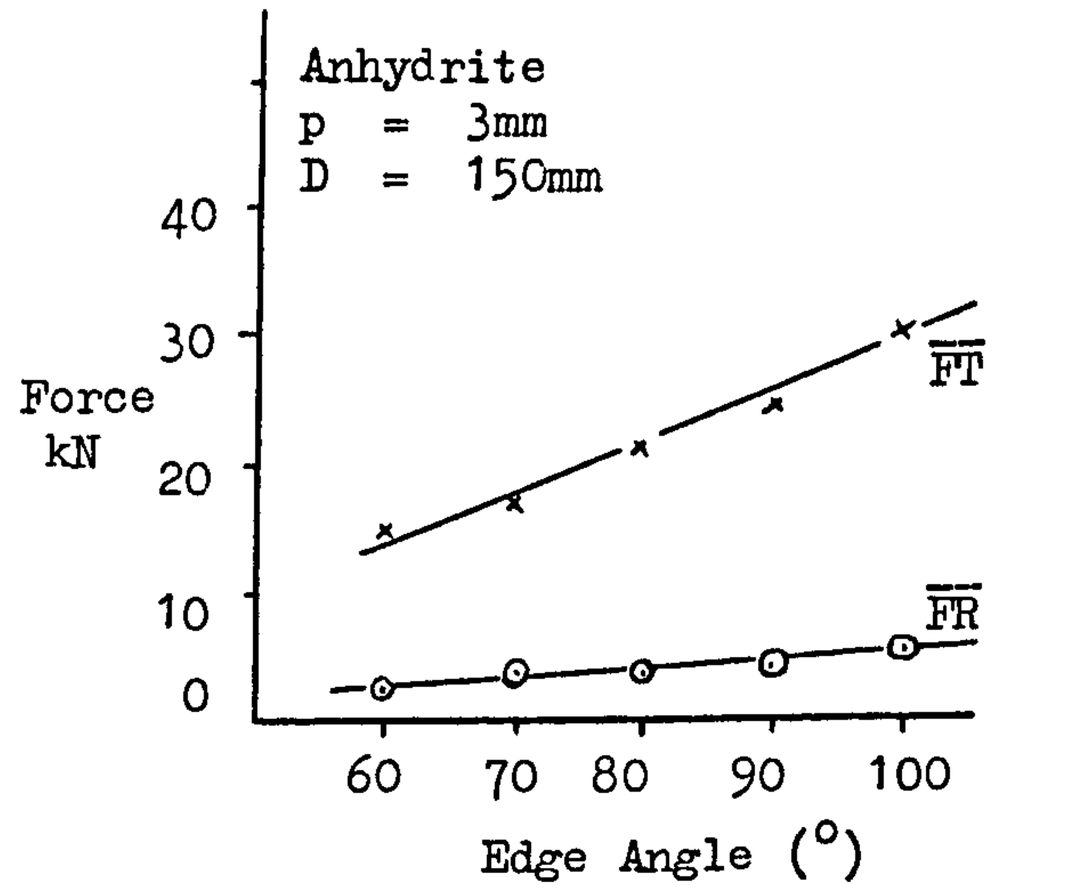

Fig.34 Variation in Disc Forces with Edge Angle.

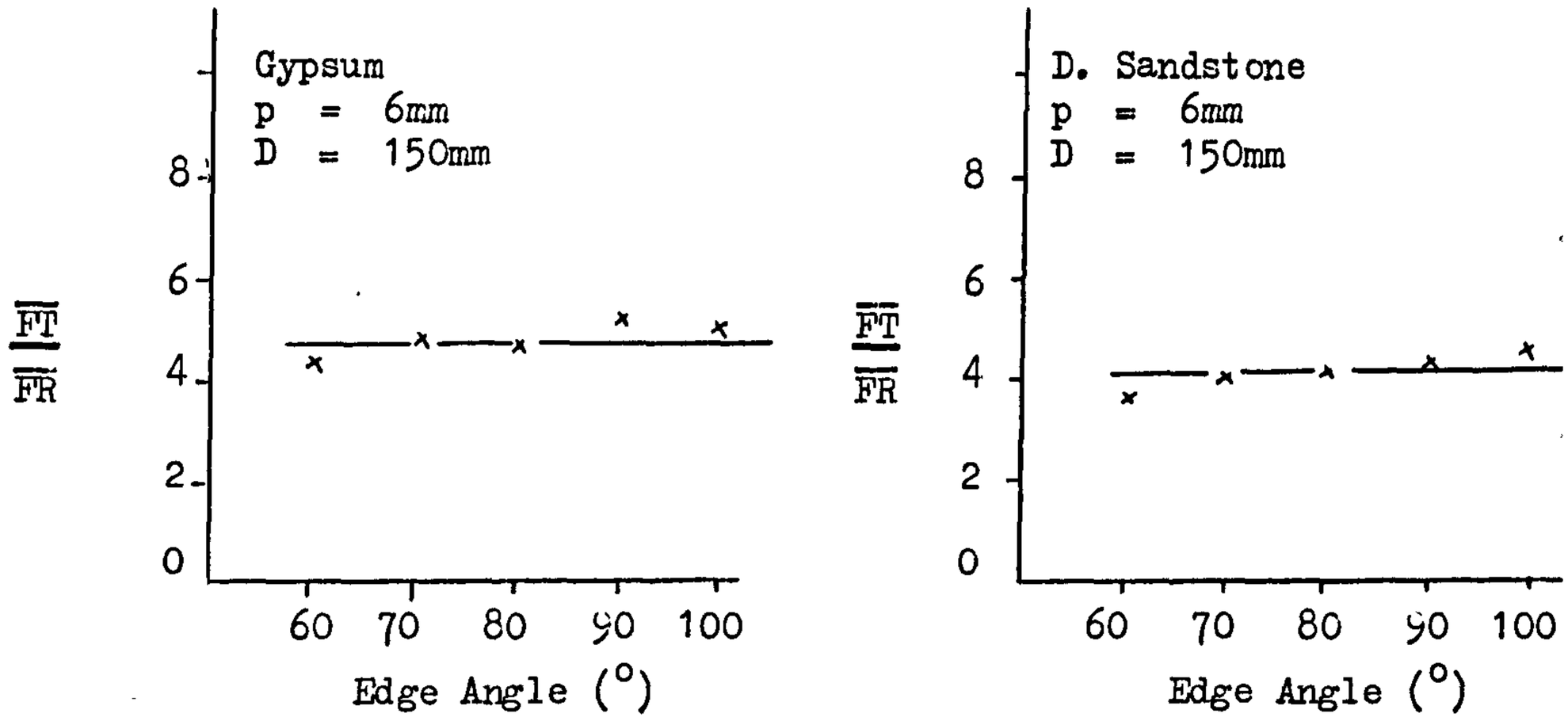

Fig.35 Variation in $\frac{\overline{FT}}{\overline{FR}}$ Ratios with Edge Angle.

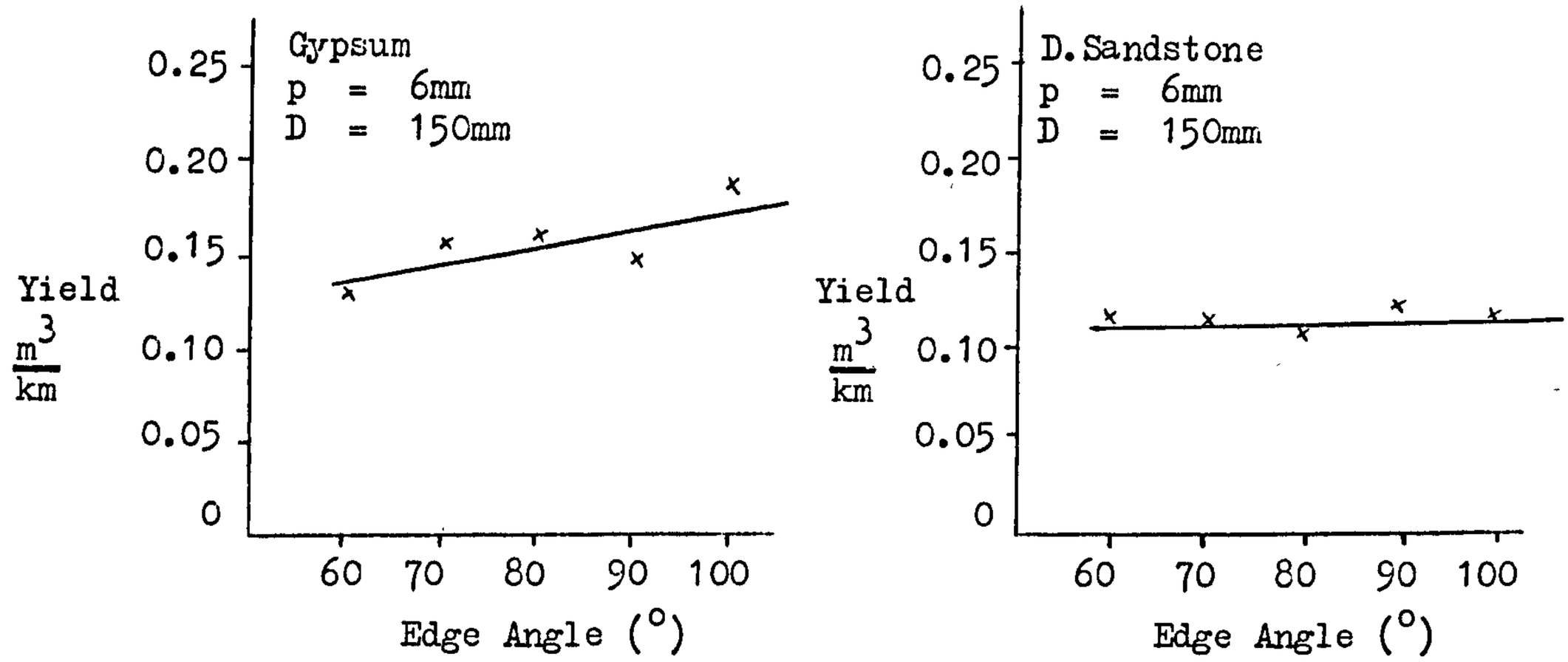

Fig.36 Variation in Yield with Disc Edge Angle.

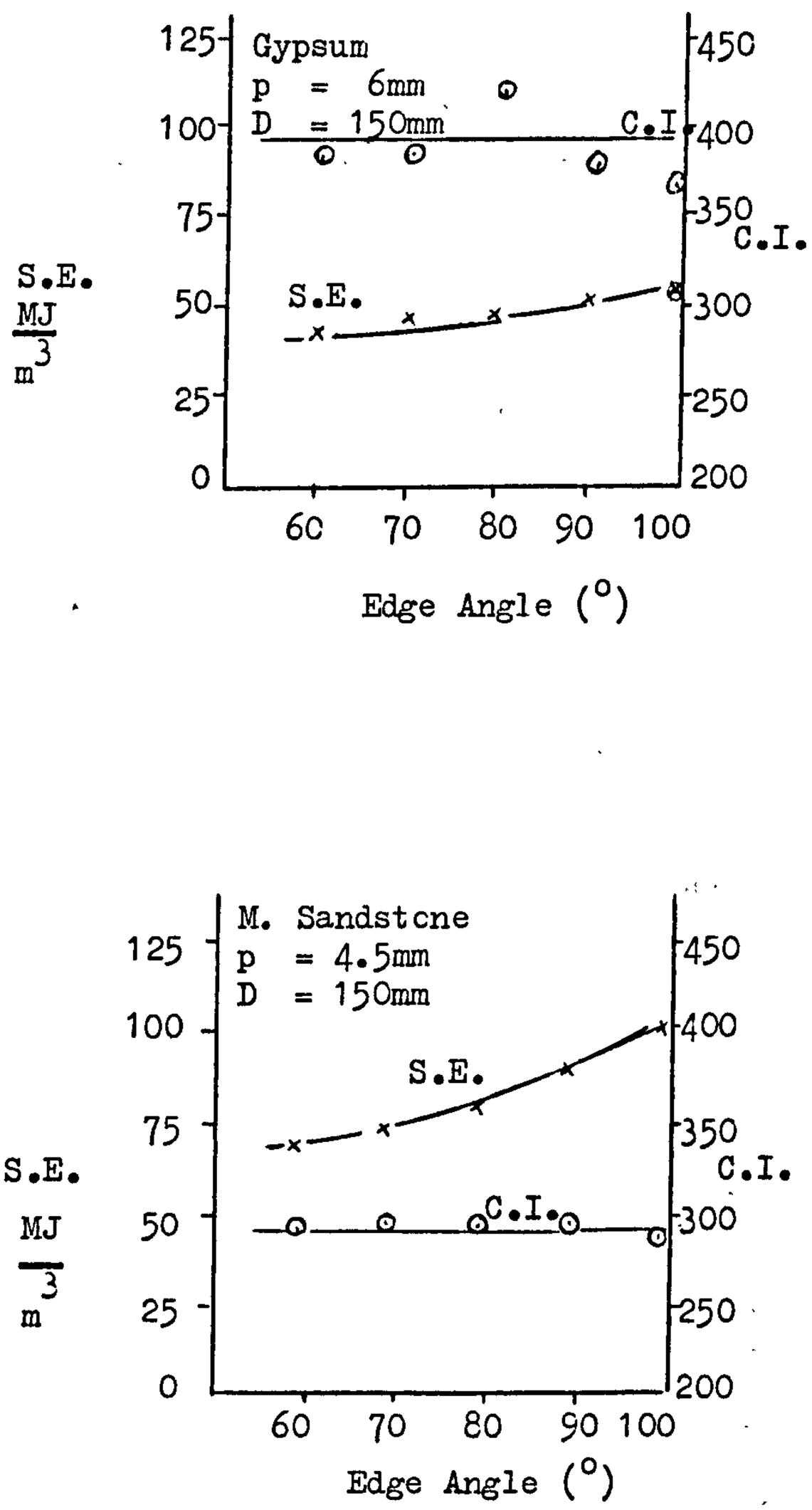

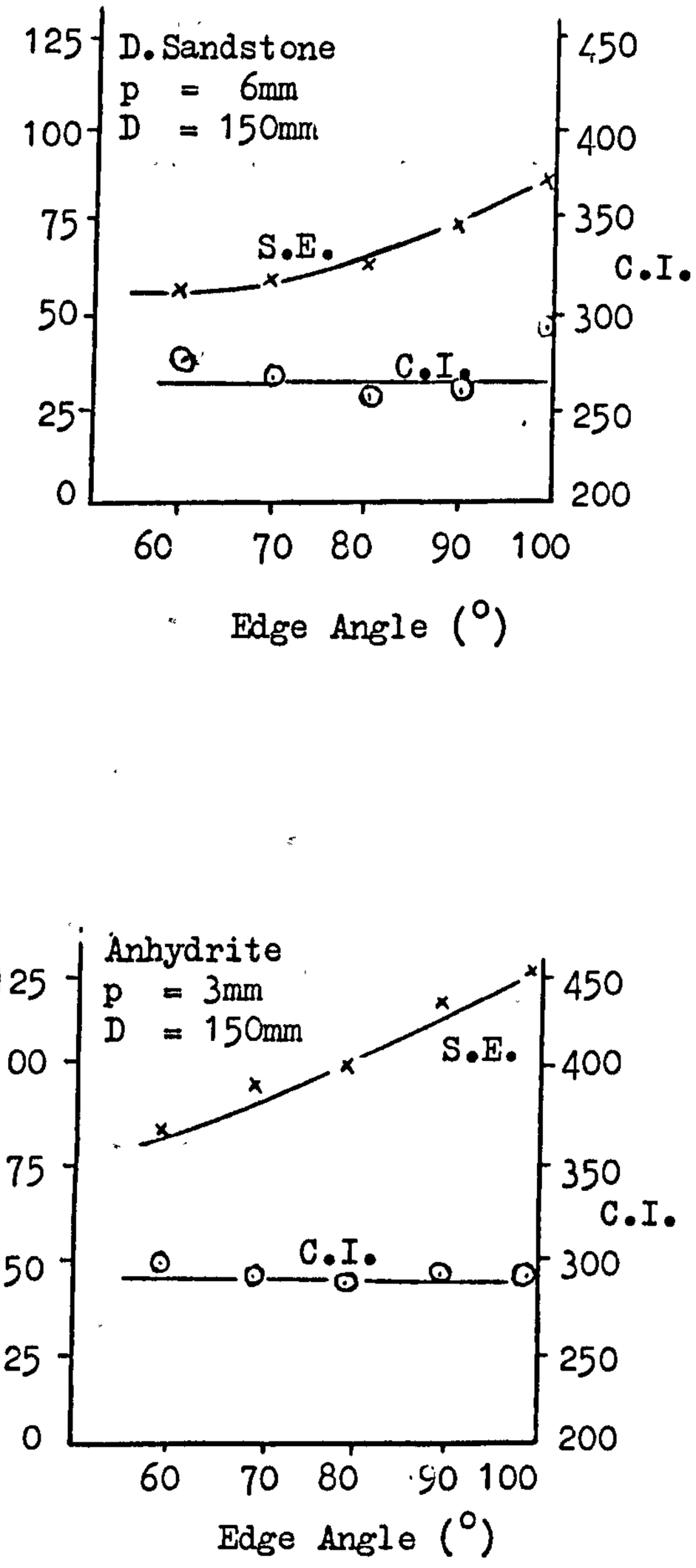

Fig.37 Variation in Specific Energy (S.E.) and Coarseness Index (C.I.) with Disc Edge Angle.

Table 19. Groove angles for different levels of Edge Angle

ϕ °	Gypsum α o	Dunhouse Sandstone α o	Mansfield Sandstone α o	Anhydrite α o
60	141.4	131.2	133.8	140.0
70	145.9	134.6	138.2	145.4
80	146.4	130.2	138.3	146.6
90	149.2	135.2	142.6	145.6
100	151.7	134.5	145.6	150.2

As show in Fig.37, disc cutters with sharp cutting edges have the lower specific energies and hence are mor efficient than discs with a mcre obtuse edge angle. Fig.37 shows that coarseness index is unaffected by edge angle.

Effect of Disc Diameter

The cutting disc diameter is of minor importance. Although it has no effect on rolling force, it can easily be seen from Fig.38 that it has a significant effect on thrust force. Yield, specific energy and coarseness index, as seen from Figs. 39 and 40, are independent of disc diameter for all experimental rocks. The calculated values of groove angles for each level of diameter at- mean values of penetration and edge angle are given in Table 20.

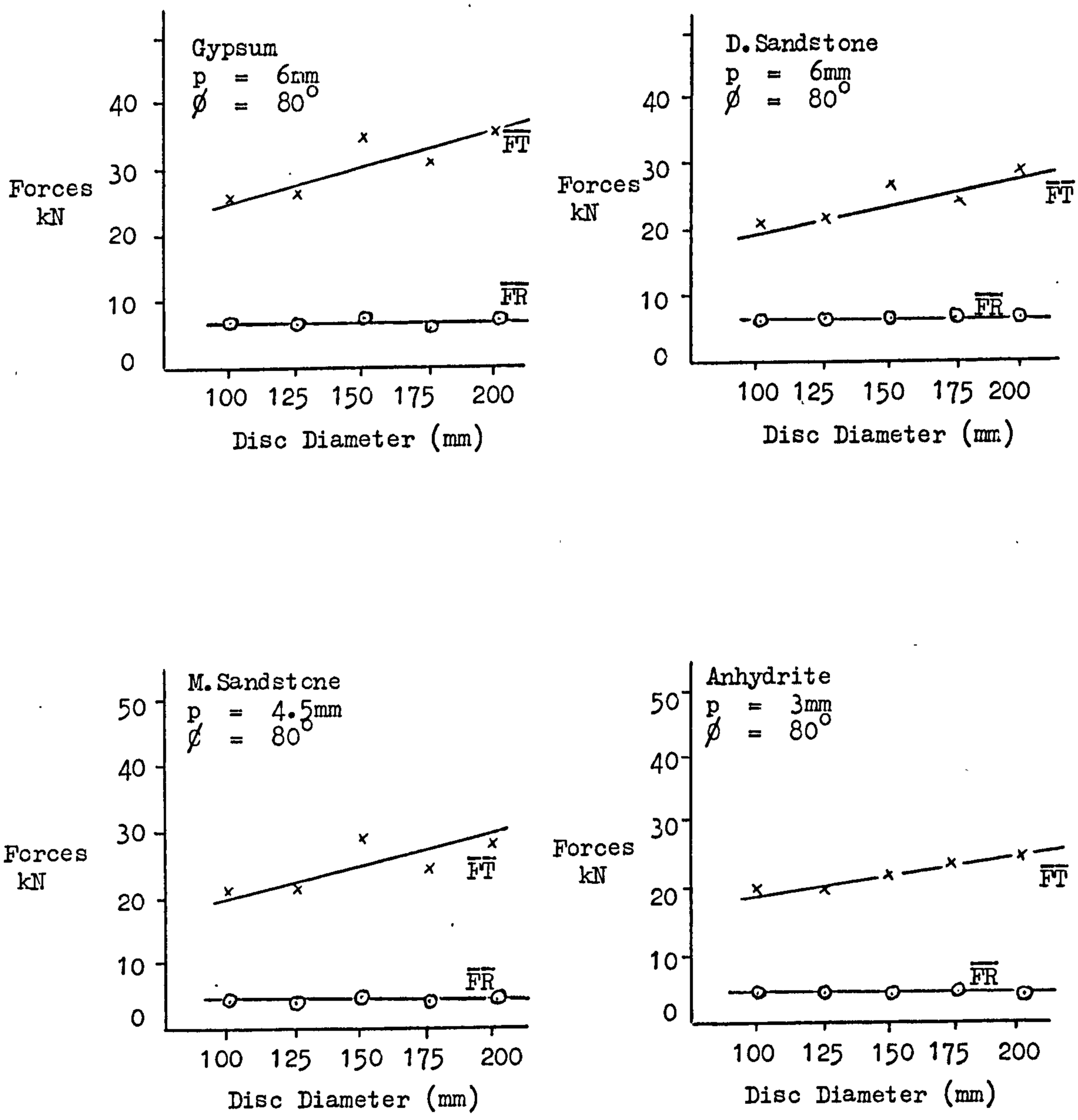

Fig.38 Variation in Disc Forces with Disc Diameter.

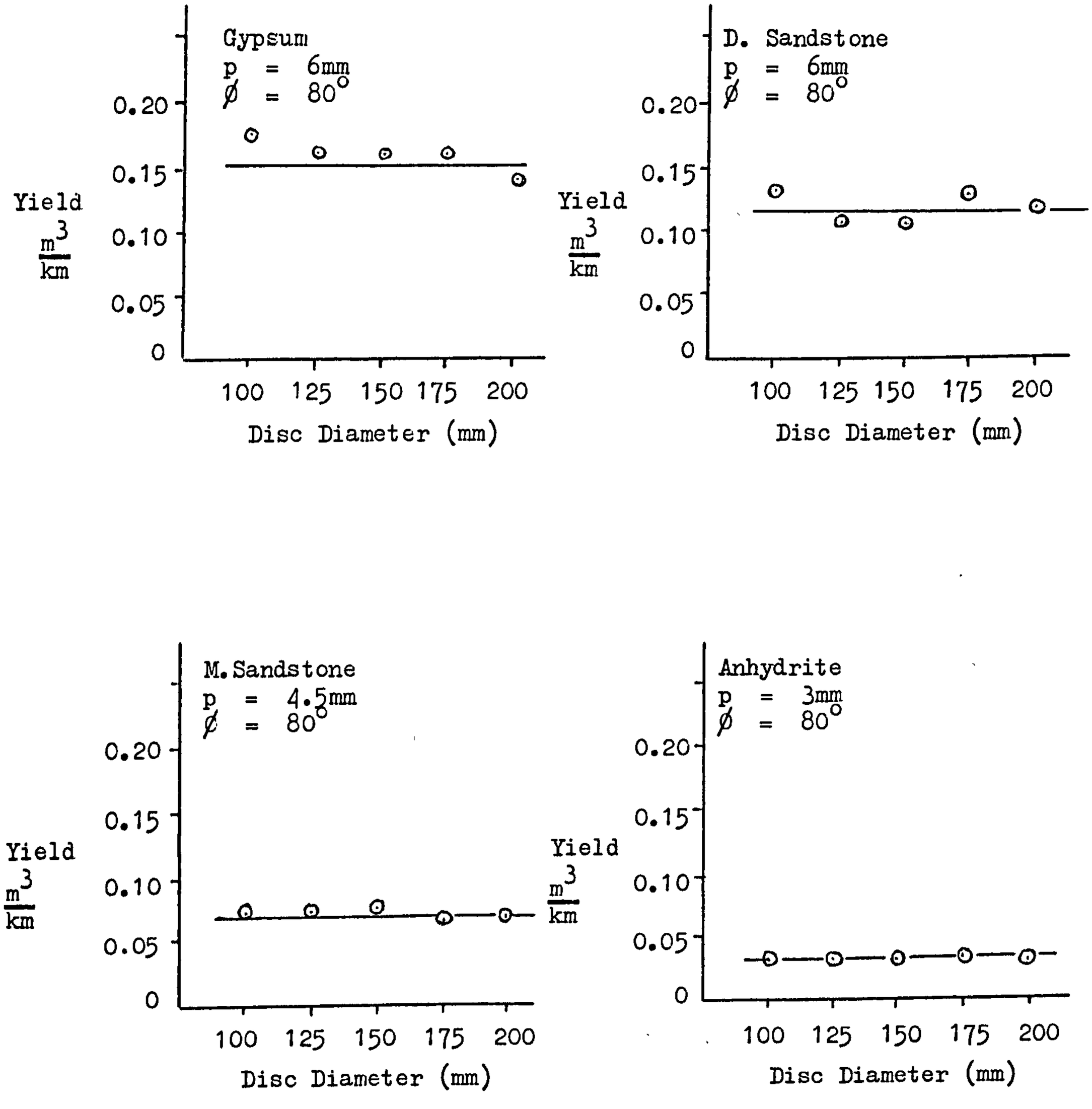

Fig.39 Variation in Yield with Disc Diameter.

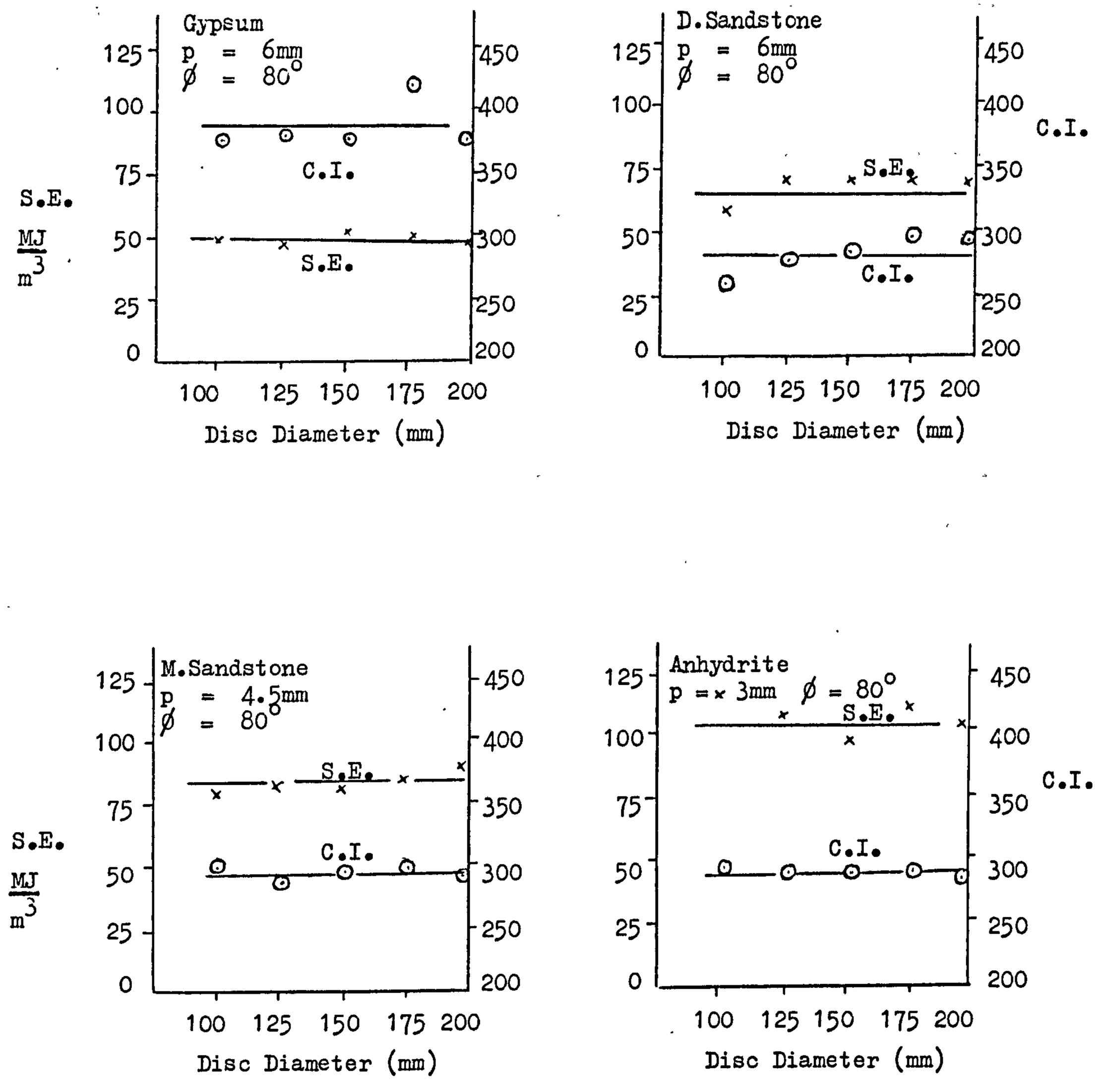

Fig.40 Variation in Specific Energy (S.E.) and Coarseness Index (C.I.) with Disc Diameter.

Table 20 Calculated values of groove angles for each level of disc diameter.

D(mm)	Gypsum α°	Dunhouse Sandstone α°	Mansfield Sandstone α°	Anhydrite α°
100	149.8	137.2	142.4	146.0
125	149.9	135.4	141.9	147.6
150	144.9	135.5	139.2	144.3
175	146.8	128.6	137.5	146.0
200	143.1	129.1	137.4	143.6

* * *

7.3 Results of Relieved Cutting Experiments

When cutting rocks with discs, spacing (S) is defined as the distance between the groove centre-lines, as shown in Fig.29. Relieved cutting experiments were carried out in 6 rocks, the experimental data being given in Appendices 7 to 11.

Effect of Spacing on Disc Forces

Fig.41 shows the effect of spacing on thrust and rolling forces. Clearly zero forces occur where the disc is cutting exactly in previous groove at zero spacing, then they increase rapidly, becoming asymptotic to the unrelieved forces.

Any relationship between dependent variables, such as FT and spacing is misleading unless the s/p ratio is considered. A shallow penetration reduces the maximum interactive spacing and higher penetration increases it. Due to this fact, spacing is usually combined with p to give an s/p ratio.

The effect of s/p on the $\frac{\text{Force Relieved}}{\text{Force Unrelieved}}$ ratios are shown in Fig.42. Each point on the figure is a result of two cuts, with one disc, having the same penetration; one cut representing the unrelieved and the other the relieved cutting. During the relieved cutting in Anhydrite, it was observed that the rock was slightly different from the one used for unrelieved cutting, so a second unrelieved cutting experiment was carried out in order to compare relieved and unrelieved cutting results. The second set of data is given in Appendix 5. The following formulae allow the calculation of the effect of spacing for different experimental conditions.

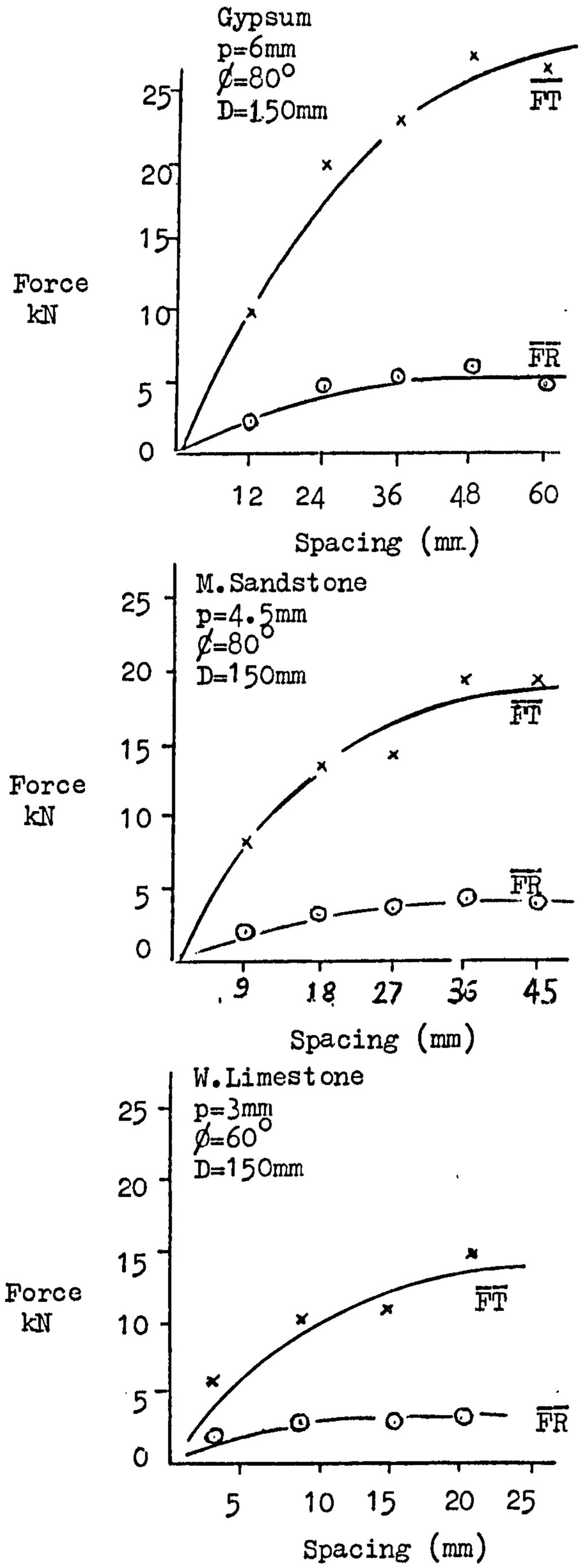

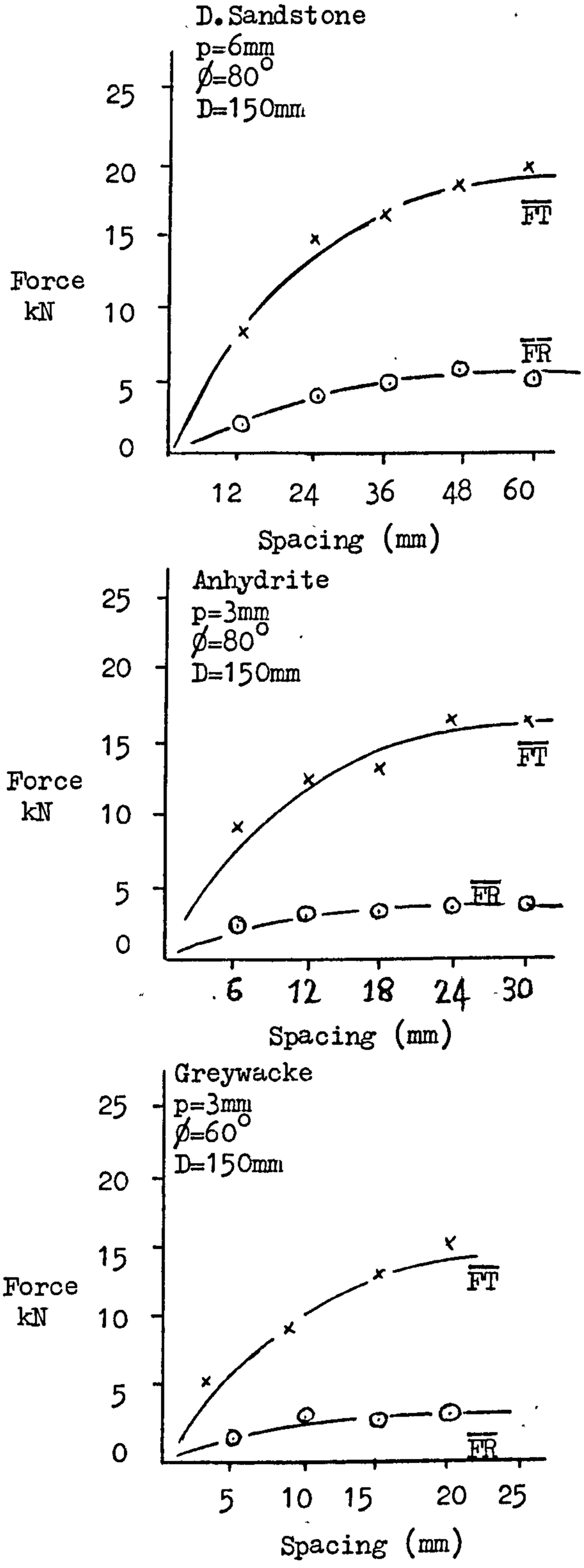

Fig.41 Effect of Spacing on Disc Forces.

Fig.42A Relieved force ratio / Unrelieved versus spacing / penetration ratio.

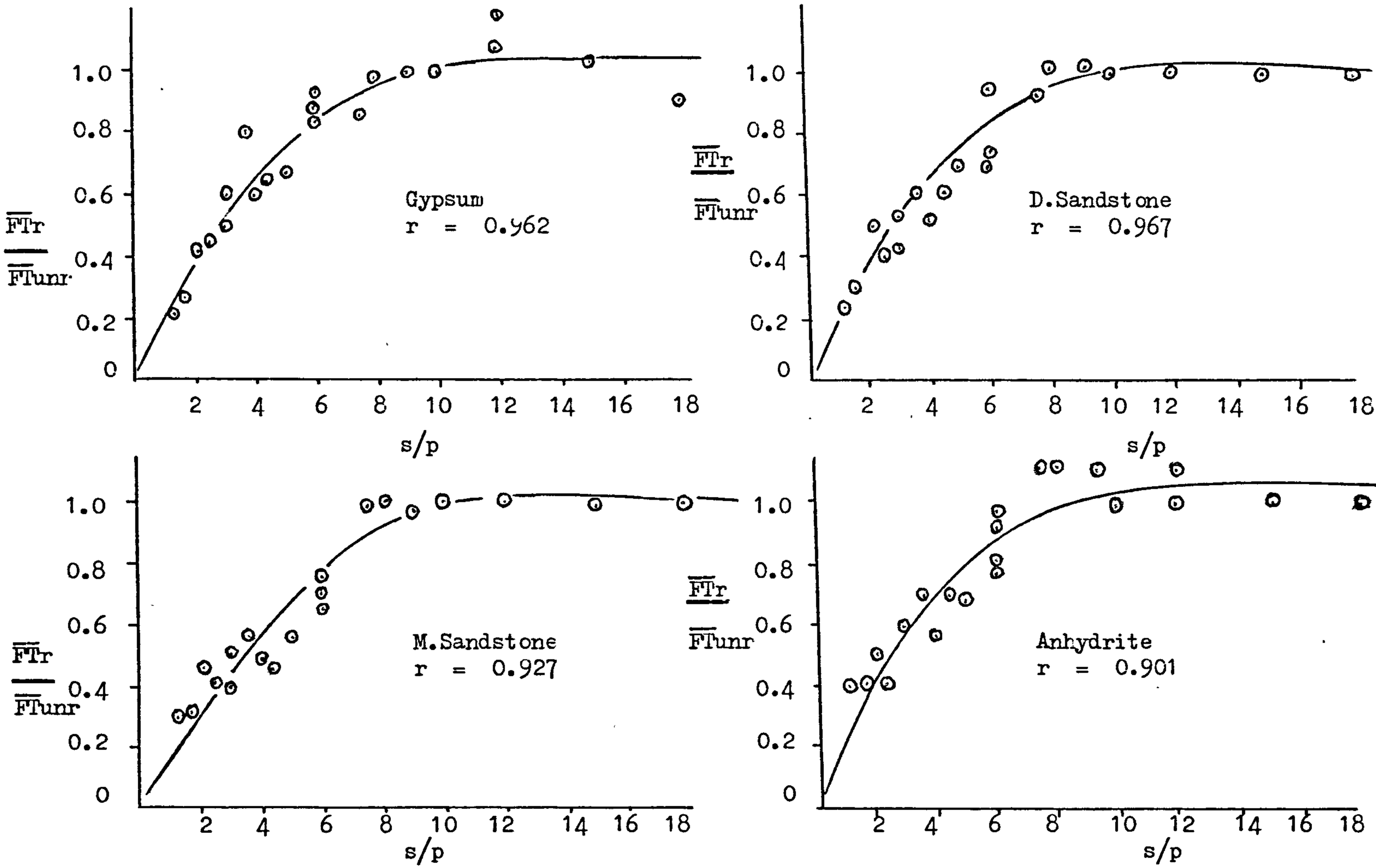

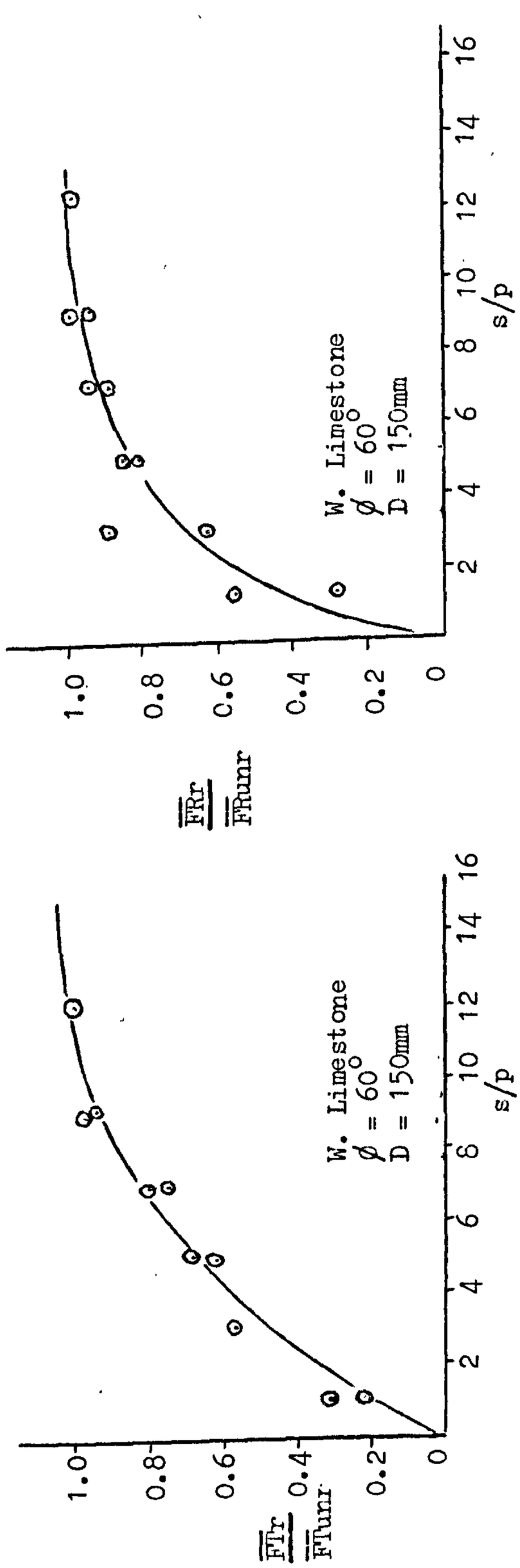

Fig. 42B $\frac{\text{Relieved}}{\text{Unrelieved}}$ force ratio versus $\frac{\text{spacing}}{\text{penetration}}$ ratio.

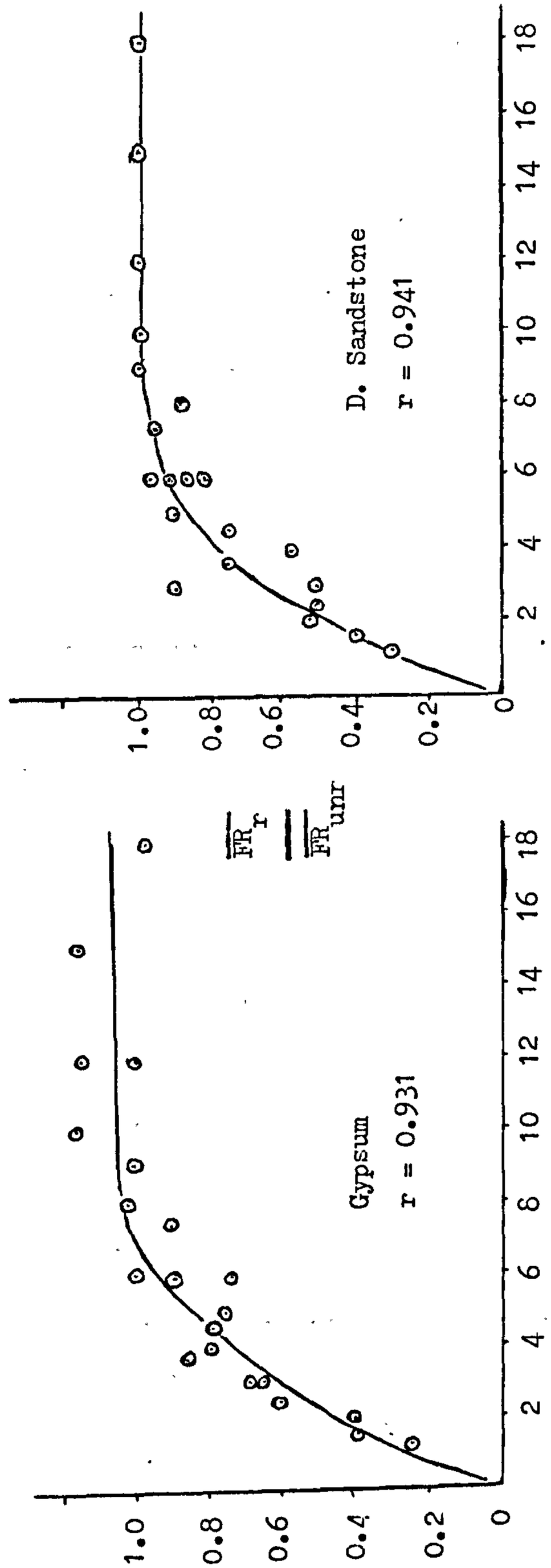

Fig. 42C Relieved force ratio versus Unrelieved

$$\overline{FT} \text{ relieved} = \overline{FT} \text{ unrelieved} \quad \frac{s/p}{a + b \times s/p} \qquad \text{- - - (7a)}$$

$$F'T \text{ relieved} = F'T \text{ unrelieved} \quad \frac{s/p}{a' + b' \times s/p} \qquad \text{- - - (7b)}$$

$$\overline{FR} \text{ relieved} = \overline{FR} \text{ unrelieved} \quad \frac{s/p}{c + d \times s/p} \qquad \text{- - - (7c)}$$

$$F'R \text{ relieved} = F'R \text{ unrelieved} \quad \frac{s/p}{c' + d' \times s/p} \qquad \text{- - - (7d)}$$

The constants of these equations are tabulated in Table 21.

Table 21 Relationships between s/p and $\frac{\text{force relieved}}{\text{force unrelieved}}$ ratios for different rocks.

Constant	Gypsum	Dunhouse Sandstone	Mansfield Sandstone	Anhydrite
a	4.970	4.040	3.315	2.353
b	0.448	0.608	0.871	0.840
a'	4.398	3.770	2.776	2.144
b'	0.474	0.664	0.884	0.836
c	3.056	2.846	1.908	0.909
d	0.655	0.716	0.863	0.931
c'	3.197	2.721	1.565	0.810
d'	0.608	0.721	0.897	0.922

The point where the interaction between adjacent cuts occurs is very critical and important for the design of the excavation systems. Fig.42 shows that the mean thrust forces for 6 rocks become asymptotic to the unrelieved forces at s/p ratios of between 6.5 - 8. The rolling

forces, however, achieve the same state at an s/p ratio of 5-6. It appears that there is a reductin in $\frac{\overline{FT}}{\overline{FR}}$ ratio as the disc approaches the previously cut groove.

However, Roxborough and Phillips[75] have postulated that the interaction between adjacent grooves occurs if $\frac{s}{p} \leqslant \frac{\sigma_c}{\sigma_3}$. The values where the interaction cccurs for mean thrust force are taken from Fig.42 and compared with the values calculated from the formula given above. From Table 22 it emerges that theoretical s/p values are in reasonable agreement with the actual values.

Table 22 Measured and Theoretical Values of s/p.

Rock	s/p measured for $\overline{FT}$	s/p Theoretical
Gypsum	7-8	10.1
Dunhouse Sandstone	5-6	5.1
Mansfield Sandstone	6-7	6.5
Anhydrite	7	9.0
Weardale Limestone	8	6.4
Greywacke	7	5.4

Effect of Spacing on Yield

Since it was shown in Figs. 36 and 39 that rock yield is independent of disc edge angle and diameter in Dunhouse Sandstone and Anhydrite, the relieved values would only be a function of penetration and spacing in these rocks. Hence the 25 values of yield

can be directed plotted against spacing for each level of penetration, as shown in Fig.43. The effect of spacing in Gypsum and Mansfield Sandstone can be illustrated more clearly after the affect of disc edge angle has been considered. Predictor equations 8 and 11 have been used to clarify the effect of spacing on these two rocks. As can be seen from Fig.43 for 4 rocks there is an optimum yield which is significantly higher than equivalent yield representing the unrelieved cutting. This optimum yield occurs at an s/p ratio of 6. In the pre-optimum region yield increases at a high rate with spacing and reaches an optimum value. In the post-optimum region there is a fall in yield to a constant value. However, this optimum yield is not clearly defined in Gypsum and Mansfield Sandstone. Fig.44 shows the relationship between s/p and Qr/Qunr ratio, where Qr is the relieved yield and Qunr the unrelieved yield. The general trend can be represented mathematically as a cubic function in the form of $Qr = (a + b\left(\frac{s}{p}\right) + c\left(\frac{s}{p}\right)^2 + d\left(\frac{s}{p}\right)^3)$ Qunr - - - (8). The constants of this equation are given in Table 23.

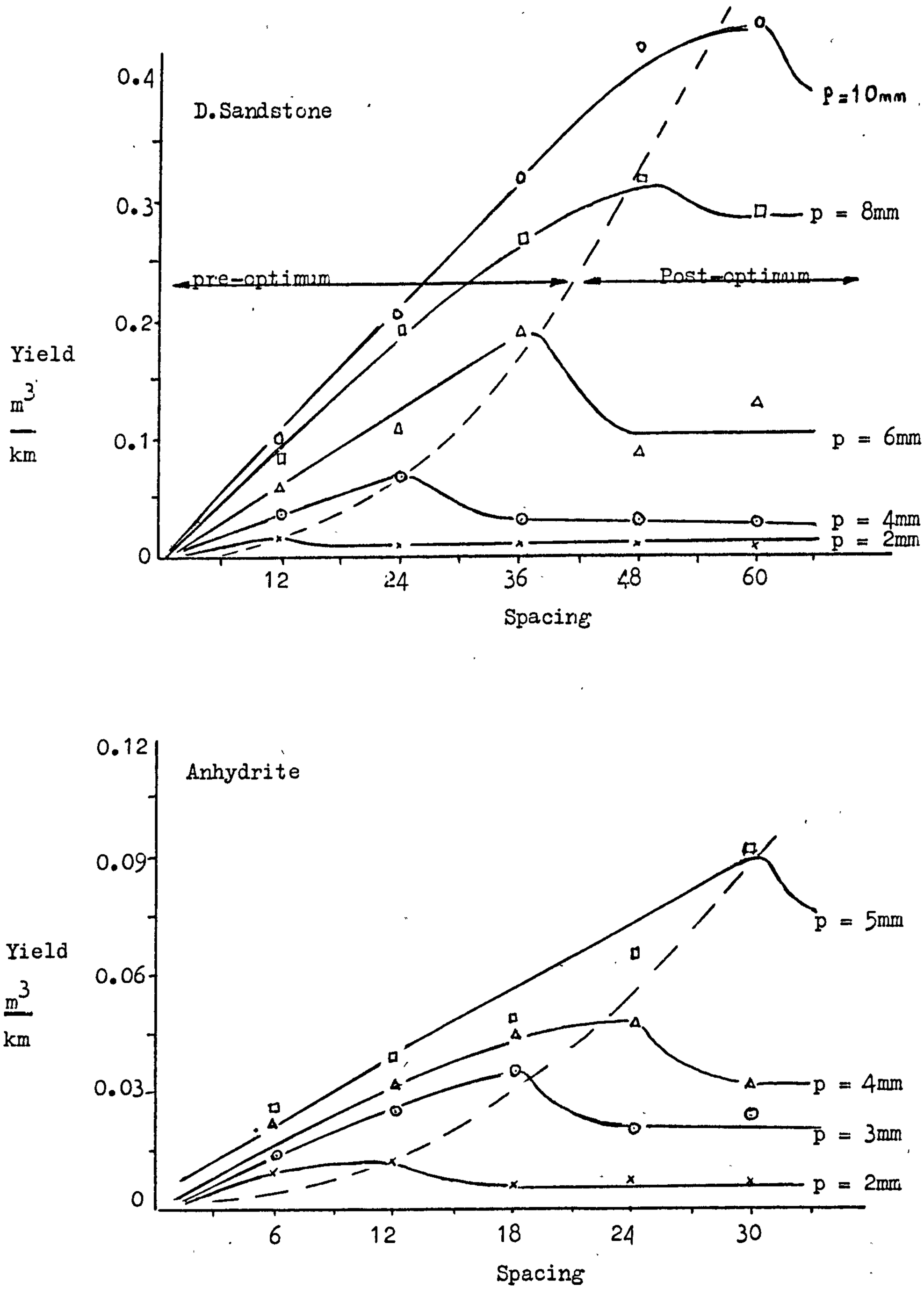

Fig.43A Variation in Yield with Spacing.

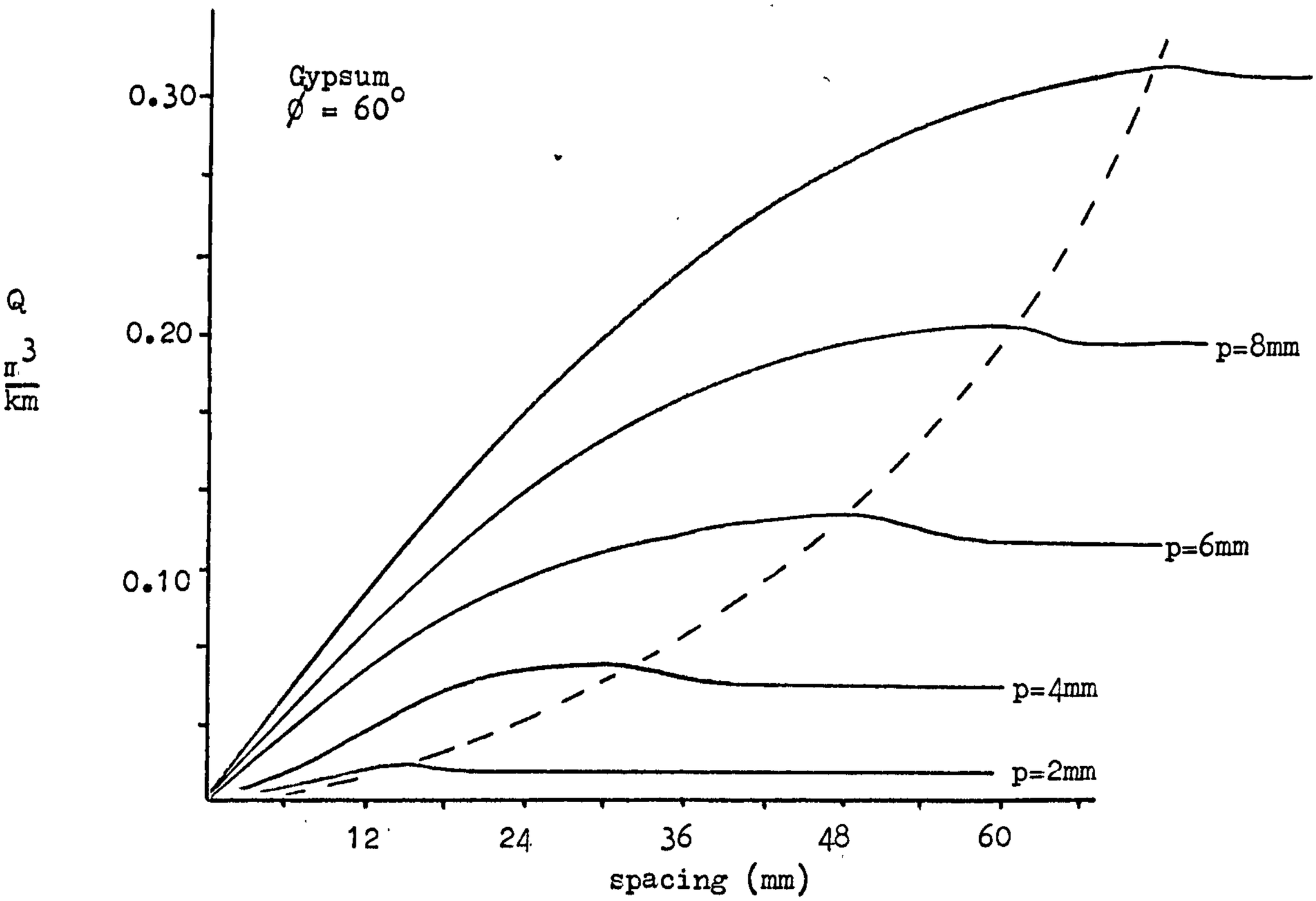

Fig.43B Variation in Yield with Spacing.

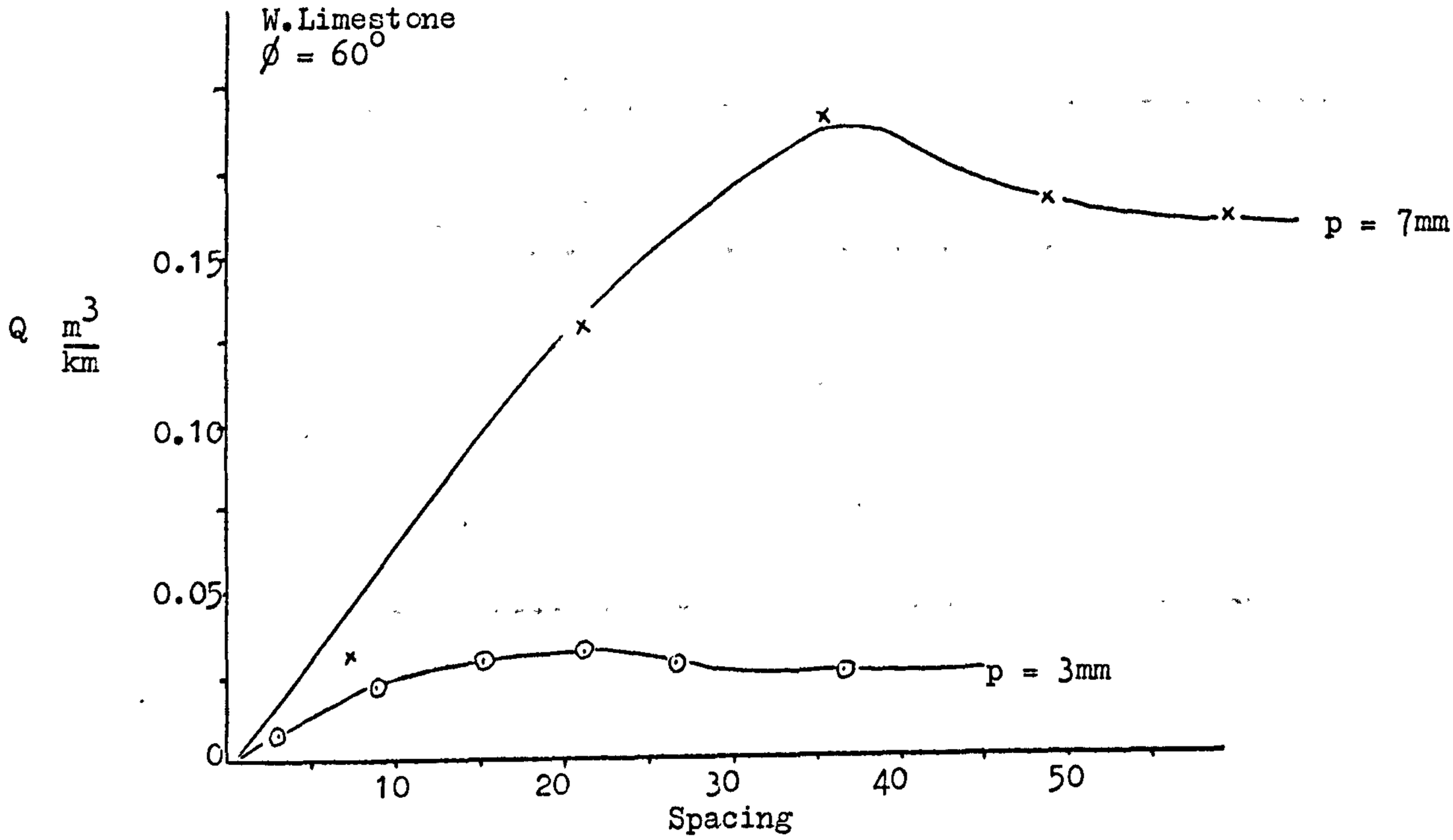

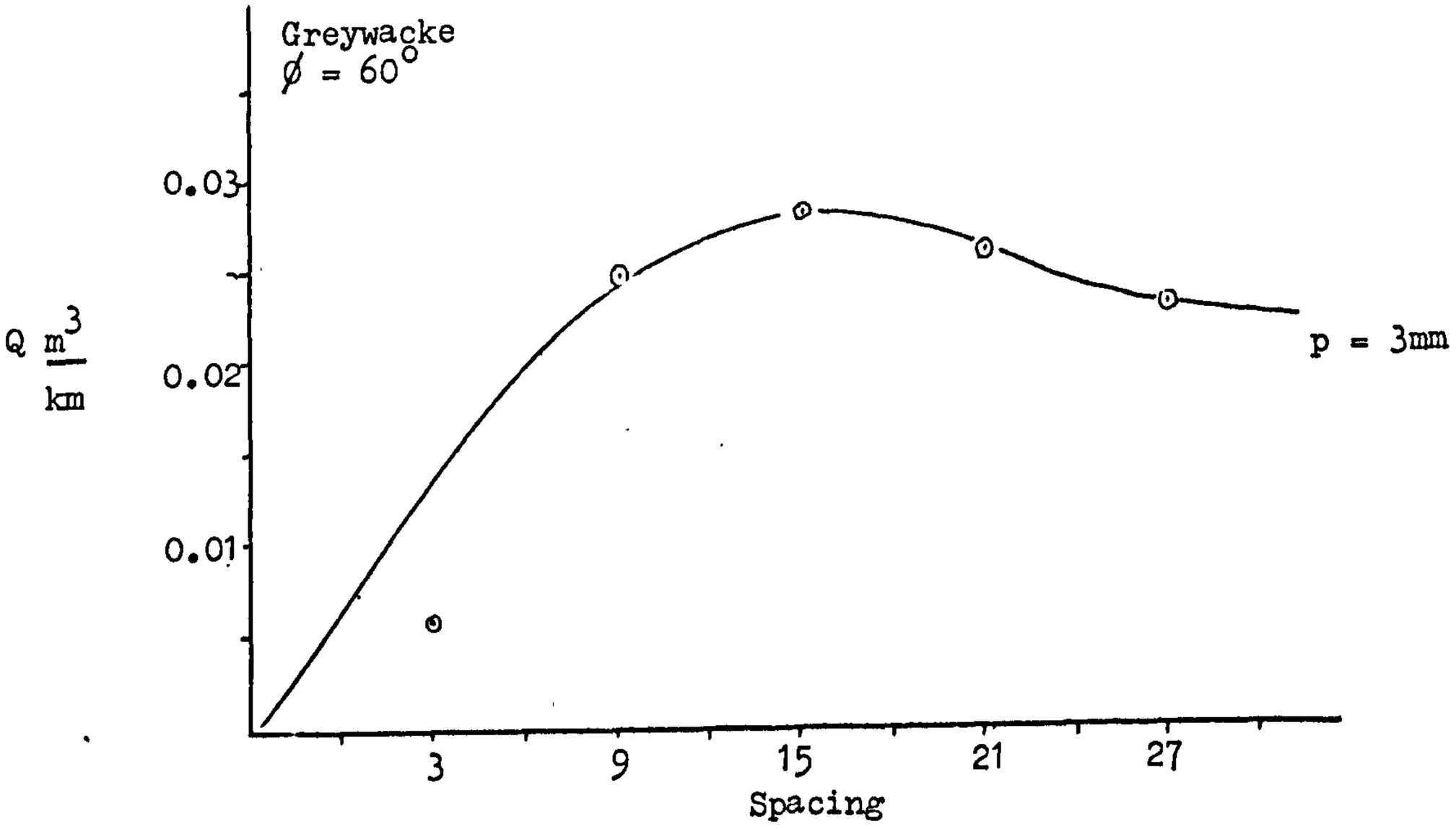

Fig.43C Variation in Yield with Spacing.

Table 23 The relationship between s/p and Qr/Qunr ratios.

Rock	$a.10^{-4}$	$b.10^{-2}$	$c.10^{-3}$	$d.10^{-4}$
Gypsum	20.3	35.5	-33.7	9.3
Dunhouse Sandstone	-686.5	59.8	-65.9	19.8
Mansfield Sandstone	- 14.0	32.5	-29.6	8.0
Anhydrite	685.6	46.8	-49.6	14.5

Note that the above equations are not valid for $\frac{s}{p} > 20$ since they give high predicted values.

Effect of Spacing on Specific Energy and Coarseness Index

Figs.44 to 47 show graphical representation of the results. There are quite definite optimum values of Specific Energy and Coarseness Index for different rocks. The minimum energy for Weardale Limestone and Greywacke occurs at s/p ratio of 5. The improvement in Specific Energy at this optimum spacing is only of the order of 30%. It is interesting to note that the optimum values of Coarseness Index corresponds almost to the same value of $\frac{s}{p} = 5$. However, the improvement in Specific Energy for the four low strength rocks is not as high as in these two high strength rocks. It has been shown by Roxborough and Phillips that the grouped data at mean penetration, disc diameter and edge angle, obscured to a certain extent the true effect of spacing on Specific Energy. In this case, Specific Energy values for different disc edge angles are calculated from the quoients of the empirical equations for mean rolling force

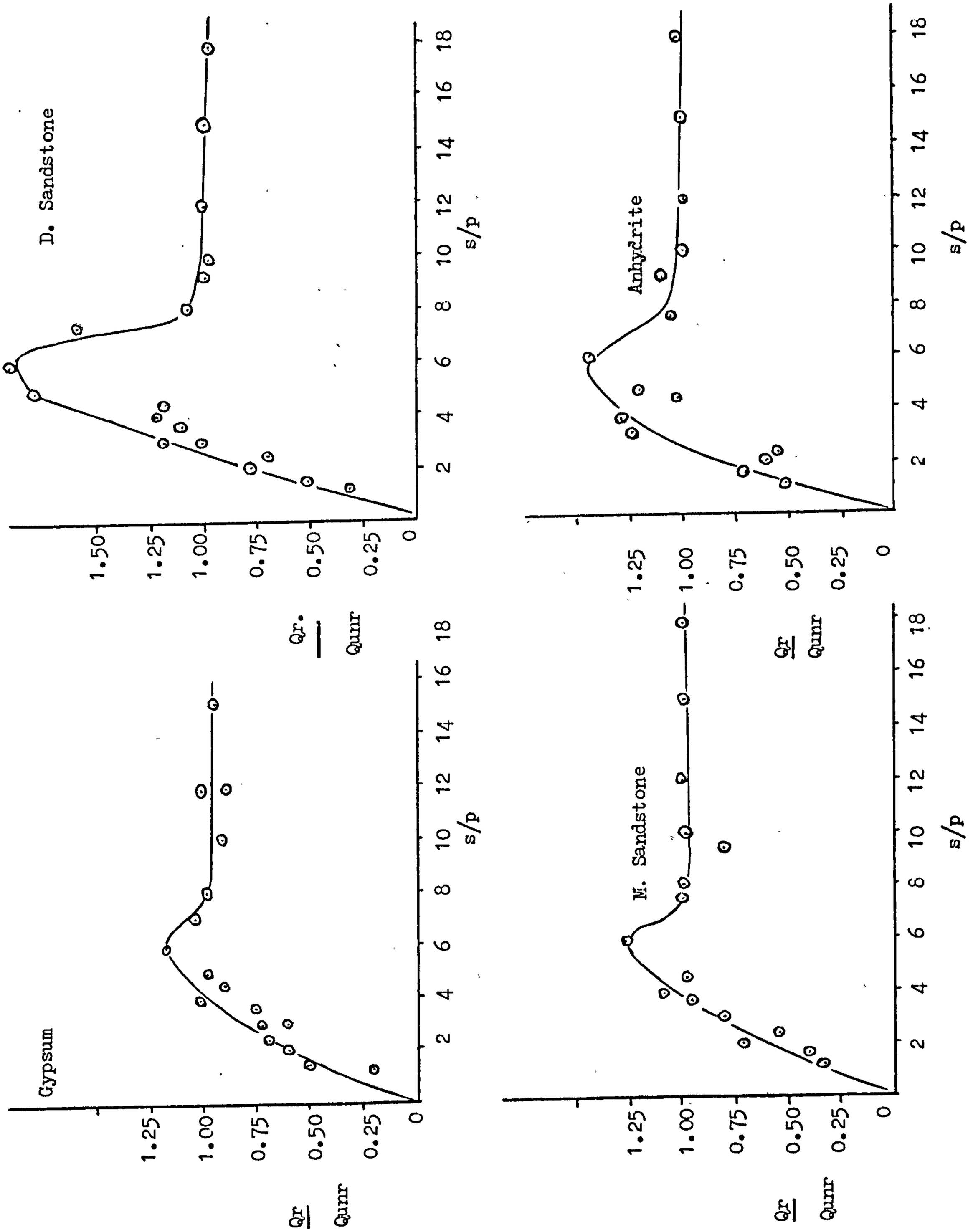

Fig.44 Relieved/Unrelieved Yield Ratios.

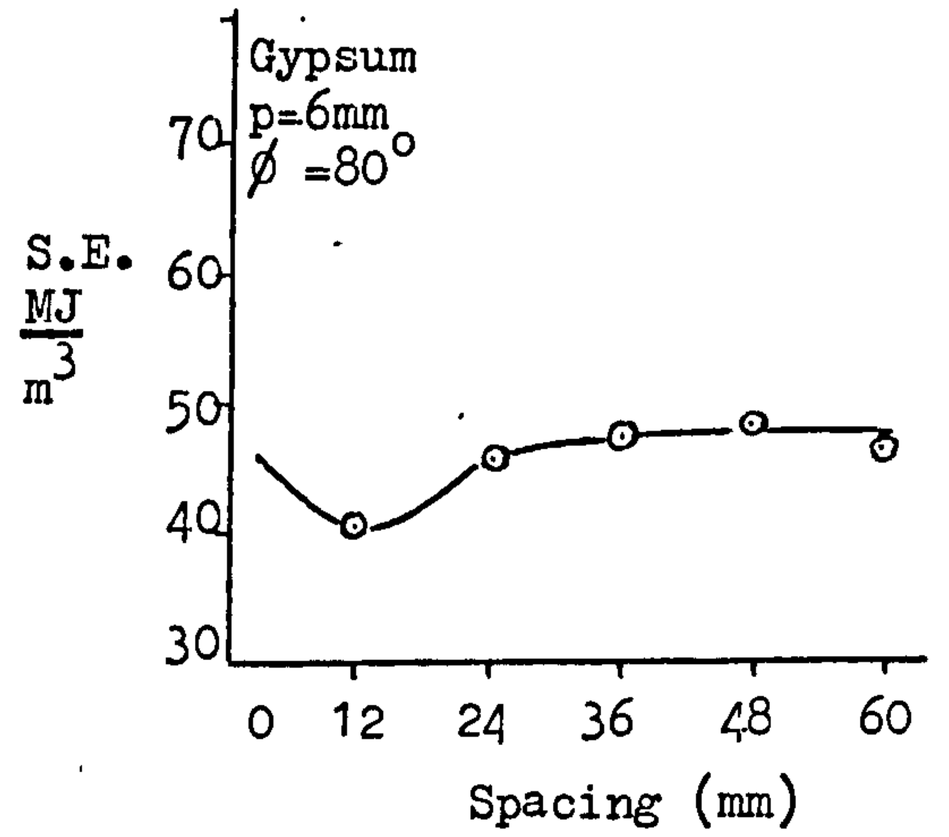

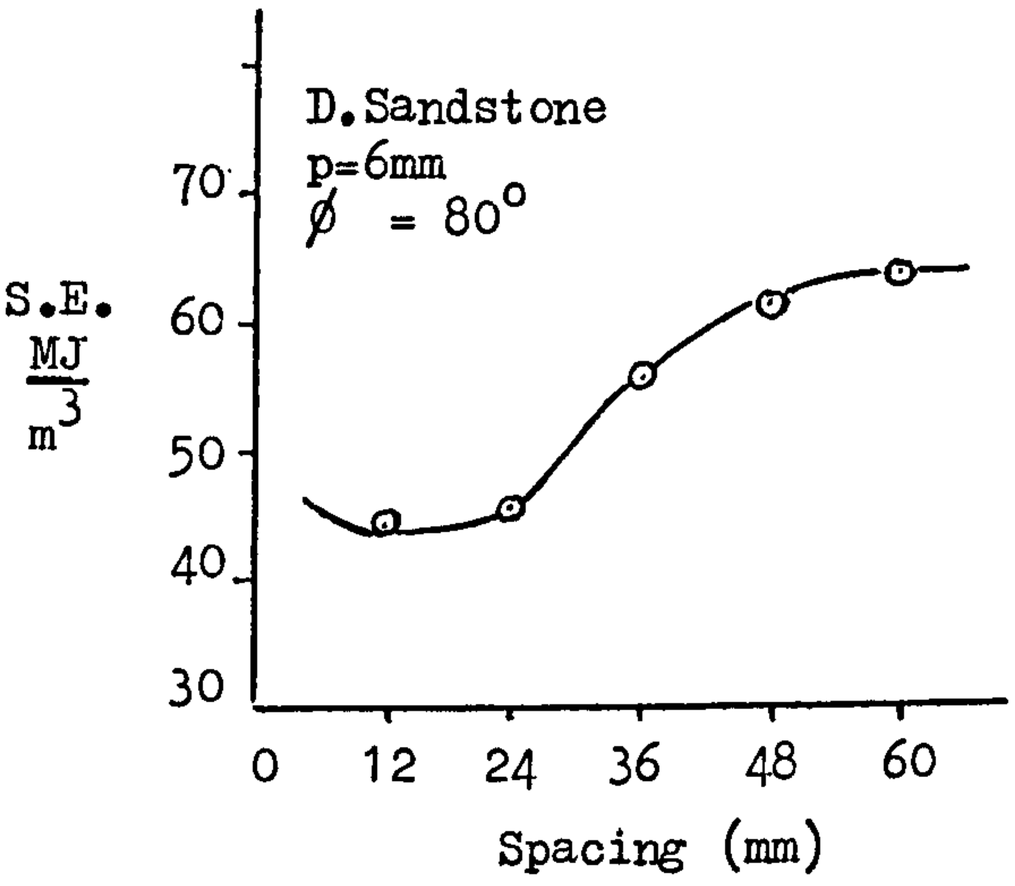

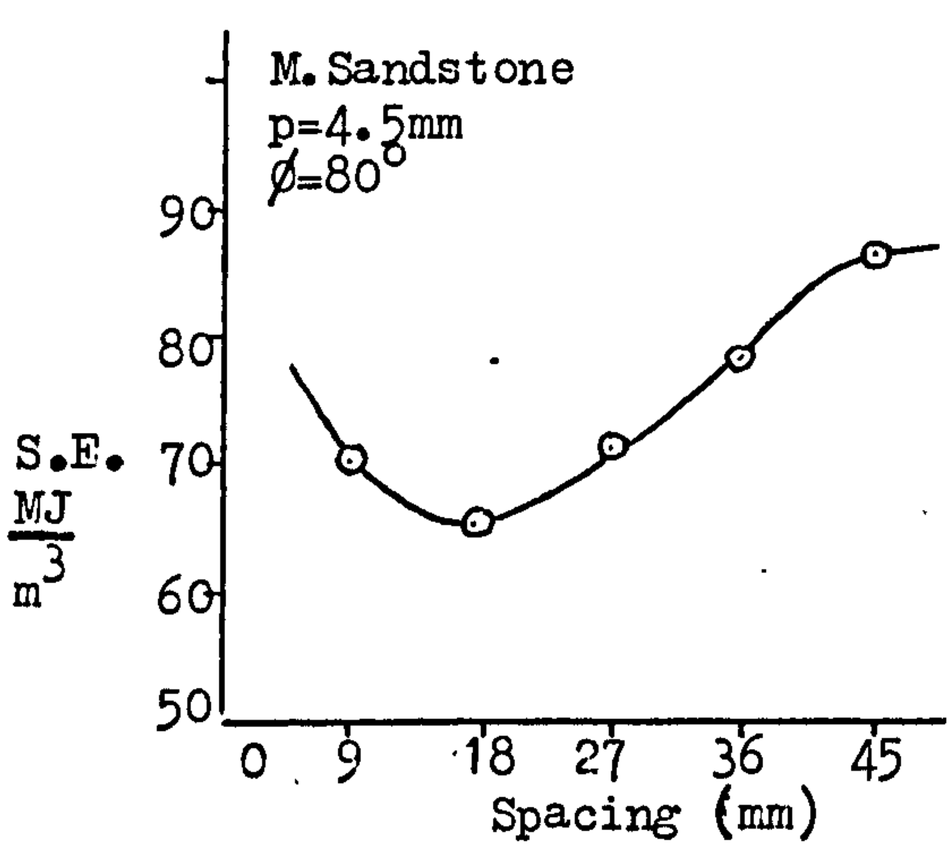

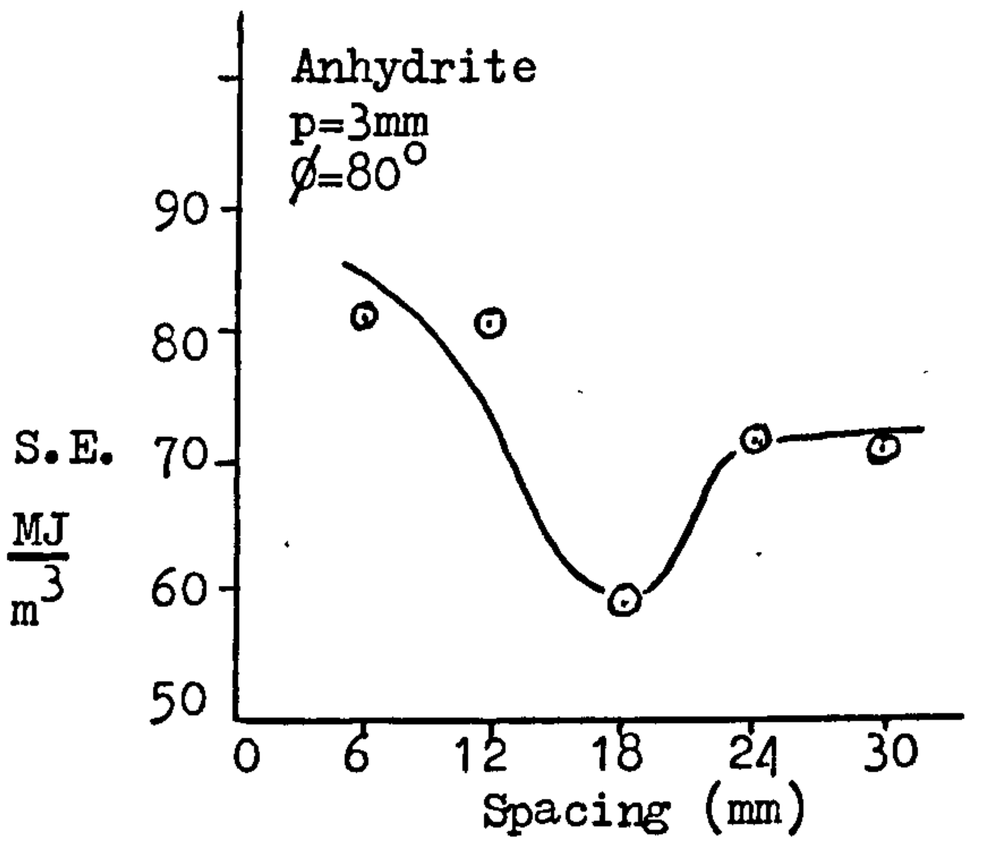

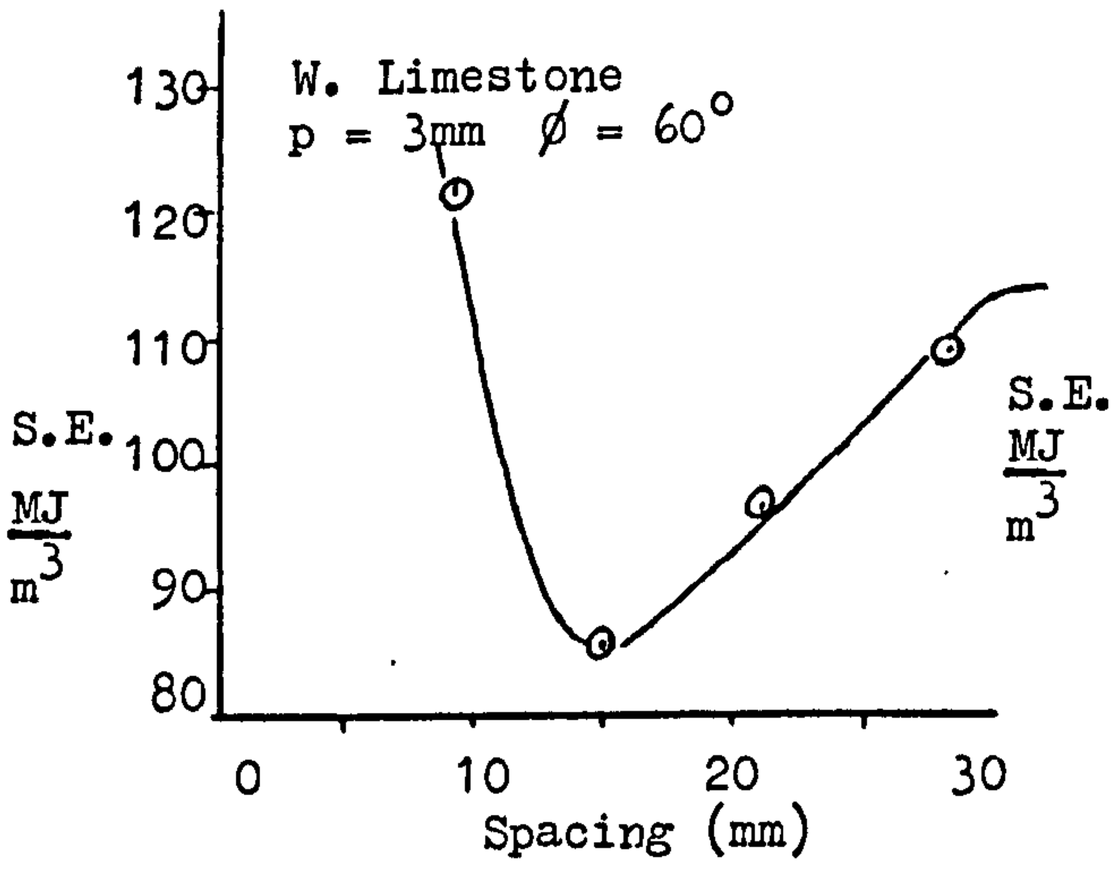

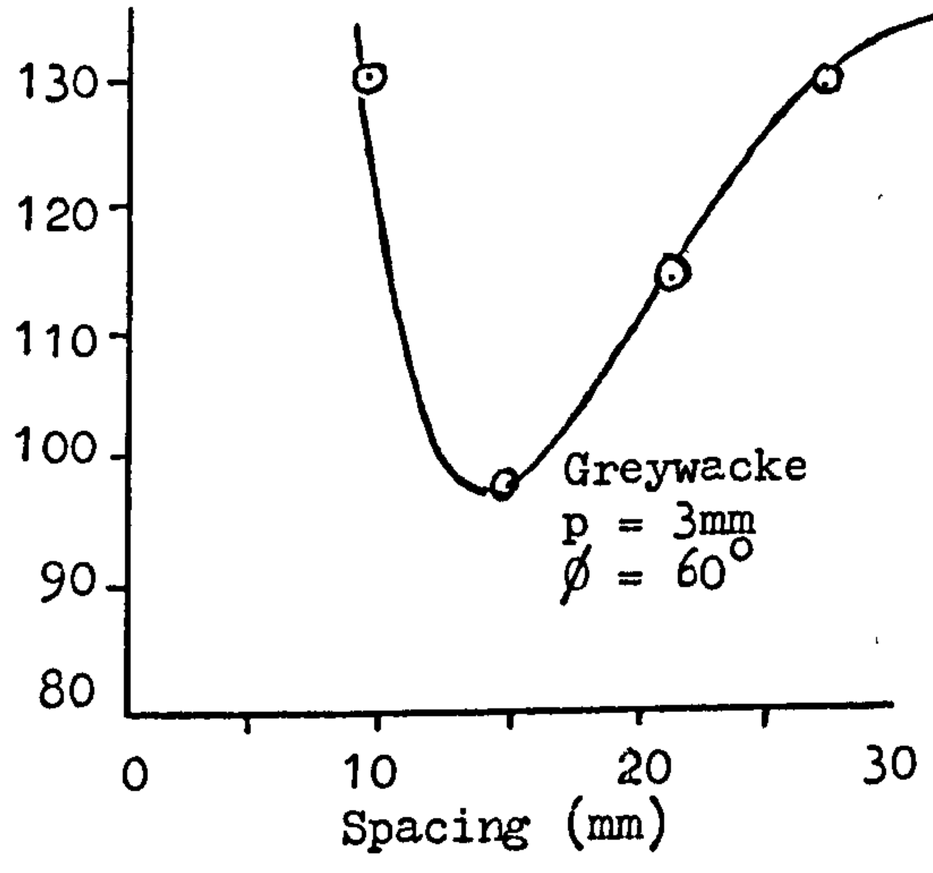

Fig.45 Variation in Specific Energy with S

(1) $\phi = 60^\circ$ (2) $\phi = 70^\circ$ (3) $\phi = 80^\circ$ (4) $\phi = 90^\circ$
(5) $\phi = 100^\circ$

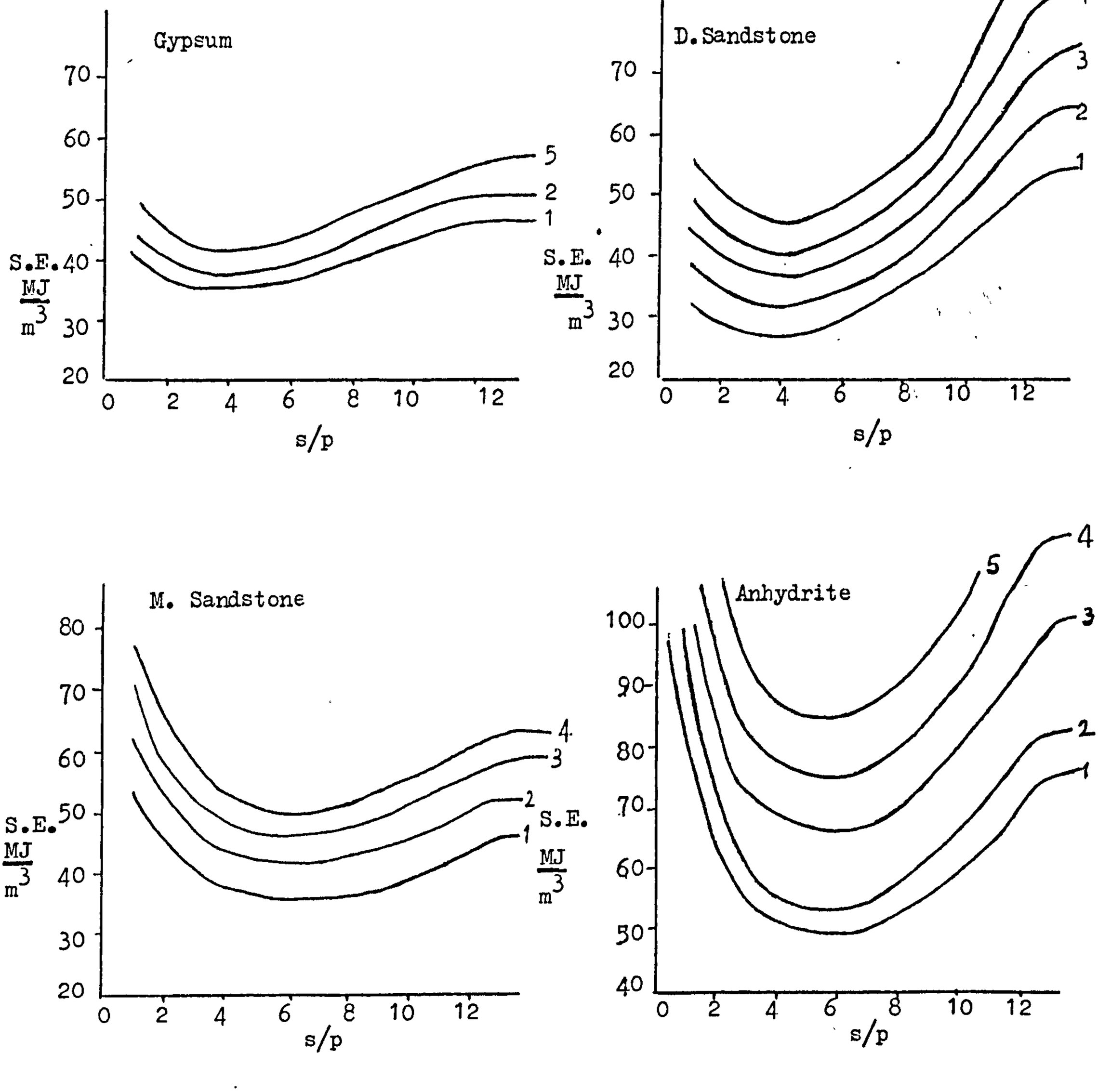

Fig.46 Effect of Spacing (p = 5mm) on Empirical Disc Specific Energy Values.

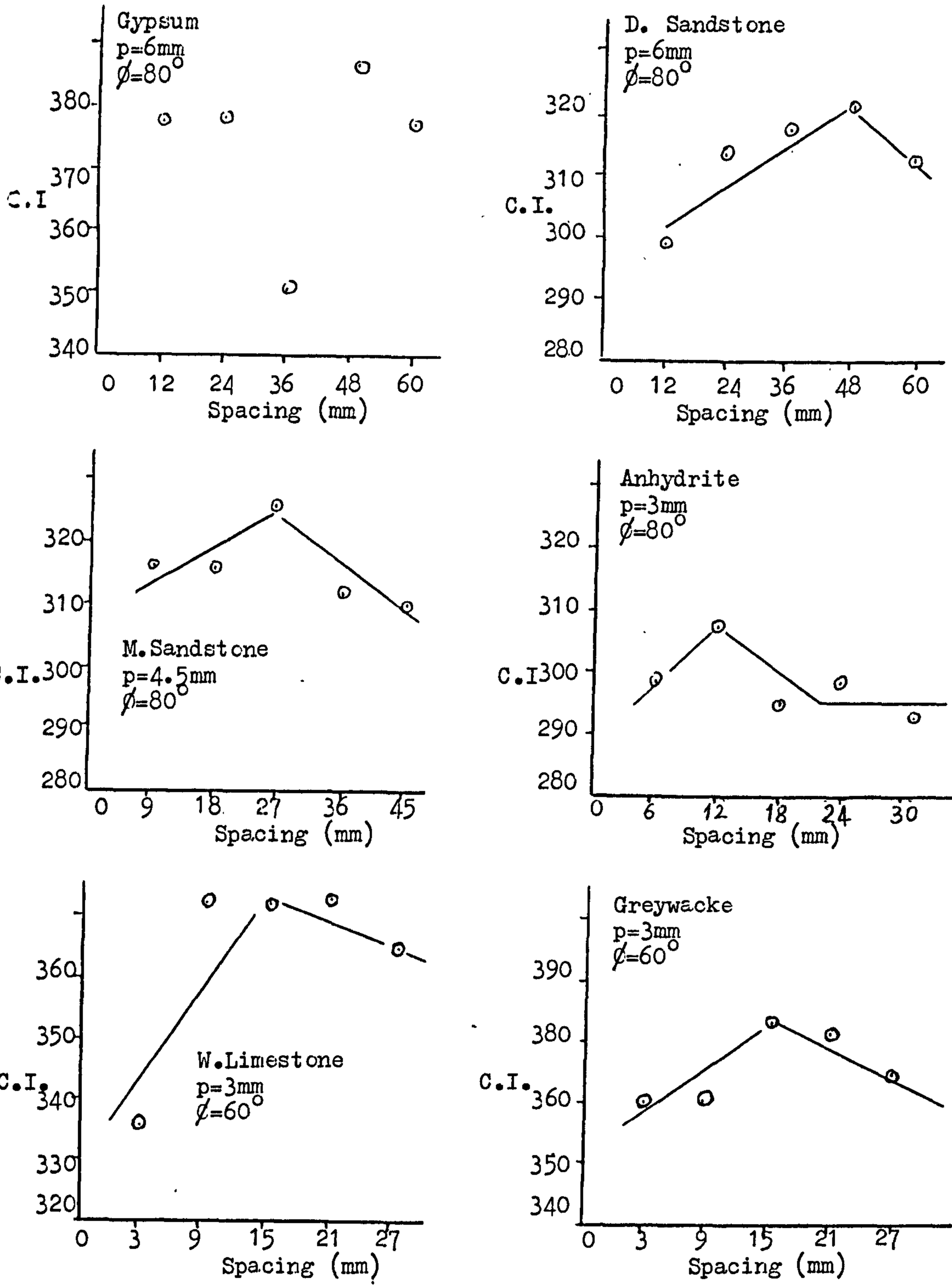

Fig.47 Variation in Coarseness Index with Spacing. D = 150mm

and yield. As can be seen from Fig.46 and Appendix 12, the s/p ratio for minimum specific energy in Gypsum and Dunhouse Sandstone is 4, in Mansfield Sandstone 7, and in Anhydrite 6. Improvement in the energy varies between 20% and 50% compared with unrelieved cutting. The angle of the disc cutting edge appears to have no influence on the optimum $\frac{s}{p}$ ratio for minimum Specific Energy. During the experiments it was observed that large pieces of rock were being consistently produced at certain spacings. Due to this fact, there is a maximum coarseness index at certain spacing (except in Gypsum) which is significantly higher than the values obtained for different spacings.

* * *

7.4 Conclusions

Observations to be made from unrelieved cutting experiments are summarised below.

(a) The ratio of peak force to mean force is found to be small being 1.05 - 1.16.

(b) In all cases, thrust and rolling forces increased with increasing penetration and edge angle.
Although disc diameter has no effect on rolling forces, it has a significant effect on thrust force.
The best functions to relate the experimental variables and forces are found to be:

$$F'T,\ \overline{FT} = (p + A)(\emptyset + B)(CD + E) \qquad ---(9)$$

$$F'R,\ \overline{FR} = (p + A)(B\emptyset + C) \qquad ---(10)$$

Constants A, B, C, E for different rocks are given in Appendix 18 where $\overline{FR}$, $\overline{FT}$ are in kN, $\emptyset$ in degrees, p and D in mm.

(c) The ratio $\frac{\overline{FT}}{\overline{FR}}$ is affected by penetration, being 14 for shallow cuts and 4 for deeper cuts. This ratio is not affected by disc edge angle.

(d) The increase in the yield was found to be proportional to the square of the penetration. The edge angle appears to have a significant effect on the Yield, both in Gypsum and Mansfield Sandstone, but not in Anhydrite and Dunhouse Sandstone.

The function which relates the yield to the two variables, in general form, is as follows:

$$Q = (p^2 + A)(B\phi + C) \text{ or } Q = (Ap^2 + B) \qquad \text{- - - (11)}$$

where A, B and C are the constants.

(e) The results of the experiments indicate that greater efficiency can be obtained by increasing the penetration and decreasing the edge angle. The experimental relationship of the specific energy to these variables suggests that this increase in efficiency beyond 8mm depth of cut would be of no practical significance. The general function of the specific energy is in the form of

$$S.E. = p^A . e^{(B\phi + C)}$$

(f) The only experimental variable which affects the coarseness index is the penetration. The function which relates the penetration to the coarseness index is

$$C.I. = Ap + B$$

Observations to be made from relieved cutting experiments are as follows:

(a) Thrust and rolling forces increase rapidly with spacing, becoming asymtotic to the un-relieved forces at s/p ratios of 6.5–8 for thrust force, and 5–6 for rolling force.

(b) It appears that there is a reduction in $\frac{FT}{FR}$ ratio as the disc approaches the previously cut groove.

(c) Relieved cutting forces are related to unrelieved cutting forces in the form of

$$FT, \overline{FR} \text{ relieved} = FT, \overline{FR} \text{ unrelieved } \frac{s/p}{a+b.s/p} .$$

(d) There is an optimum yield for relieved cutting which is significantly higher than equivalent yield produced by unrelieved cutting. This optimum yield occurs at s/p ratios of about 6.

(e) There is a quite definite optimum value of Specific Energy and Coarseness Index for s/p ratios ranging from 4 to 7.

(f) The point where the interation between adjacent grooves occurs can be predicted by the formula

$$\frac{s}{p} \leqslant \frac{\sigma_c}{\sigma_s}$$

* * *

CHAPTER EIGHT

CORRELATION OF ROCK PROPERTIES WITH THE MEASURED PERFORMANCE OF DISC CUTTERS

The cutting material directly affects the performance of a machine by its physical and mechanical properties. Laboratory cutting experiments usually give the basic data to choose the most suitable cutting tool and to design a cutting head of a tunnel boring machine for a given rock mass, but such experiments are mostly time consuming and expensive. The many advantantages of finding some relationship between a particular rock property or properties and the performance of rock cutting tools have attracted the attention of different research workers for many years.

The Twin Cities Mining Research Centre of the U.S. Bureau of Mines attempted to correlate the rock physical properties with disc cutter performance parameters. Although the predictor equations they developed gave high correlation coefficients they failed to provide all the information vital to tunnel boring machine design. The major drawback was the failure to consider the effect of disc gecmetry on tool performance. Predictor equations should provide some indication of the peak forces, so that bearings may be designed for the worst loading conditions.

The USBM suggested that the significant physical properties for use in empirical equations were:

1. Shcre Scleroscope Hardness,
2. Rock Density,
3. Tensile Strength,

4. Ccmpressive Strength,

5. Young's Modulus and

6. Shear Modulus.

These were combined into predictor equations valid for all rocks with physical properties falling into selected ranges. The inherent disadvantage of these equations are the numbers of different physical properties involved, since a rock to be investigated might easily fail to have all the physical properties conveniently within the ranges used by the USBM.

Research at the University of Newcastle upon Tyne differs from the previous work in a unique way by attempting to predict disc cutter forces using a single standard rock property. The affect of the geometry of discs was also considered in determining the predictor equations. These equations have been developed using four medium strength rocks from the Wolfson Research Programme and two further rocks used in a T.R.R.L. Project[91]. All these rocks have compressive strengths falling within a range of 45 MN/m^2 to 113 MN/m^2. Regression analysis techniques have been used for data curve fitting. A standard regression analysis programme on an H.P.2000 multiple access computer allowed the best statistical fit to be obtained from a choice of linear, power, exponential, hyperbolic and logarithmic functions.

The validity of these equations was checked on three high strength rocks, limestone, Greywacke and Granite, having the compressive strengths of 127.3 MN/m^2, 183.9 MN/m^2 and 179.1 MN/m^2 respectively.

The results obtaine by the USBM were also included in this comparative study.

8.1 Prediction of Mean Thrust Force

Initially, it was decided to investigate the relationship between thrust force and the projected area of disc contact, since several authors assumed that there was a close relation between these parameters[9,10].

The projected area of disc contact is formed by two parabolas as seen in Fig.48 and is calculated as follows:

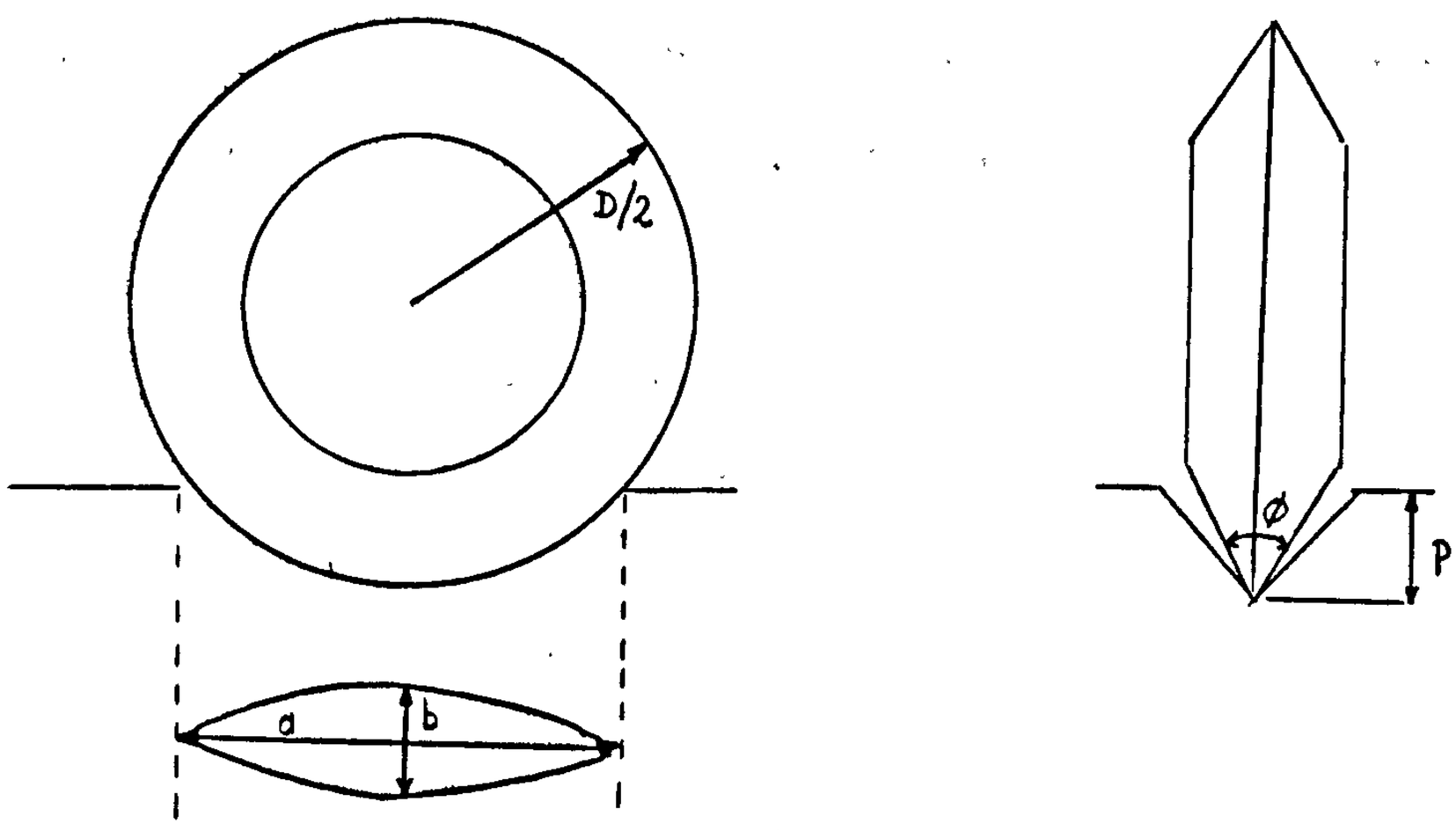

Fig.48 Geometry of Disc Penetration

The area of one parabola is $\frac{A}{2} = \frac{2}{3}$ a.b.

The whole projected area A may, therefore, be written:

$$A = \frac{8p}{3} \tan \frac{\phi}{2} \sqrt{Dp-p^2} \qquad ---(12)$$

Another mathematical approach to calculate the projected area of disc contact was done by Phillips[91]. It was formulated as:

$$A = 2 \tan \frac{\phi}{2} \left[\frac{Ra}{2} - (R-d)^2 \ln \left| \frac{\frac{a}{2} + R}{R-p} \right| \right] \quad \text{---(13)}$$

However, it is interesting to note that the difference between the areas calculated from the formulae (12) and (13) are about 1%.

The value of projected contact area (A) were calculated using the formula (12) for the 25 different experimental conditions and are shown in Appendix 13. Mean thrust forces from each experiment were regressed against the values of A, using a standard regression programme. The best statistical fit for the five different rocks was found to be a linear function and the constants of the equation are given in Table 23.

A typical relationship between mean thrust force and projected contact area for one of the experimental rocks is shown in Fig.49.

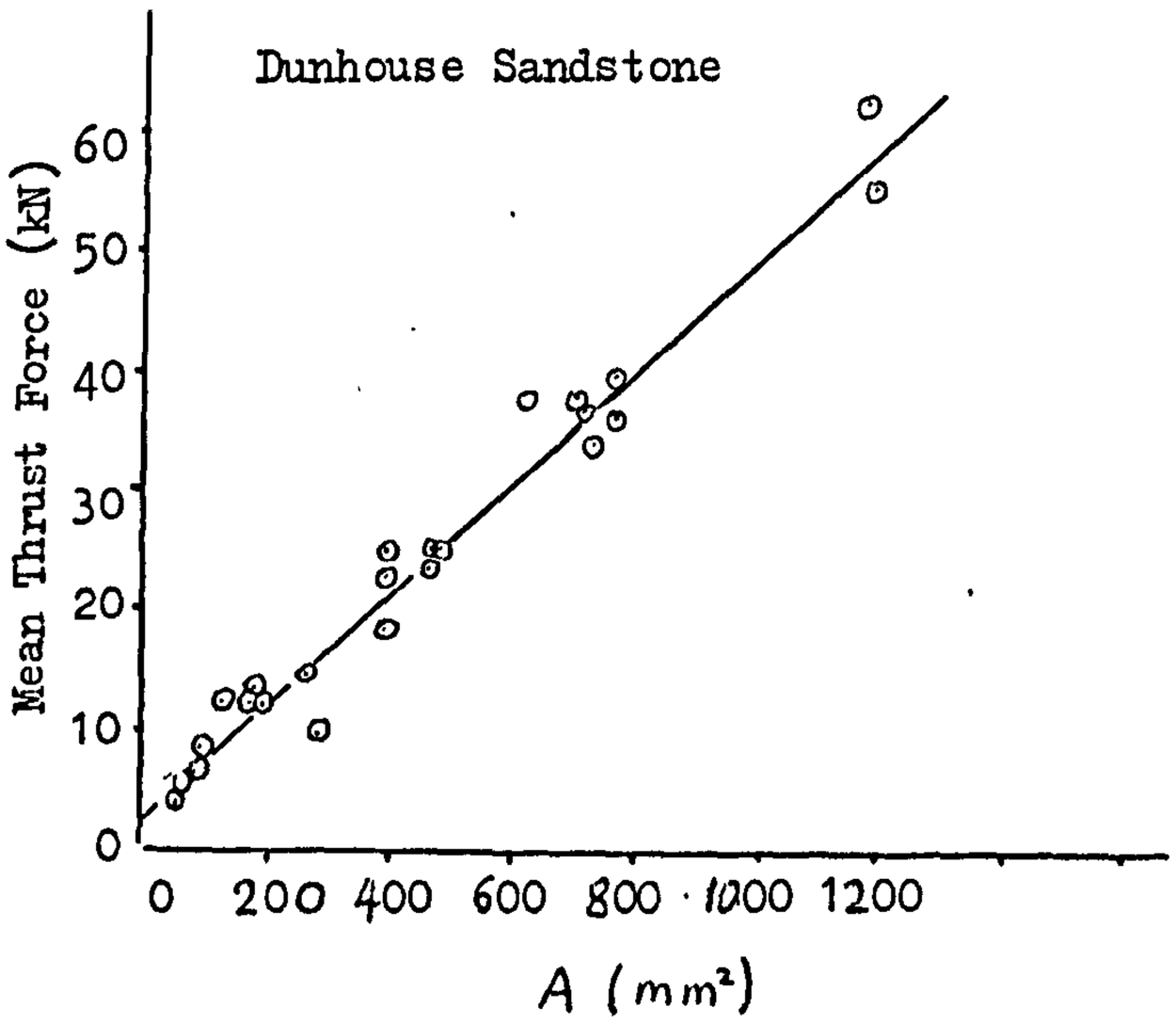

Fig.49 Mean Thrust Force versus Projected Contact Area.

Table 23 Constants of Predictor Equations

$\overline{FT} = a + b A$			$\overline{FT}$ (kN), A in (mm^2)
Rock	a	b	Correlation Coefficient
Gypsum	3.761	0.0612	0.993
Bunter Sandstone	5.399	0.0548	0.969
Dunhouse Sandstone	3.741	0.0472	0.977
Mansfield Sandstone	2.497	0.0782	0.978
Magnesian Limestone	6.089	0.1069	0.991
Anhydrite	3.713	0.1147	0.972

The second step of the analysis was to find a relationship, if indeed one exists, between the constants (a;b) and the rock physical and mechanical properties. The constants a and b were regressed against rock properties. A standard regression analysis programme allowed the best statistical fit to be obtained from a choice of linear,power, exponential, hyperbolic and logarithmic functions. It is found that there is no obvious relationship between the rock properties and the constant a. As can be seen from Appendix 14, the significant rock properties in determining the constant b are rock density, compressive strength and tensile strength, Young's Modulus and impact strength hardness. However, a close check of Appendix 14 shows that the compressive strength is the most dominant factor in determining the cutting performance of disc cutters. Hence, the compressive strength was chosen to develop the predictor equations and to compare the measured

forces with the predicted forces.

The constants 'b' and σ_c are related by a linear equation which was found to be

$$b = 0.0076 + 0.000998\ \sigma_c \qquad ---(14)$$

If a mean value of 'a' is taken for all experimental rocks considered, the final predictor equation becomes,

$$\overline{FT} = 4.2 + (0.0076 + 0.000998\ \sigma_c)A \qquad ---(15)$$

With a correlation coefficient of 0.94 for 6 rocks, in this predictor equation $\overline{FT}$ is in kN, σ_c in MN/m^2, A in mm^2.

The predicted mean thrust forces for 6 different rocks are given in Appendix 15. To demonstrate the accuracy of this equation a plot of the actual and predicted mean thrust force values for 6 different rocks are given in Figs.50, 51 and 52. The mean predicted values used to plot the graphs are directly calculated from the values tabulated in Appendix 15.

* * *

8.2 Prediction of Mean Rolling Forces

The rolling forces are likely to be directly related to the projected area of the disc in the direction of movement. This area is found to be

$$A' = p^2 \tan \frac{\phi}{2} \qquad \text{- - - (16)}$$

where p = The penetration of the disc

ϕ = The disc edge angle.

A typical relationship between mean rolling force and the projected area of the disc in the direction of movement for one of the experimental rocks is shown in Fig.53.

Mean rolling forces for the 6 different rocks were regressed against the area 'A' and the most satisfactory relationship between them was found to be a power function. The constants of the equations are given in Table 24.

Table 24 The Relationship between Mean Rolling Force and the Area 'A'

$\overline{FR} = cA'^{e}$			
Rock	c	e	Correlation Coefficient
Gypsum	0.372	0.7972	0.991
Bunter Sandstone	0.307	0.7556	0.995
Dunhouse Sandstone	0.326	0.8113	0.993
Mansfield Sandstone	0.503	0.7236	0.992
Magnesian Limestone	0.552	0.8711	0.993
Anhydrite	0.815	0.7073	0.991

- - - Predicted Values ——— Measured values

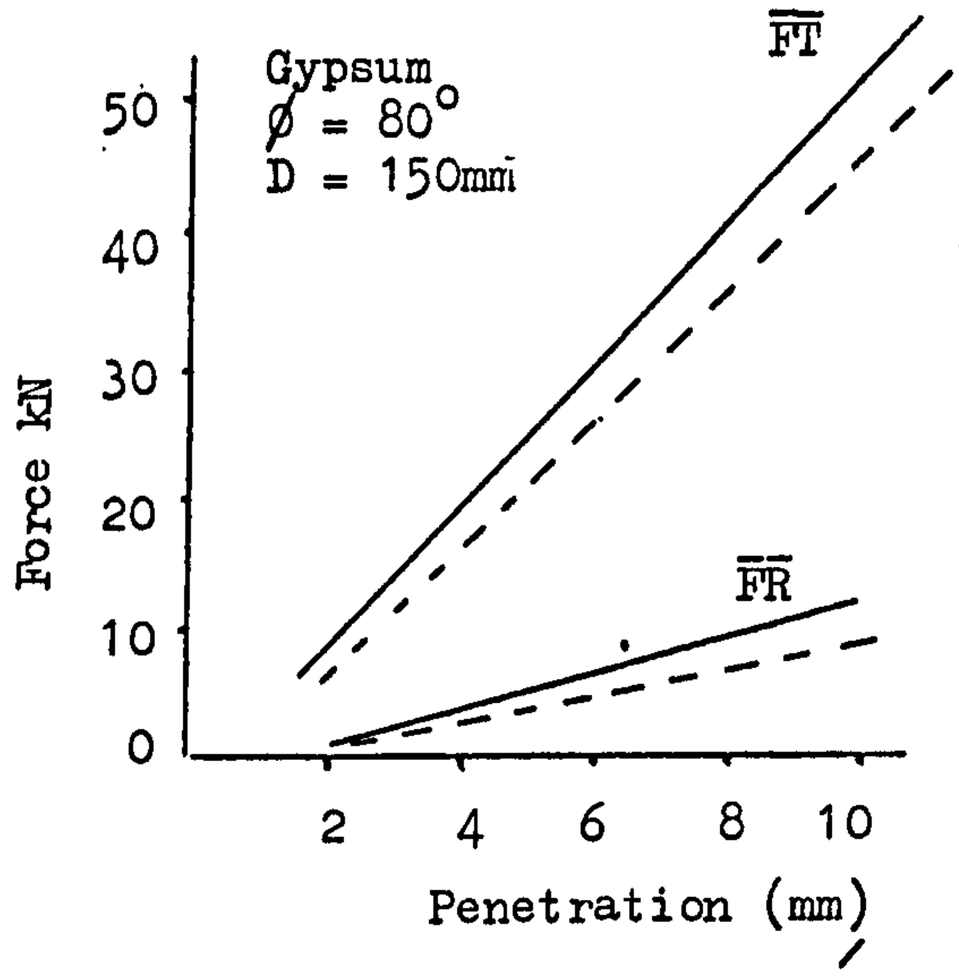

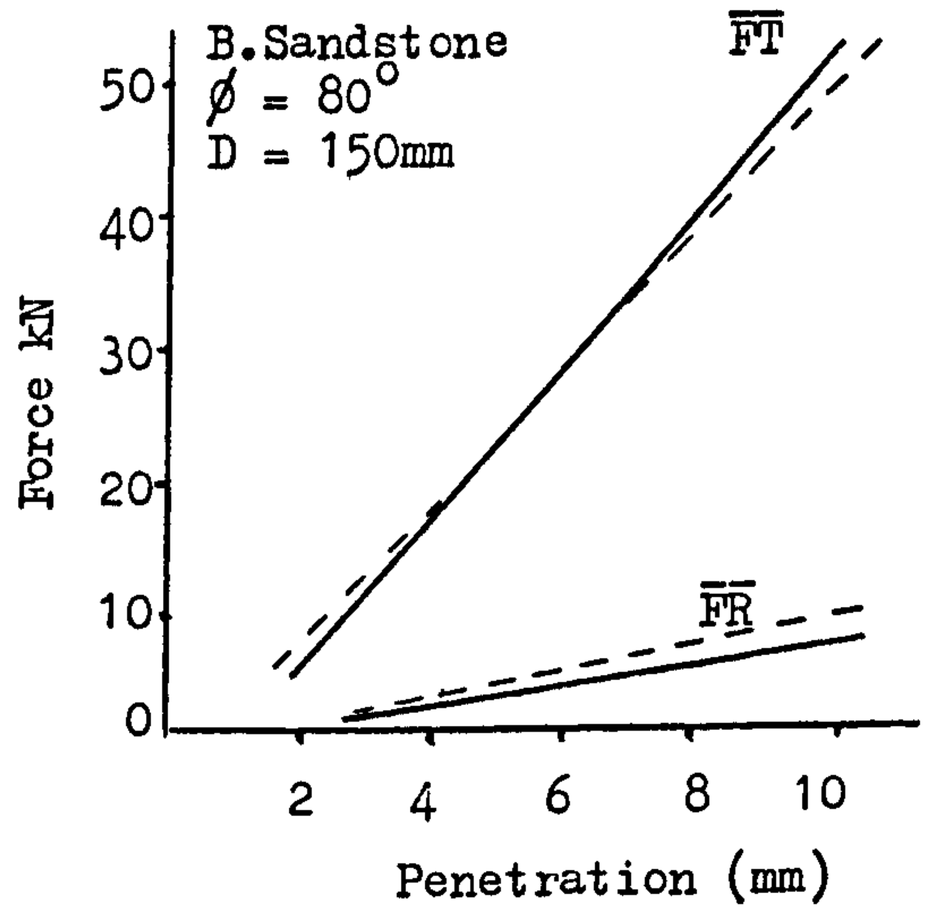

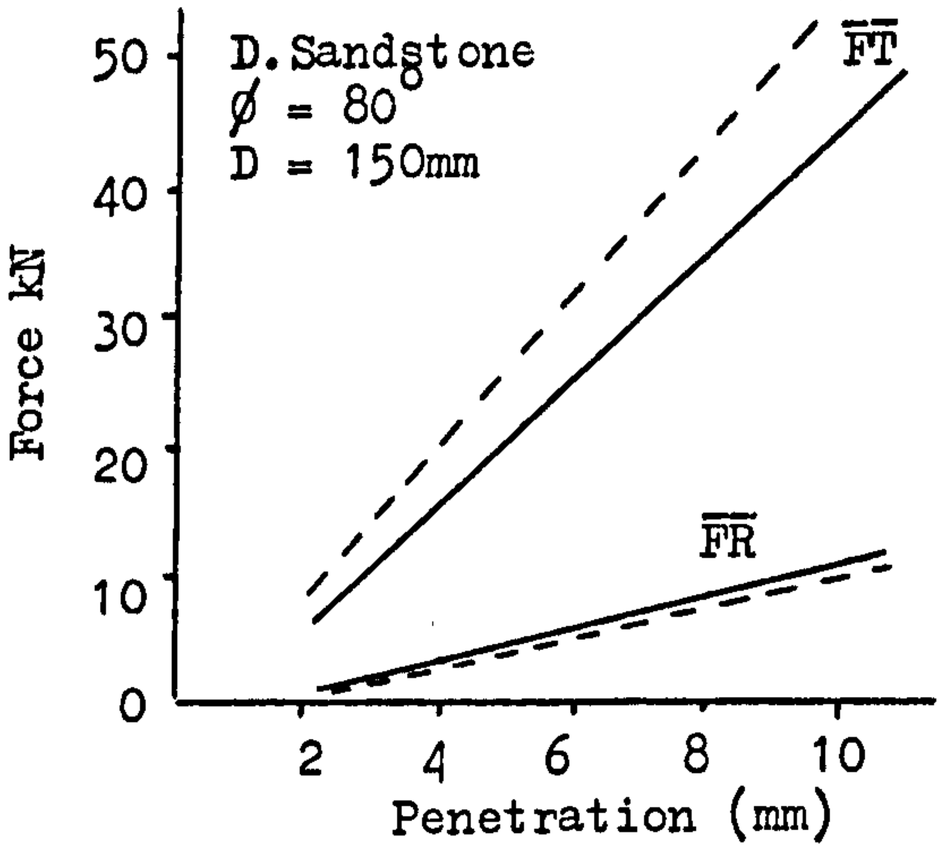

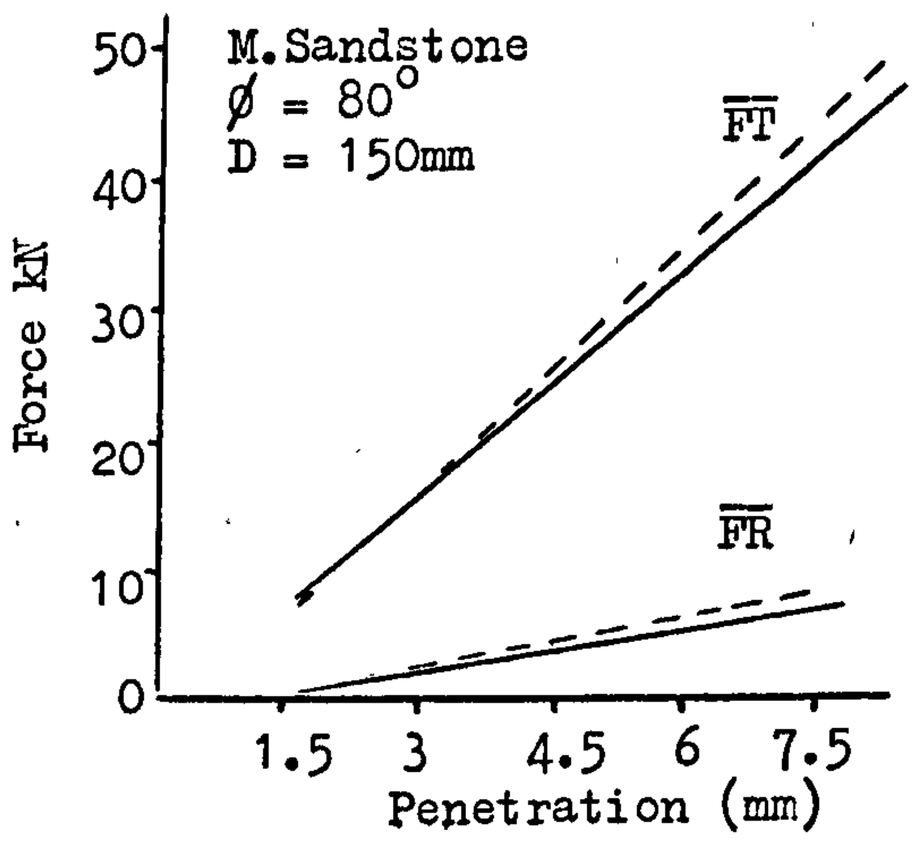

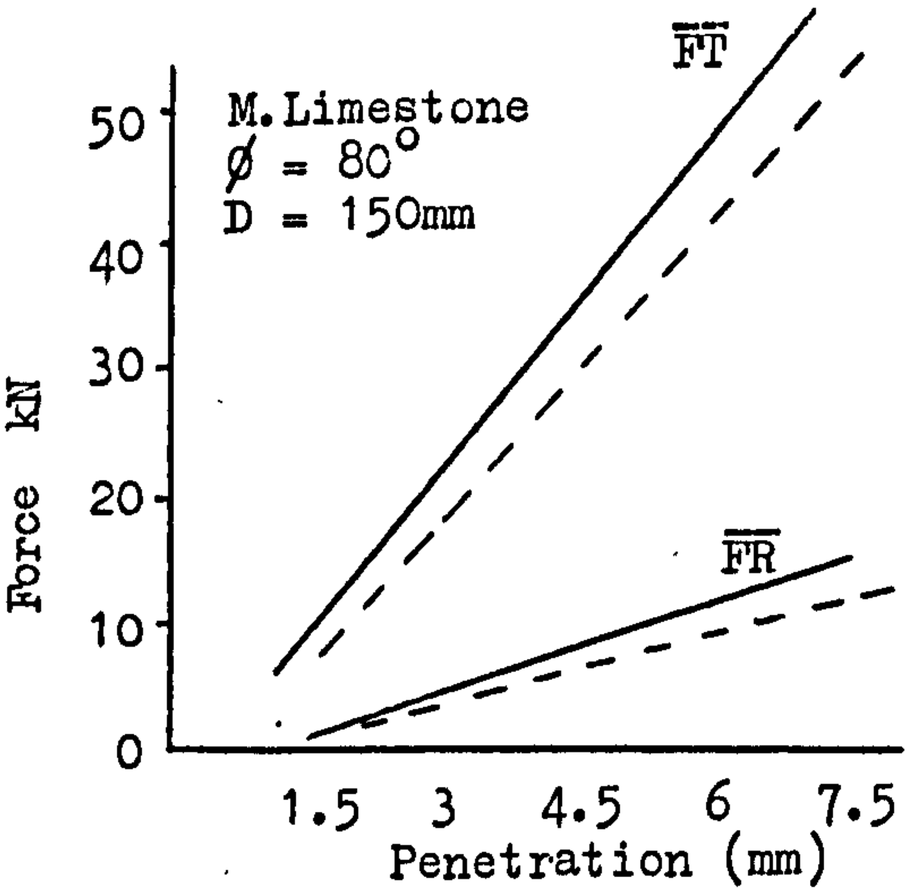

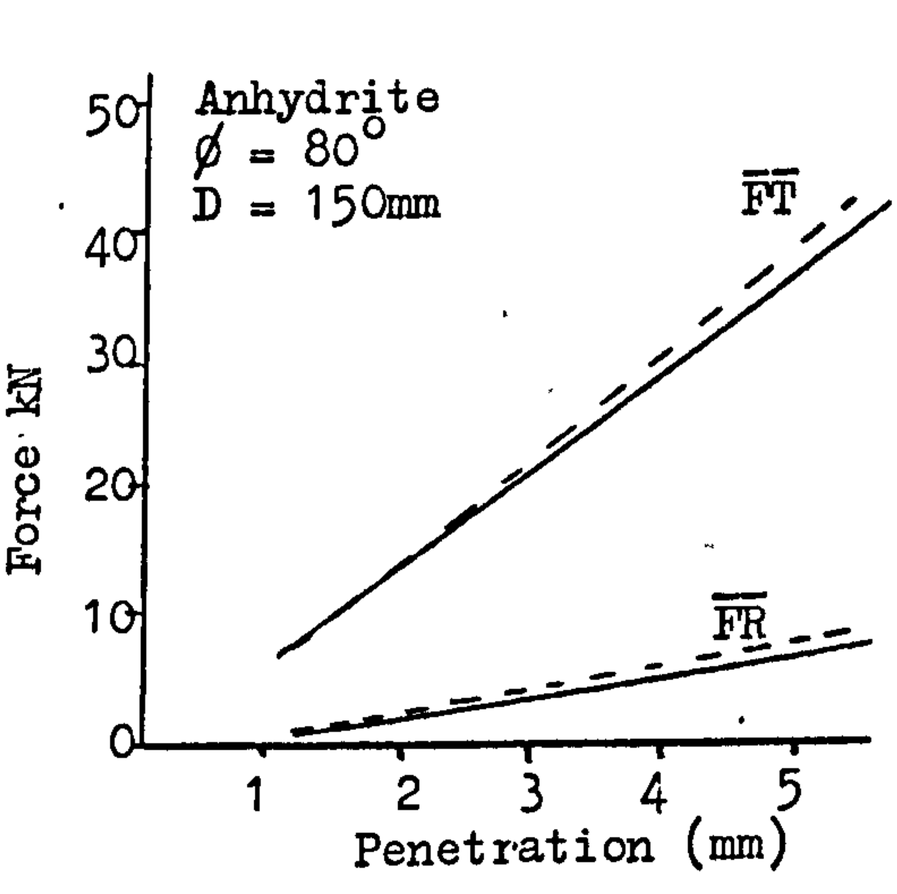

Fig.50 Variation in Measured and Predicted Forces with Disc Penetration.

- - - Predicted values ——— Measured values

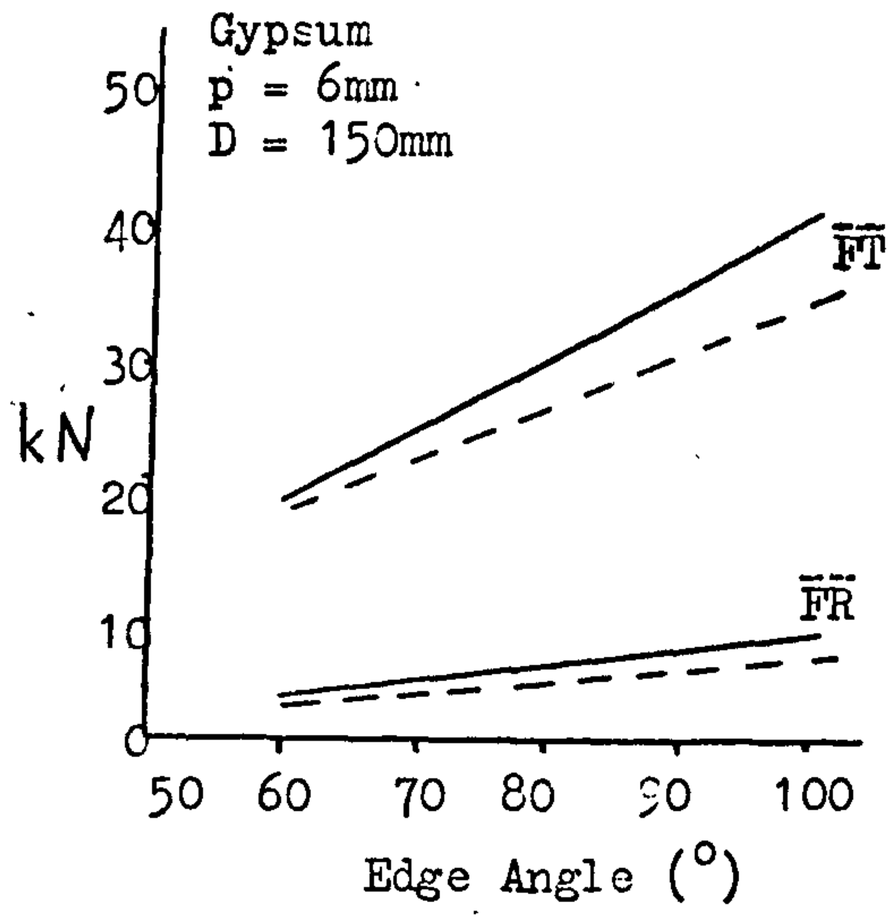

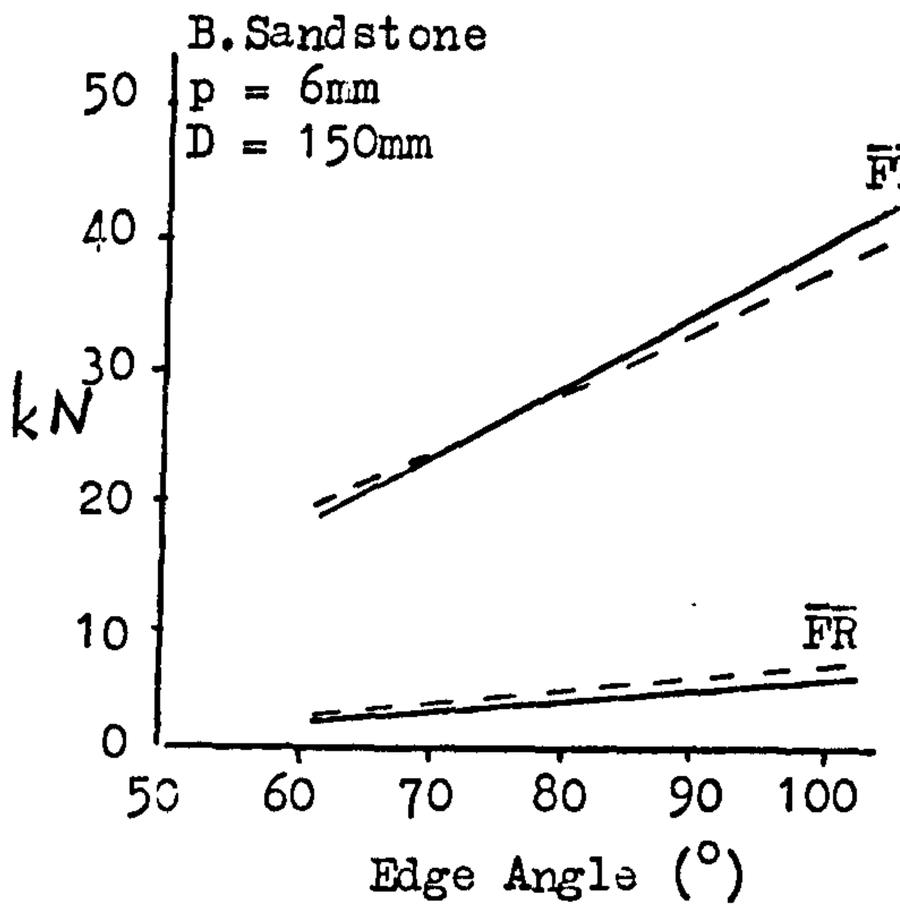

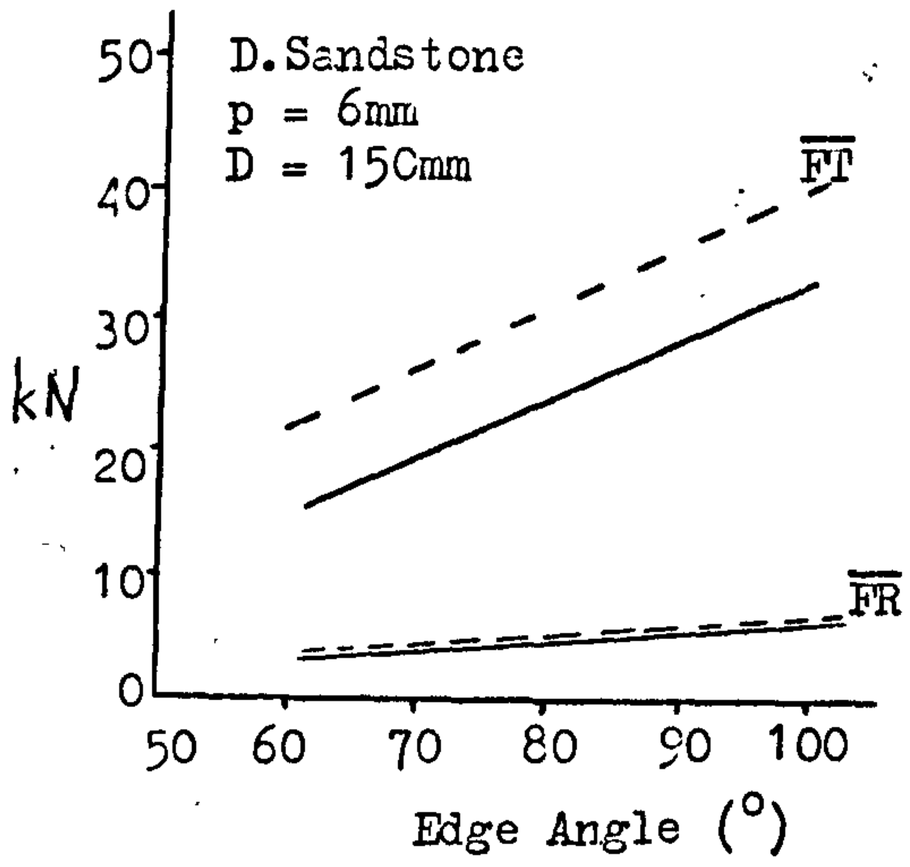

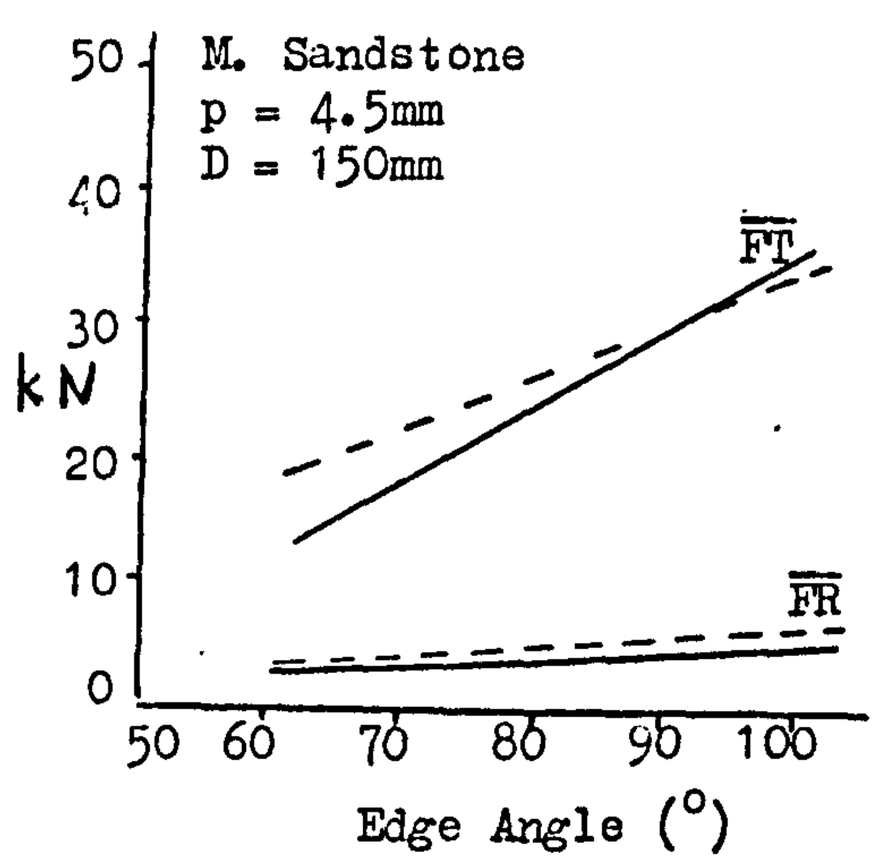

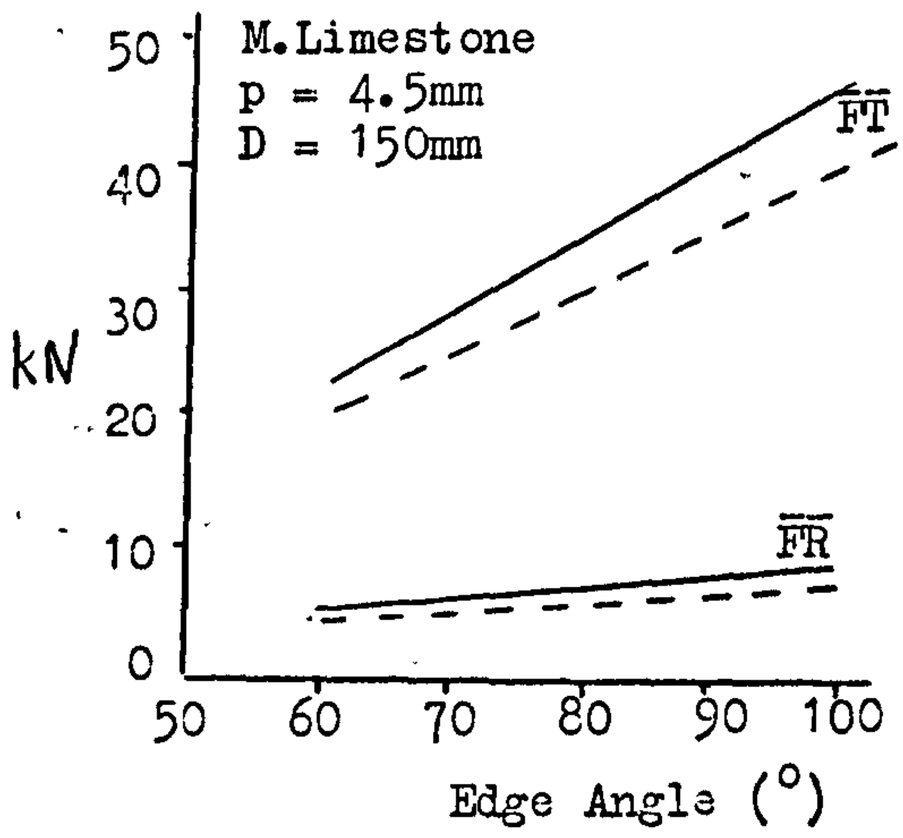

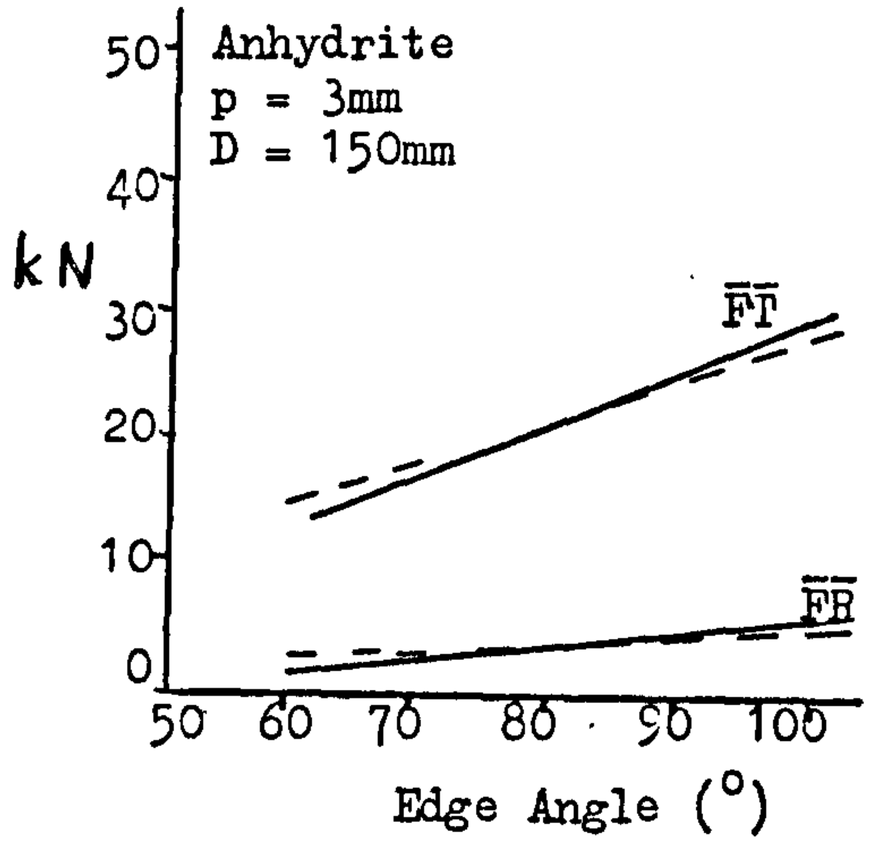

Fig.51 Variation in Measured and Predicted Forces with Disc Edge Angle.

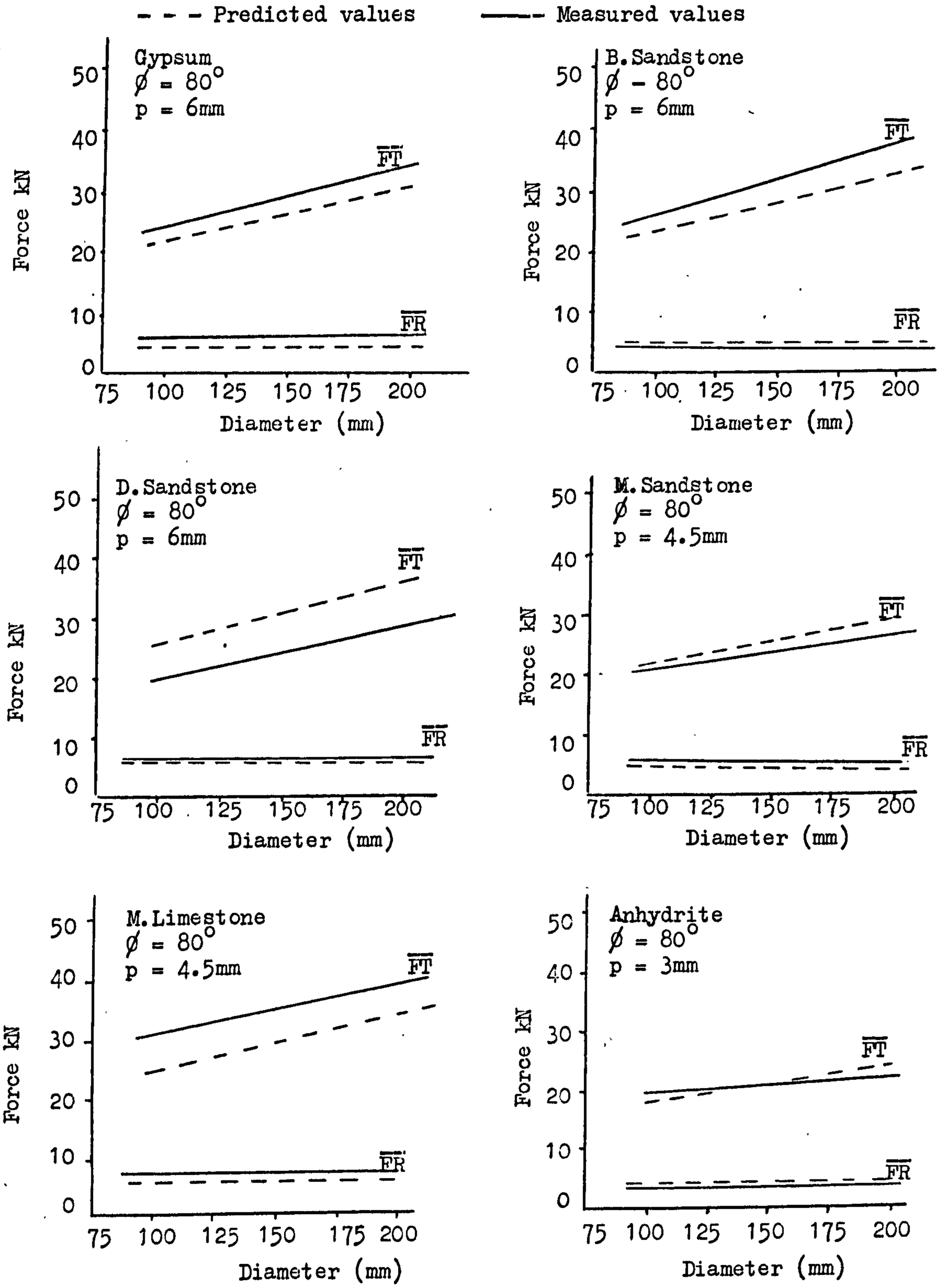

Fig.52 Variation in Measured and Predicted Values with Disc Diameter.

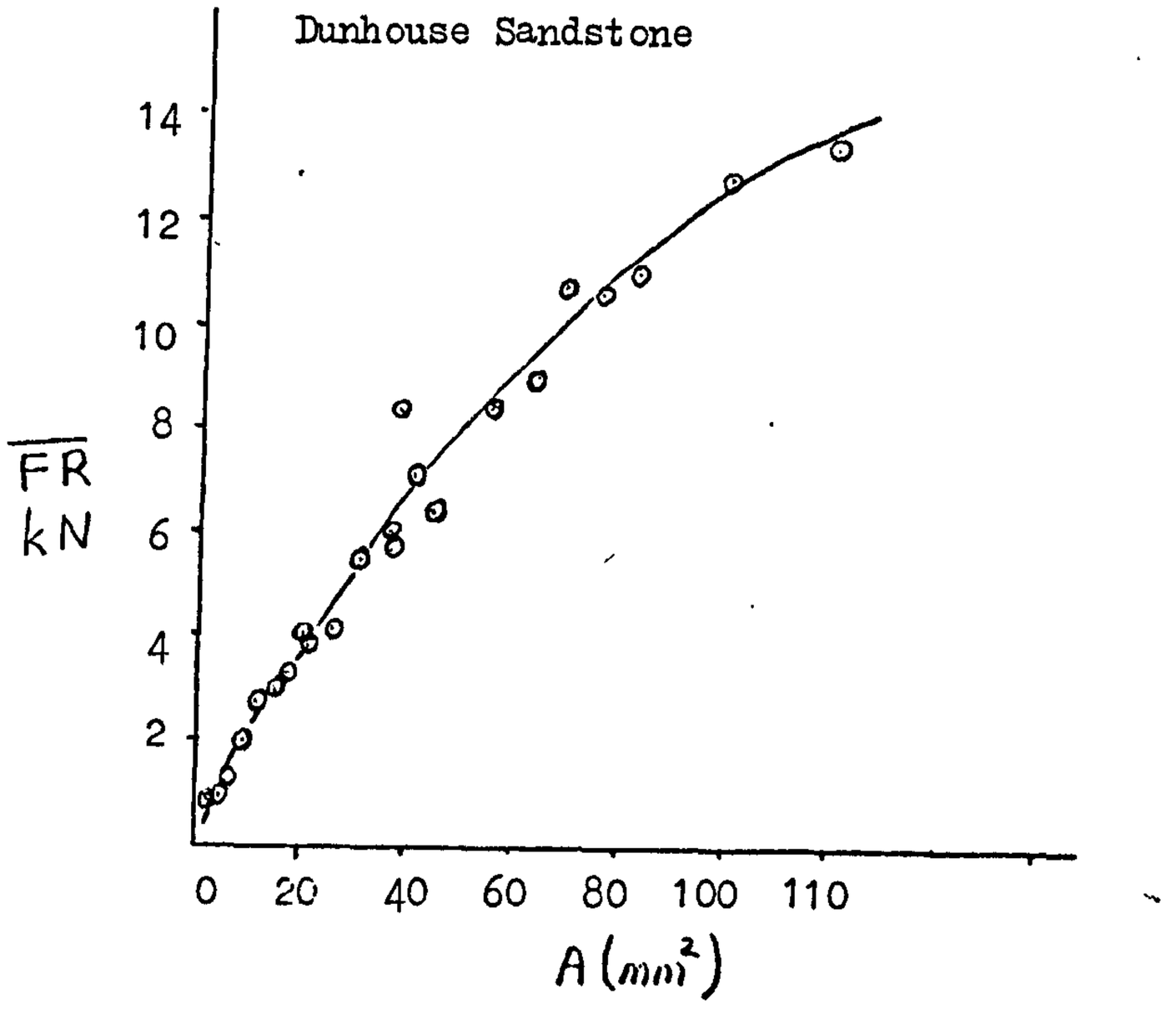

Fig.53 The Projected Area of the Disc in the Direction of Movement versus Mean Rolling Force.

From Appendix 14 it is seen that the most significant rock properties in determining the constant c are, compressive strength, rock density, tensile strength and Young's Modulus. There is no obvious relationship between the constant e and rock properties.

If a mean value of 'e' is taken for all experimental rocks, and the compressive strength is used to predict the mean rolling force, the predictor equation becomes as:

predictor equation becomes as:

$$\overline{FR} = (-0.0249 + 0.0072\ \sigma c)\ A^{0.778} \qquad ---(17)$$

with a correlation coefficient of 0.926 for 6 experimental rocks.

In this predictor equation $\overline{FR}$ is in kN, σc in MN/m^2, A in mm^2.

The predicted mean rolling forces for 6 different rocks are given in Appendix 16. To demonstrate the accuracy of this equation, a plot of the actual and predicted mean rolling forces are given in Figs.50, 51 and 52. The mean predicted values used to plot the graphs are tabulated in Appendix 16C.

* * *

8.3 Prediction of Peak Thrust and Rolling Forces

The same procedure as used in predicting the mean forces was carried out with the peak thrust force and peak rolling force data.

The constants of the linear equation which relates the projected area of disc contact to the peak thrust force are given in Table 25.

Table 25 The Relationship between Peak Thrust Forces and Projected Areas for 6 different rocks.

$F'T = a' + b'A$			
Rock	a'	b'	Correlation Coefficient
Gypsum	4.849	0.0642	0.990
Bunter Sandstone	6.729	0.0598	0.972
Dunhouse Sandstone	6.399	0.0580	0.980
Mansfield Sandstone	5.663	0.0844	0.983
Magnesian Limestone	9.861	0.1206	0.987
Anhydrite	5.356	0.1319	0.964

The significant rock properties in determining peak thrust force are rock density, compressive strength and tensile strength, as seen in Appendix 14.

The constant 'b' is a linear function of the compressive strength. There is no obvious relationship between the rock physical properties and the constant 'a'.

The final predictor equation is

$$F'T = 6.48 + (0.003 + 0.0012\ \sigma c)A \qquad ---(18)$$

Predicted F'T values for 6 rocks are tabulated in Appendix 17. These values regressed against measured F'T values give a correlation coefficient of 0.955.

Peak rolling force increases in a power manner with the projected area of the disc in the direction of movement. The constants of the power function are given in Table 26.

Table 26 The Relationship between Peak Rolling Forces and the Projected Area A'.

$F'R = c'A'^{e'}$			
Rock	c'	e'	Correlation Coefficient
Gypsum	0.414	0.7817	0.991
Bunter Sandstone	0.440	0.7417	0.995
Dunhouse Sandstone	0.462	0.7832	0.990
Mansfield Sandstone	0.625	0.7015	0.995
Magnesian Limestone	0.734	0.8054	0.990
Anhydrite	1.106	0.6792	0.989

The significant rock properties in determining the constant c' are compressive strength, rock density, tensile strength and Young's Modulus. If the mean values of e' are taken, the final predictor equation becomes

$$F'R = (0.0782 + 0.01\ \sigma c)A'^{0.75} \qquad ---(19)$$

The predicted values of F'R given in Appendix 17, when regressed against the measured F'R, give a correlation coefficient of 0.951.

* * *

8.4 Prediction of Disc Groove Angle

Disc groove angle α as defined in Fig.29, is a major factor to predict the yield and specific energy.

Evans[8] formulates α as:

$$\alpha = \frac{\pi}{2} + \theta + \psi + \phi \qquad ---(20)$$

For a wedge indentation, Paul and Sikarskie[92] formulate α as:

$$\alpha = \frac{\pi}{2} + \theta + \psi + \phi \qquad ---(21)$$

Where 2θ is Disc or Wedge Angle

ψ is Friction Angle between Rock and Cutting Tool

ϕ is Internal Friction Angle of the Rock.

The experiments carried out in 6 different rocks at the University of Newcastle upon Tyne showed that α is independent of disc edge angle for the majority of the rocks tested. The general equation relating the yield to the disc penetration was in the form of

$$Q = k p^2 + b.$$

Assuming that b is small and the yield is independent of disc edge angle, the equation shown above then becomes:

$$Q = k p^2$$

From the geometry of the disc groove the yield is

$$Q = 10^{-3} p^2 \tan \frac{\alpha}{2}$$

$$\text{i.e. } \tan \frac{\alpha}{2} = 10^3 k.$$

The mean value of $\tan\frac{\alpha}{2}$ was calculated for each experimental rock. As can be seen in Fig.54, a close relationship exists between $\tan\frac{\alpha}{2}$ and the sum of the value of internal friction angle and sliding friction angle.

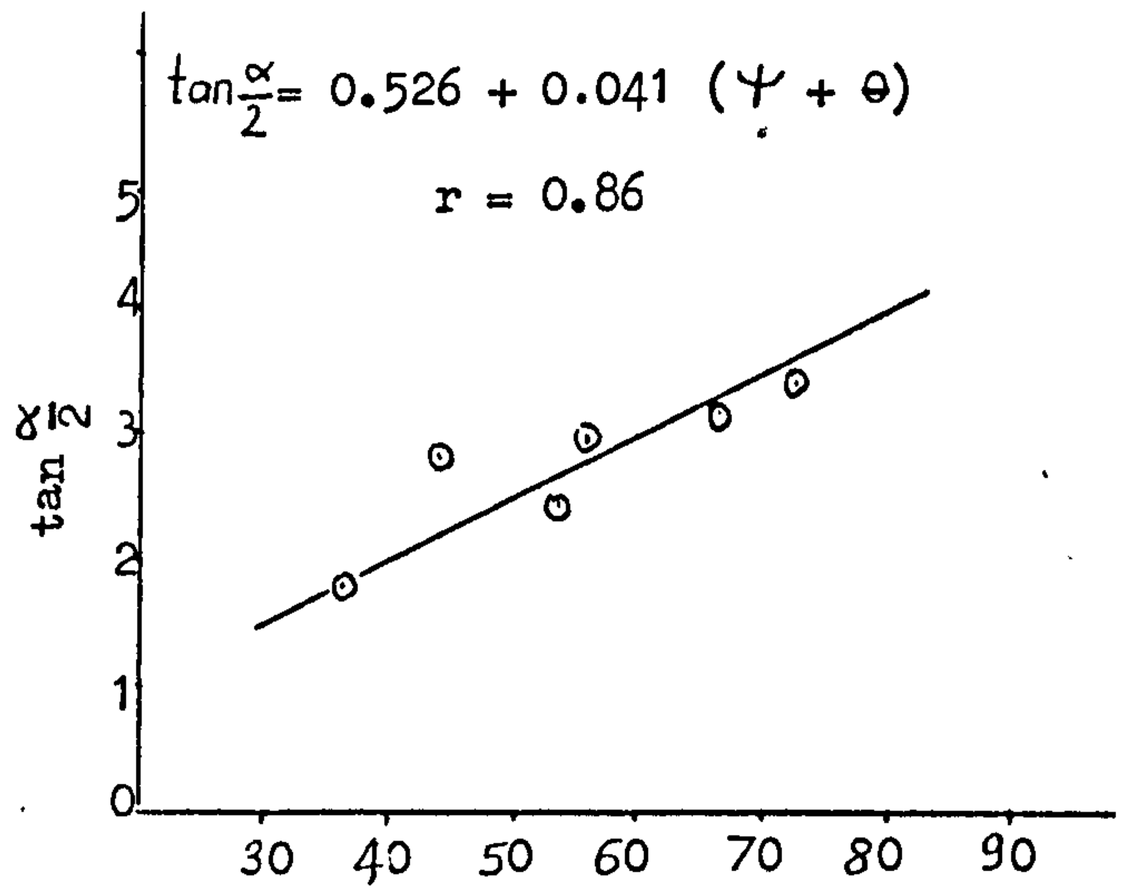

Fig.54 The relationship between the groove angle, the sum of the internal friction angle and the sliding friction angle.

The actual and predicted values of disc groove angle are given in Table 27.

Table 27 The actual and predicted values of disc groove angle.

Rock	Internal Friction Angle (°)	Sliding Friction Angle (°)	Actual Groove Angle (o)	Predicted Groove Angle (o)
Gypsum	30	42.0	147.0	147.9
Anhydrite	45	21.4	145.6	145.8
Bunter Sandstone	25	19.3	142.0	133.8
Mansfield Sandstone	47	9.6	137.8	141.3
Dunhouse Sandstone	43	10.4	133.1	139.6
Magnesian Limestone	18	18.8	119.2	127.7

* * *

8.5 The Comparison of the Predicted and Measured Performance of Disc Cutters

Experiments with one disc of 60° edge angle and 150mm diameter were carried out in Weardale Limestone, Greywacke and Granite. The main objective of these tests was to see the validity of the predictor equations for high strength rocks. As seen from Fig.55, the predicted force values of Weardale Limestone are very close to the measured force values. A disc of 1mm edge radius was used to test Granite, since the sharp edge of the other experimental discs deteriorated quickly in this rock. In this case, the measured force values should be corrected, since blunt discs give different results to sharp discs.

The following formula which were developed in Chapter 9 were used to correct the mean thrust and rolling forces:

$$\overline{FT}_r = \overline{FT}_{ro}\, e^{Ar} \qquad \text{---(23)}$$

$$\overline{FR}_r = \overline{FR}_{ro}\, e^{Br} \qquad \text{---(24)}$$

where $A = 0.0354 + \frac{0.6554}{p}$

$$B = 0.06 + \frac{0.383}{p}$$

$\overline{FT}_{ro}$, $\overline{FR}_{ro}$ = The forces for a sharp disc

FT_r, FR_r = The forces for a disc with an edge radius of r

p = Disc penetration.

—— Actual Values

- - - Predicted Values

-·-·- Corrected Predicted Values

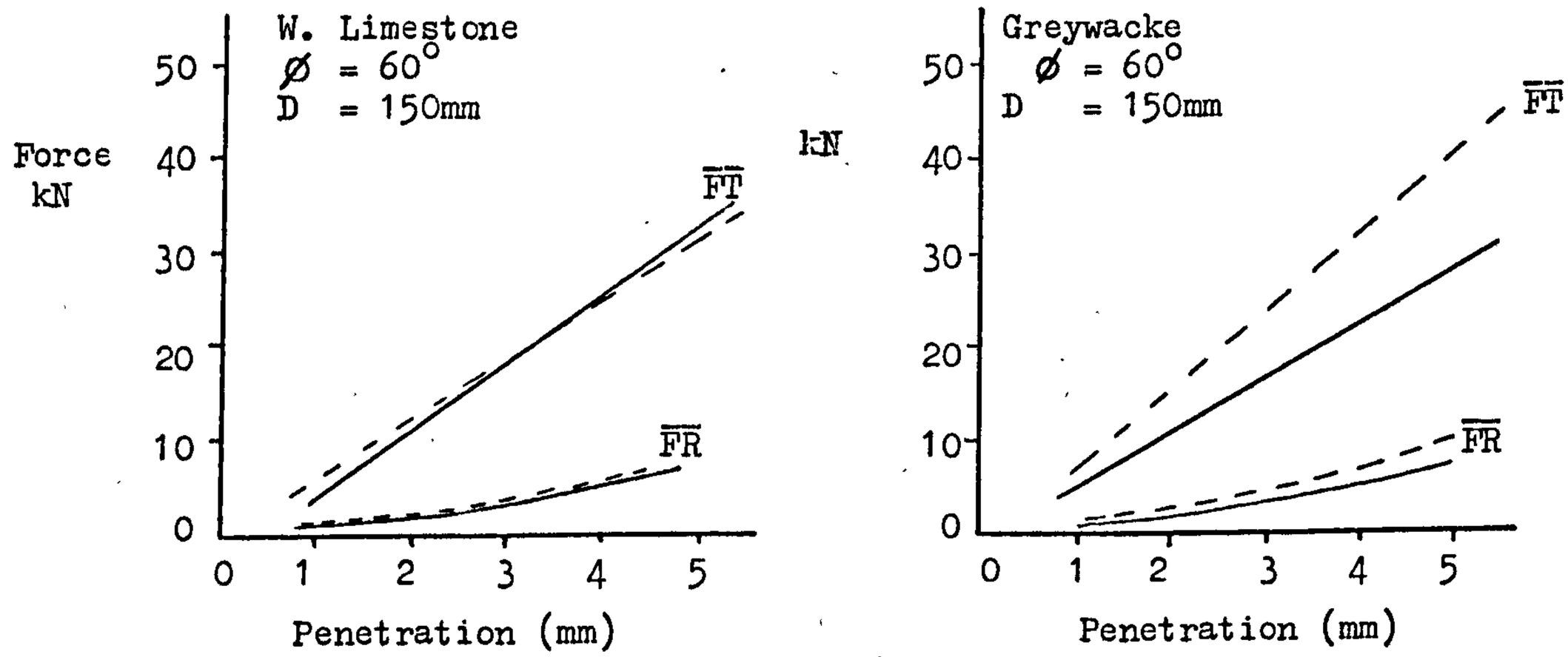

Fig.55 Mean Rolling and Thrust Forces versus Disc Penetration.

As can be seen from Fig.55, the measured mean thrust and rolling forces are about 30% higher than predicted force values in Granite and Greywacke.

Table 28 shows that the prediction of groove angles for two high strength rocks are very accurate . Granite is not included in this Table since the complexity of the effect of edge radius on groove angle makes it difficult to predict.

Table 28 Predicted and Measured Groove Angles

Rock	Internal Friction Angle(o)	Sliding Friction Angle(o)	Measured Groove Angle(o)	Predicted Groove Angle (o)
Weardale Limestone	37	23.4	144.0	143.2
Greywacke	33	11.3	136.0	133.5

* * *

8.6 The Comparison of Predicted and Measured Disc Cutter Performance for Rocks tested in U.S.B.M.

The experimental disc used in U.S.B.M. had an edge radius of 0.8mm. The measured values should be corrected according to formula mentioned above, since the predictor equations developed for the 6 experimental rocks are only valid for sharp discs.

As shown in Figs. 55 and 56, the predicted mean thrust force values are accurate for rocks with a compressive strength ranging from 64 to 118 MN/m^2. However, the predicted $\overline{FT}$ values lose their accuracy for high strength rocks.

* * *

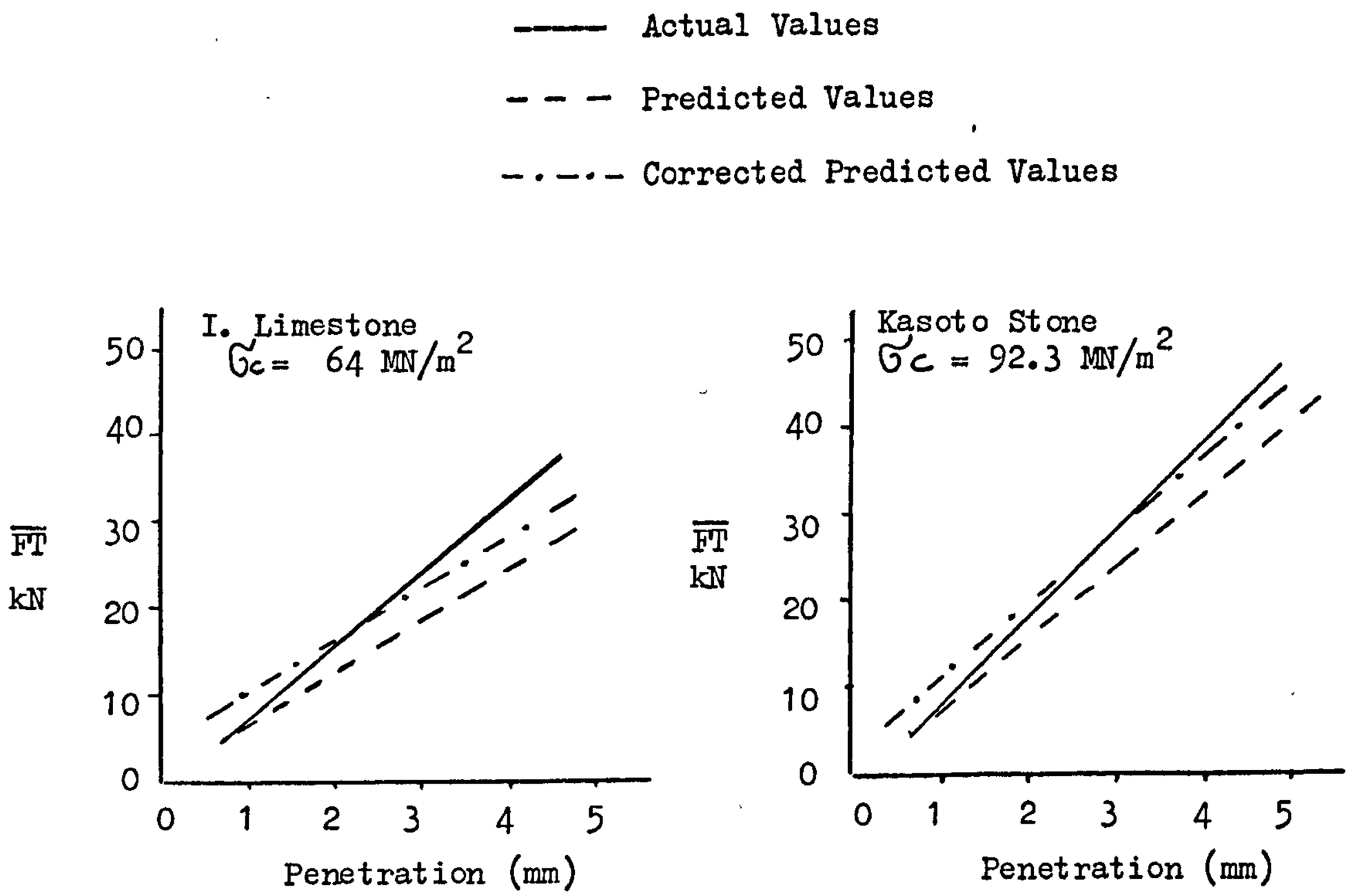

$\phi = 90°$ D = 177.8 mm

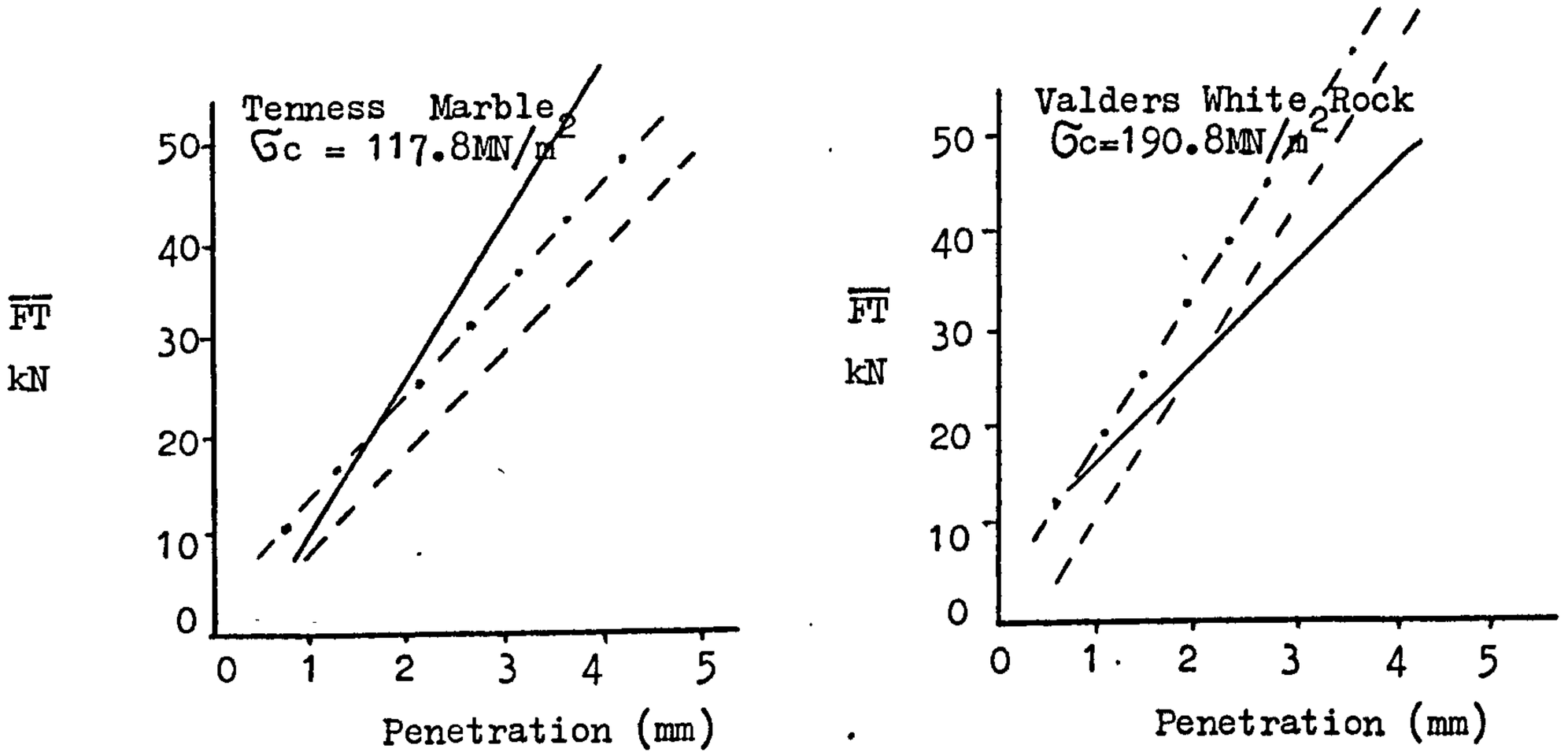

Fig.56A Mean Thrust Force versus Disc Penetration.

——— Actual Values

— — — Predicted Values

—·—·— Corrected Predicted Values

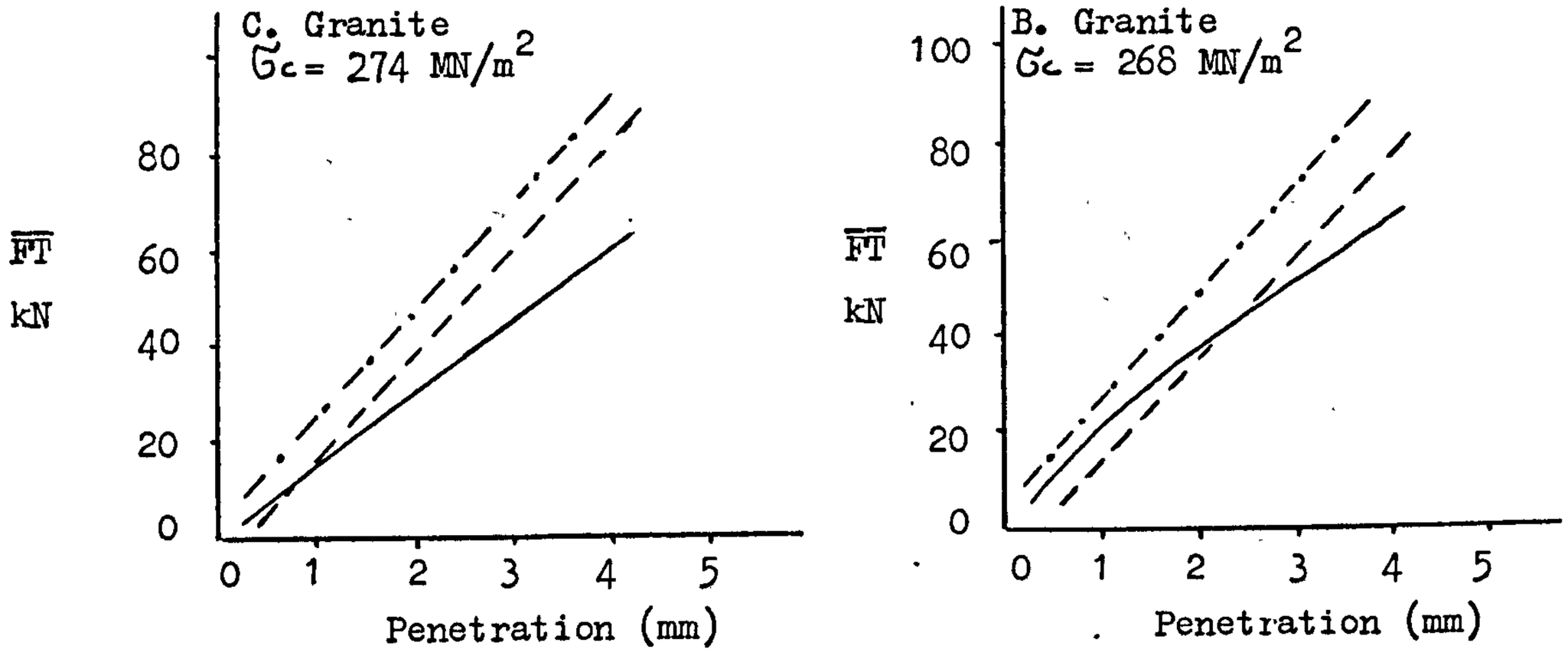

ϕ = 90° D = 177.8mm (after U.S.B.M.)

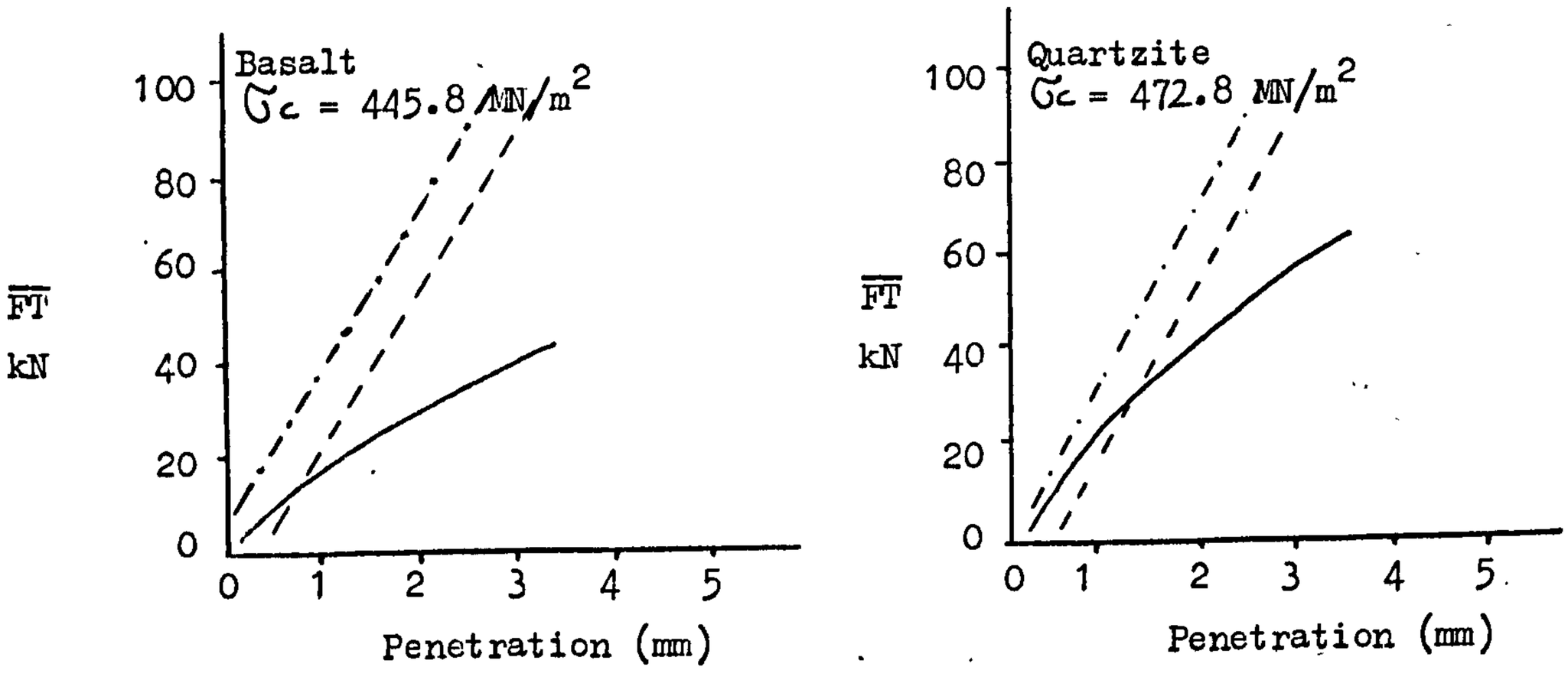

Fig.56B Mean Thrust Force versus Disc Penetration.

8.7 Conclusions

This work has provided a unique opportunity to predict disc cutter forces from a single rock property and disc geometry. The conclusions to be drawn from this analysis can be summarised as follows:

1. The most dominant rock properties in determining disc cutter forces are compressive strength, rock density and tensile strength. Young's Modulus and impact strength Index are of minor importance.

2. Thrust force is linearly related to the compressive strength of the rock and the projected area of disc contact.

3. Rolling force is a power function of the projected area of the disc in the direction of movement and correlates well with the compressive strength of the rock.

4. Disc groove angle is a function of the sum of internal friction angle of the rock and the sliding friction angle between disc and rock.

5. The predicted performance of disc cutters is reasonably good in high strength rocks.

6. The predicted mean thrust force values for the rocks tested at the U.S.B.M. are in good agreement with measured mean thrust force values in medium strength rocks, but not in high strength rocks.

* * *

CHAPTER NINE

EFFECT OF EDGE RADIUS ON THE CUTTING PERFORMANCE OF DISC CUTTERS

One of the most important factors in determining the economic success of a hard rock tunnel bore is the amount of the cutter costs. In a tunnel constructed in an abrasive and hard rock this might be as high as 57£/m^3[5]. A careful study of the wear processes of disc cutters could be a ccnsiderable help in understanding methods of reducing cutter costs. During the past few years new cutters have been developed which withstand 15-20 ton thrust force[93]. A sharp edge on a disc cutter can not resist loads of this magnitude when subjected to grinding through an abrasive rock. The experience gained by different tunnel boring machine manufacturers in abrasive and hard formations led them to use discs with different edge radius in order to prolong disc life. Although the importance of edge radius to the effective performance of a disc cutter has been acknowledged by different research workers, few results are available[19,26], and some of them are misleading due to the experimental technique which has been used, i.e. Rad, defining edge bluntness as in Fig.57, concluded that[26]

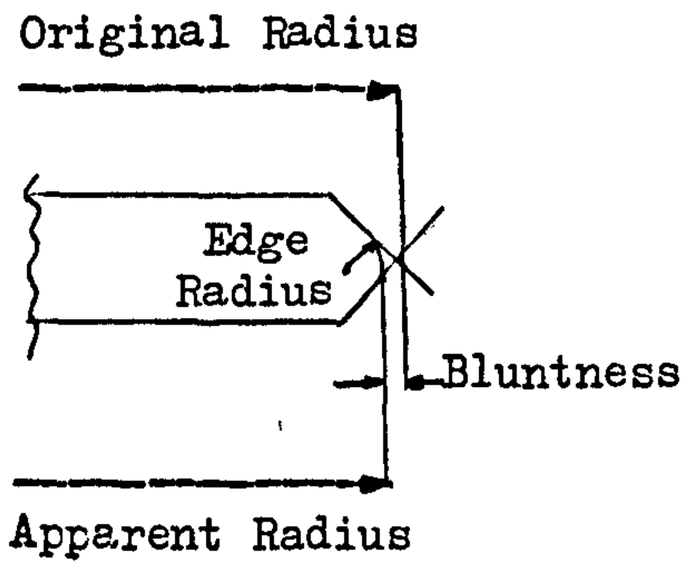

Fig.57 Definition of Disc Bluntness (after Rad)

1. For each level of thrust force, penetration, fineness modulus, yield and groove width decrease with increasing bluntness.

2. Specific energy increases considerably with increasing edge bluntness, where 'bluntness' is defined as in Fig.57.

In order to obtain a better understanding of the cutting performance of blunt discs some new experiments were designed and executed in the laboratory. Different rock materials have been tested in order to assess the affect of the rock properties on blunt disc cutting performance.

* * *

9.1 Experimental Technique and Procedure

A series of six disc cutters were manufactured of tool-steel, having a hardness of 60R, in the Department's workshop. All discs have a 60° edge angle, 150mm diameter. Each has a different edge radius, i.e. 0, 1, 1.5, 2, 2.5, 3mm respectively. Fig.58 shows the profiles of these disc cutters. The independent variables in the experiment were the penetration of the disc and the spacing between the grooves. The penetration was set at levels of 2, 3, 4, 6, 7, 8 and the spacing/penetration ratio was set at 1, 5, 6, 7, 8, 9. The initial rock material was Bunter Sandstone. Three different discs of 0, 1, 2mm edge radii were used for an experiment in Weardale Limestone at levels of 1, 3, 4, 5mm penetration. Only a sharp disc and a 1mm edge radius disc were used for Greywacke. A sharp disc generated after a few cuts in granite, thus a 1mm radius tool was used.

* * *

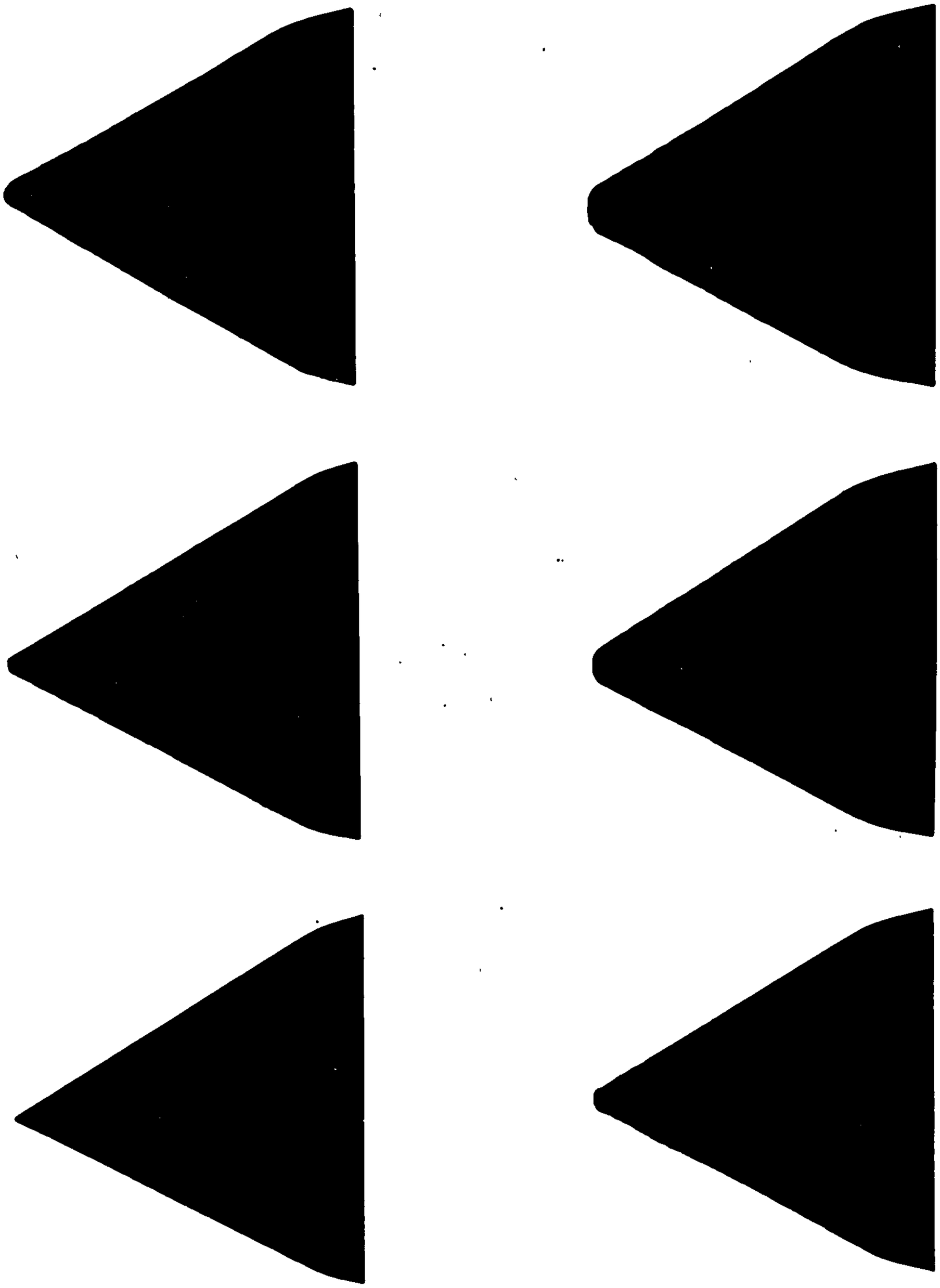

Fig.58 Disc Cutters with Different Edge Radius.

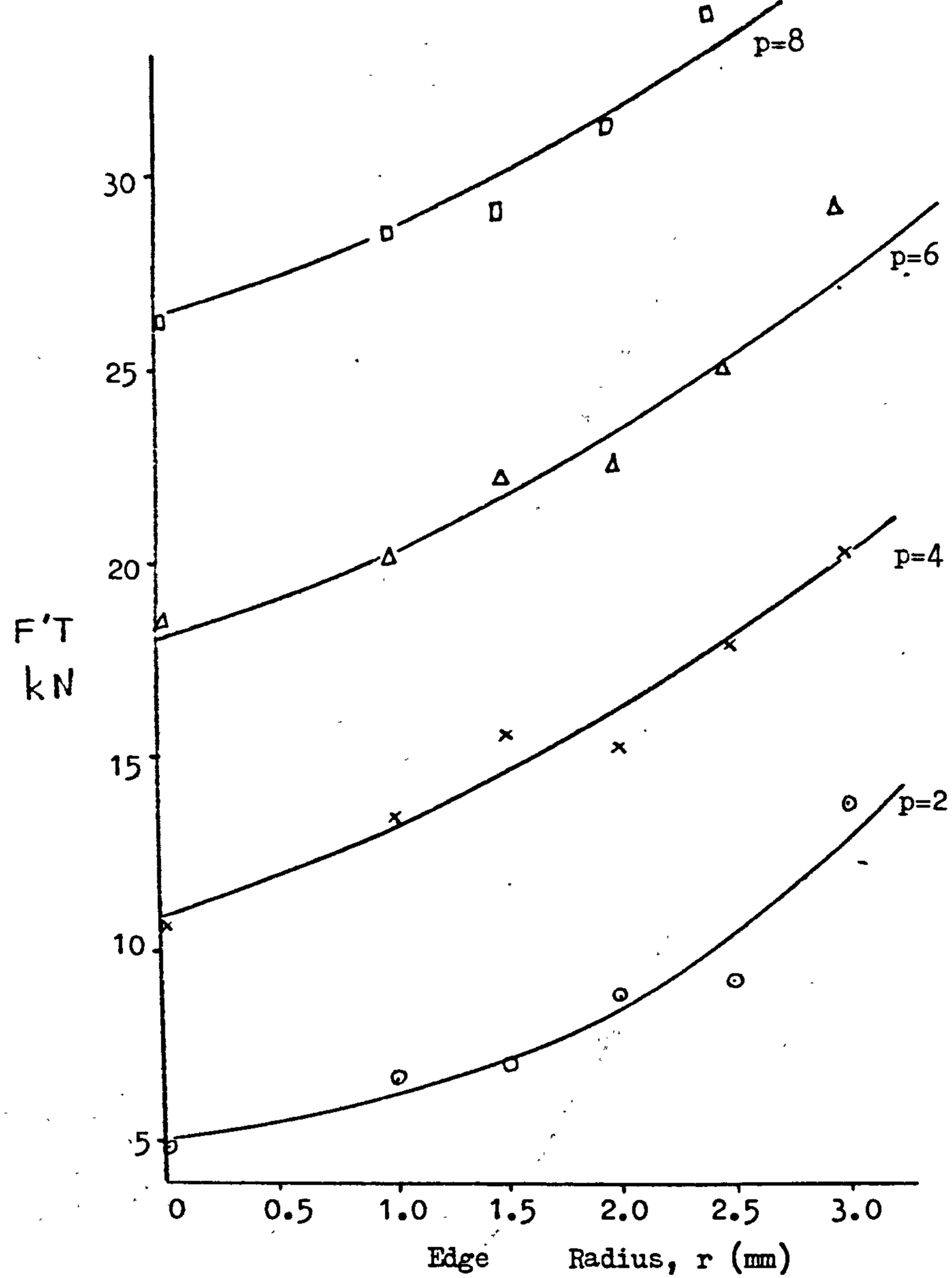

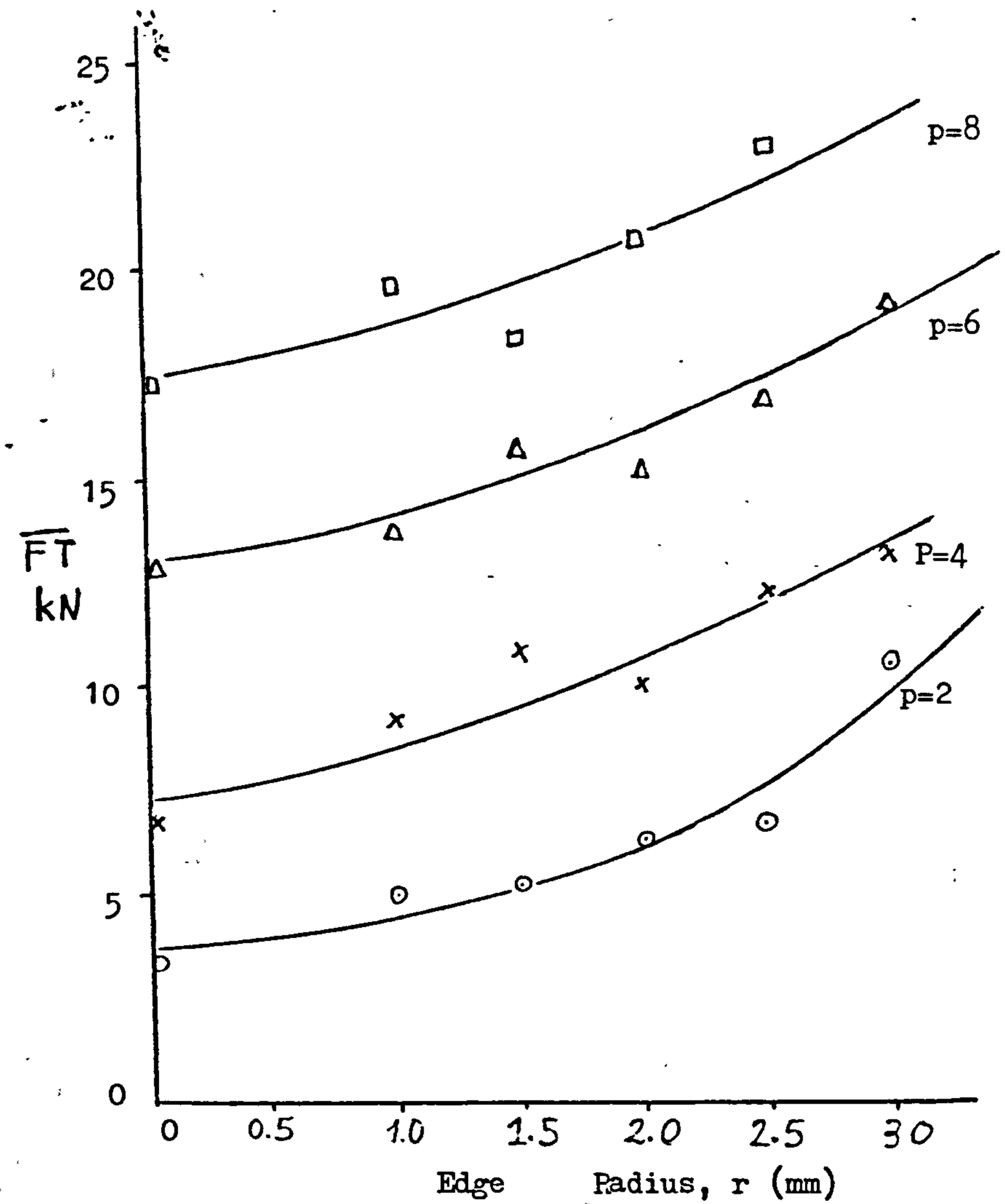

Fig.58 Variation in Thrust Forces with Edge Radius.

9.2 Effect of Edge Radius on Thrust Force

Fig.58 shows the variation of peak thrust force and mean thrust force with edge radius for each level of penetration in Bunter Sandstone. All experimental data for thrust force and the other dependent variables are given in Appendix 19. In each case thrust force increases with edge radius. A least squares regression technique has been used for the analysis of the experimental data and it is found that the thrust force is related to the edge radius in an exponential manner. All the equations are in the form of

$$F'T_r = F'T_{ro}\, e^{A'r} \qquad ---(25)$$

$$\overline{FT}_r = \overline{FT}_{ro}\, e^{Ar} \qquad ---(26)$$

where $F'T_r$, $\overline{FT}_r$ = Thrust force for a disc of r mm edge radius

$F'T_{ro}$, $\overline{FT}_{ro}$ = Thrust force for a sharp disc

A is a constant, r is edge radius.

These equations and correlation coefficients are given in Table 29.

Table 29 The relationship between edge radius and thrust force.

P mm	Equations for $F'T$	Correlation Coefficient	Equations for $\overline{FT}$	Correlation Coefficient
2	$F'T = 4.76e^{0.317r}$	0.97	$\overline{FT} = 3.31e^{0.346r}$	0.97
3	$F'T = 8.07e^{0.245r}$	0.98	$\overline{FT} = 5.27e^{0.280r}$	0.98
4	$F'T = 10.85e^{0.205r}$	0.98	$\overline{FT} = 7.18e^{0.211r}$	0.98
6	$F'T = 17.68e^{0.144r}$	0.93	$\overline{FT} = 12.58e^{0.126}$	0.95
7	$F'T = 20.56e^{0.136r}$	0.99	$\overline{FT} = 14.28e^{0.142}$	0.97
8	$F'T = 25.76e^{0.104r}$	0.96	$\overline{FT} = 17.10e^{0.102}$	0.88

As can be seen from Fig.59, the constants A' and A of the equations (25) and (26) decrease with increasing disc penetration, suggesting that the effect of edge radius on thrust force is reduced when using deeper penetrations.

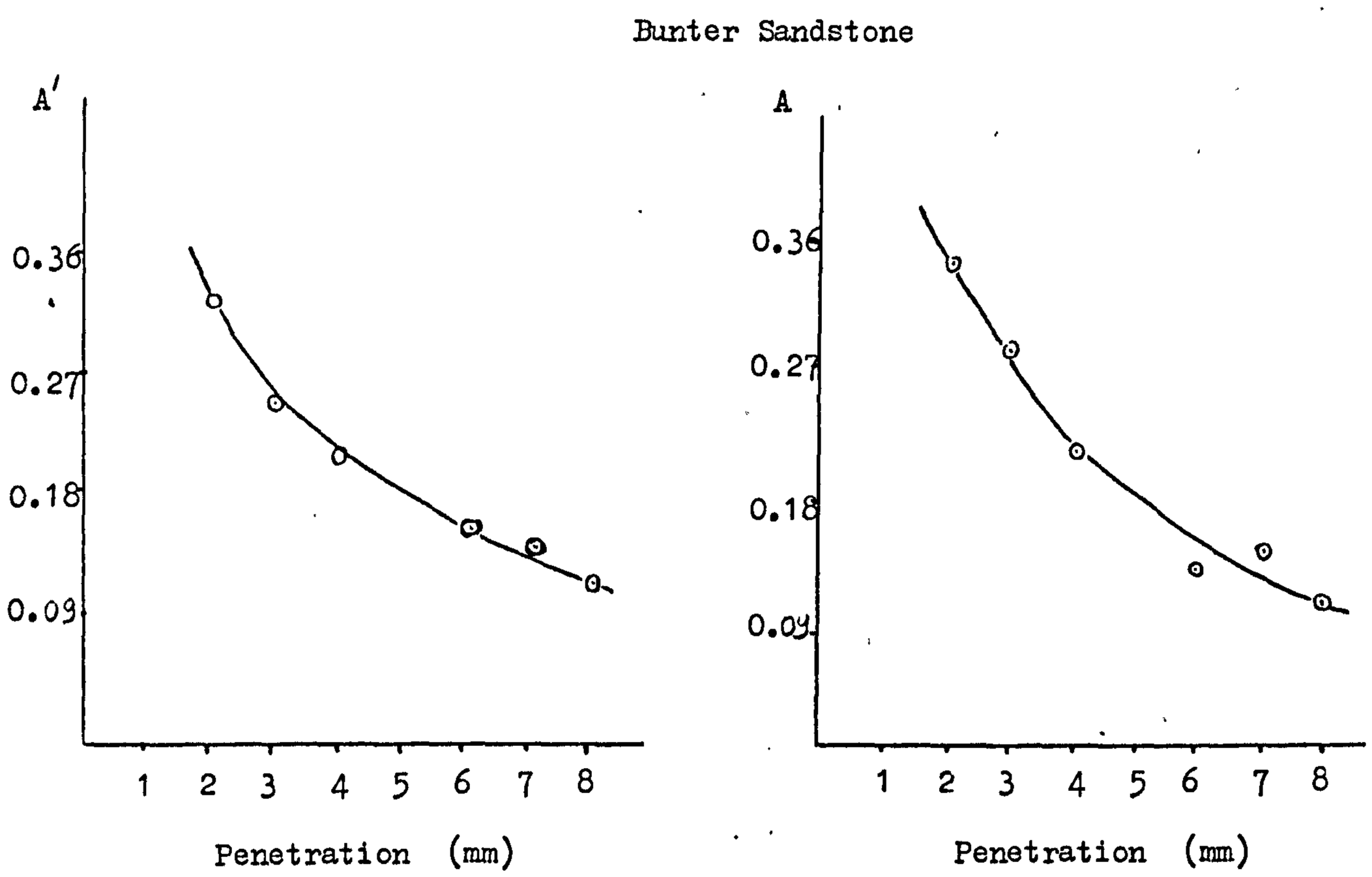

Fig.59 Blunt Disc Analysis.

The projected area of disc contact formulated in Chapter 8 is related to edge radius as shcwn below.

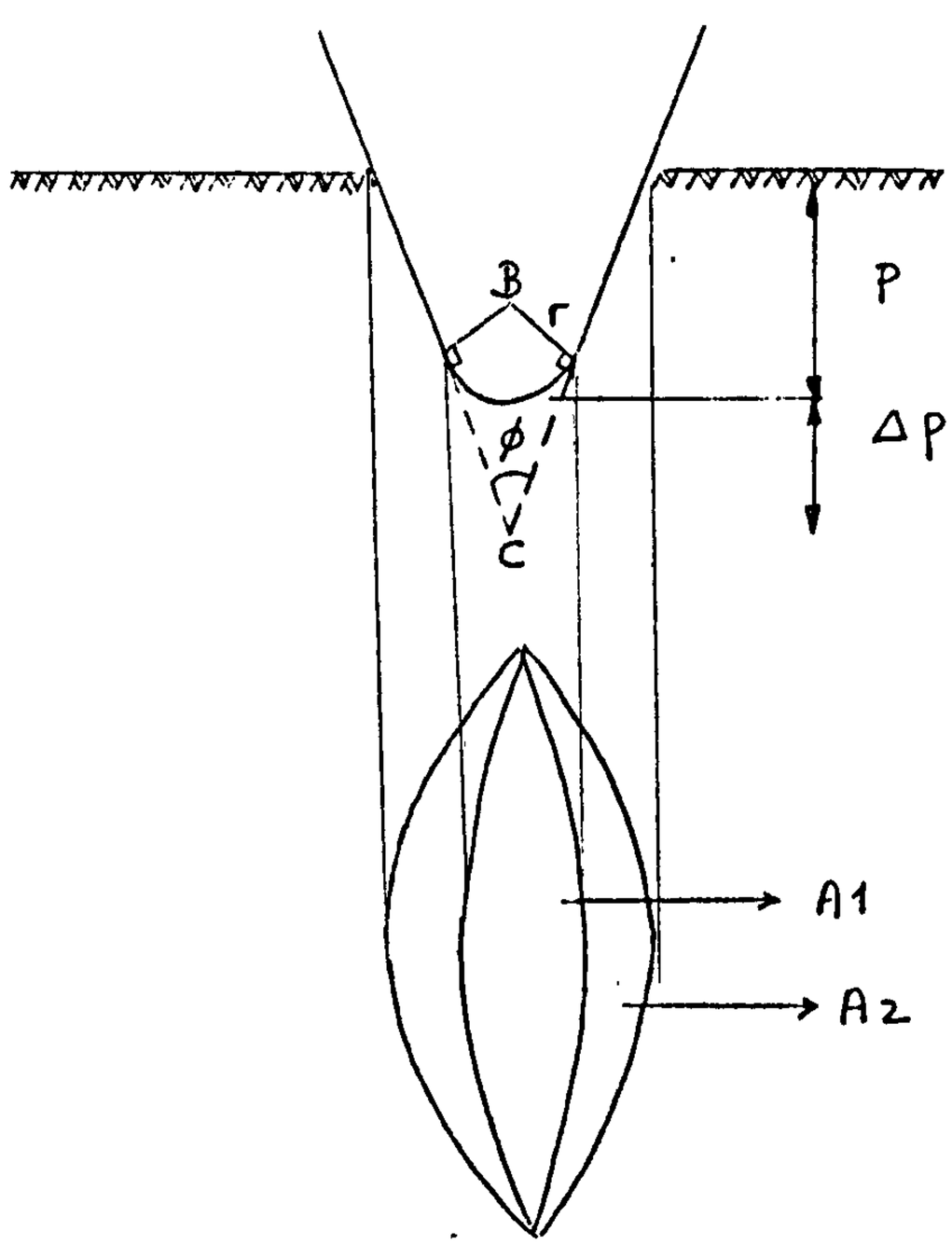

$$A1 = \frac{8}{3} \Delta p \tan \frac{\phi}{2} \sqrt{D \Delta p - \Delta p^2}$$

$$BC = \frac{r}{\sin \frac{\phi}{2}}$$

$$\Delta p = \frac{r}{\sin \frac{\phi}{2}} - r$$

$$A2 = \frac{8}{3} (p + \Delta p) \tan \frac{\phi}{2} \sqrt{\rho(D-2\Delta p) - \rho^2} \qquad ---(27)$$

Fig.60 Relationship between the Projected Area of Disc Contact and Edge Radius.

The decrease of the effect of edge radius on thrust force with deeper penetrations might be explained with the change of projected area of disc contact, as can be seen in Fig.61 (the calculated values are given in Appendix 20).

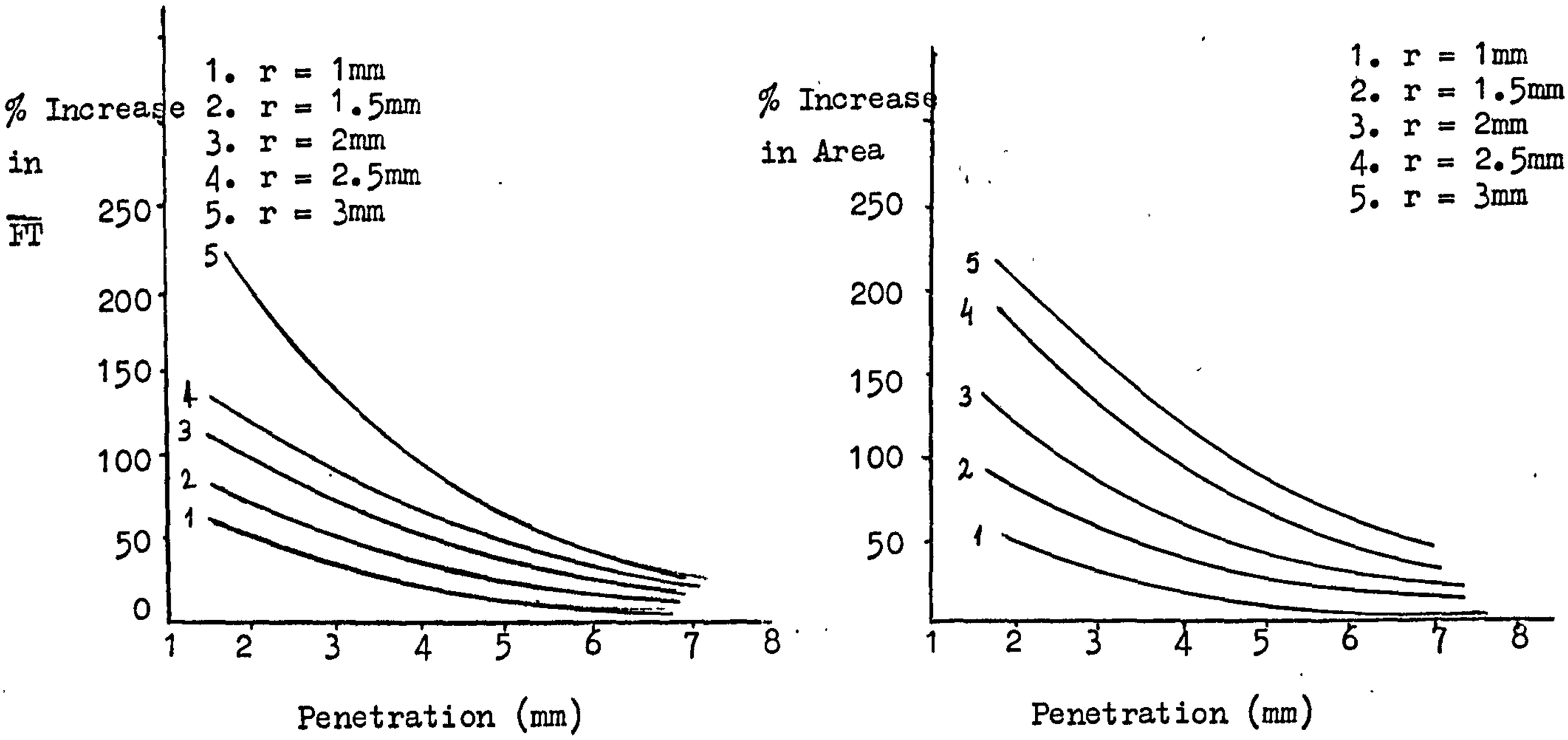

Fig.61 Relationships between % Increase in mean thrust force and % increase in projected area of disc contact.

However, the constants A' and A , equations (25) and (26) , are related to penetration in a hyperbolic form. The equations are:

$$A' = 0.0532 + \frac{0.5478}{p} \quad \text{(Correlation Coefficient - 0.99)} \quad -- (28)$$

$$A = 0.0354 + \frac{0.6554}{p} \quad \text{(Correlation Coefficient = 0.98)} \quad -- (29)$$

Further experiments have been carried out in Granite, Limestone and Greywacke in order to investigate whether the constant A for each level of penetration is dependent on rock physical properties. The equations (25), (26), (28) and (29) were used to predict the thrust force values. As can be seen from Appendix 21, the predicted thrust force values are very close to the actual values, suggesting that A is independent of rock physical properties.

Unfortunately, the sharp disc was worn out very soon after a few cuts in Granite and so the prediction of blunt disc performance in this rock was not possible.

A statistical analysis was carried out in order to see whether the predicted FT values were significantly different from the actual FT values . One of the most common tests in determining whether one process is different from another is the student 't' test, based on comparison between pairs of values[94]. The closer to zero the total of differences lies, the greater the degree of statistical confidence which can be attached to the statement that there is no difference between the processes. 't' has been calculated from the following formula:

$$t = \frac{|\overline{X} - r|}{\overline{SX}}$$; The null hypothesis is Ho: = o

$$X = \overline{X_1} - \overline{X_2}$$

where $\overline{X_1}$ = mean of first sample

$\overline{X_2}$ = mean of second sample

$$\overline{SX} = \frac{SSd}{n-1}$$

where $SSd = \sum(X_1 - X_2)^2 - (\overline{X_1} - \overline{X_2}) \leq (X_1 - X_2)$

n - 1 are degrees of freedom.

We reject the hypothesis of no difference and conclude that the two experimental processes are different when the calculated value of 't' is greater than the tabulated value of 't'.

The calculated student 't' test value for F'T is 2.19 and for $\overline{FT}$ is 1.66. It is concluded that the predicted thrust force values are not significantly different than the actual thrust force values since tabulated value of 't' 005,11 is 2.20. Thus we are 95% confident that no difference exists between actual and predicted values.

* * *

9.3 Effect of Edge Radius on Rolling Forces

As can be seen from Fig.62, the mean rolling forces increase with increasing edge radius in Bunter Sandstone. A similar statistical method has been used to analyse the rolling force values. For each level of penetration the rolling force is related to edge radius in the form of

$$F'R_r = F'R_{ro} e^{B'r} \qquad ---(30)$$

$$\overline{FR}_r = \overline{FR}_{ro} e^{Br} \qquad ---(31)$$

where $F'R_r$, $\overline{FR}_r$ = Rolling force for a disc of rmm edge radius

$F'R_{ro}$, $\overline{FR}_{ro}$ = Rolling force for a sharp disc

B is a constant, r is edge radius.

Equations and correlation coefficients are given in Table 30.

Table 30 Relationship between edge radius and rolling forces.

P mm	Equations for F'R	Coefficient Correlation	Equations for $\overline{FR}$	Coefficient Correlation
2	$F'R = 0.58 e^{0.263r}$	.98	$\overline{FR} = 0.48 e^{0.234r}$	0.98
3	$F'R = 1.17 e^{0.239r}$	.98	$\overline{FR} = 0.98 e^{0.200r}$	0.99
4	$F'R = 1.71 e^{0.222r}$	.98	$\overline{FR} = 1.27 e^{0.203r}$	0.95
6	$F'R = 3.70 e^{0.128r}$	.96	$\overline{FR} = 2.94 e^{0.076r}$	0.80
7	$F'R = 4.74 e^{0.117r}$	.99	$\overline{FR} = 3.42 e^{0.118r}$	0.95
8	$F'R = 5.90 e^{0.133r}$	.99	$\overline{FR} = 4.25 e^{0.110r}$	0.94

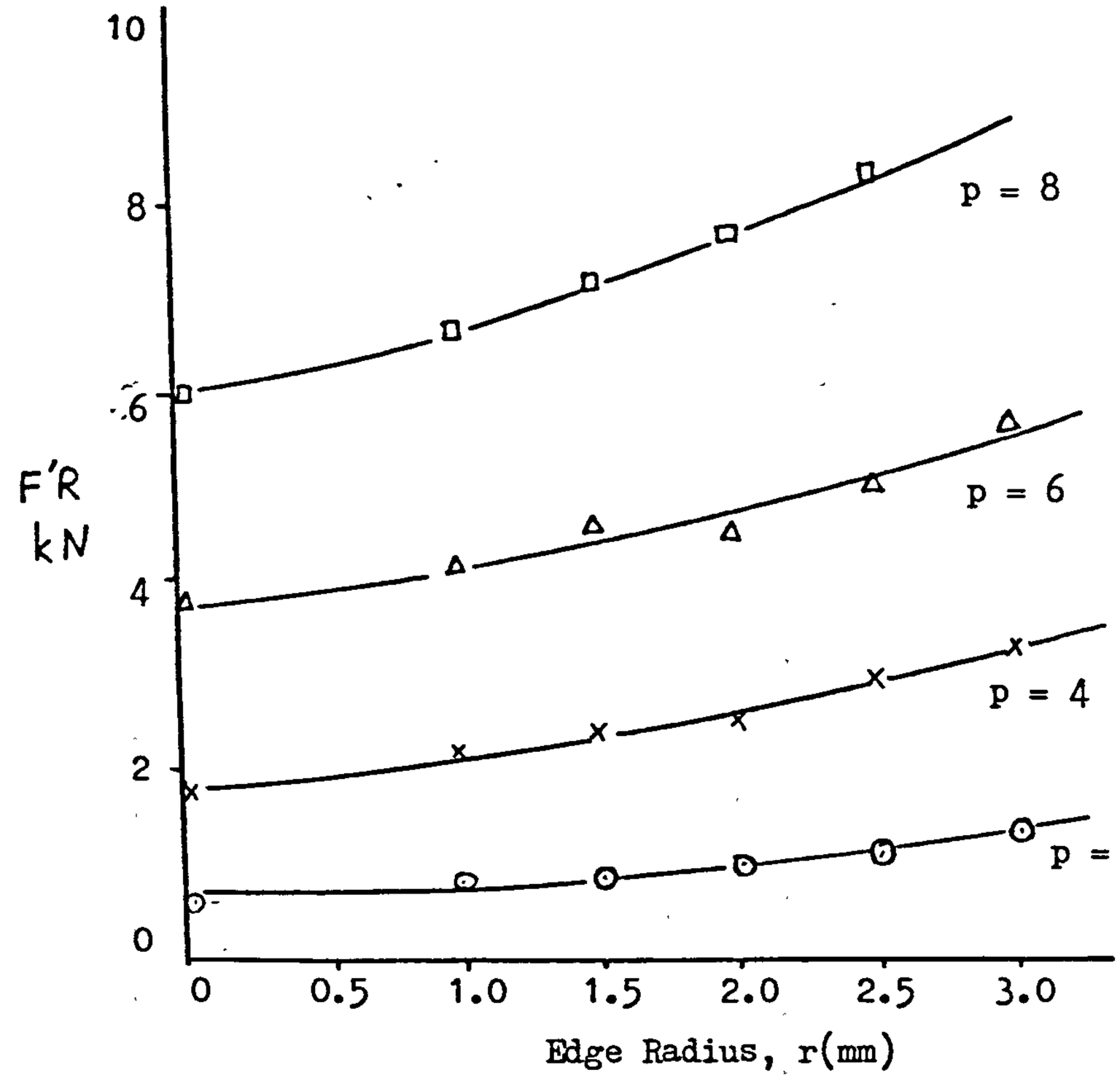

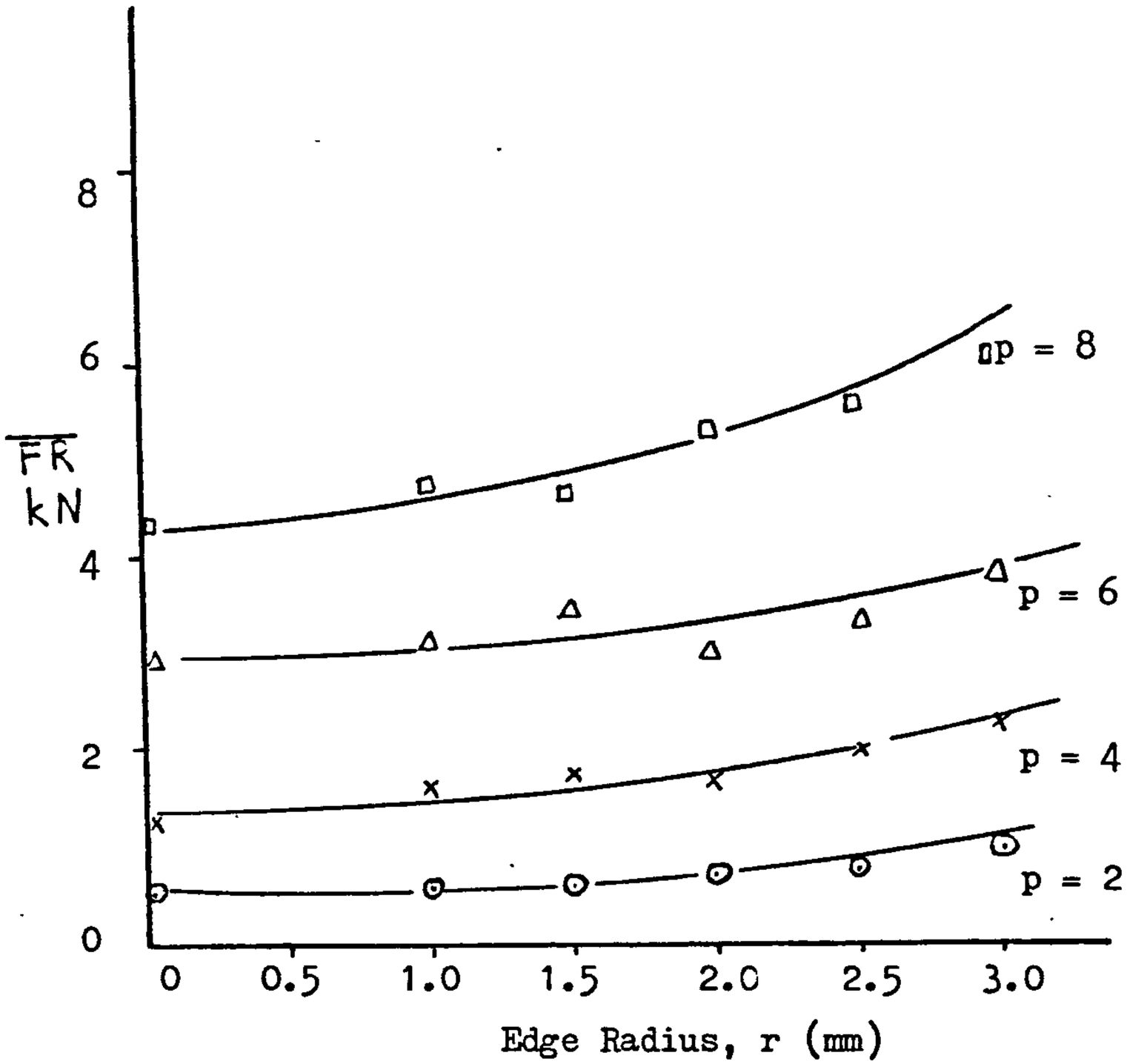

Fig.62 Variation in Rolling Forces with Edge Radius.

It can be easily seen from Table 30 that the constants B' and B of equations (28) and (29) decrease as the edge radius becomes larger.

B and B' are related to penetration in the form of

$$(30)\quad B' = 0.079 + \frac{0.4116}{p} \qquad \text{(Correlation Coefficient = 0.91)}$$

$$(31)\quad B = 0.060 + \frac{0.383}{p} \qquad \text{(Correlation Coefficient = 0.87)}$$

In Appendix 21, rolling force values in Limestone and Greywacke are compared with predicted values (obtained from formula 28, 29, 30 and 31). A student 't' test has been used to investigate whether the two sets of data are different. The student 't' test value for F'R is 0.256, for $\overline{FR}$ is 0.082. t0.05.11 = 2.20. Since the tabulated t value is greater than the calculated values, we accept the hypothesis that the predicted rolling force data is not different from the actual rolling force data.

A close check of Fig.63 and Appendix 20 shows that the affect of edge radius is reduced when cutting with deeper penetrations.

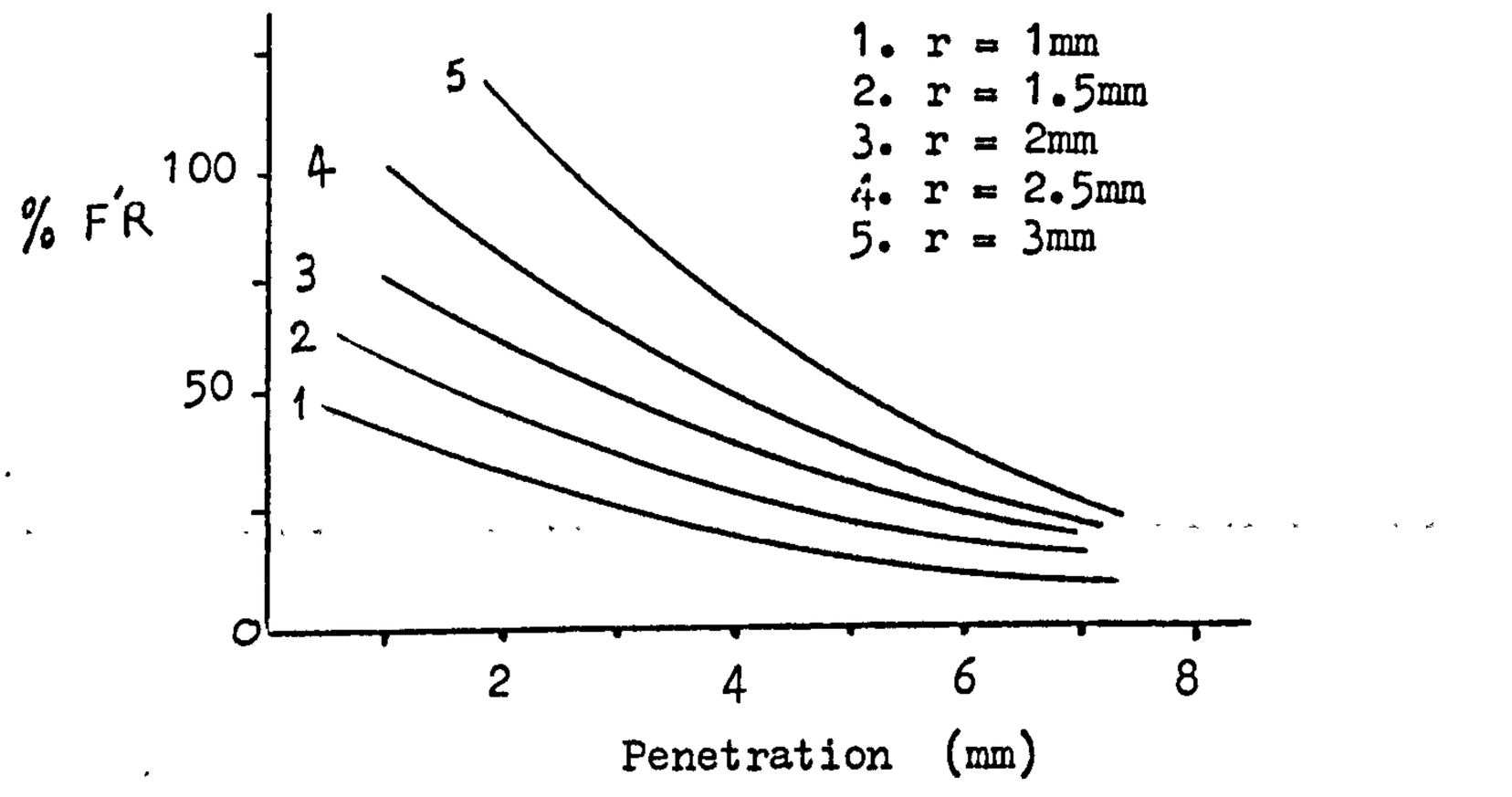

Fig.63 The Decrease of the Effect of Edge Radius on Rolling Force with Deeper Penetrations.

9.4 The Effect of Edge Radius on Yield, Specific Energy and Coarseness Index

The specific energy is a measure of cutting efficiency and is used for assessing the effect of changes in either design or operating procedure during the rock cutting process. As can be seen from Fig.64, the specific energy in Bunter Sandstone is increased very little with edge radius for penetrations deeper than 2mm. This shows that the blunt discs can be as efficient as the sharp discs. This result stems from the fact that there is a significant increase in yield with increasing edge radius (Fig.64).

This conclusion is also valid for Limestone and Greywacke since yield and specific energy show the same trend as in Bunter Sandstone (Table 31).

Table 31 Variation in Yield with Edge Radius

	Yield m^3/km					Specific Energy MJ/m^3				
	Limestone r(mm)			Greywacke r(mm)		Limestone r(mm)			Greywacke r(mm)	
P_{mm}	0	1	2	0	1	0	1	2	0	1
1	0.002	0.003	0.004	0.002	0.002	292.68	289.62	311.49	366.59	390.12
3	0.025	0.024	0.037	0.023	0.028	125.07	145.86	140.69	136.20	130.23
4	-	0.054	0.058	0.043	0.055	79.48	98.85	107.86	98.82	92.84
5	0.088	0.106	0.109	0.058	0.076	79.51	75.12	82.27	97.19	90.29

The slopes of the lines in Fig.65 are too shallow to place any reliance on these trends. It is concluded that the Edge Radius has no effect on C.I.

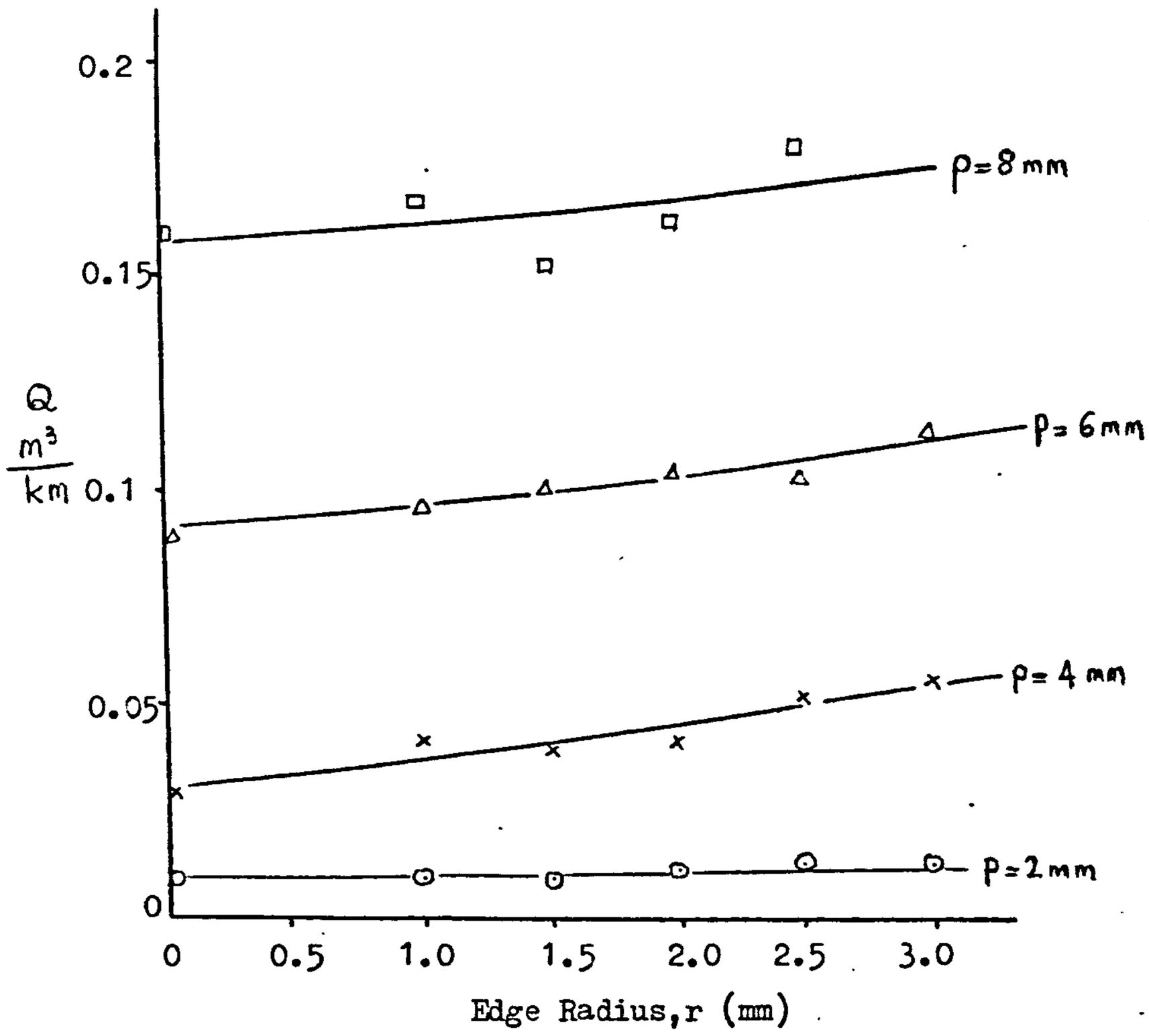

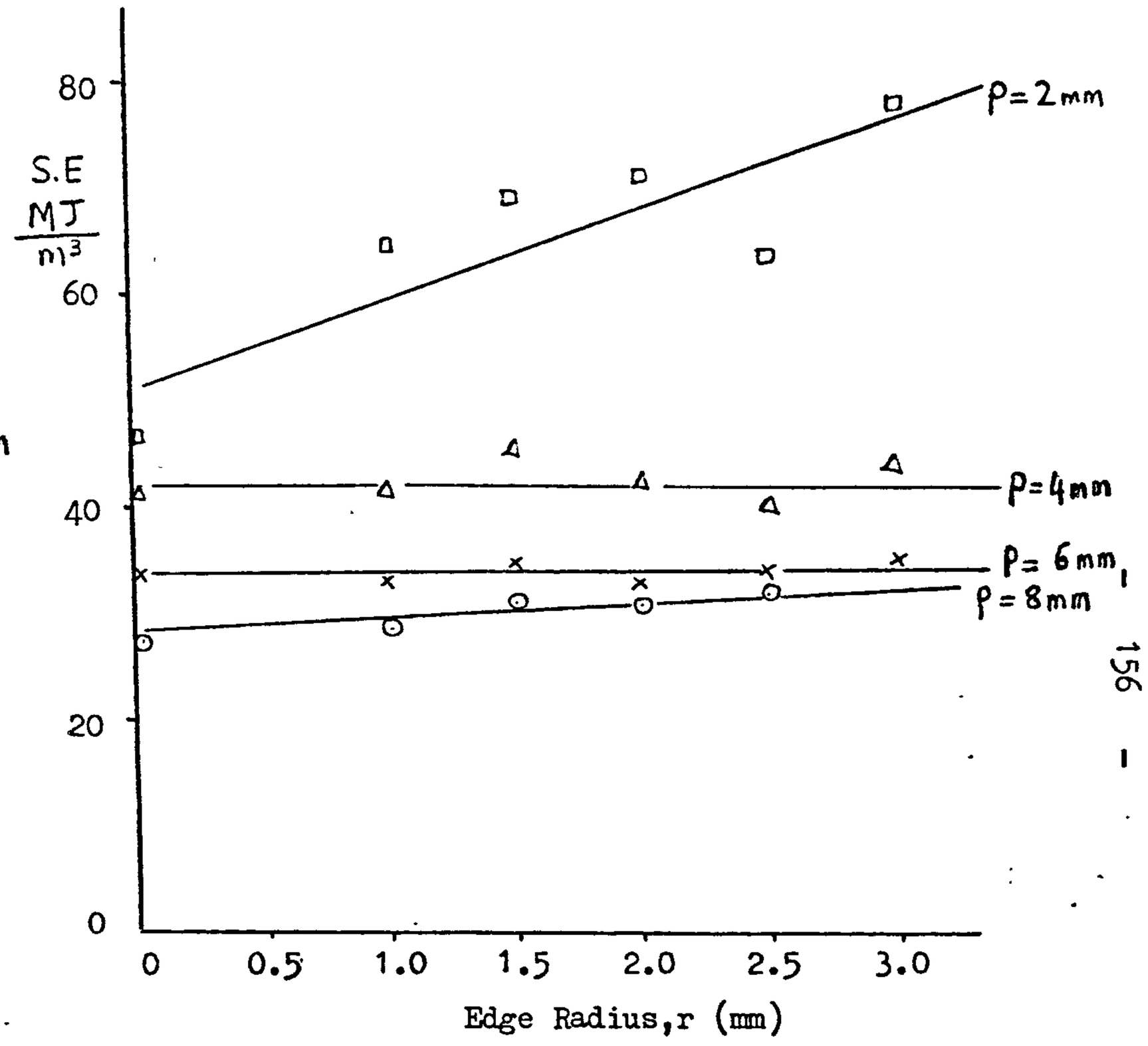

Fig.64 Variation in Yield and Specific Energy with Edge Radius.

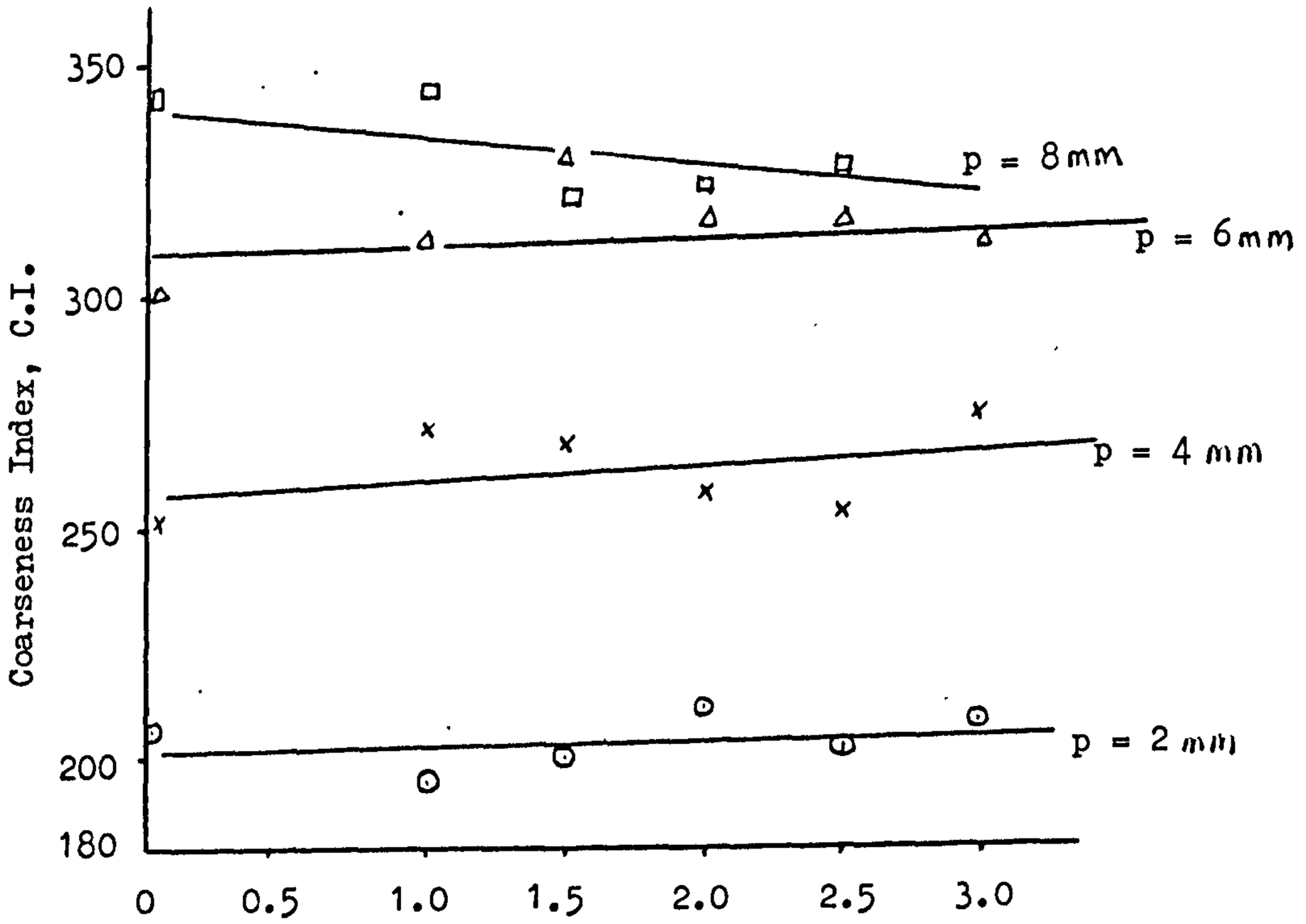

Fig.65 Variation in Coarseness Index with Edge Radius.

9.5 Relieved Cutting in Bunter Sandstone with Blunt Discs

In the previous sections, it has been shown that edge radius has caused an increase in yield. Therefore, it can be concluded that the edge radius has a significant influence on breakout angle, which might be due to high stress concentration around such discs.

Although a small amount of fundamental research has been undertaken on the operation of blunt discs, it has not been possible to obtain any information on relieved cutting of this type of cutters, so preliminary experiments were undertaken in Bunter Sandstone to investigate the effect of edge radius on relieved cutting.

Data for all the relieved cutting tests are given in Appendix 22.

Effect of Spacing on Disc Forces

Figs.66 and 67 show the relation between disc forces and spacing for two levels of penetration. Clearly, disc forces increase rapidly with spacing becoming asymtotic to the unrelieved forces.

Effect of Spacing on Yield and Specific Energy

Fig.68 shows the variation in yield with spacing/penetration ratio. The maximum yield is significantly and consistently higher than the equivalent yields obtained in unrelieved cutting. It should be noted, however, that the highest maximum yields for sharp discs occur at s/p ratio of 5, and for blunt discs at s/p ratios of 5 to 7. This important

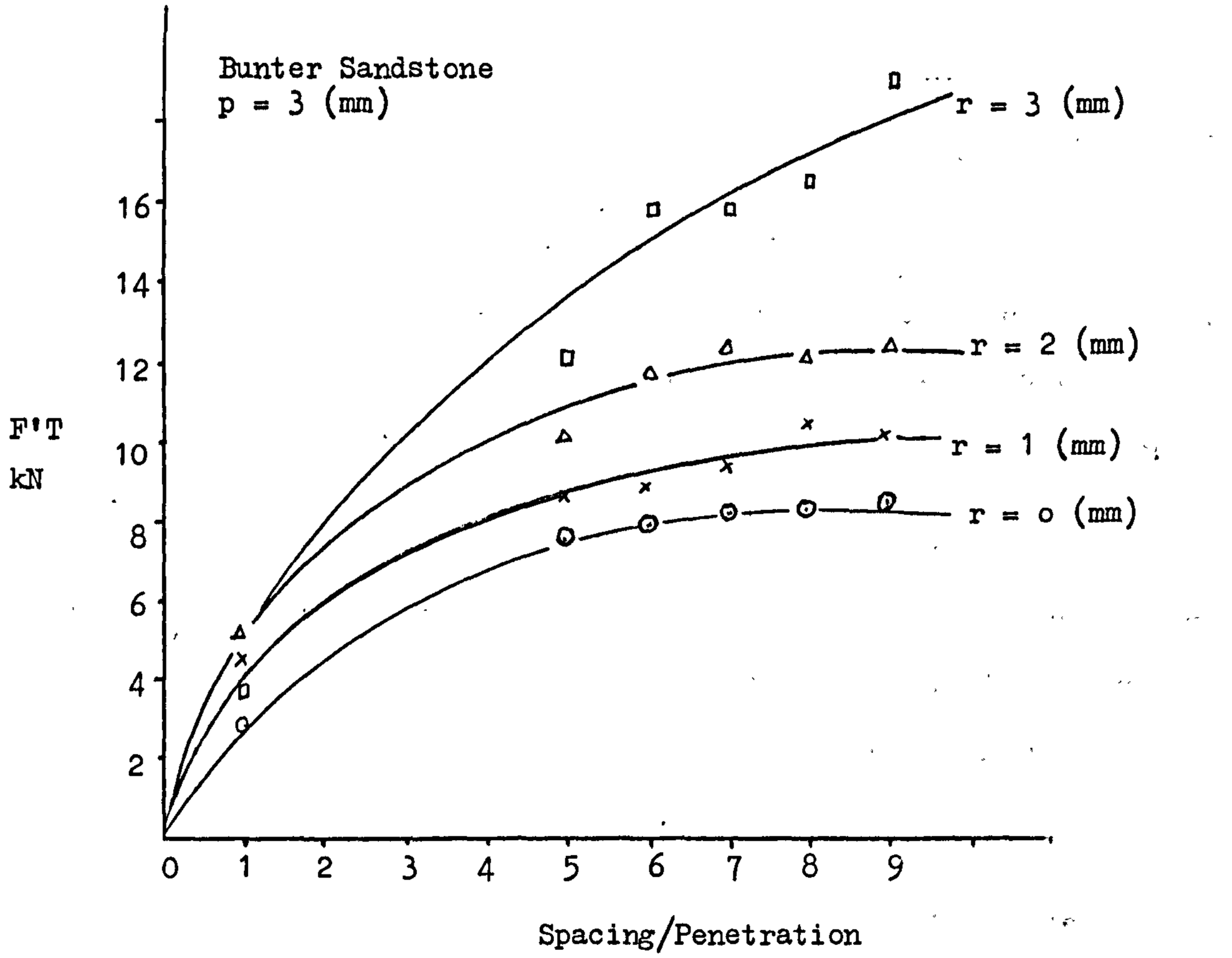

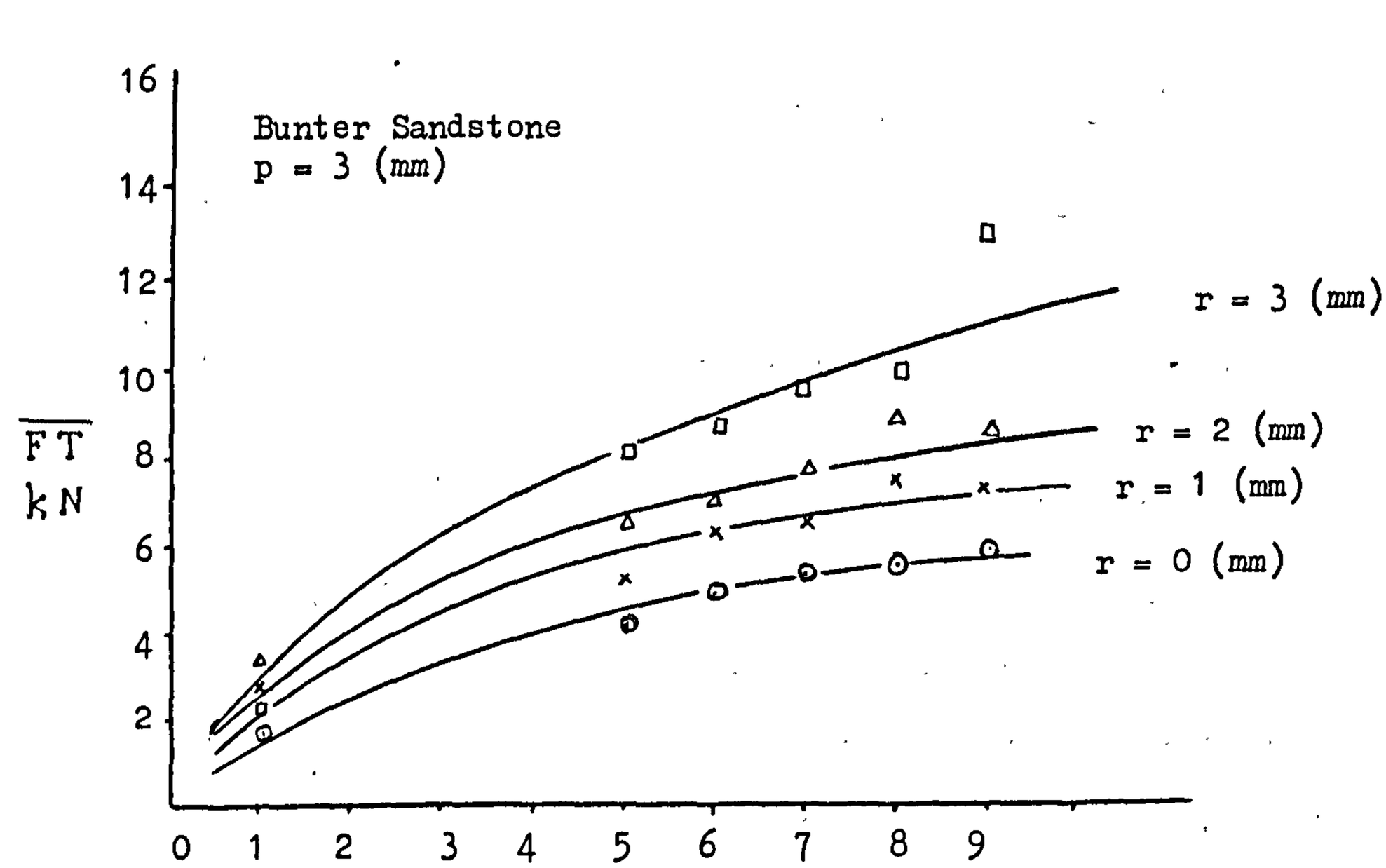

Fig.66A Variation in Thrust Forces with s/p.

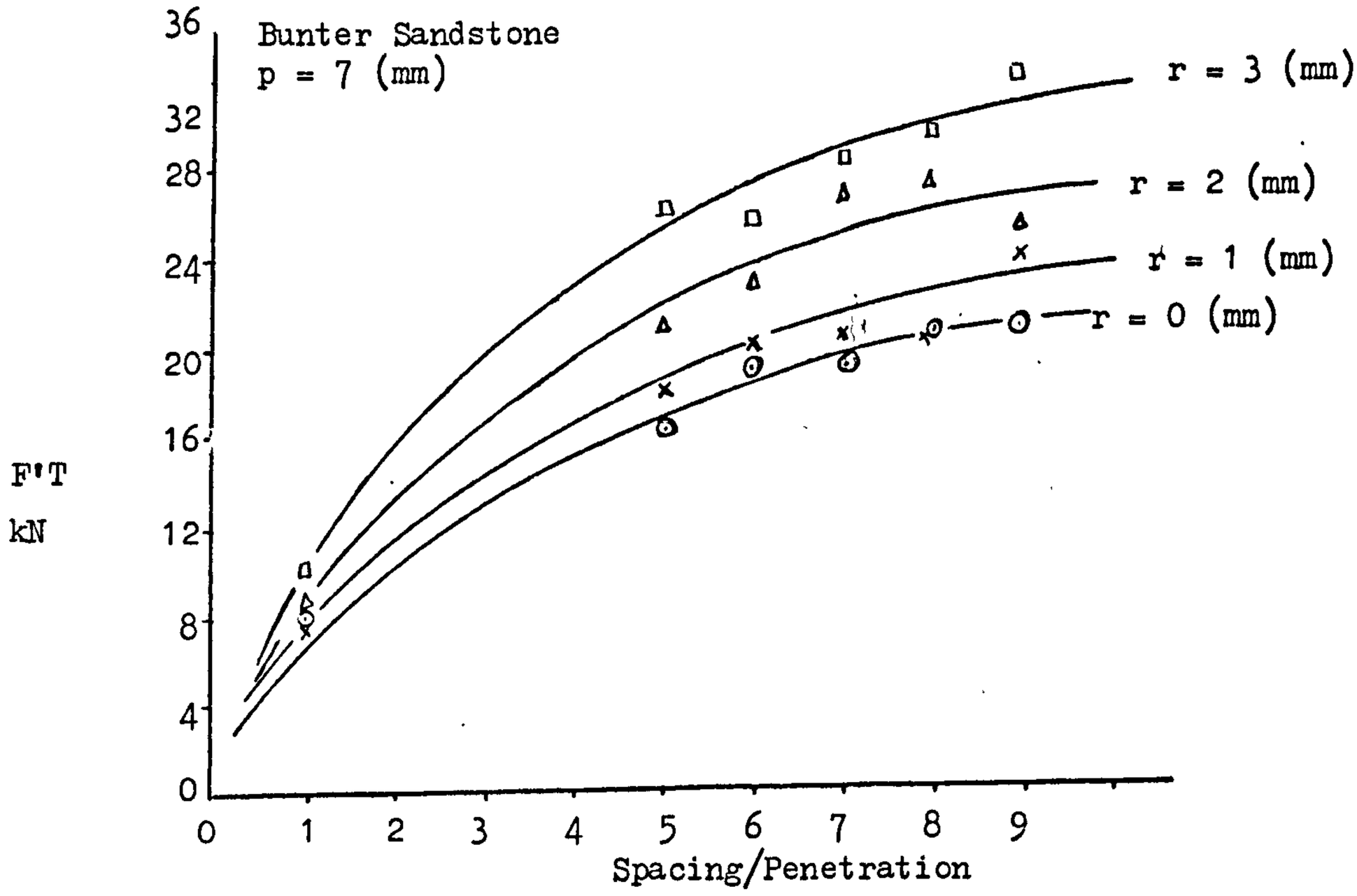

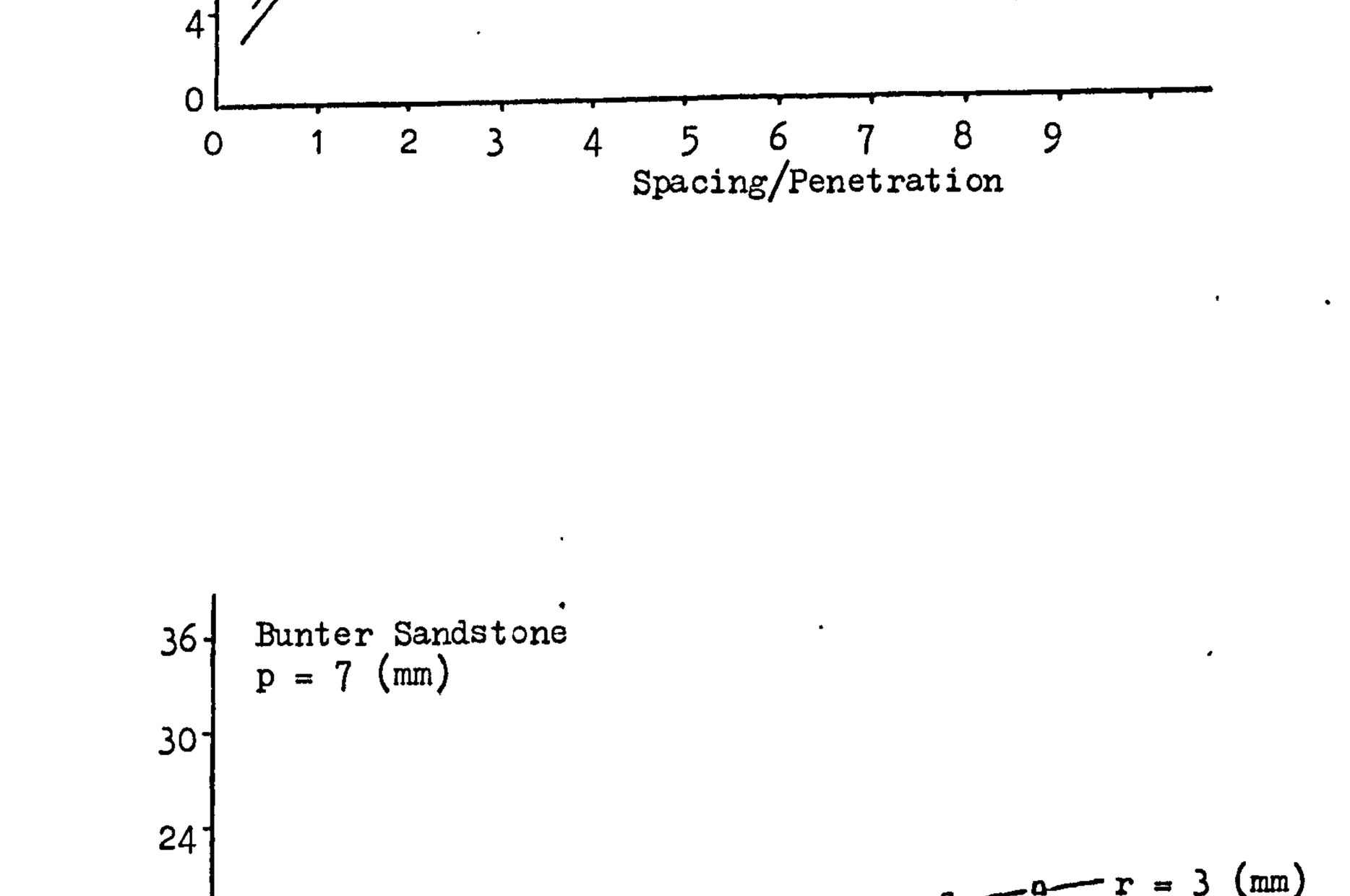

Fig.66B Variation in Thrust Forces with s/p.

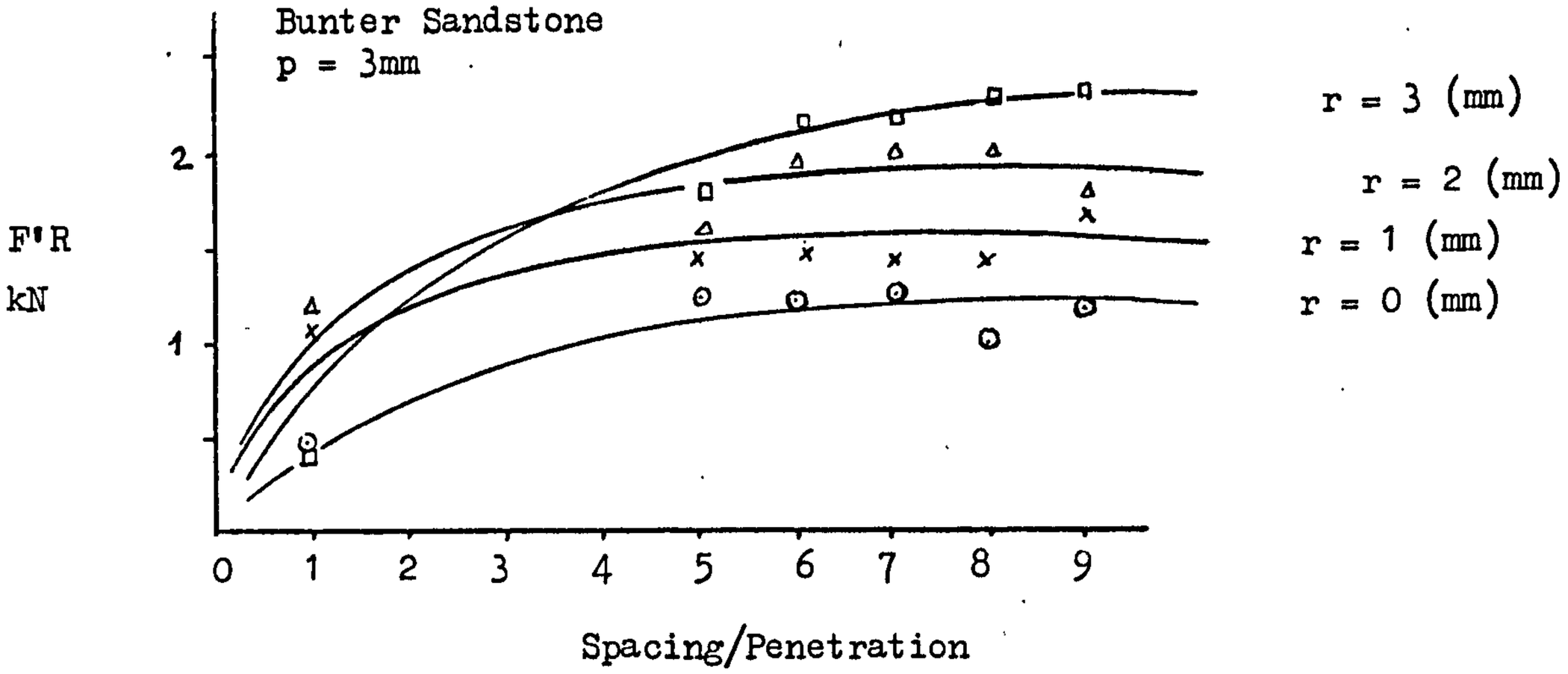

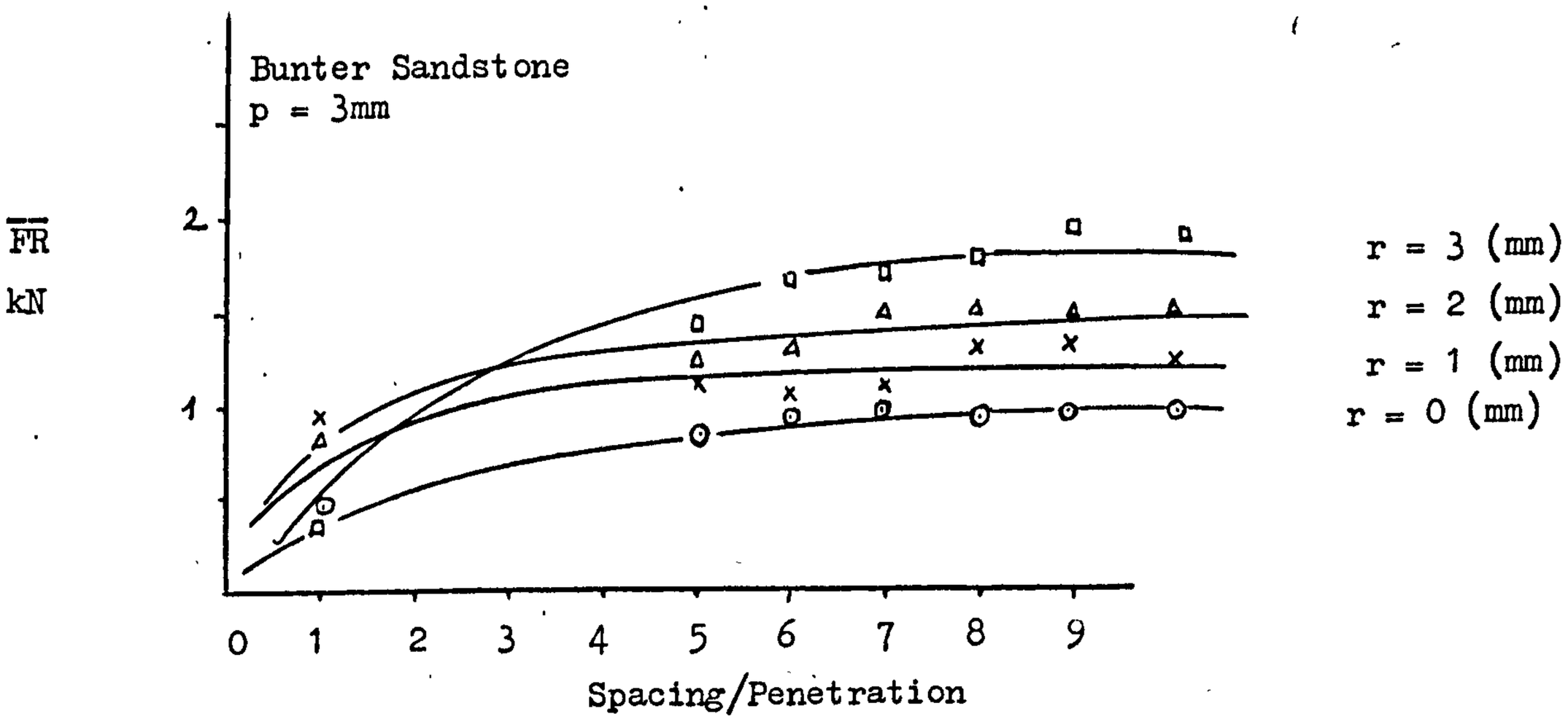

Fig.67A Variation in Rolling Forces with s/p.

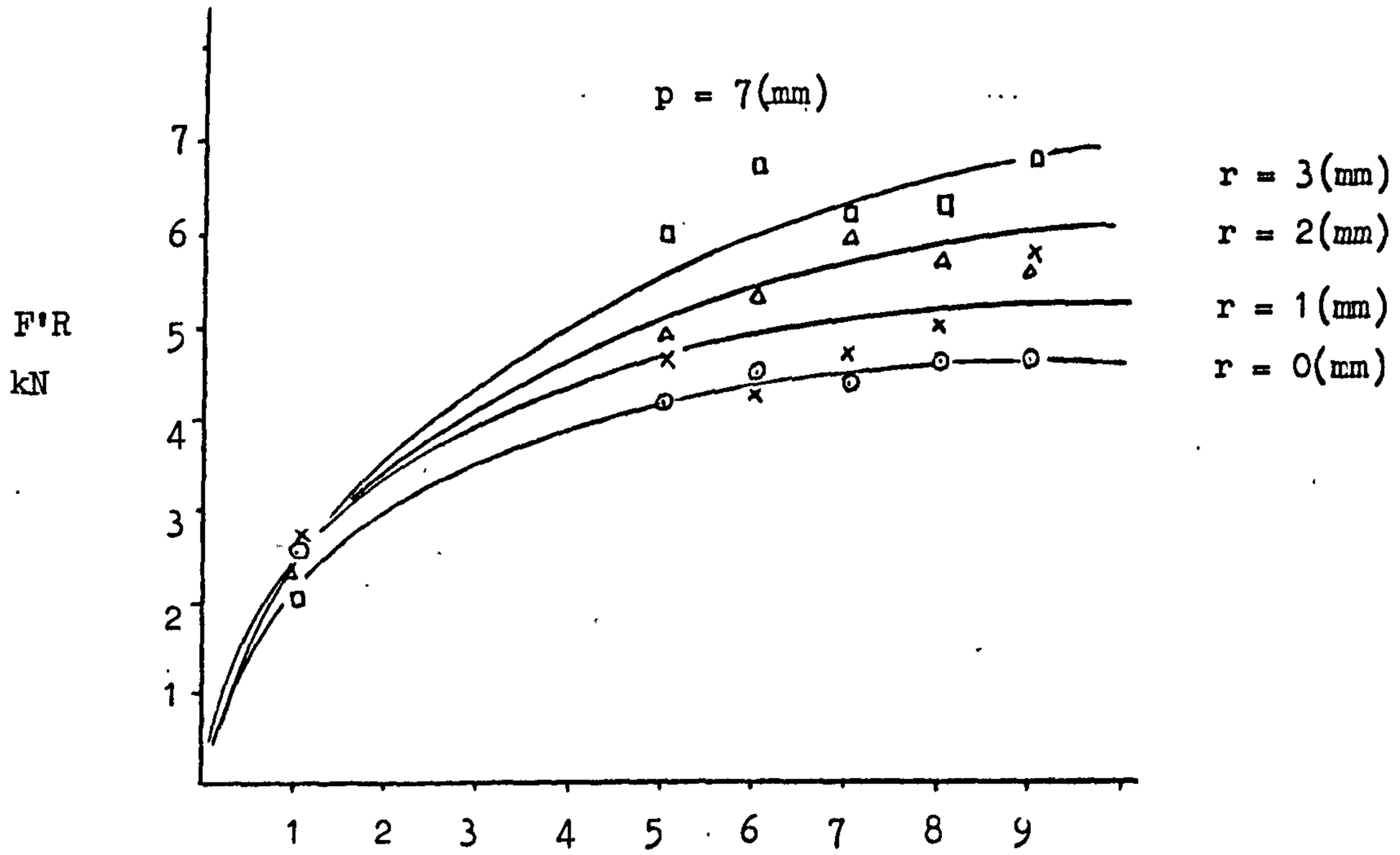

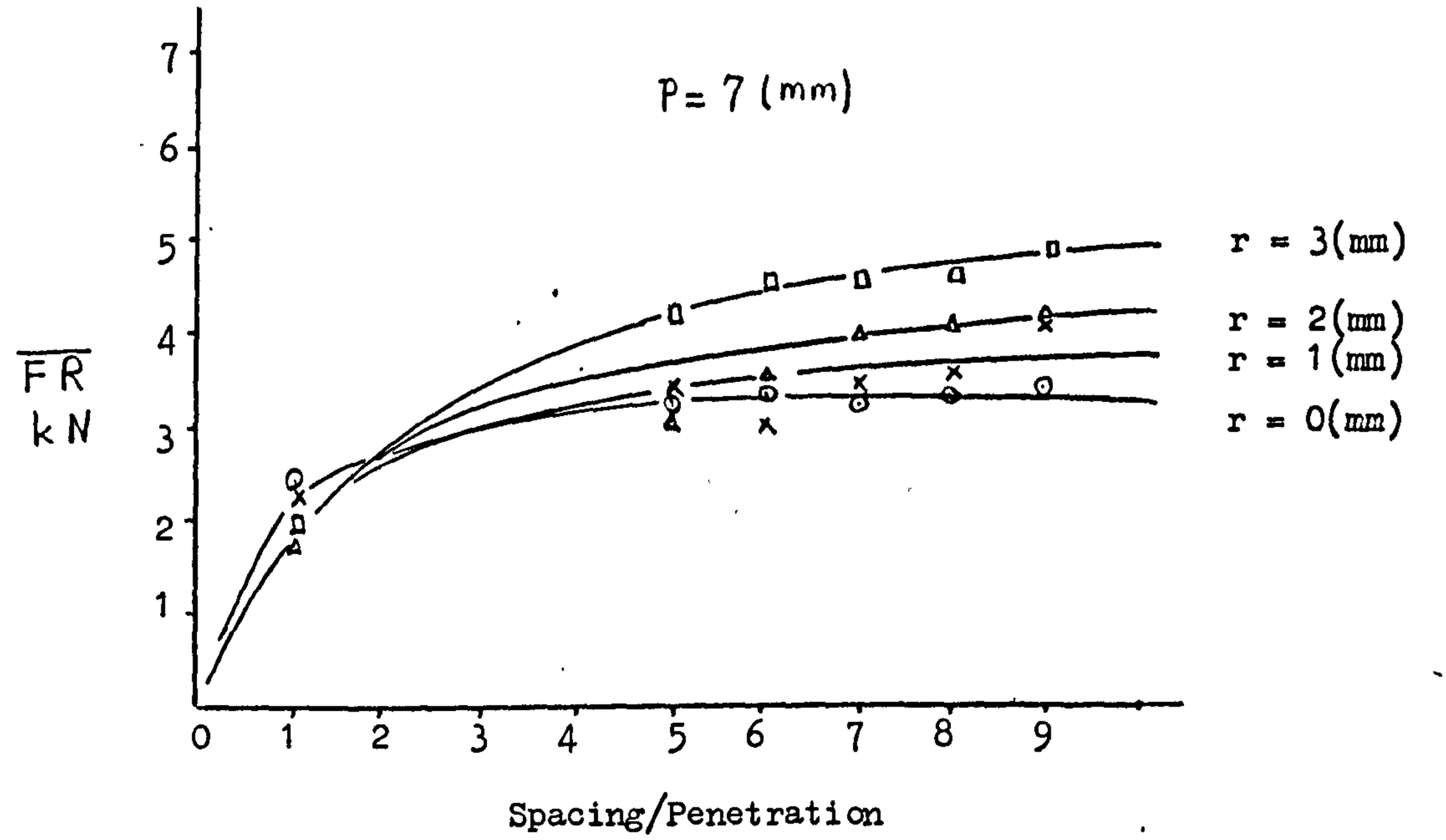

Fig.67B Variation in Rolling Forces with s/p.

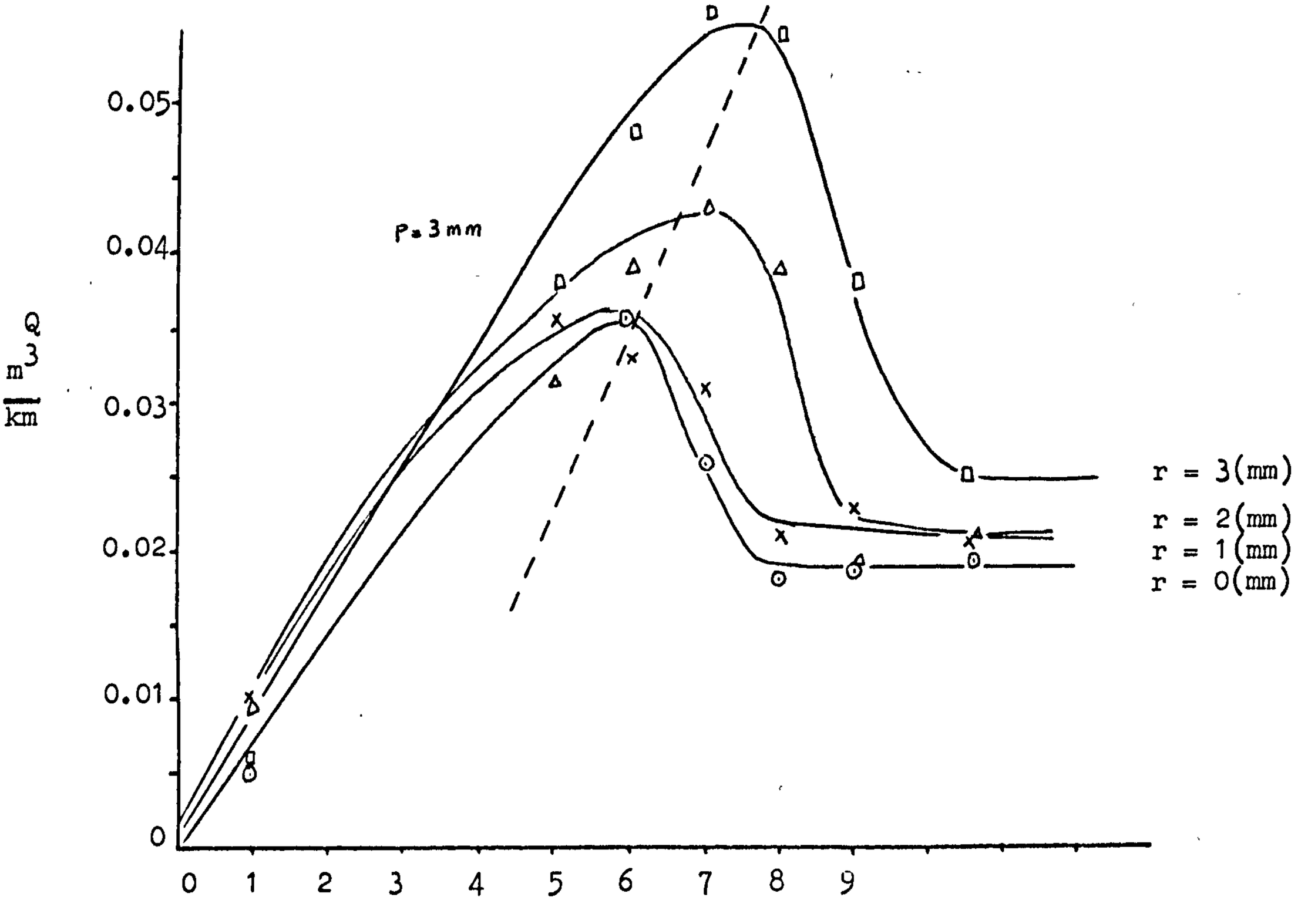

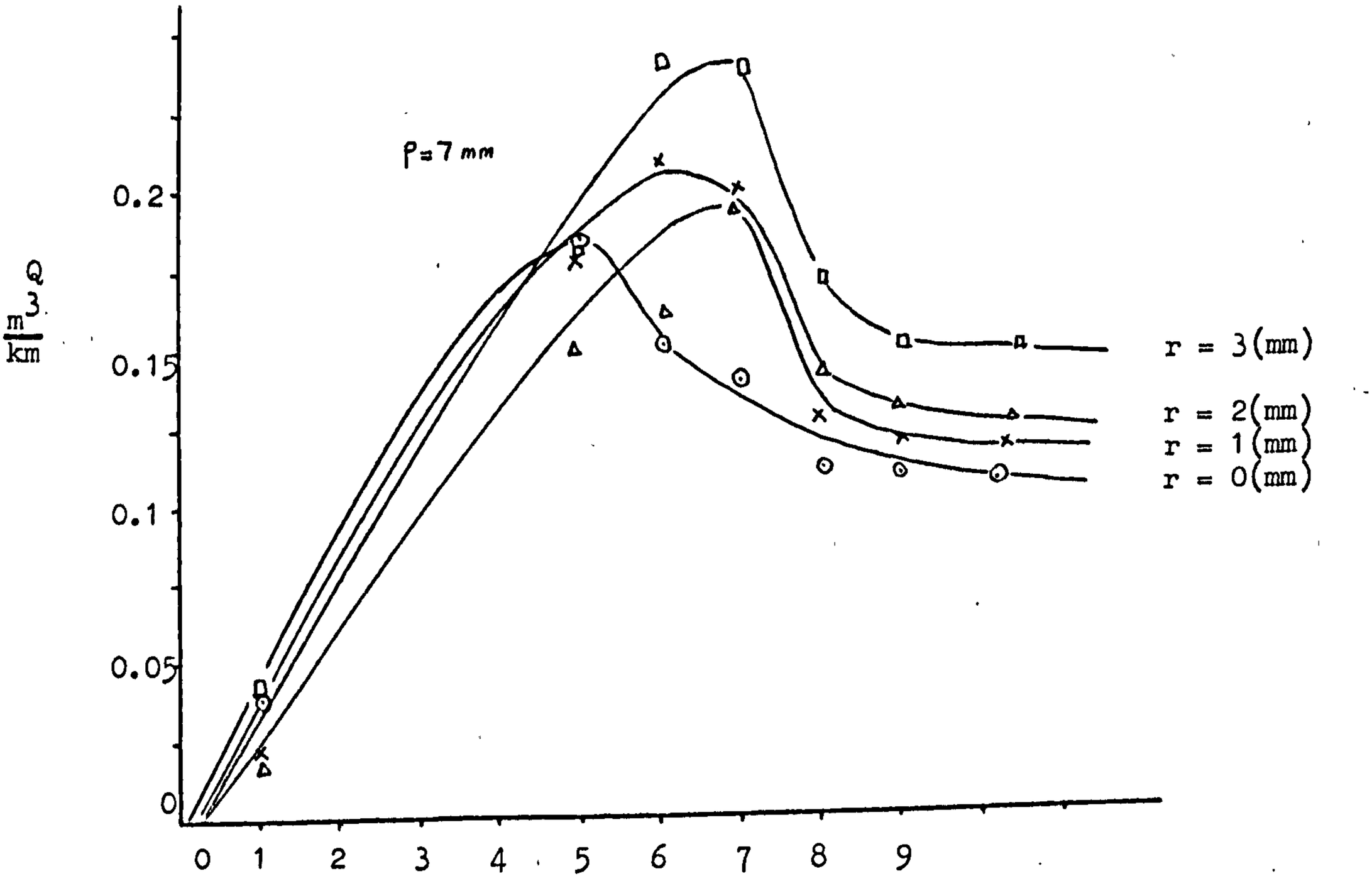

Fig.68 Variation in Yield with s/p for Different Edge Radius.

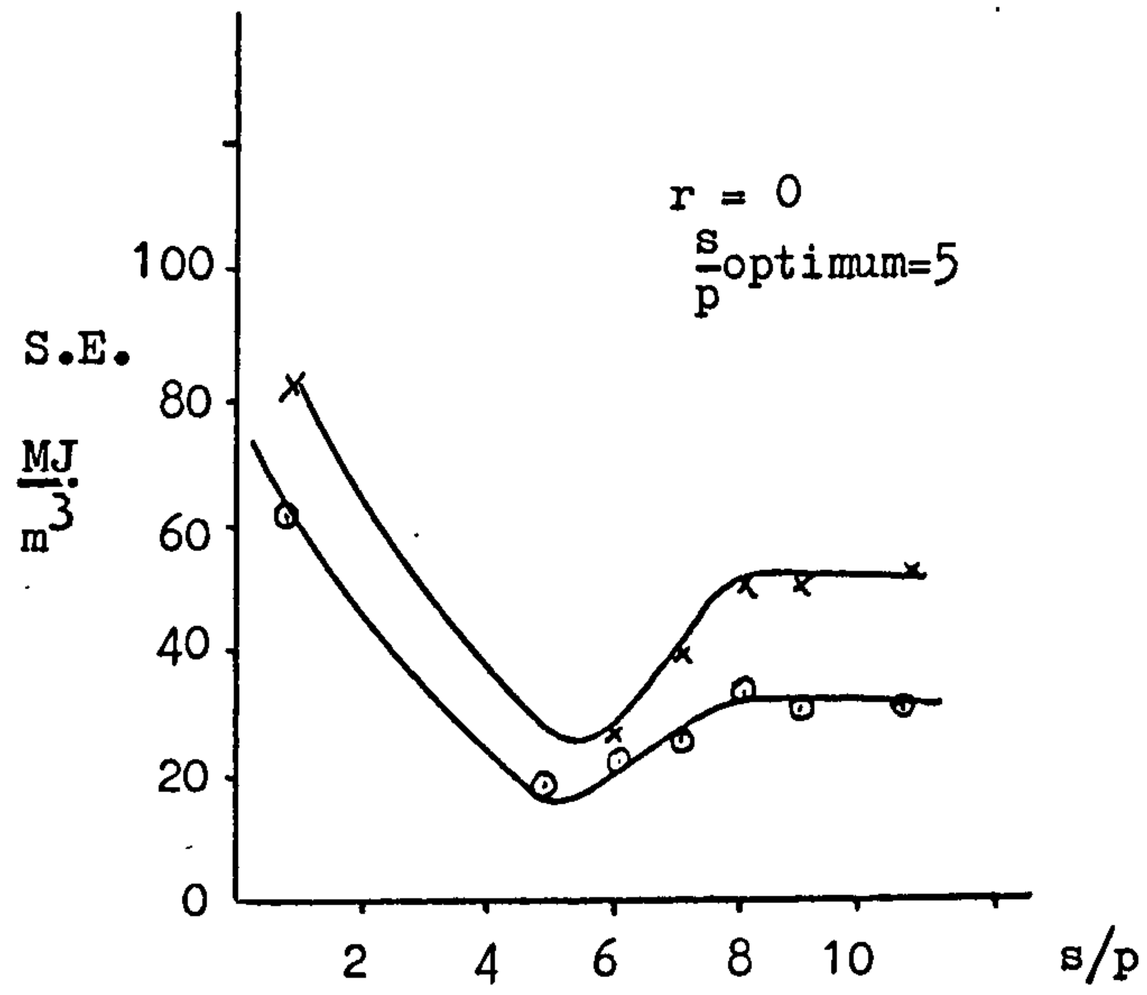

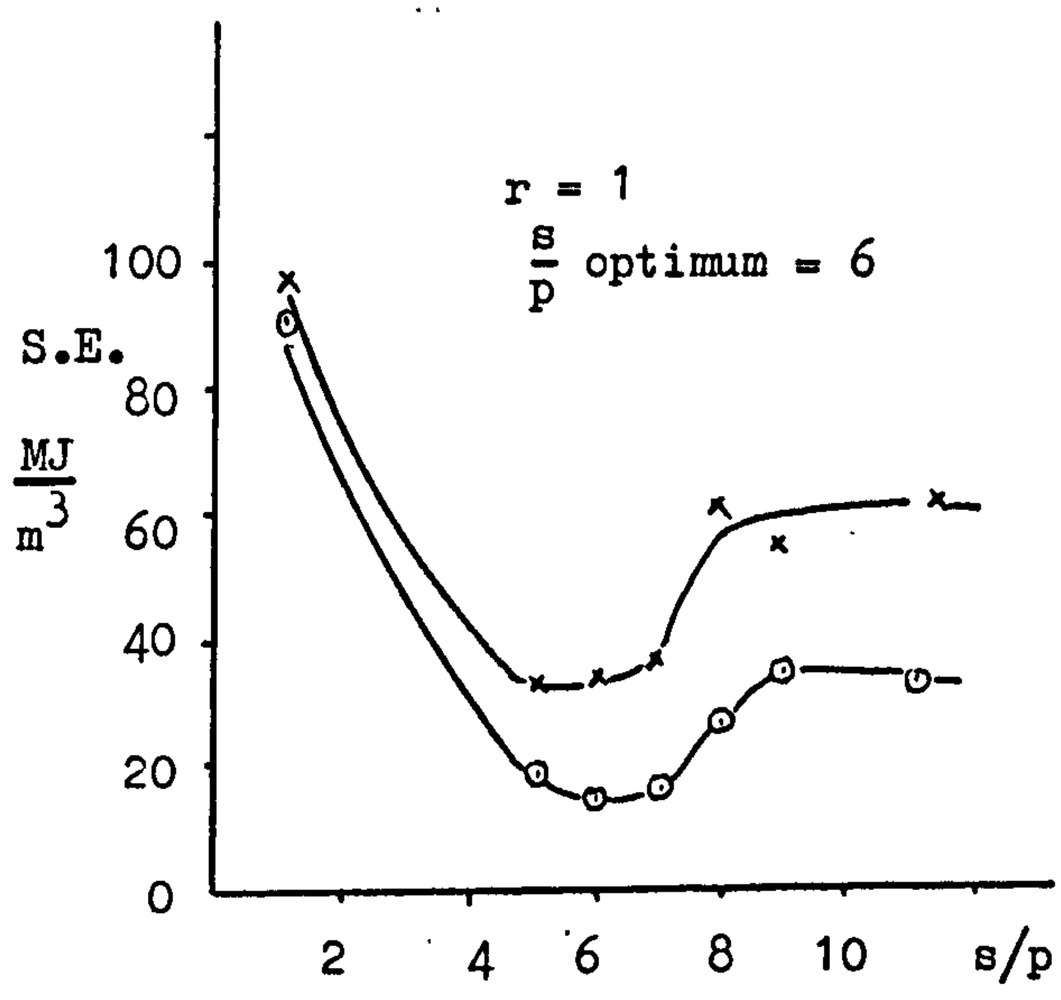

x p = 3mm

o p = 7mm

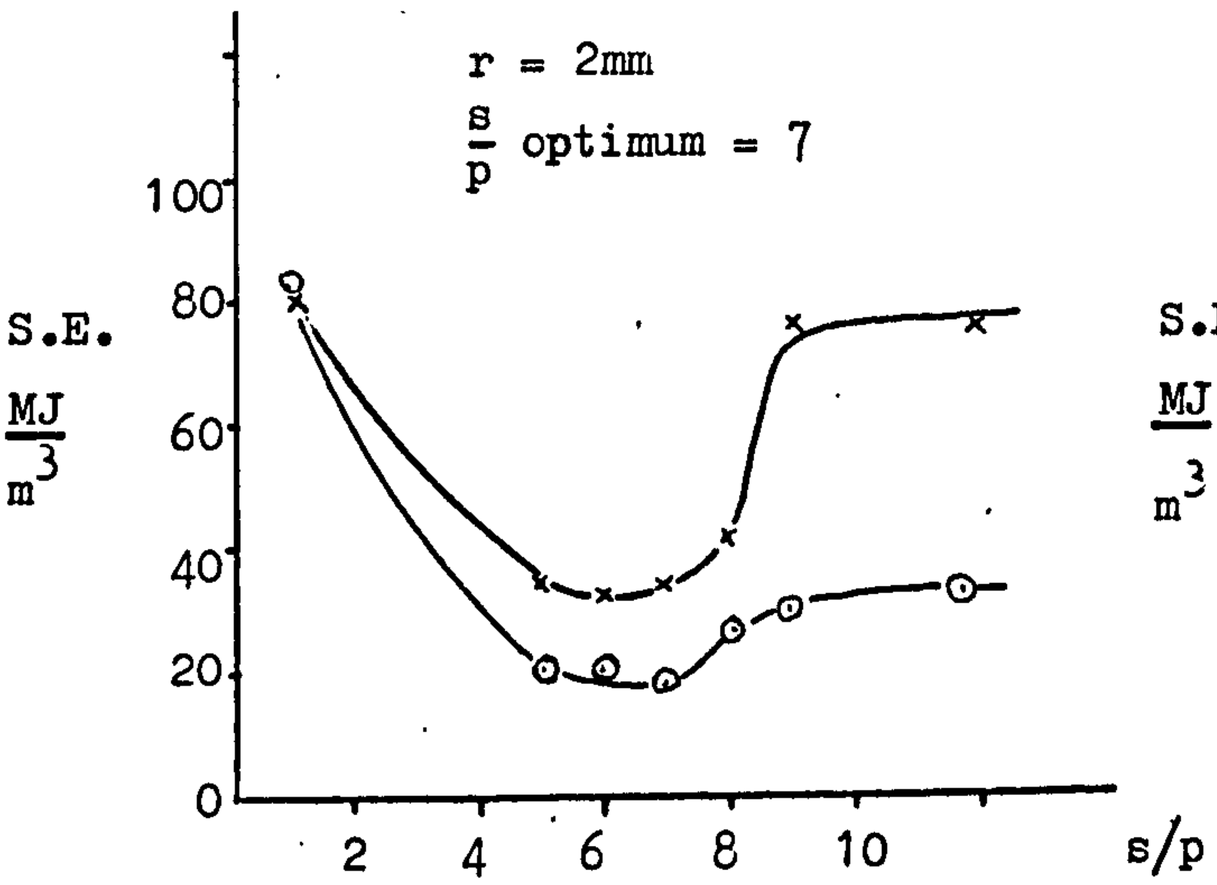

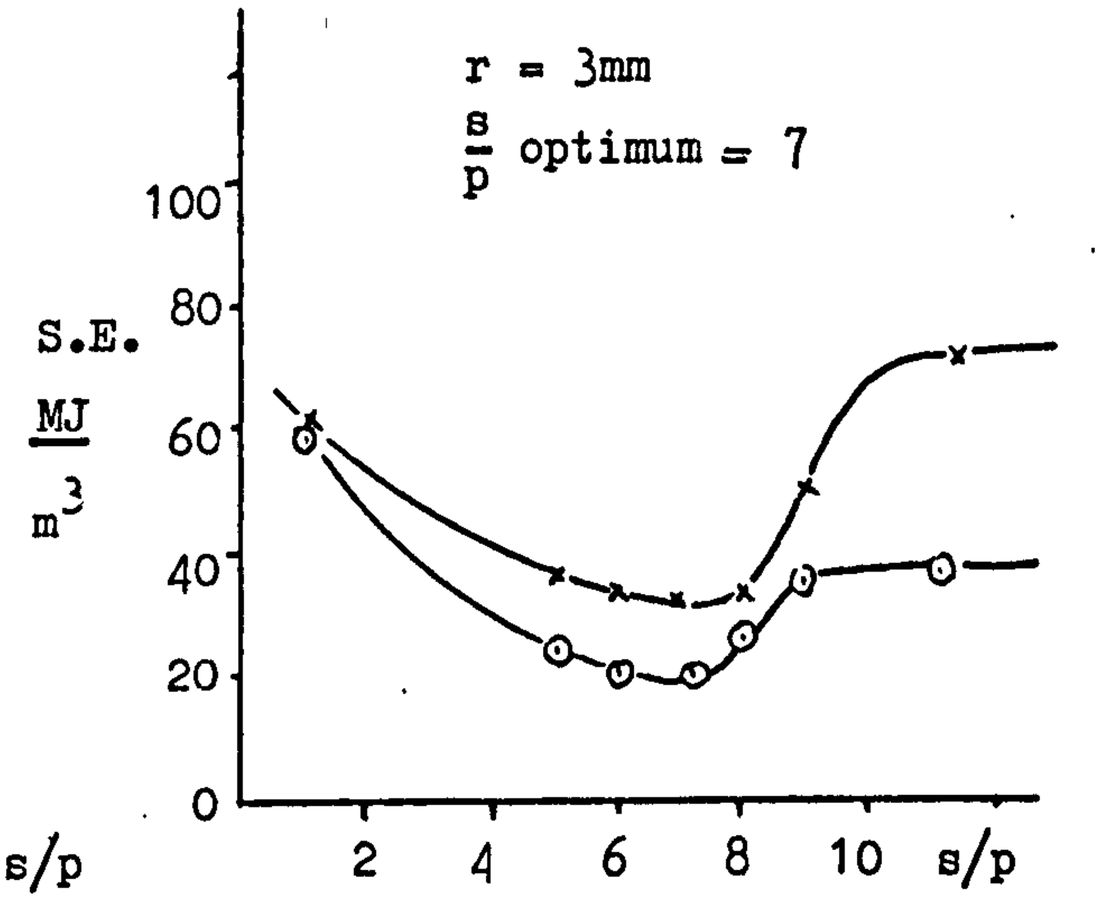

Fig.69 Variation in Specific Energy with s/p for different Edge Radius.

point is reflected in specific energy values. It can be clearly seen from Fig.69 that optimum specific energy is dependent on edge radius, and it varies by almost 40% for the range of blunt discs tested.

* * *

9.6 Conclusion

The detailed analysis of blunt discs experimental results leads to the following conclusions:-

(a) Thrust and rolling forces increase considerably with edge radius in an exponential manner in the form of:

$$FT_r = FT_{ro} e^{Ar}$$

$$FR_r = FR_{ro} e^{Br}$$

A and B are a function of disc penetration and independent of rock physical properties.

(b) The effect of edge radii is reduced when using deeper penetrations.

(c) Specific energy remains almost constant with increasing edge radius for penetrations deeper than 2mm, since bluntness causes an increase in yield.

(d) In relieved cutting situations the general trend was for optimum spacing/penetration ratio to increase as discs became duller.

* * *

CHAPTER TEN

TOOTHED ROLLER CUTTERS

Toothed roller cutters have long been in use in blast hole drilling and in the oil industry for cutting large diameter boreholes to great depths and now they are in common use on tunnel boring machines. Table 32 divides the steel toothed roller cutters into four classifications, determined by the formation strength which they are best suited to drill[95].

Table 32 Classification of Toothed Roller Cutters.

Rock Formation	Cutter Type	Design Features Cutting Action			
		T Spacing	T Depth	Gauge Hard Facing	Crushing
Soft to medium formations, shales, clays, calcites.	A				
Harder shales, hard limestone, sandstone	B				
Hard semi-abrasive formations, siliceous limestone, dolomite, sandstone.	C				
Hard abrasive formations, siliceous limestone, hard sandstone, copper ores.	C&D				

Yet the designers of boring machines are still faced with a deficiency of reliable information on the choice of this type of cutters. The main objective of this Chapter is to try to provide a basis for the comparison of the efficiency of toothed roller cutters with the other type of cutters.

10.1 Experimental Technique and Procedure

The present work is restricted to one type of toothed roller cutter which has 60° x 12 teeth, a diameter of 110mm and width of 25.4mm. This toothed roller cutter was constructed from steel and subsequently hardened. The cutter was used in Gypsum, Bunter Sandstone, Dunhouse Sandstone and Mansfield Sandstone at 5 levels of depths up to 10mm.

The cutting rig, the recording instrumentation and the method of data analysis were similar to that used for the other type of cutters.

All test values are given in Appendix 23.

* * *

10.2 Unrelieved Cutting

The results are presented in graphical form in Figs. 70 to 73. Thrust forces increased approximately linearly with penetration in Dunhouse and Mansfield Sandstones and the relationship seemed to follow a power law in Bunter Sandstone and in Gypsum. Bunter Sandstone provided the lowest thrust forces for all the values. Mansfield Sandstone was the third rock to be tested; due to high forces, the toothed roller cutter failed when cutting at 10mm depth. The experiment in Dunhouse Sandstone was carried out with a replacement toothed roller cutter identical to the previous cutting tool.

Both peak and mean rolling forces increase with depth of cut with a non-linear law relationship. Bunter Sandstone gives the lowest forces and Dunhouse Sandstone showed the highest value for the 4 different rocks.

The ratio of thrust force to rolling force remains between 10 and 4.5 for 4 rocks being high at shallow cuts and low at deep cuts. At shallow penetrations each tooth is only briefly in contact with the rock and interaction between each groove begins when the penetration is bigger than 7. Due to this fact Peak Force/Mean Force ratio decreases with penetration as can be seen in Fig.74 and levels off when penetration reaches the value of 7mm.

* * *

12 Toothed Roller Cutter Experiment

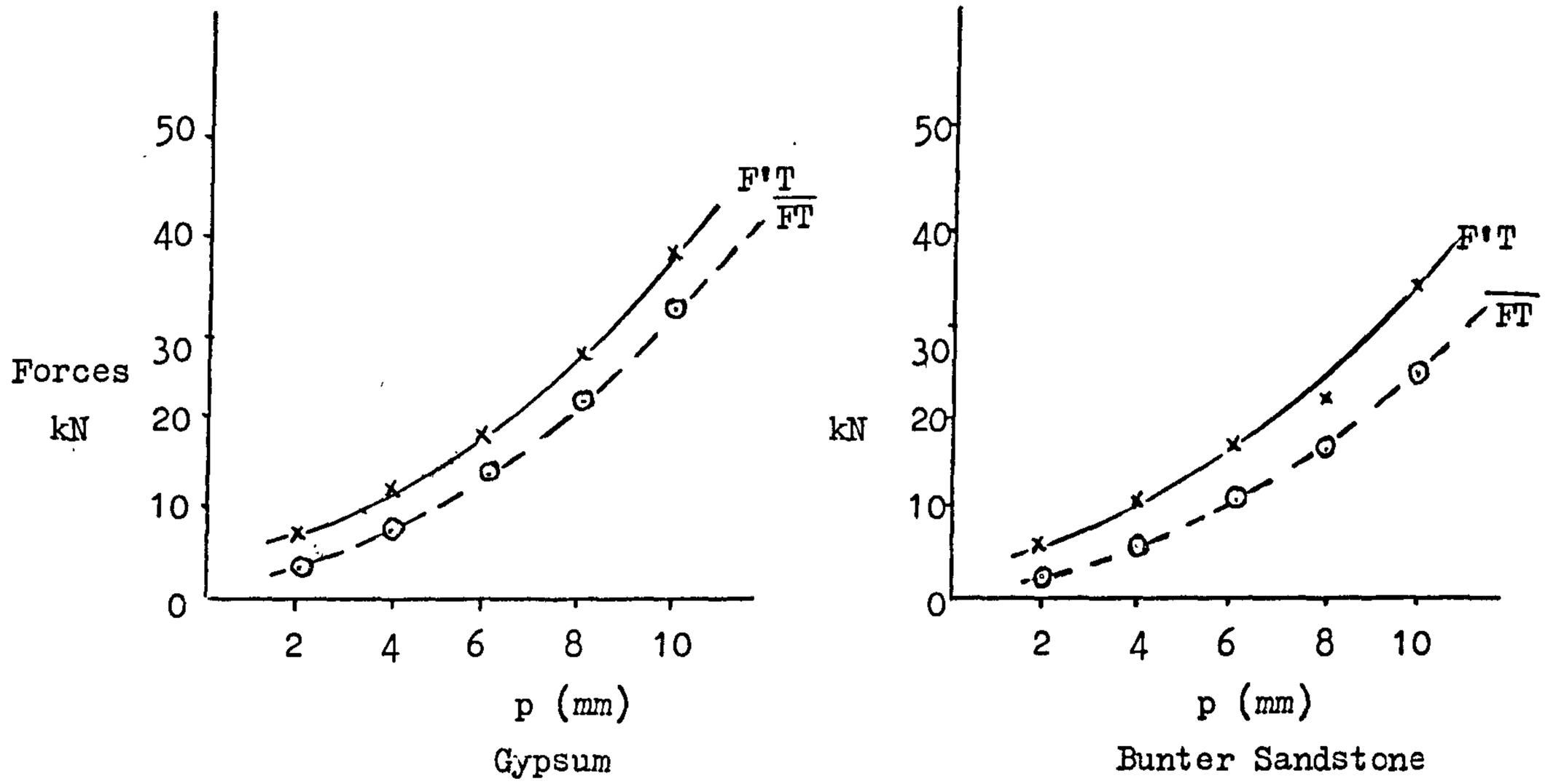

Fig.70 Variation in Thrust Forces with Penetration.

12 Toothed Roller Cutter Experiment

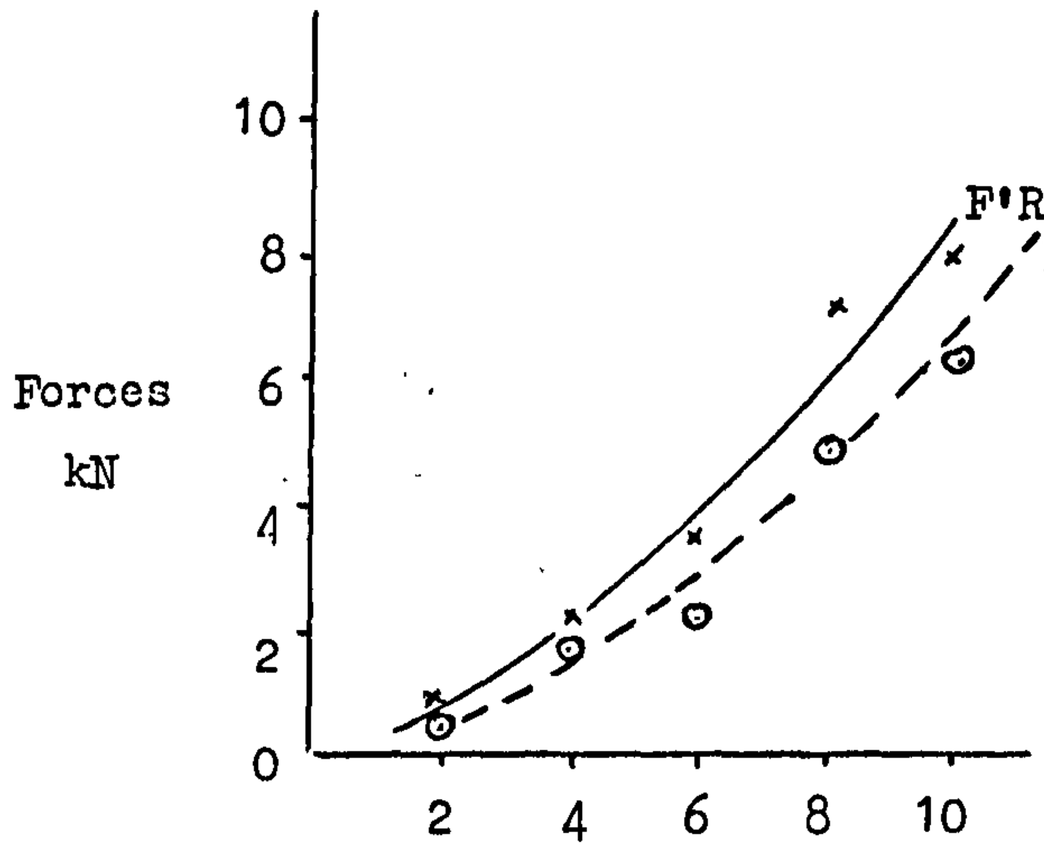

Gypsum

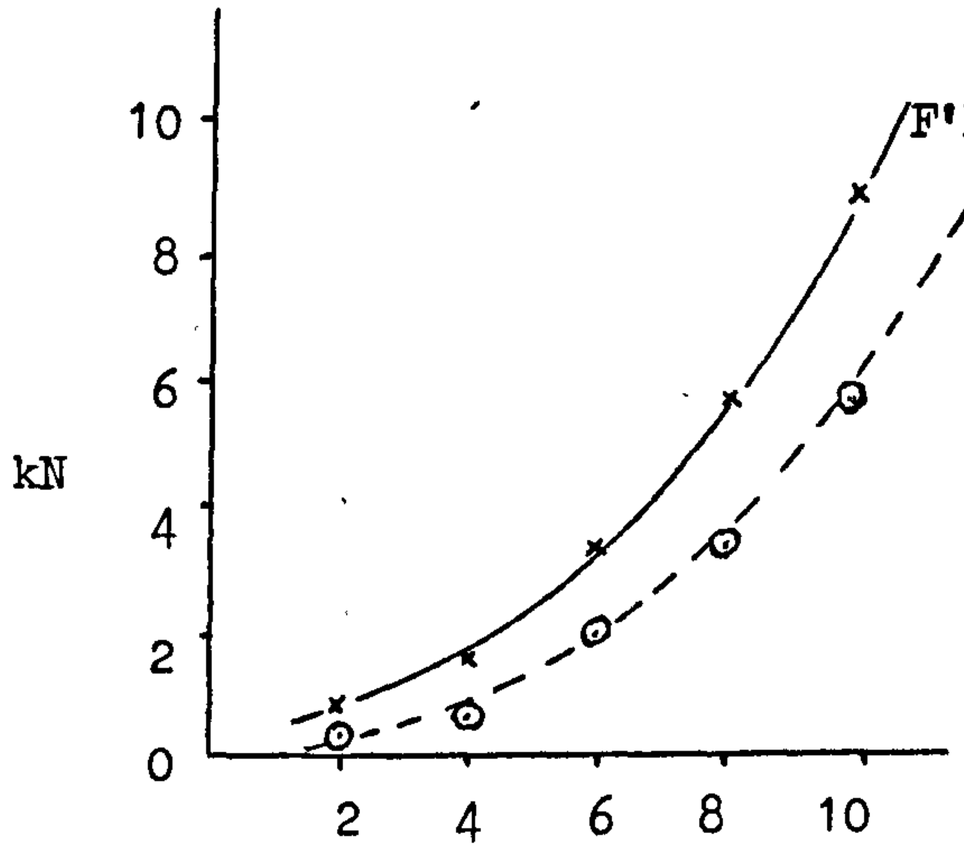

Bunter Sandstone

x Peak Rolling Force

• Mean Rolling Force

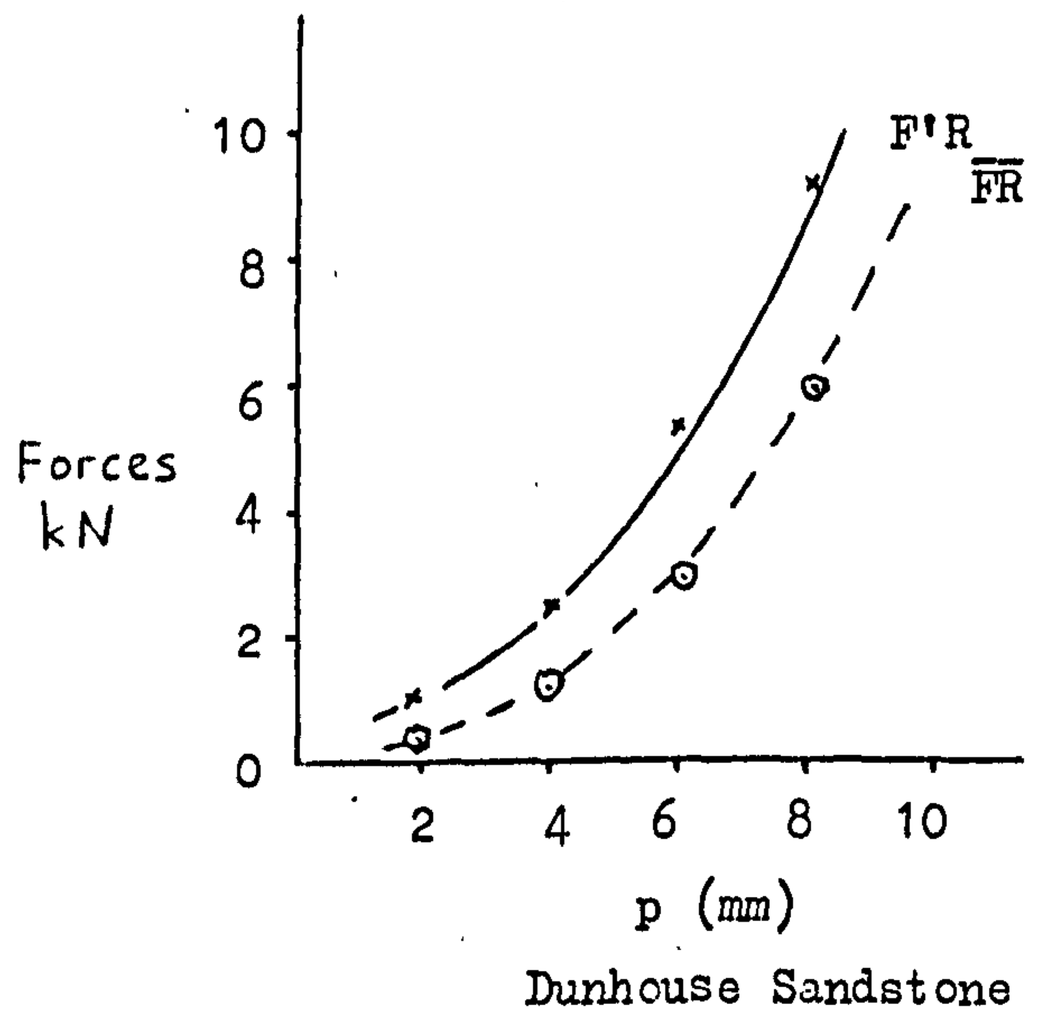

Dunhouse Sandstone

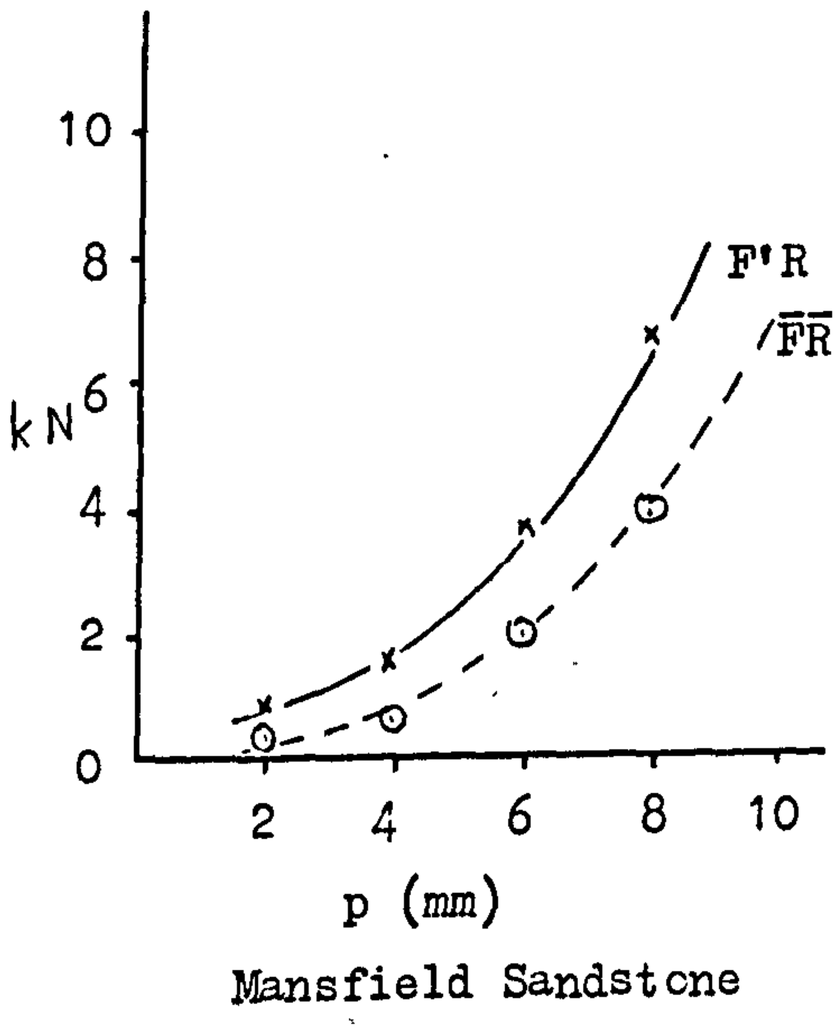

Mansfield Sandstone

Fig.71 Variation in Rolling Forces with Penetration.

12 Toothed Roller Cutter Experiment

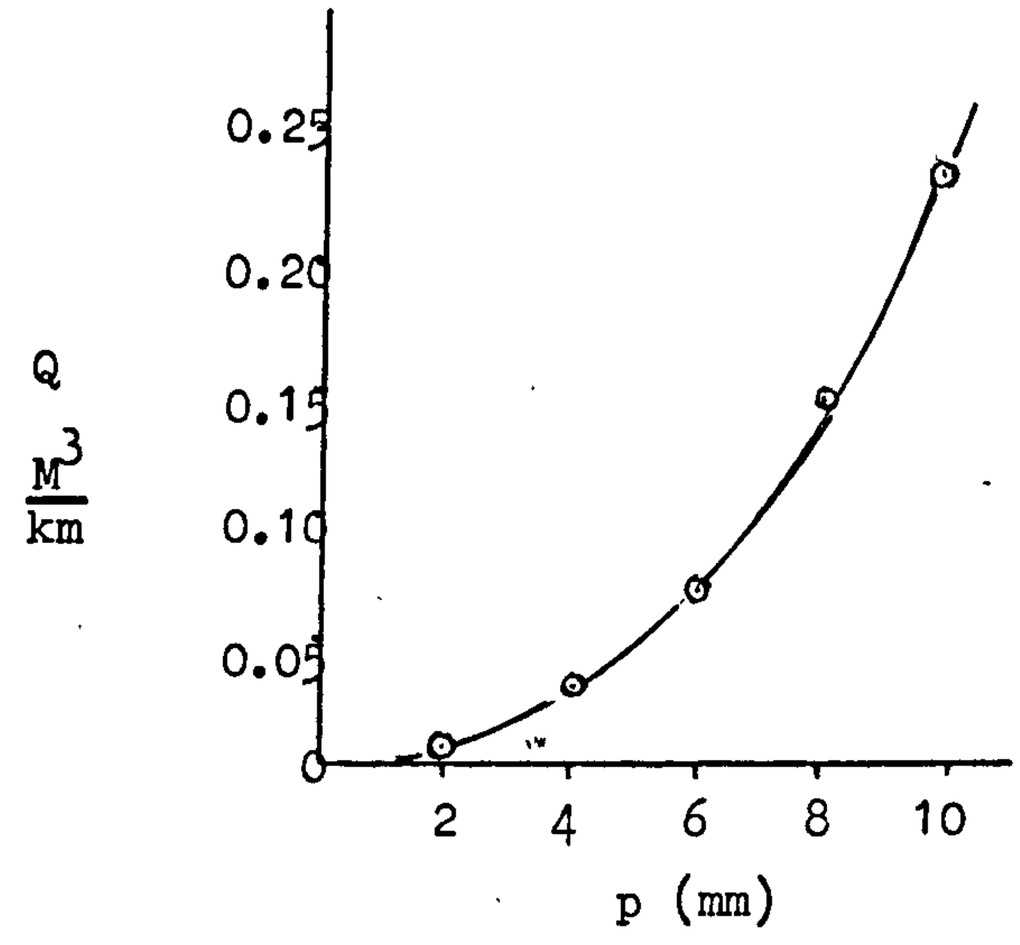

Gypsum

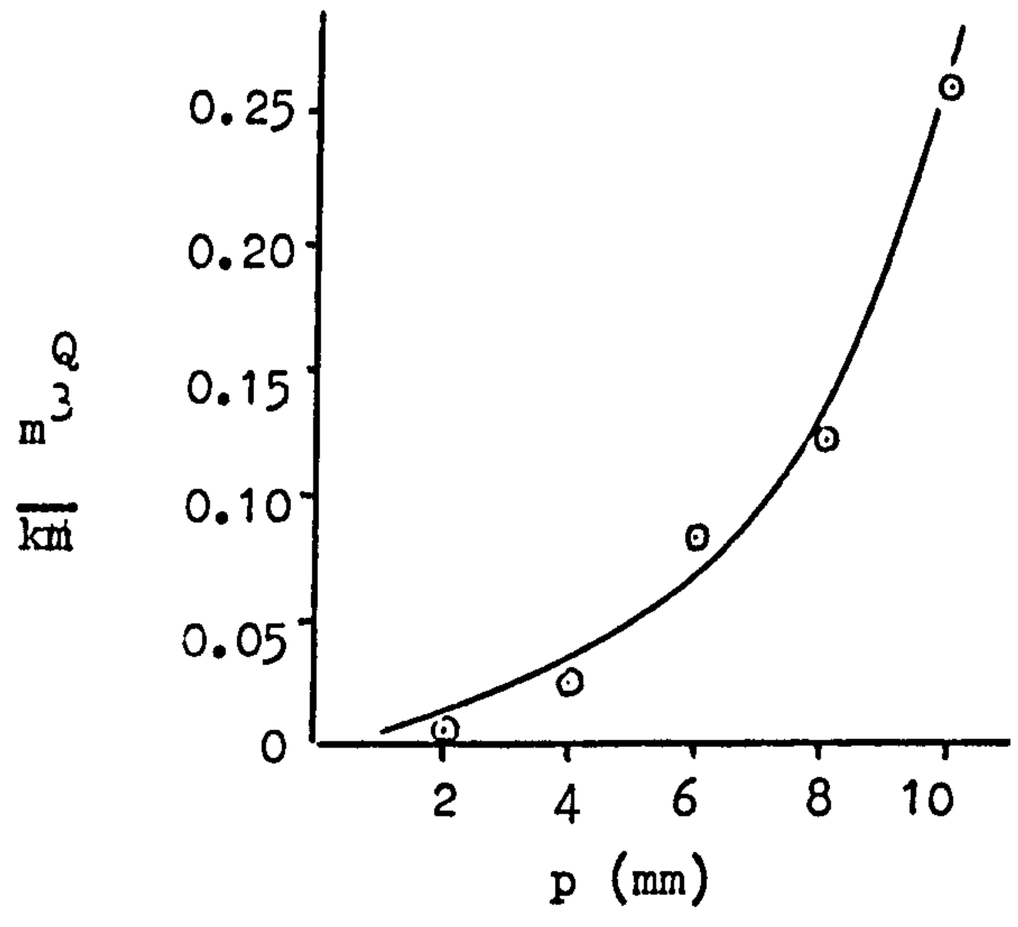

Bunter Sandstone

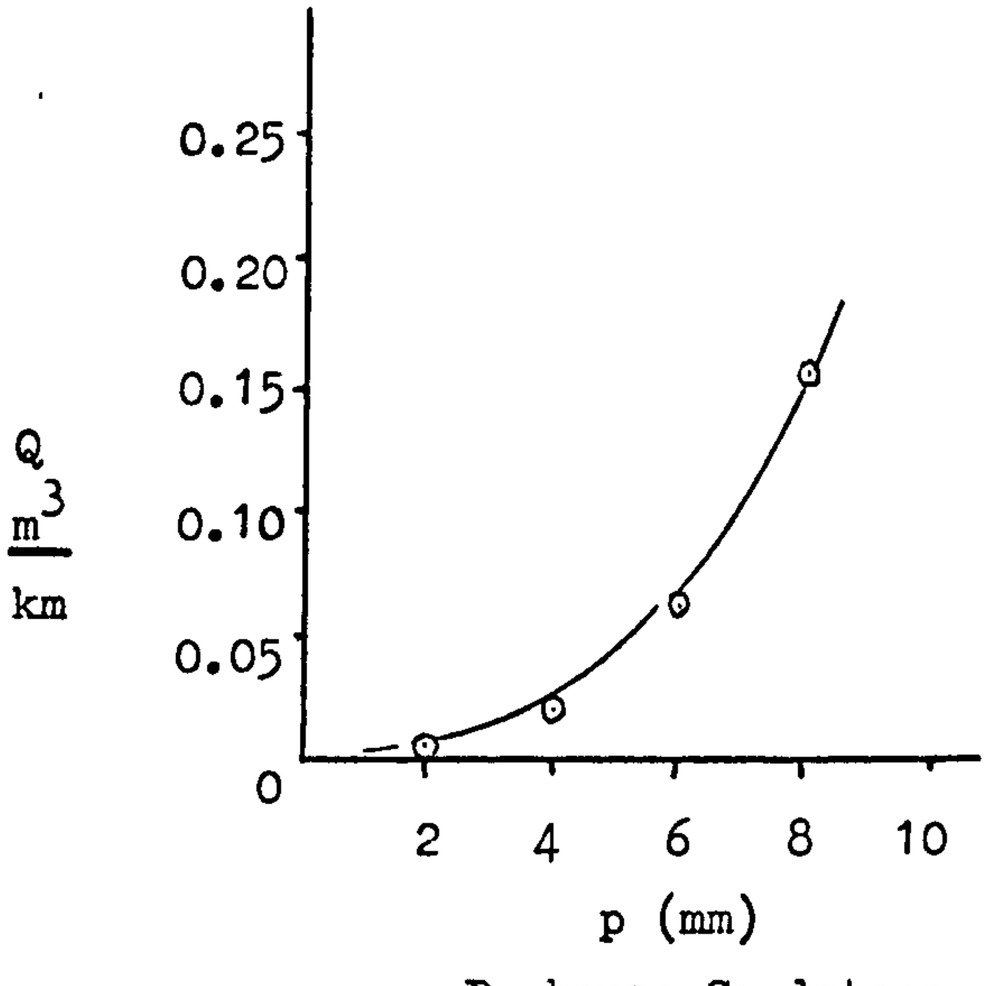

Dunhouse Sandstone

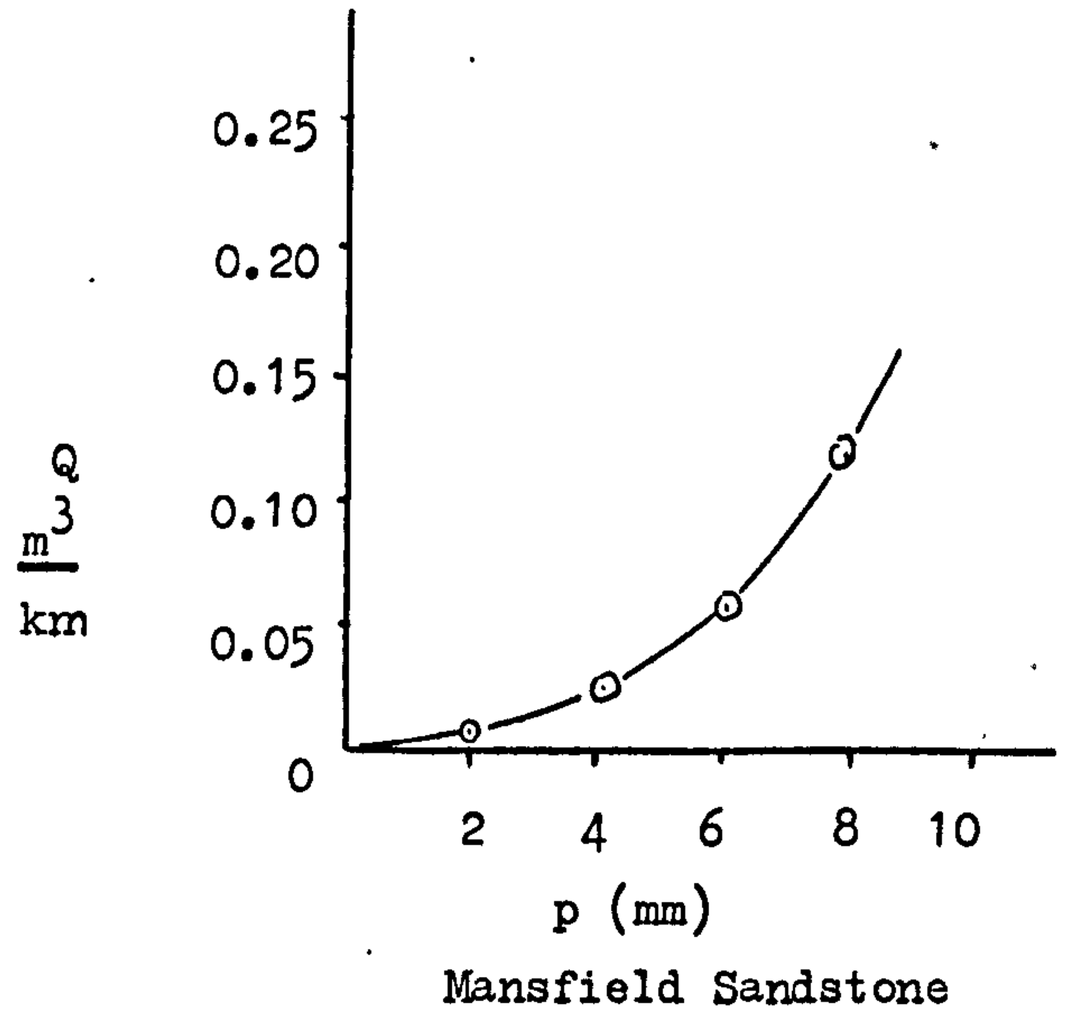

Mansfield Sandstone

Fig.72 Variation in Yield with Penetration.

12 Toothed Roller Cutter Experiment.

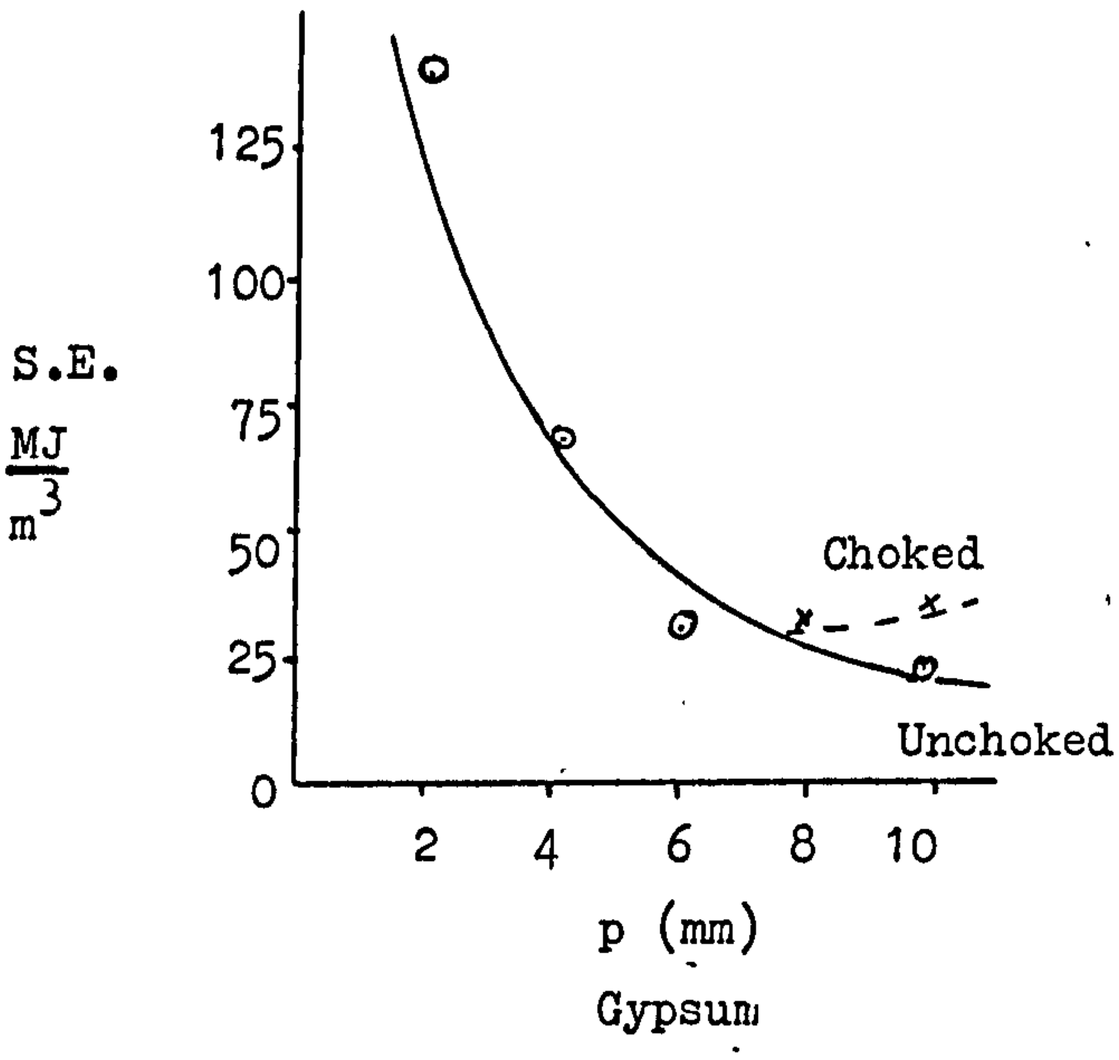

Gypsum

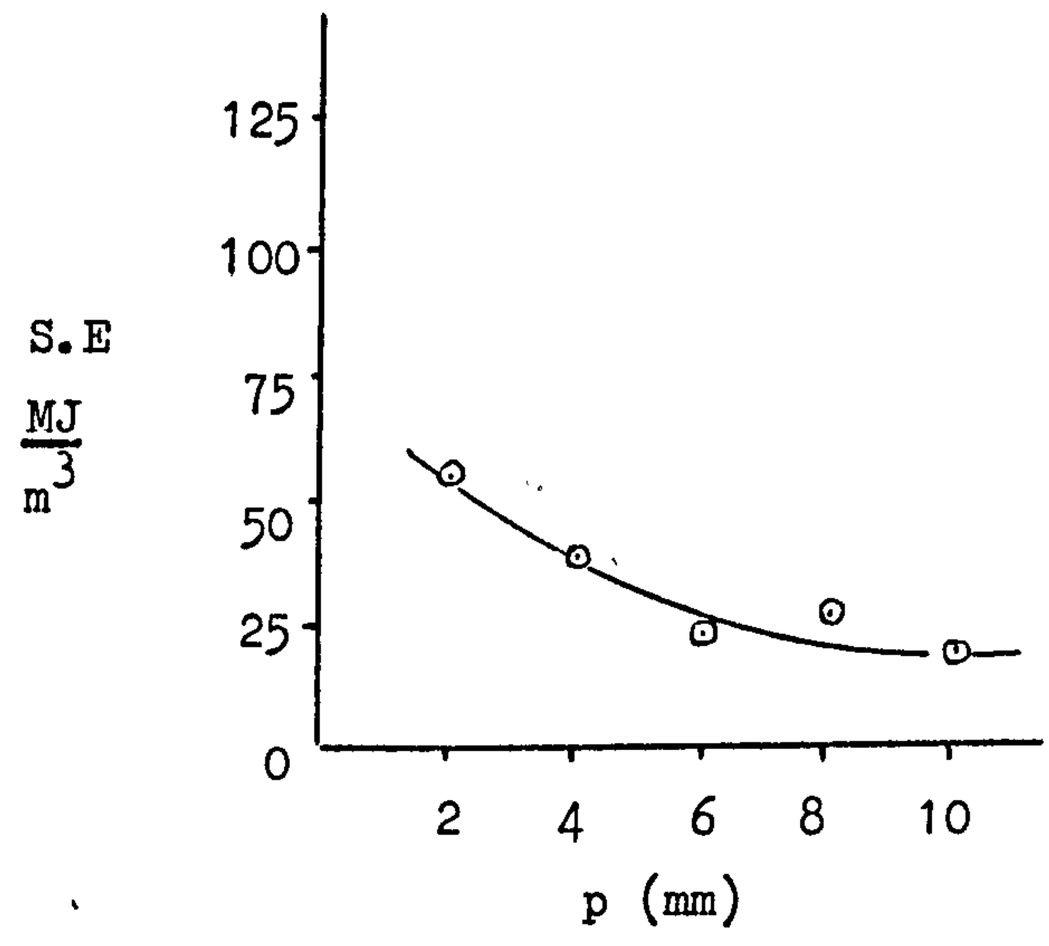

Bunter Sandstone

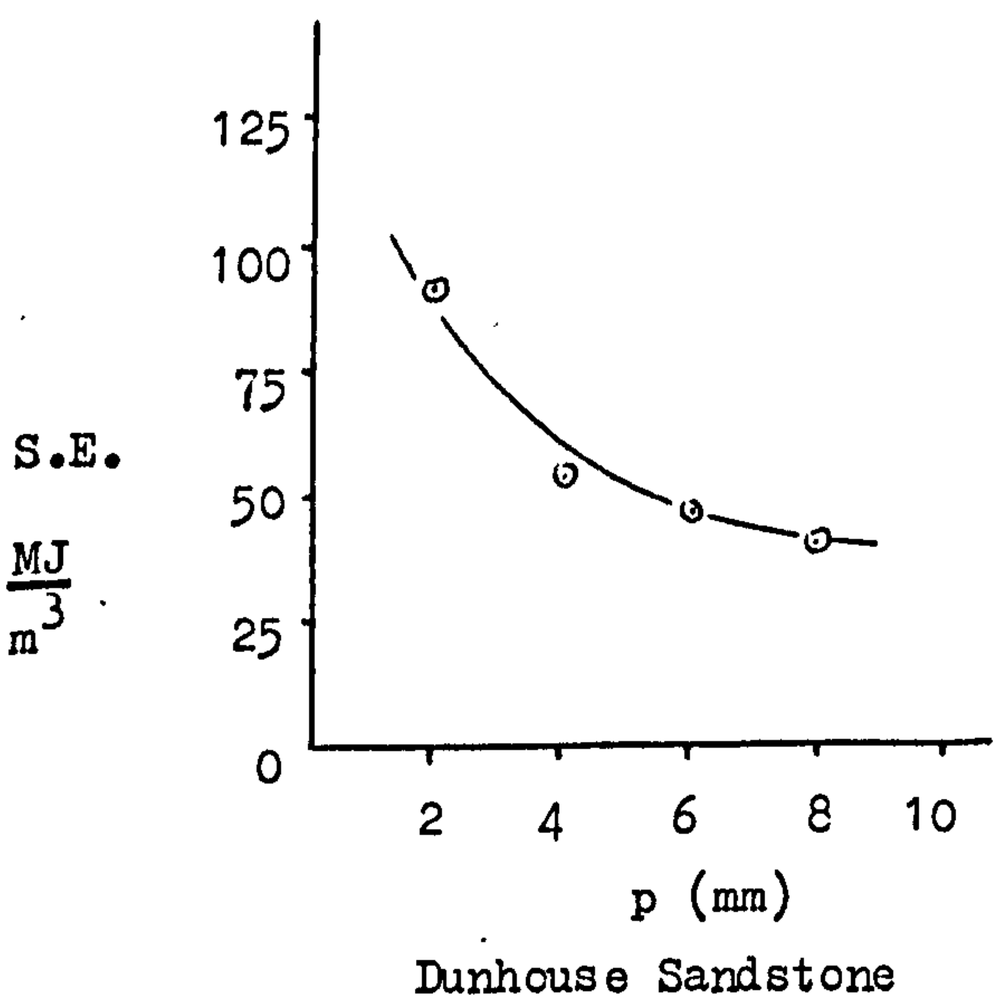

Dunhouse Sandstone

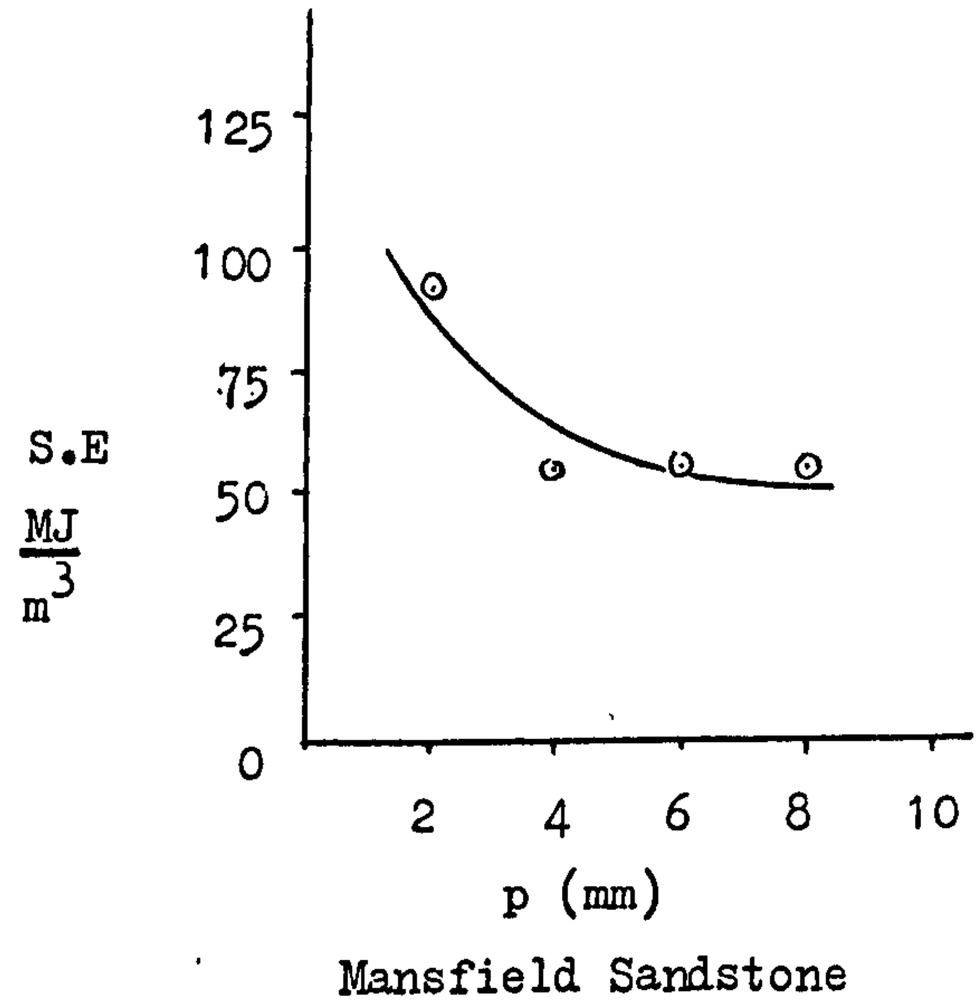

Mansfield Sandstone

Fig.73 Variations in Specific Energy with Penetration.

It was found that yield increased with the square of penetration. All the rocks exhibited a large fall in Specific Energy with increasing penetration up to about 6mm, after which improvement was much more gradual. This indicates that there is a limit to the benefit gained from deep cuts.

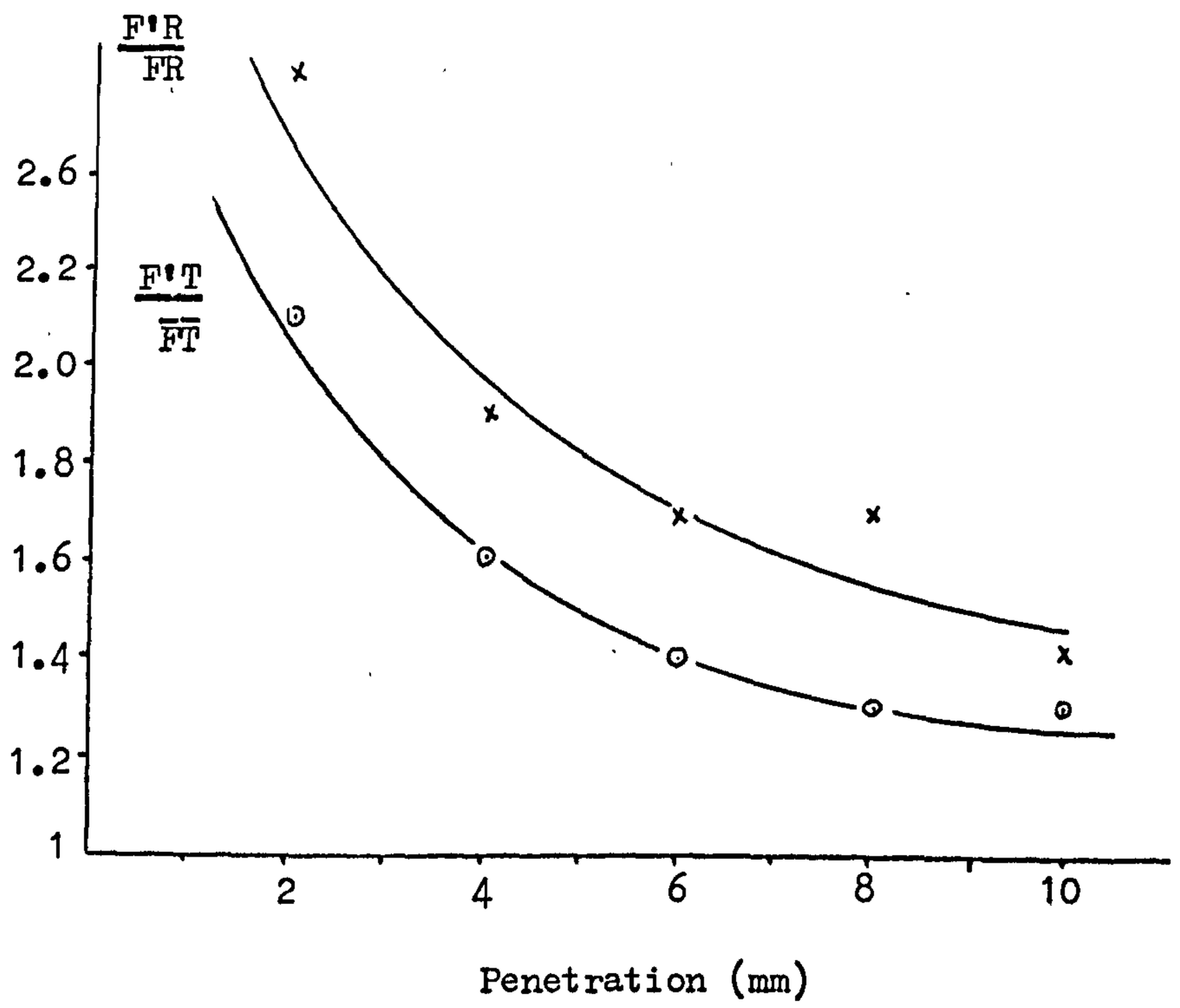

Fig.74 Peak Force /Mean Force Ratios for 4 Rocks.

* * *

10.3 Relieved Cutting

This type of tool does not in practice operate in isolation and the disposition of individual tools in an operational array must be considered for the better understanding of gear cutter performance.

The spacing tests were undertaken in three different rocks at different spacing with one depth of penetration, since the second roller cutter failed when cutting Mansfield Sandstone. Yield and Specific Energy values are plotted in Figs. 75 and 76. From these figures it can be seen that yield increases rapidly with spacing and stays asymptotic for the spacing values representing the unrelieved situation. The lowest specific energy was for an s/p ratio of approximately 1 in Bunter Sandstone, 1.5 in Dunhouse Sandstone and 0 in Mansfield Sandstone.

* * *

12 Toothed Roller Cutter Experiment

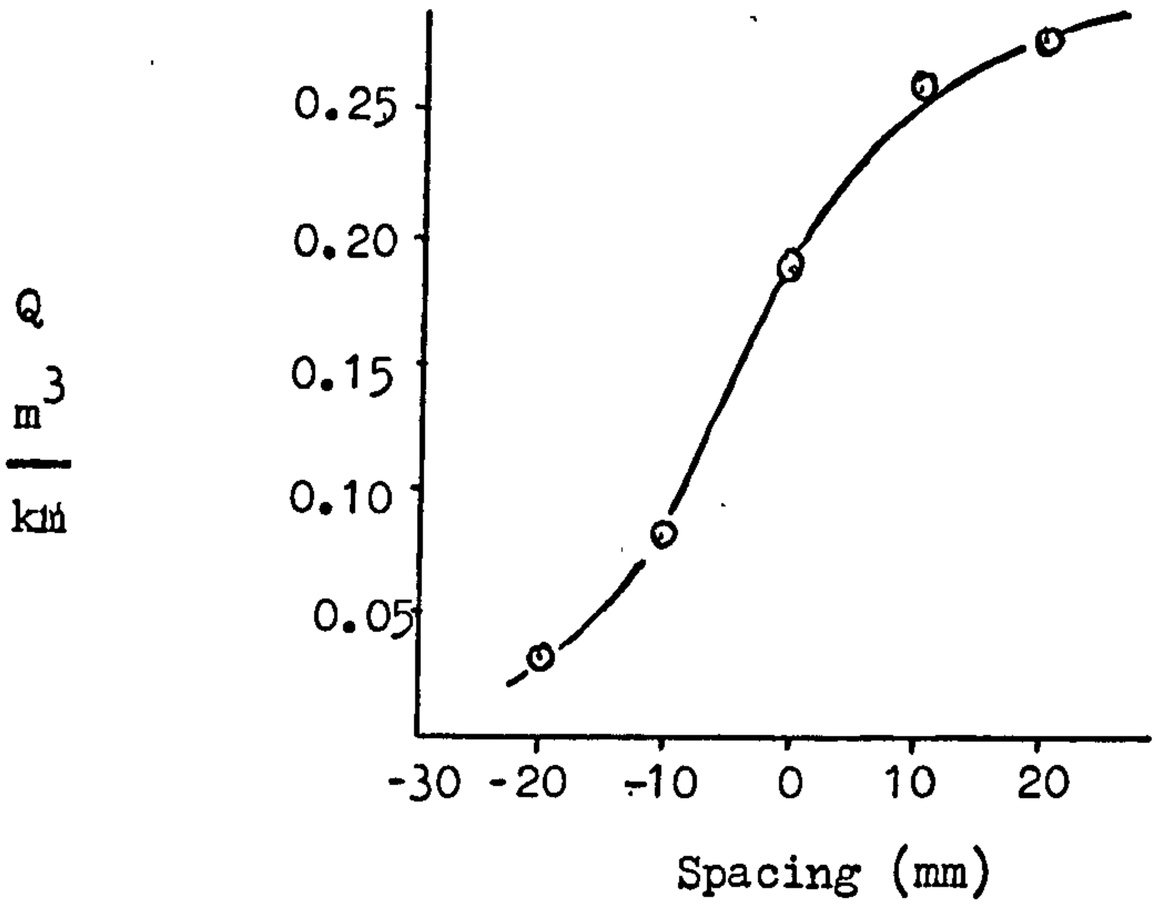

Bunter Sandstone

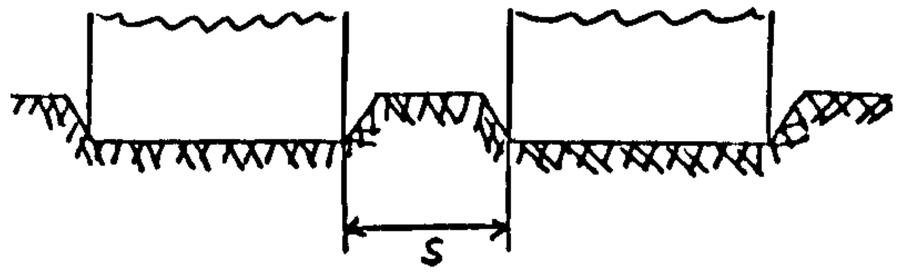

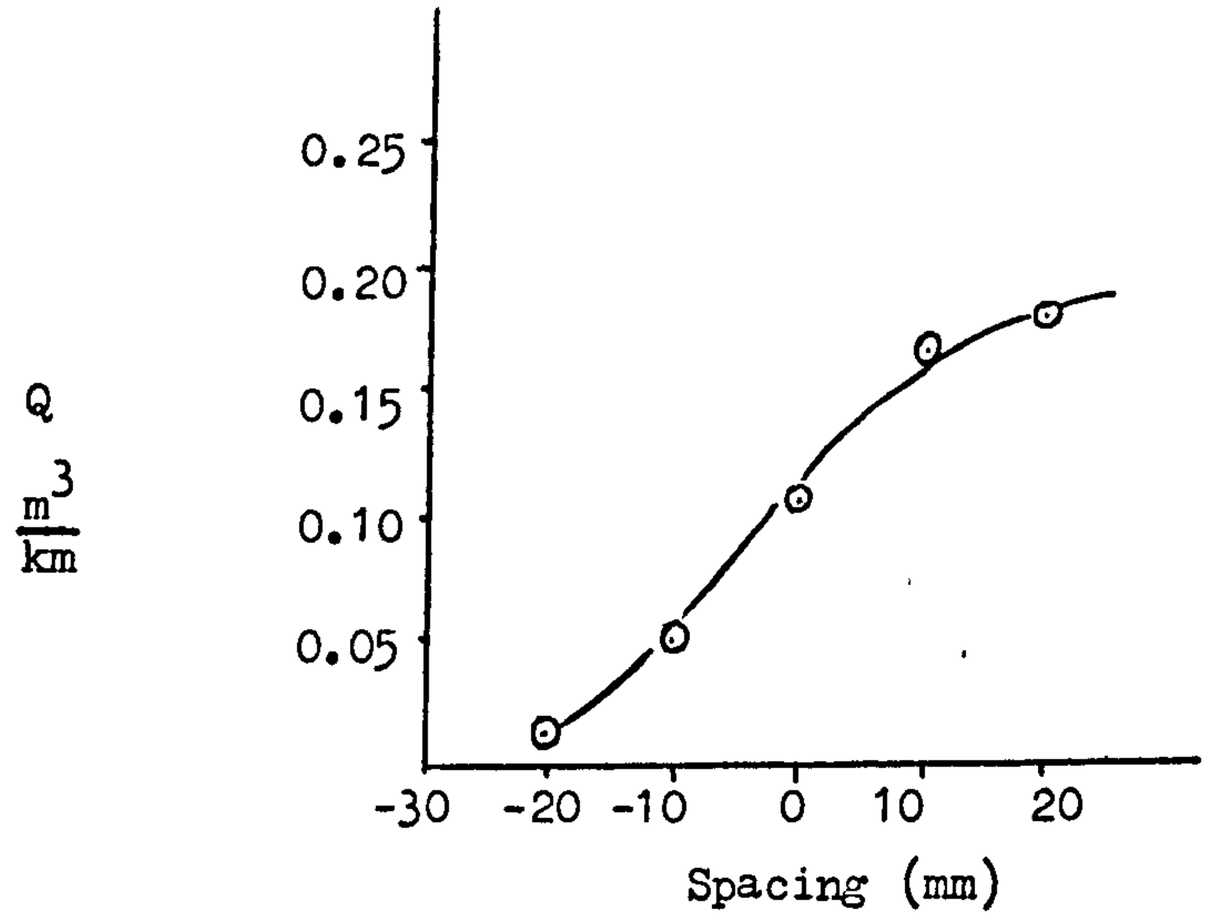

Dunhouse Sandstone

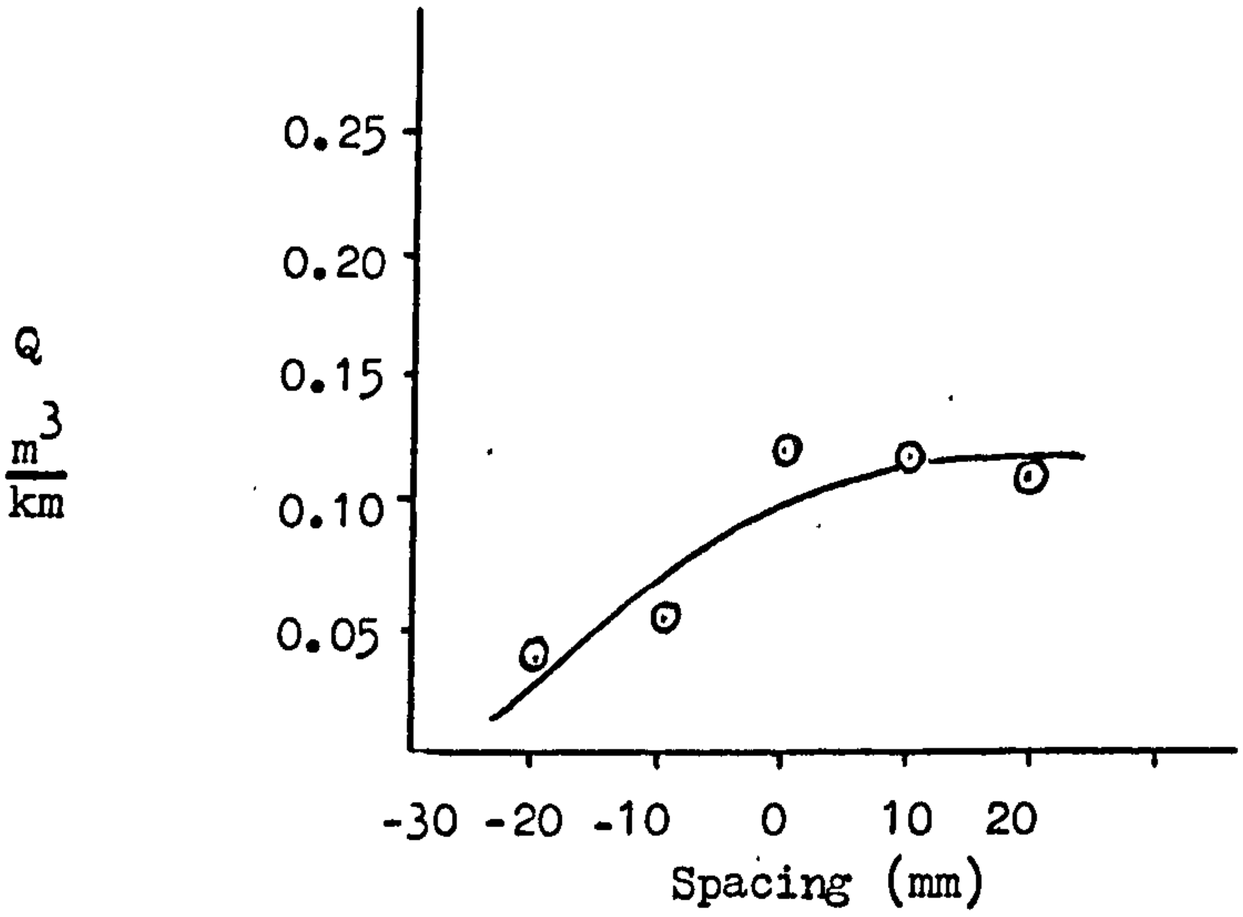

Mansfield Sandstone

Fig.75 Variation in Yield with Spacing.

12 Toothed Roller Cutter Experiment

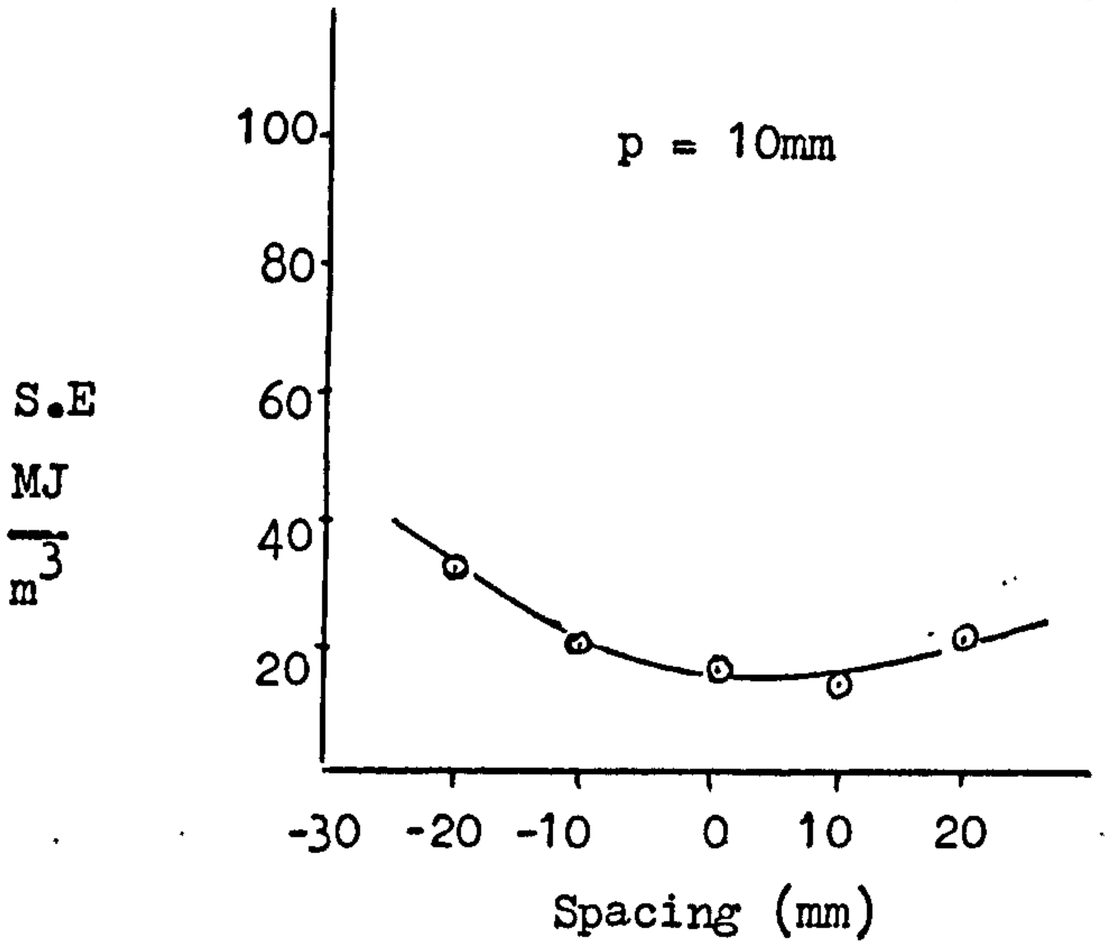

Bunter Sandstone

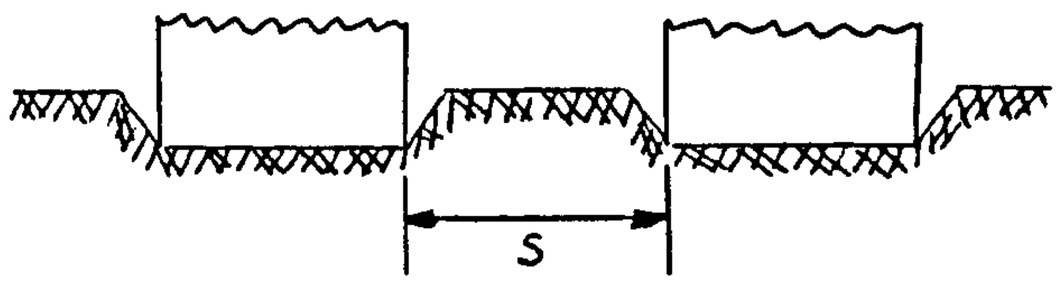

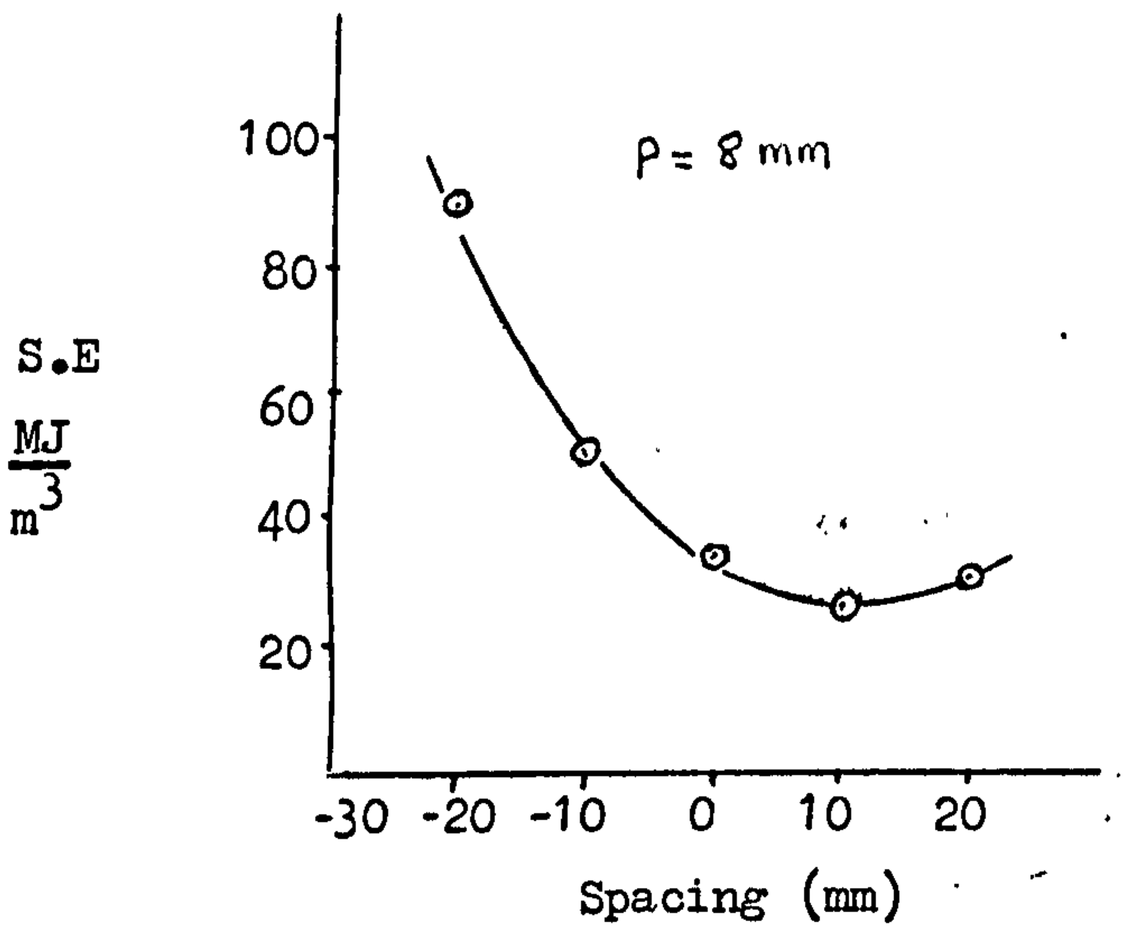

Dunhouse Sandstone

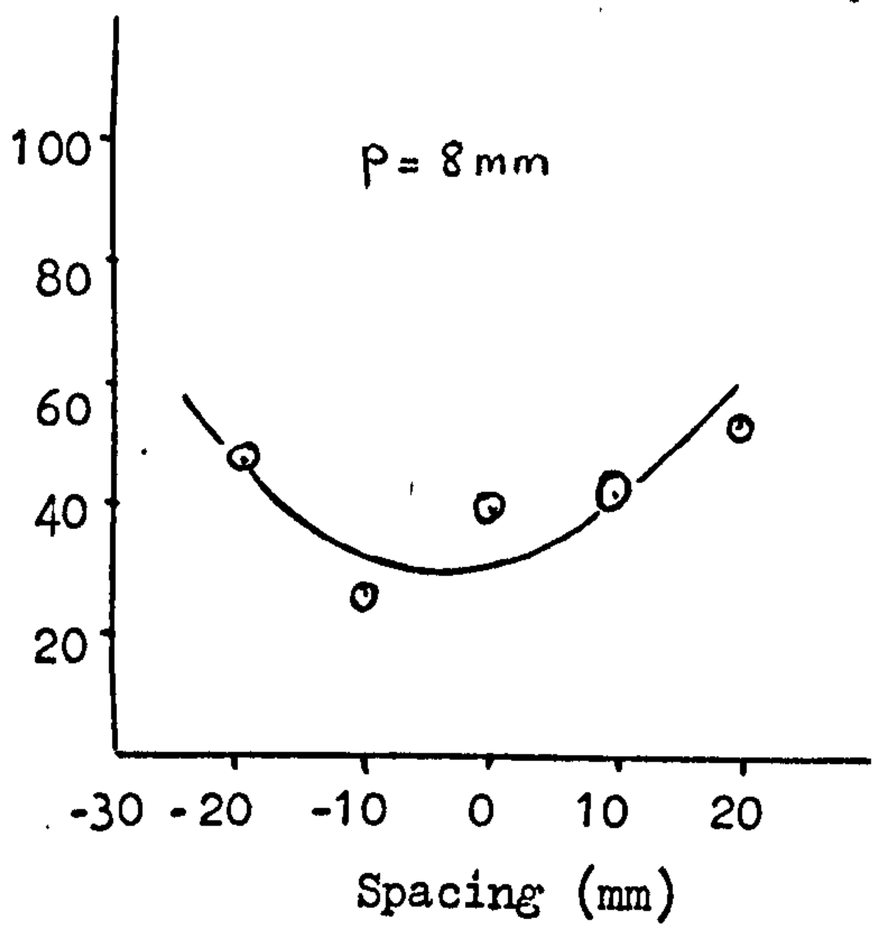

Mansfield Sandstone

Fig.76 Variation in Specific Energy with Spacing.

CHAPTER ELEVEN

CUTTING HIGH STRENGTH ROCKS WITH PICKS

Although pick cutters are mostly used in soft and medium strength rocks their application in strong and abrasive rocks is increasing[96]. Probably the main advantage of picks comes from the fact that they are relatively cheap compared to roller cutters and machines equipped with picks do not require as high values of thrust against the face as do tunnelling machines using rotary cutters. This reduces many problems associated with the design of the machine. It has lately been reported that an Atlas Copco pick machine was successfully used in a Jurassic Limestone of 120 MN/m^2 compressive strength[97].

In the following Chapter the physical laws governing the cutting performance of picks in Anhydrite, Limestone, Greywacke and Granite are reported.

11.1 Experimental Programme

The partial factorial experimental technique described in Chapter Four has been used in planning the pick cutting experiments. Pick cutter parameters are defined as follows.

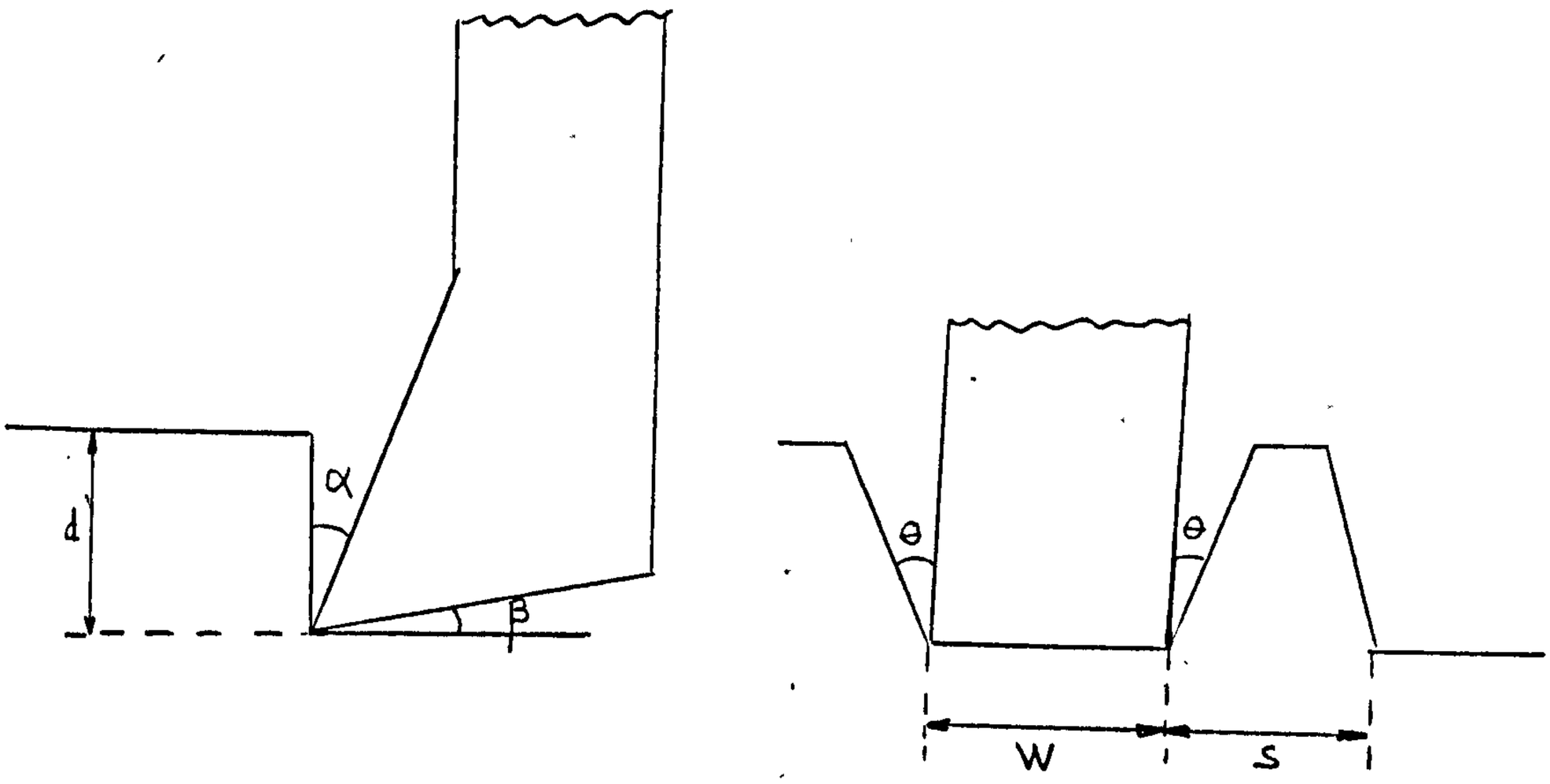

d = Depth of cut

α = Rake Angle

β = Back Clearance Angle

W = Width of Pick

S = Spacing

θ = Breakout Angle

Fig. 77 Pick Cutter Parameters.

The effect of rake angle (α), width of pick (W) and depth of cut (d) on the cutting performance of 25 different picks has been studied in four high strength rocks, all of the picks having 5° side clearance angle and 10° back clearance angle. Due to cutting experience in Anhydrite, it was felt that new, stronger picks should be designed for the other high strength rocks. A range of negative rake tools were considered as most suitable, since these would possess an inherent strength in their geometry.

A constant cutting speed of 150mm/sec was used for these experiments and each of the 25 experimental levels was replicated four times. The experimental programme carried out for relieved and unrelieved cutting is given in Tables 33 and 34.

Table 33 Experimental programme for unrelieved cutting experiments.

Rock	Independent Variable	Levels
Anhydrite	Depth of cut, d(mm) Width of Pick, W(mm) Rake Angle, α(o)	1.5 3 4.5 6 7.5 10 20 30 40 50 -10 0 10 20 30
W.Limestone Greywacke	Depth of cut, d(mm) Width of Pick, W(mm) Rake Angle, α(o)	1.5 3 4.5 6 7.5 10 15 20 25 30 0 -5 -10 -15 -20
Granite	Depth of cut, d(mm) Width of Pick, W(mm) Rake Angle, α(°)	1 2 3 4 5 10 15 20 25 30 0 -5 -10 -15 -20

Table 34 Experimental programme for relieved cutting experiments

Rock	Independent Variable and levels	s/d
Anhydrite	W=30mm, α = 10°, d=3,4.5,6mm	-0.5 1 2.5 4 5.5
Limestone Greywacke	W=20mm, α =-10° d=3,4.5,6mm	-0.5 1 2.5 4 5.5

The excessive wear and failure of some picks in Granite made the relieved cutting tests very difficult to carry out in this rock and the experiment was abandoned after a few cuts.

The measured and calculated parameters obtained for each experimental cut are defined as follows:

(a) Mean Peak Cutting Force, F'C (kN)

The average of the peak forces acting on the tool in the direction of cutting.

(b) Mean Cutting Force, $\overline{FC}$ (kN)

The average force on the tool in the direction of cutting.

(c) Mean Peak Normal Force, F'N (kN)

The average force acting normal to the direction of cutting, tending to push the tool into or out of rock.

(d) Mean Normal Force, $\overline{FN}$ (kN)

The average force on the tool acting normal to the direction of cutting.

(e) Yield, Q (m^3/km)

The volume of rock excavated per unit distance cut.

(f) Specific Energy, S.E (MJ/m^3)

The work done per unit volume of each cut.

Hence, $$S.E = \frac{\text{Mean Cutting Force}}{\text{Yield}}$$

(g) Coarseness Index

As defined in Chapter Seven.

* * *

11.2 Results of Unrelieved Cutting Experiments

Measured and predicted values for all rocks are given in Appendices 24 to 27 and the results are plotted in Figs. 78 to 86.

Effect of Depth of Cut

All forces are directly proportional to the depth of cut. The cutting force relationships are better defined than those for the normal forces which consistently showed scatter. The ratio of peak cutting force to mean cutting force is 2.1 for all rocks and for each level of experimental variable. However, the ratio of peak normal force to mean normal force is less than the previous one, being 1.3 for Granite and 1.6 for other rocks. The ratio of $\frac{FC}{FN}$, in general, increases with depth of cut as shown in Table 35. This is in good agreement with Barendsen and Wagner's observations in high strength rocks[98]. The ratios are calculated for mean values of rake angle and width of tool.

Table 35 Variation of the ratio $\frac{\overline{FC}}{\overline{FN}}$ with depth of cut.

d mm	Greywacke $\overline{FC}/\overline{FN}$	Limestone $\overline{FC}/\overline{FN}$	Anhydrite $\overline{FC}/\overline{FN}$	d mm	Granite $\overline{FC}/\overline{FN}$
1.5	0.72	1.05	0.63	1	0.67
3.0	0.89	1.24	0.68	2	0.74
4.5	1.05	1.43	0.70	3	0.80
6.0	1.23	1.45	0.66	4	0.88
7.5	1.55	1.46	0.58	5	1.05

The relationship between yield and depth of cut is found, for all rocks, to follow a square law. Specific energy decreases rapidly at shallow depths and then levels off at greater depths. This indicates that there is a limit to the benefit gained from deep cuts. Coarseness index against depth of cut follows the inverse of specific energy curves. Breakout angles, θ^{o}, are calculated directly from yield and found to be a function of depth of cut in Greywacke and in Limestone as shown below.

	Greywacke	Limestone
d mm	θ^{o}	θ^{o}
1.5	39	33
3.0	47	35
4.5	54	54
6.0	69	60
7.5	57	60

The average breakout angle for Anhydrite is 50^{o} and for Granite 25^{o}.

When cutting Granite it was noticed that third and fourth replications for each test gave significantly higher values compared to first cut, due to very abrasive nature of this rock. Fig.87 shows dramatic changes in pick cutting performance with wear. The first one is a typical wear curve suggesting that the wear is reduced in deeper cuts. All the empirical relationships for Granite are derived from sharp cutting results.

Effect of Tool Width

Cutting and normal forces are seen to increase linearly with

tool width. The linear relationship between yield and tool width gives a positive intercept which is the yield generated by breakout. Specific Energy is found to be constant for all pick widths. Breakout angles, coarseness index and the ratios of $\frac{F'C}{FC}$, $\frac{F'N}{FN}$, $\frac{FC}{FN}$ are not affected.

Rake Angle

Considerable benefit is gained by increasing the rake angle but, in practice, this must be balanced against a decrease in tool strength. Specific energy and tool forces decrease with increasing rake angle in an exponential manner. The effect of rake angle on normal forces in Anhydrite is not very well defined. Coarseness index was seen to decrease linearly with rake angle.

* * *

11.3 Comparison of Experimental Results with Evans' Tensile Theory

The following equation has been used to calculate peak cutting forces for 25 experimental combinations in each rock. The calculated values are given in Appendix 29.

$$F'C = \frac{2.\sigma t.d.w.\sin \frac{1}{2}\left(\frac{\pi}{2} - \alpha\right)}{1 - \sin \frac{1}{2}\left(\frac{\pi}{2} - \alpha\right)}$$

As can be seen from Figs. 78, 80, 82 and 84, theoretical values are in good agreement in trend and in magnitude with measured values for all rocks, best results being obtained for Greywacke. The friction between picks and rocks during the cutting process is a complex problem and probably a more comprehensive study of the influence of the friction angle on the above equation will increase the accuracy of predicted cutting force values.

* * *

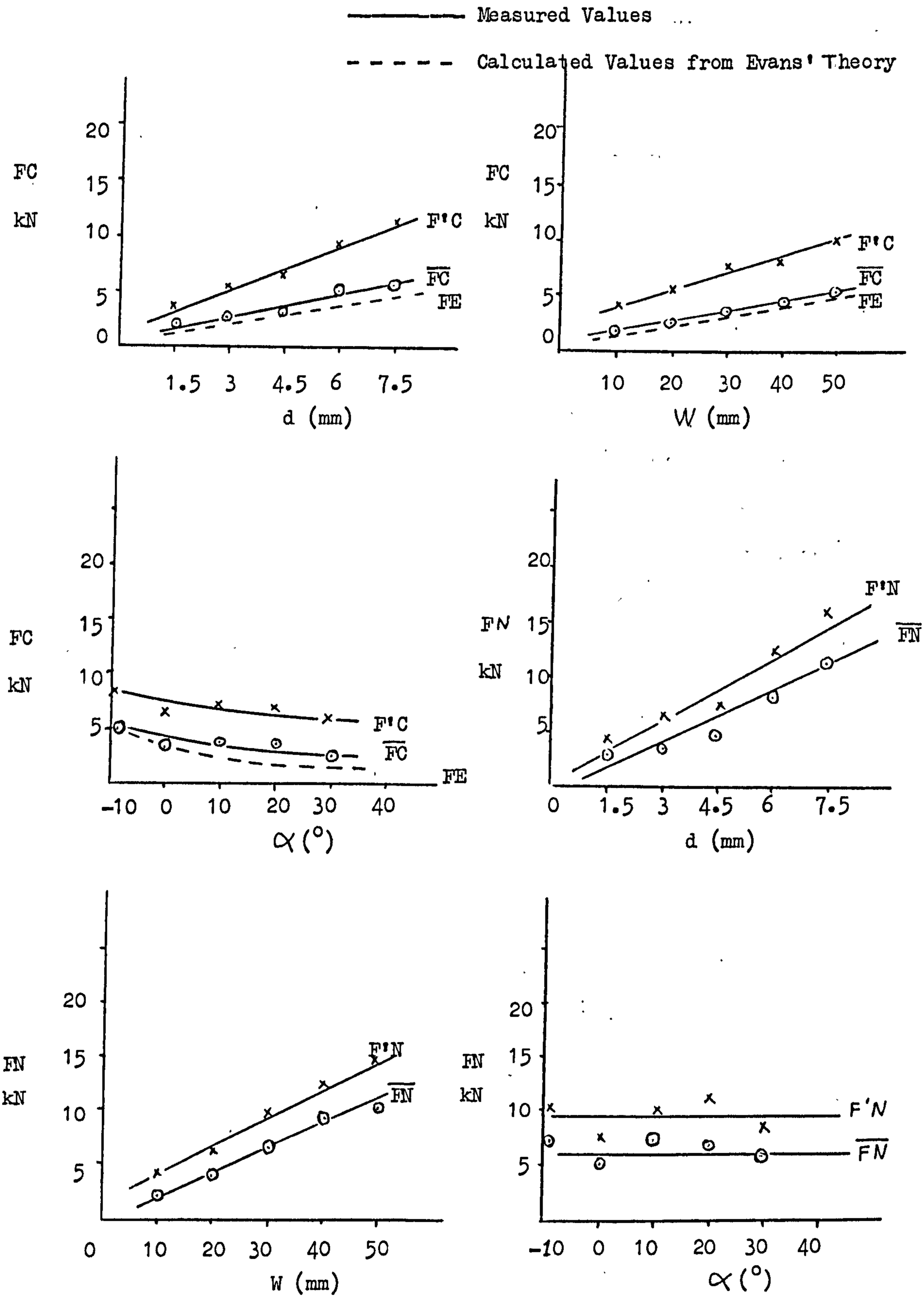

Fig.78 Variations in Forces with Pick Cutter Parameters in Anhydrite.

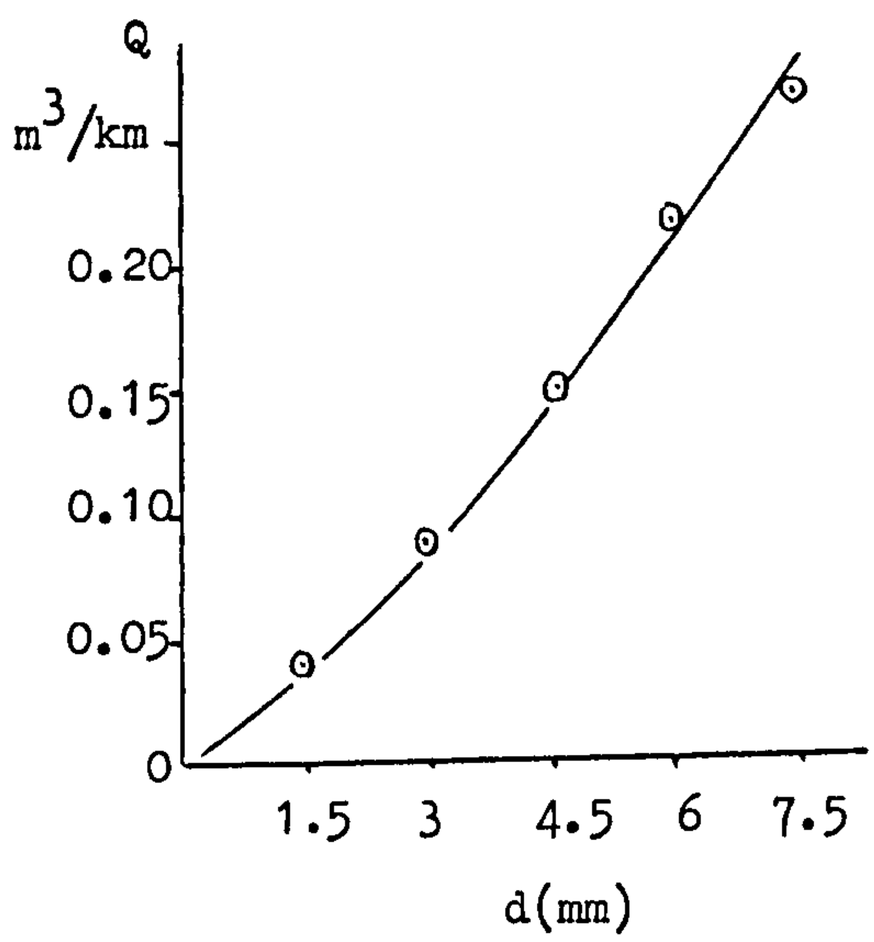

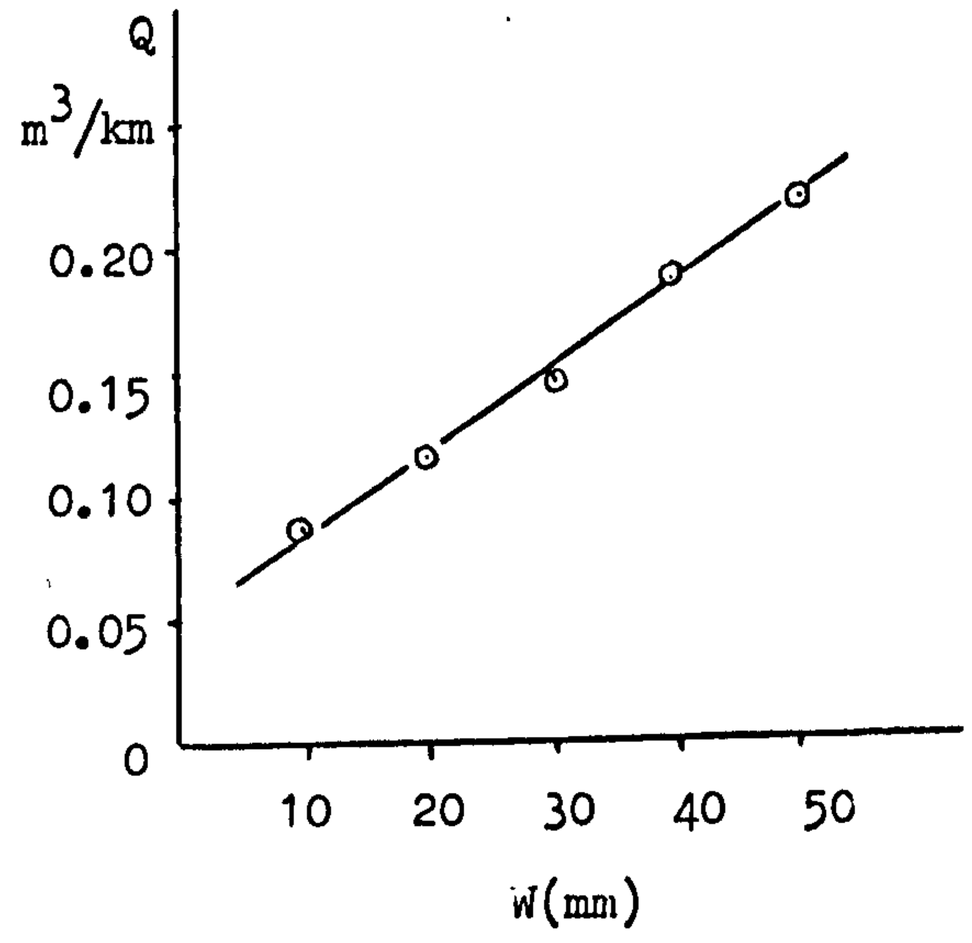

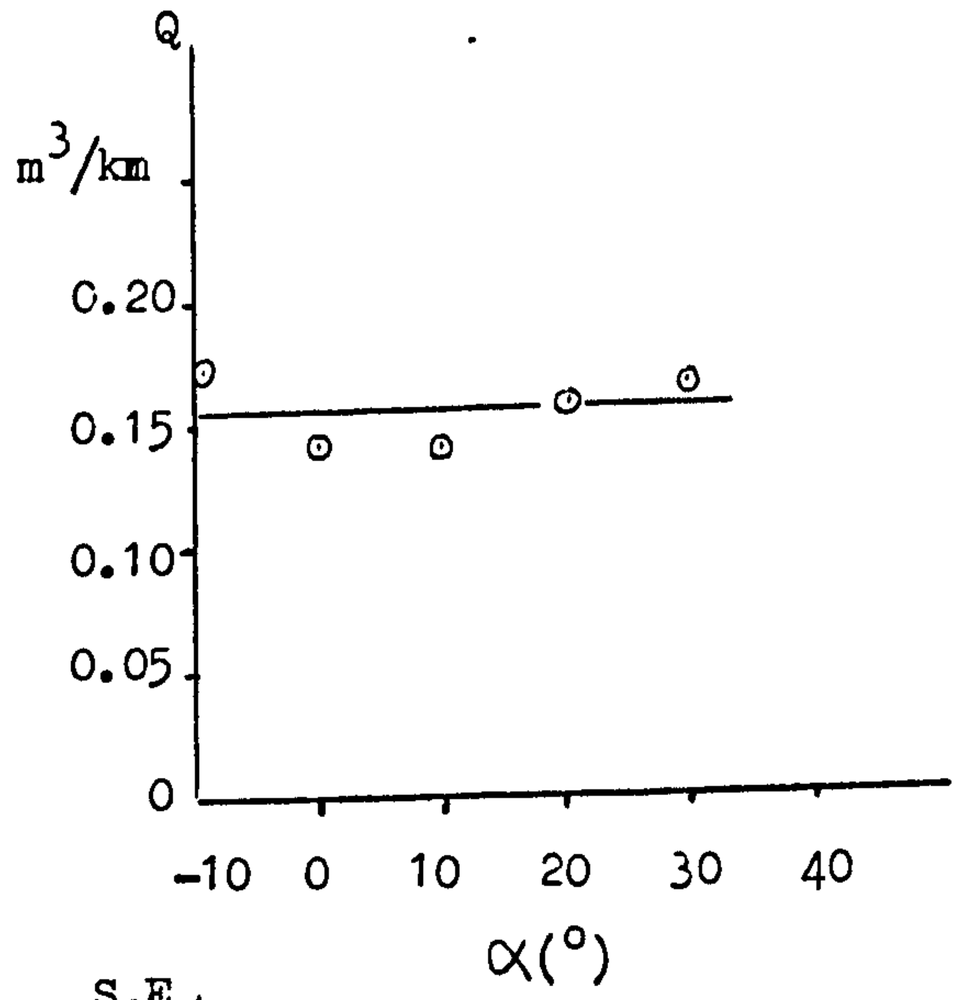

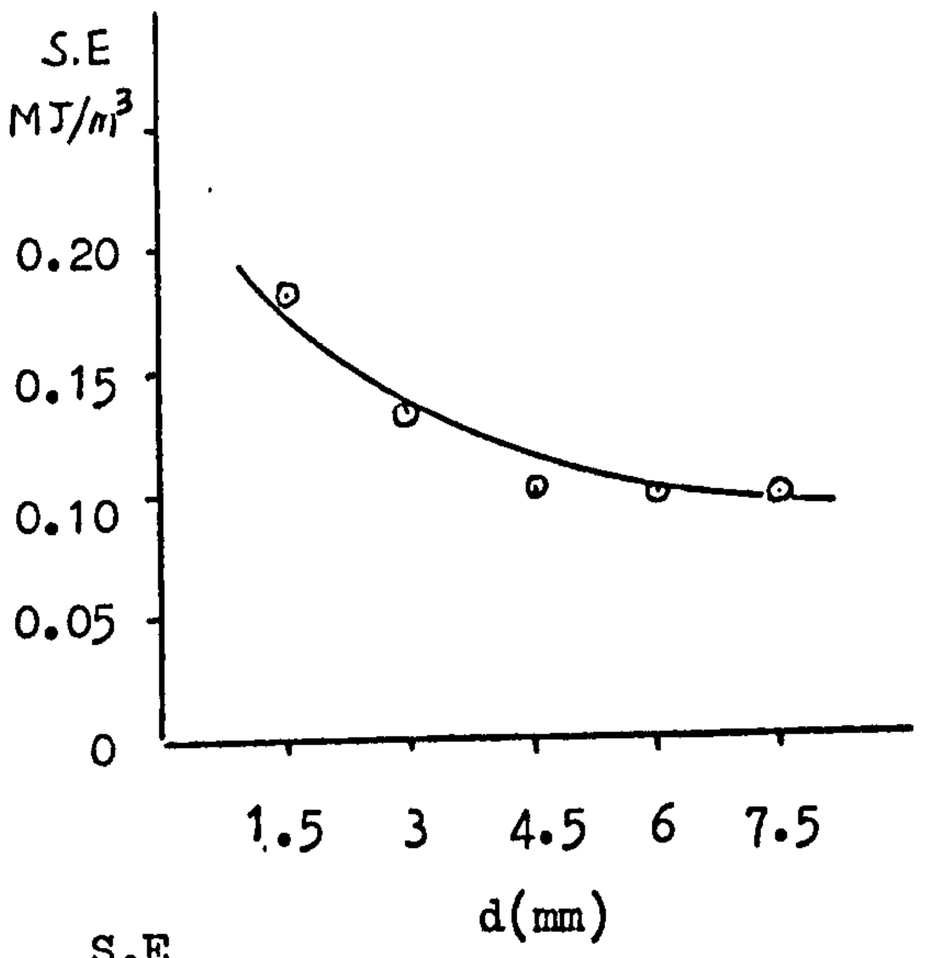

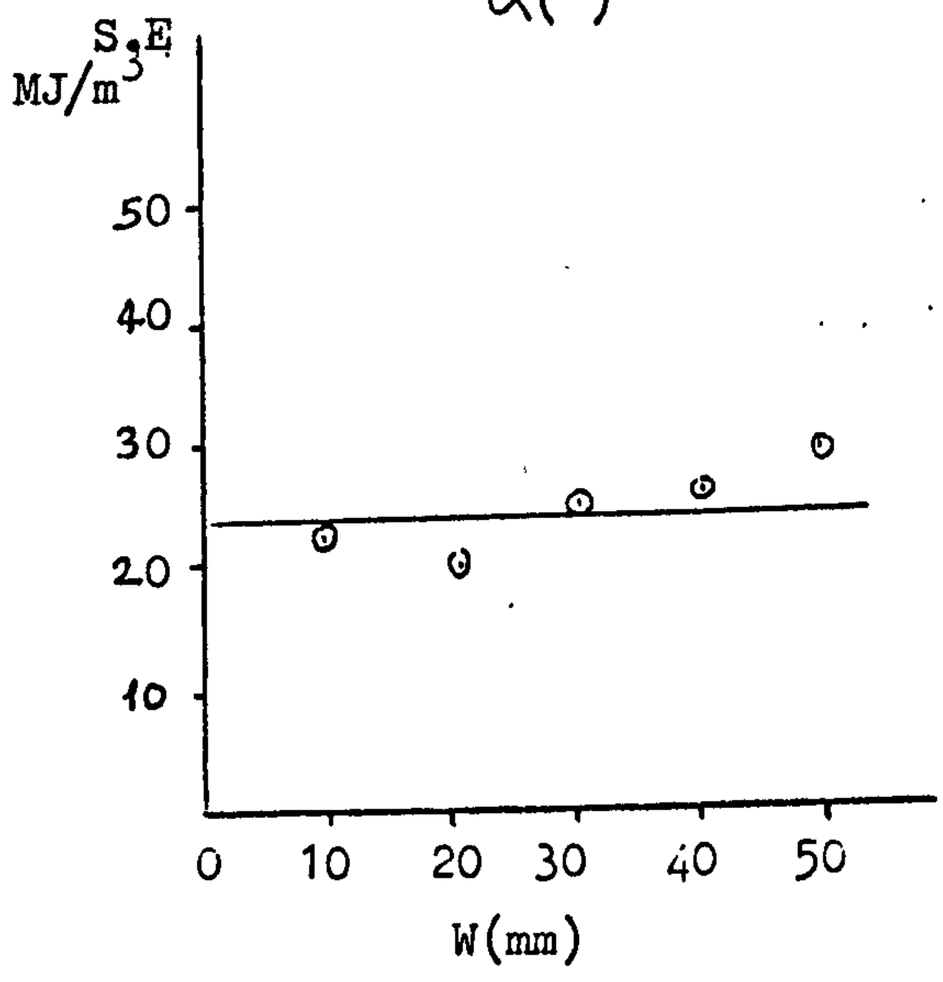

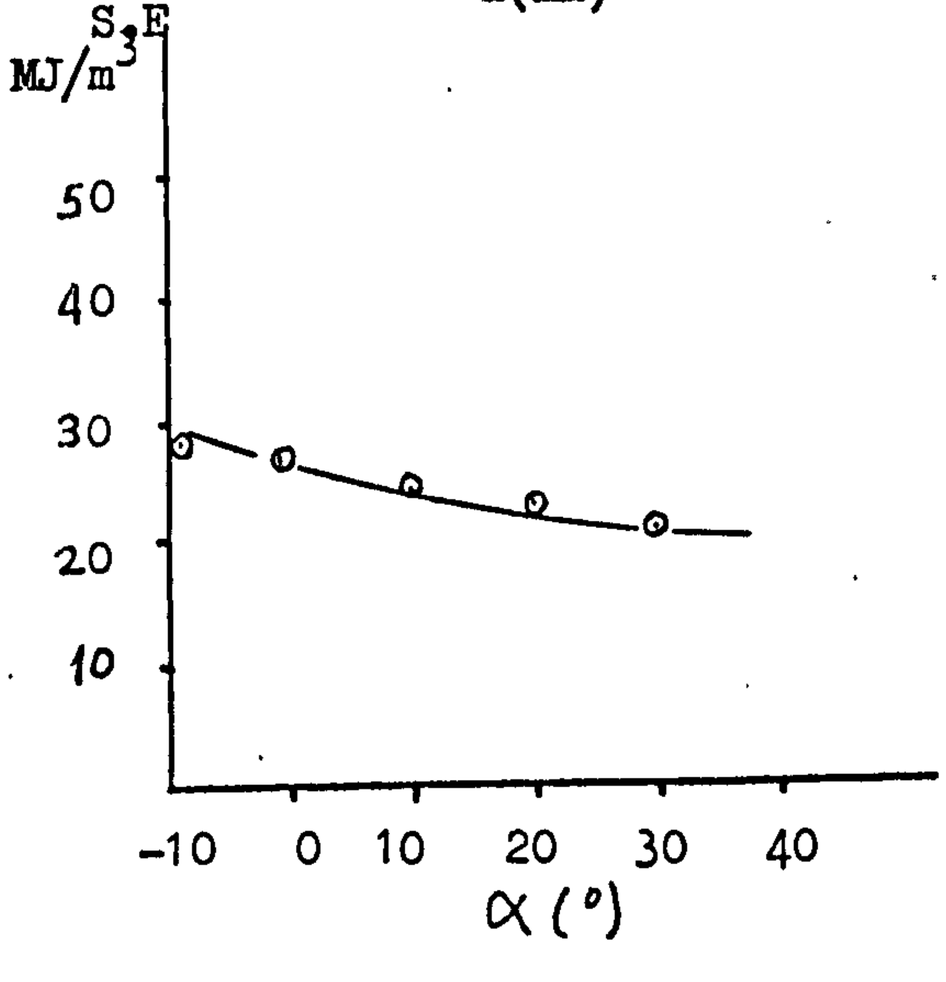

Fig.79 Variation in Yield and Specific Energy with Pick Cutter Parameters in Anhydrite.

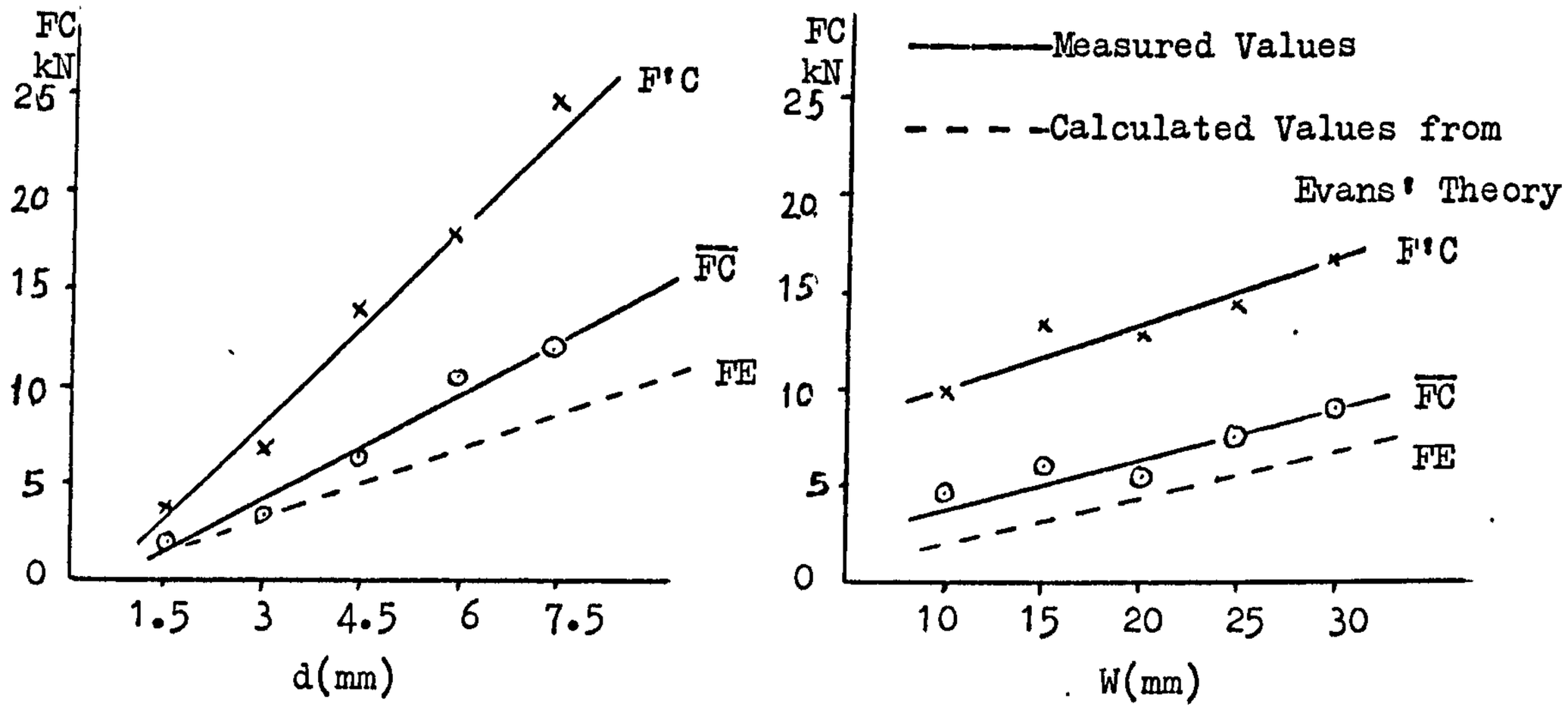

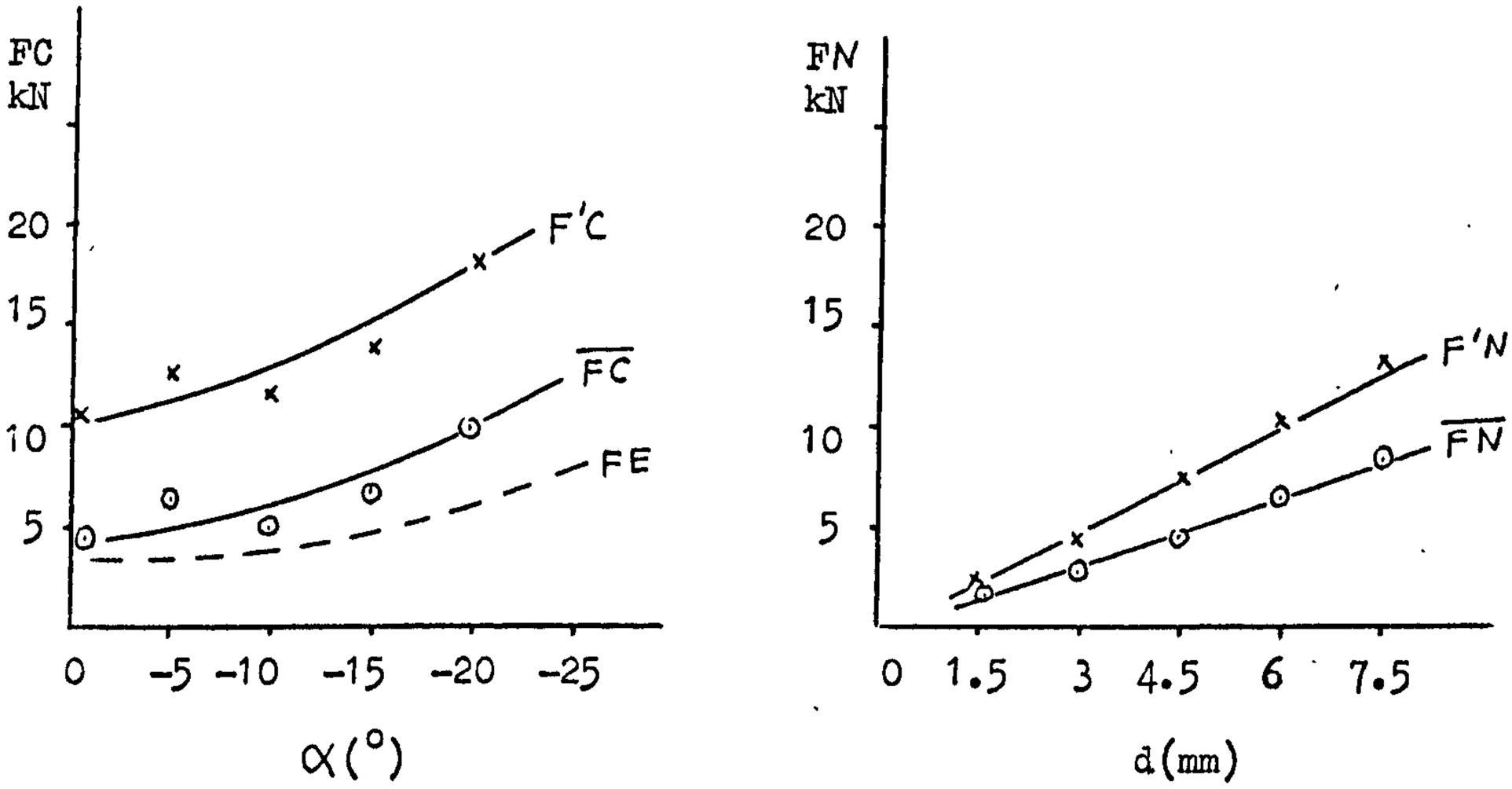

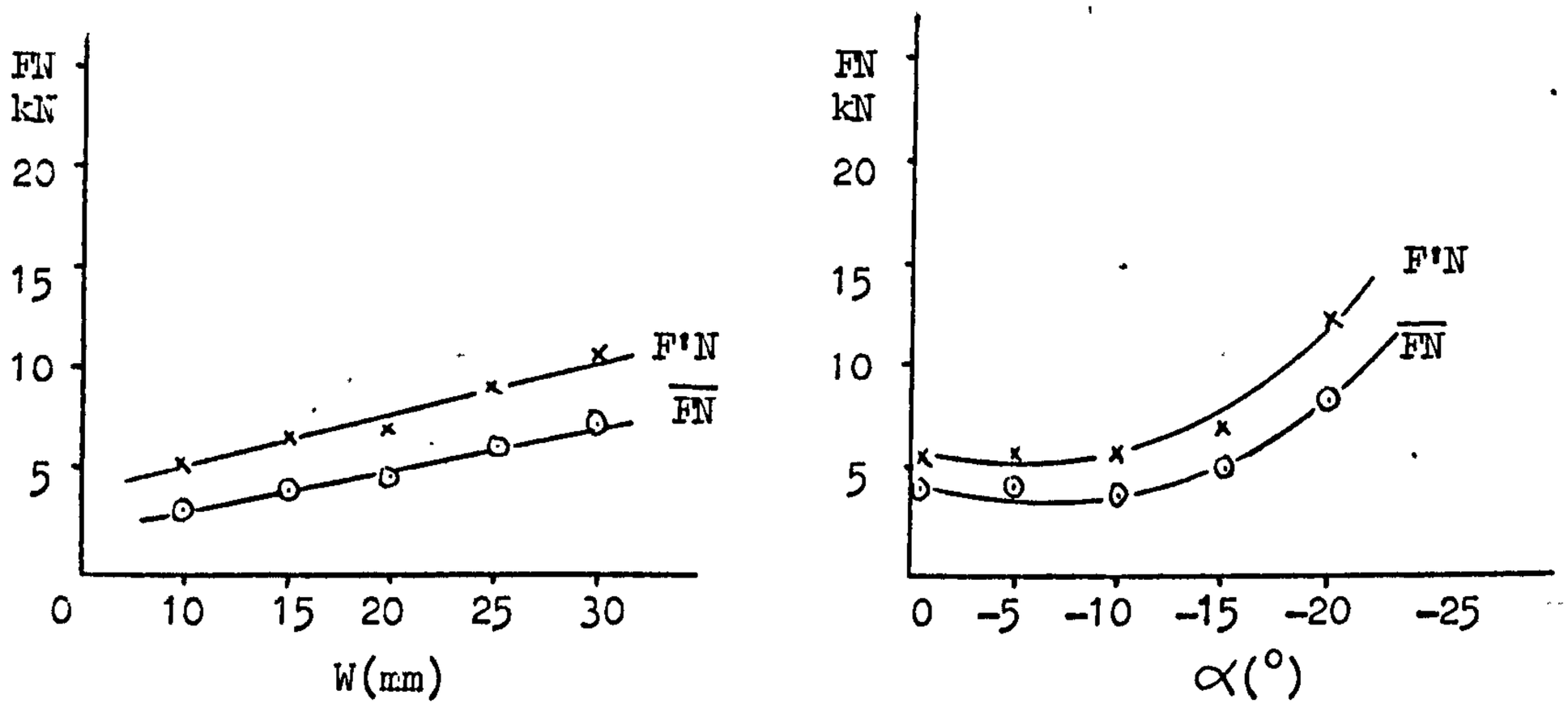

Fig.80 Variations in Forces with Pick Cutter Parameters in Limestone.

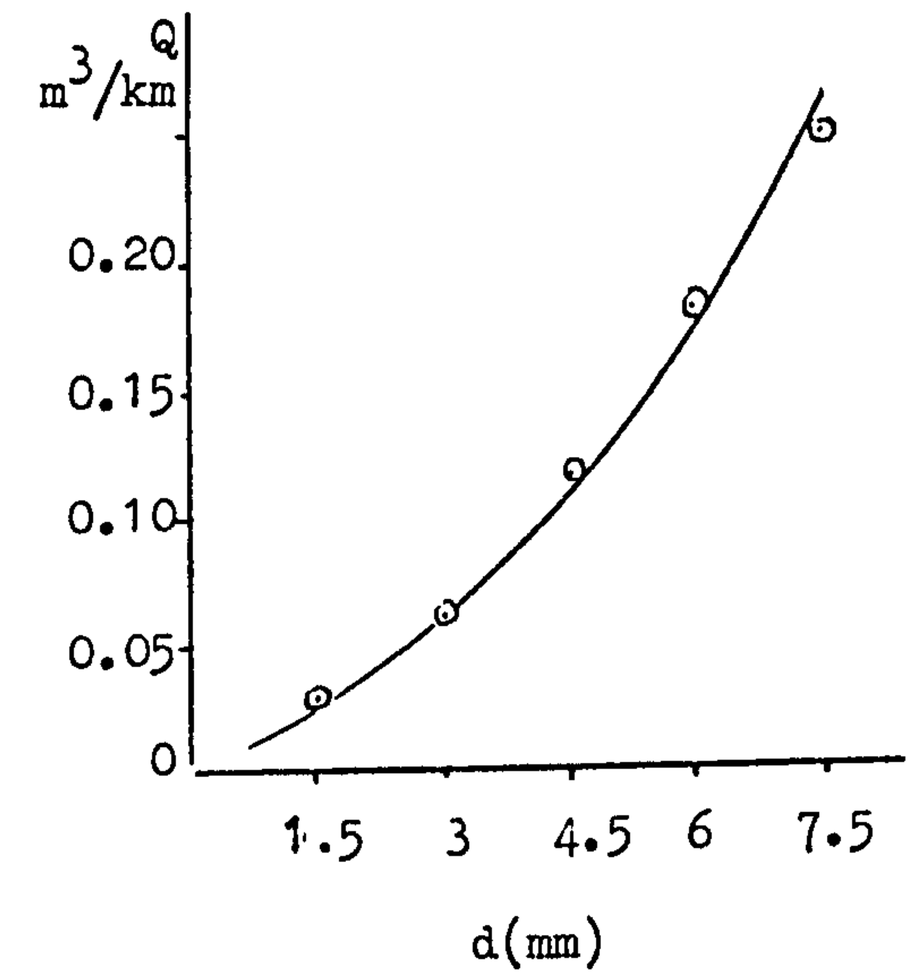

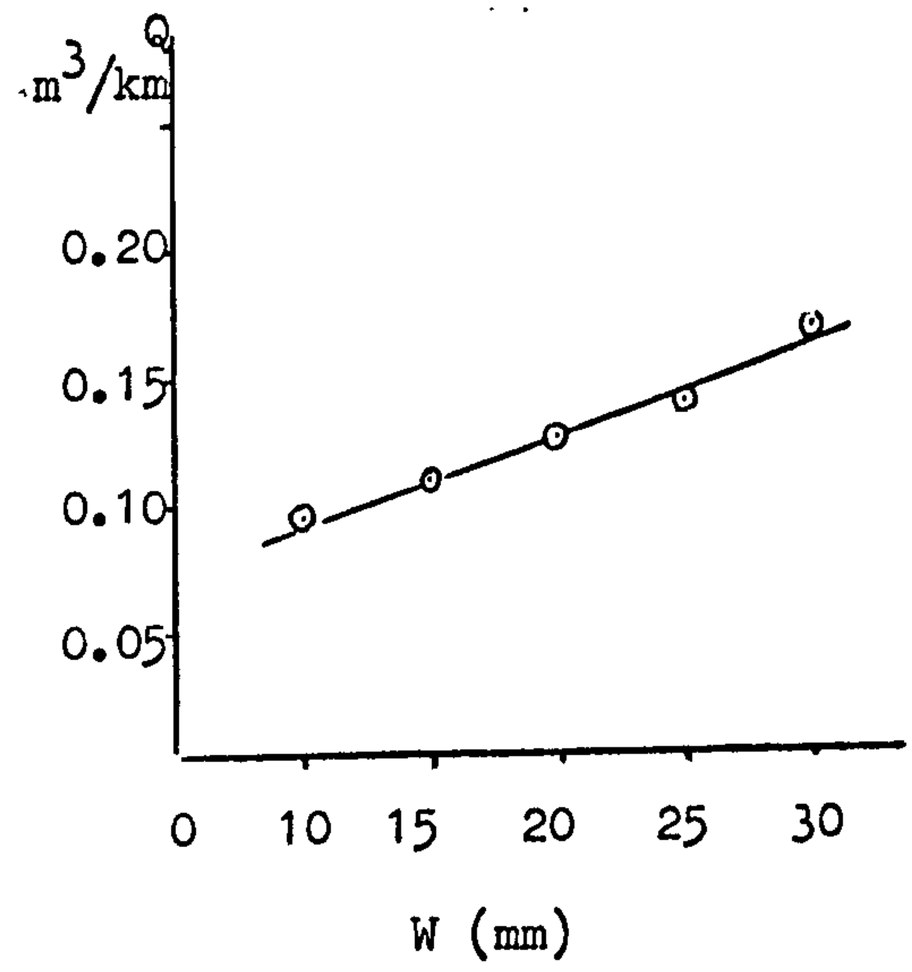

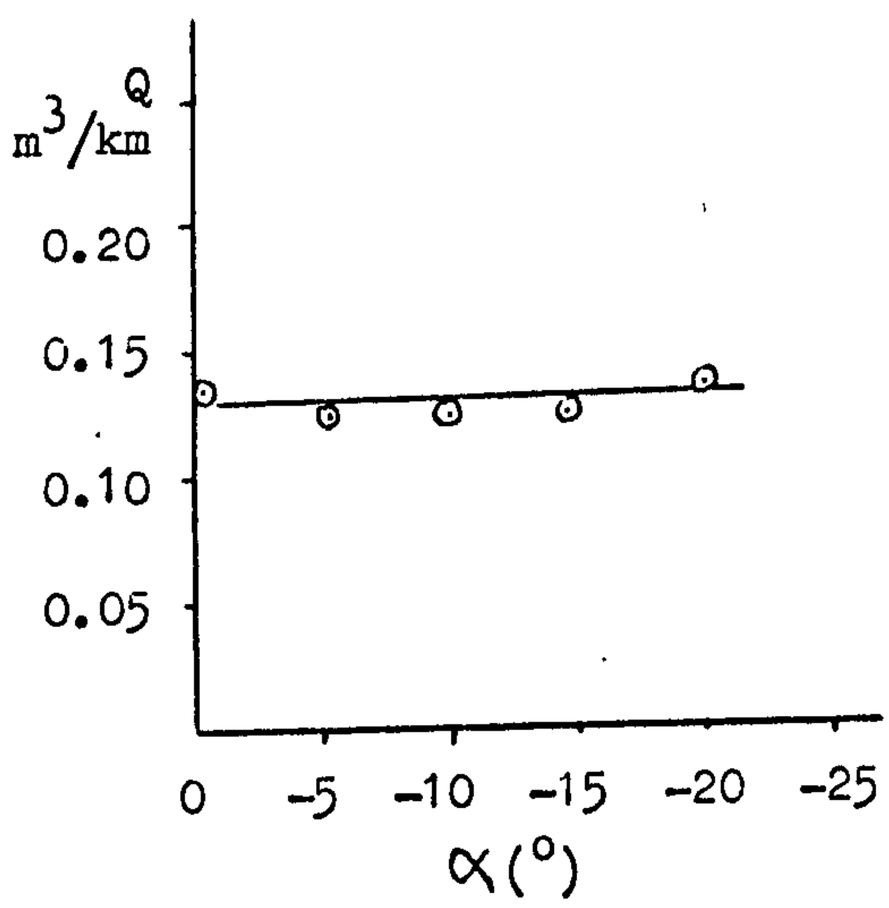

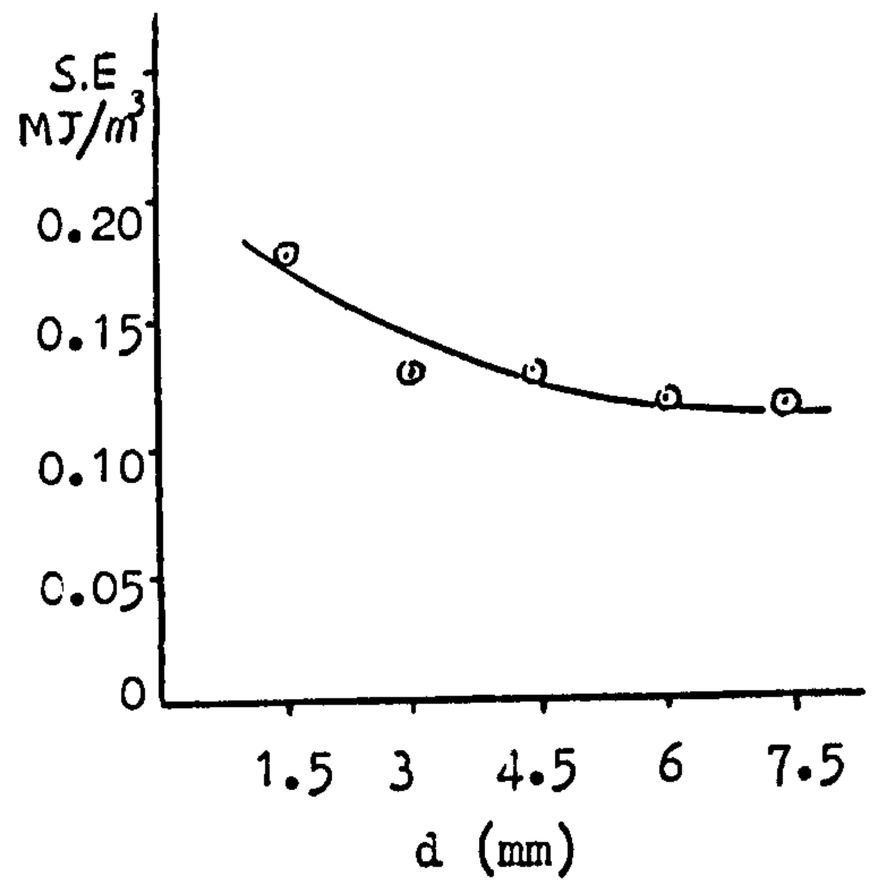

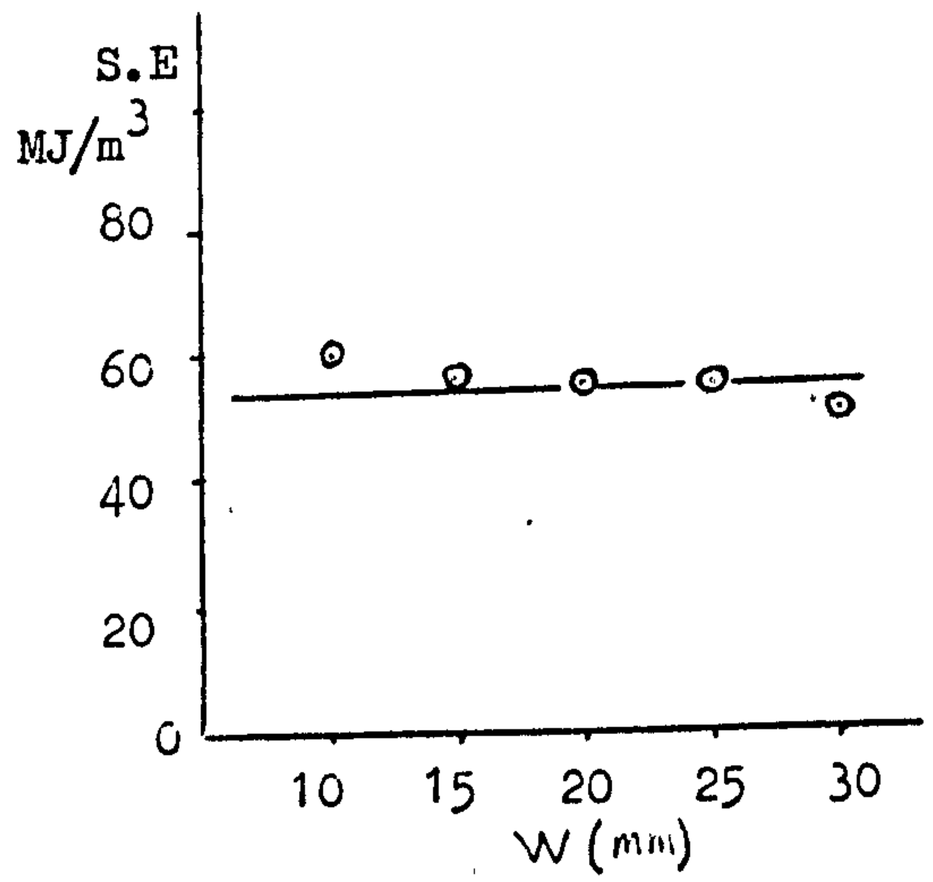

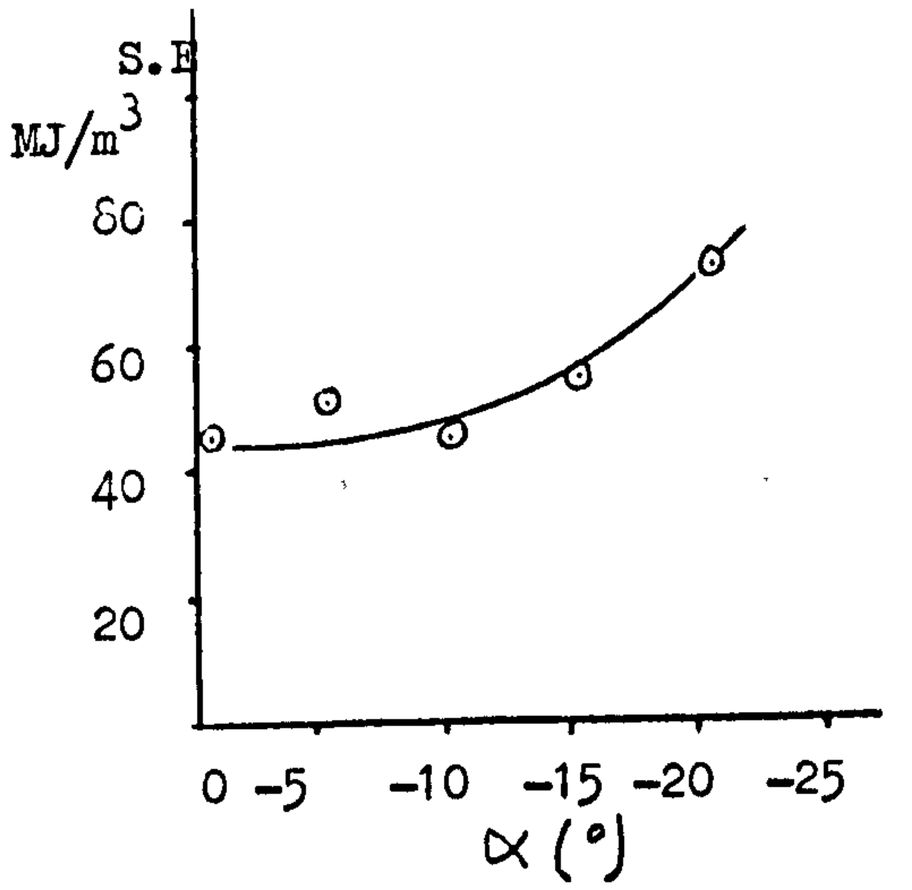

Fig.81 Variation in Yield and Specific Energy with Pick Cutter Parameters in Limestone.

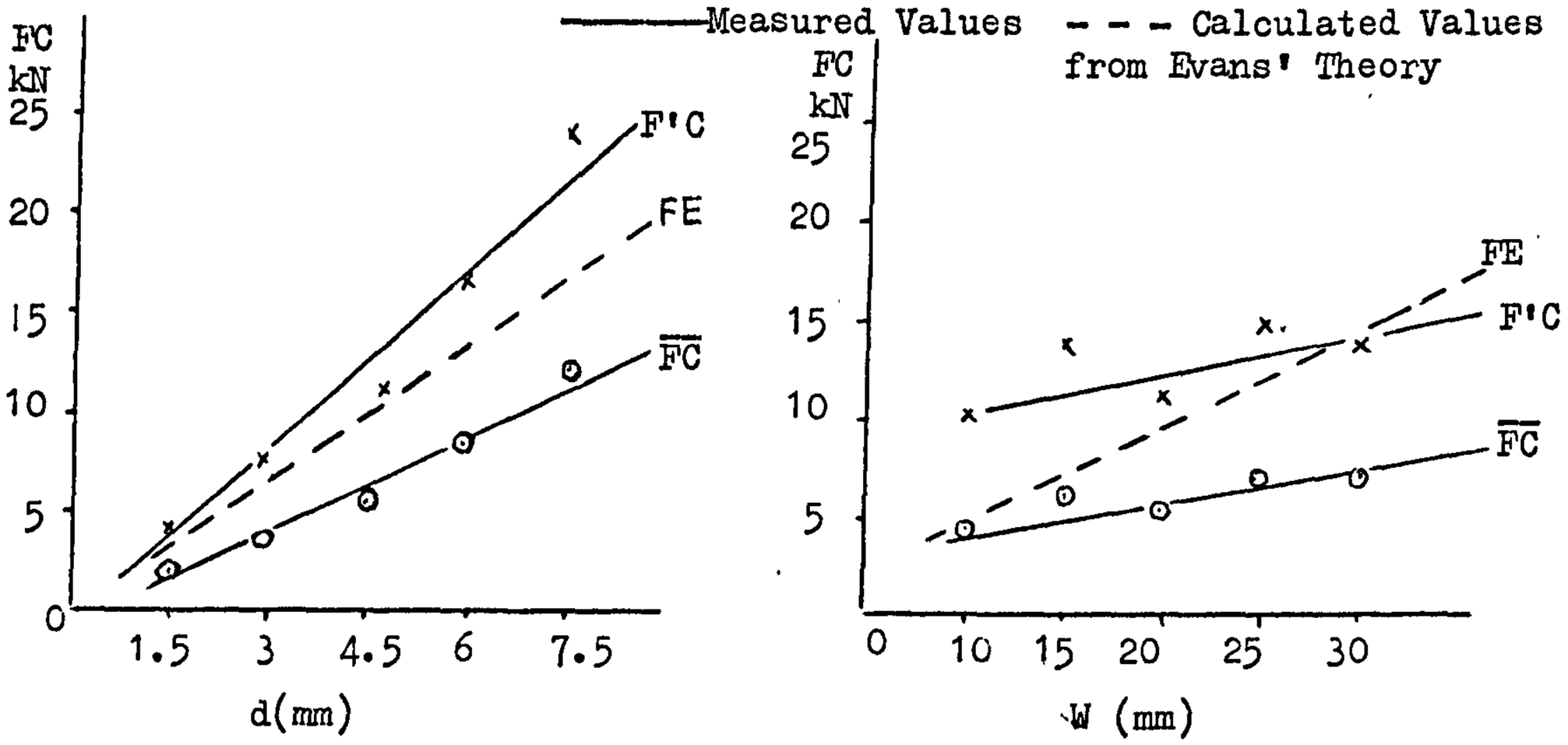

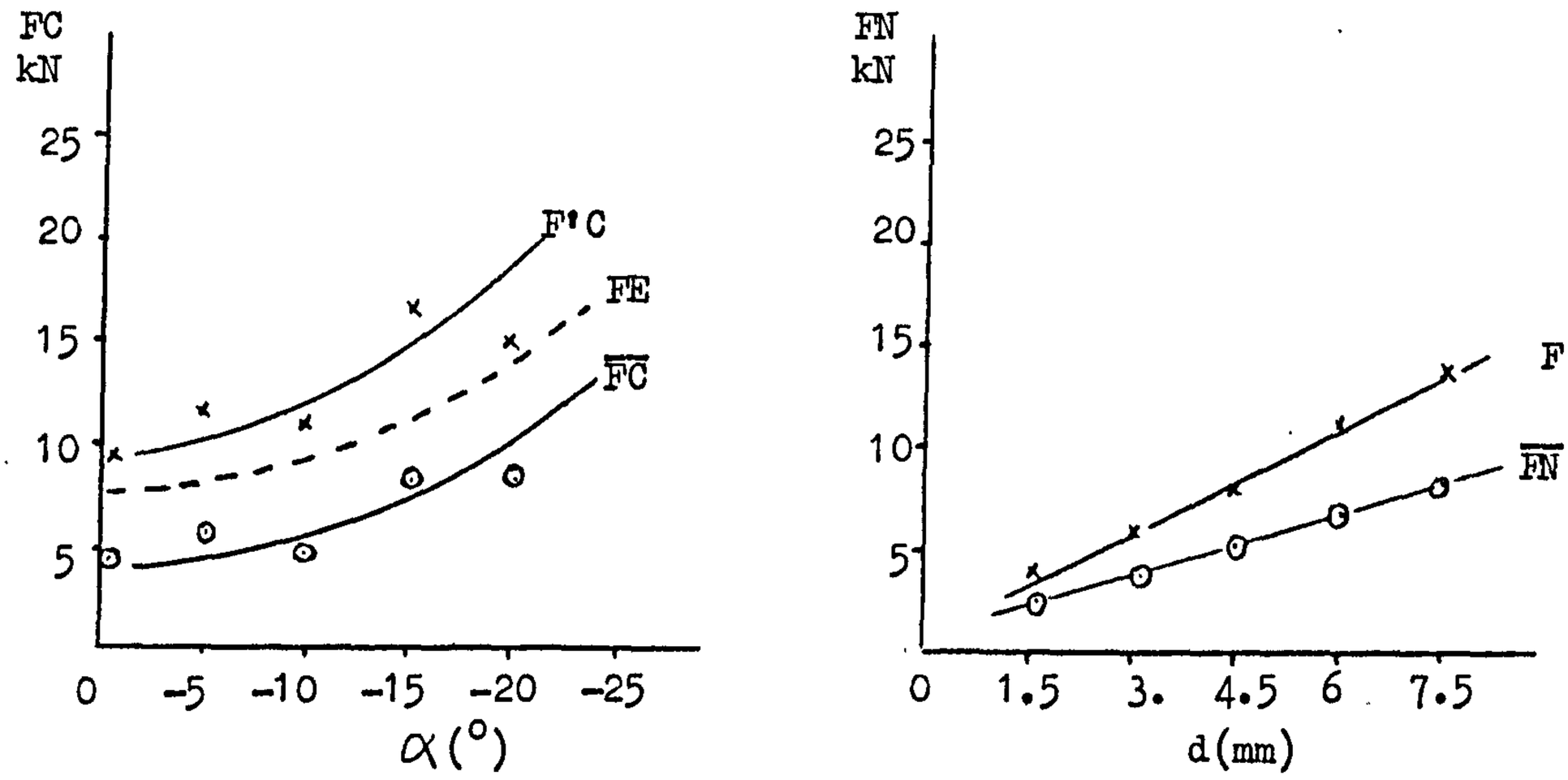

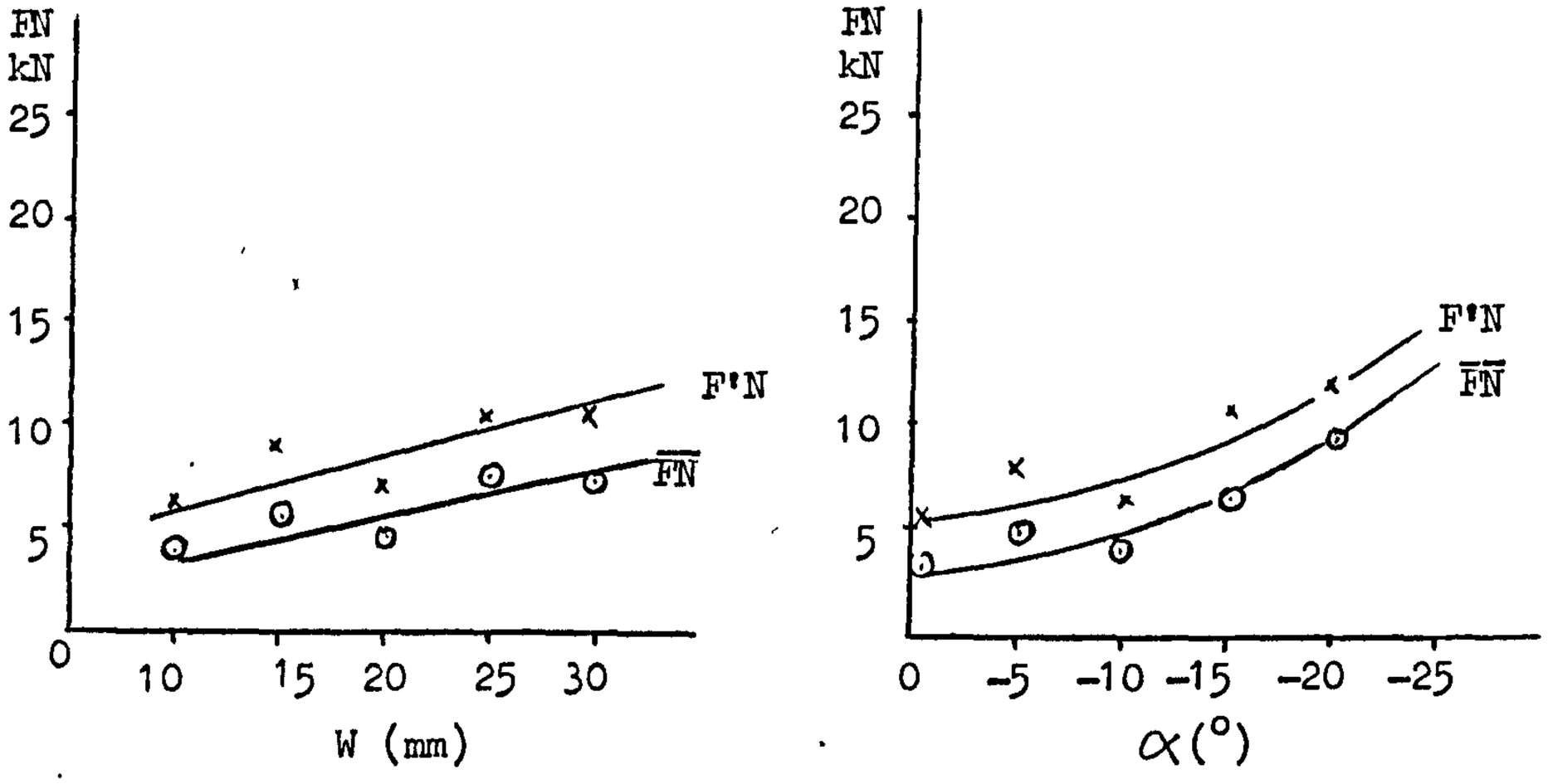

Fig.82 Variation in Forces with Pick Cutter Parameters in Greywacke.

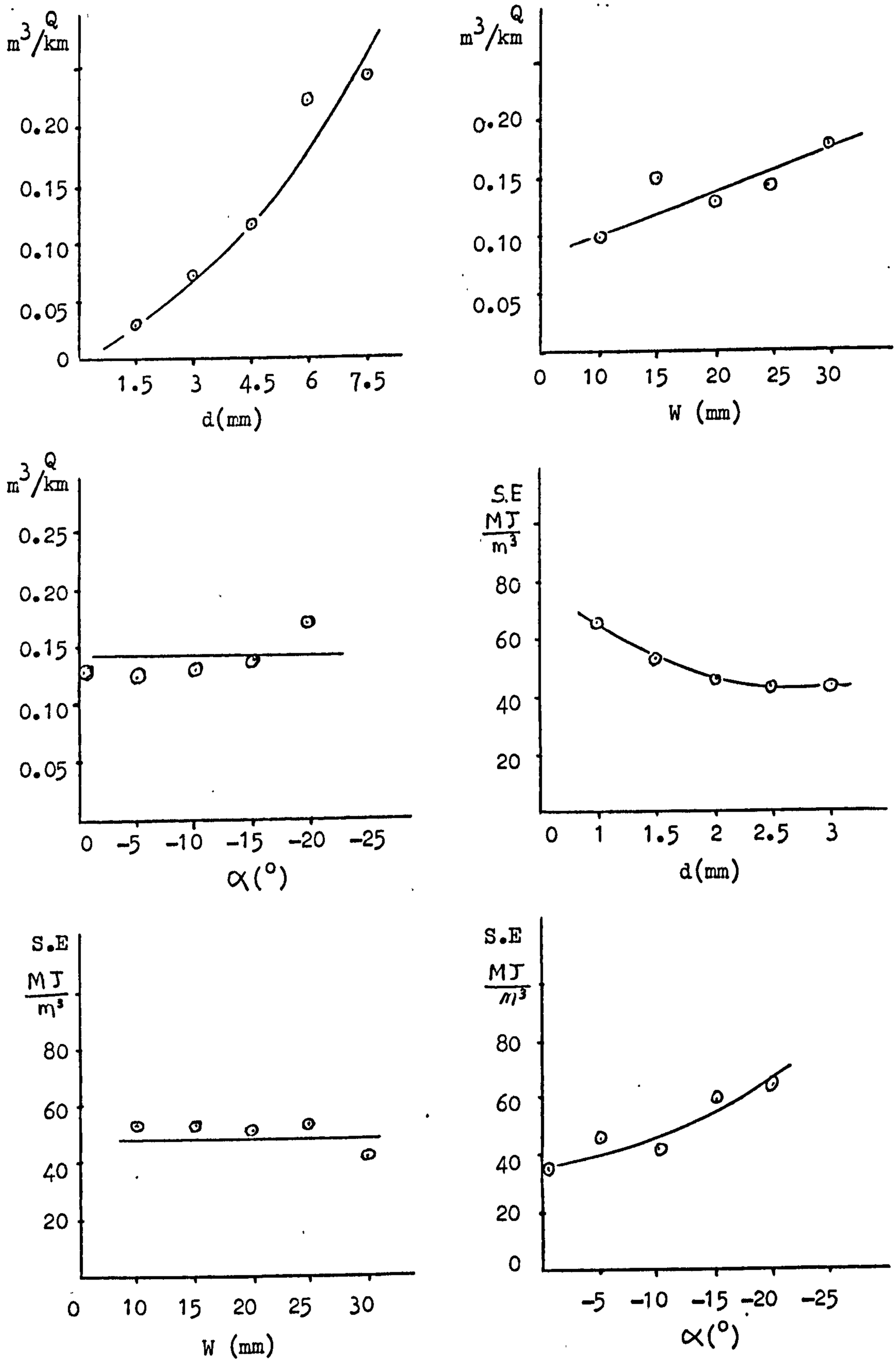

Fig.83 Variation in Yield and Specific Energy with Pick Cutter Parameters in Greywacke.

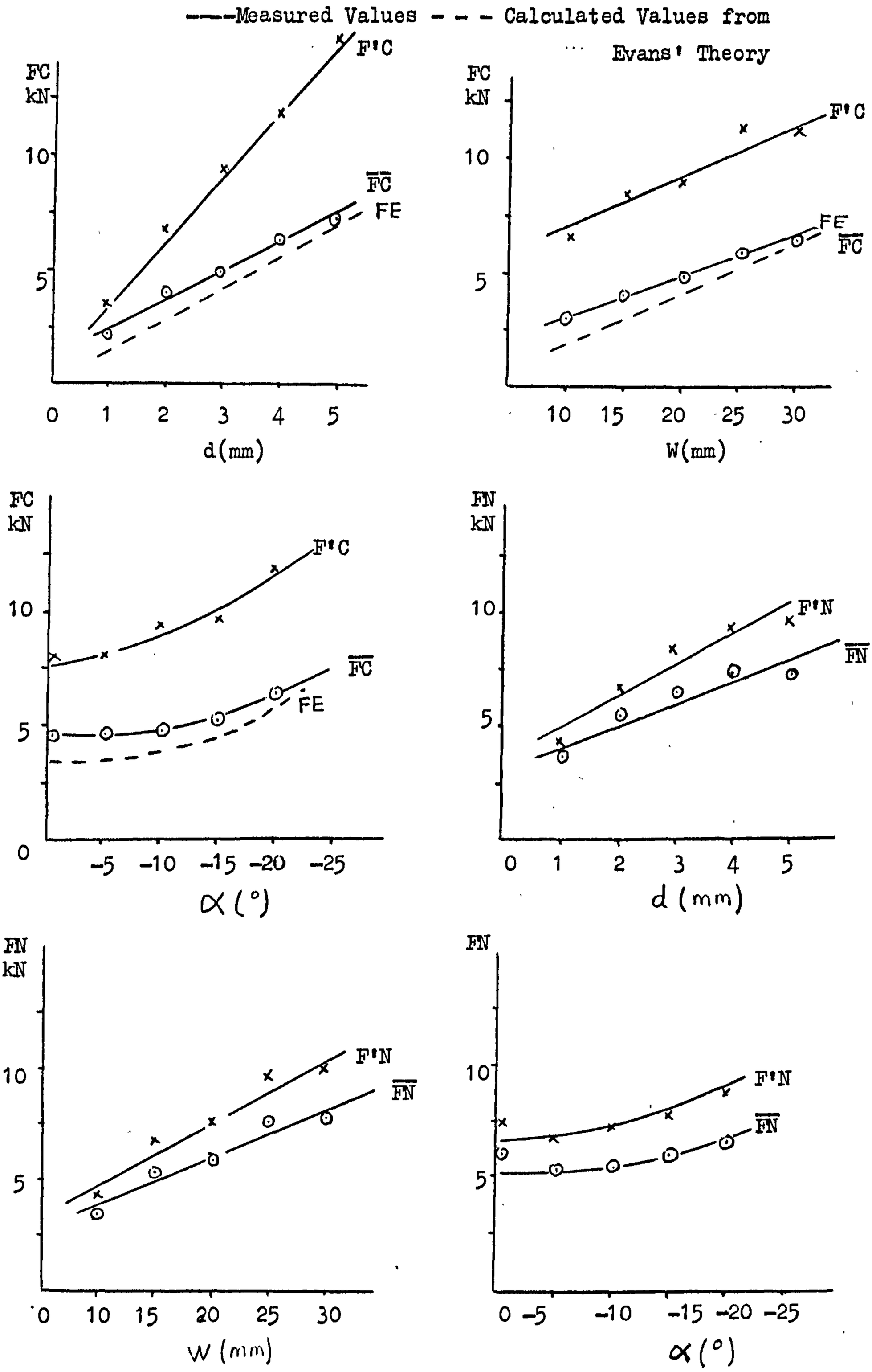

Fig.84 Variation in Forces with Pick Cutter Parameters in Granite.

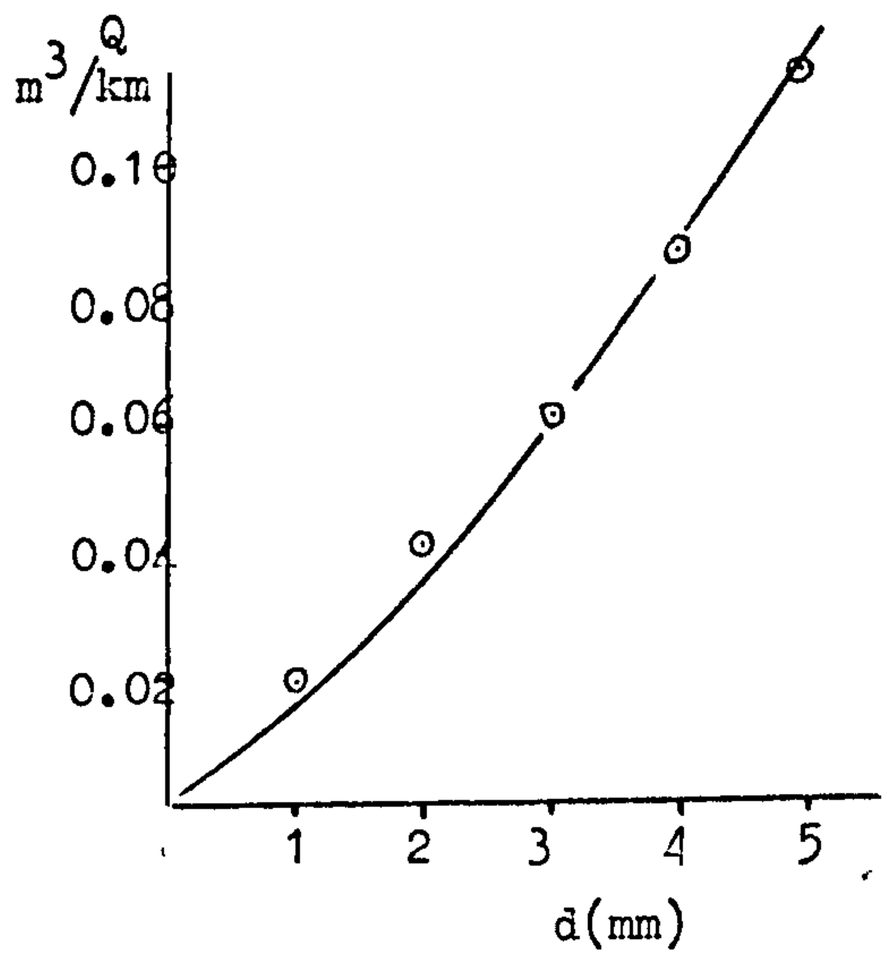

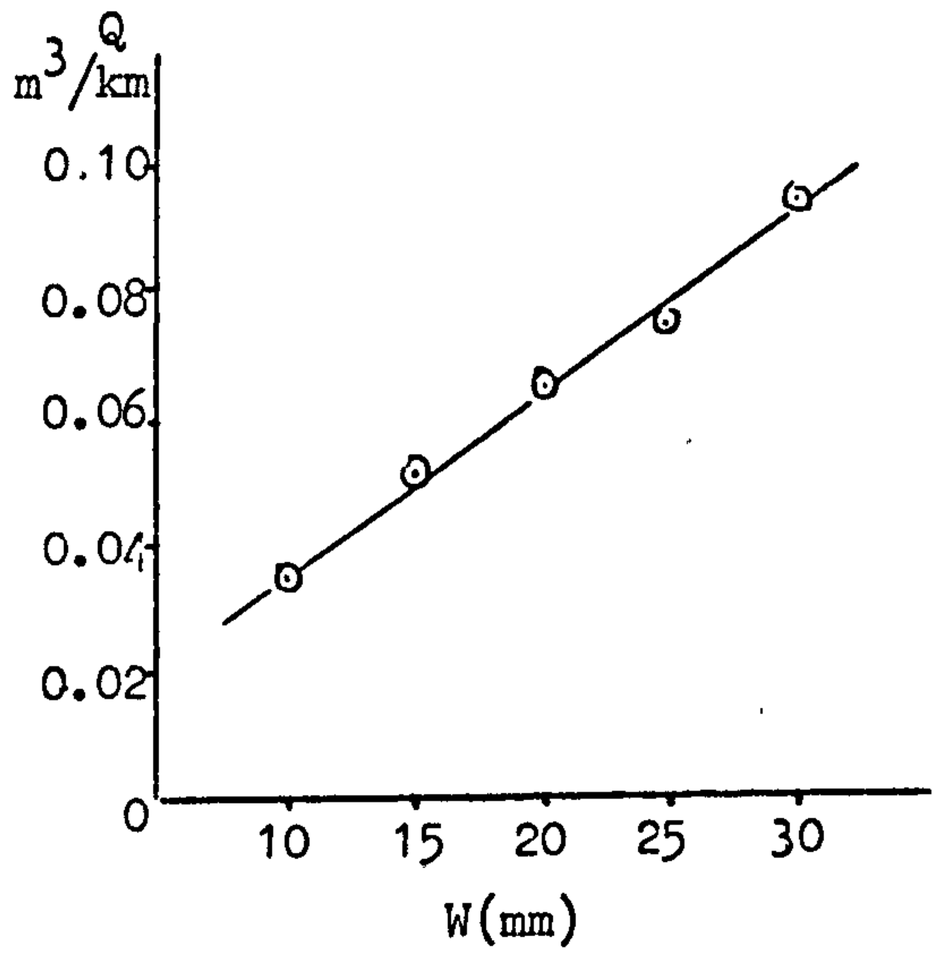

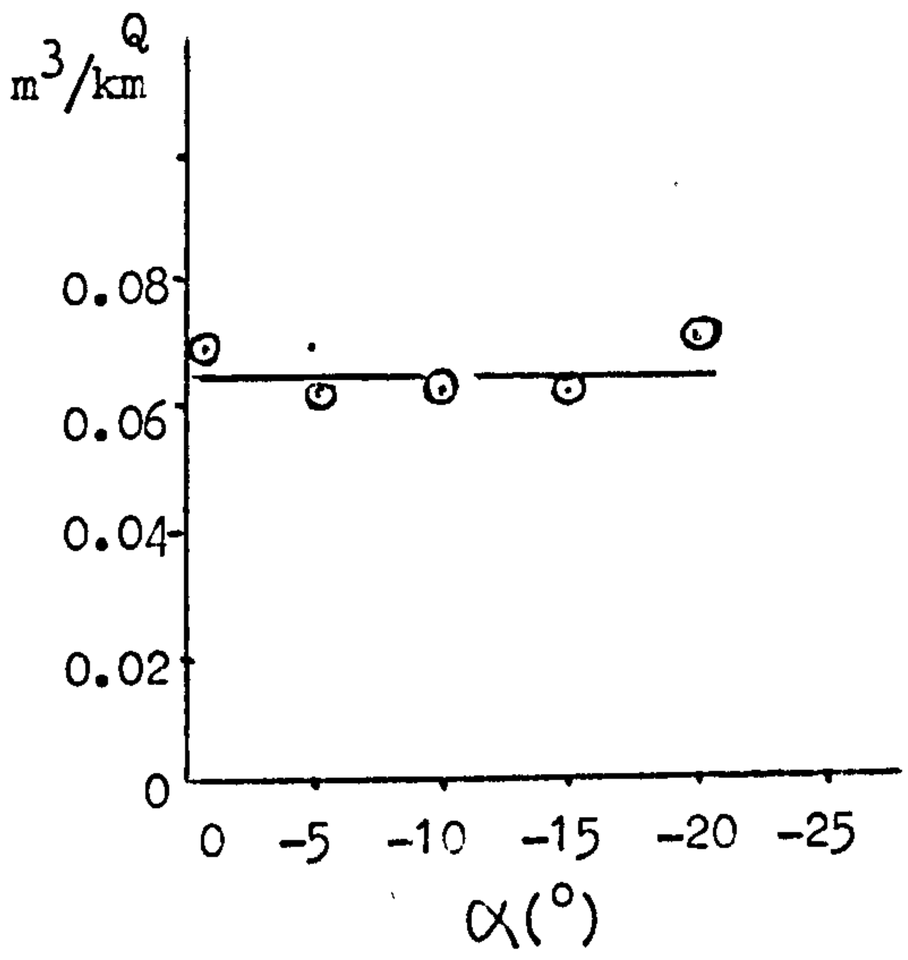

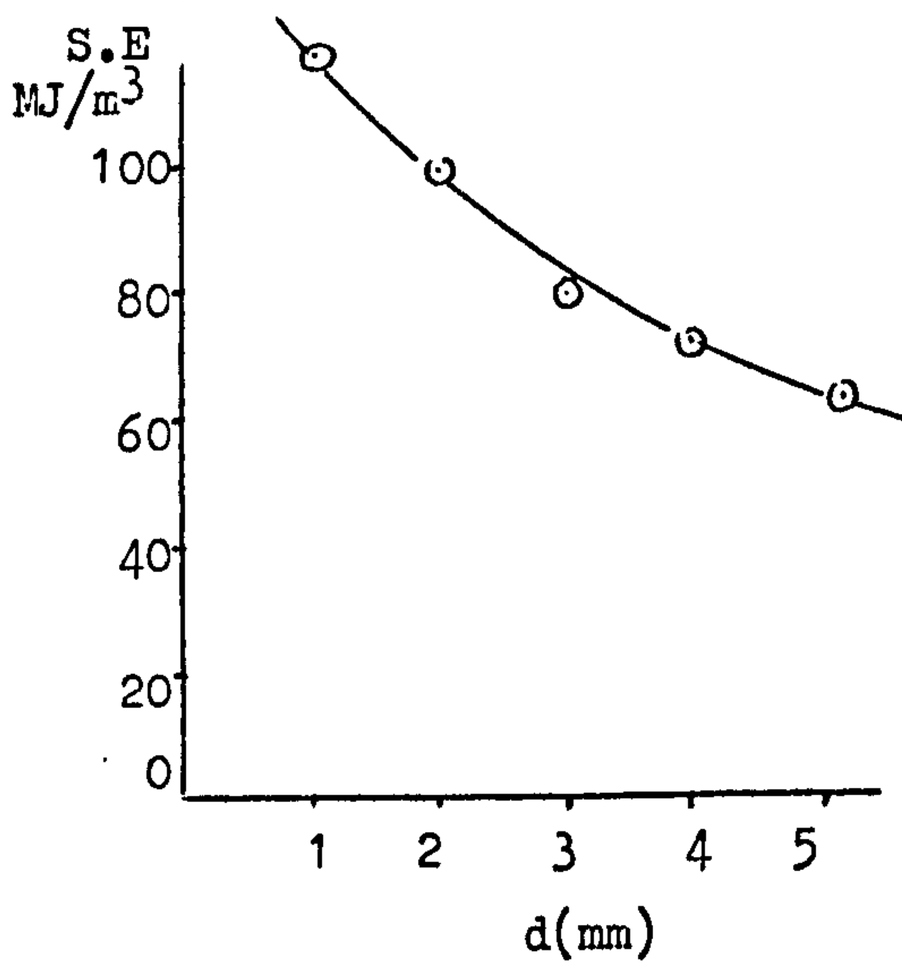

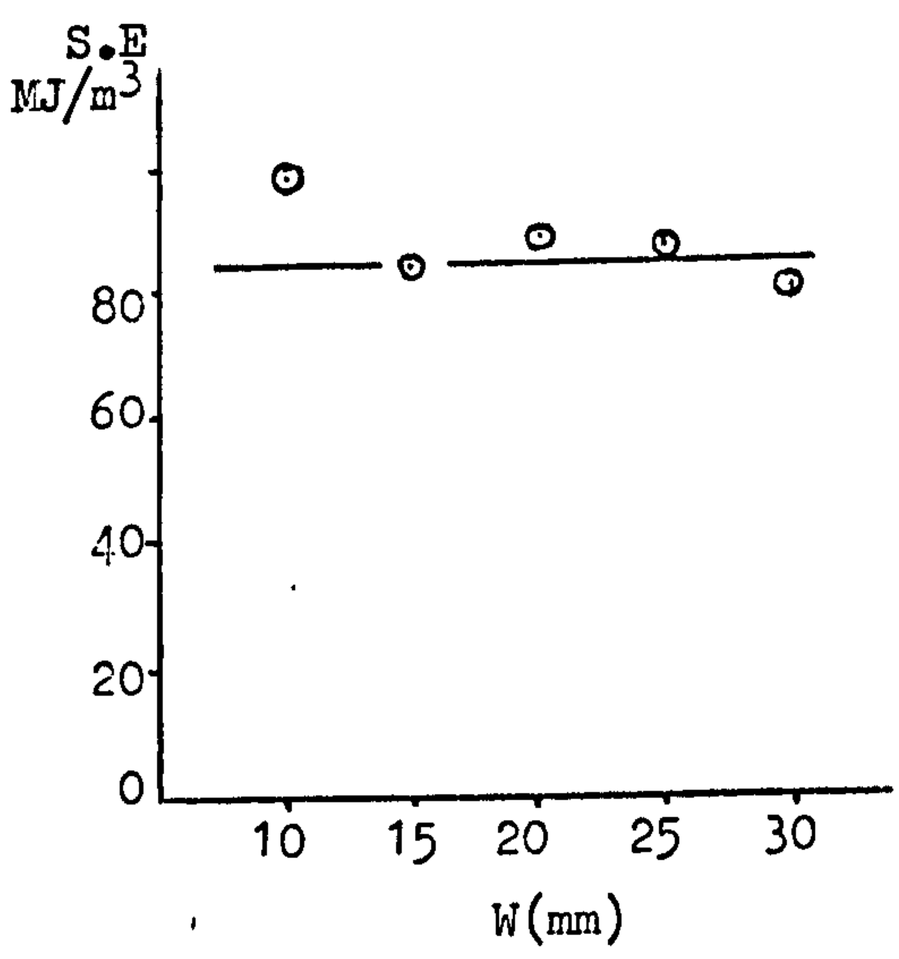

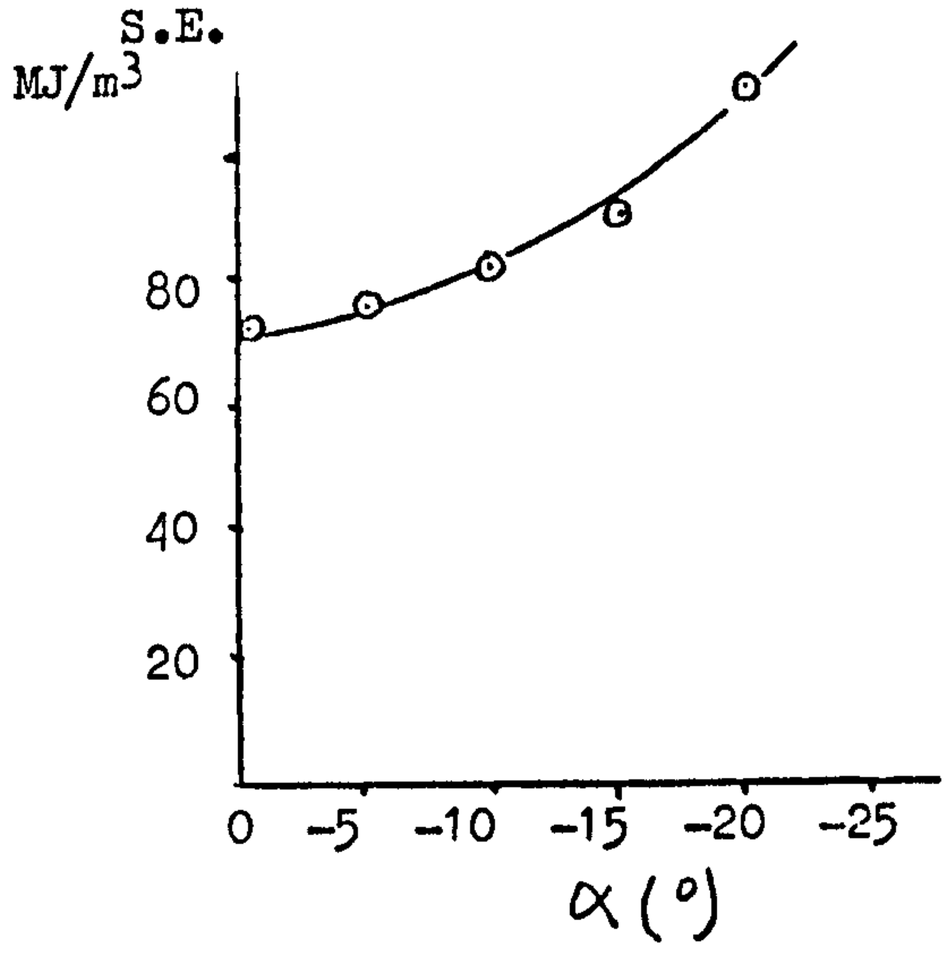

Fig.85 Variation in Yield and Specific Energy with Pick Cutter Parameters in Granite.

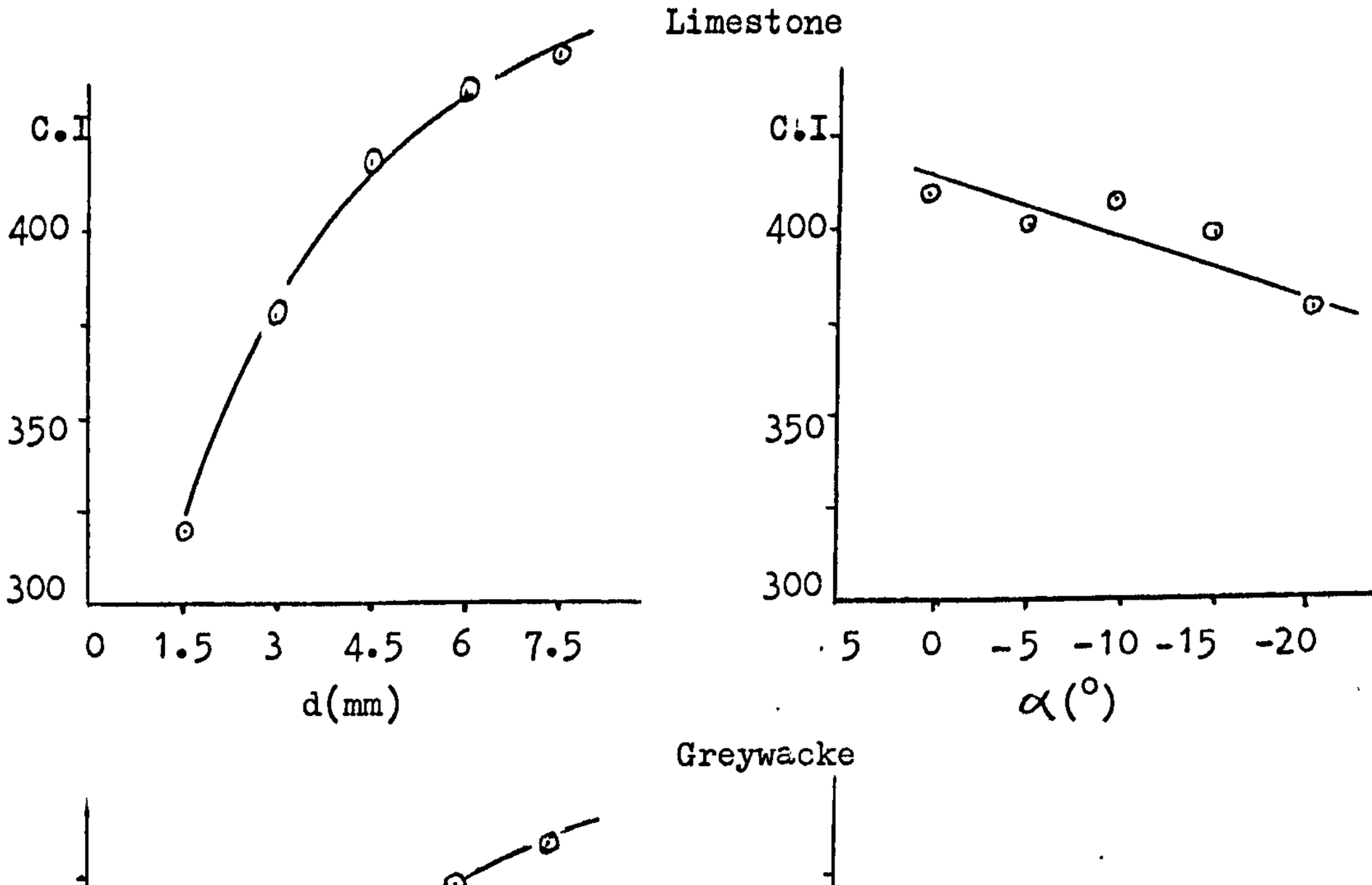

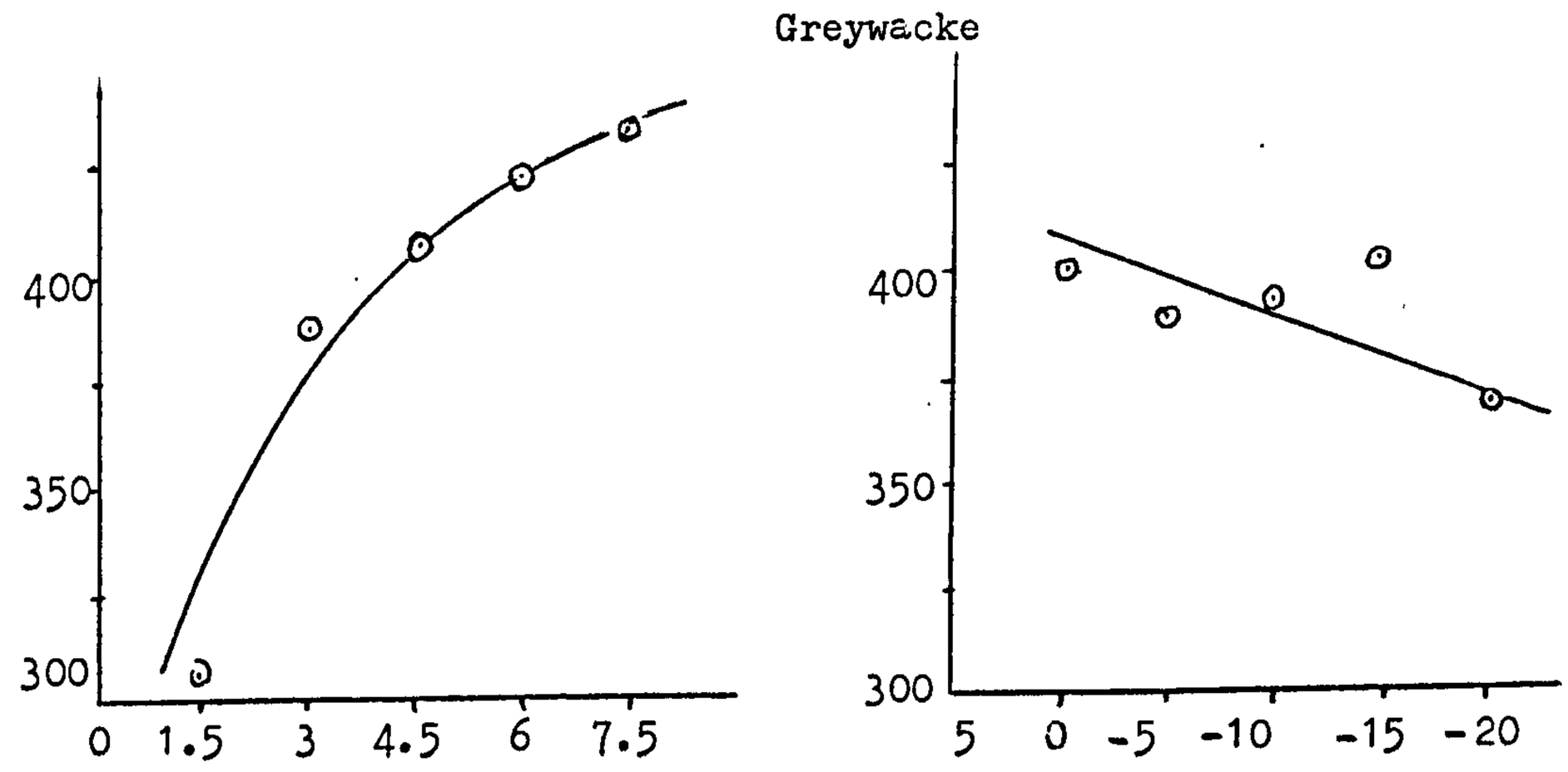

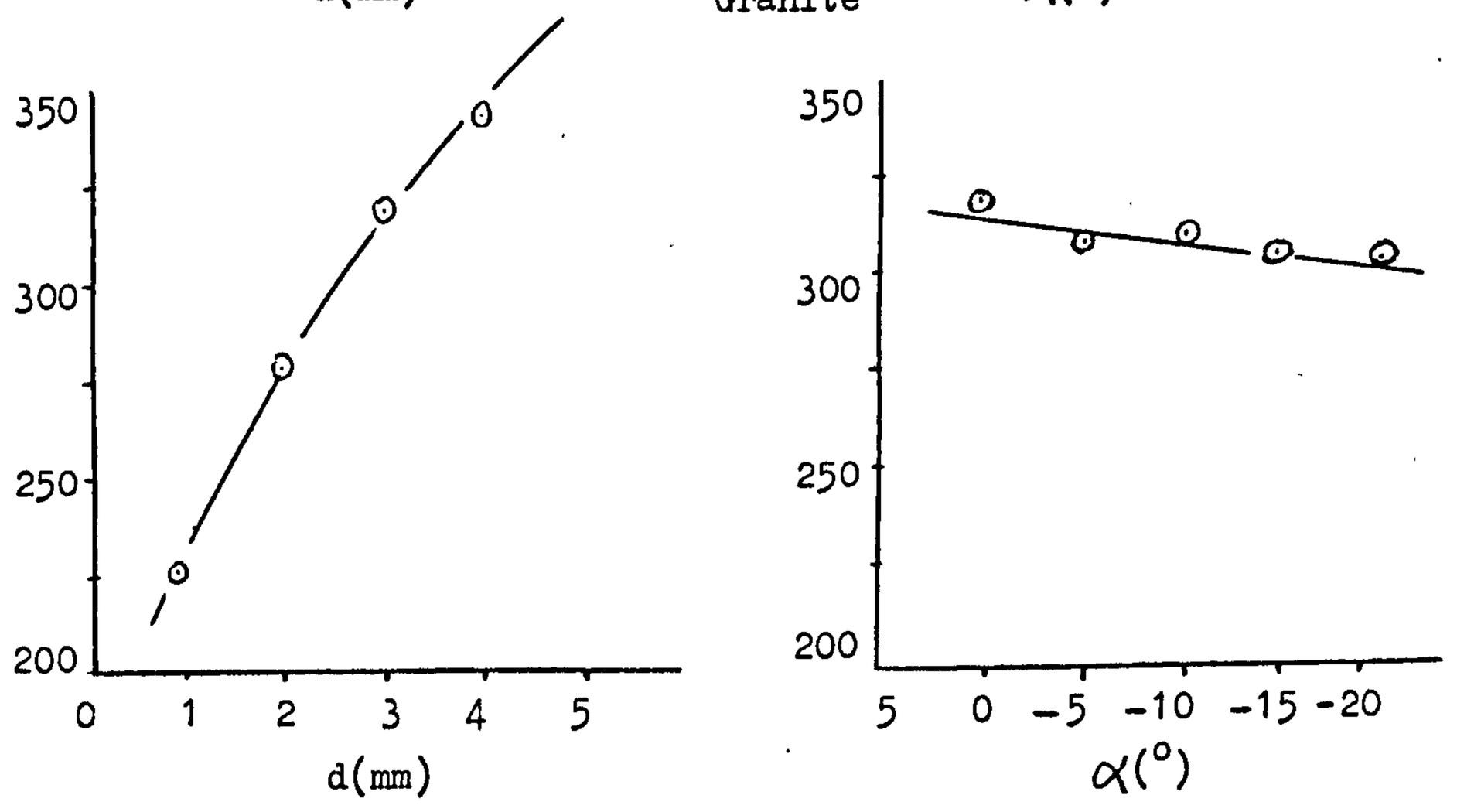

Fig.86 Variation in Coarseness Index with Depth of Cut and Rake Angle.

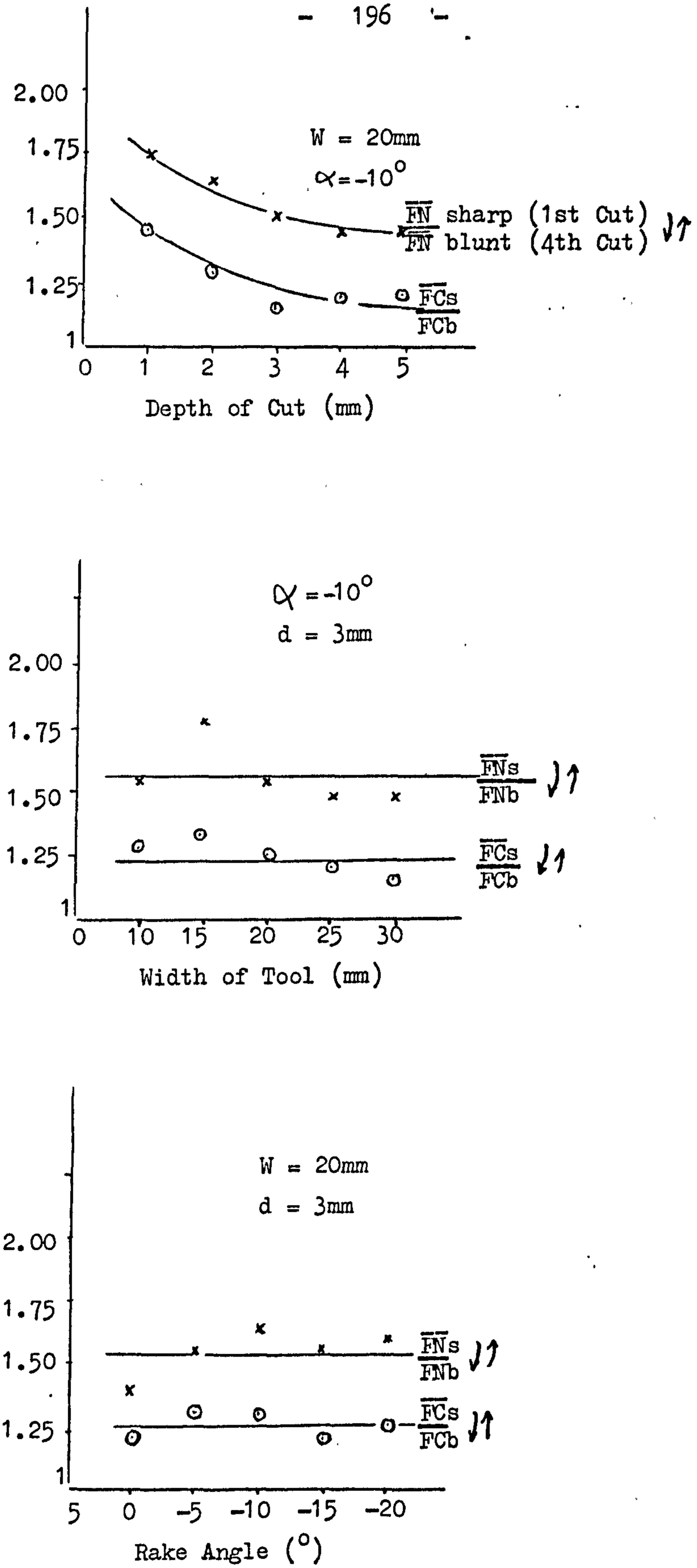

Fig.87 Effect of Tool Wear in Granite.

11.4 Relieved Cutting Results

All the relieved cutting data are given in Appendix 30. Forces are seen to increase with increasing spacing and reach a maximum at the point where no further interaction between adjacent grooves occurs.

Rock yield also increases with spacing to a maximum value and stays asymptotic to a value equivalent to the unrelieved yield (Appendix 30). Specific energy values are plotted against s/d for each level of depth of cut in Fig.88. Minimum specific energy was found in all cases to occur when the ratio s/p was around 2 for Anhydrite and Limestone and 1 for Greywacke. The improvement in specific energy for optimum spacing values, on average, is not more than 30%.

* * *

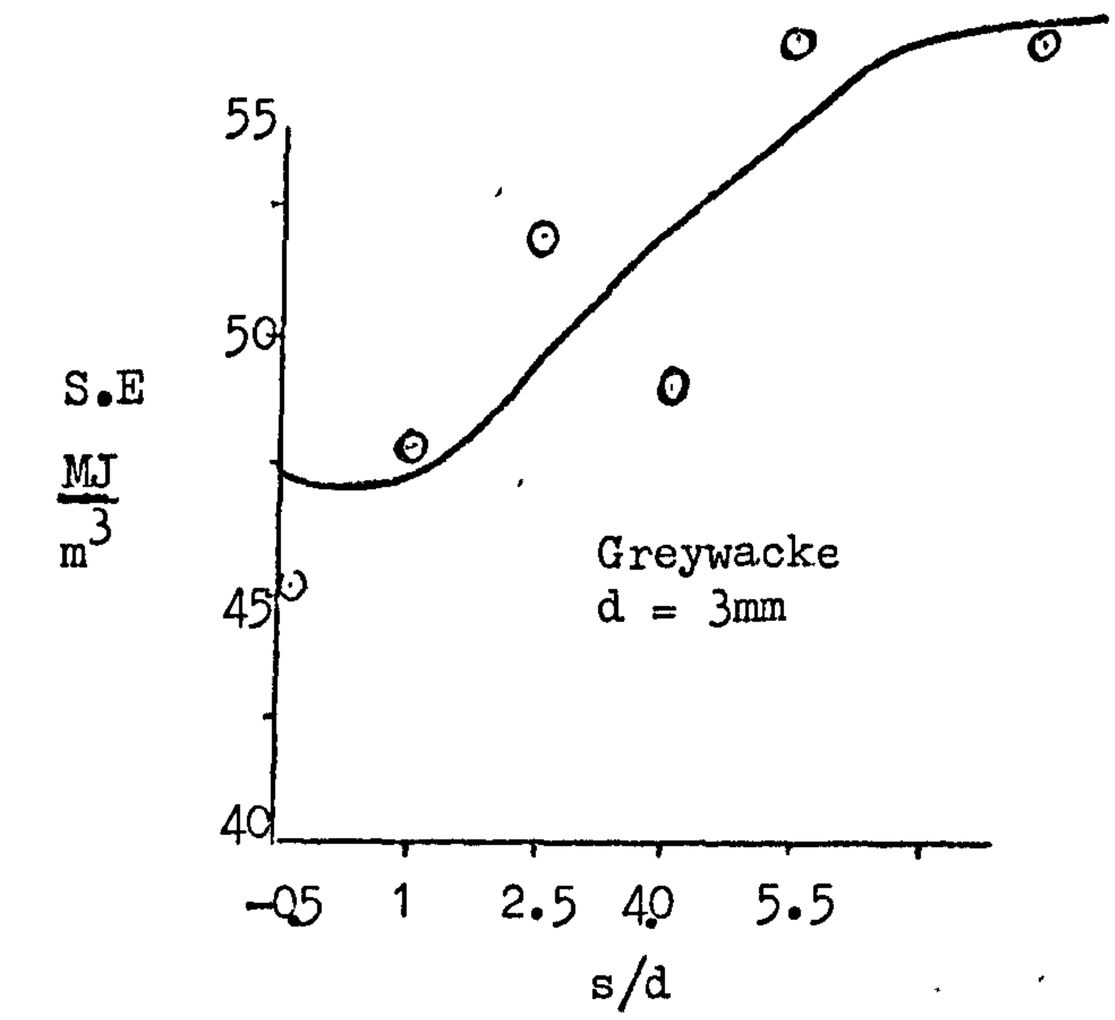

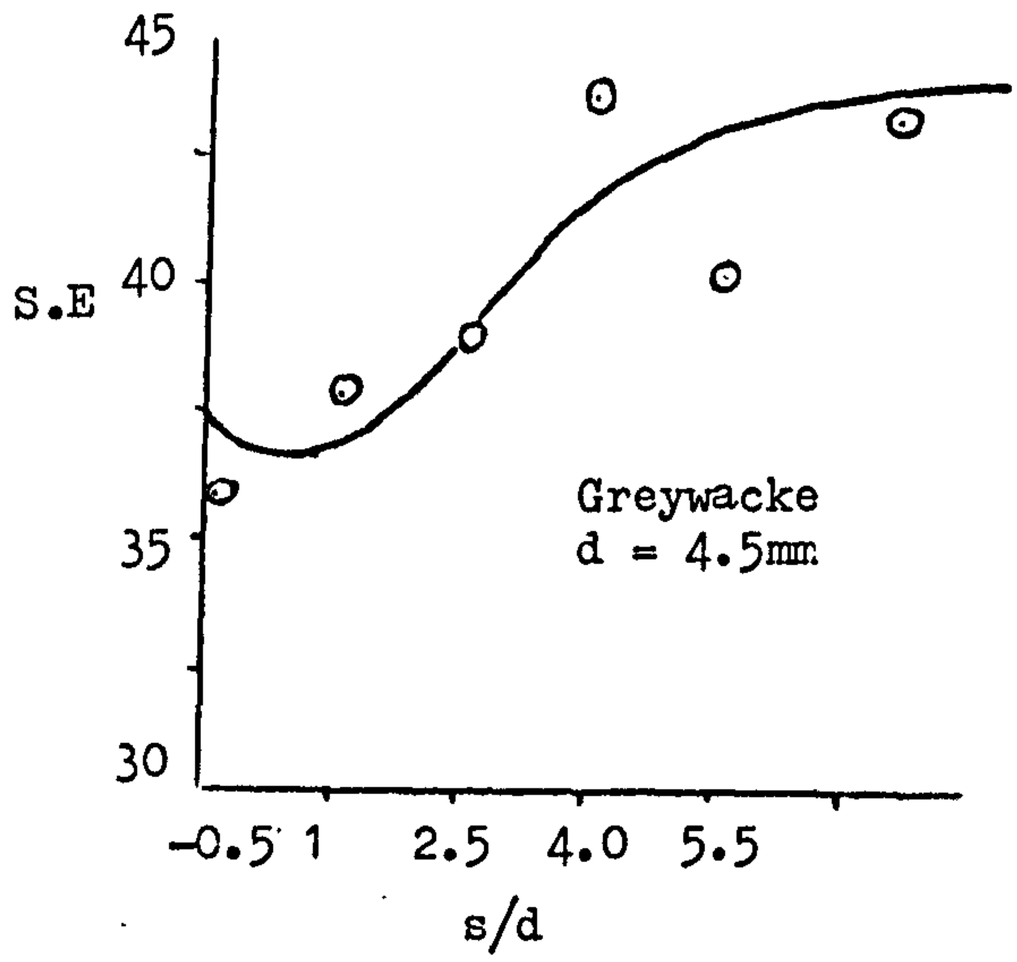

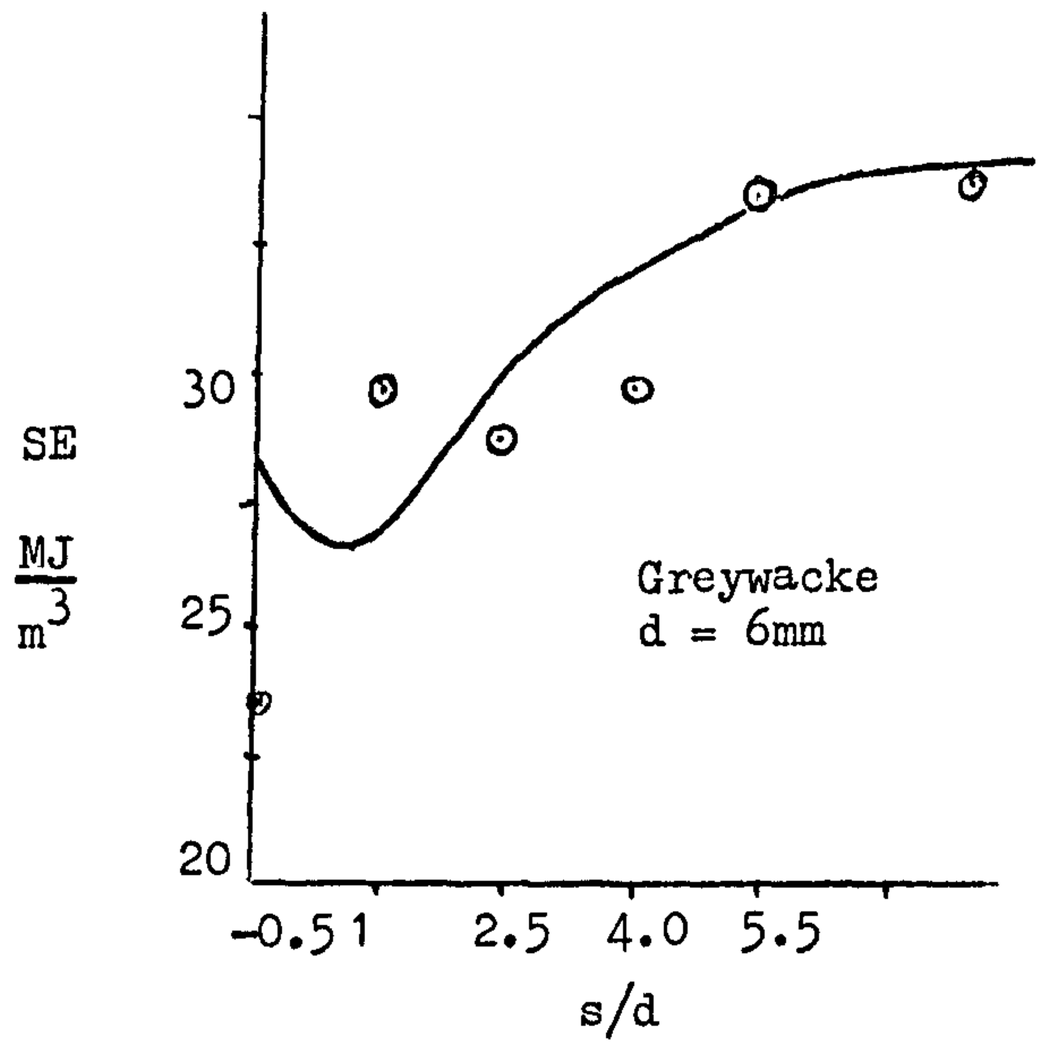

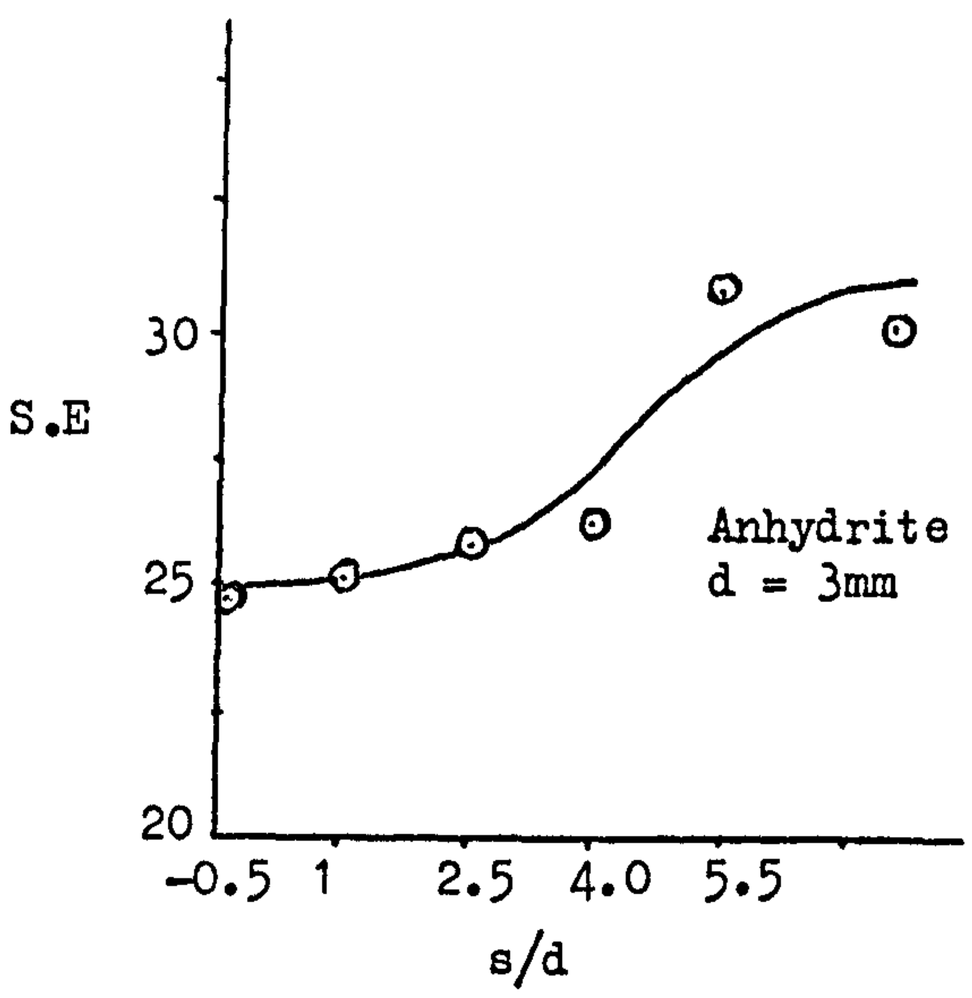

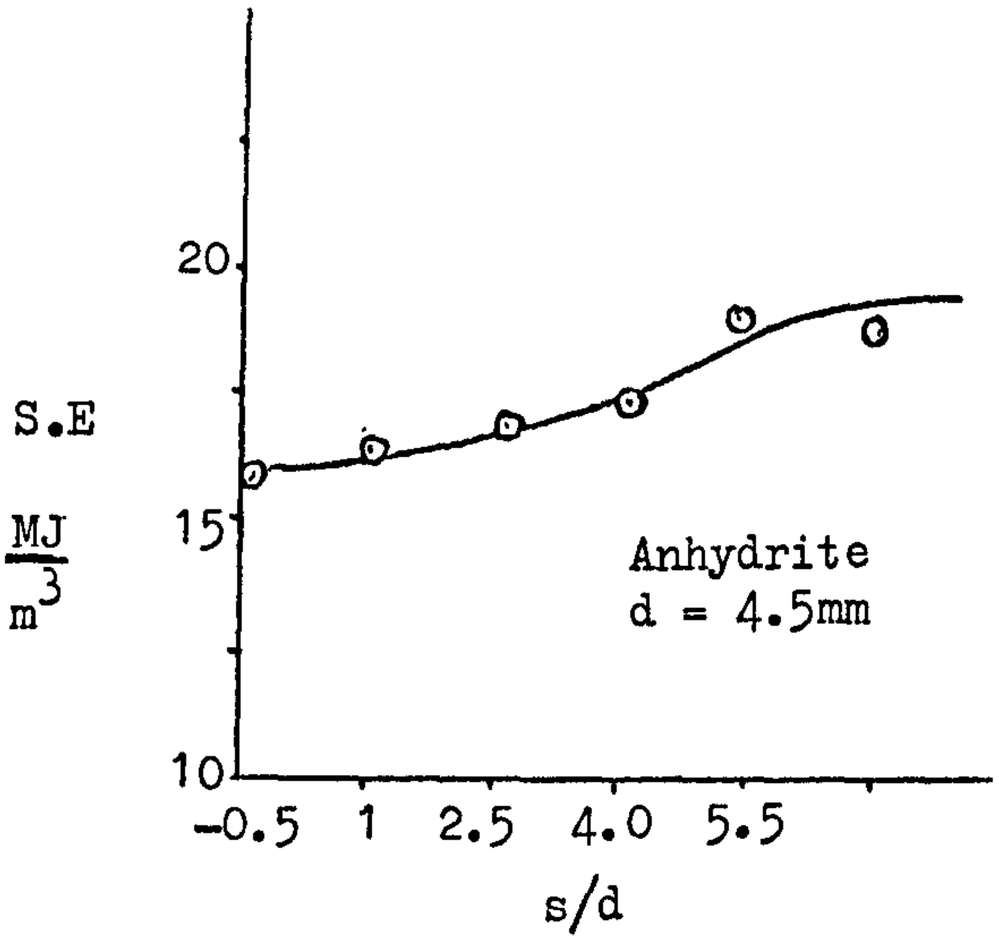

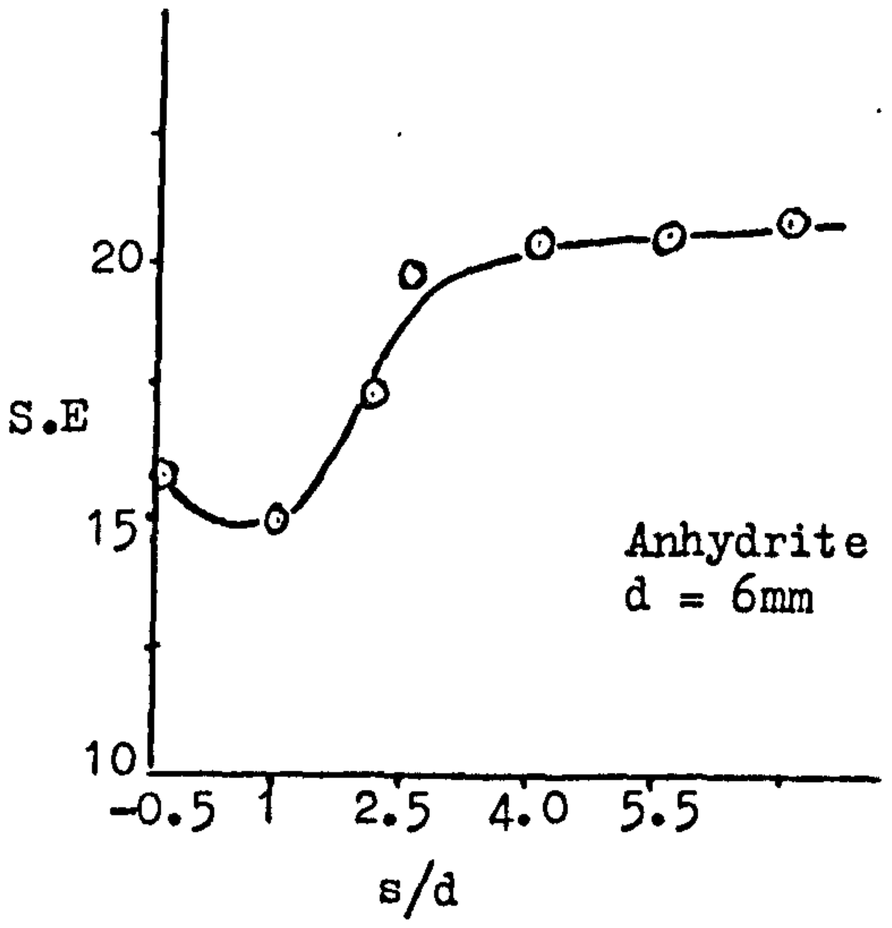

Fig.88A Variation in Specific Energy with s/d.

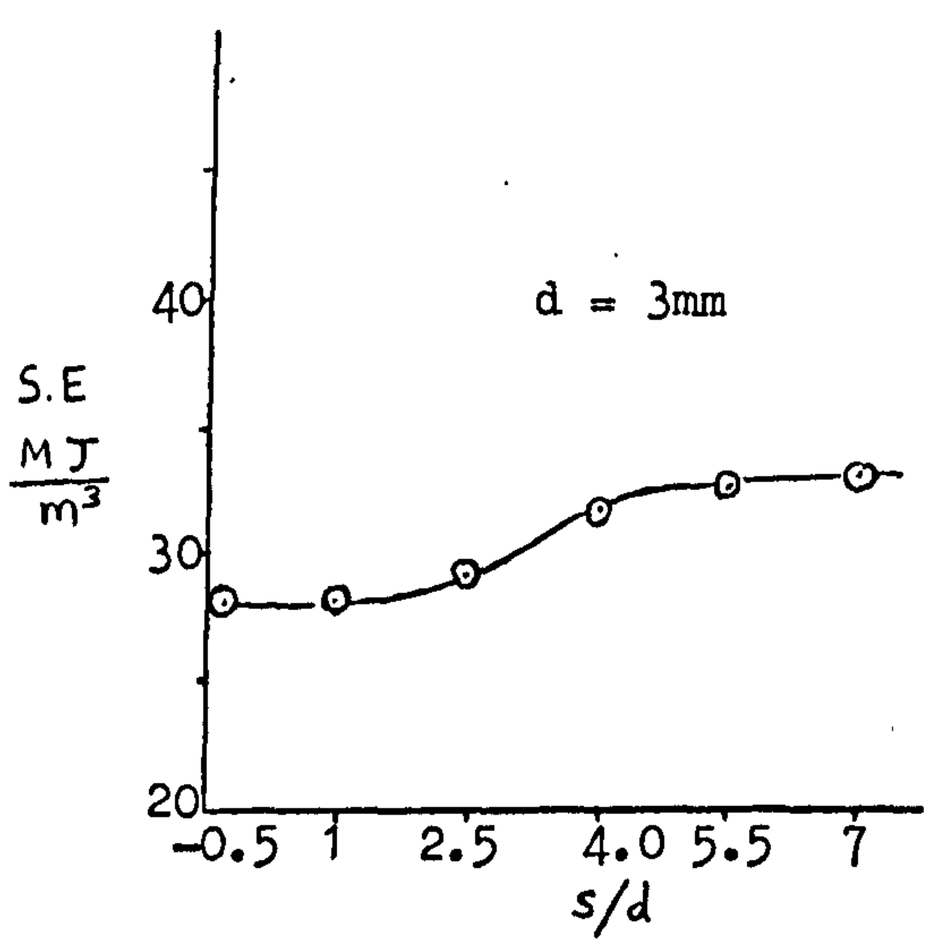

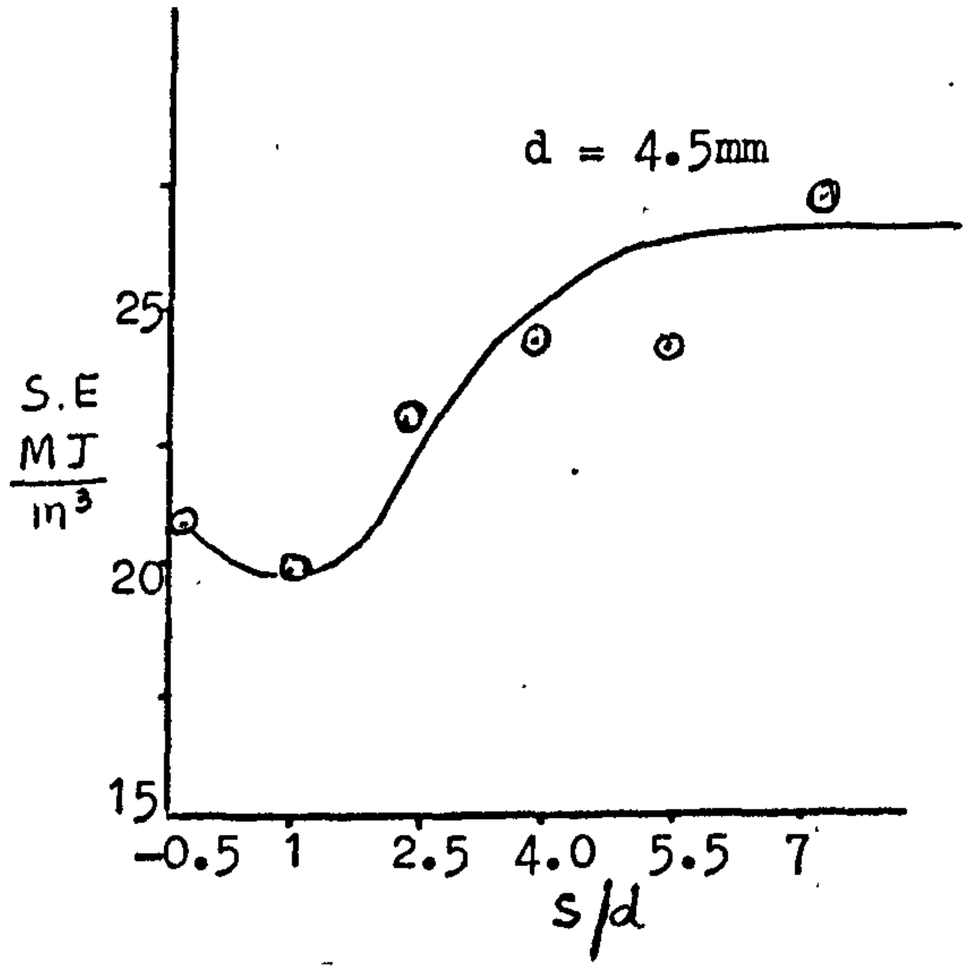

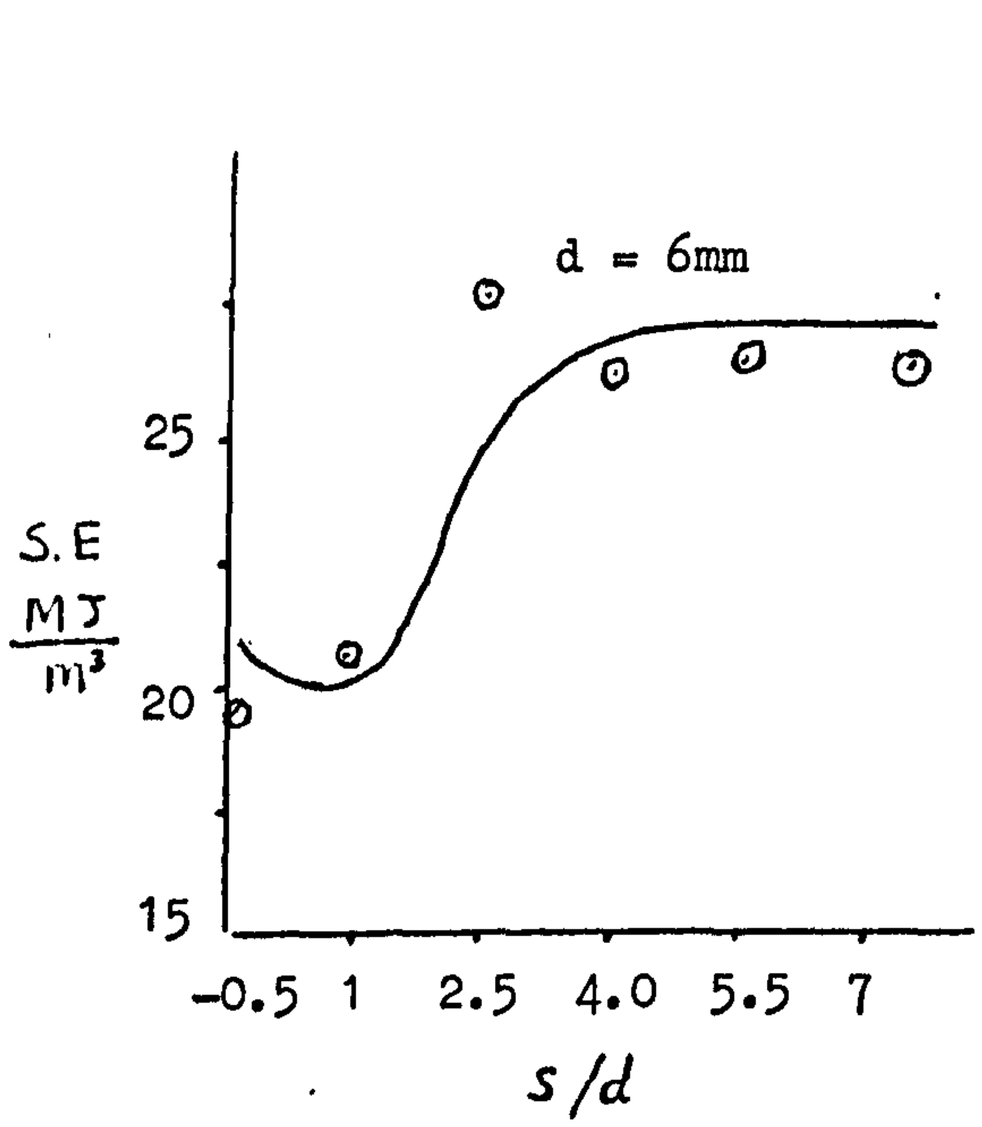

Fig.88B Variation in Specific Energy with s/d in Limestone.

11.5 Conclusions

Observations to be made from the results discussed above are summarised.

(a) The relationships between the measured values and independent variables are in the form of

$$FC,\ FN = (d + A)(W + B)\ (e^{(C \propto + D)}{}_{+E})$$

$$Q = (d^2 + A)(B\ W + C)$$

$$C.I = \frac{d + A}{d + B}\ (C \propto + D)$$

where A, B, C, D and E are the constant of the predictor equations and are given in Appendix 31.

(b) In general the ratio of $\frac{FC}{FN}$ increases with depth of cut.

(c) Specific Energy is independent of tool width but decreases rapidly with increasing depth before levelling off at greater depths.

(d) Breakout is found to be a function of depth of cut for two rocks, Greywacke and Limestone.

(e) Pick cutting performance in Granite is greatly influenced by the abrasive nature of the rock. Deeper cuts, in this rock, cause a decrease in tool wear.

(f) Considerable benefit is gained by increasing the rake angle but in practice this must be balanced against a decrease in tool strength.

(g) Cutting force values calculated from Evans' Tensile Theory give good correlation, in trend and in magnitude, with measured cutting force values.

(h) For relieved cutting, minimum specific energy occurs when the ratio s/p is around 2 for Anhydrite and Limestone and 1 for Greywacke.

(i) The improvement in specific energy, for optimum spacing, is, on average, not more than 30%.

* * *

CHAPTER TWELVE

EFFECT OF ROCK PROPERTIES ON THE WEAR PERFORMANCE OF A SINGLE PICK

Wear properties of the rocks should be considered in any type of rock machineability investigation since they affect tool cutting performance dramatically[78,79]. Rates of tool wear are very dependent on structure, composition and properties of the excavated material. High-strength rocks give rise to high stress on the cutting edge, cracks are formed and tool life is then reduced. Quartz has great influence on the wear process which in turn controls the economic success of rock machinery. Tool materials, design and operational variables, strength of the rock, shape and content of quartz affect the durability of cutting tools and makes the problem very complex indeed. Hence the following Chapter should be considered in the light of such complexity.

* * *

12.1 Experimental Programme

Bunter Sandstone, Dunhouse Sandstone, Mansfield Sandstone, Anhydrite, Weardale Limestone, Greywacke and Granite were tested in the linear cutting rig described in Chapter Five.

Each rock was cut for 100m with a pick of 1cm width and -5° rake angle. The depth of cut for all tests was 2.5mm and the cutting speed was maintained at 0.210m/sec. Pick forces and yield were recorded at various increments of cutting distance. For each increment of cutting distance the tip was cleaned in an ultrasonic cleaner, weighed and examined under a travelling microscope to measure weight loss and wear flat. Seven picks used in the wear experiments are shown in Fig.89 and all the experimental data are given in Appendix 32.

* * *

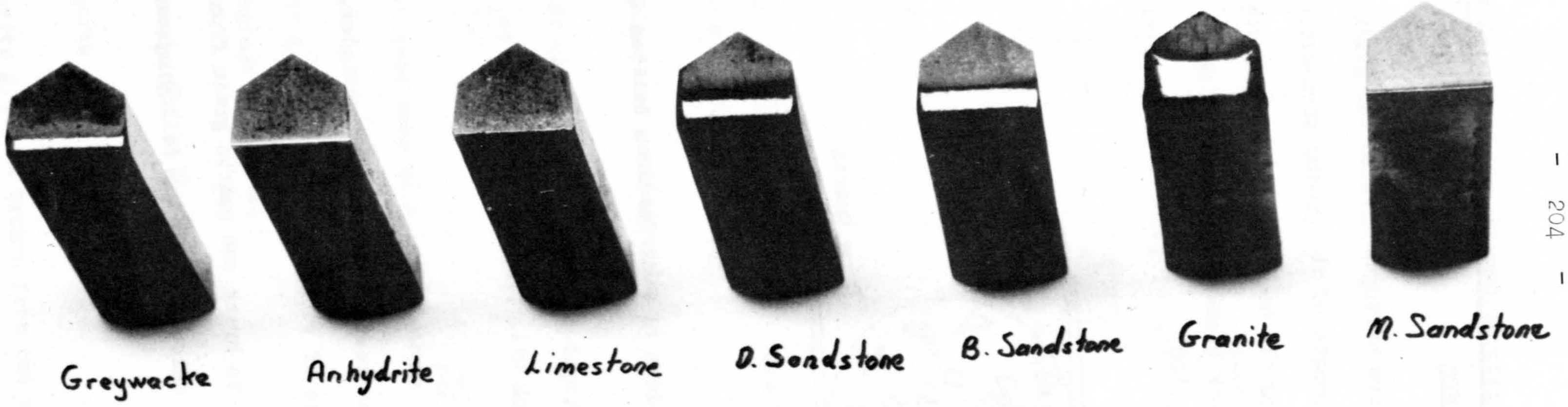

Fig. 89 Worn Tips.

12.2 Some Theoretical Considerations on the Wear Performance of Pick Cutters

The cohesive strength between the grains in most rocks is less than the strength of the grains themselves[99]. Some minerals, such as quartz, rarely have any cleavage or other microscopic weakness, so that when a rock breaks, rupture will take place between the grains of such a mineral[100]. Fig.90 illustrates such phenomenon.

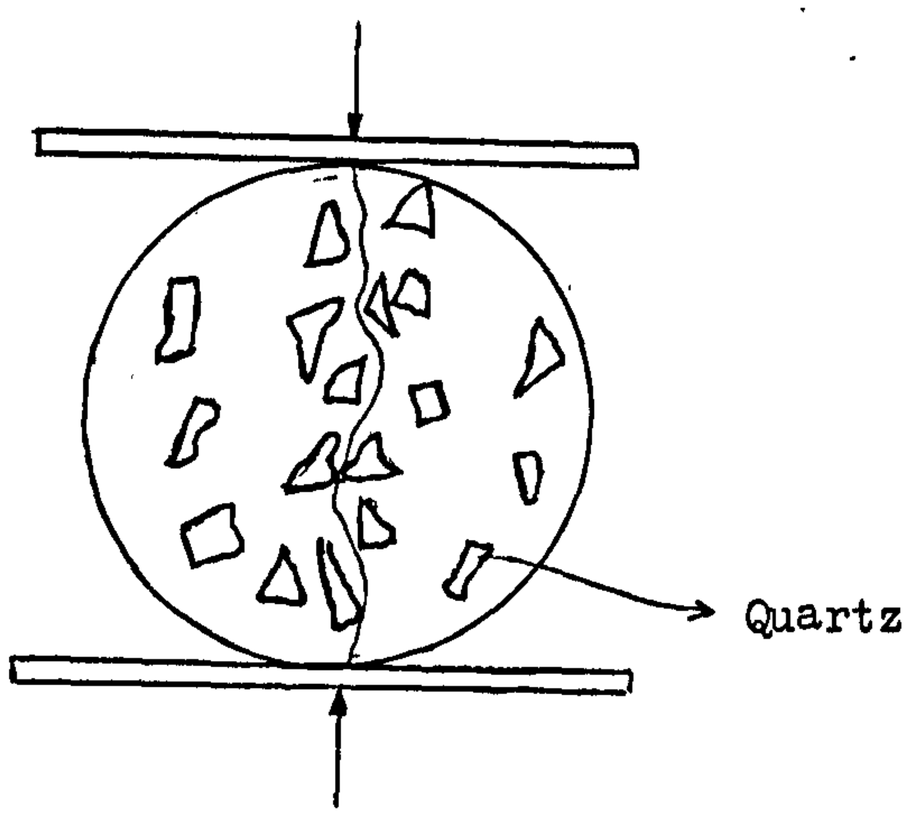

Fig.90 Failure of Rock Specimen between Quartz Grains.

If σ_{GB} is the strength of grain boundaries in rock, the tensile strength of the rock will probably be related to σ_{GB} as:

$$\sigma_{GB} = k.\sigma t \qquad \text{---(32)}$$

k being rock texture or cementation index, and different for each type of rock.

The force F, to break one quartz grain from the rock matrix or rock texture can be calculated in the following manner (Fig.91).

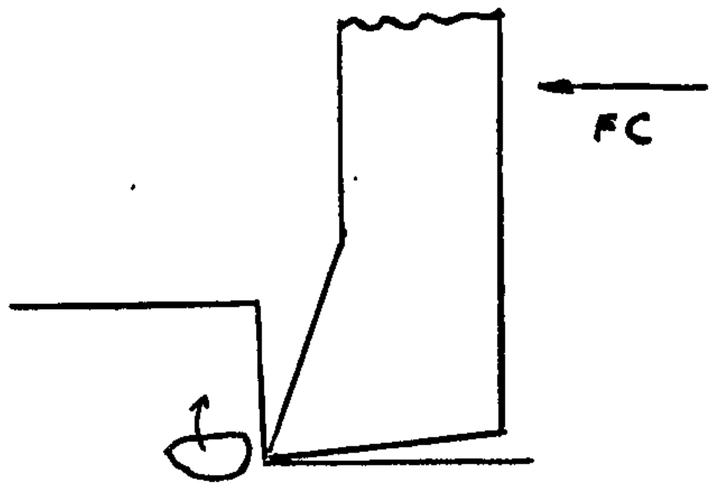

FC > F

(A)

Quartz grain is broken from the Rock Matrix.

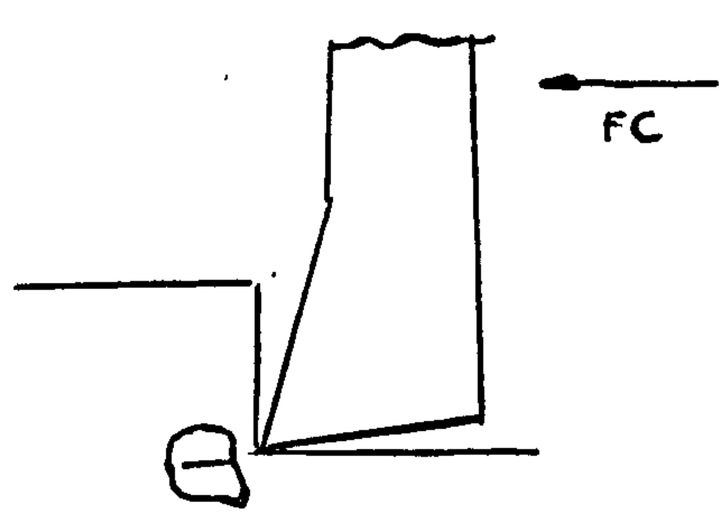

FC < F

(B)

Quartz grain is cut.

Fig.91 Theoretical consideration of cutting a Quartz Grain.

$$F = \sigma_{GB} \cdot A$$

$$F = \sigma_{GB} \cdot k_1 \cdot l \qquad \text{---(33)}$$

A is the surface area of a quartz grain

k_1 is quartz grain shape index

l is quartz grain size

$Q_j\%$ is percentage of quartz.

$$\text{hence} \leq F = k \cdot k_1 \cdot \sigma t \cdot l \cdot Q_j\% \qquad \text{---(34)}$$

if $FC < F$ Quartz grain is cut ---(35)

if $FC > F$ Quartz grain is broken from the matrix ---(36)

Hence it is obvious that the weight loss of the pick in the first case will be more than in the second case. This clearly shows that F is related to the wear. Schimazek's results in small scale drilling gives a good correlation between tip weight loss and the product. $\sigma t.l.Q_3\%$, as seen from Fig.92.

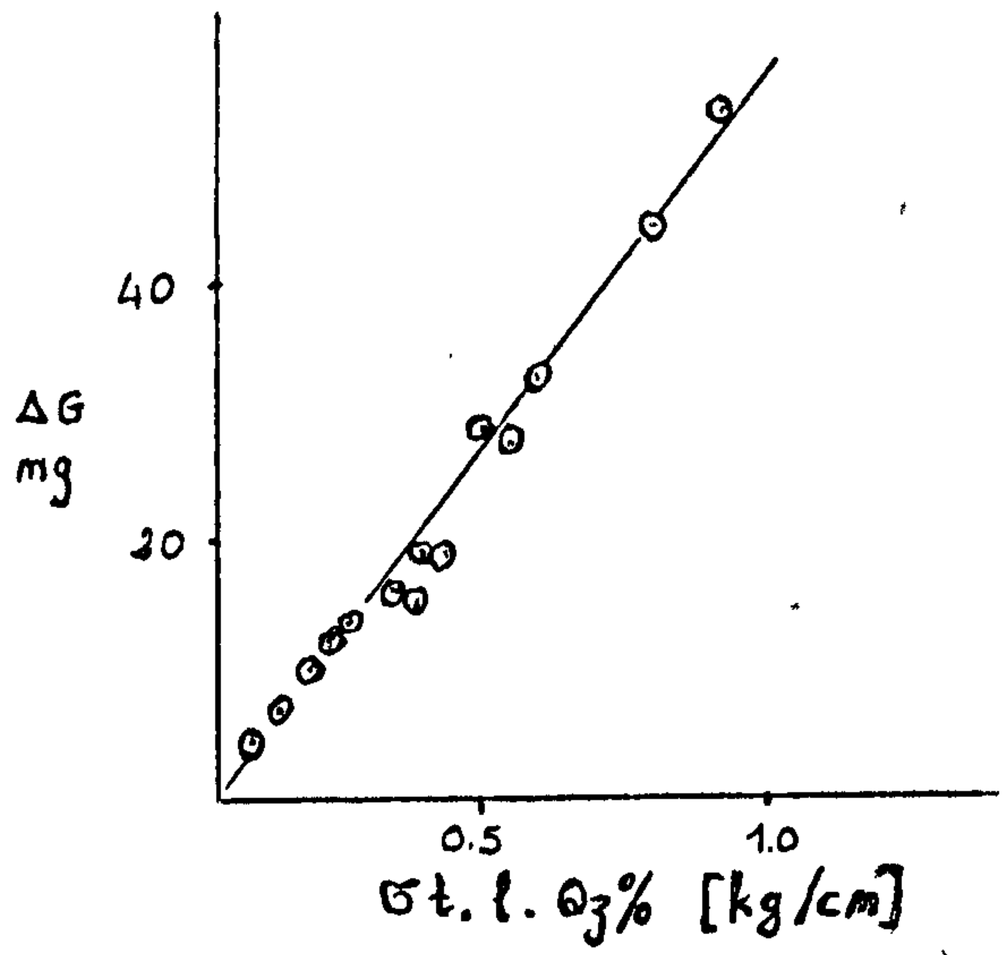

Fig.92 Relations between Tip Weight Loss and Rock Properties (after Schimazek).

However, the rock cutting process is different from drilling in its nature, so a similar relationship might not necessarily exist for cutting.

In Chapter Eleven it was shown that Evans' theory was in good agreement with experimental results in trend and magnitude. When equation (35) and the cutting force obtained from Evans' theory are combined, the following relationship is obtained.

$$\frac{2\sigma t.d.\sin\frac{1}{2}\left(\frac{\pi}{2}-\alpha\right)}{1-\sin\frac{1}{2}\left(\frac{\pi}{2}-\alpha\right)} < k.k_1.\sigma t.l.Q_3\% \quad -- (37)$$

For a given rock the second part of equation (37) will be a constant. If d increases the weight loss of tip should decrease since the relation FC $<$ F will turn to be FC $>$ F. With the same way of thinking it can be concluded that tip weight loss increases with increasing rake angle and the product of $k.k_1.l.Q_3$ %. It is interesting to note that equation (37) is independent of tensile strength. Hence the following theoretical wear curves can be drawn.

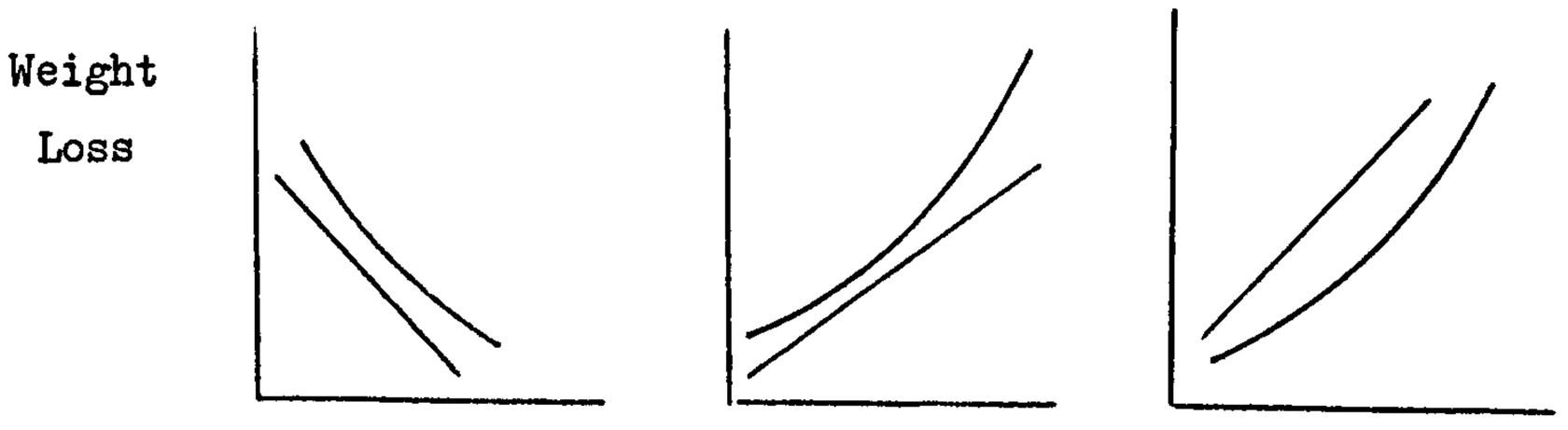

(a) Depth of Cut (b) Rake Angle (c) $k.k_1.l.Q_3$ %.

Fig.93 Theoretical Wear Curves.

The experimental results of some research workers are in good agreement with the general trend of Figs. 93A and 93B. However, one should note that the above theoretical consideration does not take into account the wear mechanism which might occur in high strength rocks, i.e. chipping, gross failure, etc.

* * *

12.3 Experimental Results and Conclusions

All the results are summarised in Tables 36 and 37 and Fig Figs.94 and 95. The tool forces and specific energy increased dramatically with distance cut, with different rates in different rocks.

Wear has a greater effect on the normal force than the cutting force. The rates $\frac{\text{Mean Peak}}{\text{Mean}}$ force is reduced when the tip starts getting blunt. Weight loss of the pick is linearly related to cutting distance, suggesting that for a given pick and depth of cut there is a constant wear rate for each type of rock. The relationships between wear flat and cutting distance are different than those for weight loss and cutting distance. The power laws governing such curves, and the different mechanisms which might occur when cutting different rock materials show that wear rate, rather than wear flat, should be used to assess a wear index. Measured values of wear rates, together with the calculated values of Q_z grain size $\times$ Q_z content and $\sigma_t \times Q_z$ grain size $\times$ Q_z content are tabulated in Table 37. From this Table and Fig.94 it can be concluded that wear rate is a function of Quartz grain size and Quartz content and is independent of the tensile strength of the rock. This conflicts with the results obtained for rock drilling, but, as previously stated, the mechanisms of rock failure in the two cases may very well be radically different.

* * *

Table 36 Variation in Pick Cutting Performance after Cutting 100m.

Rock	% Increase					Weight Loss $g_x 10^{-3}$
	F'C	$\overline{FC}$	F'N	$\overline{FN}$	SE	
W. Limestone	0	1	25	60	3	0.90
M. Sandstone	22	55	98	126	42	1.40
Anhydrite	6	15	82	190	10	1.80
Greywacke	60	90	145	209	110	23.62
D.Sandstone	118	247	343	589	290	61.20
B.Sandstone	105	168	203	428	189	78.90
Granite	200	237	598	794	310	227.00

Table 37 Variation in Wear Rate with Qz Grain Size, Qz Content and Tensile Strength.

Rock	Wear Rate *mg/m*	Qz Grain Size(mm) x Qz Content%	σ_t x Qz Grain Size (mm) x Qz Content %
W. Limestone	0.0034	0	0
M. Sandstone	0.0143	2.8	12.4
Anhydrite	0.0177	0	0
Greywacke	0.2310	11.2	184.2
D. Sandstone	0.6021	14.8	46.2
B. Sandstone	0.7844	16.4	40.3
Granite	2.7614	38	409.3

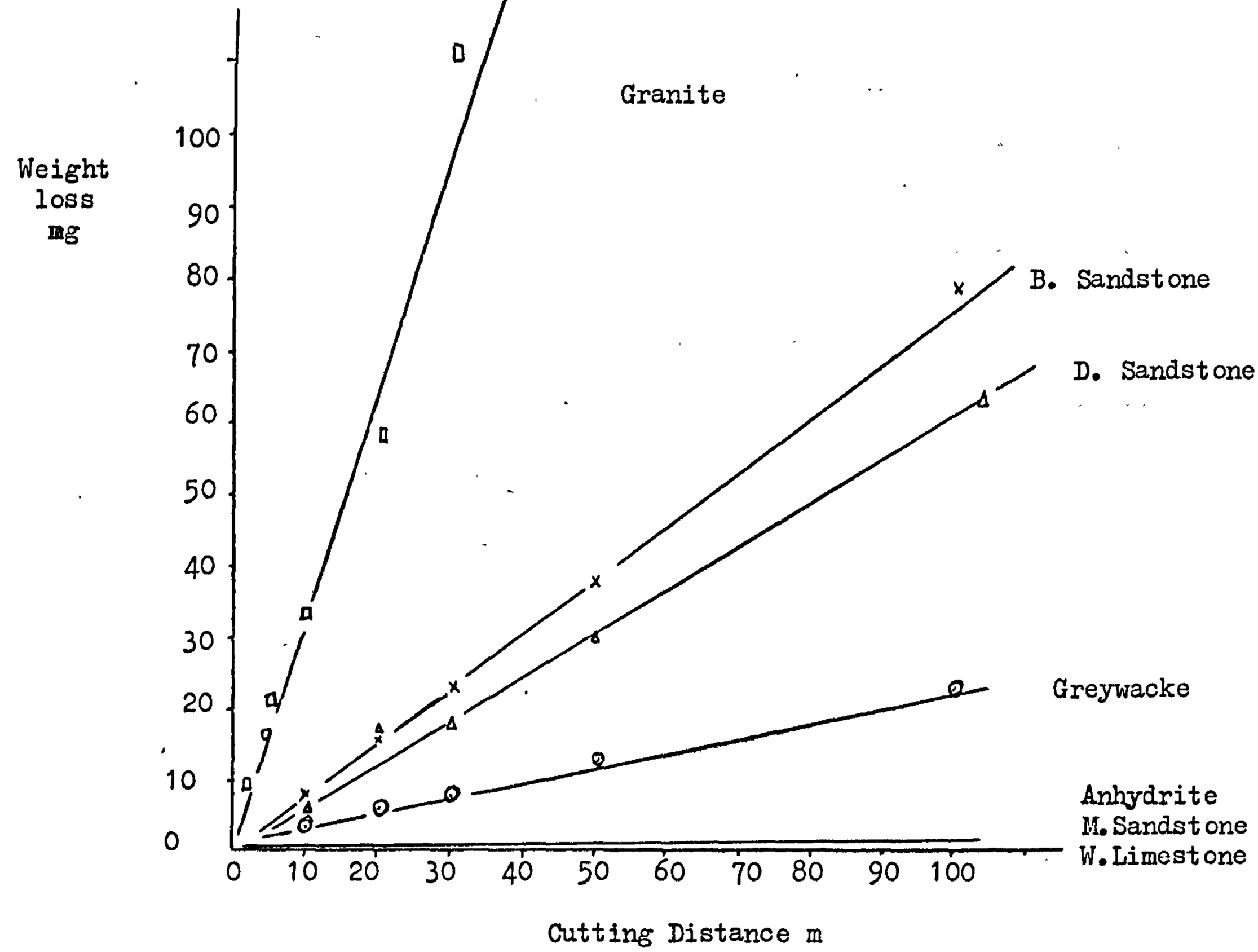

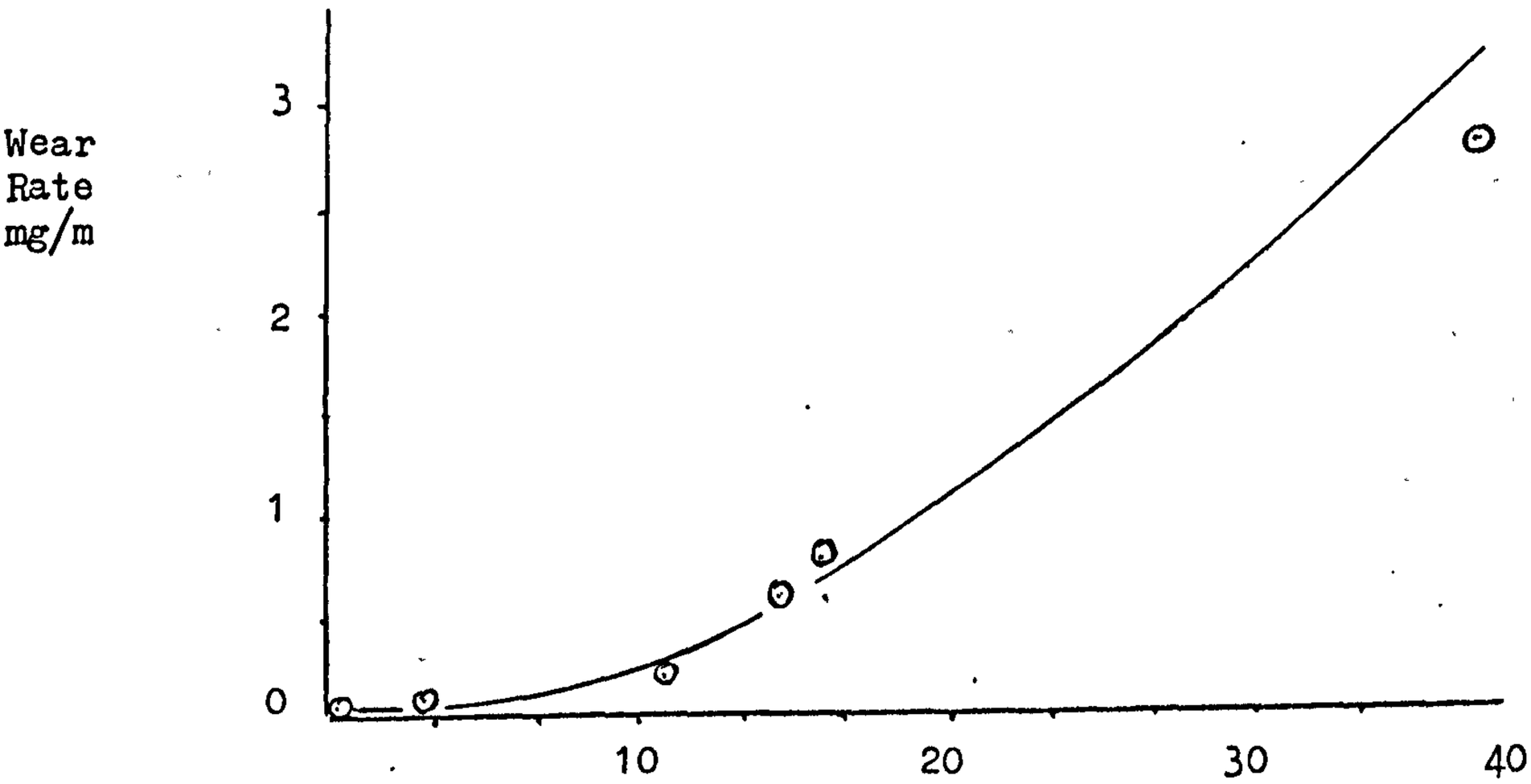

Fig.94 Effect of Quartz Content and Quartz Grain Size on Tool Wear.

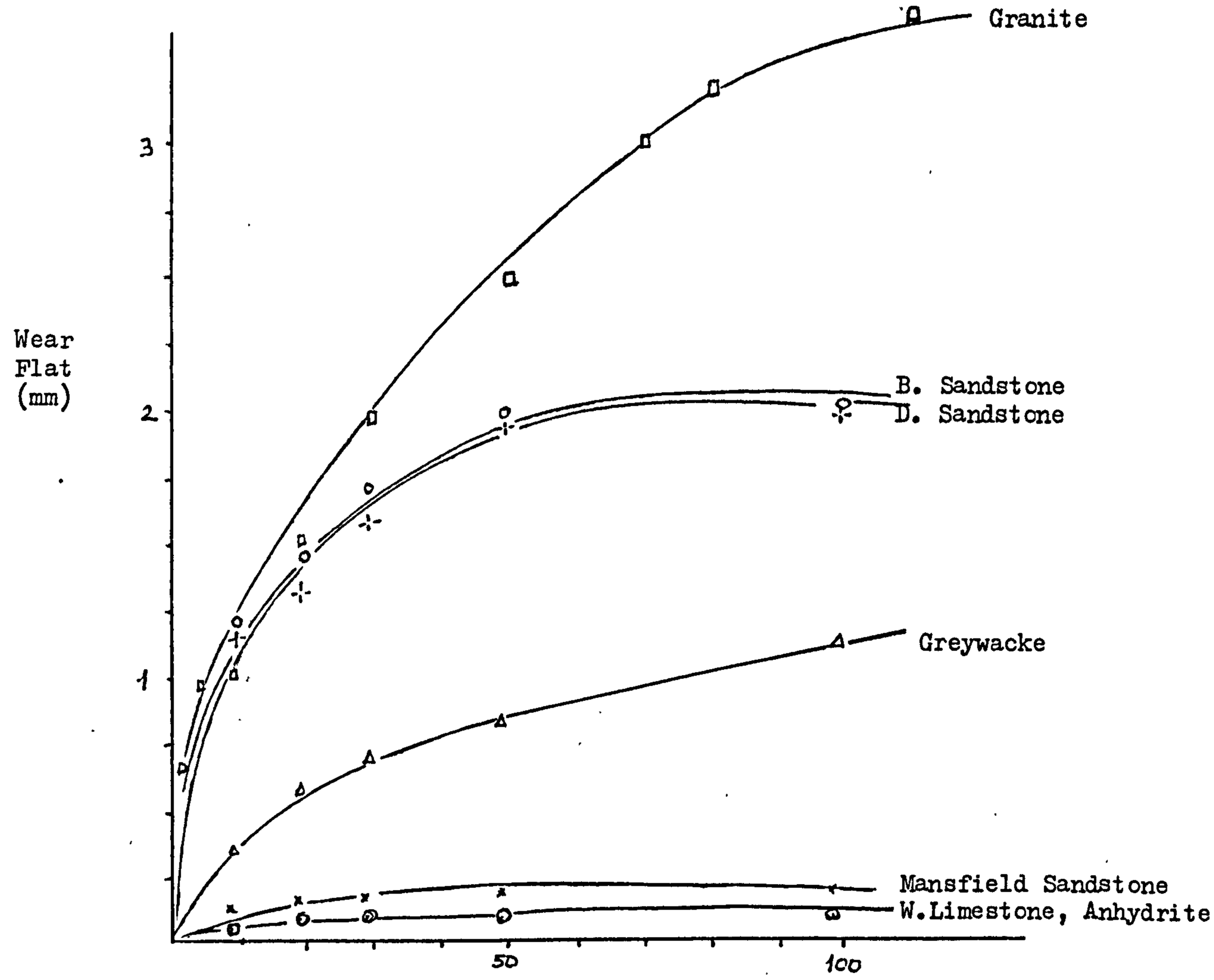

Fig.95 Effect of Cutting Distance on Wear Flat.

CHAPTER THIRTEEN

13 RELATIVE EFFICIENCY OF PICKS AND ROLLER CUTTERS

Different factors affecting specific energy should be considered in order to assess relative efficiency of picks and roller cutters. The main factors are rock properties, depth of cut, rake angle, geometrical parameters of roller cutters, wear and improvement in specific energy for relieved cutting. The effects of rock discontinuities, moisture content of the rock and the geometrical parameters of toothed roller cutters are ignored in this analysis.

Some relieved and unrelieved cutting experiments in Dunhouse and Mansfield Sandstone were carried out in order to fulfil some of the requirements of this comparative study. All the experimental data are given in Appendices 33 and 34. Pick Specific Energy values for Gypsum are taken from Fourth Wolfson Progress Report[101] and cutting results already discussed in previous Chapters are also used in this section.

* * *

13.1 Unrelieved Cutting

The comparative efficiency of picks, which is the ratio of Specific Energy for Disc Cutting to Specific Energy for Pick Cutting, is tabulated in Table 38, for different combinations of depth of cut, rake angle and edge angle. It can be easily seen that this ratio is not significantly affected by depth of cut, except in Dunhouse Sandstone. Moreover, a similar trend was noticed by Roxborough in Bunter Sandstone[102]. If rake angle is kept constant at 10° and disc edge angle changed from 60° to 100°, the relative efficiency of picks increases 20% in Gypsum, 50% in Dunhouse Sandstone, 43% in Mansfield Sandstone and 33% in Anhydrite. On the other hand, if disc edge angle is kept at 60° and rake angle changed from 0° to -20°, the comparative efficiency of picks decreases 47% in Limestone and 80% in Greywacke. Thus it may be concluded that for unrelieved cutting, picks are 4~5 times more efficient than discs in Evaporites, 6~17 times in medium strength sandstones, 1.5~3 times in Limestone and Greywacke. It is interesting to note that the theoretical studies of Evans show disc cutting is likely to take several times (roughly 2 to 5 times) as much energy per unit volume of rock broken as pick cutting[8].

As it can be seen from Table 39, the efficiency of a 10° rake angle pick compared to a single toothed roller cutter is almost the same as compared to discs.

One should bear in mind that cutting tools operate in an array and are susceptible to wear. Hence any comparative study without taking account of the relieved cutting situation and wear performance of cutting tools will not be very conclusive.

* * *

13.2 Relieved Cutting

Improvements in Specific Energy values for relieved cutting using different cutting tools are given in Table 40. Although this improvement is 3 times for discs in Dunhouse Sandstone and twice for Greywacke, there is no significant difference in the improved performance of picks and discs in the other rocks. Surprisingly, however, the benefit of relief is seen to be much greater in the case of toothed roller cutters operating in Mansfield Sandstone.

* * *

13.3 Tool Wear

Previous experiments already carried out in an abrasive sandstone showed that a 2mm wear flat was generated after only 100m of cutting, which is a very small distance in practical terms. However, this amount of wear may cause the specific energy to increase several times. It is likely that a further increase of wear flat beyond 3mm would not increase specific energy dramatically, as is shown in Fig. 96. From wear tests already discussed in Chapter Twelve it may be concluded that picks will be hardly worn in Mansfield Sandstone, Anhydrite and Limestone, but the wear flats which will be generated when cutting Dunhouse Sandstone and Greywacke will probably cause an increase of 4~5 times in the energy to excavate a unit volume of rock.

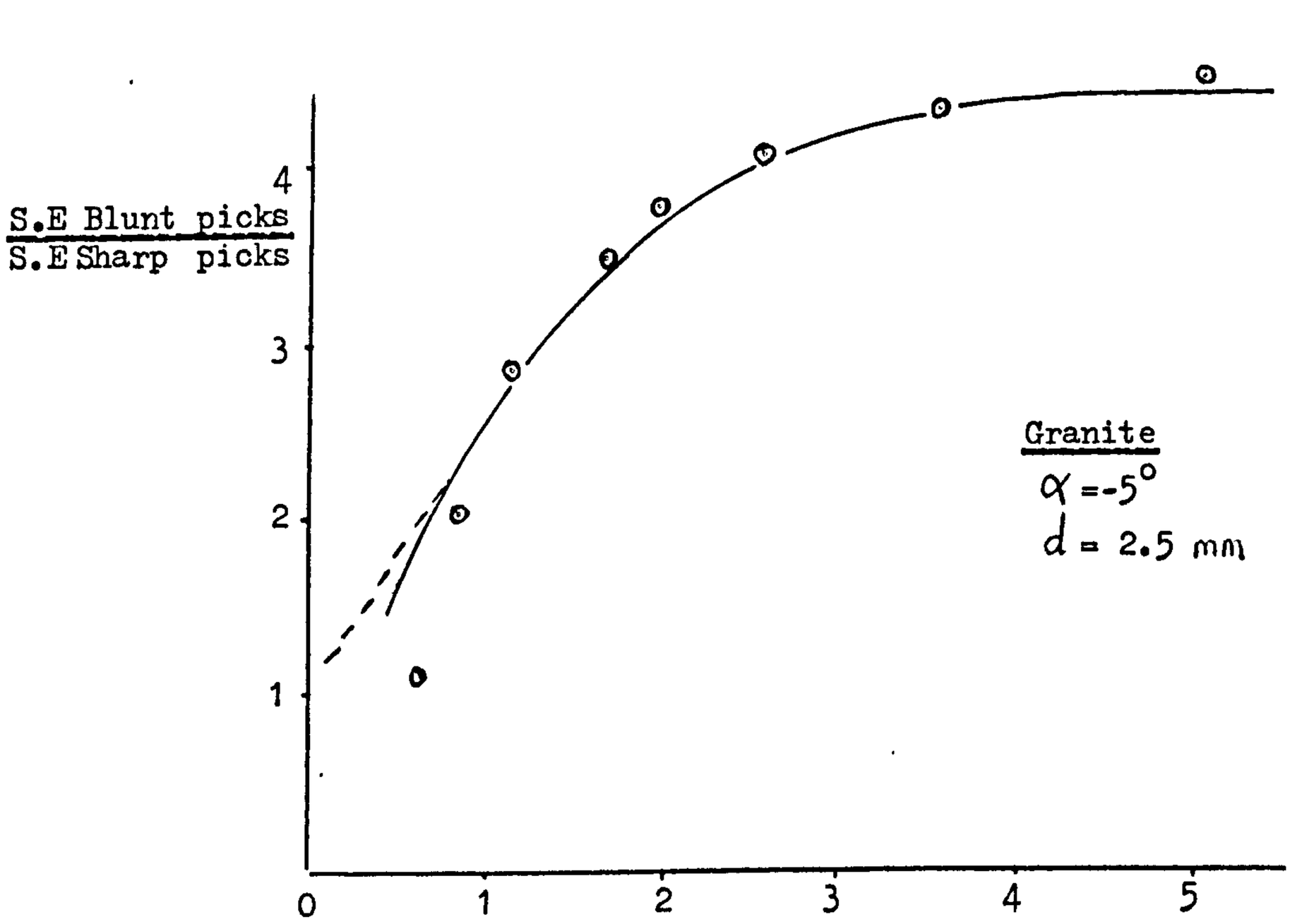

Fig.96 Variation in Specific Energy with Wear Flat.

Discs are less susceptible to wear than picks due to the fact that each point on the circumference of a disc is in contact with the rock only once during a revolution. The other advantage of the discs, is that specific energy is not greatly affected by edge radius and it is likely that discs with a radius on the cutting edge will be worn less than sharp ones.

* * *

13.4 Conclusions

1. For unrelieved cutting when rake angle, edge angle, and depth of cut are considered, it is found that picks are 4~5 times more efficient than discs in Evaporites, 6~17 times in Sandstones, 1.5~3 times in Limestone and Greywacke. The efficiency of toothed roller cutters was found to be of the same order as that for disc cutters.

2. When relieved cutting and the wear performance of different cutting tools are taken into account, discs are probably as efficient as picks when cutting in rocks such as Dunhouse Sandstone and Greywacke. However, one can still say that picks are 4-5 times more efficient than discs in Evaporites, 6-8 times in Mansfield Sandstone and 1.5 ~ 2.5 times in Limestone.

* * *

Table 38 Relative Efficiency of Picks and Discs

Rocks	Specific Energy Discs / Specific Energy Picks for Unrelieved Cutting								
	$\alpha=10^\circ$ $\phi=60^\circ$ Depth of Cut (mm)			$\alpha=10^\circ$ $\phi=80^\circ$ Depth of Cut (mm)			$\alpha=10^\circ$ $=100^\circ$ Depth of Cut (mm)		
	6	9	12	6	9	12	6	9	12
Gypsum	3.9	3.6	3.5	4.2	3.9	3.9	4.7	4.4	4.3
D. Sandstone	10.5	12.7	13.6	13.1	15.8	16.9	16.2	19.7	21.1
M. Sandstone	6.3	6.4	5.8	7.5	7.6	6.7	8.9	9.1	8.2
Anhydrite	4.0	4.8	5.5	4.5	5.6	6.4	5.2	6.4	7.4
Rock	$\alpha=0^\circ$ $=60^\circ$ Depth of Cut (mm)			$\alpha=-10^\circ\phi=60^\circ$ Depth of Cut (mm)			$\alpha=-20^\circ\phi=60^\circ$ Depth of Cut (mm)		
	3	5	7	3	5	7	3	5	7
W. Limestone	2.8	2.1	2.6	2.3	1.7	2.1	2.0	1.4	1.7
Greywacke	3.2	2.5	3.0	2.4	1.9	2.2	1.8	1.4	1.6

Table 39 Relative Efficiency of Picks and Toothed Roller Cutters Pick $\alpha = 10^\circ$, 12 Toothed Roller Cutter with 60° Wedge Angle.

Rock	Specific Energy, Roller Cutter / Specific Energy, Pick		
	Depth of Cut (mm)		
	6	9	12
Gypsum	3	3	3
D. Sandstone	11	14	17
M. Sandstone	7	9	9

Table 40 Improvement in S.E. Values for Relieved Cutting

Rock	Optimum Spacing/Penetration			Improvement in S.E. %		
	Picks	Discs	Toothed R.C.	Picks	Discs	Toothed R.C.
Gypsum	-	4	-	* -	** 30	-
D.Sandstone	4	4	1.5	25	75	20
M.Sandstone	3.5	7	0	30	30	90
Anhydrite	2	6	-	30	30	-
W.Limestone	2	5	-	30	35	-
Greywacke	1	5	-	20	40	-

* Mean values for 3 levels of depth of cut

** Mean values calculated from experimental results and disc precitor equations (except for Limestone and Greywacke.)

* * *

CHAPTER FOURTEEN

14 CONCLUSIONS AND RECOMMENDATIONS FOR FUTURE RESEARCH

The general conclusions have already been discussed in each of the Chapters and only a summary appears below.

Cutting Rocks with Discs

1. In all cases, thrust and rolling forces increased with increasing penetration and edge angle. Although disc diameter has no effect on rolling force, it has a significant effect on thrust force.

2. The ratio $\frac{FT}{FR}$ is affected by penetration, being 14 for shallow cuts and 4 for deeper cuts.

3. The increase in the yield was found to be proportional to the square of the penetration. The Edge angle appears to have a small effect on yield, both in Gypsum and Mansfield Sandstone, but not in Anhydrite and Dunhouse Sandstone.

4. Greater efficiency can be obtained by increasing the penetration and decreasing the edge angle. Specific energy is not affected by disc diameter.

5. For unrelieved cutting the only experimental variable which affects the coarseness index is the penetration.

6. Thrust and rolling forces increase rapidly with spacing, becoming asymptotic to the unrelieved forces at s/p ratios of 6.5 - 8 for thrust force, and 5-6 for rolling force.

7. There is an optimum yield for relieved cutting which is significantly higher than equivalent yield produced by unrelieved cutting. This optimum yield occurs at s/p ratios of about 6.

8. There is a quite definite optimum value of specific energy and coarseness index for s/p ratios ranging, in the different rocks, from 4 to 7.

9. The point where the interaction between adjacent grooves occurs can be predicted by the following formula.

$$\frac{s}{p} \leq \frac{\sigma c}{\sigma s}$$

10. The most dominant rock properties in determining disc cutter forces are compressive strength, rock density and tensile strength. Young's Modulus and impact strength index are of minor importance.

11. Thrust force is linearly related to the compressive strength of the rock and the projected area of disc contact.

12. Rolling force is a power function of the projected area of the disc in the direction of movement and correlates well with the compressive strength of the rock.

13. Disc groove angle is a function of the sum of internal friction angle of the rock and the sliding friction between disc and rock.

Effect of Edge Radius on the Cutting Performance of Disc Cutters

1. Thrust and rolling forces increase considerably with edge radius in an exponential manner in the form of:

$$FT_r = FT_{ro} e^{Ar}$$

$$FR_r = FR_{ro} e^{A'r}$$

A is a function of disc penetration and independent of rock properties.

2. The affect of edge radius is reduced when using deeper penetrations.

3. Specific energy remains almost constant with increasing edge radius for penetration deeper than 2mm, since bluntness causes an increase in yield.

4. In relieved cutting the general trend was for optimum spacing/penetration ratio to increase as discs became duller.

Cutting High Strength Rocks with Picks

1. Cutting and normal forces are linearly affected by depth of cut and tool width.

2. Yield increase is found to be proportional to the square of penetration.

3. Yield increases linearly with tool width giving a positive intercept attributed to breakout.

4. In general the ratio of $\frac{\overline{FC}}{FN}$ increases with depth of cut.

5. Specific energy is independent of tool width but decreases rapidly as the depth of cut is increased from zero. This decrease does, however, level off at greater depths.

6. Breakout is found to be a function of depth of cut for both Greywacke and Limestone.

7. Pick cutting performance in Granite is greatly influenced by its abrasive nature. Deeper cuts in this rock cause a decrease in the wear of picks.

8. Considerable benefit is gained by increasing the rake angle, but in practice this must be balanced against a decrease in tool strength.

9. Cutting force values calculated from Evans' Tensile Theory give good correlation, in trend and in magnitude, with the measured cutting force values.

10. For relieved cutting, minimum specific energy occurs when the ratio of s/d is around 2 for Anhydrite and Limestone and 1 for Greywacke.

11. The improvement in specific energy, at optimum spacing, was on average not more than 30% of the unrelieved value.

Wear Performance of a Single Pick in Different Experimental Rocks

1. Wear rate of the pick was found to be a function of the product of Quartz grain size and Quartz content of the rocks.

Relative Efficiency of Picks and Roller Cutters

1. For relieved cutting, when rake angle, edge angle and depth of cut are considered, it is found that picks are 4-6 times more

efficient than discs in Evaporites, 6~17 times in Sandstone, 1.5~3 times in Limestone and Greywacke.

2. The efficiency of toothed roller cutters was found to be of the same order as that for disc cutters.

3. When relieved cutting and the wear characteristics of different cutting tools are taken into account, discs are probably as efficient as picks when cutting in Dunhouse Sandstone and Greywacke. However, one can still say that picks are 4-6 times more efficient than discs in Evaporites, 6~8 times in Mansfield Sandstone and 1.5~2.5 times in Limestone.

The method of analysis developed by Protodyakanov and Teder has shown that different cutting tools behaved in substantially the same manner in the wide range of rocks tested. An overall picture of the cutting performance for picks, discs and roller cutters has been built up, and the work reported in this thesis has been an attempt to increase the available knowledge on cutting characteristics of a range of rocks. The data obtained is basic to the design of the cutting systems for the excavation of these rock materials.

* * *

Recommendations for Future Research

Any research worker dealing with rock cutting or rock mechanics is always faced with the question of how well his results represent the in-situ situation.

The disc cutting predictor equations developed in this thesis provide the ability to correlate laboratory cutting results with actual tunnel boring machine performance, since these equations are a function of disc geometrical parameters and rock properties. The values obtained from the predictor equations should be correlated with machine data if available.

Full face tunnel boring machines are usually equipped with single discs, double discs or triple discs. The relative efficiencies of the three systems has remained obscure. Comprehensive laboratory rock cutting tests should be carried out in order to investigate the efficiency of such cutters.

There is no information in the literature on the angle of attack, skew angle and corner cutting characteristics of discs and so these parameters remain to be investigated .

Rocks with different degrees of abrasivity should be tested with sharp discs, blunt discs and discs with different geometrical parameters in order to understand better the wear performance of discs.

Any research with the objective of prolonging pick or disc cutter life will be of great interest to those concerned with the economical success of tunnel boring.

* * *

Appendix 1

Details of Tool Holders

Tool No.	Angle (Degrees)	Dimension A (cm)	Dimension B (cm)	Dimension C (cm)
1	5	0.91	0	0.30
2	5	1.41	0	0.48
3	5	1.91	0.55	0.50
4	5	2.41	1.05	0.48
5	5	2.91	0.90	0.74
6	15	0.91	0	0.30
7	15	1.41	0	0.48
8	15	1.91	0.55	0.50
9	15	2.41	1.05	0.48
10	15	2.91	0.90	0.74
11	20	0.91	0	0.30
12	20	1.41	0	0.48
13	20	1.91	0.55	0.50
14	20	2.41	1.05	0.48
15	20	2.91	0.90	0.74

Appendix 2A

Results of Single Disc Experiment in Gypsum

Test No	Levels of			Thrust Forces			
				Measured Values		Predicted Values	
	∅ (o)	D (mm)	p (mm)	F'T(kN)	$\overline{FT}$(kN)	F'T(kN)	$\overline{FT}$(kN)
1	60	100	10	37.59	35.86	36.29	33.80
2	60	125	6	21.59	19.49	21.70	20.08
3	60	150	2	6.65	6.11	5.20	4.49
4	60	175	8	36.21	34.21	33.53	31.29
5	60	200	4	14.27	12.75	15.59	14.30
6	70	125	8	33.06	30.94	37.11	35.03
7	70	150	4	16.02	14.38	17.35	16.11
8	70	175	10	50.53	44.75	52.87	50.23
9	70	200	6	28.90	26.70	31.34	29.55
10	70	100	2	7.13	6.32	5.72	4.99
11	80	150	6	31.68	29.43	33.63	31.94
12	80	175	2	8.12	7.48	8.03	7.13
13	80	200	8	46.82	45.56	51.67	49.49
14	80	100	4	15.60	14.25	18.40	17.19
15	80	125	10	51.73	48.92	56.43	53.96
16	90	175	4	24.66	21.95	25.20	23.83
17	90	200	10	79.05	78.76	76.58	74.10
18	90	100	6	27.10	24.81	34.78	33.14
19	90	125	2	10.67	10.44	8.36	7.43
20	90	150	8	53.88	51.31	54.05	51.99
21	100	200	2	12.21	11.24	11.13	9.99
22	100	100	8	50.54	47.66	54.84	52.83
23	100	125	4	25.77	23.61	25.72	24.37
24	100	150	10	80.00	75.38	78.60	76.25
25	100	175	6	48.00	46.89	46.72	44.99

Appendix 2B

Results of Single Disc Experiment in Gypsum

Test No	Levels of			Rolling Forces			
				Measured Values		Predicted Values	
	ø (o)	D (mm)	p (mm)	F'R(kN)	$\overline{FR}$(kN)	F'R(kN)	$\overline{FR}$(kN)
1	60	100	10	11.95	11.42	8.31	7.81
2	60	125	6	4.75	4.45	4.63	4.33
3	60	150	2	0.84	0.77	0.95	0.85
4	60	175	8	7.21	6.77	6.47	6.07
5	60	200	4	1.98	1.81	2.79	2.59
6	70	125	8	8.26	7.74	7.50	7.12
7	70	150	4	2.56	2.42	3.24	3.04
8	70	175	10	10.28	9.72	9.63	9.16
9	70	200	6	4.59	4.27	5.37	5.08
10	70	100	2	1.22	1.09	1.11	1.00
11	80	150	6	5.74	5.35	6.11	5.83
12	80	175	2	0.89	0.83	1.26	1.14
13	80	200	8	8.87	8.45	8.53	8.17
14	80	100	4	3.26	3.01	3.68	3.48
15	80	125	10	13.21	12.81	10.96	10.51
16	90	175	4	3.67	3.34	4.13	3.93
17	90	200	10	14.72	14.67	12.28	11.86
18	90	100	6	6.53	6.02	6.85	6.58
19	90	125	2	1.39	1.37	1.41	1.29
20	90	150	8	10.58	9.98	9.57	9.22
21	100	200	2	1.13	1.03	1.56	1.43
22	100	100	8	12.7	12.03	10.60	10.26
23	100	125	4	4.15	3.78	4.57	4.38
24	100	150	10	17.08	17.31	13.61	13.20
25	100	175	6	7.06	6.99	7.59	7.32

Appendix 2C

Results of Single Disc Experiment in Gypsum

Test No	Levels of			Yield, Specific Energy and C.I.					
				Measured Values			Predicted Values		
	∅ (°)	D (mm)	p (mm)	Q(m^3/km)	SE(MJ/m^3)	C.I.	Q(m^3/km)	SE(MJ/m^3)	C.I.
1	60	100	10	0.332	34.49	397	0.278	32.08	448
2	60	125	6	0.119	37.76	397	0.103	40.23	387
3	60	150	2	0.010	85.27	321	0.016	65.44	326
4	60	175	8	0.185	37.31	39.9	0.180	35.41	417
5	60	200	4	0.045	40.18	327	0.048	48.14	356
6	70	125	8	0.223	35.30	397	0.196	37.12	417
7	70	150	4	0.054	45.02	358	0.053	50.46	356
8	70	175	10	0.378	25.74	426	0.304	33.62	448
9	70	200	6	0.111	38.58	387	0.113	42.16	387
10	70	100	2	0.013	83.76	325	0.017	68.59	326
11	80	150	6	0.136	40.23	396	0.122	44.19	387
12	80	175	2	0.011	76.28	325	0.018	71.89	326
13	80	200	8	0.231	36.21	406	0.213	38.90	417
14	80	100	4	0.061	49.80	364	0.057	52.89	356
15	80	125	10	0.353	3 7.02	619	0.329	35.24	448
16	90	175	4	0.073	46.22	367	0.062	55.43	356
17	90	200	10	0.296	48.79	427	0.354	36.94	448
18	90	100	6	0.152	39.57	384	0.131	46.32	387
19	90	125	2	0.018	74.31	339	0.019	75.35	326
20	90	150	8	0.203	49.06	408	0.229	40.78	417
21	100	200	2	0.012	82.38	324	0.021	78.98	326
22	100	100	8	0.326	37.27	408	0.245	42.74	417
23	100	125	4	0.076	51.69	365	0.066	58.10	356
24	100	150	10	0.376	46.10	406	0.380	38.72	448
25	100	175	6	0.147	47.49	399	0.141	48.55	387

Appendix 2D

Single Disc Experiment in Gypsum

Means Derived for Plotting Graphs

Variable	Units	Penetration (p) mm				
		2	4	6	8	10
F'T	kN	8.96	19.26	34.45	44.10	59.78
$\overline{FT}$	kN	8.32	17.39	29.47	41.94	56.73
F'R	kN	1.09	3.13	5.73	9.52	13.45
$\overline{FR}$	kN	1.02	2.87	5.41	8.99	13.19
Q	m^3/km	0.013	0.062	0.133	0.234	0.342
SE	MJ/m^3	78.13	46.59	40.730	39.03	38.42
C.I.	——	326.9	356.2	392.4	403.6	455.0

Variable	Units	Edge Angle (ϕ) degrees				
		60	70	80	90	100
F'T	kN	23.26	27.13	30.79	39.07	43.30
$\overline{FT}$	kN	21.69	24.62	29.13	37.46	40.96
F'R	kN	5.35	5.38	6.39	7.38	8.43
$\overline{FR}$	kN	5.04	5.05	6.09	7.07	8.23
Q	m^3/km	0.138	0.156	0.158	0.143	0.187
SE	MJ/m^3	44.75	45.67	47.91	51.60	52.97
C.I.	——	368.1	378.6	421.7	385.0	380.5

Variable	Units	Disc Diameter (D) mm				
		100	125	150	175	200
F'T	kN	27.59	28.56	37.65	33.50	36.25
$\overline{FT}$	kN	25.78	26.68	35.32	31.06	35.00
F'R	kN	7.13	6.35	7.36	5.82	6.24
$\overline{FR}$	kN	6.71	6.03	7.16	5.53	6.04
Q	m^3/km	0.177	0.158	0.156	0.159	0.134
SE	MJ/m^3	48.97	47.21	50.87	46.60	49.22
C.I.	——	375.5	423.5	377.7	383.0	374.2

APPENDIX 3A

Results of Single Disc Experiment in Dunhouse Sandstone

Test No	ø (°)	D (mm)	p (mm)	Thrust Forces			
				Measured Values		Predicted Values	
				F'T(kN)	FT(kN)	F'T(kN)	FT(kN)
1	60	100	10	33.209	25.067	36.093	23.013
2	60	125	6	24.824	14.086	21.906	14.165
3	60	150	2	6.456	4.710	5.837	3.784
4	60	175	8	36.780	23.006	33.554	22.290
5	60	200	4	16.509	12.623	16.074	10.760
6	70	125	8	34.443	25.255	35.892	25.712
7	70	150	4	17.208	12.740	17.291	12.518
8	70	175	10	51.295	40.522	50.905	37.447
9	70	200	6	26.631	18.476	30.621	22.735
10	70	100	2	6.461	4.455	6.025	4.323
11	80	150	6	35.478	24.975	32.081	24.897
12	80	175	2	8.321	6.108	8.523	6.622
13	80	200	8	51.004	37.123	48.866	38.847
14	80	100	4	17.582	12.865	17.902	13.461
15	80	125	10	50.856	36.113	53.034	40.661
16	90	175	4	10.298	9.127	24.116	19.833
17	90	200	10	71.084	62.895	70.808	59.093
18	90	100	6	29.099	23.412	32.573	25.754
19	90	125	2	10.190	8.099	8.708	6.917
20	90	150	8	46.476	34.227	50.206	40.923
21	00	200	2	14.210	12.529	11.453	9.784
22	00	100	8	47.047	38.372	50.216	41.203
23	00	125	4	27.653	25.472	24.272	20.164
24	00	150	10	71.228	55.745	71.667	60.593
25	00	175	6	45.175	37.648	43.225	36.935

APPENDIX 3B

Results of Single Disc Experiment in Dunhouse Sandstone

Test No.	Levels of			Rolling Forces			
				Measured Values		Predicted Values	
	ø (o)	D (mm)	p (mm)	F'R(kN)	$\overline{FR}$ (kN)	F'R (kN)	$\overline{FR}$ (kN)
1	60	100	10	12.042	8.683	12.107	9.103
2	60	125	6	6.775	4.283	6.396	4.755
3	60	150	2	0.892	0.648	0.685	0.407
4	60	175	8	8.511	6.170	9.252	6.929
5	60	200	4	2.773	2.052	3.541	2.581
6	70	125	8	9.049	6.448	10.218	8.108
7	70	150	4	3.334	2.603	3.911	3.021
8	70	175	10	13.423	10.835	13.371	10.652
9	70	200	6	5.545	3.944	7.064	5.564
10	70	100	2	1.074	0.711	0.757	0.477
11	80	150	6	7.217	5.598	7.732	6.373
12	80	175	2	1.021	0.740	0.829	0.546
13	80	200	8	10.327	8.458	11.183	9.287
14	80	100	4	3.884	2.923	4.280	3.460
15	80	125	10	13.594	10.790	14.635	12.201
16	90	175	4	3.834	3.317	4.650	3.899
17	90	200	10	14.287	12.814	15.899	13.749
18	90	100	6	7.819	5.774	8.400	7.182
19	90	125	2	1.340	1.062	0.900	0.615
20	90	150	8	11.595	9.002	12.150	10.466
21	100	200	2	1.182	0.943	0.972	0.685
22	100	100	8	12.786	10.561	13.115	11.645
23	100	125	4	4.768	3.980	5.020	4.338
24	100	150	10	16.298	13.355	17.163	15.298
25	100	175	6	8.016	7.048	9.067	7.991

APPENDIX 3C

Results of Single Disc Experiment in Dunhouse Sandstone

Test No.	Levels of			Yield, Specific Energy and C.I					
				Measured Values			Predicted Values		
	ø (°)	D (mm)	p (mm)	Q m^3/km	S.E MJ/m^3	C.I	Q m^3/km	S.E MJ/m^3	C.I
1	60	100	10	0.295	29.355	365	0.269	34.43	354
2	60	125	6	0.079	54.376	274	0.097	47.24	274
3	60	150	2	0.007	85.533	195	0.011	93.29	194
4	60	175	8	0.175	35.154	318	0.172	39.53	314
5	60	200	4	0.026	77.568	241	0.043	60.73	234
6	70	125	8	0.163	39.578	317	0.172	44.10	314
7	70	150	4	0.030	86.956	240	0.043	67.75	234
8	70	175	10	0.295	36.652	354	0.267	38.41	254
9	70	200	6	0.081	48.400	294	0.097	52.70	274
10	70	100	2	0.007	93.371	230	0.011	104.07	194
11	80	150	6	0.082	67.750	251	0.097	58.80	274
12	80	175	2	0.007	95.504	164	0.011	116.11	194
13	80	200	8	0.181	47.157	347	0.172	49.20	314
14	80	100	4	0.045	64.178	274	0.043	75.58	234
15	80	125	10	0.225	47.924	347	0.269	42.85	354
16	90	175	4	0.028	114.881	225	0.043	84.32	234
17	90	200	10	0.285	44.895	367	0.269	47.80	354
18	90	100	6	0.126	46.137	279	0.097	65.60	274
19	90	125	2	0.009	122.281	222	0.011	129.54	194
20	90	150	8	0.168	57.796	282	0.172	54.89	314
21	100	200	2	0.006	144.000	157	0.011	144.51	194
22	100	100	8	0.199	53.171	321	0.172	61.24	314
23	100	125	4	0.037	105.146	171	0.043	94.07	234
24	100	150	10	0.242	55.070	323	0.269	53.33	354
25	100	175	6	0.092	76.569	293	0.097	73.18	274

APPENDIX 3D

Single Disc Experiment in Dunhouse Sandstone. Means derived for Plotting Graphs.

Variable Units	Penetration (p) mm				
	2	4	6	8	10
F'T kN	9.13	17.85	32.24	43.15	55.53
$\overline{FT}$ kN	7.18	14.57	23.72	31.60	44.07
F'R kN	1.10	3.72	7.07	10.45	13.93
$\overline{FR}$ kN	0.82	2.98	5.33	8.13	11.30
Q m^3/km	0.020	0.033	0.092	0.177	0.268
S.E MJ/m^3	108.13	87.60	56.94	46.57	42.78
C.I	194	230	278	317	351

Variable Units	Edge Angle (ϕ) Degrees				
	60	70	80	90	100
F'T kN	23.56	27.21	32.65	33.43	41.06
$\overline{FT}$ kN	15.89	20.29	23.44	27.55	33.95
F'R kN	6.20	6.49	7.21	7.78	8.61
$\overline{FR}$ kN	4.37	4.91	5.70	6.39	7.18
Q m^3/km	0.116	0.116	0.108	0.123	0.116
S.E MJ/m^3	56.40	60.99	64.50	77.20	86.79
C.I	294	266	258	271	281

Variable Units	Disc Diameter (D) mm				
	100	125	150	175	200
F'T kN	26.68	29.59	35.37	30.37	35.89
$\overline{FT}$ kN	20.83	21.81	26.48	23.28	28.73
F'R kN	7.52	7.11	7.87	6.96	6.82
$\overline{FR}$ kN	5.73	5.31	6.24	5.62	5.64
Q m^3/km	0.134	0.103	0.106	0.133	0.116
S.E MJ/m^3	57.24	73.86	70.62	71.75	72.40
C.I.	279	287	277	275	253

Appendix 4A

Results of Single Disc Experiment in Mansfield Sandstone

Test No.	Levels of			Thrust Forces			
				Measured Values		Predicted Values	
	ø (o)	D (mm)	p (mm)	F'T(kN)	$\overline{FT}$(kN)	F'T(kN)	$\overline{FT}$(kN)
1	60	100	7.5	29.05	21.06	28.38	19.68
2	60	125	4.5	18.12	14.47	17.89	12.17
3	60	150	1.5	5.92	4.32	5.43	3.29
4	60	175	6.0	27.12	20.05	28.04	19.22
5	60	200	3.0	19.93	10.42	14.10	9.32
6	70	125	6.0	29.65	22.65	30.87	24.37
7	70	150	3.0	15.11	10.54	15.68	11.93
8	70	175	7.5	43.28	34.05	45.02	35.66
9	70	200	4.5	23.95	20.42	27.94	32.72
10	70	100	1.5	6.14	4.48	5.91	4.13
11	80	150	4.5	26.57	22.30	29.66	25.05
12	80	175	1.5	7.71	5.85	8.96	6.74
13	80	200	6.0	41.89	34.83	46.05	39.23
14	80	100	3.0	14.60	11.99	16.30	13.49
15	80	125	7.5	47.81	37.12	47.33	40.75
16	90	175	3.0	22.53	18.70	23.93	20.78
17	90	200	7.5	65.58	62.68	68.41	61.84
18	90	100	4.5	28.58	24.77	29.89	26.72
19	90	125	1.5	9.91	7.69	9.13	7.26
20	90	150	6.0	45.48	38.85	47.37	42.66
21	100	200	1.5	13.51	12.48	12.90	10.61
22	100	100	6.0	51.76	44.03	46.68	43.79
23	100	125	3.0	24.83	22.08	23.85	21.56
24	100	150	7.5	71.37	65.19	68.82	64.74
25	100	175	4.5	43.20	39.90	42.91	39.61

Appendix 4B

Results of Single Disc Experiment in Mansfield Sandstone

Test No.	Levels of			Rolling Forces			
				Measured Values		Predicted Values	
	ϕ (o)	D (mm)	p (mm)	F'R(kN)	$\overline{FR}$ (kN)	F'R(kN)	$\overline{FR}$ (kN)
1	60	100	7.5	6.38	5.04	6.59	5.21
2	60	125	4.5	3.78	3.17	3.62	2.86
3	60	150	1.5	0.76	0.64	0.65	0.51
4	60	175	6.0	5.55	4.39	5.11	4.03
5	60	200	3.0	1.91	1.56	2.14	1.69
6	70	125	6.0	6.41	5.28	6.03	5.01
7	70	150	3.0	2.28	1.72	2.52	2.09
8	70	175	7.5	7.33	6.31	7.79	6.46
9	70	200	4.5	3.93	3.40	4.28	3.55
10	70	100	1.5	0.94	0.75	0.77	0.64
11	80	150	4.5	4.49	4.07	4.94	4.24
12	80	175	1.5	0.80	0.63	0.89	0.76
13	80	200	6.0	6.79	5.88	6.96	5.98
14	80	100	3.0	2.69	2.20	2.91	2.50
15	80	125	7.5	8.95	7.27	8.98	7.71
16	90	175	3.0	2.97	2.61	3.30	2.91
17	90	200	7.5	9.66	8.75	10.18	8.97
18	90	100	4.5	5.60	5.22	5.59	4.93
19	90	125	1.5	1.14	0.90	1.01	0.89
20	90	150	6.0	8.09	7.08	7.89	6.95
21	100	200	1.5	1.15	1.03	1.13	1.01
22	100	100	6.0	10.15	9.23	8.82	7.92
23	100	125	3.0	3.67	3.34	3.69	3.31
24	100	150	7.5	10.94	9.85	11.38	10.22
25	100	175	4.5	6.10	5.74	6.25	5.62

Appendix 4C

Results of Single Disc Experiment in Mansfield Sandstone

Test No.	Levels of			Yield, Specific Energy and C.I					
				Measured Values			Predicted Values		
	ϕ (o)	D (mm)	p (mm)	Q m^3/km	S.E MJ/m^3	C.I	Q m^3/km	S.E MJ/m^3	C.I
1	60	100	7.5	0.130	38.70	338	0.167	41.59	366
2	60	125	4.5	0.047	68.09	293	0.06	58.72	295
3	60	150	1.5	0.005	122.32	206	0.003	123.27	224
4	60	175	6.0	0.089	49.68	327	0.106	48.36	331
5	60	200	3.0	0.021	74.68	274	0.024	77.20	259
6	70	125	6.0	0.104	51.05	346	0.114	52.80	331
7	70	150	3.0	0.022	83.76	269	0.025	84.27	259
8	70	175	7.5	0.149	42.59	362	0.180	45.40	366
9	70	200	4.5	0.049	69.32	297	0.062	64.09	295
10	70	100	1.5	0.006	126.64	217	0.003	134.54	224
11	80	150	4.5	0.049	83.61	292	0.066	69.96	295
12	80	175	1.5	0.005	122.93	208	0.004	146.85	224
13	80	200	6.0	0.090	65.25	346	0.121	57.61	331
14	80	100	3.0	0.026	86.81	267	0.027	91.98	259
15	80	125	7.5	0.179	40.72	375	0.192	40.55	366
16	90	175	3.0	0.023	122.01	253	0.029	100.39	259
17	90	200	7.5	0.183	48.49	362	0.205	54.09	366
18	90	100	4.5	0.064	81.93	316	0.071	76.36	295
19	90	125	1.5	0.006	142.29	218	0.004	160.29	224
20	90	150	6.0	0.105	68.99	340	0.129	62.88	331
21	100	200	1.5	0.005	182.61	228	0.004	174.96	224
22	100	100	6.0	0.148	62.85	314	0.137	68.63	331
23	100	125	3.0	0.030	113.17	272	0.031	109.58	259
24	100	150	7.5	0.207	48.44	364	0.217	59.04	366
25	100	200	4.5	0.059	99.14	293	0.075	83.34	295

Appendix 4D

Single Disc Experiment in Mansfield Sandstone

Means Derived for Plotting Graphs

Variable	Units	Penetration (p) mm				
		1.5	3	4.5	6	7.5
F'T	kN	8.64	19.40	28.09	39.16	51.43
$\overline{FT}$	kN	6.97	14.75	24.37	32.08	44.02
F'R	kN	0.96	2.70	4.78	7.40	8.65
$\overline{FR}$	kN	0.79	2.29	4.32	6.37	7.44
Q	m^3/km	0.005	0.024	0.054	0.107	0.170
SE	MJ/m^3	138.95	94.09	80.41	59.56	43.77
C.I		215.5	266.9	298.4	334.4	360.2

Variable	Units	Edge Angle (ϕ) degrees				
		60	70	80	90	100
F'T	kN	20.03	23.63	27.72	34.39	40.94
$\overline{FT}$	kN	14.06	18.43	22.42	30.54	35.74
F'R	kN	3.68	4.18	4.74	5.49	6.40
$\overline{FR}$	kN	2.96	3.49	4.01	4.91	5.84
Q	m^3/km	0.059	0.066	0.070	0.076	0.09
SE	MJ/m^3	70.70	74.28	79.87	90.75	101.25
C.I		287.9	298.1	297.4	297.9	294.1

Variable	Units	Disc Diameter (D) mm				
		100	125	150	175	200
F'T	kN	26.04	26.06	32.87	28.77	32.97
$\overline{FT}$	kN	21.27	20.80	28.24	23.71	28.17
F'R	kN	5.15	4.79	5.31	4.55	4.69
$\overline{FR}$	kN	4.49	3.99	4.67	3.94	4.12
Q	m^3/km	0.075	0.073	0.078	0.065	0.07
SE	MJ/m^3	78.99	83.07	81.43	85.27	88.07
C.I		290.6	300.6	294.3	288.6	301.3

Appendix 5A

Results of Single Disc Experiment in Anhydrite.

Test No.	Levels of p (mm)	D (mm)	∅ (o)	Thrust Forces: Measured Values F'T(kN)	Measured Values $\overline{FT}$(kN)	Predicted Values F'T(kN)	Predicted Values $\overline{FT}$ (kN)
1	1	100	100	9.77	7.92	9.94	7.65
2	1	125	80	8.39	6.64	7.46	5.81
3	1	150	60	5.86	4.82	4.84	3.73
4	1	175	90	10.80	9.53	9.39	7.69
5	1	200	70	7.70	6.34	6.63	5.43
6	2	125	90	19.54	15.78	19.51	16.00
7	2	150	70	6.19	4.70	13.81	11.35
8	2	175	100	28.94	25.10	23.90	20.60
9	2	200	80	7.65	8.45	17.92	15.53
10	2	100	60	11.16	8.52	10.05	7.73
11	3	150	80	25.16	19.87	26.20	22.09
12	3	175	60	20.53	16.00	16.96	14.15
13	3	200	90	33.30	28.40	32.85	29.07
14	3	100	70	19.35	15.23	20.12	15.98
15	3	125	100	34.36	26.41	34.88	29.15
16	4	175	70	32.92	27.08	29.71	25.43
17	4	200	100	56.74	48.36	51.39	46.04
18	4	100	80	29.30	23.81	33.42	27.02
19	4	125	60	24.40	19.06	21.67	17.41
20	4	150	90	37.49	31.54	42.03	35.94
21	5	200	60	29.40	25.46	29.75	25.56
22	5	100	90	47.20	39.60	49.95	40.87
23	5	125	70	38.12	32.45	35.37	29.08
24	5	150	100	55.70	48.59	61.28	52.90
25	5	175	80	46.80	40.85	45.99	39.98

Appendix 5B

Results of Single Disc Experiment in Anhydrite

Test No.	Levels of p (mm)	D (mm)	∅ (°)	Rolling Forces: Measured Values F'R(kN)	Measured Values $\overline{FR}$(kN)	Predicted Values F'R(kN)	Predicted Values $\overline{FR}$(kN)
1	1	100	100	1.71	0.88	1.05	0.62
2	1	125	80	1.10	0.85	0.80	0.49
3	1	150	60	0.65	0.50	0.55	0.36
4	1	175	90	1.02	0.83	0.93	0.56
5	1	200	70	0.73	0.58	0.68	0.43
6	2	125	90	2.54	2.16	3.33	2.60
7	2	150	70	2.06	1.68	2.43	1.99
8	2	175	100	3.76	2.93	3.78	2.90
9	2	200	80	3.00	1.86	2.88	2.29
10	2	100	60	2.10	1.67	1.97	1.69
11	3	150	80	4.09	3.14	4.95	4.09
12	3	175	60	3.20	2.38	3.40	3.01
13	3	200	90	4.46	3.49	5.73	4.64
14	3	100	70	4.14	3.48	4.17	3.55
15	3	125	100	5.53	4.26	6.50	5.18
16	4	175	70	5.67	4.49	5.92	5.12
17	4	200	100	8.19	6.97	9.23	7.46
18	4	100	80	6.31	4.98	7.03	5.90
19	4	125	60	5.09	4.00	4.82	4.33
20	4	150	90	6.71	4.46	8.13	6.68
21	5	200	60	5.46	4.56	6.25	5.66
22	5	100	90	11.37	9.32	10.53	8.72
23	5	125	70	8.70	7.37	7.67	6.68
24	5	150	100	10.84	8.75	11.95	9.73
25	5	175	80	8.64	7.10	9.10	7.70

Appendix 5C

Results of Single Disc Experiment in Anhydrite

Test No.	Levels of p (mm)	D (mm)	∅ (o)	Yield, Specific Energy and C.I — Measured Values Q m^3/km	S.E MJ/m^3	C.I	Predicted Values Q m^3/km	S.E MJ/m^3	C.I
1	1	100	100	0.004	221.34	238	0.004	222.60	254
2	1	125	80	0.005	179.0	263	0.004	192.30	254
3	1	150	60	0.003	143.66	233	0.004	166.13	254
4	1	175	90	0.003	230.39	234	0.004	206.90	254
5	1	200	70	0.003	163.81	250	0.004	178.74	254
6	2	125	90	0.013	173.74	278	0.013	153.57	274
7	2	150	70	0.011	143.37	289	0.013	132.67	274
8	2	175	100	0.018	166.15	287	0.013	165.23	274
9	2	200	80	0.014	130.82	284	0.013	142.74	274
10	2	100	60	0.012	141.62	290	0.013	123.31	274
11	3	150	80	0.026	120.30	292	0.028	119.90	293
12	3	175	60	0.025	96.36	290	0.028	103.58	293
13	3	200	90	0.027	127.60	317	0.028	129.00	293
14	3	100	70	0.028	134.90	315	0.028	111.44	293
15	3	125	100	0.031	136.95	290	0.028	138.79	293
16	4	175	70	0.049	91.40	314	0.049	98.49	312
17	4	200	100	0.058	122.06	307	0.049	122.66	312
18	4	100	80	0.048	105.41	292	0.049	105.97	312
19	4	125	60	0.046	88.77	310	0.049	91.54	312
20	4	150	90	0.048	96.94	311	0.049	114.01	312
21	5	200	60	0.051	88.48	345	0.076	83.15	331
22	5	100	90	0.084	110.67	315	0.076	103.56	331
23	5	125	70	0.086	85.26	334	0.076	89.46	331
24	5	150	100	0.082	107.46	326	0.076	111.42	331
25	5	175	80	0.075	95.78	326	0.076	96.25	331

Appendix 5D

Single Disc Experiment in Anhydrite

Means Derived for Plotting Graphs

Variable	Units	Penetration (p) mm				
		1	2	3	4	5
F'T	kN	8.50	14.70	26.54	36.17	43.44
$\overline{FT}$	kN	7.05	12.51	21.18	29.97	37.39
F'R	kN	1.04	2.69	4.29	6.39	9.00
$\overline{FR}$	kN	0.73	1.96	3.35	5.02	7.42
Q	m^3/km	0.004	0.014	0.027	0.050	0.076
SE	MJ/m^3	187.64	151.14	123.22	100.92	97.53
C.I		244	286	299	307	329

Variable	Units	Edge Angle (ϕ) degrees				
		60	70	80	90	100
F'T	kN	18.27	20.86	23.45	29.67	37.10
$\overline{FT}$	kN	14.77	17.16	20.92	24.97	31.28
F'R	kN	3.30	4.26	4.63	5.22	6.01
$\overline{FR}$	kN	2.62	3.42	3.59	4.09	4.76
Q	m^3/km	0.027	0.035	0.034	0.035	0.039
SE	MJ/m^3	111.78	123.75	126.26	147.87	150.79
C.I		294	298	291	291	290

Variable	Units	Disc Diameter (D) mm				
		100	125	150	175	200
F'T	kN	23.36	24.96	26.08	28.00	26.96
$\overline{FT}$	kN	20.02	20.07	21.90	23.71	23.40
F'R	kN	5.13	4.59	4.87	4.46	4.37
$\overline{FR}$	kN	4.07	3.73	3.64	3.55	3.49
Q	m^3/km	0.035	0.036	0.034	0.034	0.031
SE	MJ/m^3	142.79	132.74	122.35	136.01	126.55
C.I		288	295	290	290	301

Appendix 5E

Results of Single Disc Experiment No.2 in Anhydrite

Test No.	Levels of ø (o)	D (mm)	p (mm)	F'T (kN)	$\overline{FT}$ (kN)	F'R (kN)	$\overline{FR}$ (kN)	Q m^3/km	S.E MJ/m^3
1	60	100	5	25.87	21.62	6.78	5.38	0.066	81.19
2	60	125	3	13.76	11.18	2.94	2.39	0.027	89.65
3	60	150	1	3.30	2.93	0.59	0.39	0.0014	234.87
4	60	175	4	23.17	17.64	4.07	3.17	0.036	87.41
5	60	200	2	8.40	4.60	0.98	0.93	0.007	135.49
6	70	125	4	24.16	18.58	5.58	4.33	0.044	97.78
7	70	150	2	10.57	9.39	1.70	1.31	0.009	152.23
8	70	175	5	34.13	28.59	6.70	5.31	0.049	108.79
9	70	200	3	19.67	15.83	3.36	2.69	0.029	92.49
10	70	100	1	3.90	3.66	0.77	0.51	0.002	233.95
11	80	150	3	25.81	23.09	4.78	4.02	0.034	116.90
12	80	175	1	4.63	4.54	0.48	0.38	0.002	205.03
13	80	200	4	29.96	26.05	5.10	4.00	0.040	99.46
14	80	100	2	13.59	10.45	1.66	1.23	0.009	149.15
15	80	125	5	41.74	35.08	9.56	8.01	0.083	96.31
16	90	175	2	15.85	16.36	1.96	1.60	0.011	148.75
17	90	200	5	54.10	50.19	10.11	8.79	0.095	92.49
18	90	100	3	21.58	17.65	4.51	3.68	0.033	111.03
19	90	125	1	4.01	3.93	0.56	0.35	0.002	199.98
20	90	150	4	35.18	29.01	6.19	4.89	0.044	111.67
21	100	200	1	6.83	7.73	0.68	0.46	0.002	192.34
22	100	100	4	38.66	30.91	8.61	6.89	0.058	118.39
23	100	125	2	20.77	17.69	2.55	1.95	0.009	227.53
24	100	150	5	47.74	42.49	9.16	7.35	0.071	103.80
25	100	175	3	34.28	34.61	4.93	4.35	0.033	130.05

Appendix 6

Results of Single Disc Experiment in W. Limestone and Greywacke

Rock	p (mm)	F'T kN	$\overline{FT}$ kN	F'R kN	$\overline{FR}$ kN	Q m^3/km	$S.E_3$ MJ/m^3	C.I
W.Limestone	1	4.52	3.63	0.47	0.48	0.0017	292.69	285
	3	21.29	18.19	3.64	3.02	0.025	125.07	358
	4	30.10	26.00	5.80	4.70	0.047	100.00	-
	5	41.39	33.68	8.03	6.85	0.088	79.47	404
	7	59.31	50.48	13.28	12.37	0.157	79.50	444
Greywacke	1	5.72	4.99	0.88	0.64	0.0017	366.59	261
	3	23.55	16.95	4.15	3.00	0.023	136.19	360
	4	31.38	20.58	6.17	4.31	0.043	98.81	392
	5	34.81	24.77	7.63	5.62	0.058	97.19	392

Appendix 7A

Results of Relieved Cutting Experiment in Gypsum

Test No.	Level of				Thrust Forces			
					Measured Values		Predicted Values	
	ϕ (°)	D (mm)	p (mm)	S (mm)	F'T(kN)	$\overline{FT}$ (kN)	F'T(kN)	$\overline{FT}$ (kN)
1	60	100	10	12	7.84	6.81	9.08	7.82
2	60	125	6	48	21.97	18.96	21.09	18.22
3	60	150	2	24	7.31	6.88	7.91	7.08
4	60	175	8	60	33.23	29.48	34.15	30.79
5	60	200	4	36	16.24	14.82	14.83	12.75
6	70	125	8	24	21.96	19.06	17.03	14.70
7	70	150	4	60	16.34	15.07	20.87	18.45
8	70	175	10	36	41.93	34.96	29.81	24.48
9	70	200	6	12	11.85	10.31	10.81	9.10
10	70	100	2	48	6.44	5.68	10.70	9.64
11	80	150	6	36	28.99	24.27	26.23	23.04
12	80	175	2	12	7.75	6.91	6.72	5.86
13	80	200	8	48	45.94	41.58	38.77	35.67
14	80	100	4	24	14.43	12.17	12.92	11.16
15	80	125	10	60	51.41	45.19	42.83	38.30
16	90	175	4	48	23.00	23.09	29.34	25.44
17	90	200	10	24	41.61	33.97	34.31	31.27
18	90	100	6	60	30.74	27.75	29.54	26.30
19	90	125	2	36	9.68	9.51	14.83	14.41
20	90	150	8	12	14.94	13.23	15.84	13.65
21	100	200	2	60	12.58	12.52	19.66	18.32
22	100	125	8	36	36.39	30.68	34.82	30.69
23	100	100	4	12	13.85	11.87	13.27	12.21
24	100	150	10	48	61.67	48.82	57.52	50.81
25	100	175	6	24	32.13	28.02	30.48	27.71

Appendix 7B

Results of Relieved Cutting Experiment in Gypsum

Test No.	Levels of ∅ (º)	D (mm)	p (mm)	S (mm)	Rolling Forces: Measured Values F'R(kN)	$\overline{FR}$(kN)	Predicted Values F'R(kN)	$\overline{FR}$ (kN)
1	60	100	10	12	2.99	3.13	3.67	3.56
2	60	125	6	48	4.85	4.49	4.72	4.29
3	60	150	2	24	1.14	0.92	0.96	0.85
4	60	175	8	60	6.68	6.23	6.99	6.38
5	60	200	4	36	2.22	2.08	2.06	1.82
6	70	125	8	24	5.75	5.62	4.96	4.63
7	70	150	4	60	2.68	2.56	3.12	2.82
8	70	175	10	36	8.61	8.35	6.90	6.46
9	70	200	6	12	2.17	1.70	2.09	1.96
10	70	100	2	48	1.10	1.05	1.65	1.34
11	80	150	6	36	5.33	4.86	5.05	4.60
12	80	175	2	12	0.90	0.83	0.78	0.71
13	80	200	8	48	8.36	7.74	7.80	7.26
14	80	100	4	24	3.28	2.18	2.87	2.59
15	80	125	10	60	12.58	6.49	11.61	11.00
16	90	175	4	48	3.45	3.34	4.22	3.67
17	90	200	10	24	9.56	9.61	7.61	7.61
18	90	100	6	60	7.21	6.51	7.05	6.26
19	90	125	2	36	1.35	1.27	1.77	1.66
20	90	150	8	42	4.22	3.98	3.88	3.71
21	100	200	2	60	1.24	1.19	1.58	1.36
22	100	125	8	36	9.88	9.35	9.66	9.02
23	100	100	4	12	2.63	2.46	2.49	2.26
24	100	150	10	48	13.24	12.94	13.44	13.42
25	100	175	6	24	6.35	5.40	5.03	4.93

Appendix 7C

Results of Relieved Cutting Experiment in Gypsum

Test No.	Levels of				Yield, Specific Energy and C.I.				
					Measured Values			Predicted Values	
	∅ (o)	D (mm)	p (mm)	S (mm)	Q (m^3/kN)	S.E (MJ/m^3)	C.I	Q (m^3/km)	S.E (MJ/m^3)
1	60	100	10	12	0.071	44.21	383	0.127	24.65
2	60	125	6	48	0.119	37.92	379	0.138	32.54
3	60	150	2	24	0.011	87.72	315	0.010	92.00
4	60	175	8	60	0.194	32.66	413	0.215	28.98
5	60	200	4	36	0.043	48.68	328	0.052	40.00
6	70	125	8	24	0.165	34.19	409	0.176	31.93
7	70	150	4	60	0.050	50.47	356	0.048	53.33
8	70	175	10	36	0.282	30.04	426	0.335	24.93
9	70	200	6	12	0.065	26.13	376	0.065	26.15
10	70	100	2	48	0.011	89.74	313	0.026	40.40
11	80	150	6	36	0.139	34.85	393	0.152	31.97
12	80	175	2	12	0.017	48.43	329	0.012	69.17
13	80	200	8	48	0.272	28.61	441	0.259	29.88
14	80	100	4	24	0.070	31.19	383	0.068	32.06
15	80	125	10	60	0.333	19.53	419	0.395	16.43
16	90	175	4	48	0.065	52.09	370	0.074	45.14
17	90	200	10	24	0.217	44.73	400	0.199	48.29
18	90	100	6	60	0.137	47.84	369	0.169	38.52
19	90	125	2	36	0.013	95.67	273	0.016	79.38
20	90	150	8	12	0.096	41.45	393	0.094	42.34
21	100	200	2	60	0.015	81.52	328	0.065	18.31
22	100	125	8	36	0.290	32.21	337	0.327	28.59
23	100	100	4	12	0.047	48.21	404	0.060	41.00
24	100	150	10	48	0.367	36.00	432	0.388	33.35
25	100	175	6	24	0.155	35.44	386	0.138	39.13

Appendix 8A

Results of Relieved Cutting Experiment in Dunhouse Sandstone

Test No.	Levels of				Thrust Forces			
					Measured Values		Predicted Values	
	ϕ (°)	D (mm)	p (mm)	S (mm)	F'T (kN)	$\overline{FT}$ (kN)	F'T (kN)	$\overline{FT}$ (kN)
1	60	100	10	12	8.13	5.61	8.73	6.29
2	60	125	6	48	20.45	14.39	21.87	12.65
3	60	150	2	24	6.46	4.71	6.60	4.98
4	60	175	8	60	29.09	21.41	31.52	20.06
5	60	200	4	36	16.51	12.62	15.24	11.94
6	70	125	8	24	19.97	13.68	17.94	12.92
7	70	150	4	60	17.21	12.74	18.79	14.51
8	70	175	10	36	34.14	23.56	29.96	23.40
9	70	200	6	12	12.80	9.44	10.44	7.02
10	70	100	2	48	6.46	4.46	7.87	5.73
11	80	150	6	36	25.59	17.14	27.46	19.48
12	80	175	2	12	8.62	5.84	6.44	4.76
13	80	200	8	48	39.86	26.83	39.48	28.96
14	80	100	4	24	16.14	12.05	13.61	10.03
15	80	125	10	60	40.96	29.63	39.36	28.17
16	90	175	4	48	10.30	9.13	10.52	9.66
17	90	200	10	24	30.97	24.18	31.77	27.42
18	90	100	6	60	29.10	23.41	27.95	23.13
19	90	125	2	36	10.19	8.10	11.66	9.72
20	90	150	8	12	14.24	10.69	14.64	10.36
21	100	200	2	60	14.21	12.53	17.99	16.86
22	100	100	8	32	33.27	22.37	31.43	25.88
23	100	125	4	12	12.95	10.89	14.41	13.02
24	100	150	10	48	50.06	38.39	49.15	38.41
25	100	175	6	24	25.47	18.89	28.10	23.27

Appendix 8B

Results of Relieved Cutting Experiment in Dunhouse Sandstone

Test No	Levels of				Rolling Forces			
					Measured Values		Predicted Values	
	ø (o)	D (mm)	p (mm)	S (mm)	F'R (kN)	$\overline{FR}$ (kN)	F'R (kN)	$\overline{FR}$ (kN)
1	60	100	10	12	3.52	2.52	4.03	2.81
2	60	125	6	48	5.51	3.76	6.39	4.00
3	60	150	2	24	0.89	0.65	0.94	0.68
4	60	175	8	60	7.59	5.90	7.85	5.63
5	60	200	4	36	2.77	2.05	2.56	1.98
6	70	125	8	24	7.14	5.68	5.56	3.87
7	70	150	4	60	3.33	2.60	3.70	2.87
8	70	175	10	36	10.15	8.14	9.09	7.19
9	70	200	6	12	2.83	2.08	2.66	1.84
10	70	100	2	48	1.07	0.71	1.29	0.85
11	80	150	6	36	6.67	4.64	6.15	4.70
12	80	175	2	12	0.99	0.72	0.87	0.62
13	80	200	8	48	9.81	7.67	8.79	7.11
14	80	100	4	24	4.03	2.87	3.31	2.46
15	80	125	10	60	11.86	9.55	11.58	9.06
16	90	175	4	48	3.83	3.32	4.04	3.48
17	90	200	10	24	7.26	6.20	7.70	6.74
18	90	100	6	60	7.82	5.77	7.87	5.77
19	90	125	2	36	1.34	1.06	1.54	1.21
20	90	150	8	12	5.14	3.67	4.57	3.44
21	100	200	2	60	1.18	0.94	1.46	1.16
22	100	100	8	36	10.17	7.86	9.64	7.83
23	100	125	4	12	2.75	2.05	2.93	2.39
24	100	150	10	48	14.02	12.40	12.66	10.20
25	100	175	6	24	5.06	3.95	5.72	4.93

Appendix 8C

Results of Relieved Cutting Experiment in Dunhouse Sandstone

Test No.	Levels of				Yield, Specific Energy and C.I				
					Measured Values			Predicted Values	
	ϕ (o)	D (mm)	p (mm)	S (mm)	Q m^3/km	S.E MJ/m^3	C.I	Q m^3/km	S.E MJ/m^3
1	60	100	10	12	0.100	27.83	374	0.164	15.27
2	60	125	6	48	0.085	44.32	299	0.119	31.60
3	60	150	2	24	0.007	85.53	192	0.007	92.86
4	60	175	8	60	0.292	22.75	423	0.270	21.85
5	60	200	4	36	0.026	75.57	241	0.037	55.41
6	70	125	8	24	0.196	27.66	361	0.193	29.43
7	70	150	4	60	0.030	86.96	240	0.023	113.04
8	70	175	10	36	0.321	25.60	296	0.390	20.87
9	70	200	6	12	0.062	32.21	310	0.071	29.30
10	70	100	2	48	0.007	93.37	230	0.026	27.31
11	80	150	6	36	0.188	24.85	359	0.129	35.97
12	80	175	2	12	0.013	55.62	254	0.012	60.00
13	80	200	8	48	0.322	23.84	440	0.285	26.91
14	80	100	4	24	0.071	41.58	333	0.071	40.42
15	80	125	10	60	0.492	19.92	448	0.354	26.98
16	90	175	4	48	0.028	114.88	225	0.029	114.48
17	90	200	10	24	0.201	35.19	363	0.289	21.45
18	90	100	6	60	0.126	46.14	297	0.164	35.18
19	90	125	2	36	0.009	122.29	222	0.008	132.50
20	90	150	8	12	0.080	49.21	311	0.119	31.91
21	100	200	2	60	0.006	144.00	157	0.072	13.06
22	100	100	8	36	0.270	29.46	372	0.292	26.92
23	100	125	4	12	0.037	54.72	242	0.044	46.59
24	100	150	10	48	0.437	28.78	416	0.364	34.07
25	100	175	6	24	0.113	35.52	325	0.128	30.86

Appencix 9A

Results of Relieved Cutting Experiment in Mansfield Sandstone

Test No.	Levels of				Thrust Forces			
					Measured Values		Predicted Values	
	ϕ (o)	D (mm)	p (mm)	S (mm)	F'T (kN)	$\overline{FT}$ (kN)	F'T (kN)	$\overline{FT}$ (kN)
1	60	100	7.5	9	9.51	6.56	9.51	5.79
2	60	125	4.5	36	18.12	14.47	14.71	11.26
3	60	150	1.5	18	5.92	4.32	5.30	3.76
4	60	175	6	45	27.12	20.05	21.61	15.26
5	60	200	3	27	12.00	9.00	16.72	8.41
6	70	125	6	18	17.12	11.26	16.40	11.45
7	70	150	3	45	15.11	10.54	14.23	9.65
8	70	175	7.5	27	25.86	18.74	26.14	19.00
9	70	200	4.5	9	11.83	9.25	10.54	8.07
10	70	100	1.5	36	6.14	4.48	6.14	4.44
11	80	150	4.5	27	22.80	16.69	19.74	15.65
12	80	175	1.5	9	6.00	4.53	5.73	4.11
13	80	200	6	36	33.47	24.39	31.12	24.45
14	80	100	3	18	10.74	7.85	10.85	8.42
15	80	125	7.5	45	36.16	28.97	35.52	26.06
16	90	175	3	36	22.53	18.70	20.19	16.29
17	90	200	7.5	18	31.02	24.00	32.13	27.83
18	90	100	4.5	45	28.58	24.77	24.61	20.58
19	90	125	1.5	27	9.90	7.69	9.54	5.98
20	90	150	6	9	16.43	12.20	16.45	12.63
21	100	200	1.5	45	13.51	12.48	13.83	12.72
22	100	100	6	27	27.73	19.26	34.47	27.43
23	100	125	3	9	10.88	8.78	13.73	11.17
24	100	150	7.5	36	44.93	35.28	48.82	41.72
25	100	175	4.5	18	24.54	20.00	27.39	23.46

APPPENDIX 9B

Results of Relieved Cutting Experiment in Mansfield Sandstone

Test No.	Levels of				Rolling Forces			
					Measured Values		Predicted Values	
	ø (o)	D (mm)	p (mm)	S (mm)	F'R kN	$\overline{FR}$	F'R kN	$\overline{FR}$
1	60	100	7.5	9	3.31	2.56	2.90	2.06
2	60	125	4.5	36	3.78	3.17	3.46	2.88
3	60	150	1.5	18	0.76	0.64	0.74	0.63
4	60	175	6	45	5.55	4.39	5.02	3.93
5	60	200	3	27	1.68	1.46	1.78	1.45
6	70	125	6	18	4.26	3.37	4.52	3.52
7	70	150	7	45	2.28	1.72	2.28	1.72
8	70	175	7.5	27	5.92	4.61	5.50	4.53
9	70	200	4.5	9	2.05	1.66	2.34	1.87
10	70	100	1.5	36	0.94	0.75	0.98	0.80
11	80	150	4.5	27	4.17	3.47	7.88	3.45
12	80	175	1.5	9	0.59	0.66	0.69	0.53
13	80	200	6	36	5.82	5.10	5.87	4.98
14	80	100	3	18	2.29	1.91	2.32	1.86
15	80	125	7.5	45	9.35	7.82	7.73	6.16
16	90	175	3	36	2.97	2.61	2.89	2.21
17	90	200	7.5	18	6.07	5.25	6.23	5.28
18	90	100	4.5	45	5.60	5.22	5.31	4.95
19	90	125	1.5	27	1.14	0.90	1.16	0.93
20	90	150	6	9	3.79	2.79	4.17	3.31
21	100	200	1.5	45	1.15	1.03	1.21	1.11
22	100	100	6	27	7.11	5.65	8.15	7.17
23	100	125	3	9	2.86	2.32	2.59	2.23
24	100	150	7.5	36	10.58	9.18	8.95	7.81
25	100	175	4.5	18	4.29	3.33	4.73	4.28

APPENDIX 9C

Results of Relieved Cutting Experiment in Mansfield Sandstone

Test No.	Levels of				Yield, Specific Energy and C.I.				
					Measured Values			Predicted Values	
	ø (°)	D (mm)	p (mm)	S (mm)	Q m^3/km	S.E MJ/m^3	C.I	Q m^3/km	S.E MJ/m^3
1	60	100	7.5	9	0.050	51.52	376	0.045	56.89
2	60	125	4.5	36	0.047	68.08	293	0.052	60.96
3	60	150	1.5	18	0.005	122.32	206	0.005	128.00
4	60	175	6	45	0.089	49.66	327	0.099	44.34
5	60	200	3	27	0.017	84.78	374	0.023	63.48
6	70	125	6	18	0.084	39.93	352	0.076	44.34
7	70	150	3	45	0.022	83.76	269	0.020	86.00
8	70	175	7.5	27	0.143	32.27	393	0.123	37.48
9	70	200	4.5	9	0.034	50.82	329	0.026	63.85
10	70	100	1.5	36	0.006	124.64	224	0.011	68.18
11	80	150	4.5	27	0.065	53.49	363	0.052	66.73
12	80	175	1.5	9	0.007	91.22	279	0.005	132.00
13	80	200	6	36	0.118	43.59	386	0.095	53.68
14	80	100	3	18	0.031	63.34	333	0.027	70.74
15	80	125	7.5	45	0.190	41.45	409	0.189	41.38
16	90	175	3	36	0.023	111.99	253	0.023	113.48
17	90	200	7.5	18	0.100	55.21	359	0.113	46.46
18	90	100	4.5	45	0.064	81.93	316	0.070	74.57
19	90	125	1.5	27	0.006	142.30	218	0.006	150.00
20	90	150	6	9	0.046	60.78	317	0.044	63.61
21	100	200	1.5	45	0.005	182.61	228	0.024	42.92
22	100	100	6	27	0.143	42.82	381	0.138	40.94
23	100	25	3	9	0.025	96.05	280	0.022	105.45
24	100	150	7.5	36	0.203	46.16	406	0.200	45.90
25	100	175	4.5	18	0.065	51.41	333	0.052	64.04

APPENDIX 10A

Results of Relieved Cutting Experiment in Anhydrite

Test No	Levels of				Thrust Forces			
					Measured Values		Predicted Values	
	ϕ (o)	D (mm)	p (mm)	S (mm)	F'T (kN)	$\overline{FT}$ (kN)	F'T (kN)	$\overline{FT}$ (kN)
1	60	100	5	6	10.33	8.55	9.86	7.72
2	60	125	3	24	14.95	11.87	12.47	9.86
3	60	150	1	12	3.30	2.93	3.25	2.83
4	60	175	4	30	22.74	19.59	20.67	15.29
5	60	200	2	18	8.83	4.95	7.82	4.18
6	70	125	4	12	15.01	11.15	15.58	11.45
7	70	150	2	30	10.57	9.39	10.80	9.42
8	70	175	5	18	26.51	20.56	23.86	19.13
9	70	200	3	6	9.64	7.72	10.31	7.85
10	70	100	1	24	3.90	3.66	4.21	3.90
11	80	150	3	18	22.03	18.00	21.63	18.74
12	80	175	1	6	4.52	4.46	3.88	3.68
13	80	200	4	24	27.97	22.33	25.12	21.14
14	80	100	2	12	11.19	8.95	11.39	8.48
15	80	125	5	30	34.20	28.01	34.98	28.46
16	90	175	2	24	15.85	16.36	15.63	15.79
17	90	200	5	12	25.01	20.13	31.27	27.55
18	90	100	3	30	21.58	17.65	20.59	16.41
19	90	125	1	18	4.01	3.93	4.20	4.05
20	90	150	4	6	16.95	12.63	15.53	12.04
21	100	200	1	30	6.83	7.73	7.53	8.42
22	100	100	4	18	27.83	21.64	29.46	22.67
23	100	125	2	6	12.67	10.61	13.40	10.90
24	100	150	5	24	35.33	28.33	37.24	30.41
25	100	175	3	12	23.16	23.16	24.99	24.23

APPENDIX 10B

Results of Relieved Cutting Experiment in Anhydrite

Test No	Levels of				Rolling Forces			
					Measured Values		Predicted Values	
	ϕ (°)	D (mm)	p (mm)	S (mm)	F'R (kN)	$\overline{FR}$ (kN)	F'R (kN)	$\overline{FR}$ (kN)
1	60	100	5	6	5.13	3.92	4.24	3.19
2	60	125	3	24	3.08	2.47	2.87	2.29
3	60	150	1	12	0.59	0.39	0.60	0.39
4	60	175	4	30	4.59	3.25	3.95	3.01
5	60	200	2	18	1.13	1.06	0.97	0.90
6	70	125	4	12	5.11	3.55	4.68	3.51
7	70	150	2	30	1.70	1.31	1.74	1.32
8	70	175	5	18	5.33	4.25	5.84	4.49
9	70	200	3	6	2.57	2.01	2.53	1.94
10	70	100	1	24	0.77	0.51	0.81	0.53
11	80	150	3	18	4.54	3.68	4.52	3.71
12	80	175	1	6	0.59	0.38	0.45	0.35
13	80	200	4	24	5.04	3.96	4.82	3.70
14	80	100	2	12	2.09	1.64	1.57	1.14
15	80	125	5	30	9.69	7.44	9.04	7.40
16	90	175	2	24	1.96	1.60	1.98	1.59
17	90	200	5	12	6.03	5.24	7.72	6.72
18	90	100	3	30	4.51	3.68	4.66	3.60
19	90	125	1	18	0.56	0.35	0.58	0.36
20	90	150	4	6	4.16	2.49	4.23	3.18
21	100	200	1	30	0.68	0.46	0.72	0.48
22	100	100	4	18	7.18	5.12	7.81	6.08
23	100	125	2	6	2.18	1.59	2.14	1.58
24	100	150	5	24	8.03	6.24	8.40	6.56
25	100	175	3	12	4.75	3.97	4.38	3.74

Appendix 10C

Results of Relieved Cutting Experiments in Anhydrite

Test No.	Levels of				Yield, Specific Energy and C.I.				
					Measured Values			Precicted Values	
	∅ (o)	D (mm)	p (mm)	S (mm)	Q m^3/km	S.E MJ/m^3	C.I	Q m^3/km	S.E MJ/m^3
1	60	100	5	6	0.033	128.63	365	0.037	105.81
2	60	125	3	24	0.027	91.21	221	0.037	66.84
3	60	150	1	12	0.0014	234.87	192	0.0015	262.00
4	60	175	4	30	0.039	84.67	309	0.050	65.02
5	60	200	2	18	0.008	140.45	273	0.009	117.67
6	70	125	4	12	0.042	84.88	345	0.047	75.53
7	70	150	2	30	0.009	152.23	269	0.007	187.57
8	70	175	5	18	0.062	68.92	335	0.058	73.29
9	70	200	3	6	0.017	118.36	311	0.024	83.71
10	70	100	1	24	0.002	233.95	192	0.005	101.60
11	80	150	3	18	0.047	79.39	349	0.048	76.75
12	80	175	1	6	0.002	208.25	197	0.002	189.00
13	80	200	4	24	0.062	65.37	360	0.056	70.77
14	80	100	2	12	0.016	101.94	310	0.013	126.38
15	80	125	5	30	0.121	63.40	373	0.117	63.62
16	90	175	2	24	0.011	148.75	369	0.012	133.58
17	90	200	5	12	0.052	115.33	376	0.088	59.51
18	90	100	3	30	0.033	111.03	312	0.041	89.85
19	90	125	1	18	0.002	199.98	170	0.002	173.00
20	90	150	4	6	0.030	88.53	335	0.029	85.79
21	100	200	1	30	0.002	192.34	192	0.018	25.56
22	100	100	4	18	0.060	56.15	347	0.076	67.32
23	100	125	2	6	0.014	115.05	284	0.010	159.40
24	100	150	5	24	0.086	72.47	350	0.095	65.66
25	100	175	3	12	0.033	121.83	319	0.041	96.73

Appendix 11

Results of Relieved Cutting Experiment in W. Limestone

p mm	s/p	F'T kN	$\overline{FT}$ kN	F'R kN	$\overline{FR}$ kN	Q m^3/km	S.E MJ/m^3	C.I
3	1	7.84	5.76	2.25	1.70	0.007	255.26	336
	3	14.65	10.48	3.64	2.77	0.023	122.35	374
	5	16.90	11.35	2.96	2.38	0.028	85.40	372
	7	19.68	13.79	3.38	2.86	0.031	96.55	374
	9	21.10	17.05	3.50	2.98	0.027	110.37	365
	Unr	21.29	18.19	3.64	3.02	0.025	125.07	360
7.	1	13.21	9.72	4.55	3.46	0.029	146.62	409
	3	36.10	26.48	10.06	7.72	0.130	61.55	419
	5	48.71	33.81	12.59	10.37	0.193	53.79	444
	7	51.43	41.54	12.45	10.75	0.165	65.14	440
	9	58.00	48.07	13.11	12.10	0.159	76.10	425
	Unr	59.31	50.48	13.28	12.37	0.157	79.50	420

Results of Relieved Cutting Experiment in Greywacke

p mm	s/p	F'T kN	$\overline{FT}$ kN	F'R kN	$\overline{FR}$ kN	Q m^3/km	S.E MJ/m^3	C.I
3	1	7.20	5.67	2.41	1.69	0.006	306.02	360
	3	13.29	9.12	4.27	3.07	0.025	131.15	361
	5	18.44	12.77	3.97	2.72	0.028	96.83	384
	7	20.52	15.34	4.05	2.90	0.026	115.31	382
	9	23.40	16.87	4.12	2.97	0.023	129.13	364
	Unr	23.55	16.95	4.15	3.00	0.022	136.19	360

Appendix 12A

Calculated Values of Specific Energy for Relieved Cutting Experiments

$\phi = 60^\circ$ p = 5mm				
s/p	Gypsum S.E MJ/m^3	D.Sandstone S.E MJ/m^3	M.Sandstone S.E MJ/m^3	Anhydrite S.E MJ/m^3
1	41.82	37.70	55.05	82.68
2	37.05	29.09	41.86	65.65
3	35.81	27.99	41.12	53.84
5	35.63	27.96	36.71	49.48
6	36.25	29.29	34.70	48.94
7	37.53	32.54	36.09	49.68
8	39.32	35.04	35.88	51.57
9	41.55	37.05	37.71	54.88
10	42.55	42.00	39.19	58.15
12	-	52.60	43.19	70.94
Unr	47.31	54.66	44.98	74.36
s/p	$\phi = 70^\circ$ p = 5mm			
1	45.00	39.37	63.76	91.09
2	39.75	34.04	48.36	72.43
3	38.54	32.66	48.81	59.40
5	38.25	32.70	42.46	54.55
6	39.04	34.05	41.70	53.99
7	40.36	36.30	41.75	54.73
8	42.19	39.42	42.42	56.82
9	44.64	41.99	43.64	61.65
10	49.95	49.10	45.29	70.12
12	-	61.49	49.92	78.28
Unr	50.88	63.87	52.01	81.99

Appendix 12B

Calculated Values of Specific Energy for Relieved Cutting Experiments

	$\phi = 80^\circ$ p = 5mm			
$\frac{s}{p}$	Gypsum S.EMJ/m^3	D. Sandstone S.E MJ/m^3	M. Sandstone S.E MJ/m^3	Anhydrite S.E MJ/m^3
1	47.62	45.19	71.05	112.64
2	42.23	39.00	54.00	89.48
3	40.71	37.51	54.56	73.40
5	40.26	37.47	47.36	67.43
6	41.31	39.09	46.55	66.69
7	43.27	41.61	46.57	67.70
8	44.64	45.23	47.31	70.25
9	47.16	48.12	48.65	74.79
10	48.37	56.31	50.58	85.15
12	-	70.52	55.71	94.39
Unr	51.74	73.28	58.02	101.34
$\frac{s}{p}$	$\phi = 90^\circ$ p = 5mm			
1	49.85	50.89	77.50	120.84
2	44.16	43.91	58.91	101.33
3	42.66	42.24	59.52	83.08
5	42.38	42.09	51.68	76.36
6	43.25	41.81	50.78	75.52
7	44.72	46.64	50.82	76.67
8	47.06	50.94	51.61	79.55
9	49.50	54.19	53.10	84.70
10	50.70	63.40	55.18	89.77
12	-	79.40	60.82	109.50
Unr	56.37	82.51	63.31	114.77

Appendix 12C

Calculated Values of Specific Energy for Relieved Cutting Experiments

	ϕ = 100° p = 5mm			
s/p	Gypsum S.EMJ/m^3	D.Sandstone S.E MJ/m^3	M.Sandstone S.E MJ/m^3	Anhydrite S.E MJ/m^3
1	48.26	56.68	83.23	142.37
2	42.86	48.92	63.26	113.06
3	41.33	47.04	63.91	92.70
5	41.05	46.99	55.49	85.21
6	41.89	49.03	54.53	84.27
7	43.31	52.18	54.56	85.55
8	45.32	56.73	55.41	88.77
9	49.35	60.35	56.98	94.51
10	-	70.69	59.26	110.12
12	54.60	-	65.27	122.19
Unr	54.60	91.90	67.97	128.06

Appendix 13

The Values of Projected Disc Contact Areas

ϕ (°)	D (mm)	p (mm)	A_2 (mm^2)	p (mm)	A_2 (mm^2)	p (mm)	A_2 (mm^2)
60	100	7.5	304.2	10	461.9	2	43.1
60	125	4.5	161.3	6	246.9	4	135.5
60	150	1.5	34.5	2	53.0	1	18.8
60	175	6.0	294.4	8	450.2	3	104.9
60	200	3.0	112.3	4	172.5	5	240.4
70	125	6.0	299.4	8	457.0	5	228.7
70	150	3.0	117.6	4	180.5	2	64.2
70	175	7.5	496.2	10	758.5	4	195.3
70	200	4.5	249.2	6	382.2	1	26.3
70	100	1.5	34.0	2	52.3	3	95.6
80	150	4.5	257.7	6	394.6	3	141.0
80	175	1.5	54.1	2	83.2	5	326.2
80	200	6.0	458.0	8	701.6	2	89.1
80	100	3.0	114.5	4	175.4	4	175.4
80	125	7.5	415.7	10	758.8	1	24.9
90	175	3.0	181.7	4	279.0	1	35.2
90	200	7.5	759.9	10	1162.4	3	194.5
90	100	4.5	248.8	6	380.0	5	290.6
90	125	1.5	54.4	2	83.7	2	83.7
90	150	6.0	470.3	8	719.0	4	257.8
100	200	1.5	82.3	2	126.5	4	356.0
100	100	6.0	452.9	8	689.8	1	31.6
100	125	3.0	182.4	4	279.7	3	29.4
100	150	7.5	779.2	10	1189.2	5	427.9
100	175	4.5	396.1	6	607.2	2	

Appendix 14A

Predictor Equation Constants

Rock Property	$\overline{FT} = 4.2 + bA$	$\overline{FR} = c\ A_1^{0.778}$
Unconfined Compressive Strength, σc MN/m^2	b =0.00762+0.000986σc r = 0.92 Sig. Lev. 0.01	c=-0.025+0.0072 σc r = 0.971 Sig. Lev. 0.001
Unconfined Tensile Strength, σt MN/m^2	b =0.00661 +0.01723 σt r = 0.933 Sig. Lev. 0.01	$c = \frac{\sigma t}{7.617+0.268\sigma t}$ r = 0.908 Sig. Lev. 0.02
Static Modulus of Elasticity, E $MN/m^2 \times 10^4$	No significant Relationship	c =0.296+0.043 ES r = 0.847 Sig. Lev. 0.05
Dynamic Modulus of Elasticity, ED $MN/m^2 \times 10^4$	$b = \frac{ED}{11.81+9.37\ ED}$ r = 0.77 Sig. Lev. 0.1	c =0.276+0.0478 ED r = 0.876 Sig. Lev.0.05
Impact Strength Index I.S.I.	$b = \frac{ISI}{772.6+2.15\ (ISI)}$ r = 0.745 Sig. Lev. 0.1	No significant Relationship
Dry Bulk Density, D	b=-0.1192+0.08188D r = 0.948 Sig. Lev. 0.01	c=-0.901+0.575 D r =0.972 Sig. Lev. 0.001

Appendix 14B

Predictor Equation Constants

Rock Property	$F'T = 4.676 + b^1A$	$F'R = c^1A^{1\ 0.749}$
Unconfined Compressive Strength, σc MN/m^2	b^1=0.00305+0.001195 r = 0.95 Sig. Lev. 0.01	c^1=-0.078+0.01 σc r = 0.99 Sig. Lev. 0.001
Unconfined Tensile Strength, σt MN/m^2	b^1=0.00366+0.0202 σt r = 0.94 Sig. Lev. 0.01	$c^1=\frac{\sigma t}{5.885+0.186\sigma t}$ r = 0.934 Sig. Lev. = 0.01
Static Modulus of Elasticity, ES $MN/m^2 \times 10^4$	No significant Relationship	c^1=0.395+0.055 ES r = 0.787 Sig. Lev. 0.1
Dynamic Modulus of Elasticity, ED $MN/m^2 \times 10^4$	No Significant Relationship	c^1=0.369+0.062 ED r = 0.819 Sig. Lev. 0.05
Impact Strength Index I.S.I.	No Significant Relationship	No significant Relationship
Dry Bulk Density D g/cc	b^1=-0.1444+0.0962 D r = 0.962 Sig.Lev. 0.01	c^1=-1.235+0.777 D r = 0.953 Sig. Lev. 0.01

Appendix 15A

Predicted Mean Thrust Force Values (kN) from Compressive Strength

ø (o)	D (mm)	p (mm)	Gypsum	Bunter Sandstone	Dunhouse Sandstone
60	100	10	28.473	30.400	33.461
60	125	6	17.175	18.204	19.841
60	150	2	6.985	7.206	7.558
60	175	8	27.858	29.735	32.720
60	200	4	13.265	13.984	15.128
70	125	8	28.215	30.121	33.151
70	150	4	13.685	7.841	15.671
70	175	10	44.059	47.222	52.251
70	200	6	24.285	25.878	28.412
70	100	2	6.948	7.166	7.513
80	150	6	24.936	26.582	29.198
80	175	2	8.572	8.919	9.471
80	200	8	41.069	43.995	48.650
80	100	4	13.417	14.149	15.312
80	125	10	44.075	47.239	52.270
90	175	4	18.861	20.025	21.875
90	200	10	65.284	70.131	77.838
90	100	6	24.169	25.754	28.279
90	125	2	8.598	8.947	9.502
90	150	8	41.983	44.982	49.749
100	200	2	10.848	11.375	12.214
100	100	8	40.449	43.325	47.899
100	125	4	18.898	20.065	21.919
100	150	10	66.692	71.651	79.536
100	175	6	36.108	38.640	42.666

Appendix 15B

Predicted Mean Thrust Force Values (kN) from Compressive Strength

∅ (o)	D (mm)	p (mm)	Mansfield Sandstone	Magnesian Limestone	p (mm)	Anhydrite
60	100	7.5	28.164	32.393	1	8.001
60	125	4.5	16.907	19.096	1	7.195
60	150	1.5	6.918	7.386	1	6.462
60	175	6	27.393	31.388	1	9.435
60	200	3	13.047	14.571	1	7.364
70	125	6	27.787	31.850	2	14.269
70	150	3	13.465	15.060	2	11.923
70	175	7.5	43.291	50.024	2	18.423
70	200	4.5	23.832	27.214	2	14.919
70	100	1.5	6.879	7.340	2	9.385
80	150	4.5	24.502	27.999	3	21.162
80	175	1.5	8.462	9.196	3	16.819
80	200	6	40.281	46.496	3	27.598
80	100	3	13.220	14.774	3	15.701
80	125	7.5	36.949	42.590	3	26.142
90	175	3	18.514	20.980	4	27.695
90	200	7.5	64.057	74.377	4	47.027
90	100	4.5	23.800	27.177	4	25.301
90	125	1.5	8.486	9.224	4	20.501
90	150	6	41.250	47.632	4	35.213
100	200	1.5	10.684	11.800	5	33.120
100	100	6	40.376	46.025	5	39.159
100	125	3	18.562	21.045	5	31.713
100	150	7.5	65.585	76.159	5	55.676
100	175	4.5	35.405	40.780	5	43.442

Appendix 15C

Predicted Mean - $\overline{FT}$ (kN) Values for Plotting Graphs

Rock	Disc Penetration (mm)				
	2	4	6	8	10
Gypsum	8.46	15.63	25.33	35.91	49.72
Bunter Sandstone	8.72	15.81	27.01	38.43	53.32
Dunhouse Sandstone	9.25	17.98	29.68	42.43	59.07
	1.5	3	4.5	6	7.5
Mansfield Sandstone	8.29	15.36	24.89	35.42	47.61
Magnesian Limestone	8.99	17.29	28.45	40.68	55.11
	1		3	4	5
Anhydrite	17.26	18.88	22.40	24.93	31.05

Rock	Disc Edge Angle (°)				
	60	70	80	90	100
Gypsum	18.75	23.44	26.41	31.85	34.60
Bunter Sandstone	19.91	23.65	28.18	33.97	37.01
Dunhouse Sandstone	21.74	27.40	30.98	37.45	40.85
Mansfield Sandstone	18.49	23.05	24.68	31.22	34.12
Magnesian Limestone	20.97	26.30	28.21	35.88	39.16
Anhydrite	17.49	13.78	21.48	31.15	40.62

Rock	Disc Diameter (mm)				
	100	125	150	175	200
Gypsum	22.69	23.46	30.86	27.09	30.95
Bunter Sandstone	24.16	24.92	31.65	28.91	33.07
Dunhouse Sandstone	26.49	27.34	36.34	31.80	36.45
Mansfield Sandstone	22.49	21.74	30.34	26.61	30.38
Magnesian Limestone	25.54	24.76	34.85	30.47	34.89
Anhydrite	19.51	19.96	26.09	22.96	26.01

Appendix 16A

Predicted Mean Rolling Force Values (kN) from Compressive Strength

ø (o)	D (mm)	p (mm)	Gypsum	Bunter Sandstone	Dunhouse Sandstone
60	100	10	8.846	7.016	7.725
60	125	6	3.996	3.169	3.490
60	150	2	0.723	0.574	0.631
60	175	8	6.251	4.958	5.458
60	200	4	2.126	1.686	1.857
70	125	8	7.263	5.760	6.342
70	150	4	2.470	1.959	2.157
70	175	10	10.276	8.150	8.973
70	200	6	4.643	3.682	4.054
70	100	2	0.840	0.666	0.733
80	150	6	5.344	4.239	4.667
80	175	2	0.968	0.768	0.845
80	200	8	6.251	4.958	5.458
80	100	4	2.843	2.255	2.482
80	125	10	11.832	9.384	10.332
90	175	4	3.259	2.585	2.846
90	200	10	13.563	10.757	11.843
90	100	6	6.126	4.858	5.349
90	125	2	1.109	0.879	0.968
90	150	8	9.584	7.601	8.369
100	200	2	1.271	1.008	1.110
100	100	8	10.986	8.713	9.593
100	125	4	3.736	2.963	3.263
100	150	10	15.546	12.330	13.575
100	175	6	7.021	5.568	6.131

Appendix 16B

Predicted Mean Rolling Force Values (kN) from Compressive Strength

ø (o)	D (mm)	p (mm)	Mansfield Sandstone	Magnesian Limestone	p (mm)	Anhydrite
60	100	7.5	7.325	8.793	1	0.902
60	125	4.5	3.354	3.971	1	0.688
60	150	1.5	0.599	0.719	1	0.516
60	175	6.0	5.177	6.215	1	0.788
60	200	3.0	1.761	2.114	1	0.597
70	125	6.0	6.014	7.220	2	2.317
70	150	3.0	2.045	2.455	2	1.756
70	175	7.5	8.511	10.217	2	2.657
70	200	4.5	3.844	4.594	2	2.023
70	100	1.5	0.697	0.926	2	1.492
80	150	4.5	4.427	5.314	3	3.798
80	175	1.5	0.801	0.962	3	2.842
80	200	6.0	6.924	8.311	3	4.354
80	100	3.0	2.356	2.829	3	3.299
80	125	7.5	9.797	11.761	3	4.993
90	175	3.0	2.699	3.240	4	5.162
90	200	7.5	11.231	13.483	4	7.810
90	100	4.5	5.072	6.089	4	5.946
90	125	1.5	0.918	1.102	4	4.444
90	150	6.0	7.936	9.526	4	6.813
100	200	1.5	1.052	1.262	5	6.287
100	100	6.0	9.096	10.919	5	9.641
100	125	3.0	3.094	3.715	5	7.308
100	150	7.5	12.873	15.453	5	11.050
100	175	4.5	5.813	6.978	5	8.412

Appendix 16C

Predicted Mean $\overline{FR}$ (in kN) Values for Plotting Graphs

Rock	Disc Penetration (mm)				
	2	4	6	8	10
Gypsum	0.78	2.29	4.30	6.40	9.53
Bunter Sandstone	0.86	2.52	4.74	7.04	10.49
Dunhouse Sandstone	1.01	2.86	5.25	7.69	11.29
	1.5	3	4.5	6	7.5
Mansfield Sandstone	0.81	2.39	4.50	7.03	9.95
Magnesian Limestone	0.99	2.87	5.39	8.44	11.94
	1	2	3	4	5
Anhydrite	0.70	2.05	3.86	6.04	8.54

Rock	Disc Edge Angle (o)				
	60	70	80	90	100
Gypsum	3.48	4.04	4.32	5.34	6.12
Bunter Sandstone	3.83	4.45	4.76	5.88	6.73
Dunhouse Sandstone	4.25	4.90	5.23	6.41	7.31
Mansfield Sandstone	3.64	4.22	4.86	5.57	6.39
Magnesian Limestone	4.36	5.08	5.84	6.69	7.67
Anhydrite	3.12	3.62	4.17	4.78	5.48

Rock	Disc Diameter (mm)				
	100	125	150	175	200
Gypsum	4.70	4.43	4.54	4.41	4.42
Bunter Sandstone	5.18	4.88	5.88	4.85	4.86
Dunhouse Sandstone	5.68	5.36	6.39	5.34	5.33
Mansfield Sandstone	4.91	4.64	5.58	4.60	4.96
Magnesian Limestone	5.91	5.55	6.69	5.52	5.95
Anhydrite	4.26	3.95	4.79	3.97	4.21

Appendix 17A

Predicted Peak Thrust Force Values (kN) from Compressive Strength

∅ (o)	D (mm)	p (mm)	Gypsum	Bunter Sandstone	Dunhouse Sandstone
60	100	10	32.735	35.042	38.686
60	125	6	20.666	21.744	23.705
60	150	2	9.489	9.754	10.174
60	175	8	32.070	34.316	37.891
60	200	4	16.283	17.143	18.513
70	125	8	32.456	34.737	38.365
70	150	4	16.737	17.559	19.071
70	175	10	49.597	53.382	59.404
70	200	6	28.204	30.111	33.146
70	100	2	9.442	8.579	10.125
80	150	6	28.909	30.878	34.011
80	175	2	11.206	11.621	12.282
80	200	8	46.362	49.863	55.434
80	100	4	16.447	17.323	18.715
80	125	10	49.614	53.400	59.425
90	175	4	22.337	23.729	25.945
90	200	10	72.558	78.353	87.588
90	100	6	28.079	29.976	32.992
90	125	2	11.234	11.652	12.317
90	150	8	47.351	50.939	56.648
100	200	2	13.668	14.299	17.303
100	100	8	45.691	49.133	54.610
100	125	4	22.377	23.773	25.993
100	150	10	74.082	80.016	89.458
100	175	6	40.995	44.025	48.846

Appendix 17B

Predicted Peak Thrust Force Values (kN) from Compressive Strength

ø (°)	D (mm)	p (mm)	Mansfield Sandstone	Magnesian Limestone	p (mm)	Anhydrite
60	100	7.5	33.322	38.267	1	10.837
60	125	4.5	20.711	23.332	1	9.912
60	150	1.5	9.521	10.081	1	9.070
60	175	6	32.457	37.241	1	11.334
60	200	3	16.386	18.211	1	10.105
70	125	6	32.898	37.763	2	18.027
70	150	3	16.854	18.765	2	15.336
70	175	7.5	50.266	58.329	2	22.792
70	200	4.5	28.468	32.517	2	18.772
70	100	1.5	9.477	10.029	2	12.424
80	150	4.5	29.218	33.406	3	25.934
80	175	1.5	11.250	12.129	3	20.952
80	200	6.0	46.896	54.337	3	33.317
80	100	3.0	16.581	18.441	3	19.669
80	125	7.5	43.135	49.917	3	31.647
90	175	3.0	22.511	25.464	4	33.427
90	200	7.5	73.537	85.886	4	55.604
90	100	4.5	28.433	32.476	4	30.681
90	125	1.5	11.277	12.161	4	25.175
90	150	6.0	47.980	55.591	4	42.052
100	200	1.5	13.739	15.076	5	39.651
100	100	6.0	46.444	54.462	5	46.579
100	125	3.0	22.573	25.537	5	38.037
100	150	7.5	75.246	87.902	5	65.526
100	175	4.5	41.432	47.868	5	51.492

Appendix 17C

Predicted Peak Rolling Force Values (kN) from Compressive Strength

ø (O)	D (mm)	p (mm)	Gypsum	Bunter Sandstone	Dunhouse Sandstone
60	100	10	7.760	8.637	10.014
60	125	6	3.611	4.019	4.659
60	150	2	0.694	0.775	0.899
60	175	8	5.555	6.182	7.168
60	200	4	1.967	2.189	2.538
70	125	8	6.418	7.143	8.282
70	150	4	2.272	2.529	2.932
70	175	10	8.964	9.977	11.567
70	200	6	4.172	4.643	5.383
70	100	2	0.804	0.895	1.038
80	150	6	4.777	5.317	6.164
80	175	2	0.992	1.042	1.190
80	200	8	5.555	6.182	7.168
80	100	4	2.602	2.895	3.357
80	125	10	10.268	11.427	13.249
90	175	4	2.967	3.303	3.829
90	200	10	11.710	13.032	15.109
90	100	6	5.448	6.063	7.029
90	125	2	1.051	1.169	1.356
90	150	8	8.382	9.329	10.816
100	200	2	1.199	1.334	1.547
100	100	8	9.560	10.640	12.336
100	125	4	3.385	3.767	4.367
100	150	10	13.354	14.862	17.231
100	175	6	6.212	6.914	8.016

Appendix 17D

Predicted Peak Rolling Force Values (kN) from Compressive Strength

ϕ (o)	D (mm)	p (mm)	Mansfield Sandstone	Magnesi Limestone	p (mm)	Anhydrite
60	100	7.5	8.673	10.453	1	1.197
60	125	4.5	4.005	4.862	1	0.923
60	150	1.5	0.773	0.934	1	0.699
60	175	6.0	6.164	7.484	1	1.051
60	200	3.0	2.183	2.651	1	0.805
70	125	6.0	7.121	8.646	2	2.969
70	150	3.0	2.520	3.062	2	2.273
70	175	7.5	9.948	12.078	2	3.388
70	200	4.5	4.628	5.619	2	2.606
70	100	1.5	0.894	1.086	2	1.968
80	150	4.5	5.301	6.437	3	4.778
80	175	1.5	1.023	1.242	3	3.614
80	200	6.0	8.155	9.921	3	5.450
80	100	3.0	2.889	3.508	3	4.172
80	125	7.0	11.391	13.830	3	6.217
90	175	3.0	3.292	3.997	4	6.420
90	200	7.5	12.992	15.774	4	9.565
90	100	4.5	6.043	7.338	4	7.356
90	125	1.5	1.166	1.415	4	5.559
90	150	6.0	9.299	11.291	4	8.386
100	200	1.5	1.329	1.613	5	7.762
100	100	6.0	10.604	12.876	5	11.715
100	125	3.0	3.756	4.560	5	8.972
100	150	7.5	14.815	17.988	5	13.359
100	175	4.5	6.891	8.367	5	10.273

Appendix 18

Constant of Predictor Equations for Unrelieved Cutting

Rocks	Cutting Parameters	A	B	C 10^{-4}	E 10^{-2}	Correlation Coefficient
Gypsum	F'T kN	-0.828	-17.092	2.229	6.992	0.992
	$\overline{FT}$ kN	-0.930	-20.198	2.341	7.024	0.988
	F'R kN	-0.963	0.0147	387.9	-	0.984
	$\overline{FR}$ kN	-1.025	0.0150	-319.3	-	0.980
	Q m^3/km	1.711	0.00003	12.338	-	0.968
	S.E MJ/m^3	-0.443	0.0047	42059	-	0.906
	C.I	15.18	295.7	-	-	0.744
Dunhouse Sandstone	F'T kN	-0.652	-8.053	1.811	5.622	0.982
	$\overline{FT}$ kN	-0.672	-28.727	2.450	5.439	0.975
	F'R kN	-1.520	0.0149	5334	-	0.995
	$\overline{FR}$ kN	-1.625	0.0185	-227.04	-	0.993
	Q m^3/km	0.0027	-0.00009	-	-	0.974
	S.E MJ/m^3	-0.619	0.0109	43084	-	0.925
	C.I	20.1	153.4	-	-	0.919
Mansfield Sandstone	F'T kN	-0.322	-22.948	3.544	7.127	0.991
	$\overline{FT}$ kN	-0.492	-38.162	4.164	8.693	0.994
	F'R kN	-0.841	0.0178	-895.3	-	0.980
	$\overline{FR}$ kN	-0.841	0.0188	-3475	-	0.992
	Q m^3/km	-1.239	0.00002	16.795	-	0.989
	S.E MJ/m^3	-0.675	0.0088	45628	-	0.968
	C.I	23.8	188	-	-	0.974
Anhydrite	F'T kN	-0.168	-26.054	1.973	14.192	0.971
	$\overline{FT}$ kN	-0.233	-28.745	3.157	10.839	0.976
	F'R kN	-0.613	0.0325	-5270	-	0.980
	$\overline{FR}$ kN	-0.726	0.0238	-1065	-	0.972
	Q m^3/km	0.003	0.0010	-	-	0.972
	S.E MJ/m^3	-0.430	0.0073	4.6738	-	0.952
	C.I	19.24	235.1	-	-	0.912

Appendix 19

Results of Blunt Disc Experiment in Bunter Sandstone

r (mm)	p(mm)	F'T(kN)	$\overline{FT}$(kN)	F'R(kN)	$\overline{FR}$(kN)	Q m^3/km	S.E.MJ/m^3	C.I
0	2	4.94	3.30	0.59	0.49	0.0105	46.95	205
	4	10.67	6.80	1.71	1.21	0.0293	41.70	252
	6	18.61	12.88	3.77	2.97	0.0883	33.77	300
	8	26.25	17.30	5.95	4.33	0.1570	27.57	343
1.0	2	6.72	5.12	0.80	0.62	0.0096	65.45	195
	4	13.48	9.26	2.20	1.70	0.0403	42.35	271
	6	20.19	13.85	4.19	3.18	0.0949	33.05	313
	8	28.52	19.71	6.68	4.78	0.1649	29.01	345
1.5	2	7.11	5.32	0.79	0.65	0.0094	70.15	200
	4	15.72	10.93	2.44	1.78	0.0383	46.55	268
	6	22.18	15.88	4.59	3.50	0.1000	35.24	330
	8	28.98	18.27	7.16	4.70	0.1493	31.48	321
2.0	2	8.94	6.36	0.99	0.76	0.0106	72.06	211
	4	15.34	10.09	2.50	1.71	0.0401	43.16	257
	6	22.66	15.08	4.50	3.12	0.1022	30.90	317
	8	31.20	20.91	7.67	5.37	0.1599	33.61	322
2.5	2	9.34	6.81	1.10	0.81	0.0127	64.71	201
	4	18.01	12.28	2.90	2.06	0.0515	40.54	253
	6	25.10	17.05	4.99	3.42	0.1009	34.38	316
	8	34.57	22.96	8.32	5.74	0.1771	32.46	328
3.0	2	13.94	10.72	1.34	1.04	0.0132	78.93	207
	4	20.35	13.25	3.51	2.41	0.0537	44.95	274
	6	29.22	19.19	5.72	3.95	0.1118	35.51	312

Appendix 20A

Increase of the Projected Area of Disc Contact (%)

p(mm)	r = 1mm	r = 1.5mm	r = 2mm	r = 2.5mm	r = 3mm
2	49.0	97.2	144.8	191.8	238.1
4	24.1	47.2	71.4	94.4	117.2
6	15.9	31.5	46.8	61.9	76.9
8	11.7	23.2	34.6	47.0	56.6

Mean Peak Thrust Force Increase (%)

p(mm)	r = 1mm	r = 1.5mm	r = 2mm	r = 2.5mm	r = 3mm
2	36.0	43.9	81.0	89.1	182.2
4	28.2	47.3	43.8	68.8	90.7
6	8.5	19.2	21.8	34.9	57.0
8	8.6	10.3	18.9	31.7	—

Mean Thrust Force Increase (%)

p(mm)	r = 1mm	r = 1.5mm	r = 2mm	r = 2.5mm	r = 3mm
2	55.0	61.2	92.7	106.4	224.8
4	36.2	60.7	48.4	80.6	94.9
6	7.5	23.3	17.1	32.4	49.0
8	13.9	7.5	20.9	32.7	-

Appendix 20B

Mean Peak Rolling Force Increase %					
p(mm)	r = 1mm	r = 1.5mm	r = 2mm	r = 2.5mm	r = 3mm
2	35.6	33.9	67.8	86.4	127.0
4	28.7	42.7	46.2	69.6	105.3
6	11.1	21.8	19.4	32.4	51.7
8	12.3	20.3	28.9	39.8	-

Mean Rolling Force Increase %					
p(mm)	r = 1mm	r = 1.5mm	r = 2mm	r = 2.5mm	r = 3mm
2	26.5	32.7	55.1	65.3	112.2
4	40.5	47.1	41.3	70.2	99.2
6	7.1	17.8	5.1	15.2	-
8	10.4	8.5	24.0	32.6	-

Appendix 21 A

Actual and Predicted Thrust Force Values for Blunt Discs

Limestone				Greywacke				Granite			
p mm	r mm	F'T (kN) Pred	F'T (kN) Act.	p mm	r mm	F'T (kN) Pred.	F'T (kN) Act.	p mm	r mm	F'T (kN) Act.	
1	0	-	4.51	1	0	-	5.72	1	0	-	
3	0	-	21.29	3	0	-	23.55	3	0	-	
4	0	-	30.10	4	0	-	31.38	4	0	-	
5	0	-	41.39	5	0	-	34.81	5	0		
1	1	8.24	10.41	1	1	10.44	8.98	1	1	12.47	
3	1	26.98	26.48	3	1	29.84	29.56	3	1	29.87	
4	1	36.44	35.16	4	1	37.98	34.81	4	1	39.89	
5	1	48.76	45.45	5	1	41.00	41.25	5	1	50.25	
1	2	15.03	13.36								
3	2	34.18	35.52								
4	2	44.11	41.36								
5	2	57.43	52.40								

Limestone				Greywacke				Granite			
p mm	r mm	$\overline{FT}$ (kN) Pred.	$\overline{FT}$ (kN) Act	p mm	r mm	$\overline{FT}$ (kN) Pred.	$\overline{FT}$ (kN) Act.	p mm	r mm	$\overline{FT}$(kN) Act.	
1	0	-	3.63	1	0	-	4.99	1	0	-	
3	0	-	18.19	3	0	-	16.95	3	0	-	
4	0	-	26.00	4	0	-	20.58	4	0	-	
5	0	-	33.68	5	0	-	24.78	5	0	-	
1	1	8.74	7.25	1	1	9.96	7.30	1	1	9.47	
3	1	23.39	23.44	3	1	21.85	19.86	3	1	29.87	
4	1	28.03	31.73	4	1	25.11	24.70	4	1	39.89	
5	1	35.01	29.78	5	1	29.26	29.47	5	1	50.25	
1	2	14.46	10.73								
3	2	30.22	28.36								
4	2	38.73	31.67								
5	2	46.99	43.63								

Appendix 21B

Actual and Predicted Rolling Force Values for Blunt Discs

Limestone				Greywacke				Granite		
p mm	r mm	$\overline{FR}$(kN) Predicted	$\overline{FR}$(kN) Actual	p mm	r mm	$\overline{FR}$(kN) Predicted	$\overline{FR}$(kN) Actual	p mm	r mm	FR(kN) Actual
1	0	-	0.48	1	0	-	0.62	1	0	-
3	0	-	3.02	3	0	-	3.00	3	0	
4	0	-	4.70	4	0	-	4.31	4	0	-
5	0	-	6.85	5	0	-	5.62	5	0	-
1	1	0.74	0.95	1	1	0.97	0.78	1	1	1.06
3	1	3.65	3.40	3	1	3.62	3.50	3	1	3.60
4	1	5.49	5.24	4	1	5.04	5.05	4	1	5.32
5	1	7.85	7.49	5	1	6.44	6.99	5	1	8.44
1	2	1.15	1.14							
3	2	4.40	5.04							
4	2	6.42	6.29							
5	2	8.99	8.97							

Limestone				Greywacke				Granite		
p mm	r mm	F'R(kN) Predicted	F'R(kN) Actual	p mm	r mm	F'R(kN) Predicted	F'R(kN) Actual	p mm	r mm	F'R(kN) Actual
1	0	-	0.47	1	0	-	0.88	1	0	-
3	0	-	3.64	3	0	-	4.15	3	0	-
4	0	-	5.80	4	0	-	6.17	4	0	-
5	0	-	8.03	5	0	-	7.63	5	0	-
1	1	0.76	1.08	1	1	1.44	1.02	1	1	1.53
3	1	4.52	4.23	3	1	5.16	4.97	3	1	4.97
4	1	6.96	6.76	4	1	7.40	7.03	4	1	7.01
5	1	9.45	9.25	5	1	8.97	9.48	5	1	11.38
1	2	1.24	1.42							
3	2	5.51	6.33							
4	2	8.35	8.56							
5	2	11.11	11.08							

Appendix 22A

Relieved Disc Cutting Results in Bunter Sandstone

s/p	F'T(kN)	$\overline{FT}$(kN)	F'R(kN)	$\overline{FR}$(kN)	Q(m^3/km)	S.E(MJ/m^3)
	p = 3mm r = 0mm					
Unr	8.498	5.490	1.120	0.979	0.0189	51.873
1	2.704	1.888	0.487	0.439	0.0051	84.893
5	7:584	4.140	1.248	0.814	0.0315	25.966
6	7.820	4.802	1.209	0.940	0.0362	26.134
7	8.164	5.307	1.244	0.948	0.0274	39.073
8	8.238	5.451	1.030	0.924	0.01754	52.656
9	8.468	5.739	1.188	0.964	0.0186	52.193
	p = 3mm r = 1mm					
Unr	9.719	6.810	1.561	1.196	0.0197	61.058
1	4.370	2.893	1.118	0.981	0.0104	98.284
5	8.384	5.291	1.525	1.134	0.0360	31.791
6	8.593	6.271	1.432	1.067	0.0326	33.648
7	9.244	6.420	1.425	1.155	0.0311	37.790
8	10.372	7.418	1.747	1.296	0.0211	61.677
9	9.995	7.153	1.673	1.281	0.0232	55.397
	p = 3mm r = 2mm					
Unr	12.677	8.601	1.968	1.480	0.0200	76.801
1	4.947	3.402	1.128	0.803	0.0105	83.084
5	10.040	6.440	1.530	1.185	0.0321	36.735
6	11.671	6.889	1.943	1.290	0.0387	33.592
7	12.271	7.713	2.002	1.476	0.0433	35.042
8	12.093	8.912	2.050	1.496	0.0391	41.717
9	12.246	8.357	1.798	1.443	0.0191	76.174

Appendix 22B

Relieved Disc Cutting Results in Bunter Sandstone

$\frac{s}{p}$	F'T(kN)	$\overline{FT}$(kN)	F'R(kN)	$\overline{FR}$(kN)	Q(m^3/km)	Q(MJ/m^3)
	p = 3mm r = 3mm					
Unr	17.575	12.926	2.299	1.774	0.0245	73.441
1	3.588	2.357	0.478	0.365	0.0062	59.668
5	11.987	7.999	1.828	1.422	0.0379	37.358
6	15.509	8.630	2.180	1.659	0.0475	34.912
7	15.550	9.469	2.194	1.659	0.0562	29.549
8	16.277	9.861	2.273	1.748	0.0552	32.354
9	17.872	14.711	2.265	1.915	0.0384	49.776
	p = 7mm r = 0mm					
Unr	20.535	14.543	4.659	3.451	0.1177	31.061
1	7.241	5.394	2.638	2.406	0.0411	59.546
5	16.426	11.841	4.198	3.260	0.1852	17.614
6	19.032	12.545	4.535	3.298	0.1502	21.995
7	19.550	13.886	4.418	3.390	0.1396	25.207
8	20.535	14.543	4.659	3.451	0.1177	31.061
9	20.535	14.543	4.659	3.451	0.1177	31.061
	p = 7mm r = 1mm					
Unr	24.013	16.464	5.474	3.935	0.1234	33.355
1	7.562	5.663	2.637	2.202	0.0235	96.352
5	17.977	11.411	4.716	3.272	0.1773	18.836
6	17.610	10.756	4.334	2.920	0.2145	14.307
7	20.096	13.820	4.694	3.396	0.2089	16.226
8	20.218	13.612	5.085	3.397	0.1260	27.275
9	24.607	16.777	5.841	4.193	0.1185	35.456

Appendix 22C

Relieved Disc Cutting Results in Bunter Sandstone

s/p	F'T(kN)	$\overline{FT}$(kN)	F'R(kN)	$\overline{FR}$(kN)	(Qm^3/km)	S.E(MJ/m^3)
	p = 7mm r = 2mm					
Unr	26.092	17.961	5.987	4.046	0.1232	32.874
1	8.990	6.937	2.434	1.869	0.0221	84.742
5	20.700	13.661	4.942	3.043	0.1468	20.728
6	23.314	14.302	5.412	3.457	0.1611	21.433
7	26.556	17.296	6.094	3.984	0.1994	19.979
8	27.365	14.184	5.757	3.974	0.1400	28.392
9	25.610	17.143	5.685	3.928	0.1259	31.193
	p = 7mm r = 3mm					
Unr	31.431	22.681	6.674	5.069	0.1507	34.311
1	10.861	9.218	2.023	1.850	0.0391	59.075
5	26.838	16.680	6.064	4.202	0.0183	24.285
6	25.293	18.893	6.705	4.620	0.2350	20.235
7	28.078	19.283	6.273	4.631	0.2384	19.756
8	29.813	21.312	6.295	4.600	0.1704	27.433
9	32.693	23.400	6.840	5.162	0.1535	34.232

Appendix 23A

Results of Unrelieved Cutting Experiments with a Gear Cutter

	Gypsum		Bunter Sandstone		Dunhouse Sandstone		Mansfield Sandstone	
Penetration (p_{mm})	F'T (kN)	$\overline{FT}$ (kN)	F'T (kN)	$\overline{FT}$ (kN)	F'T (kN)	$\overline{FT}$ (kN)	F'T (kN)	$\overline{FT}$ (kN)
2	7.6	4.0	6.7	3.0	9.7	4.5	10.3	4.9
4	12.8	8.2	11.3	6.6	17.5	11.0	17.9	11.1
6	17.3	14.4	16.8	11.3	26.9	19.6	25.6	20.2
8	27.4	21.8	21.9	16.7	35.6	29.8	37.3	30.8
10	37.6	31.7	35.6	26.4	-	-	-	-

Penetration p (mm)	F'R (kN)	$\overline{FR}$ (kN)	F'R (kN)	$\overline{FR}$ (kN)	F'R (kN)	$\overline{FR}$ (kN)	F'R (kN)	$\overline{FR}$ (kN)
2	1.0	0.4	0.8	0.3	1.3	0.5	1.2	0.5
4	2.1	1.1	1.7	0.9	2.6	1.4	2.3	1.3
6	3.5	2.3	3.4	2.0	5.8	3.2	5.5	3.2
8	7.4	4.9	5.8	3.5	10.5	6.0	9.3	6.2
10	8.4	6.3	9.1	5.9	-	-	-	-

Penetration p (mm)	Q m^3/km	S.E MJ/m^3	Q m^3/km	S.E MJ/m^3	Q m^3/km	S.E MJ/m^3	Q m^3/km	S.E MJ/m^3
2	0.005	143.5	0.006	55.01	0.006	92.64	0.005	93.85
4	0.031	69.61	0.024	37.96	0.024	54.97	0.027	54.51
6	0.074	31.64	0.086	23.95	0.066	48.62	0.059	55.70
8	0.149	33.22	0.128	27.00	0.151	42.49	0.124	54.04
10	0.242	26.22	0.272	22.13	-	-	-	-
10	0.150*	42.49*	-	-	-	-	-	-

* Two sets of readings were obtained for Gypsum at 10mm of penetration, since the spaces between the tooth became packed with debris.

Appendix 23B

Results of Spacing Experiments with a Gear Cutter

Bunter Sandstone

d (mm)	S (mm)	F'T kN	$\overline{FT}$ kN	F'R kN	$\overline{FR}$ kN	Q m^3/km	S.E MJ/m^3
10	-20	7.6	5.1	2.2	1.2	0.033	34.530
10	-10	11.8	8.0	3.3	1.7	0.087	20.500
10	0	19.6	14.3	5.7	3.4	0.197	17.130
10	10	24.0	16.8	6.9	4.0	0.261	15.490
10	20	35.0	25.9	9.9	5.8	0.286	20.341

Mansfield Sandstone

d (mm)	S (mm)	F'T kN	$\overline{FT}$ kN	F'R kN	$\overline{FR}$ kN	Q m^3/km	S.E MJ/m^3
8	-20	12.0	8.7	3.2	1.9	0.042	45.91
8	-10	12.1	7.4	2.6	1.3	0.051	25.55
8	0	24.5	23.5	7.4	4.7	0.118	39.60
8	10	31.4	24.7	8.7	5.4	0.122	43.37
8	20	31.9	26.5	9.2	5.9	0.110	53.94

Dunhouse Sandstone

d (mm)	S (mm)	F'T kN	$\overline{FT}$ kN	F'R kN	$\overline{FR}$ kN	Q m^3/km	S.E MJ/m^3
8	-20	11.7	8.0	3.2	1.7	0.018	90.36
8	-10	21.0	13.1	5.7	2.7	0.055	48.88
8	0	26.3	18.7	7.0	3.9	0.110	35.74
8	10	29.0	22.5	8.3	4.6	0.169	26.85
8	20	35.0	27.0	9.7	5.5	0.183	29.72

APPENDIX 24A

Results of Single Pick Experiment in Anhydrite

Test No.	Levels of d (mm)	W (mm)	α (o)	Cutting Forces: Measured Values F'C (kN)	Measured Values $\overline{FC}$ (kN)	Predicted Values F'C (kN)	Predicted Values $\overline{FC}$ (kN)
1	1.5	10	-10	1.46	0.70	2.02	0.71
2	4.5	20	-10	6.75	3.08	6.15	2.84
3	7.5	30	-10	13.25	6.00	12.20	6.32
4	3.0	40	-10	6.24	3.02	7.08	3.75
5	6.0	50	-10	15.94	9.72	14.56	8.25
6	3.0	20	0	3.68	1.40	4.28	1.92
7	6.0	30	0	8.67	4.57	9.57	4.89
8	1.5	40	0	5.46	2.35	4.25	2.14
9	4.5	50	0	10.04	5.90	10.91	6.08
10	7.5	10	0	6.21	3.17	6.42	2.43
11	4.5	30	10	8.50	3.22	7.17	3.60
12	7.5	40	10	13.44	8.53	13.51	7.32
13	3.0	50	10	7.57	4.24	7.58	4.11
14	6.0	10	10	5.81	1.86	5.04	1.88
15	1.5	20	10	1.74	0.82	2.57	1.10
16	6.0	40	20	10.79	6.50	10.60	5.66
17	1.5	50	20	5.05	2.77	4.55	2.35
18	4.5	10	20	4.20	1.25	3.77	1.38
19	7.5	20	20	9.82	3.66	8.16	3.75
20	3.0	30	20	6.22	2.51	4.99	2.44
21	7.5	50	30	13.03	6.02	14.46	8.03
22	3.0	10	30	2.99	1.34	2.62	0.94
23	6.0	20	30	5.20	2.70	6.40	2.90
24	1.5	30	30	3.40	1.98	2.99	1.39
25	4.5	40	30	4.43	1.57	7.95	4.17

Appendix 24B

Results of Single Pick Experiment in Anhydrite

Test No.	Levels of d (mm)	W (mm)	α (o)	Normal Forces: Measured Values F'N (kN)	Measured Values $\overline{FN}$ (kN)	Predicted Values F'N (kN)	Predicted Values $\overline{FN}$ (kN)
1	1.5	10	-10	1.56	0.90	1.49	0.65
2	4.5	20	-10	5.41	3.35	6.98	4.44
3	7.5	30	-10	17.45	11.70	16.14	11.45
4	3.0	40	-10	6.14	3.81	8.75	5.98
5	6.0	50	-10	21.19	15.61	20.67	15.40
6	3.0	20	0	3.09	1.61	4.77	2.91
7	6.0	30	0	9.42	5.32	13.01	9.12
8	1.5	40	0	6.91	4.65	4.70	2.84
9	4.5	50	0	13.80	10.22	15.71	11.46
10	7.5	10	0	6.02	2.73	6.64	3.55
11	4.5	30	10	10.48	5.53	9.89	6.78
12	7.5	40	10	24.60	22.73	20.89	15.40
13	3.0	50	10	9.25	5.77	10.74	7.51
14	6.0	10	10	3.96	2.34	5.35	2.82
15	1.5	20	10	1.60	0.96	2.56	1.38
16	6.0	40	20	21.51	13.39	16.84	12.26
17	1.5	50	20	8.42	5.70	5.77	3.56
18	4.5	10	20	5.00	2.32	4.07	2.10
19	7.5	20	20	13.62	8.11	11.39	7.50
20	3.0	30	20	7.77	4.86	6.76	4.44
21	7.5	50	30	20.82	13.88	25.64	19.36
22	3.0	10	30	5.03	2.75	2.78	1.38
23	6.0	20	30	8.48	5.43	9.18	5.97
24	1.5	30	30	4.80	3.76	3.63	2.11
25	4.5	40	30	3.76	1.71	12.80	9.12

Appendix. 24C

Results of Single Pick Experiment in Anhydrite

Test No.	Levels of d (mm)	W (mm)	∝ (o)	Yield, Specific Energy: Measured Values Q (m^3/km)	S.E (MJ/m^3)	Predicted Values Q (m^3/km)	S.E (MJ/m^3)
1	1.5	10	-10	0.0171	34.54	0.0227	31.28
2	4.5	20	-10	0.1130	23.27	0.1105	25.70
3	7.5	30	-10	0.3014	22.75	0.3495	18.08
4	3.0	40	-10	0.1130	31.36	0.1022	36.69
5	6.0	50	-10	0.3322	26.83	0.3490	23.64
6	3.0	20	0	0.0685	25.49	0.0623	30.82
7	6.0	30	0	0.2260	22.89	0.2349	20.82
8	1.5	40	0	0.0480	45.38	0.0548	39.05
9	4.5	50	0	0.2089	27.42	0.2167	28.06
10	7.5	10	0	0.1781	16.09	0.1798	13.52
11	4.5	30	10	0 1370	23.48	0.1459	24.67
12	7.5	40	10	0.2808	22.25	0.4343	16:85
13	3.0	50	10	0.1301	29.35	0.1222	33.63
14	6.0	10	10	0.1027	15.80	0.1209	15.55
15	1.5	20	10	0.0377	37.23	0.0334	32.93
16	6.0	40	20	0.2911	21.87	0.2920	19.38
17	1.5	50	20	0.0685	43.01	0.0655	35.88
18	4.5	10	20	0.0925	15.80	0.0751	18.38
19	7.5	20	20	0.2397	17.67	0.2647	14.17
20	3.0	30	20	0.0925	25.14	0.0822	29.68
21	7.5	50	30	0.5548	20.79	0.5191	15.47
22	3.0	10	30	0.0480	17.70	0.0423	22.22
23	6.0	20	30	0.1678	17.34	0.1779	16.30
24	1.5	30	30	0.0514	35.04	0.0441	31.52
25	4.5	40	30	0.2123	21.99	0.1813	23.00

Appendix 24D

Single Pick Experiment in Anhydrite

Means Derived for Plotting Graphs

Variable		F'C kN	$\overline{FC}$ kN	F'N kN	$\overline{FN}$ kN	Q m^3/km	S.E MJ/m^3
		W = 30mm $\alpha = 10^\circ$					
Depth of cut d(mm)	1.5	3.40	1.70	4.66	3.20	0.0445	37.67
	3.0	5.34	2.50	4.30	3.30	0.0890	27.04
	4.5	6.80	3.00	7.70	4.60	0.1507	20.148
	6.0	9.30	5.10	12.90	4.80	0.2226	20,73
	7.5	11.20	5.50	16.50	11.80	0.2705	20.15
		d = 4.5mm $\alpha = 10^\circ$					
Width of Tool W(mm)	10	4.10	1.60	4.31	2.20	0.0890	23.36
	20	5.40	2.30	6.40	3.90	0.1233	20.15
	30	8.00	3.70	10.00	6.20	0.1473	25.70
	40	8.07	4.40	12.60	9.30	0.1884	26.57
	50	10.30	5.70	14.70	10.20	0.2158	29.78
		d = 4.5mm W = 30mm					
Rake Angle α(o)	-10	8.70	4.50	10.35	7.10	0.1747	28.32
	0	6.80	3.50	7.80	4.90	0.1473	27.16
	10	7.40	3.70	10.00	7.50	0.1370	25.40
	20	7.20	3.30	11.30	6.90	0.1575	23.07
	30	5.80	2.70	8.60	5.50	0.1644	21.61

Appendix 25A

Results of Single Pick Experiment in Limestone

Test No.	Levels of			Cutting Forces			
				Measured Values		Predicted Values	
	d (mm)	W (mm)	α (o)	F'C (kN)	$\overline{FC}$ (kN)	F'C (kN)	$\overline{FC}$ (kN)
1	1.5	10	0	2.715	1.594	1.841	0.860
2	4.5	15	0	9.683	3.548	10.437	4.716
3	7.5	20	0	18 707	7.406	21.152	9.833
4	3.0	25	0	7.442	3.622	7.869	3.864
5	6.0	30	0	15.254	7.114	20.173	9.927
6	3.0	15	-5	5.674	2.612	6.847	3.194
7	6.0	20	-5	20.469	9.941	17.964	8.525
8	1.5	25	-5	3.868	2.247	2.887	1.548
9	4.5	30	-5	16.738	8.325	15.739	7.930
10	7.5	10	-5	18.08	9.199	17.877	7.721
11	4.5	20	-10	12.479	5.110	14.016	6.810
12	7.5	25	-10	21.314	9.450	28.044	13.896
13	3.0	30	-10	8.696	3.895	10.325	5.371
14	6.0	10	-10	11.902	4.121	15.183	6.694
15	1.5	15	-10	3.085	1.734	2.512	1.280
16	6.0	25	-15	20.021	11.356	23.817	12.049
17	1.5	30	-15	4.378	2.676	3.789	2.152
18	4.5	10	-15	10.734	4.348	11.846	5.347
19	7.5	15	-15	28.95	12.835	24.402	11.488
20	3.0	20	-15	8.207	3.912	9.145	4.613
21	7.5	30	-20	40.155	22.490	36.80	19.318
22	3.0	10	-20	5.625	2.717	7.77	3.622
23	6.0	15	-20	21.286	10.41	20.72	9.961
24	1.5	20	-20	4.304	2.402	3.374	1.848
25	4.5	25	-20	19.853	10.603	18.582	9.625

Appendix 25B

Results of Single Pick Experiment in Limestone

Test No	Levels of			Normal Forces			
				Measured Values		Predicted Values	
	d (mm)	W (mm)	α (o)	F'N (kN)	$\overline{FN}$ (kN)	F'N (kN)	$\overline{FN}$ (kN)
1	1.5	10	0	2.378	1.850	1.287	0.802
2	4.5	15	0	4.234	2.478	5.488	3.293
3	7.5	20	0	12.472	7.597	11.035	6.691
4	3.0	25	0	5.070	3.437	4.725	2.996
5	6.0	30	0	7.188	4.007	11.282	7.076
6	3.0	15	-5	3.616	2.273	3.860	2.450
7	6.0	20	-5	9.992	5.416	9.574	6.070
8	1.5	25	-5	3.130	2.334	2.286	1.593
9	4.5	30	-5	8.657	5.153	9.106	5.991
10	7.5	10	-5	8.312	4.500	8.564	5.113
11	4.5	20	-10	6.116	3.366	7.272	5.063
12	7.5	25	-10	9.521	5.502	15.206	10.007
13	3.0	30	-10	5.126	3.060	6.406	4.394
14	6.0	10	-10	5.367	2.888	7.430	4.569
15	1.5	15	-10	2.214	1.632	1.867	1.283
16	6.0	25	-15	14.230	11.356	13.192	8.837
17	1.5	30	-15	2.991	2.227	3.099	2.273
18	4.5	10	-15	5.239	3.268	5.967	3.766
19	7.5	15	-15	8.756	5.150	12.422	7.965
20	3.0	20	-15	4.294	2.696	5.435	3.666
21	7.5	30	-20	28.499	20.553	20.613	13.971
22	3.0	10	-20	3.428	2.156	4.218	2.701
23	6.0	15	-20	14.735	8.770	10.777	6.966
24	1.5	20	-20	2.971	2.095	2.629	1.879
25	4.5	25	-20	13.564	8.500	10.648	7.213

Appendix 25C

Results of Single Pick Experiment in Limestone

Test No.	Levels of			Yield, Specific Energy, Coarseness Index					
				Measured Values			Predicted Values		
	d (mm)	W (mm)	α (o)	Q (m^3/km)	S.E (MJ/m^3)	C.I	Q (m^3/km)	S.E (MJ/m^3)	C.I
1	1.5	10	0	0.0164	97.20	324	0.0248	34.68	330
2	4.5	15	0	0.1064	33.67	437	0.0899	52.46	429
3	7.5	20	0	0.2429	30.48	473	0.2505	39.25	463
4	3.0	25	0	0.0820	44.17	386	0.0760	50.84	396
5	6.0	30	0	0.2351	30.33	445	0.2306	43.05	449
6	3.0	15	-5	0.0508	51.27	380	0.0534	59.81	391
7	6.0	20	-5	0.1810	55.00	433	0.1708	49.91	443
8	1.5	25	-5	0.0393	57.80	316	0.0448	34.55	323
9	4.5	30	-5	0.1633	50.96	420	0.1470	53.27	423
10	7.5	10	-5	0.2000	46.00	470	0.1629	47.40	456
11	4.5	20	-10	0.1143	44.75	424	0.1089	62.53	417
12	7.5	25	-10	0.2541	37.14	453	0.2943	47.22	449
13	3.0	30	-10	0.0971	40.15	390	0.0873	61.52	385
14	6.0	10	-10	0.1315	31.72	452	0.1111	60.25	436
15	1.5	15	-10	0.0239	72.55	327	0.0315	40.63	321
16	6.0	25	-15	0.2050	55.69	440	0.2007	60.03	430
17	1.5	30	-15	0.0464	55.67	308	0.0515	41.79	316
18	4.5	10	-15	0.0774	58.45	421	0.0708	75.52	411
19	7.5	15	-15	0.2300	55.88	456	0.2067	55.58	443
20	3.0	20	-15	0.0653	59.91	377	0.0647	71.30	379
21	7.5	30	-20	0.3224	69.76	388	0.3381	57.14	436
22	3.0	10	-20	0.0370	73.57	387	0.0421	86.03	274
23	6.0	15	-20	0.1508	70.34	423	0.1410	70.65	424
24	1.5	20	-20	0.0314	76.50	322	0.0381	48.50	311
25	4.5	25	-20	0.1332	79.63	395	0.1279	75.25	405

Appendix 25D

Single Pick Experiment in Limestone

Means Derived for Plotting Graph

Variable		F'C kN	$\overline{FC}$ kN	F'N kN	$\overline{FN}$ kN	Q m^3/km	S.E MJ/m^3	C.I
		W = 20 mm $\alpha = -10^\circ$						
Depth of Cut d (mm)	1.5	3.670	2.131	2.737	2.028	0.0315	71.944	319
	3.0	7.129	3.352	4.307	2.724	0.0664	53.814	384
	4.5	13.897	6.387	7.562	4.553	0.1189	53.492	419
	6.0	17.786	10.736	10.308	6.487	0.1807	48.615	439
	7.5	25.441	12.276	13.512	8.660	0.2499	47.850	448
		d = 4.5mm $\alpha = -10^\circ$						
Width of tool W(mm)	10	9.811	4.396	4.945	2.932	0.0925	61.385	411
	15	13.736	6.228	6.711	4.061	0.1124	56.742	405
	20	12.833	5.754	7.169	4.234	0.1270	53.329	406
	25	14.500	7.456	9.103	6.226	0.1427	54.886	398
	30	17.044	8.900	10.492	7.000	0.1728	49.374	390
		d = 4.5mm W = 20mm						
Rake Angle $\alpha(^\circ)$	0	10.760	4.657	6.268	3.874	0.1366	47.171	413
	-5	12.966	6.465	6.741	3.935	0.1269	52.205	403
	-10	11.500	4.862	5.669	3.290	0.1242	45.261	409
	-15	14.458	7.025	7.102	4.439	0.1248	57.118	400
	-20	18.245	9.724	12.639	8.415	0.1350	73.960	383

Appendix 26A

Results of Single Pick Experiment in Greywacke

Test No.	Levels of d (mm)	W (mm)	α (o)	Cutting Forces: Measured Values F'C (kN)	Measured Values $\overline{FC}$ (kN)	Predicted Values F'C (kN)	Predicted Values $\overline{FC}$ (kN)
1	1.5	10	0	3.03	1.03	2.15	0.82
2	4.5	15	0	8.01	3.18	9.72	4.36
3	7.5	20	0	15.29	9.55	18.57	8.72
4	3.0	25	0	7.44	3.25	7.09	3.28
5	6.0	30	0	13.35	6.13	16.90	8.27
6	3.0	15	-5	5.97	2.83	6.77	3.06
7	6.0	20	-5	16.15	7.39	16.34	7.88
8	1.5	25	-5	3.89	2.30	3.10	1.34
9	4.5	30	-5	11.11	5.60	13.75	6.88
10	7.5	10	-5	20.79	10.11	17.50	7.93
11	4.5	20	-10	10.56	4.15	13.29	6.56
12	7.5	25	-10	20.72	8.37	25.24	12.98
13	3.0	30	-10	9.22	4.01	9.58	4.83
14	6.0	10	-10	10.84	4.07	15.40	7.17
15	1.5	15	-10	3.79	1.81	2.96	1.25
16	6.0	25	-15	26.08	14.54	22.21	11.73
17	1.5	30	-15	5.96	2.54	4.19	1.97
18	4.5	10	-15	12.30	5.53	12.52	5.97
19	7.5	15	-15	33.84	15.55	24.12	12.12
20	3.0	20	-15	10.05	5.14	9.26	4.61
21	7.5	30	-20	30.62	16.80	34.12	19.12
22	3.0	10	-20	6.38	2.94	8.73	4.19
23	6.0	15	-20	18.20	10.34	21.22	10.95
24	1.5	20	-20	4.69	2.37	4.05	1.88
25	4.5	25	-20	15.46	9.32	18.07	9.76

Appendix 26B

Results of Single Pick Experiment in Greywacke.

Test No.	Levels of d (mm)	W (mm)	α (o)	Normal Forces: Measured Values F'N (kN)	Measured Values $\overline{FN}$ (kN)	Predicted Values F'N (kN)	Predicted Values $\overline{FN}$ (kN)
1	1.5	10	0	2.57	1.26	2.18	1.38
2	4.5	15	0	5.17	3.00	5.67	3.26
3	7.5	20	0	6.13	5.00	9.91	5.56
4	3.0	25	0	5.90	3.61	5.00	3.02
5	6.0	30	0	9.15	4.69	9.80	5.63
6	3.0	15	-5	5.04	3.99	4.75	2.95
7	6.0	20	-5	9.93	5.74	9.48	5.62
8	1.5	25	-5	4.40	3.39	3.53	2.40
9	4.5	30	-5	8.59	6.48	8.91	5.46
10	7.5	10	-5	11.53	7.46	9.18	5.28
11	4.5	20	-10	6.93	3.05	8.63	5.44
12	7.5	25	-10	10.59	6.63	14.91	9.15
13	3.0	30	-10	7.24	3.95	7.46	4.93
14	6.0	10	-10	5.68	2.83	8.78	5.33
15	1.5	15	-10	4.14	3.16	3.35	2.34
16	6.0	25	-15	18.52	11.79	14.26	9.27
17	1.5	30	-15	4.78	2.82	5.27	3.92
18	4.5	10	-15	8.44	5.00	7.99	5.17
19	7.5	15	-15	16.86	6.87	14.15	8.95
20	3.0	20	-15	7.34	4.52	7.22	4.92
21	7.5	30	-20	24.53	17.28	22.22	14.98
22	3.0	10	-20	5.54	4.39	6.69	4.67
23	6.0	15	-20	14.38	11.83	13.53	9.05
24	1.5	20	-20	4.57	3.80	5.10	3.91
25	4.5	25	-20	12.66	10.88	12.97	8.98

Appendix 26C

Results of Single Pick Experiment in Greywacke

Test No.	Levels of d (mm)	W (mm)	∝ (o)	Yield, Specific Energy and Coarseness Index — Measured Values Q (m^3/km)	S.E (MJ/m^3)	C.I	Predicted Values Q (m^3/km)	S.E (MJ/m^3)	C.I
1	1.5	10	0	0.0169	61.49	309	0.0275	29.82	317
2	4.5	15	0	0.1022	31.80	426	0.1067	40.86	406
3	7.5	20	0	0.2079	29.56	465	0.2916	29.90	428
4	3.0	25	0	0.0809	40.00	370	0.0765	42.82	369
5	6.0	30	0	0.2599	23.60	430	0.2436	33.95	409
6	3.0	15	-5	0.0509	55.16	367	0.0600	51.00	377
7	6.0	20	-5	0.2101	35.22	420	0.1959	40.22	418
8	1.5	25	-5	0.0393	58.52	302	0.0408	32.84	307
9	4.5	30	-5	0.1532	36.79	407	0.1510	45.56	393
10	7.5	10	-5	0.1899	53.69	458	0.2206	35.95	437
11	4.5	20	-10	0.1288	32.28	412	0.1215	53.99	401
12	7.5	25	-10	0.2532	32.63	441	0.3271	39.68	424
13	3.0	30	-10	0.1022	39.65	375	0.0849	56.89	365
14	6.0	10	-10	0.1419	28.76	437	0.1482	48.38	426
15	1.5	15	-10	0.0243	74.64	313	0.0319	39.18	314
16	6.0	25	-15	0.2255	64.56	423	0.2198	53.37	413
17	1.5	30	-15	0.0468	54.33	291	0.0452	43.58	304
18	4.5	10	-15	0.0873	64.51	411	0.0919	64.96	410
19	7.5	15	-15	0.2689	42.48	437	0.2561	47.33	433
20	3.0	20	-15	0.0670	76.58	461	0.0683	67.50	373
21	7.5	30	-20	0.3124	53.88	374	0.3626	52.73	419
22	3.0	10	-20	0.0745	66.06	373	0.0517	81.04	381
23	6.0	15	-20	0.3285	61.38	410	0.1721	63.63	422
24	1.5	20	-20	0.0318	74.69	311	0.0364	51.65	310
25	4.5	25	-20	0.1300	71.53	381	0.1362	71.66	397

Appendix 26D

Single Pick Experiment in Greywacke

Means Derived for Plotting Graphs

Variable		$F'C$ kN	$\overline{FC}$ kN	$F'N$ kN	$\overline{FN}$ kN	Q m^3/km	S.E MJ/m^3	C.I
		W = 20mm $\alpha = -10^\circ$						
Depth of Cut d(mm)	1.5	4.27	2.01	4.09	2.89	0.0318	64.73	305
	3.0	7.81	3.63	6.21	4.09	0.0751	55.49	389
	4.5	11.49	5.56	8.36	5.68	0.1203	47.38	407
	6.0	16.92	8.49	11.53	7.38	0.2332	42.70	424
	7.5	24.25	12.08	13.93	8.65	0.2465	42.45	435
		d = 4.5mm $\alpha = -10^\circ$						
Width of Tool W(mm)	10	10.67	4.74	6.75	4.19	0.1021	54.90	398
	15	13.96	6.74	9.12	5.77	0.1550	53.09	391
	20	11.35	5.72	6.98	4.42	0.1291	49.66	414
	25	14.72	7.56	10.41	7.26	0.1458	53.45	383
	30	14.05	7.02	10.86	7.04	0.1750	41.65	375
		d = 4.5mm W = 20mm						
Rake Angle α (o)	0	9.43	4.63	5.78	3.51	0.1336	37.29	400
	-5	11.58	5.65	7.90	5.41	0.1287	47.88	391
	-10	11.03	4.48	6.92	3.92	0.1301	41.59	396
	-15	17.65	8.66	11.19	6.20	0.1391	60.49	405
	-20	15.07	8.35	12.34	9.64	0.1754	65.51	370

Appendix 27A

Results of Single Pick Experiment in Granite

Test No.	Levels of			Cutting Forces			
				Measured Values		Predicted Values	
	d (mm)	W (mm)	α (o)	F'C (kN)	$\overline{FC}$ (kN)	F'C (kN)	$\overline{FC}$ (kN)
1	1	10	0	2.064	1.284	2.319	1.362
2	3	15	0	7.448	3.659	6.809	3.442
3	5	20	0	12.936	6.034	12.466	6.280
4	2	25	0	7.346	4.859	6.109	3.764
5	4	30	0	11.995	6.987	12.641	7.169
6	2	15	-5	4.808	2.394	5.221	2.831
7	4	20	-5	10.413	5.752	11.111	5.716
8	1	25	-5	3.800	2.850	3.812	2.770
9	3	30	-5	10.473	6.584	10.663	6.273
10	5	10	-5	10.488	4.592	10.277	4.335
11	3	20	-10	10.526	5.618	9.372	5.002
12	5	25	-10	17.510	7.798	16.892	8.818
13	2	30	-10	8.082	4.810	8.177	5.159
14	4	10	-10	8.300	3.500	9.160	3.946
15	1	15	-10	3.102	1.764	3.258	2.083
16	4	25	-15	15.712	9.043	15.056	8.027
17	1	30	-15	4.500	3.400	5.103	3.796
18	3	10	-15	6.099	2.672	7.727	3.453
19	5	15	-15	14.511	6.658	14.438	6.632
20	2	20	-15	7.387	4.127	7.187	4.114
21	5	30	-20	21.426	11.887	22.610	12.085
22	2	10	-20	6.692	3.475	5.925	2.840
23	4	15	-20	13.582	6.976	12.869	6.037
24	1	20	-20	4.762	2.920	4.485	3.027
25	3	25	-20	13.185	7.058	12.700	7.023

Appendix 27B

Results of Single Pick Experiment in Granite

Test No.	Levels of d (mm)	W (mm)	∝ (o)	Normal Forces			
				Measured Values		Predicted Values	
				F'N (kN)	$\overline{FN}$ (kN)	F'N (kN)	$\overline{FN}$ (kN)
1	1	10	0	2.792	2.072	2.936	2.514
2	3	15	0	6.225	4.692	5.783	4.524
3	5	20	0	9.675	7.529	9.541	7.108
4	2	25	0	9.849	8.409	7.045	5.593
5	4	30	0	11.399	8.581	11.487	8.608
6	2	15	-5	4.351	3.871	4.985	4.027
7	4	20	-5	8.856	7.012	8.647	6.562
8	1	25	-5	5.400	4.100	5.821	4.839
9	3	30	-5	11.034	7.732	10.193	7.821
10	5	10	-5	4.530	4.172	6.157	4.706
11	3	20	-10	8.665	6.351	7.673	5.954
12	5	25	-10	10.031	6.475	12.208	9.047
13	2	30	-10	8.706	7.423	9.786	6.951
14	4	10	-10	5.700	4.300	5.580	4.338
15	1	15	-10	3.217	2.676	4.119	3.479
16	4	25	-15	11.944	9.160	11.064	8.329
17	1	30	-15	6.200	5.200	7.260	5.998
18	3	10	-15	4.172	3.457	4.951	3.932
19	5	15	-15	10.776	8.015	8.638	6.496
20	2	20	-15	6.325	4.527	6.614	5.285
21	5	30	-20	13.103	9.018	15.255	11.186
22	2	10	-20	4.787	3.665	4.268	3.486
23	4	15	-20	9.650	7.340	7.829	5.973
24	1	20	-20	4.525	3.962	5.465	4.555
25	2	25	-20	11.800	10.010	9.818	7.540

Appendix 27C

Results of Single Pick Experiment in Granite

Test No.	Levels of d (mm)	W (mm)	∝ (°)	Cutting Forces kN					
				$F'C_2$	$F'C_3$	$F'C_4$	$\overline{FC}_2$	$\overline{FC}_3$	$\overline{FC}_4$
1	1	10	0	2.363	1.845	3.241	1.229	1.129	2.100
2	3	15	0	8.090	7.750	9.234	3.881	4.241	4.313
3	5	20	0	13.196	15.587	15.451	7.399	8.275	7.782
4	2	25	0	8.146	8.252	8.925	5.008	5.433	6.164
5	4	30	0	14.847	14.964	14.363	8.555	8.947	8.379
6	2	15	-5	4.891	5.582	6.052	2.786	3.178	3.872
7	4	20	-5	12.297	12.513	12.569	7.413	7.999	8.500
8	1	25	-5	4.824	5.705	6.300	3.405	3975	4.200
9	3	30	-5	9.761	10.987	11.795	5.712	7.224	7.038
10	5	10	-5	12.101	13.000	13.450	4.314	5.000	5.200
11	3	20	-10	10.957	10.654	11.636	5.923	6.173	7.470
12	5	25	-10	17.445	20.648	21.200	8.809	9.822	10.000
13	2	30	-10	7.974	9.189	9.924	4.924	5.863	6.723
14	4	10	-10	8.426	8.917	9.200	3.688	3.692	3.810
15	1	15	-10	3.454	3.700	4.004	1.971	2.200	2.618
16	4	25	-15	13.900	13.906	14.681	8.100	8.149	8.925
17	1	30	-15	4.916	6.218	6.617	3.688	4.588	4.978
18	3	10	-15	6.205	5.956	6.477	2.665	2.571	3.092
19	5	15	-15	15.640	15.527	14.613	7.454	7.512	7.658
20	2	20	-15	6.133	9.034	8.241	3.745	5.494	4.789
21	5	30	-20	17.550	27.417	28.992	9.709	15.728	14.464
22	2	10	-20	5.352	5.600	6.065	2.718	3.000	3.271
23	4	15	-20	16.452	14.741	14.700	8.823	8.226	8.200
24	1	20	-20	4.798	6.076	5.194	2.940	4.301	3.790
25	3	25	-20	11.859	12.293	12.660	7.058	6.839	7.362

Appendix 27D

Results of Single Pick Experiment in Granite

Test No.	Levels of d (mm)	W (mm)	α (o)	Normal Forces kN $F'N_2$	$F'N_3$	$\overline{F'N_4}$	$\overline{FN_2}$	$\overline{FN_3}$	$\overline{FN_4}$
1	1	10	0	3.134	2.440	4.000	2.582	2.006	3.250
2	3	15	0	7.630	9.122	9.932	5.960	6.482	7.631
3	5	20	0	11.156	13.398	13.594	7.594	9.542	9.524
4	2	25	0	11.424	12.854	14.246	9.522	10.849	12.830
5	4	30	0	16.594	17.898	18.211	13.243	14.422	14.427
6	2	15	-5	5.772	7.688	6.054	4.564	6.316	7.388
7	4	20	-5	10.834	11.911	14.358	10.100	9.781	11.553
8	1	25	-5	6.780	9.024	10.673	5.294	7.482	8.815
9	3	30	-5	12.491	15.601	16.412	10.731	13.347	13.071
10	5	10	-5	7.742	8.300	8.500	5.348	6.000	6.200
11	3	20	-10	11.541	13.353	14.092	9.460	10.879	10.423
12	5	25	-10	12.917	14.467	15.200	9.315	10.526	11.000
13	2	30	-10	11.079	13.635	14.017	9.037	11.012	11.739
14	4	10	-10	6.819	7.264	7.420	4.824	5.006	5.200
15	1	15	-10	4.445	4.800	5.321	3.423	3.200	3.968
16	4	25	-15	12.900	13.299	15.032	11.200	11.491	11.620
17	1	30	-15	6.682	8.881	9.604	5.778	7.596	8.369
18	3	10	-15	4.850	5.228	5.689	3.623	3.645	4.684
19	5	15	-15	11.387	13.602	13.847	9.404	10.200	11.391
20	2	20	-15	7.227	10.053	10.111	6.155	8.029	8.198
21	5	30	-20	13.699	18.477	19.682	9.084	13.088	12.883
22	2	10	-20	5.531	6.300	6.799	4.209	5.000	5.391
23	4	15	-20	13.045	11.977	13.412	10.350	9.214	10.101
24	1	20	-20	6.138	7.530	8.636	5.360	6.583	7.896
25	3	25	-20	11.965	13.519	14.487	10.010	9.466	11.852

Appendix 27E

Results of Single Pick Experiment in Granite

Test No.	Levels of d (mm)	W (mm)	α (o)	Yield, Specific Energy, Coarseness Index — Measured Values Q (m^3/km)	S.E_3 (MJ/m^3)	C.I.	Predicted Values Q (m^3/km)	S.E_3 (MJ/m^3)	C.I
1	1	10	0	0.0104	123.34	232	0.0119	114.45	201
2	3	15	0	0.0531	68.91	345	0.0459	74.99	310
3	5	20	0	0.1115	54.18	391	0.1347	46.62	346
4	2	25	0	0.0515	94.42	283	0.0438	85.94	274
5	4	30	0	0.1258	55.54	353	0.1338	53.58	332
6	2	15	-5	0.0315	76.10	277	0.0277	102.20	271
7	4	20	-5	0.0874	65.84	352	0.0923	61.93	328
8	1	25	-5	0.0253	112.74	230	0.0264	104.77	199
9	3	30	-5	0.0929	70.84	305	0.0860	72.94	307
10	5	10	-5	0.0732	62.73	384	0.0740	58.58	342
11	3	20	-10	0.0617	91.05	324	0.0593	84.35	303
12	5	25	-10	0.1300	59.98	380	0.1650	53.44	338
13	2	30	-10	0.0617	77.95	378	0.0518	99.59	267
14	4	10	-10	0.0480	72.98	344	0.0507	77.83	324
15	1	15	-10	0.0154	110.32	236	0.0167	124.73	197
16	4	25	-15	0.1041	86.87	338	0.1130	71.04	320
17	1	30	-15	0.0304	114.32	211	0.0313	121.28	194
18	3	10	-15	0.0320	83.58	315	0.0326	105.92	299
19	5	15	-15	0.0997	66.77	380	0.1043	63.59	334
20	2	20	-15	0.0431	96.71	287	0.0357	115:24	264
21	5	30	-20	0.1692	70.27	367	0.1953	61.88	330
22	2	10	-20	0.0229	152.01	281	0.0196	144.90	261
23	4	15	-20	0.0672	103.82	340	0.0715	84.43	316
24	1	20	-20	0.0204	142.82	219	0.0216	140.14	192
25	3	25	-20	0.0781	90.41	311	0.0726	96.74	295

Appendix 27F

Single Pick Experiment in Granite
Means Derived for Plotting Graphs

Variable		F'C kN	$\overline{FC}$ kN	F'N kN	$\overline{FN}$ kN	Q m^3/km	S.E. MJ/m^3
		W = 20mm $\alpha = -10^\circ$					
Depth of Cut d(mm)	1	3.65	2.44	4.43	3.60	0.0204	120.71 226
	2	6.86	2.93	6.80	5.58	0.0421	99.44 281
	3	9.55	5.12	8.38	6.45	0.0636	80.96 320
	4	12.00	6.45	9.51	7.28	0.0865	77.01 345
	5	15.37	7.39	9.62	7.04	0.1167	62.77 380
		d = 3mm $\alpha = -10^\circ$					
Width of Tool W (mm)	10	6.73	3.11	4.40	3.53	0.0373	98.93 311
	15	8.69	4.29	6.84	5.32	0.0534	85.18 316
	20	9.21	4.89	7.61	5.87	0.0648	90.11 315
	25	11.51	6.32	9.81	7.63	0.0778	88.88 308
	30	11.30	6.73	10.09	7.59	0.0960	77.78 303
		d = 3mm W = 20mm					
Rake Angle α(o)	0	8.36	4.57	7.99	6.26	0.0705	79.27 321
	-5	8.00	4.43	6.83	5.38	0.0620	77.65 310
	-10	9.50	4.70	7.26	5.45	0.0634	82.46 312
	-15	9.64	5.18	7.88	6.07	0.0619	89.65 306
	-20	11.93	6.46	8.77	6.80	0.0715	111.87 304

Appendix 28

Force Ratios

Test No.	Anhydrite $\overline{FC}/\overline{FN}$	Limestone $\overline{FC}/\overline{FN}$	Greywacke $\overline{FC}/\overline{FN}$	Granite $\overline{FC}/\overline{FN}$
1	0.78	0.86	0.82	0.62
2	0.92	1.43	1.06	0.78
3	0.51	0.97	1.91	0.80
4	0.79	1.05	0.90	0.58
5	0.62	1.78	1.31	0.81
6	0.82	1.15	0.71	0.62
7	0.87	1.84	1.29	0.82
8	0.51	0.96	0.68	0.70
9	0.58	1.62	0.86	0.85
10	1.16	2.04	1.36	1.10
11	0.58	1.52	1.36	0.88
12	0.36	1.72	1.26	1.20
13	0.73	1.27	1.02	0.65
14	0.79	1.43	1.44	0.81
15	0.85	1.06	0.57	0.66
16	0.49	1.00	1.23	0.99
17	0.49	1.20	0.90	0.65
18	0.54	1.33	1.11	0.77
19	0.45	2.49	2.26	0.83
20	0.52	1.45	1.14	0.91
21	0.44	1.09	0.97	1.32
22	0.49	1.26	0.67	0.95
23	0.50	1.19	0.87	0.95
24	0.53	1.15	0.62	0.74
25	0.92	1.25	0.86	0.71

Appendix 29A

Cutting Force Predictions using Evans' Theory

Test No.	Levels of d (mm)	W (mm)	α (o)	Anhydrite F'C(kN)	Levels of d (mm)	W (mm)	α (o)	Granite F'C(kN)
1	1.5	10	-10	0.54	1	10	0	0.52
2	4.5	20	-10	3.22	3	15	0	2.34
3	7.5	30	-10	8.06	5	20	0	5.20
4	3.0	40	-10	4.30	2	25	0	2.60
5	6.0	50	-10	10.74	4	30	0	6.24
6	3.0	20	0	1.58	2	15	-5	1.81
7	6.0	30	0	4.75	4	20	-5	4.84
8	1.5	40	0	1.58	1	25	-5	1.51
9	4.5	50	0	5.94	3	30	-5	5.44
10	7.5	10	0	1.98	5	10	-5	3.02
11	4.5	30	10	2.66	3	20	-10	4.23
12	7.5	40	10	5.91	2	25	-10	8.81
13	3.0	50	10	2.95	2	30	-10	4.23
14	6.0	10	10	1.18	4	10	-10	2.82
15	1.5	20	10	0.59	1	15	-10	1.06
16	6.0	40	20	3.53	4	25	-15	8.27
17	1.5	50	20	1.10	1	30	-15	2.48
18	4.5	10	20	0.66	3	10	-15	2.48
19	7.5	20	20	2.21	5	15	-15	6.20
20	3.0	30	20	1.32	2	20	-15	3.31
21	7.5	50	30	4.10	5	30	-20	14.64
22	3.0	10	30	0.33	2	10	-20	1.95
23	6.0	20	30	1.31	4	15	-20	5.86
24	1.5	30	30	0.49	1	20	-20	1.95
25	4.5	40	30	1.97	3	25	-20	7.32

Appendix 29B

Cutting Force Predictions using Evans' Theory

Test No.	Levels of d (mm)	W (mm)	α (o)	Limestone F'C(kN)	Greywacke F'C(kN)
1	1.5	10	0	0.55	1.19
2	4.5	15	0	2.46	5.36
3	7.5	20	0	5.46	11.90
4	3.0	25	0	2.73	5.95
5	6.0	30	0	6.55	14.29
6	3.0	15	-5	1.90	4.16
7	6.0	20	-5	5.08	11.08
8	1.5	25	-5	1.59	3.46
9	4.5	30	-5	5.71	12.47
10	7.5	10	-5	3.17	6.93
11	4.5	20	-10	4.44	9.69
12	7.5	25	-10	9.26	20.19
13	3.0	30	-10	4.44	9.69
14	6.0	10	-10	2.96	6.46
15	1.5	15	-10	1.11	2.42
16	6.0	25	-15	8.69	18.95
17	1.5	30	-15	2.61	5.69
18	4.5	10	-15	2.61	5.69
19	7.5	15	-15	6.51	14.21
20	3.0	20	-15	3.47	7.58
21	7.5	30	-20	15.37	33.54
22	3.0	10	-20	2.05	4.47
23	6.0	15	-20	6.15	13.42
24	1.5	20	-20	2.05	4.47
25	4.5	25	-20	7.69	16.77

Appendix 30A

Relieved Cutting Results in Anhydrite

$\alpha = 10^{o}$ W = 30mm

Spacing / Depth	F'C kN	$\overline{FC}$ kN	F'N kN	$\overline{FN}$ kN	Q m^3/km	S.E MJ/m^3	C.I
d = 3mm							
-0.5	3.947	1.942	1.832	1.157	0.0784	24.71	376
1.0	4.400	2.260	2.070	1.317	0.0890	25.31	373
2.5	4.731	2.440	2.089	1.381	0.0925	26.35	377
4.0	4.616	2.386	2.215	1.451	0.0914	26.03	373
5.5	4.558	2.764	2.285	1.560	0.089	31.01	370
Unr.	4.944	2.877	2.335	1.601	0.0928	30.98	373
d = 4.5mm							
-0.5	5.264	1.981	1.979	1.142	0.1219	16.23	408
1.0	6.162	2.481	2.424	1.496	0.1490	16.67	414
2.5	6.182	2.657	2.410	1.496	0.1572	16.88	416
4.0	6.514	2.743	2.489	1.657	0.1568	17.53	415
5.5	6.987	2.969	2.564	1.669	0.1538	19.30	410
Unr.	6.745	2.939	2.327	1.393	0.1558	18.85	408
d = 6mm							
-0.5	6.632	2.484	2.219	1.261	0.1531	16.31	435
1.0	7.496	2.985	2.585	1.532	0.2021	14.98	436
2.5	10.024	4.446	3.638	2.207	0.2182	20.36	430
4.0	9.981	4.490	3.446	2.074	0.2178	20.70	430
5.5	10.405	4.454	3.468	2.164	0.2151	20.74	420
Unr.	11.355	4.501	3.759	2.268	0.2151	20.93	423

Appendix 30B

Relieved Cutting Results in Weardale Limestone

$\alpha = -10^{\circ}$ W = 20mm

Spacing / Depth	F'C kN	$\overline{FC}$ kN	F'N kN	$\overline{FN}$ kN	Q m^3/km	S.E. MJ/m^3	C.I
			d = 3mm				
-0.5	3.722	1.515	1.741	0.924	0.0523	29.18	384
1.0	4.161	1.898	1.967	1.115	0.0662	28.95	388
2.5	4.431	2.025	2.061	1.181	0.0680	29.61	393
4.0	4.563	2.176	2.183	1.247	0.0673	32.31	397
5.5	4.704	2.131	2.227	1.206	0.0662	32.81	-
Unr.	4.581	2.174	2.184	1.200	0.0665	32.59	386
			d = 4.5mm				
-0.5	5.426	1.807	2.135	1.015	0.0870	20.81	433
1.0	5.433	2.063	2.389	1.266	0.1030	10.04	435
2.5	7.02	2.787	2.620	1.535	0.1214	23.56	439
4.0	7.583	3.160	3.022	1.702	0.1259	25.13	445
5.5	7.977	2.945	3.013	1.647	0.1233	24.41	456
Unr.	7.573	3.606	3.192	2.044	0.1267	28.43	434
			d = 6mm				
-0.5	6.600	1.995	2.545	1.263	0.1015	19.81	450
1.0	8.044	3.000	3.484	1.968	0.1400	21.43	442
2.5	10.069	4.436	4.471	2.598	0.1609	27.58	441
4.0	10.305	4.497	4.426	2.646	0.1778	26.33	467
5.5	10.847	4.678	4.049	2.352	0.1789	26.36	458
Unr.	11.768	4.660	4.131	2.457	0.1800	25.89	462

Appendix 30C

Relieved Cutting Results in Greywacke

$\alpha = -10^{\circ}$ W = 20mm

Spacing / Depth	F'C kN	$\overline{FC}$ kN	F'N kN	$\overline{FN}$ kN	Q m^3/km	S.E. MJ/m3	C.I
d = 3mm							
-0.5	5.948	2.449	3.358	2.075	0.0539	45.15	383
1.0	7.763	3.076	4.296	2.636	0.0640	48.11	381
2.5	7.348	3.299	4.653	2.763	0.0648	52.37	378
4.0	7.017	2.852	4.050	2.358	0.0592	48.90	377
5.5	7.890	3.504	4.907	2.894	0.0629	55.80	370
Unr.	8.244	3.526	4.471	2.797	0.0625	56.19	374
d = 4.5mm							
-0.5	8.270	2.585	3.694	2.005	0.0719	35.75	417
1.0	9.534	3.648	4.827	2.610	0.0966	37.66	411
2.5	9.647	4.176	5.593	3.057	0.1067	39.01	412
4.0	10.956	4.616	5.782	3.190	0.1041	44.30	409
5.5	10.444	4.453	5.015	3.322	0.1112	40.03	411
Unr.	10.394	4.652	5.290	2.796	0.1112	43.61	415
d = 6mm							
-0.5	8.709	2.273	3.840	2.110	0.0963	23.61	437
1.0	13.419	4.666	6.878	3.543	0.1551	30.02	433
2.5	14.258	4.822	7.148	3.909	0.1674	28.71	451
4.0	16.403	5.436	7.106	3.494	0.1835	29.57	453
5.5	14.345	5.729	8.070	4.815	0.1637	34.97	449
Unr.	16.471	5.817	7.775	3.933	0.1670	34.83	430

Appendix 31

Predictor Equation Constants for Pick Cutting

Rocks	Cutting Parameters	A	B	C $x10^{-2}$	D	E	Correlation Coefficient
Anhydrite	F'C	1.0642	14.7407	-0.4982	-3.4969	0	0.955
	$\overline{FC}$	0.7947	3.6930	-0.5670	-3.8458	0	0.932
	F'N	0.2433	0.0613	24.4150	0	0	0.904
	$\overline{FN}$	-0.1461	0.0537	-5.5152	0	0	0.866
	Q	5.5409	0.00014	0.1538	0	0	0.966
	C.I	-	-	-	-	-	-
Weardale Limestone	F'C	-0.7404	24.312	-1.7510	-2.6505	0	0.961
	$\overline{FC}$	-0.6632	14.152	-2.0926	-3.1689	0	0.938
	F'N	-0.3157	14.222	-1.8424	-3.1037	0	0.894
	$\overline{FN}$	-0.1921	10.2543	-0.0829	0.0298	-1	0.868
	Q	7.4452	0.00014	0.1182	0	0	0.985
	C.I	0.2492	1.0000	150.640	528.68	0	0.964
Greywacke	F'C	-0.5417	42.457	-2.2986	-3.1529	0	0.927
	$\overline{FC}$	-0.6863	26.475	-2.9506	-3.5919	0	0.918
	F'N	0.7963	28.452	-3.0977	-3.7026	0	0.932
	$\overline{FN}$	1.3112	25.192	-3.9566	-4.2717	0	0.910
	Q	5.4445	0.00012	0.0243	0	0	0.906
	C.I	0.1260	1.000	101.44	494.34	0	0.898
Granite	F'C	0.3174	20.167	-1.8656	-2.8411	0	0.989
	$\overline{FC}$	1.0809	7.299	-1.7126	-3.2747	0	0.977
	F'N	2.9155	6.457	-0.7333	-3.0887	0	0.913
	$\overline{FN}$	3.9847	7.580	-0.0073	1.1081	-3	0.850
	Q	3.5802	0.00021	0.00047	0	0	0.986
	C.I	-0.0377	1.000	110.41	462.49	0	0.928

Appendix 32A

Results of Wear Experiments

Cut Dist (m)	Weight loss (mg)	Wear Flat (mm)	F'C kN	$\overline{FC}$ kN	F'N kN	$\overline{FN}$ kN	m^3Q/km	S.E. MJ/m^3
Limestone								
Sharp	-	-	2.91	1.30	1.37	0.73	0.035	37.02
10	0.3	0.067	3.12	1.35	1.72	1.06	0.035	38.71
20	0.4	0.082	2.88	1.33	1.82	1.15	0.034	39.61
30	0.7	0.095	2.77	1.24	1.75	1.09	0.033	38.00
50	0.9	0.099	2.50	1.24	1.73	1.12	0.033	37.98
100	0.9	0.100	2.70	1.30	1.69	1.17	0.034	37.78
Anhydrite								
Sharp	-	-	2.75	1.07	1.18	0.55	0.032	33.30
10	0.2	0.042	2.49	1.011	1.33	0.75	0.028	33.39
20	0.6	0.064	-	-	-	-	-	-
30	0.7	0.078	2.99	1.22	1 61	1.08	0.035	34.46
50	1.1	0.105	2.91	1.15	1.83	1.29	0.034	33.61
100	1.8	0.160	2.73	1.23	2.15	1.60	0.030	36.63
M. Sandstone								
Sharp	-	-	0 88	0.38	0.39	0.19	0.026	14.89
10	0.2	0.157	1.06	0.51	0.59	0.30	0.027	19.14
20	0.2	0.175	1.14	0.54	0.66	0.34	0.027	19.73
30	0.7	0.187	1.15	0.51	0.63	0.31	0.029	17.68
50	1.0	0.228	1.17	0.53	0.67	0.40	0.028	19.73
100	1.4	0.228	1.20	0.59	0.77	0.43	0.028	21.15

Appendix 32B

Results of Wear Experiments

Cut Dist (m)	Weight Loss (mg)	Wear Flat (mm)	F'C kN	FC kN	F'N kN	FN kN	Q m^3/km	SE_3 MJ/m^3
Greywacke								
Sharp	-	-	2.39	1.01	2.49	1.41	0.027	38.29
10	3.6	0.411	3.22	1.55	4.06	2.45	0.029	58.66
20	5.9	0.613	3.16	1.55	4.71	2.94	0.026	62.43
30	8.1	0.723	3.39	1.79	5.41	3.39	0.027	66.97
50	13.1	0.871	3.59	1.74	5.64	3.47	0.024	72.54
100	23.6	1.185	3.83	1.94	6.11	4.37	0.025	80.03
B. Sandstone								
Sharp	-	-	1.36	0.47	0.83	0.31	0.031	14.86
10	8.0	1.200	1.78	0.72	0.32	0.65	0.029	25.12
20	16.0	1.450	2.10	0.90	1.63	0.85	0.029	31.03
30	23.2	1.720	2.29	0.81	1.77	0.96	0.031	25.87
50	37.8	1.970	2.46	0.96	2.02	1.15	0.031	31.39
100	78.9	2.140	2.79	1.25	2.52	1.61	0.029	43.00
D. Sandstone								
Sharp	-	-	0.76	0.33	0.44	0.20	0.034	9.54
10	6.2	1.183	1.00	0.55	0.97	0.57	0.028	19.42
20	16.7	1.277	1.30	0.72	1.27	0.77	0.033	21.92
30	17.4	1.561	1.32	0.76	1.38	0.79	0.033	23.21
50	30.5	1.953	1.47	0.95	1.62	1.14	0.032	29.15
100	61.2	2.001	1.67	1.13	1.94	1.38	0.030	37.24

Appendix 32C

Results of Wear Experiments

Granite

Cut Dist (m)	Weight Loss (mg)	Wear Flat (mm)	F'C kN	$\overline{FC}$ kN	F'N kN	$\overline{FN}$ kN	Q m^3/km	S.E. MJ/m^3
0.4	-	-	4.96	2.35	2.89	1.81	0.029	81.32
0.7	-	-	4.96	2.49	3.52	2.68	0.027	90.52
1.1	-	-	6.16	2.71	4.44	3.31	0.029	94.42
1.5	9.6	0.612	5.78	2.56	4.51	3.25	0.029	89.35
3.4	16.1	0.848	-	-	-	-	-	-
5.3	21.2	0.912	-	-	-	-	-	-
10	33.3	1.087	10.22	5.16	10.11	6.94	0.024	218.69
20	58.0	1.554	10.98	6.00	12.57	9.55	0.021	302.65
30	111.2	1.893	11.92	6.39	14.31	10.71	0.023	297.55
50	157.1	2.473	13.78	7.72	17.45	13.52	0.023	343.29
70	211.1	3.000	-	-	-	-	-	-
80	230.7	3.200	-	-	-	-	-	-
90	253.0	-	-	-	-	-	-	-
100	277.0	3.500	14.87	7.91	16.20	16.20	0.024	333.76

Appendix 33

Relieved Cutting Results in Mansfield Sandstone

$\alpha = 10^{\circ}$ W = 30mm

Spacing / Depth	F'C kN	$\overline{FC}$ kN	F'N kN	$\overline{FN}$ kN	Q m^3/km	S.E MJ/m^3	C.I
d = 6mm							
-0.5	2.694	1.029	1.172	0.480	0.1522	6.83	437
1.0	3.060	1.286	1.280	0.802	0.2017	6.35	455
2.5	3.175	1.365	1.357	0.829	0.2350	5.87	460
4.0	3.642	1.573	1.636	1.031	0.2308	7.199	440
6.0	4.256	1.846	1.615	0.921	0.2414	7.68	442
Unr.	4.250	1.847	1.630	1.000	0.2412	7.66	446
d = 9mm							
-0.5	3.178	1.262	1.157	0.635	0.1882	6.71	477
1.0	5.082	2.438	2.161	1.012	0.3852	6.23	484
2.5	5.826	2.459	2.194	1.071	0.3928	5.96	481
4.0	5.897	2.212	1.914	1.162	0.4405	5.14	502
6.0	5.977	3.046	2.386	1.29	0.5291	5.76	476
Unr.	6.000	3.040	2.380	1.27	0.5300	5.74	476
d = 12mm							
-0.5	3.540	1.569	1.510	0.695	0.2342	6.70	491
1.0	6.497	3.540	2.348	1.286	0.5591	6.33	528
2.5	7.539	2.857	2.421	0.971	0.5477	5.22	515
4.0	8.332	3.163	2.268	0.997	0.7030	4.50	531
6.0	8.233	3.200	2.638	1.300	0.4831	5.24	470
Unr.	8.327	3.170	2.577	1.279	0.4827	6.49	468

Appendix 34

Relieved Cutting Results in Dunhouse Sandstone

$\alpha = 10^{\circ}$ W = 30mm

Spacing Depth	F'C kN	$\overline{FC}$ kN	F'N kN	$\overline{FN}$ kN	Q m^3/km	S.E MJ/m^3	C.I
d = 6mm							
-0.5	1.807	0.650	0.901	0.350	0.1279	5.08	434
1.0	2.121	0.872	1.030	0.441	0.1918	4.55	456
2.5	2.110	0.900	9.870	0.573	0.2210	4.07	459
4.0	2.155	1.013	9.870	0.513	0.2626	3.85	437
6.0	2.305	1.008	1.201	0.717	0.2233	4.51	442
Unr.	2.315	1.000	1.300	0.720	0.2300	4.33	443
d = 9mm							
-0.5	2.059	0.748	0.988	0.42	0.2142	3.49	475
1.0	2.203	1.133	1.101	0.578	0.3388	3.34	483
2.5	2.250	0.916	1.000	0.603	0.3954	2.33	480
4.0	2.851	1.239	1.130	0.644	0.5548	2.23	497
6.0	3.068	1.224	1.600	0.844	0.4251	2.88	473
Unr.	3.100	1.250	1.591	0.840	0.4310	2.90	474
d = 12mm							
-0.5	2.970	0.989	1.026	0.562	0.3009	3.29	484
1.0	3.935	1.155	1.516	0.809	0.3986	2.90	523
2.5	3.935	1.244	1.699	0.876	0.6553	2.40	513
4.0	5.612	1.375	2.083	0.930	0.7817	1.76	530
6.0	5.300	1.950	2.500	0.931	0.8767	2.25	467
Unr.	5.401	1.877	2.527	0.941	0.8760	2.14	465

REFERENCES

1. JANSSON, B. - "Underground Forecast"
   Tunnels and Tunnelling, Vol.6, No.1
   Jan-Feb 1974.

2. TREGELLES, P.G.
   WOODLEY, J.N.L. - "High-Speed Tunnelling",
   Symposium on Mining Methods, Harrogate.
   pp.11, October 1975.

3. FECKLER, W.
   LUCKER, A. - "Experience with a Two-Stage Full-Face Heading Machine at Consolidation Colliery'
   Glückauf, No.22, pp.1083-7,
   25 October 1973.

4. BARKING, E.H.
   BOLDT, H. - "First Practical Experience in Mechanised Drivage of Hard Headings at Rheinland Combine"
   Glückauf, No.1, pp.5-10, 9 January 1975.

5. GRAHAM, P.C. - "Some Problems Associated with the Use of a Tunnel Machine in Deep-Level Gold Mines"
   Tunnelling 76 Conference, London,
   p.7, March 1976..

6. SIMONIN, L. - "Underground Life or Mines and Miners"
   London, Chapman and Hall, 193, Picadilly,
   1869.

7. WANG, F. et al. - "Improvement Underground Excavation Through the Application of Hydraulic Water Jet Assisted, etc."
   Colorado School of Mines, Golden Excav.
   Eng. and Earth Mechanics Institute,
   p.173, Feb. 1976.

8. EVANS, I. - "Relative Efficiency of Picks and Discs for Cutting Rocks" Advance in Rock Mechanics, Reports of Current Research, National Academy of Sciences, Washington. Vol.II, part B.,pp.1407-12, 1974.

9. ROXBOROUGH, F.F. PHILLIPS, H.R. - "Rock Excavation by Disc Cutter" Int.J. Rock Mech. and Min. Sci., Vol.12, pp.361-6, 1975.

10. HEWITT, K. - "Aspects of the Design and Application of Cutting Systems for Rock Excavation" Ph.D. Thesis, University of Newcastle upon Tyne, p.250, 1976.

11. PHILLIPS, H.R. - "Rock Cutting Mechanics Related to the Design of Primary Excavation Systems" Ph.D. Thesis, University of Newcastle upon Tyne, October 1975.

12. BARON, L.L. ZAGORSKII, S.L. LOGOUNTZOW, B.M. - "Fragmentation des Roches par des Taillants a Molettes Biseautées" Translation of Cerchar, Translation No. 232-63, p.19, January 1962.

13. ROXBOROUGH, F.F. RISPIN, A. - "The Mechanical Cutting Characteristics of the Lower Chalk" Tunnell and Tunnelling, pp.45-67, January 1973.

14. TAKAOKA, S.
HAYAMIZU, H.
MISAWA, S.
- "Rock Cutting by Disc Cutters"
Tunnel and Tunnelling, pp.181-5,
March 1973.

15. TAKAOKA, S.
HAYAMIZU, H.
MISAWA, S.
KURIYAGAWA, M
- "Mechanical Fracture Characteristics of Rock with a Cutter Bit and a Disc Cutter"
Advance in Rock Mechanics, National Academy of Sciences, Washington, pp.1723-9, 1974.

16. MORREL, R.J.
BRUCE, W.E.
LARSON, D.A.
-"Disc Cutters Experiments in Sedimentary and Metamorfic Rocks"
U.S.B.M.,R.I. 7410, p.32, 1970.

17. MORREL, R.J.
LARSON, D.A.
-"Disc Cutter Experiments in Metamorfic and Igneous Rocks"
U.S.B.M., R.I. 7961,p50 , 1974.

18. ROSS, N.
HUSTRULID, W.A.
-"Development of a Tunnel Boreability Index"
Colorado School of Mines, Golden Dept. of Mining,
p.378, Feb. 72.

19. OZDEMIR, L.
- "A Laboratory and Field Investigation of Tunnel Boreability"
Colorado School of Mines, Golden Dept. of Mining, p.201, 6 May 1975.

20. RAD, P.F.
SCHMIDT, R.L.
- "Development of an Experimental Full Scale Rock Cutting Device" U.S.B.M, I.R. 7787, p.18, 1973.

21. RAD, P.F.
McGARRY, F.J.
- "Thermally Assisted Cutting of Granite" Proc. 12th Symp. on Rock Mech., University of Missouri - - Rolla, Nov.16-18, 1970, AIME, New York, pp.721-57.

22. RAD, P.F.
OLSON, R.C.
- "Interaction Between Disc-Cutter Grooves in Rocks" U.S.B.M., R.I. 7881, p.21, 1974.

23. RAD, P.F.
- "Muck Evaluates Machines" Tunnels and Tunnelling, pp.30-3, January, 1975.

24. ROBBINS, J.
- "Economic Factors in Tunnel Boring" The South African Tunnelling Conference, pp.1-8, July 1970.

25. INNAURADO, N.
MANCINI, R.
PELIZZA, S.
- "Consideration of Rock Boring Machines: Analyses of Italian Operation" Tunnelling Conference, London. p.5, March 76.

26. RAD, P.F.
- "Bluntness and Wear of Rolling Disc Cutters" Int.J.Rock Mech.Min.Sci. and Geomech. Abstr.Vol.12, pp.93-9, 1975.

27. HIGNETT, H.J.
BODEN, J.B.
- "Chinnor Tunnelling Trials - Background and Progress"
Tunnels and Tunnelling,
pp.65-70, No.6, 1974.

28. O'REILLY, M.P.
ROXBOROUGH, F.F.
HIGNETT, H.J.
- "Programme of Laboratory Pilot and Full-Scale Experiments in Tunnel Boring"
Tunnelling Conference, London.
p.15, March 76.

29. RAD, P.F.
- "Correlation of Laboratory Data with Tunnel Boring Machine Performance"
U.S.B.M., R.I. 7883,
p.19, 1974.

30. HUSTRULID, W.A.
- "A Theoretical and Experimental Study of Tunnel Boring by Machine"
Colorado School of Mines, Golden
Dept. of Mining Eng., Feb.72.

31. WANG, F.
MILLER, R.J.
- "A Theoretical and Experimental Study of Tunnel Boring by Machine",
Colorado School of Mines, Golden
Dept. of Mining Eng., Aug. 72.

32. HUSTRULID, W.A.
- "A comparison of Laboratory Cutting Results and Actual Boring Performance"
1st North American Rapid Excavation and Tunnelling Conference, Chicago, Illinois,
Proceedings, Vol.2, pp.1299-323, June 72.

33. WANG, F.
MILLER R.
OZDEMIR, L.
- "Improving Hard Rock Tunnelling through Comparison of Laboratory and Field Tunnel Boring Studies"
Proceedings, Rapid Excavation and Tunnelling Conference, San Francisco, California, June 74, Vol.2, pp.1742-57.

34. GOBETZ, F.W.
- "Development of a Boring Machine cutter Instrumentation"
Aircraft Research Labs., East Hartford, Conn. Varl., p.175, June 1973.

35. HIGGINS, R.J.
HIGNETT, H.J.
- "Monitoring Forces on Rock Cutting Tools"
Tunnels and Tunnelling, No.4, pp.39-41, 1975.

36. NEW, B.M.
TEMPORAL, J.
- "Tunnelling Machine Data Acquisition and Processing System"
Tunnelling Conference, London. p.11, March 1976.

37. MELLOR, M.
HAWKES, I.
- "How to Rate a Hard-Rock Borer"
World Construction, pp.21-3, September, 1972.

38. MELLOR, M.
HAWKES, I.
- "Hard Rock Tunnelling Machine Characteristics"
1st North American Rapid Excavational Tunnelling Conference, Chicago, pp.1149-58, 1972.

39. NIZAMOĞLU, S. - "Etude des Liaisons Entre les Parametres de Fonctionnement d'un Tunnelier dans un Terrain Donne"
Laboratoire de Mecanique des Terrains Cerchar. Ecole des Mines de Nancy. 75-73-2100 No.153, p.13, September 1975.

40. GAYE, F. - "Efficient Excavation"
Tunnels and Tunnelling, pp.39-48, January 1972, Part II pp.135-43, March 1972.

41. REES, P.B.
HUGHES, H.M.
HAY, J.D. - "Full-Face Tunnelling Machines in British Coal Mines"
Tunnelling Conference, London, p.10, March 76.

42. HIBBARD, R.R.
HYMAN, O.S.
MURPHY, F.H. - "Hard Rock Tunnelling Evaluation and Computer Simulation"
General Research Corp. Arlington, Sept.71.

43. TARKOY, P.J. - "Rock Index Properties to Predict Turnell Boring Machine Penetration Rates"
Illinois Univ.Urbans., Dept. of Civil Eng., p.48, June 76.

44. TARKOY, P.J. - "Rock Hardness Index Properties and Geotechnical Parameters for Predicting Tunnel Boring Machine Performance" Illinois Univ. at Urbana - Champaign, Dept. of Civil Eng., p.347, Sept.75.

45. MILLER, P.P. - "Eng. Classification of Index Properties of Intact Rock" Ph.D. Thesis, University of Illinois Urbana, pp.333, 1965.

46. NIZAMOĞLU, S. - "Essais de Sclerometrie dans la Galerie et Explication de la Vitesse du Tunnelier par la Dureté au Rebondissement" Laboratoire de Mecanique des Terrains Cerchar - Ecole des Mines de Nancy, 75-73-2100 No.152, p.20, Aout 1975.

47. COMES - "Le Creusement d'une Galerie d'Amenée D'ouvrage Hydroélectrique à L'Aide d'une Machine Foreuse" Advances in Rock Mechanics. Proceedings of a Third Congress of the International Society for Rock Mechanics. Denver, 1974, II B, pp.1476-80.

48. TEALE, R. - "The Mechanical Excavation of Rock - Experiments with Roller Cutters" Int.J. Rock Mech. and Mining Sic., Vol.1, pp.63-78, 1963.

49. BIGGS, M.D.
CHEATHAM, J.B.
- "Theoretical Forces for Prescribed Motion of a Roller Bit"
Society of Petroleum Eng. of AIME, 1969.
Paper No. SPE 2391.

50. PETERSON, C.R.
- "Roller Cutter Forces"
Society of Petroleum Eng. Journal of AIME, pp.57-65, March 1970.

51. PRICE, N.J.
SHEPHERD, R.
- "Roller Bit Penetration Experiments in Concretes"
Proc. of a Conference on the Mechanical Properties of non-Metallic Brittle Materials, pp.336-45, London, 1958

52. ROXBOROUGH, F.F.
RISPIN, A.
- "The Mechanical Cutting Characteristics of the Lower Chalk"
Report to T.R.R.L.
University of Newcastle upon Tyne,
p. 197[illegible],May 1972.

53. MILLER, M.H.
- "On the Penetration of Rocks by Three-Dimensional Indentors"
Int. J. Rock Mech.Min.Sci.,
Vol 5, pp.375-98, 1968.

54. HAMBACH, P.
- "An Inclined Gallery Through Hard Rock"
Tunnels and Tunnelling,
May-June 1970.

55. HAMBACH, P. - "Excavation of Inclined Shaft by Reaming in Two Stages" Rapid Excavation and Tunnelling Conference, California, Proceedings Vol.2., pp.1651-63, 1974.

56. SEILER, W.K. - "Hard Rock Boring with Tungsten Carbide Insert Big Cutters" 1st North American Rapid Excavation and Tunnelling Conference, Chicago, Proceedings Volume 2, pp.1149-58, 1972.

57. HANDEWITH, H.J. - "Predicting the Economic Success of Continuous Tunnelling in Hard Rock" Canadian Mining and Metallurgical Bulletin pp.595-9, May 1970.

58. HANDEWITH, H.J. - "Machine Boring and the Mechanical Properties of Hard Rock" Australian Geomechanics Society, Symposium on Raise and Tunnel Boring p.5 14-15 August 1970.

59. MORRIS, R.I. - "Rock Drillability Related to a Roller Cone Bit" Proceedings of Society of Petroleum Engineers of AIME. Paper No. SPE 2389, pp.79-86,1969.

60. LIGHTFOOT, R.M. - "Drillability and Wear Prediction by Laboratory Techniques and Correlation with Operating Experience" Australian Geomechanics Society Symposium on Raise and Tunnel Boring. p.15, 14-15 August 1970.

61. CALDER, P.N. - "Rock Mechanics Aspects of Large Hole Boring Machine Design" 8th Canadian Rock Mechanics Symposium. pp.159-75, 1972.

62. EVANS, I. POMEROY, C.O. - "The Strength, Fracture and Workability of Coal" Pergamon, London, p.256, 1966.

63. ROXBOROUGH, F.F. - "Cutting Rocks with Picks" The Mining Engineer, Vol.132, pp.445-54, June 1973.

64. ROXBOROUGH, F.F. RISPIN, A. - "A Laboratory Investigation into the Application of Picks for Mechanised Tunnel Boring in the Lower Chalk" The Mining Engineer, Vol.133, pp.1-13. October 1973.

65. EVANS, I. - "Energy Requirements for Impact Breakage" Conference on Fluid Power Equipment in Mining, Quarrying and Tunnelling. pp.1-8, February 1974.

66. NISHIMATSU, Y. - "The Mechanics of Rock Cutting" Int.J. Rock Mech. Min.Sci. Vol.9. pp.261-70, 1972.

67. BARKER, J.S. - "A Laboratory Investigation of Rock Cutting using Large Picks" Int.J.Rock Mech.Min.Sci.,Vol.1., pp.519-34, 1964.

68. BARKER, J.S.
POMEROY, C.O.
WHITTAKER, D. - "The M.R.E. Large Pick Shearer Drum" The Mining Engineer, p.323. February 1966.

69. POTTS, E.L.J.
SHUTTLEWORTH, P. - "A Study on the Ploughability of Coal" Trans. Inst. Min. Engrs. Vol.117, No.8, p.512, May 1959.

70. POTTS, E.L.J.
ROXBOROUGH, F.F.
WHITTAKER, B.N. - "Experiments with the Automatic Variable Geometry Coal Plough" The Mining Engineer, p.539, May 1967.

71. ROXBOROUGH, F.F.
ESKIKAYA, S. - "An Investigation into some Aspects of Coal Plough System Design using a $\frac{1}{4}$ Scale Dynamic Model" The Mining Engineer, No.134, pp.55-68, November 1971.

72. ALLINGTON, A.V. - "The Machining of Rock Materials" Ph.D. Thesis, University of Newcastle upon Tyne, p.192, September 1969.

73. RISPIN, A. - "An Investigation into the Application of Linear Cutting Tools to the Machining of Strong and Abrasive Rock Materials" Ph.D. Thesis, University of Newcastle upon Tyne, p.325, October 1970.

74. FOWELL, R.J. - "Studies on the Application of Percussively Activated Tools to Relief Slotting in Some South African Quartzites" Ph.D. Thesis, University of Newcastle upon Tyne, 1973.

75. ROXBOROUGH, F.F. PHILLIPS, H.R. - "The Mechanical Properties and Cutting Characteristics of the Bunter Sandstone" Report to T.R.R.L., University of Newcastle upon Tyne, p.217, 1975.

76. DUNN, P. - "An Investigation into the Mechanical Cutting of Hard Rock Materials in Relation to the Design of Effective Tunnelling Systems" Ph.D. Thesis, University of Newcastle upon Tyne, p.132, February 1975.

77. HOOD, M. - "Cutting Strong Rock with a Drag Bit Assisted by High-Pressure Water Jets" Journal of the South African Institute of Mining and Metallurgy, pp.79-90, November 1976.

78. KENNY P
JOHNSON, S.N.
- "The Effect of Wear on the Performance of Mineral-Cutting Tools"
Colliery Guardian, June, pp.246-52, 1976.

79. KENNY, P
JOHNSON, S.N.
- "An Investigation of the Abrasive Wear of Mineral-Cutting Tools"
Wear, Vol.36, pp.337-61, 1976.

80. HARLE, M.
- "Private Communication"

81. FOWELL, R.J.
McFEAT-SMITH, I.
- "Factors Influencing the Cutting Performance of a Selective Tunnelling Machine".
Tunnelling 76,
Symposium, London, March 1976.

82. McFEAT-SMITH, I.
FOWELL, R.J.
- "Correlation of Rock Properties and the Cutting Performance of Tunnelling Machines"
Proc. on Rock Engineering,
Newcastle upon Tyne, pp.581-602,
4-7th April 1977.

83. PROTODYAKANOV, M.M.
TEDER, R.I.
- "Application of Statistical Curves to Laboratory Experiments"
U.S.S.R. Academy of Sciences,
Nauka - Moskow.
p.73, 1970.

84. PROTODYAKANOV, M.M.
TEDER, R.I.
- "Rational Methods of Planning Experiments"
Proc. 12th Symp. on Rock Mechanics, Rolla.
pp.129-49, 1970.

85. YATES, F. - "Experimental Design - Selected Papers"
Griffin, London.
p. 293, 1970.

86. NOTHOLT, A.J.G.
HIGHLEY, O.E. - "Gypsum and Anhydrite"
Mineral Resources Consultative Committee
Department of Industry, p. 38, 1970.

87. ARTHURTON, R.S.
HEMINGWAY, T.E. - "The St. Bees Evaporites"
Proc. Yorkshire Geol. Soc., Vol.38,
Part 4, No.24, January 1972.

88. MILLER, R.P. - "Eng. Classification and Index Properties of Intact Rock"
Ph.D. Thesis, University of Illinois,
Urbana, p.333, 1965.

89. McFEAT-SMITH, I. - "Rock Property Testing for the Assessment of Tunnelling Machine Performance"
Tunnels and Tunnelling, pp.29-33,
March 1977.

90. SZLAVIN, J. - "Relationships between some Physical Properties of Rocks Determined by Laboratory Tests"
Int.J.Rock Mech.Min.Sci. and Geomech.Abst.,
Vol.11, pp.57-66, 1974.

91. PHILLIPS, H.R. - "The Mechanical Cutting Characteristics and Properties of Selected Rock Formations" Report to T.R.R.L., University of Newcastle upon Tyne, p.218, December 1975.

92. PAUL, B. SIKARSKIE, D.L. - "A Preliminary theory of Static Penetration by a Rigid Wedge into a Brittle Material" VII Symposium on Rock Mechanics, Pennsylvania State University, pp.119-48, 1965.

93. ROBBINS, R.J. - "Mechanized Tunnelling - Progress and Expectations" Tunnels and Tunnelling, pp.47-52, May-June 1976.

94. LAWRENCE, J.R. - "Applied Engineering Statistics for Practising Engineers" Barnes and Nobe, inc.New York, 1970.

95. - - - - "Blast Hole Bit Handbook" Hughes Tool Company, p.28, 1975.

96. - - - - "Rockbreaking without Explosives" Research Review, Chamber of Mines of South Africa, pp.1-11, 1973.

97. BARENDSEN, P. - "Machine-Bored Small-Size Tunnels in Rock, with Some Case Studies" Tunnelling 76, March, London.

98. MORTON, W.A.T. - "Tunnelling Machines and Systems" South African Tunnelling Conference. pp.64-70, 1970.

99. SAVANICK, G.A. JOHNSON, D. - "Measurements of the Strength of Grain Boundaries in Rock" J.Rock Mech.Min.Sci. and Geomech.Abs. Vol.11, pp.173-80, 1974.

100. RZHEVSKY, V. NOVIK, G. - "The Physics of Rocks" Mir Publishers, Moscow, p.320, 1971.

101. RISPIN, A. COOPER, I. - "Fourth Progress Report to the Wolfson Foundation in Rock Cutting Mechanics" University of Newcastle upon Tyne, p.56, October 1974.

102. ROXBOROUGH, F.F. - "A Comparative Study of Picks and Discs" Second Australian Tunnelling Conference, Melbourn, 1976.

* * *